OPTICAL MICROSCOPY

Michael W. Davidson[1] and Mortimer Abramowitz[2]

[1] National High Magnetic Field Laboratory, The Florida State University, 1800 E. Paul Dirac Dr., Tallahassee, Florida 32306, davidson@magnet.fsu.edu, http://microscopy.fsu.edu

[2] Olympus America, Inc., 2 Corporate Center Dr., Melville, New York 11747, abramm@olympus.com, http://www.olympus.com

Keywords: microscopy, phase contrast, differential interference contrast, DIC, polarized light, Hoffman modulation contrast, photomicrography, fluorescence microscopy, numerical aperture, CCD electronic cameras, CMOS active pixel sensors, darkfield microscopy, Rheinberg illumination.

Introduction

The past decade has witnessed an enormous growth in the application of optical microscopy for micron and sub-micron level investigations in a wide variety of disciplines (reviewed in references 1-5). Rapid development of new fluorescent labels has accelerated the expansion of fluorescence microscopy in laboratory applications and research (6-8). Advances in digital imaging and analysis have also enabled microscopists to acquire quantitative measurements quickly and efficiently on specimens ranging from photosensitive caged compounds and synthetic ceramic superconductors to real-time fluorescence microscopy of living cells in their natural environment (2, 9). Optical microscopy, with help of digital video, can also be used to image very thin optical sections, and confocal optical systems are now in operation at most major research institutions (10-12).

Early microscopists were hampered by optical aberration, blurred images, and poor lens design, which floundered until the nineteenth century. Aberrations were partially corrected by the mid-nineteenth century with the introduction of Lister and Amici achromatic objectives that reduced chromatic aberration and raised numerical apertures to around 0.65 for dry objectives and up to 1.25 for homogeneous immersion objectives (13). In 1886, Ernst Abbe's work with Carl Zeiss led to the production of apochromatic objectives based for the first time on sound optical principles and lens design (14). These advanced objectives provided images with reduced spherical aberration and free of color distortions (chromatic aberration) at high numerical apertures.

Several years later, in 1893, Professor August Köhler reported a method of illumination, which he developed to optimize photomicrography, allowing microscopists to take full advantage of the resolving power of Abbe's objectives. The last decade of the nineteenth century saw innovations in optical microscopy, including metallographic microscopes, anastigmatic photolenses, binocular microscopes with image-erecting prisms, and the first stereomicroscope (14).

Early in the twentieth century, microscope manufacturers began parfocalizing objectives, allowing the image to remain in focus when the microscopist exchanged objectives on the rotating nosepiece. In 1824, Zeiss introduced a LeChatelier-style metallograph with infinity-corrected optics, but this method of correction would not see widespread application for another 60 years.

Shortly before World War II, Zeiss created several prototype ***phase contrast*** microscopes based on optical principles advanced by Frits Zernike. Several years later the same microscopes were modified to produce the first time-lapse cinematography of cell division photographed with phase contrast optics (14). This contrast-enhancing technique did not become universally recognized until the 1950s and is still a method of choice for many cell biologists today.

Physicist Georges Nomarski introduced improvements in Wollaston prism design for another powerful contrast-generating microscopy theory in 1955 (15). This technique is commonly referred to as ***Nomarski interference*** or ***differential interference contrast*** (DIC) microscopy and, along with phase contrast, has allowed scientists to explore many new arenas in biology using living cells or unstained tissues. Robert Hoffman (16) introduced another method of increasing contrast in living material by taking advantage of phase gradients near cell membranes. This technique is now termed Hoffman Modulation Contrast, and is available as optional equipment on most modern microscopes.

The majority of microscopes manufactured around the world had fixed mechanical tube lengths (ranging from 160 to 210 millimeters) until the late 1980s, when manufacturers largely migrated to infinity-corrected optics. Ray paths through both finite tube length and infinity-corrected microscopes are illustrated in Figure 1. The upper portion of the figure contains the essential optical elements and ray traces defining the optical train

of a conventional finite tube length microscope (17). An object (**O**) of height **h** is being imaged on the retina of the eye at **O"**. The objective lens ($\mathbf{L_{ob}}$) projects a real and inverted image of **O** magnified to the size **O**' into the intermediate image plane of the microscope. This occurs at the eyepiece diaphragm, at the fixed distance **fb + z'** behind the objective. In this diagram, **fb** represents the back focal length of the objective and **z'** is the optical tube length of the microscope. The aerial intermediate image at **O'** is further magnified by the microscope eyepiece ($\mathbf{L_{ey}}$) and produces an erect image of the object at **O"** on the retina, which appears inverted to the microscopist. The magnification factor of the object is calculated by considering the distance (**a**) between the object (**O**) and the objective ($\mathbf{L_{ob}}$) , and the front focal length of the objective lens (**f**). The object is placed a short distance (**z**) outside of the objective's front focal length (**f**), such that **z + f = a**. The intermediate image of the object, **O'**, is located at distance **b**, which equals the back focal length of the objective (**fb**) plus (**z'**), the optical tube length of the microscope. Magnification of the object at the intermediate image plane equals **h'**. The image height at this position is derived by multiplying the microscope tube length (**b**) by the object height (**h**), and dividing this by the distance of the object from the objective: **h' = (h x b)/a**. From this argument, we can conclude that the lateral or transverse magnification of the objective is equal to a factor of **b/a** (also equal to **f/z** and **z'/fb**), the back focal length of the objective divided by the distance of the object from the objective. The image at the intermediate plane (**h'**) is further magnified by a factor of 25 centimeters (called the ***near*** distance to the eye) divided by the focal length of the eyepiece. Thus, the total magnification of the microscope is equal to the magnification by the objective times that of the eyepiece. The visual image (virtual) appears to the observer as if it were 10 inches away from the eye.

Most objectives are corrected to work within a narrow range of image distances, and many are designed to work only in specifically corrected optical systems with matching eyepieces. The magnification inscribed on the objective barrel is defined for the tube length of the microscope for which the objective was designed.

The lower portion of Figure 1 illustrates the optical train using ray traces of an infinity-corrected microscope system. The components of this system are labeled in a similar manner to the finite-tube length system for easy comparison. Here, the magnification of the objective is the ratio **h'/h**, which is determined by the tube lens ($\mathbf{L_{tb}}$). Note the ***infinity space*** that is defined by parallel light beams in every azimuth between the objective and the tube lens. This is the space used by microscope manufacturers to add accessories such as vertical illuminators, DIC

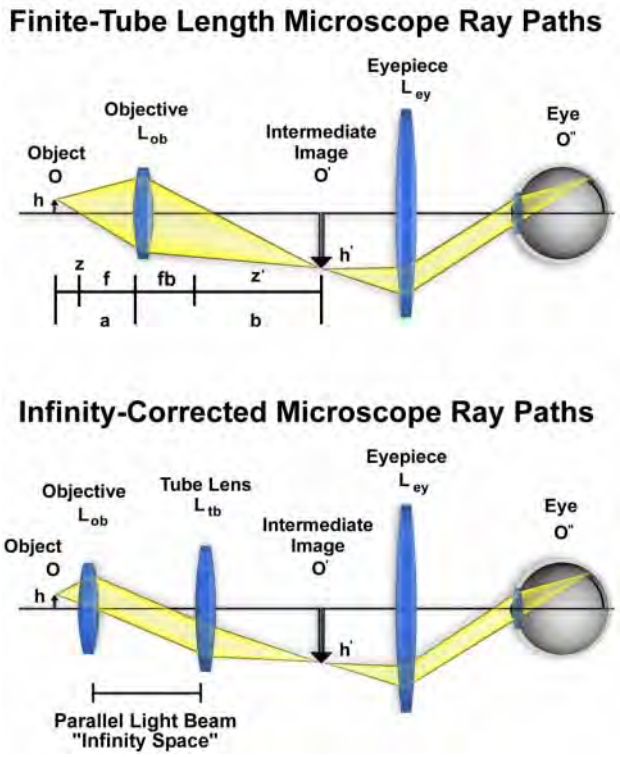

Figure 1. Optical trains of finite-tube and infinity-corrected microscope systems. (Upper) Ray traces of the optical train representing a theoretical finite-tube length microscope. The object (**O**) is a distance (**a**) from the objective (L**ob**) and projects an intermediate image (**O'**) at the finite tube length (**b**), which is further magnified by the eyepiece (**Ley**) and then projected onto the retina at **O**". (Lower) Ray traces of the optical train representing a theoretical infinity-corrected microscope system.

prisms, polarizers, retardation plates, etc., with much simpler designs and with little distortion of the image (18). The magnification of the objective in the infinity-corrected system equals the focal length of the tube lens divided by the focal length of the objective.

Fundamentals of Image Formation

In the optical microscope, when light from the microscope lamp passes through the condenser and then through the specimen (assuming the specimen is a light absorbing specimen), some of the light passes both around and through the specimen undisturbed in its path. Such light is called direct light or undeviated light. The background light (often called the surround) passing around the specimen is also undeviated light.

Some of the light passing through the specimen is deviated when it encounters parts of the specimen. Such deviated light (as you will subsequently learn, called diffracted light) is rendered one-half wavelength or 180

degrees out of step (more commonly, out of phase) with the direct light that has passed through undeviated. The one-half wavelength out of phase, caused by the specimen itself, enables this light to cause destructive interference with the direct light when both arrive at the intermediate image plane located at the fixed diaphragm of the eyepiece. The eye lens of the eyepiece further magnifies this image which finally is projected onto the retina, the film plane of a camera, or the surface of a light-sensitive computer chip.

What has happened is that the direct or undeviated light is projected by the objective and spread evenly across the entire image plane at the diaphragm of the eyepiece. The light diffracted by the specimen is brought to focus at various localized places on the same image plane, where the diffracted light causes destructive interference and reduces intensity resulting in more or less dark areas. These patterns of light and dark are what we recognize as an image of the specimen. Because our eyes are sensitive to variations in brightness, the image becomes a more or less faithful reconstitution of the original specimen.

To help understand the basic principles, it is suggested that readers try the following exercise and use as a ***specimen*** an object of known structure, such as a stage micrometer or similar grating of closely spaced dark lines. To proceed, place the finely ruled grating on the microscope stage and bring it into focus using first a 10x and then the 40x objective (18). Remove the eyepiece and, in its place, insert a phase telescope so the rear focal plane of the objective can be observed. If the condenser aperture diaphragm is closed most of the way, a bright white central spot of light will appear at the back of the objective, which is the image of the aperture diaphragm. To the right and left of the central spot, a series of spectra (also images of the aperture diaphragm) will be present, each colored blue on the part closest to the central spot and colored red on the part of the spectrum farthest from the central bright spot (as illustrated in Figure 2). The intensity of these colored spectra decreases according to how far the spectrum is from the central spot (17,18).

Those spectra nearer the periphery of the objective are dimmer than those closer to the central spot. The diffraction spectra illustrated in Figure 2 using three different magnifications. In Figure 2(b), the diffraction pattern visible at the rear focal plane of the 10X objective contains two diffraction spectra. If the grating is removed from the stage, as illustrated in Figure 2(a), these spectra disappear and only the central image of the aperture diaphragm remains. If the grating is reinserted, the spectra reappear once again. Note that the spaces between the colored spectra appear dark. Only a single pair of spectra can be observed if the grating is examined with the 10x objective. In this case, one diffraction spot appears to the left and one appears to the right of the central aperture opening. If the line grating is examined with a 40x objective (as shown in Figure 2(c)), several diffraction spectra appear to the left and right of the central aperture. When the magnification is increased to 60x (and assuming it has a higher numerical aperture than the 40x objective), additional spectra (Figure 2(d)) appear to the right and left than are visible with the 40x objective in place.

Because the colored spectra disappear when the grating is removed, it can be assumed that it is the specimen itself that is affecting the light passing through, thus producing the colored spectra. Further, if the aperture diaphragm is closed down, we will observe that objectives of higher numerical aperture ***grasp*** more of these colored spectra than do objectives of lower numerical aperture. The crucial importance of these two statements for understanding image formation will become clear in the ensuing paragraphs.

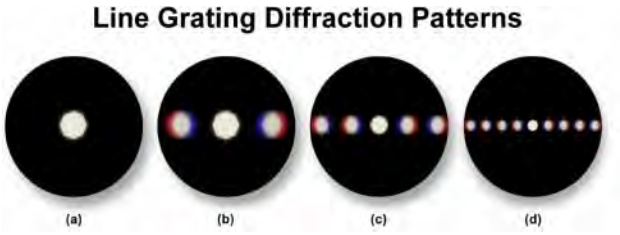

Figure 2. Diffraction spectra seen at the rear focal plane of the objective through a focusing telescope when imaging a closely spaced line grating. (a) Image of the condenser aperture diaphragm with an empty stage. (b) Two diffraction spectra from a 10x objective when a finely ruled line grating is placed on the microscope stage. (c) Diffraction spectra of the line grating from a 40x objective. (d) Diffraction spectra of the line grating from a 60x objective.

The central spot of light (image of the condenser aperture diaphragm) represents the direct or undeviated light passing through the specimen or around the specimen undisturbed (illustrated in Figure 3(b)). It is called the 0th or zeroth order. The fainter images of the aperture diaphragm on each side of the zeroth order are called the 1st, 2nd, 3rd, 4th, etc. orders respectively, as represented by the simulated diffraction pattern in Figure 3(a) that would be observed at the rear focal plane of a 40x objective. All the ***captured*** orders represent, in this case, the diffraction pattern of the line grating as seen at the rear focal plane of the objective (18).

The fainter diffracted images of the aperture diaphragm are caused by light deviated or diffracted, spread out in fan shape, at each of the openings of the line grating (Figure 3(b)). The blue wavelengths are diffracted at a lesser angle than the green wavelengths, which are diffracted at a lesser angle than the red wavelengths.

At the rear focal plane of the objective, the blue wavelengths from each slit interfere constructively to produce the blue area of the diffracted image of each spectrum or order; similarly for the red and green areas (Figure 3(a)). Where the diffracted wavelengths are 1/2 wave out of step for each of these colors, the waves destructively interfere. Hence the dark areas between the spectra or orders. At the position of the zeroth order, all wavelengths from each slit add constructively. This produces the bright white light you see as the zeroth order at the center of the rear focal plane of the objective (Figures 2, 3 and 4).

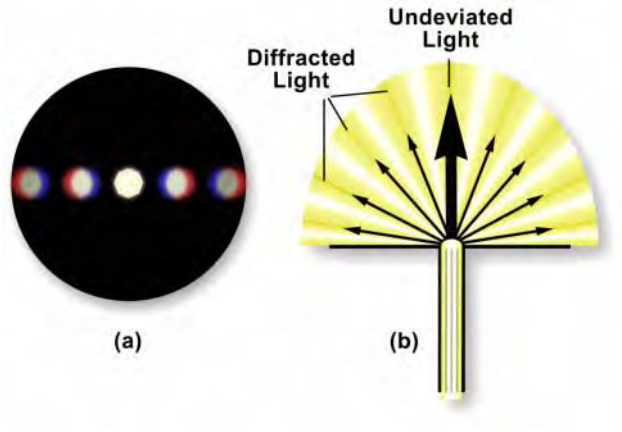

Figure 3. Diffraction spectra generated at the rear focal plane of the objective by undeviated and diffracted light. (a) Spectra visible through a focusing telescope at the rear focal plane of a 40x objective. (b) Schematic diagram of light both diffracted and undeviated by a line grating on the microscope stage.

The closer the spacing of a line grating, the fewer the spectra that will be captured by a given objective, as illustrated in Figure 4(a-c). The diffraction pattern illustrated in Figure 4(a) was captured by a 40x objective imaging the lower portion the line grating in Figure 4(b), where the slits are closer together (17, 18). In Figure 4(c), the objective is focused on the upper portion of the line grating (Figure 4(b)) where the slits are farther apart, and more spectra are captured by the objective. The direct light and the light from the diffracted orders continue on, being focused by the objective, to the intermediate image plane at the fixed diaphragm of the eyepiece. Here the direct and diffracted light rays interfere and are thus reconstituted into the real, inverted image that is ***seen*** by the eye lens of the eyepiece and further magnified. This is illustrated in Figure 4 (d-g) with two types of diffraction gratings. The square grid illustrated in Figure 4(d) represents the orthoscopic image of the grid (i.e. the usual specimen image) as seen through the full aperture of the objective. The diffraction pattern derived from this grid is shown as a conoscopic image that would be seen

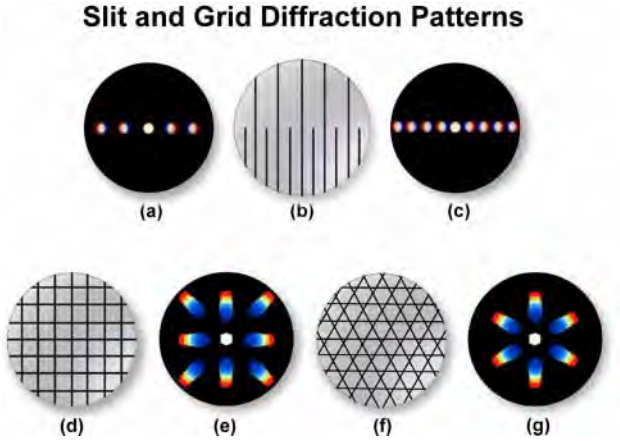

Figure 4. Diffraction patterns generated by narrow and wide slits and by complex grids. (a) Conoscopic image of the grid seen at the rear focal plane of the objective when focused on the wide slit pattern in (b). (b) Orthoscopic image of the grid with greater slit width at the top and lesser width at the bottom. (c) Conoscopic image of the narrow width portion of the grid (lower portion of (b)). (d) and (f) Orthoscopic images of grid lines arranged in a square pattern (d) and a hexagonal pattern (f). (e) and (g) Conoscopic images of patterns in (d) and (f), respectively.

at the rear focal plane of the objective (Figure 4(e). Likewise, the orthoscopic image of a hexagonally arranged grid (Figure 4(f)) produces a corresponding hexagonally arranged conoscopic image of first order diffraction patterns (Figure 4(g)).

Microscope specimens can be considered as complex gratings with details and openings of various sizes. This concept of image formation was largely developed by Ernst Abbe, the famous German microscopist and optics theoretician of the 19th century. According to Abbe (his theories are widely accepted at the present time), the details of a specimen will be resolved if the objective captures the 0th order of the light and at least the 1st order (or any two orders, for that matter). The greater the number of diffracted orders that gain admittance to the objective, the more accurately the image will represent the original object (2, 14, 17, 18).

Further, if a medium of higher refractive index than air (such as immersion oil) is used in the space between the front lens of the objective and the top of the cover slip (as shown in Figure 5(a)), the angle of the diffracted orders is reduced and the fans of diffracted light will be compressed. As a result, an oil immersion objective can capture more diffracted orders and yield better resolution than a dry objective (Figure 5(b)). Moreover, because blue light is diffracted at a lesser angle than green light or red light, a lens of a given aperture may capture more orders of light when the wavelengths are in the blue region of the visible light spectrum. These two principles explain

the classic Rayleigh equation often cited for resolution (2, 18-20):

$$d = 1.22 (l / 2NA) \qquad (1)$$

Where **d** is the space between two adjacent particles (still allowing the particles to be perceived as separate), l is the wavelength of illumination, and **NA** is the numerical aperture of the objective.

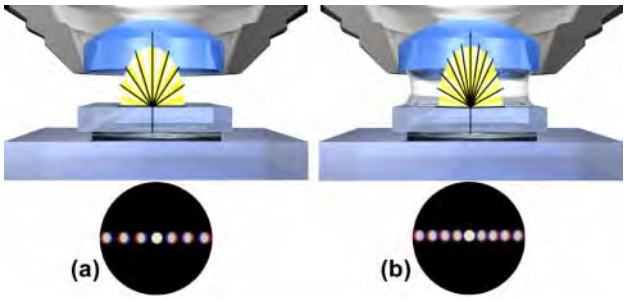

Figure 5. Effect of imaging medium refractive index on diffracted orders captured by the objective. (a) Conoscopic image of objective back focal plane diffraction spectra when air is the medium between the cover slip and the objective front lens. (b) Diffraction spectra when immersion oil of refractive index similar to glass is used in the space between the cover slip and the objective front lens.

The greater the number of higher diffracted orders admitted into the objective, the smaller the details of the specimen that can be clearly separated (resolved). Hence the value of using high numerical aperture for such specimens. Likewise, the shorter the wavelength of visible light used, the better the resolution. These ideas explain why high numerical aperture, apochromatic lenses can separate extremely small details in blue light.

Placing an opaque mask at the back of the objective blocks the outermost diffracted orders. This either reduces the resolution of the grating lines, or any other object details, or it destroys the resolution altogether so that the specimen is not visible. Hence the usual caution not to close down the condenser aperture diaphragm below the suggested 2/3 to 9/10 of the objective's aperture.

Failure of the objective to grasp any of the diffracted orders results in an unresolved image. In a specimen with very minute details, the diffraction fans are spread at a very large angle, requiring a high numerical aperture objective to capture them. Likewise, because the diffraction fans are compressed in immersion oil or in water, objectives designed for such use can give better resolution than dry objectives.

If alternate diffracted orders are blocked out (still assuming the grating as our specimen), the number of lines in the grating will appear doubled (a spurious resolution). The important caveat is that actions introduced at the rear of the objective can have significant effect upon the eventual image produced (18). For small details in a specimen (rather than a grating), the objective projects the direct and diffracted light onto the image plane of the eyepiece diaphragm in the form of small, circular diffraction disks known as Airy disks (illustrated in Figure 6). High numerical aperture objectives capture more of the diffracted orders and produce smaller size disks than do low numerical aperture objectives. In Figure 6, Airy disk size is shown steadily decreasing from Figure 6(a)

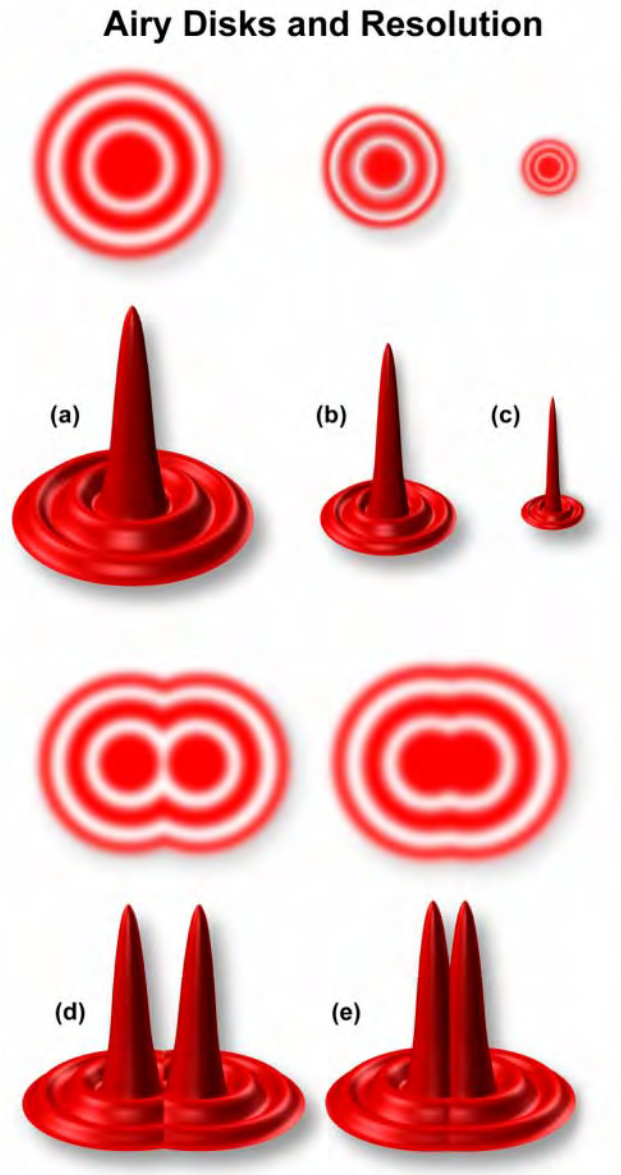

Figure 6. Airy disks and resolution. (a-c) Airy disk size and related intensity profile (point spread function) as related to objective numerical aperture, which decreases from (a) to (c) as numerical aperture increases. (e) Two Airy disks so close together that their central spots overlap. (d) Airy disks at the limit of resolution.

through Figure 6(c). The larger disk sizes in Figures 6(a) and (b) are produced by objectives with lower numerical aperture, while the very sharp Airy disk in Figure 6(c) is produced by an objective of very high numerical aperture (2, 18).

The resulting image at the eyepiece diaphragm level is actually a mosaic of Airy disks which are perceived as light and dark regions of the specimen. Where two disks are so close together that their central black spots overlap considerably, the two details represented by these overlapping disks are not resolved or separated and thus appear as one (illustrated in Figure 6(d)). The Airy disks shown in Figure 6(e) are just far enough apart to be resolved.

The basic principle to be remembered is that the combination of direct and diffracted light (or the manipulation of direct or diffracted light) is critically important in image formation. The key places for such manipulation are the rear focal plane of the objective and the front focal plane of the substage condenser. This principle is fundamental to most of the contrast improvement methods in optical microscopy (18, and see the section on **Contrast Enhancing Techniques**); it is of particular importance at high magnification of small details close in size to the wavelength of light. Abbe was a pioneer in developing these concepts to explain image formation of light-absorbing or ***amplitude*** specimens (2, 18-20).

Köhler Illumination

Proper illumination of the specimen is crucial in achieving high-quality images in microscopy and critical photomicrography. An advanced procedure for microscope illumination was first introduced in 1893 by August Köhler, of the Carl Zeiss corporation, as a method of providing optimum specimen illumination. All manufacturers of modern laboratory microscopes recommend this technique because it produces specimen illumination that is uniformly bright and free from glare, thus allowing the user to realize the microscope's full potential.

Most modern microscopes are designed so that the collector lens and other optical components built into the base will project an enlarged and focused image of the lamp filament onto the plane of the aperture diaphragm of a properly positioned substage condenser. Closing or opening the condenser diaphragm controls the angle of the light rays emerging from the condenser and reaching the specimen from all azimuths. Because the light source is not focused at the level of the specimen, illumination at specimen level is essentially grainless and extended, and does not suffer deterioration from dust and imperfections on the glass surfaces of the condenser. The opening size of the condenser aperture diaphragm, along with the aperture of the objective, determines the realized numerical aperture of the microscope system. As the condenser diaphragm is opened, the working numerical aperture of the microscope increases, resulting in greater light transmittance and resolving power. Parallel light rays that pass through and illuminate the specimen are brought to focus at the rear focal plane of the objective, where the image of the variable condenser aperture diaphragm and the light source are observed in focus simultaneously.

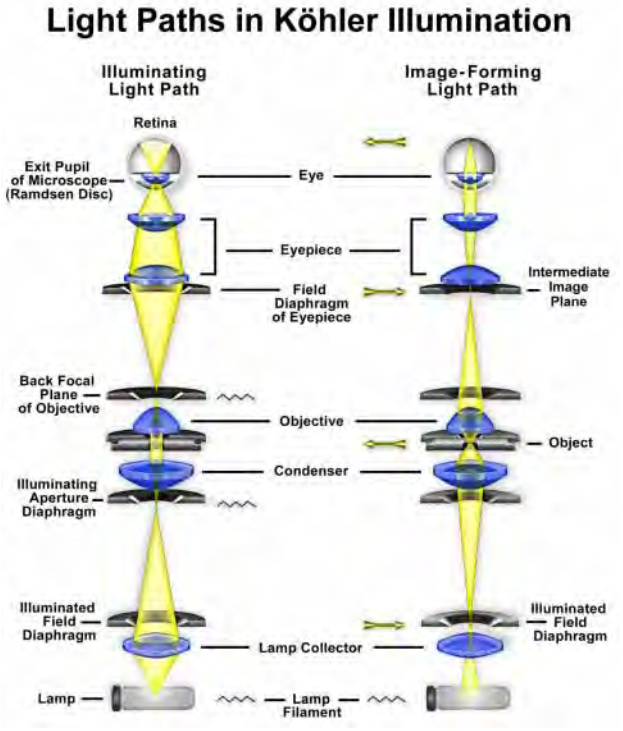

Figure 7. Light paths in Kohler illumination. The illuminating ray paths are illustrated on the left side and the image-forming ray paths on the right. Light emitted from the lamp passes through a collector lens and then through the field diaphragm. The aperture diaphragm in the condenser determines the size and shape of the illumination cone on the specimen plane. After passing through the specimen, light is focused at the back focal plane of the objective and then proceeds to and is magnified by the ocular before passing into the eye.

Light pathways illustrated in Figure 7 are schematically drawn to represent separate paths taken by the specimen-illuminating light rays and the image forming light rays (17). This is not a true representation of any real segregation of these pathways, but a diagrammatic representation presented for purposes of visualization and discussion. The left-hand diagram in Figure 7 demonstrates that the ray paths of illuminating light produce a focused image of the lamp filament at the plane

of the substage condenser aperture diaphragm, the rear focal plane of the objective, and the eyepoint (also called the ***Ramsden disk***) above the eyepiece. These areas in common focus are often referred to as conjugate planes, a principle that is critical in understanding the concept of Köhler illumination (2, 17-21). By definition, an object that is in focus at one plane is also in focus at other conjugate planes of that light path. In each light pathway (both image forming and illumination), there are four separate planes that together make up a conjugate plane set.

Conjugate planes in the path of the illuminating light rays in Köhler illumination (left-hand diagram in Figure 7) include the lamp filament, condenser aperture diaphragm (at the front focal plane of the condenser), the rear focal plane of the objective, and the eyepoint of the eyepiece. The eyepoint is located approximately one-half inch (one centimeter) above the top lens of the eyepiece, at the point where the observer places the front of the eye during observation.

Likewise, the conjugate planes in the image-forming light path in Köhler illumination (right-hand diagram in Figure 7) include the field diaphragm, the focused specimen, the intermediate image plane (i.e., the plane of the fixed diaphragm of the eyepiece), and the retina of the eye or the film plane of the camera. The presence of conjugate focal planes is often useful in troubleshooting a microscope for contaminating dust, fibers, and imperfections in the optical elements. When such artifacts are in sharp focus, it follows that they must reside on or near a surface that is part of the imaging-forming set of conjugate planes. Members of this set include the glass element at the microscope light port, the specimen, and the graticule (if any) in the eyepiece. Alternatively, if these contaminants are out of focus, then they occur near the illuminating set of elements that share conjugate planes. Suspects in this category are the condenser top lens (where dust and dirt often accumulate), the exposed eyepiece lens element (contaminants from eyelashes), and the objective front lens (usually fingerprint smudges).

In Köhler illumination, light emitted from the tungsten-halide lamp filament first passes through a collector lens located close to the lamp housing, and then through a field lens that is near the field diaphragm. A sintered or frosted glass filter is often placed between the lamp and the collector lens to diffuse the light and ensure an even intensity of illumination. In this case, the image of the lamp filament is focused onto the front focal plane of the condenser while the diffuser glass is temporarily removed from the light path. The focal length of the collector lens must be carefully matched to the lamp filament dimensions to ensure that a filament image of the appropriate size is projected into the condenser aperture. For proper Köhler illumination, the image of the filament should completely fill the condenser aperture.

The field lens is responsible for bringing the image of the filament into focus at the plane of the substage condenser aperture diaphragm. A first surface mirror (positioned at a 45-degree angle to the light path) reflects focused light leaving the field lens through the field diaphragm and into the substage condenser. The field diaphragm iris opening serves as a virtual light source for the microscope, and its image is focused by the condenser (raised or lowered) onto the specimen plane. Optical designs for the arrangement of these elements may vary by microscope manufacturer, but the field diaphragm should be positioned at a sufficient distance from the field lens to eliminate dust and lens imperfections from being imaged in the plane of the specimen.

The field diaphragm in the base of the microscope controls only the width of the bundle of light rays reaching the condenser—it does not affect the optical resolution, numerical aperture, or the intensity of illumination. Proper adjustment of the field diaphragm (i.e., focused by adjusting the height of the condenser and centered in the optical path, then opened so as to lie just outside of the field of view) is important for preventing glare, which can reduce contrast in the observed image. The elimination of unwanted light is particularly important when attempting to image specimens with inherently low contrast. When the field diaphragm is opened too far, scattered light originating from the specimen and light reflected at oblique angles from optical surfaces can act to degrade image quality.

The substage condenser is typically mounted directly beneath the microscope stage in a bracket that can be raised or lowered independently of the stage. Control of the aperture diaphragm opening size occurs with either a swinging arm, a lever, or by rotating a collar on the condenser housing. The most critical aspect of achieving proper Köhler illumination is correct adjustment of the substage condenser. Condenser misalignment and an improperly adjusted condenser aperture diaphragm are the main sources of image degradation and poor quality photomicrography (19).

When properly adjusted, light from the condenser will fill the rear focal plane of the objective and project a cone of light into the field of view. The condenser aperture diaphragm is responsible for controlling the angle of the illuminating light cone and, consequently, the working numerical aperture of the condenser. It is important to note, with respect to the size and shape of condenser light cones, that reducing the size of the field diaphragm only serves to slightly decrease the size of the lower portions of the light cone. The angle and numerical aperture of

the light cone remains essentially unchanged with reduction in field diaphragm size (21). Illumination intensity should not be controlled through opening and closing the condenser aperture diaphragm, or by shifting the condenser up and down or axially with respect to the optical center of the microscope. It should only be controlled through the use of neutral density filters placed into the light path or by reducing voltage to the lamp (although the latter is not usually recommended, especially for photomicrography). To ensure the maximum performance of the tungsten-halide lamp, refer to the manufacturer's instrument manual to determine the optimum lamp voltage (usually 5-10 volts) and use that setting. Adding or removing neutral density filters can then easily control brightness of the illumination without affecting color temperature.

The size of the substage condenser aperture diaphragm opening should not only coincide with the desired numerical aperture, but also the quality of the resulting image should be considered. In general, the diaphragm should be set to a position that allows 2/3 to 9/10 (60 to 90 percent) of the entire light disc size (visible at the rear focal plane of the objective after removal of the eyepiece or with a Bertrand lens). These values may vary with extremes in specimen contrast.

The condenser aperture diaphragm should be set to an opening size that will provide a compromise of resolution and contrast that depends, to a large degree, on the absorption, diffraction, and refraction characteristics of the specimen. This adjustment must be accomplished without overwhelming the image with artifacts that obscure detail and present erroneous enhancement of contrast. The amount of image detail and contrast necessary to produce the best photomicrograph is also dependent upon refractive index, optical characteristics, and other specimen-dependent parameters.

When the aperture diaphragm is erroneously closed too far, resulting diffraction artifacts cause visible fringes, banding, and/or pattern formation in photomicrographs. Other problems, such as refraction phenomena, can also produce apparent structures in the image that are not real (21). Alternatively, opening the condenser aperture too wide causes unwanted glare and light scattering from the specimen and optical surfaces within the microscope, leading to a significant loss of contrast and washing out of image detail. The correct setting will vary from specimen to specimen, and the experienced microscopist will soon learn to accurately adjust the condenser aperture diaphragm (and numerical aperture of the system) by observing the image without necessarily having to view the diaphragm in the rear focal plane of the objective. In fact, many microscopists (including the authors) believe that critical adjustment of the numerical aperture of the microscope system to optimize image quality is the single most important step in photomicrography.

The illumination system of the microscope, when adjusted for proper Köhler illumination, must satisfy several requirements. The illuminated area of the specimen plane must no larger than the field of view for any given objective/eyepiece combination. Also, the light must be of uniform intensity and the numerical aperture may vary from a maximum (equal to that of the objective) to a lesser value that will depend upon the optical characteristics of the specimen. Table 1 contains a list of objective numerical apertures versus the field of view diameter (for an eyepiece of field number 22 with no tube lens present – see discussion on field number) for each objective, ranging from very low to very high magnifications.

Many microscopes are equipped with specialized substage condensers that have a swing-out top lens, which can be removed from the optical path for use with lower power objectives (2x through 5x). This action changes the performance of the remaining components in the light path, and some adjustment is necessary to achieve the best illumination conditions. The field diaphragm can no longer be used for alignment and centering of the substage condenser and is now ineffective in limiting the area of the specimen under illumination. Also, much of the unwanted glare once removed by the field diaphragm is reduced because the top lens of the condenser produces a light cone having a much lower numerical aperture, allowing light rays to pass through the specimen at much lower angles. Most important, the optical conditions for

Table 1 Viewfield Diameters (FN 22) (SWF 10x Eyepiece)

Objective Magnification	Diameter (mm)
1/2x	44.0
1x	22.0
2x	11.0
4x	5.5
10x	2.2
20x	1.1
40x	0.55
50x	0.44
60x	0.37
100x	0.22
150x	0.15
250x	0.088

[a] Source: Nikon

Köhler illumination no longer apply.

For low power objectives (2x to 5x), alignment of the microscope optical components and the establishment of Köhler illumination conditions should always be undertaken at a higher (10x) magnification before removing the swing-out condenser lens for work at lower (5x and below) magnifications. The height of the condenser should then not be changed. Condenser performance is radically changed when the swing-out lens is removed (18, 21). The image of the lamp filament is no longer formed in the aperture diaphragm, which ceases to control the numerical aperture of the condenser and the illumination system. In fact, the aperture diaphragm should be opened completely to avoid vignetting, a gradual fading of light at the edges of the viewfield.

Contrast adjustment in low magnification microscopy is then achieved by adjustment of the field diaphragm (18, 19, 21). When the field diaphragm is wide open (greater than 80 percent), specimen details are washed out and a significant amount of scattering and glare is present. Closing the field diaphragm to a position between 50 and 80 percent will yield the best compromise on specimen contrast and depth of field. This adjustment is now visible at the rear focal plane of the objective when the eyepiece is removed or a Bertrand lens is inserted into the eye tube. Objectives designed for low magnification are significantly simpler in design than their higher magnification counterparts. This is due to the smaller angles of illuminating light cones produced by low magnification condensers, which require objectives of lower numerical aperture.

Measurement graticules, which must be in sharp focus and simultaneously superimposed on the specimen image, can be inserted into any of several conjugate planes in the image-forming path. The most common eyepiece (ocular) measuring and photomicrography graticules are placed in the intermediate image plane, which is positioned at the fixed diaphragm within the eyepiece. It is theoretically possible to also place graticules in any image-forming conjugate plane or in the plane of the illuminated field diaphragm. Stage micrometers are specialized ***graticules*** placed on microslides, which are used to calibrate eyepiece graticules and to make specimen measurements.

Color and neutral density filters are often placed in the optical pathway to reduce light intensity or alter the color characteristics of the illumination. There are several locations within the microscope stand where these filters are usually placed. Some modern laboratory microscopes have a filter holder sandwiched between the lamp housing and collector lens, which serves as an ideal location for these filters. Often, neutral density filters along with color correction filters and a frosted diffusion filter are placed together in this filter holder. Other microscope designs provide a set of filters built internally into the body, which can be toggled into the light path by means of levers. A third common location for filters is a holder mounted on the bottom of the substage condenser, below the aperture diaphragm, that will accept gelatin or glass filters.

It is important not to place filters in or near any of the image-forming conjugate planes to avoid dirt or surface imperfections on the filters being imaged along with the specimen (22). Some microscopes have an attachment for placing filters near the light port at the base (near the field diaphragm). This placement is probably too close to the field diaphragm, and surface contamination may be either in sharp focus or appear as blurred artifacts superimposed onto the image. It is also not wise to place filters directly on the microscope stage for the same reasons.

Microscope Objectives, Eyepieces, Condensers, and Optical Aberrations

Finite microscope objectives are designed to project a diffraction-limited image at a fixed plane (the **intermediate** image plane) that is dictated by the microscope tube length and located at a pre-specified distance from the rear focal plane of the objective. Specimens are imaged at a very short distance beyond the front focal plane of the objective through a medium of defined refractive index, usually air, water, glycerin, or specialized immersion oils. Microscope manufacturers offer a wide range of objective designs to meet the performance needs of specialized imaging methods (2, 6, 9, 18-21, and see the section on **Contrast Enhancing Techniques**), to compensate for cover glass thickness variations, and to increase the effective working distance of the objective.

All of the major microscope manufacturers have now changed their design to infinity-corrected objectives. Such objectives project emerging rays in parallel bundles from every azimuth to infinity. They require a tube lens in the light path to bring the image into focus at the intermediate image plane.

The least expensive (and most common) objectives are the achromatic objectives, which are corrected for axial chromatic aberration in two wavelengths (red and blue) that are brought into the same focus. Further, they are corrected for spherical aberration in the color green, as described in Table 2. The limited correction of achromatic objectives leads to problems with color microscopy and photomicrography. When focus is chosen in the red-blue region of the spectrum, images will have a green halo (often termed ***residual color***). Achromatic

Table 2 Objective Lens Types and Corrections [a]

	Corrections for Aberrations		
Type	**Spherical**	**Chromatic**	**Flatness Correction**
Achromat	* [b]	2 [c]	No
Plan Achromat	* [b]	2 [c]	Yes
Fluorite	3 [d]	< 3 [d]	No
Plan Fluorite	3 [d]	< 3 [d]	Yes
Plan Apochromat	4 [e]	> 4 [e]	Yes

[a] Source: Nikon Instrument Group
[b] Corrected for two wavelengths at two specific aperture angles.
[c] Corrected for blue and red - broad range of the visible spectrum.
[d] Corrected for blue, green and red - full range of the visible spectrum.
[e] Corrected for dark blue, blue, green and red.

objectives yield their best results with light passed through a green filter (often an interference filter) and using black and white film when these objectives are employed for photomicrography. The lack of correction for flatness of field (or field curvature) further hampers achromat objectives. In the past few years, most manufacturers have begun providing flat field corrections for achromat objectives and have given these corrected objectives the name of plan achromats.

The next higher level of correction and cost is found in objectives called fluorites or semi-apochromats illustrated by the center objective in Figure 8. This figure depicts three major classes of objectives: The achromats with the least amount of correction, as discussed above; the fluorites (or semi-apochromats) that have additional spherical corrections; and, the apochromats that are the most highly corrected objectives available. Fluorite objectives are produced from advanced glass formulations that contain materials such as fluorspar or newer synthetic substitutes (5). These new formulations allow for greatly improved correction of optical aberration. Similar to the achromats, the fluorite objectives are also corrected chromatically for red and blue light. In addition, the fluorites are also corrected spherically for two colors. The superior correction of fluorite objectives compared to achromats enables these objectives to be made with a higher numerical aperture, resulting in brighter images. Fluorite objectives also have better resolving power than achromats and provide a higher degree of contrast, making them better suited than achromats for color photomicrography in white light.

The highest level of correction (and expense) is found in apochromatic objectives, which are corrected chromatically for three colors (red, green, and blue), almost eliminating chromatic aberration, and are corrected spherically for two colors. Apochromatic objectives are the best choice for color photomicrography in white light. Because of their high level of correction, apochromat objectives usually have, for a given magnification, higher numerical apertures than do achromats or fluorites. Many of the newer high-end fluorite and apochromat objectives are corrected for four colors chromatically and four colors spherically.

All three types of objectives suffer from pronounced field curvature and project images that are curved rather than flat. To overcome this inherent condition, lens designers have produced flat-field corrected objectives that yield flat images. Such lenses are called plan achromats, plan fluorites, or plan apochromats, and although this degree of correction is expensive, these objectives are now in routine use due to their value in photomicrography.

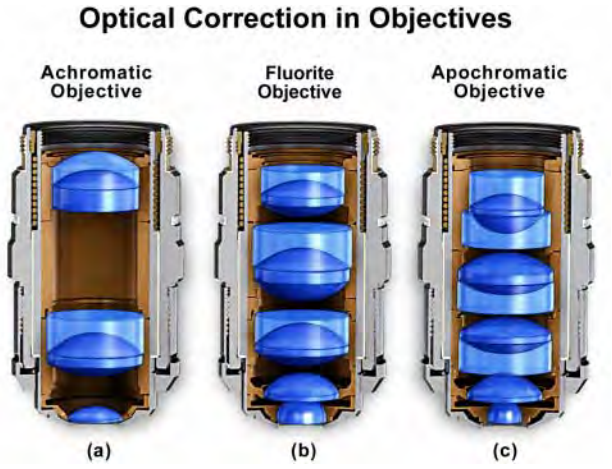

Figure 8. Levels of optical correction for aberration in commercial objectives. (a) Achromatic objectives, the lowest level of correction, contain two doublets and a single front lens; (b) Fluorites or semi-apochromatic objectives, a medium level of correction, contain three doublets, a meniscus lens, and a single front lens; and (c) Apochromatic objectives, the highest level of correction, contain a triplet, two doublets, a meniscus lens, and a single hemispherical front lens.

Uncorrected field curvature is the most severe aberration in higher power fluorite and apochromat objectives, and it was tolerated as an unavoidable artifact for many years. During routine use, the viewfield would have to be continuously refocused between the center and the edges to capture all specimen details. The introduction of flat-field (plan) correction to objectives perfected their use for photomicrography and video microscopy, and today these corrections are standard in both general use and high-performance objectives. Correction for field

curvature adds a considerable number of lens elements to the objective, in many cases as many as four additional lenses. This significant increase in the number of lens elements for plan correction also occurs in already overcrowded fluorite and apochromat objectives, frequently resulting in a tight fit of lens elements within the objective barrel (4, 5, 18).

Before the transition to infinity-corrected optics, most objectives were specifically designed to be used with a set of oculars termed ***compensating eyepieces***. An example is the former use of compensating eyepieces with highly corrected high numerical aperture objectives to help eliminate lateral chromatic aberration.

There is a wealth of information inscribed on the barrel of each objective, which can be broken down into several categories (illustrated in Figure 9). These include the linear magnification, numerical aperture value, optical corrections, microscope body tube length, the type of medium the objective is designed for, and other critical factors in deciding if the objective will perform as needed. Additional information is outlined below (17):

Figure 9. Specifications engraved on the barrel of a typical microscope objective. These include the manufacturer, correction levels, magnification, numerical aperture, immersion requirements, tube length, working distance, and specialized optical properties.

· **Optical Corrections:** These are usually abbreviated as **Achro** (achromat), **Apo** (apochromat), and **Fl, Fluar, Fluor, Neofluar, or Fluotar** (fluorite) for better spherical and chromatic corrections, and as **Plan, Pl, EF, Acroplan, Plan Apo** or **Plano** for field curvature corrections. Other common abbreviations are: **ICS** (infinity corrected system) and **UIS** (universal infinity system), **N** and **NPL** (normal field of view plan), **Ultrafluar** (fluorite objective with glass that is transparent down to 250 nanometers), and **CF** and **CFI** (chrome-free; chrome-free infinity).

· **Numerical Aperture:** This is a critical value that indicates the light acceptance angle, which in turn determines the light gathering power, the resolving power, and depth of field of the objective. Some objectives specifically designed for transmitted light fluorescence and darkfield imaging are equipped with an internal iris diaphragm that allows for adjustment of the effective numerical aperture. Designation abbreviations for these objectives include **I, Iris, W/Iris**.

· **Mechanical Tube Length:** This is the length of the microscope body tube between the nosepiece opening, where the objective is mounted, and the top edge of the observation tubes where the oculars (eyepieces) are inserted. Tube length is usually inscribed on the objective as the size in number of millimeters (160, 170, 210, etc.) for fixed lengths, or the infinity symbol (∞) for infinity-corrected tube lengths.

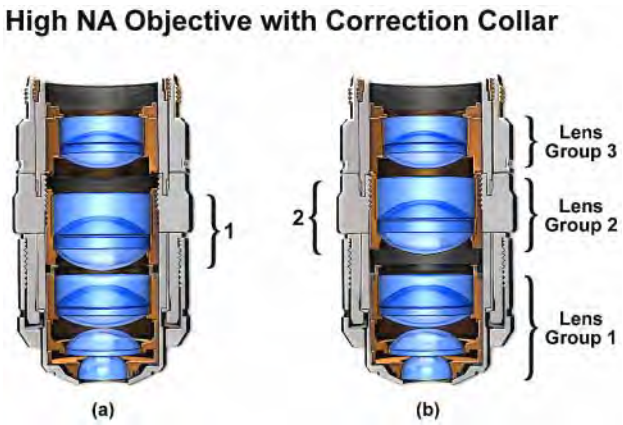

Figure 10. Objective with three lens groups and correction collar for varying cover glass thicknesses. (a) Lens group 2 rotated to the forward position within the objective. This position is used for the thinnest cover slips. (b) Lens group 2 rotated to the rearward position within the objective. This position is used for the thickest coverslips.

· **Cover Glass Thickness:** Most transmitted light objectives are designed to image specimens that are covered by a cover glass (or cover ***slip***). The thickness of these small glass plates is now standardized at 0.17 mm for most applications, although there is some variation in thickness within a batch of cover slips. For this reason, some of the high numerical aperture dry objectives have a correction collar adjustment of the internal lens elements to compensate for this variation (Figure 10). Abbreviations for the correction collar adjustment include **Corr, w/Corr,** and **CR,** although the presence of a movable, knurled collar and graduated scale is also an

indicator of this feature.

· **Working Distance:** This is the distance between the objective front lens and the top of the cover glass when the specimen is in focus. In most instances, the working distance of an objective decreases as magnification increases. Working distance values are not included on all objectives and their presence varies depending upon the manufacturer. Common abbreviations are: **L, LL, LD,** and **LWD** (long working distance); **ELWD** (extra-long working distance); **SLWD** (super-long working distance), and **ULWD** (ultra-long working distance).

· **Objective Screw Threads:** The mounting threads on almost all objectives are sized to standards of the Royal Microscopical Society (RMS) for universal compatibility. This standard specifies mounting threads that are 20.32 mm in diameter with a pitch of 0.706, which is currently used in the production of infinity-corrected objectives by manufacturers Olympus and Zeiss. Leica and Nikon have broken from the standard with the introduction of new infinity-corrected objectives that have a wider mounting thread size, making Leica and Nikon objectives usable only on their own microscopes. Abbreviations commonly used are: **RMS** (Royal Microscopical Society objective thread), **M25** (metric 25-mm objective thread), and **M32** (metric 32-mm objective thread).

· **Immersion Medium:** Most objectives are designed to image specimens with air as the medium between the objective and the cover glass. To attain higher working numerical apertures, many objectives are designed to image the specimen through another medium that reduces refractive index differences between glass and the imaging medium. High-resolution plan apochromat objectives can achieve numerical apertures up to 1.40 when the immersion medium is special oil with a refractive index of 1.51. Other common immersion media are water and glycerin. Objectives designed for special immersion media usually have a color-coded ring inscribed around the circumference of the objective barrel as listed in Table 3 and described below.

· **Color Codes:** Many microscope manufacturers label their objectives with color codes to help in rapid identification of the magnification. The dark blue color code on the objective illustrated in Figure 9 indicates the linear magnification is 60x. This is very helpful when you have a nosepiece turret containing 5 or 6 objectives and you must quickly select a specific magnification. Some specialized objectives have an additional color code that indicates the type of immersion medium necessary to achieve the optimum numerical aperture. Immersion lenses intended for use with oil have a black color ring, while those intended for use with glycerin have an orange ring. Objectives designed to image living organisms in aqueous media are designated ***water immersion*** objectives with a white ring and highly specialized objectives for unusual immersion media often are engraved with a red ring. Table 3 lists current magnification and imaging media color codes in use by most manufacturers.

Table 3 Color-Coded Rings on Microscope Objectives

Immersion color code [a]	**Immersion type**
Black	Oil immersion
Orange	Glycerol immersion
White	Water immersion
Red	Special
Magnification color code [b]	**Magnification**
Black	1x, 1.25x
Brown	2x, 2.5x
Red	4x, 5x
Yellow	10x
Green	16x, 20x
Turquoise blue	25x, 32x
Light blue	40x, 50x
Cobalt (dark) blue	60x, 63x
White (cream)	100x

[a] Narrow colored ring located near the specimen end of objective.
[b] Narrow band located closer to the mounting thread than the immersion code.

· **Specialized Optical Properties:** Microscope objectives often have design parameters that optimize performance under certain conditions. For example, there are special objectives designed for polarized illumination (signified by the abbreviations **P, Po, Pol,** or **SF,** and/or having all barrel engravings painted red), phase contrast (**PH**, and/or green barrel engravings), differential interference contrast (**DIC**), and many other abbreviations for additional applications. The apochromat objective illustrated in Figure 9 is optimized for DIC photomicrography and this is indicated on the barrel. The capital H beside the DIC marking indicates that the objective must be used with a specific DIC prism optimized for high-magnification applications.

There are some applications that do not require objectives designed to be corrected for cover glass thickness. These include objectives used to observe uncovered specimens in reflected light metallurgical specimens, integrated circuit inspection, micro machinery, biological smears, and other applications that require observation of uncovered objects. Other common abbreviations found on microscope objective barrels, which are useful in identifying specific properties, are listed in Table 4 (17).

Table 4 Specialized Objective Designations

Abbreviation	Type
Phase, PHACO, PC, Ph 1,2, 3, etc.	Phase contrast, using phase condenser annulus 1, 2, 3, etc.
DL, DM, PLL, PL, PM, PH, NL, NM, NH	Phase contrast: dark low, dark medium, positive low, positive low, positive medium, positive high contrast (regions with higher refractive index appear darker); negative low, negative medium, negative high contrast (regions with higher refractive index appear lighter)
P, Po, Pol, SF	Strain-free, low birefringence, for polarized light
U, UV, Universal	UV transmitting (down to approx. 340 nm), for UV-excited epifluorescence
M	Metallographic (no coverslip)
NC, NCG	No coverslip
EPI	Surface illumination (specimen illuminated through objective lens), as contrasted to dia- or transillumination
TL	Transmitted light
BBD, HD, B\D	For use in bright or dark field (hell, dunkel)
D	Dark field
H	Designed primarily for heating stage
U, UT	Designed to be used with universal stage (magnification/NA applied for use with glass hemisphere; divine both values by 1.51 when hemisphere is not used)
DI; MI; TI Michelson	Interferometry; noncontact; multiple beam (Tolanski)

[a] Many of the designation codes are manufacturer specific.

Optical Aberrations

Lens errors or aberrations in optical microscopy are caused by artifacts arising from the interaction of light with glass lenses (2-5, 19-24). There are two primary causes of aberration: (i) geometrical or spherical aberrations are related to the spherical nature of the lens and approximations used to obtain the Gaussian lens equation; and (ii) chromatic aberrations that arise from variations in the refractive indices of the wide range of frequencies found in visible light.

In general, the effects of optical aberrations are to induce faults in the features of an image being observed through a microscope. These artifacts were first addressed in the eighteenth century when physicist John Dollond discovered that chromatic aberration would be reduced or corrected by using a combination of two different types of glass (flint and crown) in the fabrication of lenses (13). Later, during the nineteenth century, achromatic objectives with high numerical aperture were developed, although there were still geometrical problems with the lenses. Modern glass formulations coupled with advanced grinding and manufacturing techniques have all but eliminated most aberrations from today's microscope objectives, although careful attention must still be paid to these effects, especially when conducting quantitative high-magnification video microscopy and photomicrography (23).

Spherical Aberration: These artifacts occur when light waves passing through the periphery of a lens are not brought into identical focus with those passing closer to the center. Waves passing near the center of the lens are refracted only slightly, whereas waves passing near the periphery are refracted to a greater degree resulting in the production of different focal points along the optical axis. This is one of the most serious resolution artifacts because the image of the specimen is spread out rather than being in sharp focus. Spherical aberrations are very important in terms of the resolution of the lens because they affect the coincident imaging of points along the optical axis and degrade the performance of the lens, which will seriously affect specimen sharpness and clarity. These lens defects can be reduced by limiting the outer edges of the lens from exposure to light using diaphragms and also by utilizing aspherical lens surfaces within the system. The highest-quality modern microscope objectives address spherical aberrations in a number of ways including special lens-grinding techniques, additional lens elements of different curvatures, improved glass formulations, and better control of optical pathways.

Chromatic Aberration: This type of optical defect is a result of the fact that white light is composed of numerous wavelengths. When white light passes through a convex lens, the component wavelengths are refracted according to their frequency. Blue light is refracted to the greatest extent followed by green and red light, a phenomenon commonly referred to as dispersion. The inability of the lens to bring all of the colors into a

common focus results in a slightly different image size and focal point for each predominant wavelength group. This leads to color fringes surrounding the image.

Lens corrections were first attempted in the latter part of the 18th century when Dollond, Lister and others devised ways to reduce longitudinal chromatic aberration (13). By combining crown glass and flint glass (each type has a different dispersion of refractive index), they succeeded in bringing the blue rays and the red rays to a common focus, near but not identical with the green rays. This combination is termed a lens doublet where each lens has a different refractive index and dispersive properties. Lens doublets are also known as achromatic lenses or achromats for short, derived from the Greek terms a meaning without and ***chroma*** meaning color. This simple form of correction allows the image points at 486 nanometers in the blue region and 656 nanometers in the red region to now coincide. This is the most widely used objective lens and is commonly found on laboratory microscopes. Objectives that do not carry a special inscription stating otherwise are likely to be achromats. Achromats are satisfactory objectives for routine laboratory use, but because they are not corrected for all colors, a colorless specimen detail is likely to show, in white light, a pale green color at best focus (the so-called secondary spectrum).

A proper combination of lens thickness, curvature, refractive index, and dispersion allows the doublet to reduce chromatic aberration by bringing two of the wavelength groups into a common focal plane. If fluorspar is introduced into the glass formulation used to fabricate the lens, then the three colors red, green, and blue can be brought into a single focal point resulting in a negligible amount of chromatic aberration (23). These lenses are known as apochromatic lenses and they are used to build very high-quality chromatic aberration-free microscope objectives. Modern microscopes utilize this concept and today it is common to find optical lens triplets made with three lens elements cemented together, especially in higher-quality objectives. For chromatic aberration correction, a typical 10x achromat microscope objective is built with two lens doublets (Figure 8(a)). Apochromat objectives usually contain two lens doublets and a lens triplet (Figure 8(c)) for advanced correction of both chromatic and spherical aberrations.

Despite longitudinal (or axial) chromatic aberration correction, apochromat objectives also exhibit another chromatic defect. Even when all three main colors are brought to identical focal planes axially, the point images of details near the periphery of the field of view, are not the same size; e.g., the blue image of a detail is slightly larger than the green image or the red image in white light, thus causing color ringing of specimen details at the outer regions of the field of view (23). This defect is known as lateral chromatic aberration or chromatic difference of magnification. It is the compensating eyepiece, with chromatic difference of magnification just the opposite of that of the objective, which is utilized to correct for lateral chromatic aberration. Because this defect is also found in higher magnification achromats, compensating eyepieces are frequently used for such objectives, too. Indeed, many manufacturers design their achromats with a standard lateral chromatic error and use compensating eyepieces for all their objectives. Such eyepieces often carry the inscription **K** or **C** or **Compens**. As a result, compensating eyepieces have build-in lateral chromatic error and are not, in themselves, perfectly corrected.

Coverslip Correction: It is possible for the user to inadvertently introduce spherical aberration into a well-corrected system (2, 23). For example, when using high magnification and high numerical aperture dry objectives (NA = 0.85-0.95), the correct thickness of the cover glass (suggested 0.17 mm) is critical; hence the inclusion of a correction collar on such objectives to enable adjustment for incorrect cover glass thickness. Similarly, the insertion of accessories in the light path of finite tube length objectives may introduce aberrations, apparent when the specimen is refocused, unless such accessories have been properly designed with additional optics. Figure 10 illustrates how internal lenses operate in an objective designed for coverslip correction.

Other Geometrical Aberrations: These include a variety of effects including astigmatism, field curvature, and comatic aberrations, which are corrected with proper lens fabrication.

Curvature of field in the image is an aberration that is familiar to most experienced microscopists. This artifact is the natural result of using lenses that have curved surfaces. When visible light is focused through a curved lens, the image plane produced by the lens will be curved. When the image is viewed in the eyepieces (oculars) of a microscope, it either appears sharp and crisp in the center or on the edges of the viewfield but not both. Normally, this is not a serious problem when the microscopist is routinely scanning samples to observe their various features. It is a simple matter to use the fine focus knob to correct small deficiencies in specimen focus. However, for photomicrography, field curvature can be a serious problem, especially when a portion of the photomicrograph is out of focus.

Modern microscopes deal with field curvature by correcting this aberration using specially designed flat-field objectives. These specially corrected objectives have been named plan or plano and are the most common type of objective in use today. Plan objectives are also corrected for other optical artifacts such as spherical and

chromatic aberrations. In the case of a plan objective that also has been mostly corrected for chromatic aberration, the objective is referred to as a plan achromat. This is also the case for fluorite and apochromatic objectives, which have the modified names: plan fluorite and plan apochromat.

Adding field curvature lens corrections to an objective that has already been corrected for optical aberrations can often add a significant number of lens elements to the objective. For example, the typical achromat objective has two lens doublets and a hemispherical lens, making of total of five lens elements. In contrast, a comparable plan achromat objective has three doublets and three single lenses for a total of nine lens elements, making it considerably more difficult to fabricate. As we have seen, the number of lens elements increases as lenses are corrected for spherical errors as well as chromatic and field curvature aberrations. Unfortunately, as the number of lens elements increases so does the cost of the objective.

Sophisticated plan apochromatic objectives that are corrected for spherical, chromatic, and field curvature aberrations can contain as many as eighteen to twenty separate lens elements, making these objectives the most expensive and difficult to manufacture. Plan apochromatic objectives can cost upward of $3,000 to $5,000 each for high-magnification units that also have a high numerical aperture. For most photomicrography applications, however, it is not absolutely necessary to have the best correction, although this is heavily dependent upon the purpose, the specimen, and the desired magnification range. When cost is important (when isn't it?), it is often wise to select more modestly priced plan fluorite objectives that have a high degree of correction, especially the more modern versions. These objectives provide crisp and sharp images with minimal field curvature, and will be sufficient for most photomicrography applications.

Field curvature is very seldom totally eliminated, but it is often difficult to detect edge curvature with most plan-corrected objectives and it does not show up in photomicrographs (19, 23). This artifact is more severe at low magnifications and can be a problem with stereo microscopes. Manufacturers have struggled for years to eliminate field curvature in the large objectives found in stereo microscopes. In the past ten years, companies like Leica, Nikon, Olympus, and Zeiss, have made great strides in the quality of optics used to build stereo microscopes and, while the artifacts and aberrations have not been totally eliminated, high-end models are now capable of producing superb photomicrographs.

Comatic aberrations are similar to spherical aberrations, but they are mainly encountered with off-axis objects and are most severe when the microscope is out of alignment (23). In this instance, the image of a point is asymmetrical, resulting in a comet-like (hence, the term coma) shape. The comet shape may have its ***tail*** pointing toward the center of the field of view or away depending upon whether the comatic aberration has a positive or negative value. Coma may occur near the axial area of the light path, and/or the more peripheral area. These aberrations are usually corrected along with spherical aberrations by designing lens elements of various shapes to eliminate this error. Objectives that are designed to yield excellent images for wide field of view eyepieces, have to be corrected for coma and astigmatism using a specially-designed multi-element optic in the tube lens to avoid these artifacts at the periphery of the field of view.

Astigmatism aberrations are similar to comatic aberrations, however these artifacts depend more strongly on the obliquity of the light beam (23). This defect is found at the outer portions of the field of view of uncorrected lenses. The off-axis image of a specimen point appears as a line instead of a point. What is more, depending on the angle of the off-axis rays entering the lens, the line image may be oriented in either of two different directions, tangentially or radially. Astigmatism errors are usually corrected by design of the objectives to provide precise spacing of individual lens elements as well as appropriate lens shapes and indices of refraction. The correction of astigmatism is often accomplished in conjunction with the correction of field curvature aberrations.

Eyepieces (Oculars)

Eyepieces work in combination with microscope objectives to further magnify the intermediate image so that specimen details can be observed. Ocular is an alternative name for eyepieces that has been widely used in the literature, but to maintain consistency during this discussion we will refer to all oculars as eyepieces. Best results in microscopy require that objectives be used in combination with eyepieces that are appropriate to the correction and type of objective. Inscriptions on the side of the eyepiece describe its particular characteristics and function.

The eyepiece illustrated in Figure 11 is inscribed with **UW** (not illustrated), which is an abbreviation for the ultra wide viewfield. Often eyepieces will also have an **H** designation, depending upon the manufacturer, to indicate a high-eyepoint focal point that allows microscopists to wear glasses while viewing samples. Other common inscriptions often found on eyepieces include **WF** for wide field; **UWF** for ultra wide field; **SW** and **SWF** for

super wide field; **HE** for high eyepoint; and **CF** for eyepieces intended for use with CF corrected objectives (2, 3, 5, 19, 23, 24). As discussed above, compensating eyepieces are often inscribed with **K, C, Comp**, or **Compens**, as well as the magnification. Eyepieces used with flat-field objectives are sometimes labeled **Plan-Comp**. Magnification factors of common eyepieces range from 5x to 25x, and usually contain an inscription, such as **A/24**, which indicates the field number is 24, in reference to the diameter (in millimeters) of the fixed diaphragm in the eyepiece. Many eyepieces also have a focus adjustment and a thumbscrew that allows their position to be fixed. Manufactures now often produce eyepieces having rubber eye-cups that serve both to position the eyes the proper distance from the front lens, and to block room light from reflecting off the lens surface and interfering with the view.

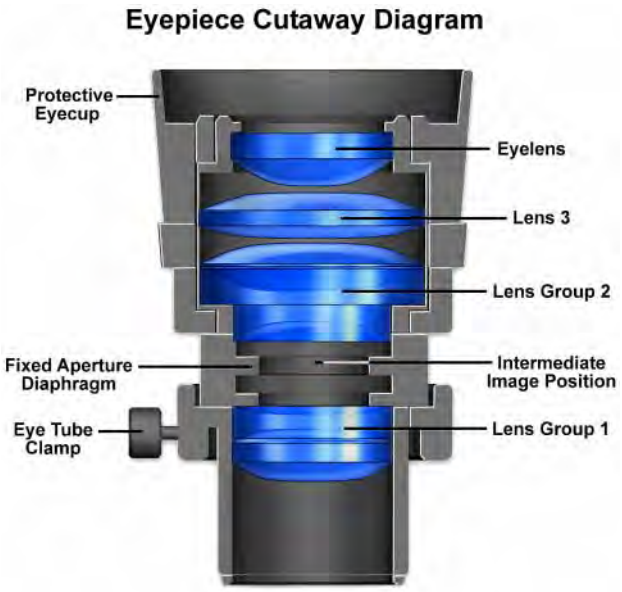

Figure 11. Cutaway diagram of a typical periplan eyepiece. The fixed aperture diaphragm is positioned between lens group 1 and lens group 2, where the intermediate image is formed. The eyepiece has a protective eyecup that makes viewing the specimen more comfortable for the microscopist.

There are two major types of eyepieces that are grouped according to lens and diaphragm arrangement: the **negative** eyepieces with an internal diaphragm between the lenses, and **positive** eyepieces that have a diaphragm below the lenses of the eyepiece. Negative eyepieces have two lenses: the upper lens, which is closest to the observer's eye, is called the eye-lens and the lower lens (beneath the diaphragm) is often termed the field lens. In their simplest form, both lenses are plano-convex, with convex sides facing the specimen. Approximately mid-way between these lenses there is a fixed circular opening or internal diaphragm which, by its size, defines the circular field of view that is observed in looking into the microscope. The simplest kind of negative eyepiece, or Huygenian eyepiece, is found on most routine microscopes fitted with achromatic objectives. Although the Huygenian eye and field lenses are not well corrected, their aberrations tend to cancel each other out. More highly corrected negative eyepieces have two or three lens elements cemented and combined together to make the eye lens. If an unknown eyepiece carries only the magnification inscribed on the housing, it is most likely to be a Huygenian eyepiece, best suited for use with achromatic objectives of 5x-40x magnification.

The other main type of eyepiece is the positive eyepiece with a diaphragm below its lenses, commonly known as the **Ramsden** eyepiece. This eyepiece has an eye lens and field lens that are also plano-convex, but the field lens is mounted with the curved surface facing towards the eye lens. The front focal plane of this eyepiece lies just below the field lens, at the level of the eyepiece fixed diaphragm, making this eyepiece readily adaptable for mounting graticules. To provide better correction, the two lenses of the Ramsden eyepiece may be cemented together.

Simple eyepieces such as the Huygenian and Ramsden and their achromatized counterparts will not correct for residual chromatic difference of magnification in the intermediate image, especially when used in combination with high magnification achromatic objectives as well as fluorite or apochromatic objectives. To remedy this in finite microscopy systems, manufacturers produce compensating eyepieces that introduce an equal, but opposite, chromatic error in the lens elements. Compensating eyepieces may be either of the positive or negative type, and must be used at all magnifications with fluorite, apochromatic and all variations of plan objectives (they can also be used to advantage with achromatic objectives of 40x and higher).

In recent years, modern microscope objectives have their correction for chromatic difference of magnification either built into the objectives themselves (Olympus and Nikon) or corrected in the tube lens (Leica and Zeiss), thus eliminating the need for compensation correction of the eyepieces.

Compensating eyepieces play a crucial role in helping to eliminate residual lateral chromatic aberrations inherent in the design of highly corrected objectives. Hence, it is preferable that the microscopist uses the compensating eyepieces designed by a particular manufacturer to accompany that manufacturer's higher-corrected objectives. Use of an incorrect eyepiece with an apochromatic objective designed for a finite (160 or

170 millimeter) tube length microscope results in dramatically increased contrast with red fringes on the outer diameters and blue fringes on the inner diameters of specimen detail. Additional problems arise from a limited flatness of the viewfield in simple eyepieces, even those corrected with eye-lens doublets.

More advanced eyepiece designs resulted in the Periplan eyepiece (Figure 11), which contains seven lens elements that are cemented into a doublet, a triplet, and two individual lenses. Design improvements in periplan eyepieces lead to better correction for residual lateral chromatic aberration, increased flatness of field, and a general overall better performance when used with higher power objectives.

Modern microscopes feature vastly improved plan-corrected objectives in which the primary image has much less curvature of field than older objectives. In addition, most microscopes now feature much wider body tubes that have accommodated greatly increased the size of intermediate images. To address these new features, manufacturers now produce wide-eyefield eyepieces that increase the viewable area of the specimen by as much as 40 percent. Because the strategies of eyepiece-objective correction techniques vary from manufacturer to manufacturer, it is very important (as stated above) to use only eyepieces recommended by a specific manufacturer for use with their objectives.

Our recommendation is to carefully choose the objective first, then purchase an eyepiece that is designed to work in conjunction with the objective. When choosing eyepieces, it is relatively easy to differentiate between simple and more highly compensating eyepieces. Simple eyepieces such as the Ramsden and Huygenian (and their more highly corrected counterparts) will appear to have a blue ring around the edge of the eyepiece diaphragm when viewed through the microscope or held up to a light source. In contrast, more highly corrected compensating eyepieces with have a yellow-red-orange ring around the diaphragm under the same circumstances. Modern non-compensating eyepieces are fully corrected and show no color. Most of the modern microscopes have all corrections done in the objectives themselves or have a final correction in the tube lens. Such microscopes do not need compensating eyepieces.

The properties of several common commercially available eyepieces are listed according to type in Table 5 (19, 23). The three major types of eyepieces listed in Table 5 are finder, wide field, and super wide field. The terminology used by various manufacturers can be very confusing and careful attention should be paid to their sales brochures and microscope manuals to ensure that the correct eyepieces are being used with a specific objective. In Table 5, the abbreviations that designate wide field and super widefield eyepieces are coupled to their design for high eyepoint, and are **WH** and **SWH**, respectively. The magnifications are either 10x or 15x and the Field Numbers range from 14 to 26.5, depending upon the application. The diopter adjustment is approximately the same for all eyepieces and many also contain either a photomask or micrometer graticule.

Light rays emanating from the eyepiece intersect at the exit pupil or eyepoint (Ramsden disc) where the front of the microscopist's eye should be placed in order to see the entire field of view (usually 8-10 mm above the eye lens). By increasing the magnification of the eyepiece, the eyepoint is drawn closer to the upper surface of the eye lens, making it much more difficult for microscopists to use, especially if he or she wears eyeglasses. Specially designed high eyepoint eyepieces have been manufactured that feature eyepoint viewing distances approaching 20-25 mm above the surface of the eye lens. These improved eyepieces have larger diameter eye lenses that contain more optical elements and usually feature improved flatness of field. Such eyepieces are often designated with the inscription "**H**" somewhere on the eyepiece housing, either alone or in combination with other abbreviations, as discussed above. We should mention that high-eyepoint eyepieces are especially useful for microscopists who wear eyeglasses to correct for near or far sightedness, but they do not correct for several other visual defects, such as astigmatism. Today, high eyepoint eyepieces are very popular, even with people who do not wear eyeglasses, because the large eye clearance reduces fatigue and makes viewing images through the microscope much more comfortable.

At one time, eyepieces were available in a wide range of magnifications extending from 6.3x to 30x and sometimes even higher for special applications. These eyepieces are very useful for observation and photomicrography with low-power objectives. Unfortunately, with higher power objectives, the problem of empty magnification (magnification without increased clarity) becomes important when using very high magnification eyepieces and these should be avoided. Today most manufacturers restrict their eyepiece offerings to those in the 10x to 20x ranges. The diameter of the viewfield in an eyepiece is expressed as a ***field of view number*** or ***field number*** (**FN**), as discussed above. Information about the field number of an eyepiece can yield the real diameter of the object viewfield using the formula (23):

$$\textbf{Viewfield Diameter} = \textbf{FN} / (\mathbf{M_O} \times \mathbf{M_T}) \quad (2)$$

Where **FN** is the field number in millimeters, $\mathbf{M_O}$ is the magnification of the objective, and $\mathbf{M_T}$ is the tube lens

Table 5 Properties of Commercial Eyepieces

Eyepiece Type	Finder Eyepieces			Super Wide Field Eyepieces	Wide Field Eyepieces		
Descriptive Abbreviation	PSWH 10x	PWH 10x	35 SWH 10x	SWH 10x H	CROSSWH 10x H	WH 15x	WH 10x H
Field Number	26.5	22	26.5	26.5	22	14	22
Diopter Adjustment	-8 ~ +2	-8 ~ +2	-8 ~ +2	-8 ~ +2	-8 ~ +2	-8 ~ +2	-8 ~ +2
Remarks	31/4 x "41/4" photo mask	31/4 x "41/4" photo mask	35mm photo mask	diopter correction	diopter correction crossline		diopter correction
Diameter of Micrometer Graticule	—	—	—	—	—	24	24

magnification factor (if any). Applying this formula to the super wide field eyepiece listed in Table 5, we arrive at the following for a 40x objective with a tube lens magnification of 1.25:

Viewfield Diameter = 26.5 / 40 x 1.25 = 0.53 mm (3)

Table 1 lists the viewfield diameters over the common range of objectives that would occur using this eyepiece.

Table 6 Range of Useful Magnification (500-1000 x NA of Objective)

Objective (NA)	Eyepieces 10x	12.5x	15x	20x	25x
2.5x (0.08)	—	—	—	x	x
4x (0.12)	—	—	x	x	x
10x (0.35)	—	x	x	x	x
25x (0.55)	x	x	x	x	—
40x (0.70)	x	x	x	—	—
60x (0.95)	x	x	x	—	—
100x (1.42)	x	x	—	—	—

Care should be taken in choosing eyepiece/objective combinations to ensure the optimal magnification of specimen detail without adding unnecessary artifacts. For instance, to achieve a magnification of 250x, the microscopist could choose a 25x eyepiece coupled to a 10x objective. An alternative choice for the same magnification would be a 10x eyepiece with a 25x objective. Because the 25x objective has a higher numerical aperture (approximately 0.65) than does the 10x objective (approximately 0.25), and considering that numerical aperture values define an objective's resolving power, it is clear that the latter choice would be the best. If photomicrographs of the same viewfield were made with each objective/eyepiece combination described above, it would be obvious that the 10x eyepiece/25x objective duo would produce photomicrographs that excelled in specimen detail and clarity when compared to the alternative combination.

Numerical aperture of the objective/condenser system defines the ***range of useful magnification*** for an objective/eyepiece combination (19, 22-24). There is a minimum magnification necessary for the detail present in an image to be resolved, and this value is usually rather arbitrarily set as 500 times the numerical aperture (500 x NA). At the other end of the spectrum, the maximum useful magnification of an image is usually set at 1000 times the numerical aperture (1000 x NA). Magnifications higher than this value will yield no further useful information or finer resolution of image detail, and will usually lead to image degradation. Exceeding the limit of useful magnification causes the image to suffer from the phenomenon of ***empty magnification*** (19), where increasing magnification through the eyepiece or intermediate tube lens only causes the image to become

more magnified with no corresponding increase in detail resolution. Table 6 lists the common objective/eyepiece combinations that fall into the range of useful magnification.

Eyepieces can be adapted for measurement purposes by adding a small circular disk-shaped glass graticule at the plane of the fixed aperture diaphragm of the eyepiece. Graticules usually have markings, such as a measuring rule or grid, etched onto the surface. Because the graticule lies in the same conjugate plane as the fixed eyepiece diaphragm, it appears in sharp focus superimposed on the image of the specimen. Eyepieces using graticules usually contain a focusing mechanism (helical screw or slider) that allows the image of the graticule to be brought into focus. A stage micrometer is needed to calibrate the eyepiece scale for each objective.

Condenser Systems

The substage condenser gathers light from the microscope light source and concentrates it into a cone of light that illuminates the specimen with parallel beams of uniform intensity from all azimuths over the entire viewfield. It is critical that the condenser light cone be properly adjusted to optimize the intensity and angle of light entering the objective front lens. Each time an objective is changed, a corresponding adjustment must be performed on the substage condenser aperture iris diaphragm to provide the proper light cone for the numerical aperture of the new objective.

A simple two-lens Abbe condenser is illustrated in Figure 12. In this figure, light from the microscope illumination source passes through the aperture or condenser diaphragm, located at the base of the condenser, and is concentrated by internal lens elements, which then project light through the specimen in parallel bundles from every azimuth. The size and numerical aperture of the light cone is determined by adjustment of the aperture diaphragm. After passing through the specimen (on the microscope slide), the light diverges to an inverted cone with the proper angle (2q in Figure 12) to fill the front lens of the objective (2, 18-24).

Aperture adjustment and proper focusing of the condenser are of critical importance in realizing the full potential of the objective. Specifically, appropriate use of the adjustable aperture iris diaphragm (incorporated into the condenser or just below it) is most important in securing correct illumination, contrast, and depth of field. The opening and closing of this iris diaphragm controls the angle of illuminating rays (and thus the aperture) which pass through the condenser, through the specimen and then into the objective. Condenser height is controlled by a rack and pinion gear system that allows the condenser focus to be adjusted for proper illumination of the specimen. Correct positioning of the condenser with relation to the cone of illumination and focus on the specimen is critical to quantitative microscopy and optimum photomicrography. Care must be taken to guarantee that the condenser aperture is opened to the correct position with respect to objective numerical aperture. When the aperture is opened too much, stray light generated by refraction of oblique light rays from the specimen can cause glare and lower the overall contrast. On the other hand, when the aperture is closed too far, the illumination cone is insufficient to provide adequate resolution and the image is distorted due to refraction and diffraction from the specimen.

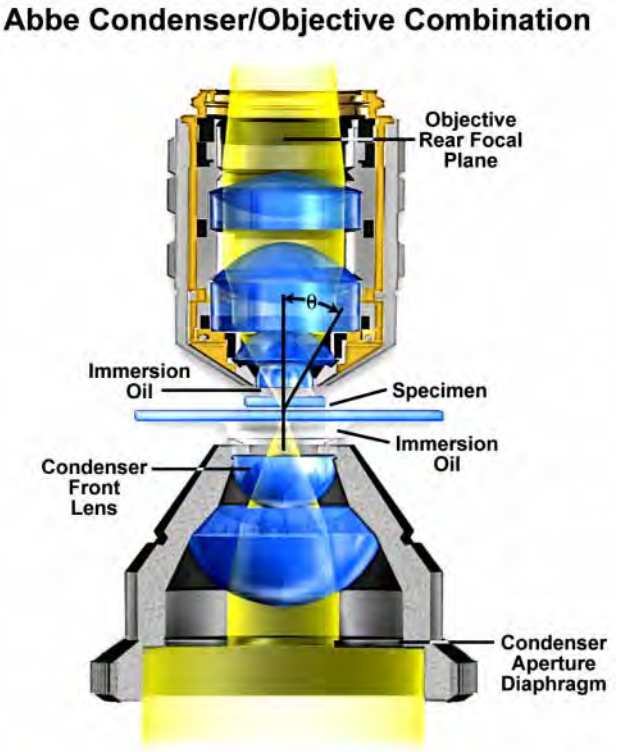

Figure 12. Condenser/objective configuration for optical microscopy. An Abbe two-lens condenser is illustrated showing ray traces through the optical train of the microscope. The aperture diaphragm restricts light entering the condenser before it is refracted by the condenser lens system into the specimen. Immersion oil is used in the contact beneath the underside of the slide and the condenser top lens, and also between the objective and cover slip. The objective angular aperture ( ) controls the amount of light entering the objective.

The simplest and least corrected (also the least expensive) condenser is the Abbe condenser that, in its simplest form, has two optical lens elements which produce an image of the illuminated field diaphragm that

is not sharp and is surrounded by blue and red color at the edges. As a result of little optical correction, the Abbe condenser is suited mainly for routine observation with objectives of modest numerical aperture and magnification. The primary advantages of the Abbe condenser are the wide cone of illumination that the condenser is capable of producing as well as its ability to work with long working distance objectives. The manufacturers supply most microscopes with an Abbe condenser as the default and these condensers are real workhorses for routine laboratory use.

Table 7 Condenser Aberration Corrections

Condenser Type	Aberrations Corrected	
	Spherical	Chromatic
Abbe	—	—
Aplanatic	x	—
Achromatic	—	x
Aplanatic-achromatic	x	x

The next highest level of condenser correction is split between the aplanatic and achromatic condensers that are corrected exclusively for either spherical (aplanatic) or chromatic (achromatic) optical aberrations.

Achromatic condensers typically contain four lens elements and have a numerical aperture of 0.95, the highest attainable without requiring immersion oil (5). This condenser is useful for both routine and critical laboratory analysis with dry objectives and also for black and white or color photomicrography.

A critical factor in choosing substage condensers is the numerical aperture performance, which will be necessary to provide an illumination cone adequate for the objectives. The condenser numerical aperture capability should be equal to or slightly less than that of the highest objective numerical aperture. Therefore, if the largest magnification objective is an oil-immersion objective with a numerical aperture of 1.40, then the substage condenser should also have an equivalent numerical aperture to maintain the highest system resolution. In this case, immersion oil would have to be applied between the condenser top lens in contact with the underside of the microscope slide to achieve the intended numerical aperture (1.40) and resolution. Failure to use oil will restrict the highest numerical aperture of the system to 1.0, the highest obtainable with air as the imaging medium (2, 5, 17-24).

Aplanatic condensers are well corrected for spherical aberration (green wavelengths) but not for chromatic aberration. These condensers feature five lens elements and are capable of focusing light in a single plane. Aplanatic condensers are capable of producing excellent black and white photomicrographs when used with green light generated by either a laser source or by use of an interference filter with tungsten-halide illumination.

The highest level of correction for optical aberration is incorporated in the aplanatic-achromatic condenser (2, 5). This condenser is well corrected for both chromatic and spherical aberrations and is the condenser of choice for use in critical color photomicrography with white light. A typical aplanatic-achromatic condenser features eight internal lens elements cemented into two doublets and four single lenses.

Engravings found on the condenser housing include its type (achromatic, aplanatic, etc.), the numerical aperture, and a graduated scale that indicates the approximate adjustment (size) of the aperture diaphragm. As we mentioned above, condensers with numerical apertures above 0.95 perform best when a drop of oil is applied to their upper lens in contact with the undersurface of the specimen slide. This ensures that oblique light rays emanating from the condenser are not reflected from underneath the slide, but are directed into the specimen without deviation. In practice, this can become tedious and is not commonly done in routine microscopy, but is essential when working at high resolutions and for accurate photomicrography using high-power (and numerical aperture) objectives.

Another important consideration is the thickness of the microscope slide, which is as crucial to the condenser as coverslip thickness is to the objective. Most commercial producers offer slides that range in thickness between 0.95 and 1.20 mm with the most common being very close to 1.0 mm. A microscope slide of thickness 1.20 mm is too thick to be used with most high numerical aperture condensers that tend to have a very short working distance. While this does not greatly matter for routine specimen observation, the results can be devastating with precision photomicrography. We recommend that microscope slides be chosen that have a thickness of 1.0 ± 0.05 mm, and that they be thoroughly cleaned prior to use.

When the objective is changed, for example from a 10x to 20x, the aperture diaphragm of the condenser must also be adjusted to provide a light cone that matches the numerical aperture of the new objective. There is a small painted arrow or index mark located on this knurled knob or lever that indicates the relative size of the aperture when compared to the linear gradation on the condenser housing. Many manufacturers will synchronize this gradation to correspond to the approximate numerical

aperture of the condenser. For example, if the microscopist has selected a 10x objective of numerical aperture 0.25, then the arrow would be placed next the value 0.18-0.20 (about 80 percent of the objective numerical aperture) on the scale inscribed on the condenser housing.

Often, it is not practical to use a single condenser with an entire range of objectives (2x to 100x) due to the broad range of light cones that must be produced to match objective numerical apertures. With low-power objectives in the range 2x to 5x, the illumination cone will have a diameter between 6-10 mm, while the high-power objectives (60x to 100x) need a highly focused light cone only about 0.2-0.4 mm in diameter. With a fixed focal length, it is difficult to achieve this wide range of illumination cones with a single condenser (18).

In practice, this problem can be solved in several ways. For low power objectives (below 10x), it may be necessary to unscrew the top lens of the condenser in order to fill the field of view with light. Other condensers are produced with a flip-top upper lens to accomplish this more readily. Some manufacturers now produce a condenser that flips over completely when used with low power objectives. Other companies incorporate auxiliary correction lenses in the light path for securing proper illumination with objectives less than 10x, or produce special low-power and low-numerical aperture condensers. When the condenser is used without its top lens, the aperture iris diaphragm is opened wide and the field diaphragm, now visible at the back of the objective,

Table 8 Substage Condenser Applications

Condenser Type	Brightfield	Darkfield	Phase Contrast	DIC	Polarizing
Achromat / Aplanat N.A. 1.3	• [10x~100x]				
Achromat Swing-out N.A. 0.90	• [4x~100x]				
Low-Power N.A. 0.20	• [1x~10x]				
Phase Contrast Abbe N.A. 1.25	•	• [up to N.A. 0.65]	• [10x~100x]		
Phase Contrast Achromat N.A. 0.85	•	• [up to N.A. 0.70]	• [4x~100x]		
DIC Universal Achromat / Aplanat	•	• [up to N.A. 0.70]	• [10x~100x]	• [10x, 20x, 40x, 100x]	
Darkfield, dry N.A. 0.80~0.95		• [4x~40x]			
Darkfield, oil N.A. 1.20~1.43		• [4x~100x]			
Strain-Free Achromat Swing-out N.A. 0.90	•				• [4x~100x]

Table 9 Depth of Field and Image Depth [a]

Magnification	Numerical Aperture	Depth of Field (M)	Image Depth (mm)
4x	0.10	15.5	0.13
10x	0.25	8.5	0.80
20x	0.40	5.8	3.8
40x	0.65	1.0	12.8
60x	0.85	0.40	29.8
100x	0.95	0.19	80.0

[a] Source: Nikon

serves as if it were the aperture diaphragm. Flip-top condensers are manufactured in a variety of configurations with numerical apertures ranging from 0.65 to 1.40. Those condensers having a numerical aperture value of 0.95 or less are intended for use with dry objectives. Flip-top condensers that have a numerical aperture greater than 0.95 are intended for use with oil-immersion objectives and they must have a drop of oil placed between the underside of the microscope slide and the condenser top lens when examining critical samples.

In addition to the common brightfield condensers discussed above, there are a wide variety of specialized models suited to many different applications. Substage condensers have a great deal of interchangeability among different applications. For instance, the DIC universal achromat/aplanat condenser is useful for brightfield, darkfield, and phase contrast, in addition to the primary DIC application. Other condensers have similar interchangeability.

Depth of Field and Depth of Focus

When considering resolution in optical microscopy, a majority of the emphasis is placed on point-to-point resolution in the plane perpendicular to the optical axis. Another important aspect to resolution is the ***axial resolving power*** of an objective, which is measured parallel to the optical axis and is most often referred to as depth of field (2, 4, 5, 22). Axial resolution, like horizontal resolution, is determined by the numerical aperture of the objective only, with the eyepiece merely magnifying the details resolved and projected in the intermediate image plane.

Just as in classical photography, depth of field is determined by the distance from the nearest object plane in focus to that of the farthest plane also simultaneously in focus. In microscopy depth of field is very short and usually measured in terms of microns. The term ***depth of focus***, which refers to image space, is often used interchangeably with depth of field, which refers to object space. This interchange of terms can lead to confusion, especially when the terms are both used specifically in terms of depth of field.

The geometric image plane might be expected to represent an infinitely thin section of the specimen, but even in the absence of aberrations, each image point is spread into a diffraction figure that extends above and below this plane (2, 4, 17). The Airy disk, discussed in the section on **Image Formation**, represents a section through the center of the image plane. This increases the effective in-focus depth of the Z-axis Airy disk intensity profile that passes through slightly different specimen planes.

Depth of focus varies with numerical aperture and magnification of the objective, and under some conditions, high numerical aperture systems (usually with higher magnification power) have deeper focus depths than do those systems of low numerical aperture, even though the depth of field is less (4). This is particularly important in photomicrography because the film emulsion or digital camera sensor must be exposed at a plane that is in focus. Small errors made to focus at high magnification are not as critical as those made with very low magnification objectives. Table 9 presents calculated variations in the depth of field and image depth in the intermediate image plane in a series of objectives with increasing numerical aperture and magnification.

Reflected Light Microscopy

Reflected light microscopy is often referred to as incident light, epi-illumination, or metallurgical microscopy, and is the method of choice for fluorescence and for imaging specimens that remain opaque even when ground to a thickness of 30 microns (25). The range of specimens falling into this category is enormous and includes most metals, ores, ceramics, many polymers, semiconductors (unprocessed silicon, wafers, and integrated circuits), slag, coal, plastics, paint, paper, wood, leather, glass inclusions, and a wide variety of specialized

materials (25-28). Because light is unable to pass through these specimens, it must be directed onto the surface and eventually returned to the microscope objective by either specular or diffused reflection. As mentioned above, such illumination is most often referred to as episcopic illumination, epi-illumination, or vertical illumination (essentially originating from above), in contrast to diascopic (transmitted) illumination that passes through a specimen. Today, many microscope manufacturers offer models that permit the user to alternate or simultaneously conduct investigations using vertical and transmitted illumination. Reflected light microscopy is frequently the domain of industrial microscopy, especially in the rapidly growing semiconductor arena, and thus represents a most important segment of microscopical studies.

A typical upright compound reflected light (illustrated in Figure 13) microscope also equipped for transmitted light has two eyepiece viewing tubes and often a trinocular tube head for mounting a conventional or digital/video camera system. Standard equipment eyepieces are usually of 10x magnification, and most microscopes are equipped with a nosepiece capable of holding four to six objectives. The stage is mechanically controlled with a specimen holder that can be translated in the X- and Y-directions and the entire stage unit is capable of precise up and down movement with a coarse and fine focusing mechanism. Built-in light sources range from 20 and 100 watt tungsten-halide bulbs to higher energy mercury vapor or xenon lamps that are used in fluorescence microscopy. Light passes from the lamp house through a vertical illuminator interposed above the nosepiece but below the underside of the viewing tube head. The specimen's top surface is upright (usually without a cover slip) on the stage facing the objective, which has been rotated into the microscope's optical axis. The vertical illuminator is horizontally oriented at a 90-degree angle to the optical axis of the microscope and parallel to the table top, with the lamp housing attached to the back of the illuminator. The coarse and fine adjustment knobs raise or lower the stage in large or small increments to bring the specimen into sharp focus.

Another variation of the upright reflected light microscope is the inverted microscope—of the Le Chatelier design (25). On the inverted stand, the specimen is placed on the stage with its surface of interest facing downward. The primary advantage of this design is that samples can be easily examined when they are far too large to fit into the confines of an upright microscope. Also, the only the side facing the objectives need be perfectly flat. The objectives are mounted on a nosepiece under the stage with their front lenses facing upward towards the specimen and focusing is accomplished either by moving the nosepiece or the entire stage up and down. Inverted microscope stands incorporate the vertical illuminator into the body of the microscope. Many types of objectives can be used with inverted reflected light microscopes, and all modes of reflected light illumination may be possible: brightfield, darkfield, polarized light, differential interference contrast, and fluorescence. Many

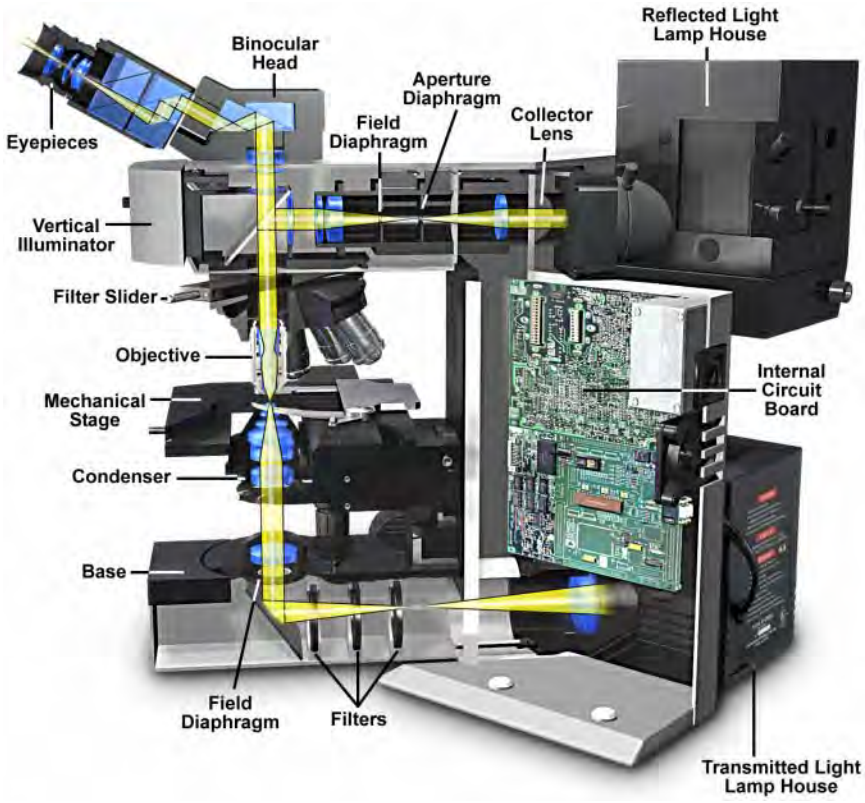

Figure 13. Components of a modern microscope configured for both transmitted and reflected light. This cutaway diagram reveals the ray traces and lens components of the microscope's optical trains. Also illustrated are the basic microscope components including two lamp houses, the microscope built-in vertical and base illuminators, condenser, objectives, eyepieces, filters, sliders, collector lenses, field, and aperture diaphragms.

of the inverted microscopes have built-in 35 millimeter and/or large format cameras or are modular to allow such accessories to be attached. Some of the instruments include a magnification changer for zooming in on the image, contrast filters, and a variety of reticules. Because an inverted microscope is a favorite instrument for metallographers, it is often referred to as a metallograph (25, 27). Manufacturers are largely migrating to using infinity-corrected optics in reflected light microscopes, but there are still thousands of fixed tube length microscopes in use with objectives corrected for a tube length between 160 and 210 millimeters.

In the vertical illuminator, light travels from the light source, usually a 12 volt 50 or 100 watt tungsten halogen lamp, passes through collector lenses, through the variable aperture iris diaphragm opening and through the opening of a variable and centerable pre-focused field iris diaphragm. The light then strikes a partially silvered plane glass reflector (Figure 13), or strikes a fully silvered periphery of a mirror with elliptical opening for darkfield illumination. The plane glass reflector is partially silvered on the glass side facing the light source and anti-reflection coated on the glass side facing the observation tube in brightfield reflected illumination. Light is thus deflected downward into the objective. The mirrors are tilted at an angle of 45 degrees to the path of the light travelling along the vertical illuminator.

The light reaches the specimen, which may absorb some of the light and reflect some of the light, either in a specular or diffuse manner. Light that is returned upward can be captured by the objective in accordance with the objective's numerical aperture and then passes through the partially silvered mirror. In the case of infinity-corrected objectives, the light emerges from the objective in parallel (from every azimuth) rays projecting an image of the specimen to infinity (25). The ***parallel*** rays enter the body tube lens, which forms the specimen image at the plane of the fixed diaphragm opening in the eyepiece (intermediate image plane). It is important to note, that in these reflected light systems, the objective serves a dual function: on the way down as a matching well-corrected condenser properly aligned; on the way up as an image-forming objective in the customary role of an objective projecting the image-carrying rays toward the eyepiece.

Optimal performance is achieved in reflected light illumination when the instrument is adjusted to produce Köhler illumination. A function of Köhler illumination (aside from providing evenly dispersed illumination) is to ensure that the objective will be able to deliver excellent resolution and good contrast even if the source of light is a coil filament lamp.

Some modern reflected light illuminators are described as universal illuminators because, with several additional accessories and little or no dismantling, the microscope can easily be switched from one mode of reflected light microscopy to another. Often, reflectors can be removed from the light path altogether in order to perform transmitted light observation. Such universal illuminators may include a partially reflecting plane glass surface (the half-mirror) for brightfield, and a fully silvered reflecting surface with an elliptical, centrally located clear opening for darkfield observation. The best-designed vertical illuminators include condensing lenses to gather and control the light, an aperture iris diaphragm and a pre-focused, centerable iris diaphragm to permit the desirable Köhler illumination (2, 25).

The vertical illuminator should also make provision for the insertion of filters for contrast and photomicrography, polarizers, analyzers, and compensator plates for polarized light and differential interference contrast illumination. In vertical illuminators designed for with infinity-corrected objectives, the illuminator may also include a body tube lens. Affixed to the back end of the vertical illuminator is a lamphouse, which usually contains a tungsten-halide lamp. For fluorescence work, the lamphouse can be replaced with one containing a mercury burner. The lamp may be powered by the electronics built into the microscope stand, or in fluorescence, by means of an external transformer or power supply.

In reflected light microscopy, absorption and diffraction of the incident light rays by the specimen often lead to readily discernible variations in the image, from black through various shades of gray, or color if the specimen is colored. Such specimens are known as amplitude specimens and may not require special contrast methods or treatment to make their details visible. Other specimens show so little difference in intensity and/or color that their feature details are extremely difficult to discern and distinguish in brightfield reflected light microscopy. Such specimens behave much like the phase specimens so familiar in transmitted light work. Such objects require special treatment or contrast methods that will be described in the next section.

Contrast Enhancing Techniques

Some specimens are considered amplitude objects because they absorb light partially or completely, and can thus be readily observed using conventional brightfield microscopy. Others that are naturally colored or artificially stained with chemical color dyes can also be seen. These stains or natural colors absorb some part of the white light passing through and transmit or reflect other colors. Often, stains are combined to yield contrasting

colors, e.g. blue haemotoxylin stain for cell nuclei combined with pink eosin for cytoplasm. It is a common practice to utilize stains on specimens that do not readily absorb light, thus rendering such objects visible to the eye.

Contrast produced by the absorption of light, brightness, or color has been the classical means of imaging specimens in brightfield microscopy. The ability of a detail to stand out against the background or other adjacent details is a measure of specimen contrast. In terms of a simple formula, contrast can be described as (18):

$$\textbf{Percent Contrast} = ((B_I - S_I) \times 100)/B_I \qquad (4)$$

Where B_I is the intensity of the background and S_I is the specimen intensity. From this equation, it is evident that specimen contrast refers to the relationship between the highest and lowest intensity in the image.

For many specimens in microscopy, especially unstained or living material, contrast is so poor that the object remains essentially invisible regardless of the ability of the objective to resolve or clearly separate details. Often, for just such specimens, it is important not to alter them by killing or treatment with chemical dyes or fixatives. This necessity has led microscopists to experiment with contrast-enhancing techniques for over a hundred years in an attempt to improve specimen visibility and to bring more detail to the image. It is a common practice to reduce the condenser aperture diaphragm below the recommended size or to lower the substage condenser to increase specimen contrast. Unfortunately, while these maneuvers will indeed increase contrast, they also seriously reduce resolution and sharpness.

An early and currently used method of increasing contrast of stained specimens utilizes color contrast filters, gelatin squares (from Kodak), or interference filters in the light path (18, 19). For example, if a specimen is stained with a red stain, a green filter will darken the red areas thus increasing contrast. On the other hand, a green filter will lighten any green stained area. Color filters are very valuable aids to specimen contrast, especially when black and white photomicrography is the goal. Green filters are particularly valuable for use with achromats, which are spherically corrected for green light, and phase contrast objectives, which are designed for manipulation of wavelength assuming the use of green light, because phase specimens are usually transparent and lack inherent color. Another simple technique for contrast improvement involves the selection of a mounting medium with a refractive index substantially different from that of the specimen. For example, diatoms can be mounted in a variety of contrast-enhancing mediums such as air or the commercial medium Styrax. The difference in refractive indices improves the contrast of these colorless objects and renders their outlines and markings more visible. The following sections describe many of the more complex techniques used by present-day microscopists to improve specimen contrast.

Darkfield Microscopy

Darkfield illumination requires blocking out of the central light rays that ordinarily pass through or around the specimen and allowing only oblique rays to illuminate the specimen. This method is a simple and popular method for imaging unstained specimens, which appear as brightly illuminated objects on a dark background. Oblique light rays emanating from a darkfield condenser strike the specimen from every azimuth and are diffracted, reflected, and refracted into the microscope objective (5, 18, 19, 28). This technique is illustrated in Figure 14. If no specimen is present and the numerical aperture of the condenser is greater than that of the objective, the oblique rays cross and all such rays will miss entering the objective because of the obliquity. The field of view will appear dark.

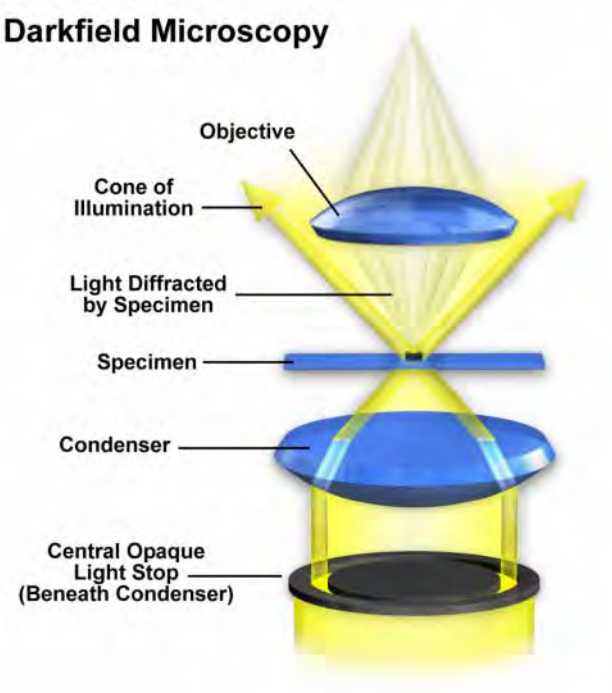

Figure 14. Schematic configuration for darkfield microscopy. The central opaque light stop is positioned beneath the condenser to eliminate zeroth order illumination of the specimen. The condenser produces a hollow cone of illumination that strikes the specimen at oblique angles. Some of the reflected, refracted, and diffracted light from the specimen enters the objective front lens.

In terms of Fourier optics, darkfield illumination removes the zeroth order (unscattered light) from the diffraction pattern formed at the rear focal plane of the objective (5). Oblique rays, now diffracted by the specimen and yielding 1st, 2nd, and higher diffracted orders at the rear focal plane of the objective, proceed onto the image plane where they interfere with one another to produce an image of the specimen. This results in an image formed exclusively from higher order diffraction intensities scattered by the specimen. Specimens that have smooth reflective surfaces produce images due, in part, to reflection of light into the objective (18, 19). In situations where the refractive index is different from the surrounding medium or where refractive index gradients occur (as in the edge of a membrane), light is refracted by the specimen. Both instances of reflection and refraction produce relatively small angular changes in the direction of light allowing some to enter the objective. In contrast, some light striking the specimen is also diffracted, producing a 180-degree arc of light that passes through the entire numerical aperture range of the objective. The resolving power of the objective is the same in darkfield illumination as found under brightfield conditions, but the optical character is the image is not as faithfully reproduced.

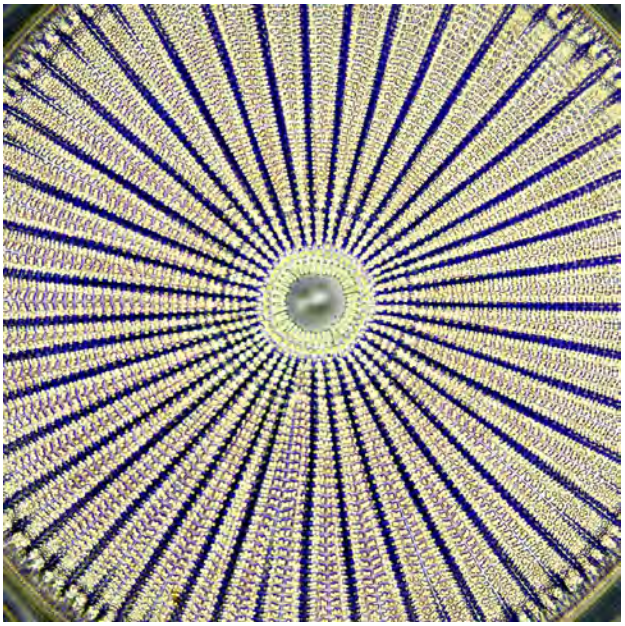

Figure 15. Darkfield photomicrograph of the diatom *Arachnoidiscus ehrenbergi* taken at high magnification using oil immersion optics and a 100x objective.

There are several pieces of equipment that are utilized to produce darkfield illumination. The simplest is a ***spider stop*** (Figure 14) placed just under the bottom lens (in the front focal plane) of the substage condenser (5, 18, 19, 28). Both the aperture and field diaphragms are opened wide to pass oblique rays. The central opaque stop (you can make one by mounting a coin on a clear glass disk) blocks out the central rays. This device works fairly well, even with the Abbe condenser, with the 10x objective up to 40x or higher objectives having a numerical aperture no higher than 0.65. The diameter of the opaque stop should be approximately 16-18 millimeters for a 10x objective of numerical aperture 0.25 to approximately 20-24 millimeters for 20x and 40x objectives of numerical apertures approaching 0.65.

For more precise work and blacker backgrounds, use a condenser designed especially for darkfield, i.e. to transmit only oblique rays (28, 29). There are several varieties including dry darkfield condensers with air between the top of the condenser and the underside of the slide. Immersion darkfield condensers are also available. These require the use of a drop of immersion oil (some are designed to use water instead) establishing contact between the top of the condenser and the underside of the specimen slide. The immersion darkfield condenser has internal mirrored surfaces and passes rays of great obliquity and free of chromatic aberration, producing the best results and blackest background.

Darkfield objects are quite spectacular to see and objects of very low contrast in brightfield shine brilliantly in darkfield. Such illumination is best for revealing outlines, edges, and boundaries. A high magnification darkfield image of a diatom is illustrated in Figure 15.

Rheinberg Illumination

Rheinberg illumination, a form of optical staining, was initially demonstrated by the British microscopist Julius Rheinberg to the Royal Microscopical Society and the Quekett Club (England) nearly a hundred years ago (18, 28). This technique is a striking variation of low to medium power darkfield illumination using colored gelatin or glass filters to provide rich color to both the specimen and background. The central opaque darkfield stop is replaced with a transparent, colored, circular stop inserted into a transparent ring of a contrasting color (illustrated in Figure 16). These stops are placed under the bottom lens of the condenser. The result is a specimen rendered in the color of the ring with a background having the color of the central spot. An example of photomicrography using Rheinberg illumination is illustrated in Figure 17 with the spiracle and trachea of a silkworm larva.

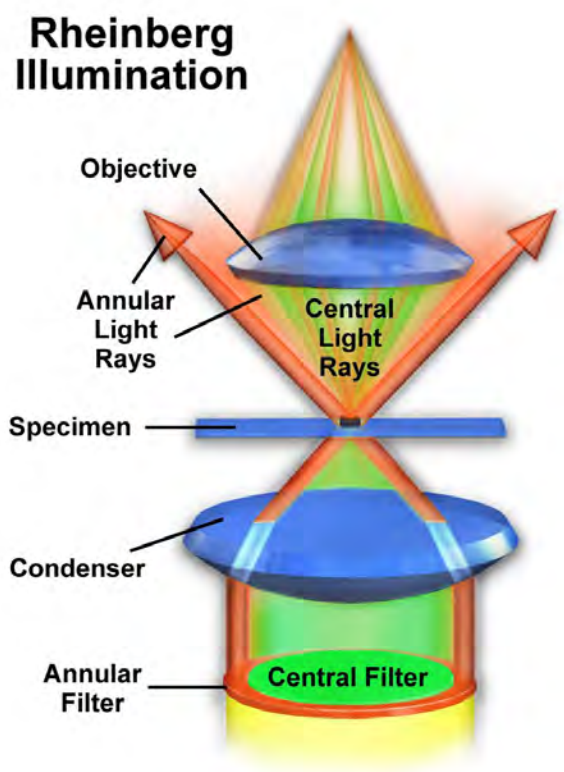

Figure 16. Schematic microscope configuration for Rheinberg illumination. Light passes through the central/annular filter pack prior to entering the condenser. Zeroth order light from the central filter pervades the specimen and background and illuminates it with higher order light from the annular filter. The filter colors in this diagram are a green central and red annular.

Phase Contrast Microscopy

Research by Frits Zernike during the early 1930s uncovered phase and amplitude differences between zeroth order and deviated light that can be altered to produce favorable conditions for interference and contrast enhancement (30, 31). Unstained specimens that do not absorb light are called phase objects because they slightly alter the phase of the light diffracted by the specimen, usually by retarding such light approximately 1/4 wavelength as compared to the undeviated direct light passing through or around the specimen unaffected. Unfortunately, our eyes as well as camera film are unable to detect these phase differences. To reiterate, the human eye is sensitive only to the colors of the visible spectrum or to differing levels of light intensity (related to wave amplitude).

In phase specimens, the direct zeroth order light passes through or around the specimen undeviated. However, the light diffracted by the specimen is not reduced in amplitude as it is in a light-absorbing object, but is slowed by the specimen because of the specimen's refractive index or thickness (or both). This diffracted light, lagging behind by approximately 1/4 wavelength, arrives at the image plane ***out of step*** (also termed ***out of phase***) with the undeviated light but, in interference, essentially undiminished in intensity. The result is that the image at the eyepiece level is so lacking in contrast as to make the details almost invisible.

Zernike succeeded in devising a method—now known as Phase Contrast microscopy—for making unstained, phase objects yield contrast images as if they were amplitude objects. Amplitude objects show excellent contrast when the diffracted and direct light are out of step (display a phase difference) by 1/2 of a wavelength (18). Zernike's method was to ***speed up*** the direct light by 1/4 wavelength so that the difference in wavelength between the direct and deviated light for a phase specimen would now be 1/2 wavelength. As a result, the direct and diffracted light arriving at the image level of the eyepiece would be able to produce destructive interference (see the section on **image formation** for absorbing objects previously described). Such a procedure results in the details of the image appearing darker against a lighter background. This is called dark or positive phase contrast. A schematic illustration of the basic phase contrast microscope configuration is illustrated in Figure 18.

Another possible course, much less often used, is to arrange to ***slow down*** the direct light by 1/4 wavelength so that the diffracted light and the direct light arrive at the eyepiece in step and can interfere constructively (2, 5, 18). This arrangement results in a bright image of the details of the specimen on a darker background, and is called negative or bright contrast.

Phase contrast involves the ***separation*** of the direct zeroth order light from the diffracted light at the rear focal plane of the objective. To do this, a ring annulus is placed in position directly under the lower lens of the condenser at the front focal plane of the condenser, conjugate to the objective rear focal plane. As the hollow cone of light from the annulus passes through the specimen undeviated, it arrives at the rear focal plane of the objective in the shape of a ring of light. The fainter light diffracted by the specimen is spread over the rear focal plane of the objective. If this combination were allowed, as is, to proceed to the image plane of the eyepiece, the diffracted light would be approximately 1/4 wavelength behind the direct light. At the image plane, the phase of the diffracted light would be out of phase with the direct light, but the amplitude of their interference would be almost the same as that of the direct light (5, 18). This would result in very little specimen contrast.

To speed up the direct undeviated zeroth order light, a phase plate is installed with a ring shaped ***phase shifter*** attached to it at the rear focal plane of the objective. The

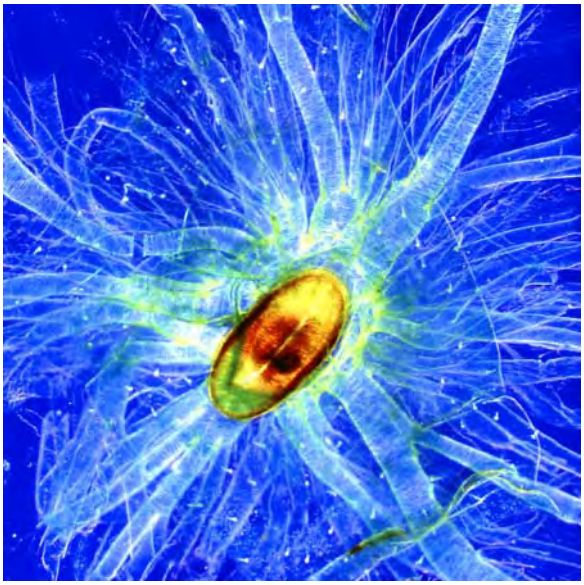

Figure 17. Spiracle and trachea from silkworm larva photographed at low magnification under Rheinberg illumination using a blue central and yellow annulus filters and a 2x objective.

narrow area of the phase ring is optically thinner than the rest of the plate. As a result, undeviated light passing through the phase ring travels a shorter distance in traversing the glass of the objective than does the diffracted light. Now, when the direct undeviated light and the diffracted light proceed to the image plane, they are 1/2 wavelength out of phase with each other. The diffracted and direct light can now interfere destructively so that the details of the specimen appear dark against a lighter background (just as they do for an absorbing or amplitude specimen). This is a description of what takes place in positive or dark phase contrast.

If the ring phase shifter area of the phase plate is made optically thicker than the rest of the plate, direct light is slowed by 1/4 wavelength. In this case, the zeroth order light arrives at the image plane in step (or in phase) with the diffracted light, and constructive interference takes place. The image appears bright on a darker background. This type of phase contrast is described as ***negative*** or ***bright contrast*** (2, 5, 18, 19).

Because undeviated light of the zeroth order is much brighter than the faint diffracted light, a thin absorptive transparent metallic layer is deposited on the phase ring to bring the direct and diffracted light into better balance of intensity to increase contrast. Also, because speeding up or slowing down of the direct light is calculated on a 1/4 wavelength of green light, the phase image will appear best when a green filter is placed in the light path (a green interference filter is preferable). Such a green filter also helps achromatic objectives produce their best images, because achromats are spherically corrected for green light.

The accessories needed for phase contrast work are a substage phase contrast condenser equipped with annuli and a set of phase contrast objectives, each of which has a phase plate installed. The condenser usually has a brightfield position with an aperture diaphragm and a rotating turret of annuli (each phase objective of different magnification requires an annulus of increasing diameter as the magnification of the objective increases). Each phase objective has a darkened ring on its back lens. Such objectives can also be used for ordinary brightfield transmitted light work with only a slight reduction in image quality. A photomicrograph of a hair cross sections from a fetal mouse taken using phase contrast illumination is illustrated in Figure 19.

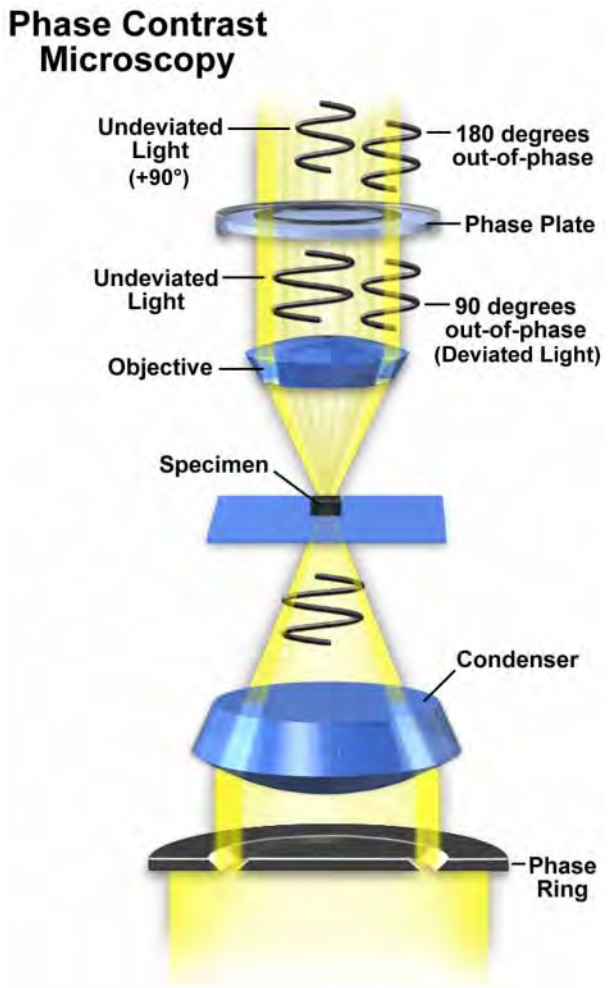

Figure 18. Schematic configuration for phase contrast microscopy. Light passing through the phase ring is first concentrated onto the specimen by the condenser. Undeviated light enters the objective and is advancedd by the phase plate before interference at the rear focal plane of the objective.

Polarized Light

Many transparent solids are optically isotropic, meaning that the index of refraction is equal in all directions throughout the crystalline lattice. Examples of isotropic solids are glass, table salt (sodium chloride), many polymers, and a wide variety of both organic and inorganic compounds (32, 33).

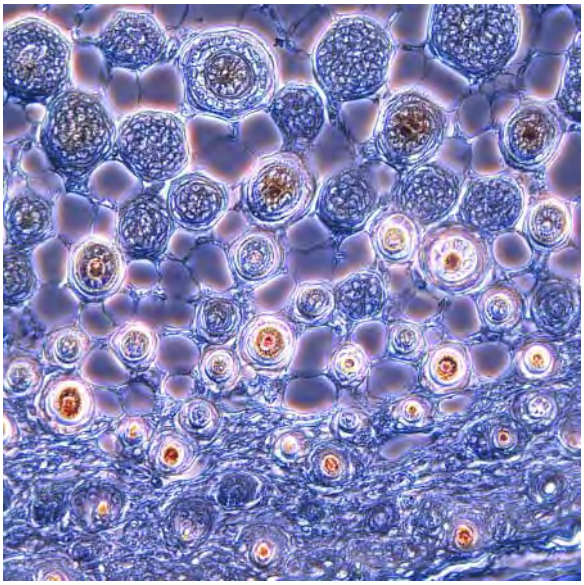

Figure 19. Photomicrograph of hair cross sections from a fetal mouse taken using phase contrast optics and a 20x objective.

Crystals are classified as being either isotropic or anisotropic depending upon their optical behavior and whether or not their crystallographic axes are equivalent. All isotropic crystals have equivalent axes that interact with light in a similar manner, regardless of the crystal orientation with respect to incident light waves. Light entering an isotropic crystal is refracted at a constant angle and passes through the crystal at a single velocity without being polarized by interaction with the electronic components of the crystalline lattice.

Anisotropic crystals, on the other hand, have crystallographically distinct axes and interact with light in a manner that is dependent upon the orientation of the crystalline lattice with respect to the incident light. When light enters the optical axis of anisotropic crystals, it acts in a manner similar to interaction with isotropic crystals and passes through at a single velocity. However, when light enters a non-equivalent axis, it is refracted into two rays each polarized with their vibration directions oriented at right angles to one another, and traveling at different velocities. This phenomenon is termed ***double*** or ***bi-refraction*** and is seen to a greater or lesser degree in all anisotropic crystals (32-34).

When anisotropic crystals refract light, the resulting rays are polarized and travel at different velocities. One of the rays travels with the same velocity in every direction through the crystal and is termed the ordinary ray. The other ray travels with a velocity that is dependent upon the propagation direction within the crystal. This light ray is termed the extraordinary ray. The retardation between the ordinary and extraordinary ray increases with increasing crystal thickness. The two independent refractive indices of anisotropic crystals are quantified in terms of their birefringence, a measure of the difference in refractive index. Thus, the birefringence (**B**) of a crystal is defined as:

$$\mathbf{B} = |\mathbf{n}_{high} - \mathbf{n}_{low}| \qquad (5)$$

Where $\mathbf{n}_{high}$ is the largest refractive index and $\mathbf{n}_{low}$ is the smallest. This expression holds true for any part or fragment of an anisotropic crystal with the exception of light waves propagated along the optical axis of the crystal. As mentioned above, light that is doubly refracted through anisotropic crystals is polarized with the vibration directions of the polarized ordinary and extraordinary light waves being oriented perpendicular to each other. We can now examine how anisotropic crystals behave under polarized illumination in a polarizing microscope.

A polarizer place beneath the substage condenser is oriented such that polarized light exiting the polarizer is plane polarized in a vibration direction that is east-west with respect to the optic axis of the microscope stand. Polarized light enters the anisotropic crystal where it is refracted and divided into two separate components vibrating parallel to the crystallographic axes and perpendicular to each other. The polarized light waves then pass through the specimen and objective before reaching a second polarizer (usually termed the analyzer) that is oriented to pass a polarized vibration direction perpendicular to that of the substage polarizer. Therefore, the analyzer passes only those components of the light waves that are parallel to the polarization direction of the analyzer. The retardation of one ray with respect to another is caused the difference in speed between the ordinary and extraordinary rays refracted by the anisotropic crystal (33, 34). A schematic illustration of microscope configuration for crossed polarized illumination is presented in Figure 20.

Now we will consider the phase relationship and velocity differences between the ordinary and extraordinary rays after they pass through a birefringent crystal. These rays are oriented so that they are vibrating at right angles to each other. Each ray will encounter a slightly different electrical environment (refractive index)

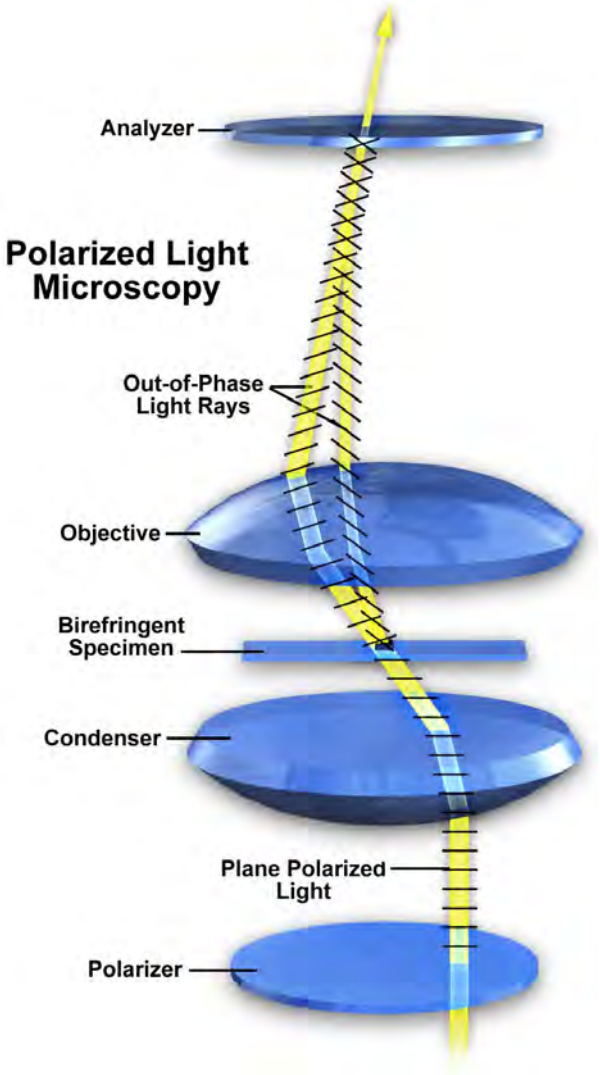

Figure 20. Schematic microscope configuration for observing birefringent specimens under crossed polarized illumination. White light passing through the polarizer is plane polarized and concentrated onto the birefringent specimen by the condenser. Light rays emerging from the specimen interfere when they are recombined in the analyzer, subtracting some of the wavelengths of white light, thus producing a myriad of tones and colors.

as it enters the crystal and this will affect the velocity at which ray passes through the crystal (32, 33). Because of the difference in refractive indices, one ray will pass through the crystal at a slower rate than the other ray. In other words, the velocity of the slower ray will be retarded with respect to the faster ray. This retardation can be quantified using the following equation:

$$\textbf{Retardation (G) = thickness (t) x Birefringence (B)} \quad (6)$$

$$\textbf{or}$$

$$\Gamma = t \times |n_{high} - n_{low}| \quad (7)$$

Where Γ is the quantitative retardation of the material, **t** is the thickness of the birefringent crystal (or material) and **B** is birefringence as defined above (33). Factors contributing to the value of retardation are the magnitude of the difference in refractive indices for the environments seen by the ordinary and extraordinary rays and also the sample thickness. Obviously, the greater the difference in either refractive indices or thickness, the greater the degree of retardation. Early observations made on the mineral calcite indicated that thicker calcite crystals caused greater differences in splitting of the images seen through the crystals. This agrees with the equation above that states retardation will increase with crystal (or sample) thickness.

When the ordinary and extraordinary rays emerge from the birefringent crystal, they are still vibrating at right angles with respect to one another. However, the component vectors of these waves that pass through the analyzer are vibrating in the same plane. Because one wave is retarded with respect to the other, interference (either constructive or destructive) occurs between the waves as they pass through the analyzer. The net result is that some birefringent samples (in white light) acquire a spectrum of color when observed through crossed polarizers.

Polarized light microscopy requires strain-free objectives and condensers to avoid depolarization effects on the transmitted light (32-34). Most polarized

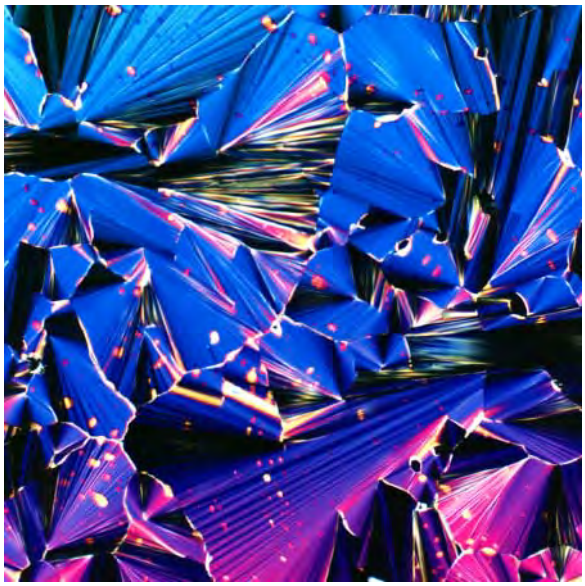

Figure 21. Photomicrograph of high-density columnar-hexatic liquid crystalline calf thymus DNA at a concentration of approximately 450 milligrams/milliliter. This concentration of DNA is approaching that found in sperm heads, virus capsids, and dinoflagellate chromosomes. The image was recorded using a polarized light microscope and the 10x objective.

microscopes are equipped with a centerable stage that has free 360-degree rotation about the optical axis of the microscope. A Bertrand lens is commonly inserted into the light path so that conoscopic images of birefringence patterns can be observed at the back of the objective. Manufacturers also offer a wide range of compensators and light retarders (full-wave and quarter-wave plates) for quantitative birefringence measurements and for adding color to polarized light photomicrographs. Birefringent DNA liquid crystals photographed using crossed polarized illumination are illustrated in Figure 21.

Hoffman Modulation Contrast

The Hoffman Modulation Contrast system is designed to increase visibility and contrast in unstained and living material by detecting optical gradients (or slopes) and converting them into variations of light intensity. This ingenious technique was invented by Dr. Robert Hoffman in 1975, and employs several accessories that have been adapted to the major commercial microscopes (16, 18). A schematic illustration of microscope configuration for Hoffman modulation contrast is presented in Figure 22.

An optical amplitude spatial filter, termed a ***modulator*** by Hoffman, is inserted at the rear focal plane of an achromat or planachromat objective (although higher correction can also be used). Light intensity passing through this system varies above and below an average value, which by definition, is then said to be modulated. Objectives useful for modulation contrast can cover the entire magnification range of 10x to 100x. The modulator has three zones: a small, dark zone near the periphery of the rear focal plane which transmits only one percent of light; a narrow gray zone which transmits 15 percent; and the remaining clear or transparent zone, covering most of the area at the back of the objective, which transmits 100 percent of the light (5, 16, 18). Unlike the phase plate in phase contrast microscopy, the Hoffman modulator is designed not to alter the phase of light passing through any of the zones. When viewed under modulation contrast optics, transparent objects that are essentially invisible in ordinary brightfield microscopy take on an apparent three-dimensional appearance dictated by phase gradients. The modulator does not introduce changes in the phase relationship of light passing through the system, but influences the principal zeroth order maxima. Higher order diffraction maxima are unaffected. Measurements using a Michelson interferometer confirm that the spatial coherency of light passed through a Hoffman-style modulator varies (if any) by a factor of less than l/20 (5).

Below the stage, a condenser with rotating turret is utilized to hold the remaining components of the Hoffman

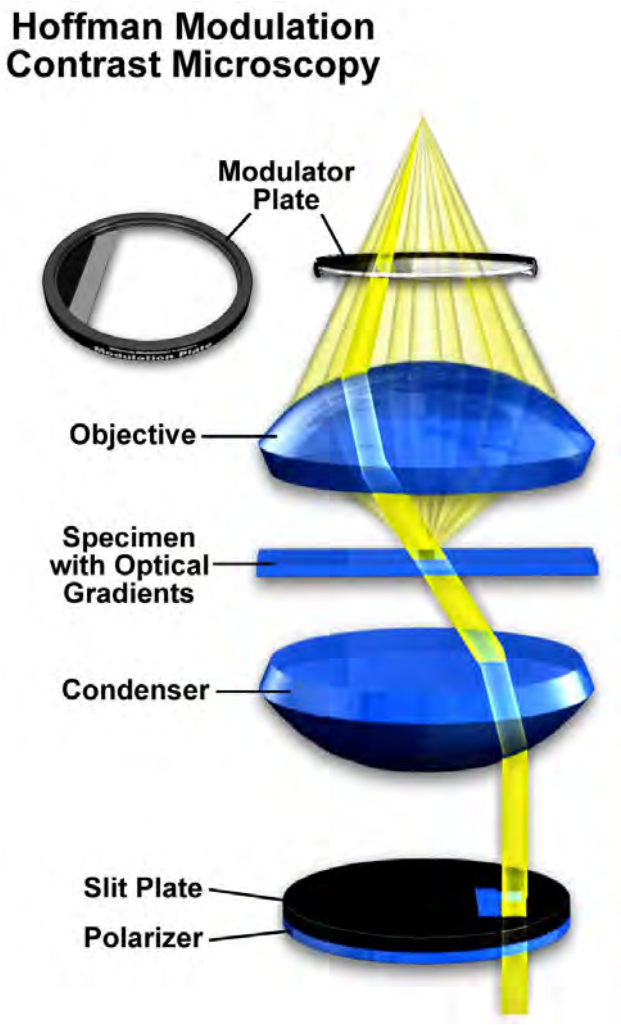

Figure 22. Schematic illustration of microscope configuration for Hoffman modulation contrast. Light passing through the polarizer and slit is concentrated onto the specimen by the condenser. After passing through the specimen light enters the objective and is filtered by the modulator plate in the rear focal plane of the objective.

Modulation Contrast system. The turret condenser has a brightfield opening with an aperture iris diaphragm for regular brightfield microscopy and for alignment and establishing proper conditions of Köhler illumination for the microscope. At each of the other turret openings, there is an off-center slit that is partially covered with a small rectangular polarizer. The size of the slit/polarizer combination is different for each objective of different magnification; hence the need for a turret arrangement. When light passes through the off-axis slit, it is imaged at the rear focal plane of the objective (also termed the Fourier plane) where the modulator has been installed. Like the central annulus and phase ring in phase contrast microscopy, the front focal plane of the condenser

containing the off-axis slit plate is optically conjugate to the modulator in objective rear focal plane. Image intensity is proportional to the first derivative of the optical density in the specimen, and is controlled by the zeroth order of the phase gradient diffraction pattern.

Below the condenser, a circular polarizer is placed on the light exit port of the microscope (note that both polarizers are below the specimen). The rotation of this polarizer can control the effective width of the slit opening. For example, a ***crossing*** of both polarizers at 90 degrees to each other results in ***narrowing*** the slit so that its image falls within the gray area of the modulator (16, 18). The part of the slit controlled by the polarizer registers on the bright area of the modulator. As the polarizer is rotated, contrast can be varied for best effect. A very narrow slit produces images that are very high in contrast with a high degree of coherence. Optical section imaging is also optimized when the slit is adjusted to its narrowest position. When the circular polarizer is oriented with its vibration direction parallel to that of the polarizer in the slit, the effective slit width is at a maximum. This reduces overall image contrast and coherence, but yields much better images of thicker objects where large differences in refractive index exist.

In modern advanced modulation contrast systems, both the modulator and the slit are offset from the optical axis of the microscope (18). This arrangement permits fuller use of the numerical aperture of the objective and results in good resolution of specimen detail. Shapes and details are rendered in shadowed, pseudo three-dimensional appearance. These appear brighter on one side, gray in the central portion, and darker on the other side, against a gray background. The modulator converts optical phase gradients in details (steepness, slope, rate of change in refractive index, or thickness) into changes in the intensity of various areas of the image at the plane of the eyepiece diaphragm. Resulting images have an apparent three-dimensional appearance with directional sensitivity to optical gradients. The contrast (related to variations in intensity) of the dark and bright areas against the gray gives a shadowed pseudo-relief effect. This is typical of modulation contrast imaging. Rotation of the polarizer alters the contrast achieved and the orientation of the specimen on the stage (with respect to the polarizer and offset slit) may dramatically improve or degrade contrast.

There are numerous advantages as well as limitations to modulation contrast. Some of the advantages include fuller use of the numerical aperture of the objective yielding excellent resolution of details along with good specimen contrast and visibility. Although many standard modulation contrast objectives are achromats or planachromats, it is also possible to use objectives with a higher degree of correction for optical aberration. Many major microscope manufacturers now offer modulation contrast objectives in fluorite-correction grades, and apochromats can be obtained by special order. Older objectives can often be retrofitted with a modulator made by Modulation Optics, Inc., the company founded by Dr. Robert Hoffman specifically to build aftermarket and custom systems.

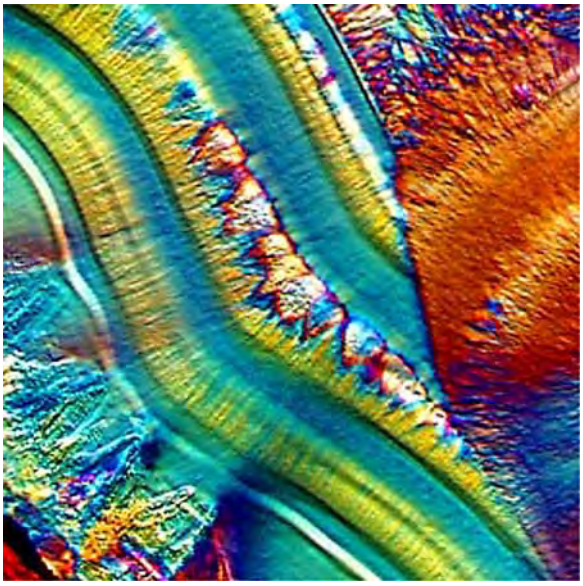

Figure 23. Duck-billed dinosaur bone thin section photographed using a combination of Hoffman modulation contrast and polarized light illumination using a 20x objective. Note the pseudo three-dimensional relief evident throughout the photomicrograph as a result of amplitude gradients (Hoffman modulation contrast). The vivid colors are due to interference of white light at the analyzer (polarized light).

In addition to the advantages of using higher numerical apertures with modulation contrast, it is also possible to do ***optical sectioning*** with this technique (16, 18). Sectioning allows the microscopist to focus on a single thin plane of the specimen without interference from confusing images arising in areas above or below the plane that is being focused on. The depth of a specimen is measured in a direction parallel to the optical axis of the microscope. Focusing the image establishes the correct specimen-to-image distance, allowing interference of the diffracted waves to occur at a pre-determined plane (the image plane) positioned at a fixed distance from the eyepiece. This enables diffracting objects that occur at different depth levels in the specimen to be viewed separately, provided there is sufficient contrast. The entire depth of a specimen can be optically sectioned by sequentially focusing on each succeeding plane. In this system, depth of field is defined as the distance from one level to the next where imaging of distinct detail occurs,

and is controlled by the numerical aperture of the objective (5, 16, 18). Higher numerical aperture objectives exhibit very shallow depths of field and the opposite holds for objectives of lower numerical aperture. The overall capability of an objective to isolate and focus on a specific optical section diminishes as the optical homogeneity of the specimen decreases.

Birefringent objects (rock thin sections, crystals, bone, etc.), that can confuse images in DIC, can be examined because the specimen is ***not*** situated between the two polarizers (18). Further, specimens can be contained in plastic or glass vessels without deterioration of the image due to polarization effects, because such vessels are also above both polarizers, not between them. This allows the Hoffman system to be far more useful than DIC in the examination and photomicrography of cell, tissue, and organ culture performed in plastic containers.

Hoffman modulation contrast can be simultaneously combined with polarized light microscopy to achieve spectacular effects in photomicrography. Figure 23 illustrates a dinosaur bone thin section photographed with a combination of Hoffman modulation contrast and plane polarized illumination. Note the pseudo three-dimensional relief apparent throughout the micrograph and the beautiful coloration provided by polarized light.

Differential Interference Contrast

In the mid 1950s a French optics theoretician named Georges Nomarski improved the method for detecting optical gradients in specimens and converting them into intensity differences (15). Today there are several implementations of this design, which are collectively called differential interference contrast (DIC). Living or stained specimens, which often yield poor images when viewed in brightfield illumination, are made clearly visible by optical rather than chemical means (2, 4, 5, 15, 18-22).

In transmitted light DIC, light from the lamp is passed through a polarizer located beneath the substage condenser, in a manner similar to polarized light microscopy. Next in the light path (but still beneath the condenser) is a modified Wollaston prism that ***splits*** the entering beam of polarized light into two beams traveling in slightly different direction (illustrated in Figure 24). The prism is composed of two halves cemented together (36). Emerging light rays vibrate at 90 degrees relative to each other with a slight path difference. A different prism is needed for each objective of different magnification. A revolving turret on the condenser allows the microscopist to rotate the appropriate prism into the light path when changing magnifications.

The plane polarized light, vibrating only in one direction perpendicular to the propagation direction of the light beam, enters the beam-splitting modified Wollaston prism and is split into two rays, vibrating perpendicular to each other (Figure 24). These two rays travel close together but in slightly different directions. The rays intersect at the front focal plane of the condenser, where they pass traveling parallel and extremely close together with a slight path difference, but they are vibrating perpendicular to each other and are therefore unable to cause interference. The distance between the rays, called the shear, is so minute that it is less than the resolving ability of the objective (5, 18, 36).

The split beams enter and pass through the specimen where their wave paths are altered in accordance with the specimen's varying thickness, slopes, and refractive

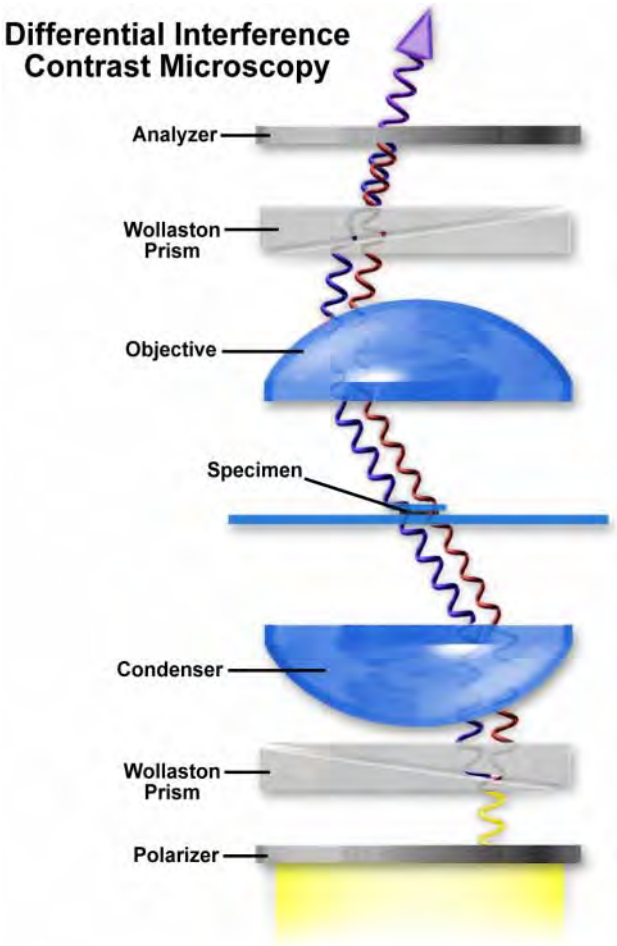

Figure 24. Schematic illustration of microscope configuration for differential interference contrast. Light is polarized in a single vibration plane by the polarizer before entering the lower modified Wollaston prism that acts as a beam splitter. Next, the light passes through the condenser and sample before the image is reconstructed by the objective. Above the objective, a second Wollaston (Nomarski) prism acts as a beam-combiner and passes the light to the analyzer, where it interferes both constructively and destructively.

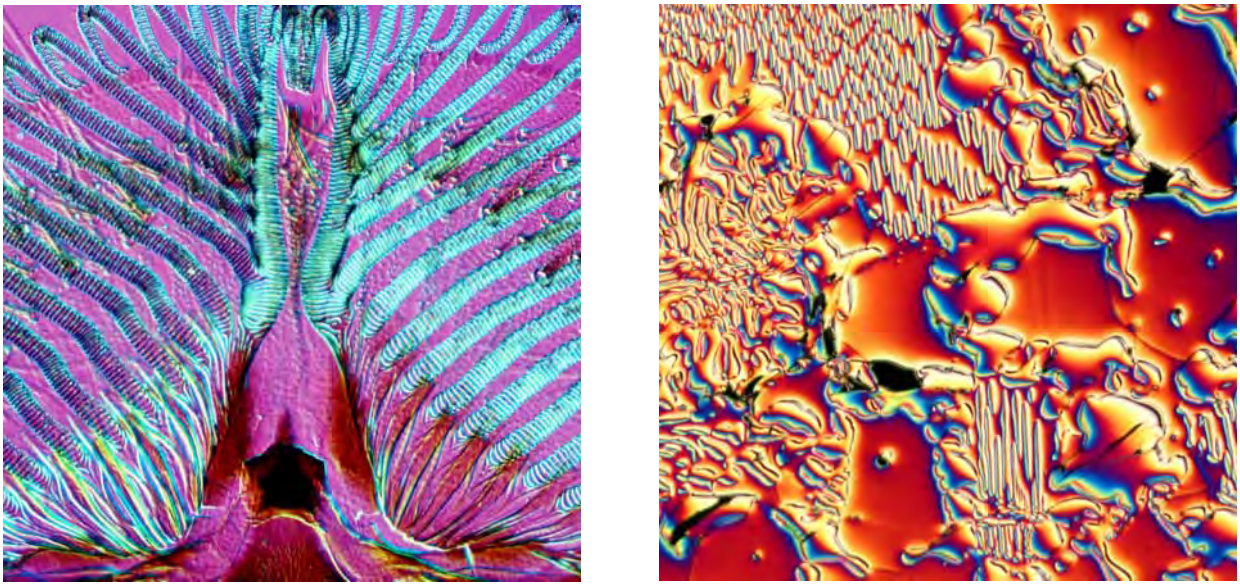

(a) **(b)**

Figure 25 (a) Nomarski transmitted light differential interference contrast (DIC) photomicrograph of mouthparts from a blowfly. **(b)** Reflected light differential interference contrast photomicrograph illustration defects on the surface of a ferro-silicon alloy. Both images were captured using the 10x objective and a first-order retardation plate.

indices. These variations cause alterations in the wave path of both beams passing through areas of the specimen details lying close together. When the parallel beams enter the objective, they are focused above the rear focal plane where they enter a second modified Wollaston prism that combines the two beams. This removes the shear and the original path difference between the beam pairs. As a result of having traversed the specimen, the paths of the parallel beams are not of the same length (optical path difference) for differing areas of the specimen.

In order for the beams to interfere, the vibrations of the beams of different path length must be brought into the same plane and axis. This is accomplished by placing a second polarizer (analyzer) above the upper Wollaston beam-combining prism. The light then proceeds toward the eyepiece where it can be observed as differences in intensity and color. The design results in one side of a detail appearing bright (or possibly in color) while the other side appears darker (or another color). This shadow effect bestows a pseudo three-dimensional appearance to the specimen (18).

In some microscopes, the upper modified Wollaston prism is combined in a single fitting with the analyzer incorporated above it. The upper prism may also be arranged so it can be moved horizontally. This allows for varying optical path differences by moving the prism, providing the user a mechanism to alter the brightness and color of the background and specimen. Because of the prism design and placements, the background will be homogeneous for whatever color has been selected.

The color and/or light intensity effects shown in the image are related especially to the rate of change in refractive index, specimen thickness, or both. Orientation of the specimen can have pronounced effect on the relief-like appearance and often, rotation of the specimen by 180 degrees changes a ***hill*** into a ***valley*** or visa versa. The three-dimensional appearance is not representing the true geometric nature of the specimen, but is an exaggeration based on ***optical thickness***. It is not suitable for accurate measurement of actual heights and depths.

There are numerous advantages in DIC microscopy as compared particular to phase and Hoffman modulation contrast microscopy. With DIC, it is also possible to make fuller use of the numerical aperture of the system and to provide optical staining (color). DIC also allows the microscope to achieve excellent resolution. Use of full objective aperture enables the microscopist to focus on a thin plane section of a thick specimen without confusing images from above or below the plane. Annoying ***halos***, often encountered in phase contrast, are absent in DIC images, and common achromat and fluorite objectives can be used for this work. A downside is that plastic tissue culture vessels and other birefringent specimens yield confusing images in DIC. Also, high-quality apochromatic objectives are now designed to be suitable for DIC. Figure 24 presents transmitted and reflected light DIC photomicrographs of the mouthparts of a blowfly

(transmitted DIC) and surface defects in a ferro-silicate alloy (reflected DIC). Both photomicrographs were made using a retardation plate with a 10x objective.

Fluorescence Microscopy

Fluorescence microscopy is an excellent tool for studying material which can be made to fluoresce, either in its natural form (primary or autofluorescence) or when treated with chemicals capable of fluorescing (secondary fluorescence). This form of optical microscopy is rapidly reaching maturity and is now one of the fastest growing areas of investigation using the microscope (6-8).

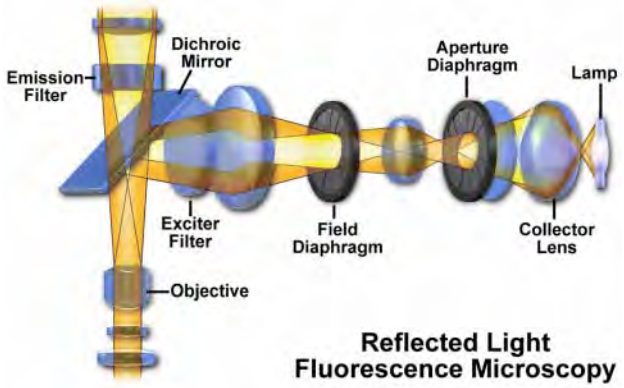

Figure 26. Schematic diagram of the configuration of reflected light fluorescence microscopy. Light emitted from a mercury burner is concentrated by the collector lens before passing through the aperture and field diaphragms. The exciter filter passes only the desired excitation wavelengths, which are reflected down through the objective to illuminate the specimen. Longer wavelength fluorescence emitted by the specimen passes back through the objective and dichroic mirror before finally being filtered by the emission filter.

The basic task of the fluorescence microscope is to permit excitation light to irradiate the specimen and then to separate the much weaker re-radiating fluorescent light from the brighter excitation light. Thus, only the emission light reaches the eye or other detector. The resulting fluorescing areas shine against a dark background with sufficient contrast to permit detection. The darker the background of the non-fluorescing material, the more efficient the instrument. For example, ultraviolet (UV) light of a specific wavelength or set of wavelengths is produced by passing light from a UV-emitting source through the exciter filter. The filtered UV light illuminates the specimen, which emits fluorescent light of longer wavelengths while illuminated with ultraviolet light. Visible light emitted from the specimen is then filtered through a barrier filter that does not allow reflected UV light to pass. It should be noted that this is the only mode of microscopy in which the specimen, subsequent to excitation, gives off its own light (6). The emitted light re-radiates spherically in all directions, regardless of the direction of the exciting light. A schematic diagram of the configuration for fluorescence microscopy is presented in Figure 26.

Fluorescence microscopy has advantages based upon attributes not as readily available in other optical microscopy techniques. The use of fluorochromes has made it possible to identify cells and sub-microscopic cellular components and entities with a high degree of specificity amidst non-fluorescing material. What is more, the fluorescence microscope can reveal the presence of fluorescing material with exquisite sensitivity. An extremely small number of fluorescing molecules (as few as 50 molecules per cubic micron) can be detected (6-8). In a given sample, through the use of multiple staining, different probes will reveal the presence of different target molecules. Although the fluorescence microscope cannot provide spatial resolution below the diffraction limit of the respective objectives, the presence of fluorescing molecules below such limits is made visible.

Techniques of fluorescence microscopy can be applied to organic material, formerly living material, or to living material (with the use of in vitro or in vivo fluorochromes). These techniques can also be applied to inorganic material (especially in the investigation of contaminants on semiconductor wafers). There are also a burgeoning number of studies using fluorescent probes to monitor rapidly changing physiological ion concentrations (calcium, magnesium, etc.) and pH values in living cells (1, 7, 8).

There are specimens that fluoresce when irradiated with shorter wavelength light (primary or autofluorescence). Autofluorescence has been found useful in plant studies, coal petrography, sedimentary rock petrology, and in the semiconductor industry. In the study of animal tissues or pathogens, autofluorescence is often either extremely faint or of such non-specificity as to make autofluorescence of minimal use. Of far greater value for such specimens are the fluorochromes (also called fluorophores) which are excited by irradiating light and whose eventual yield of emitted light is of greater intensity. Such fluorescence is called secondary fluorescence.

Fluorochromes are stains, somewhat similar to the better-known tissue stains, which attach themselves to visible or sub-visible organic matter. These fluorochromes, capable of absorbing and then re-radiating light, are often highly specific in their attachment targeting and have significant yield in absorption-emission ratios. This makes them extremely valuable in biological

application. The growth in the use of fluorescence microscopes is closely linked to the development of hundreds of fluorochromes with known intensity curves of excitation and emission and well-understood biological structure targets (6). When deciding which label to use for fluorescence microscopy, it should be kept in mind that the chosen fluorochrome should have a high likelihood of absorbing the exciting light and should remain attached to the target molecules. The fluorochrome should also be capable of providing a satisfactory yield of emitted fluorescence light. Illustrated in Figure 27 is a photomicrograph of cat brain cells infected with Cryptococcus. The image was made using a combination of fluorescence and DIC microscopy, taking advantage of the features from both contrast enhancing techniques. Infected neurons are heavily stained with the DNA-specific fluorescent dye acridine orange, and the entire image is rendered in a pseudo three-dimensional effect by DIC.

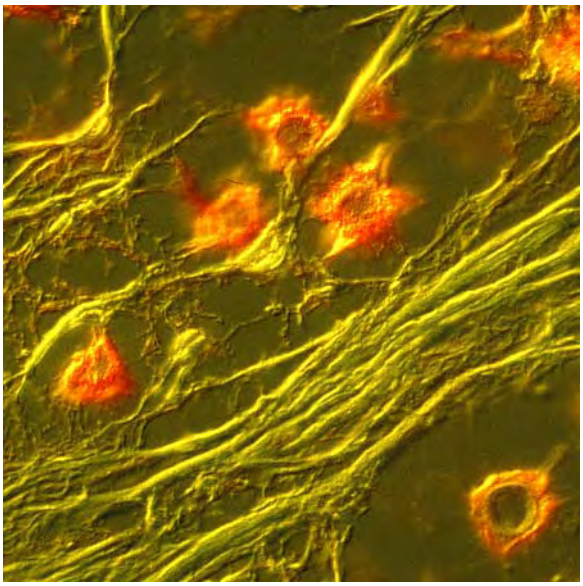

Figure 27. Fluorescence/DIC combination photomicrograph of cat brain tissue infected with Cryptococcus. Infected neurons are heavily stained with the DNA-specific fluorescent dye acridine orange. Note the pseudo three-dimensional effect that occurs when these two techniques are combined. The micrograph was recorded using a 40x objective.

Photomicrography and Digital Imaging

The use of photography to capture images in a microscope dates back to the invention of the photographic process (37). Early photomicrographs were remarkable for their quality, but the techniques were laborious and burdened with long exposures and a difficult process for developing emulsion plates. The primary medium for photomicrography was film until the past decade when improvements in electronic camera and computer technology made digital imaging cheaper and easier to use than conventional photography. This section will address photomicrography both on film and with electronic analog and digital imaging systems.

The quality of a photomicrograph, either digital or recorded on film, is dependent upon the quality of the microscopy. Film is a stern judge of how good the microscopy has been prior to capturing the image. It is essential that the microscope be configured using Köhler illumination, and that the field and condenser diaphragms are adjusted correctly and the condenser height is optimized. When properly adjusted, the microscope will yield images that have even illumination over the entire field of view and display the best compromise of contrast and resolution.

Photographic Films

Films for photography are coated with a light-sensitive emulsion of silver salts and/or dyes. When light is allowed to expose the emulsion, ***active centers*** combine to form a latent image that must be developed by use of photographic chemicals (19, 37-39). This requires exposure of the film in a darkened container to a series of solutions that must be controlled with respect to temperature, development time, and with the appropriate agitation or mixing of the solutions. The developing process must then be halted by means of a ***stop*** solution. Next, the unexposed emulsion material, which consists of silver salts and dyes, is cleared and the film fixed, then washed and dried for use. The development, stop, fixing, and clearing must be done under darkroom conditions or in light-tight developing tanks, and film must be handled in complete darkness. The rigors of temperature, duration, and agitation are usually dependent upon the film being used. For example, the Kodachrome K14 process is far more demanding than the E6 process used for Ektachrome and Fujichrome (19, 37). The emulsion speed determines how much light must be used to expose the film in a given time period. Films are rated according to their ASA or ISO number, which gives an indication of the relative film speed. Larger ISO numbers indicate faster films with an ISO of 25 being one of the slowest films available and ISO 1600 one of the fastest. Because the microscope is a relatively stable platform with good illumination properties, films in the 50-200 ISO range are commonly used for photomicrography.

Film is divided into a number of categories depending upon whether it is intended for black/white or color

photography. Color films are subdivided into two types: color films that yield positive transparencies (colors like those of the image being observed) and color negatives (colors complementary to those in the microscope image, e.g., green for magenta). The color films can be further subdivided into two groups: films designed to receive light of daylight quality and those designed to receive indoor or tungsten light. As a rule, but with some exceptions, transparency or positive films (slides) have the suffix ***chrome***, such as Kodachrome, Ektachrome, Fujichrome, Agfachrome, etc. Color negative films usually end with the suffix ***color***, such as Kodacolor, Ektacolor, Fujicolor, Agfacolor, etc. (37). Each of these film types is offered in a variety of film speeds or ISO ratings. Film packages usually display the ISO of the film and whether the film is intended for daylight or an indoor/tungsten balanced illumination. Modern film magazines have a code (termed the DX number) that allows camera backs to automatically recognize the film speed.

The color temperature of tungsten-halide lamps found in modern microscopes varies between 2900K and 3200K, depending upon the voltage applied to the lamp filament. Film manufacturers offer film balanced for this illumination, and usually indicate on the magazine that the film is intended for indoor or scientific use. Fuji offers a very nice transparency film, Fujichrome 64T, that has a rather slow emulsion speed intended for tungsten illumination, but is designed to perform well with ***push*** film processing. To push a film, it is first underexposed by one or several f-stops, then the development time in the first developer is increased to decrease film density. This technique often will increase the color saturation of the image (19, 37).

Daylight-balanced film, by far the most common film available at retailers at a wide variety of ISOs, can also be used with the microscope, provided an appropriate filter is added to the light path. Manufacturers usually add a daylight conversion light filter to their microscope packages as standard equipment and high-end research microscopes usually have this filter (called a daylight color temperature conversion filter) in a cassette housed in the base of the microscope. Almost any color print or transparency film can be used for microscopy, provided the daylight-balanced filter is in place for those films designed for a 5500K color temperature or removed if the film is balanced for tungsten illumination (3200K).

For many applications, securing the photomicrograph almost immediately is a necessity or a great advantage. Here the Polaroid films are unrivaled. These films for photomicrography are available in three sizes: 35 millimeter Polachrome (color transparency), and Polapan (black/white) in 3¼" x 4¼" film packs and 4" x 5" individual film packets (37, 39). Larger formats are available in color (ID numbers 668/669 or 58/59) or black/white (ID numbers 667, 52, 665, 55, etc.).

The Polaroid large format films produce a paper negative and a paper positive print. After the positive print has been made, the paper negative is peeled away and discarded. This can be accomplished within a matter of a few minutes. The color films, with the exception of the film pack 64T and the large format 64T, are balanced for daylight (5500 Kelvin) color temperature. All microscope manufacturers supply adapters for their photomicrographic cameras that accept large format Polaroid film sizes.

Polaroid black/white films 665 P/N and 55 P/N require special mention. These films produce a paper positive print and a polymer-based negative. If the negative is bathed in an 18% sodium sulfite solution for a few minutes, washed, and hung up to dry, it will produce a permanent negative of high quality and high resolution suitable for use in printing (37, 39).

The Polaroid 35mm films deserve more popular use. They are loaded into the usual 35mm camera back and exposed in the typical manner according to their rated ISO and color temperature requirements. When the film is purchased, the container includes the film cassette and a small box of developer. The film is processed in a tabletop processor that measures approximately 4" x 5" x 9" in size. All processing is carried out in daylight after the processor has been loaded and closed. The finished strip of positive color or positive black/white transparencies is removed and ready for examination and for cutting apart for mounting in frame holders for projection. The actual processing takes only five minutes and produces micrographs of quite accurate color and good resolution.

Recently, Polaroid has marketed a relatively inexpensive photomicrographic camera call the MicroCam. This camera is lightweight and can be inserted into one of the eyetubes or phototube of the microscope. It contains an exposure meter, an eyepiece and an automatically controlled shutter. The camera accepts 339 color film packs or 331 black/white film packs. These films, approximately 3" x 3" in size, are self-developing and do not require peeling apart. Although the films have only about half the resolution of the more common large format Polaroid films, the resulting print is easily obtained and may be quite adequate for many applications.

Digital Photomicrography

Over the past decade, the quality of digital cameras has greatly improved and today, the market has exploded with at least 40 manufacturers offering a wide variety of models to suit every application. The cameras operate by

capturing the image projected directly onto a computer chip without the use of film. In recent years, the number of pixels of information capable of being captured and stored by the best digital cameras is approaching, but still short of, the resolution available with traditional film (37). Digital images offer many opportunities for computer-controlled image manipulation and enhancement as well as the advantage of permanence of digital storage. The highest quality digital cameras can cost many thousands of dollars.

Selection of an electronic camera must be preceded by careful consideration of its proposed use. This includes examination of fixed specimens or live specimens, need for grayscale or true color images, sensitivity to low light levels as in fluorescence, resolution, speed of image acquisition, use in qualitative or quantitative investigations, and the video feed rate into a computer or VCR (1, 2, 9, 37).

The two general types of electronic cameras available for microscopy are the tube cameras (Vidicon family) or CCD (charge coupled device) cameras. Either type can be intensified for increased sensitivity to low light. The SIT (silicon intensified tube) or ISIT is useful for further intensification of tube cameras, while the ICCD is an intensified CCD camera. CCD cameras can also be cooled to increase sensitivity by giving a better signal to noise ratio. These kinds of cameras can be designed to respond to light levels undetectable by the human eye (2, 37).

The criteria for selection of an electronic camera for microscopy include sensitivity of the camera, quantum efficiency, signal to noise ratio, spectral response, dynamic range capability, speed of image acquisition and readout, linearity or response, speed of response in relation to changes in light intensity, geometric accuracy, and ready adaptability to the microscope. A very important criterion for the newer digital CCD cameras is resolution. Current chips range from as few as 64 x 64 pixels up to 2048 x 2048 and above for very specialized applications, but larger arrays are continuously being introduced and, at some not-to-distant time, digital image resolution will rival that of film.

The purchaser must also decide whether or not the camera will operate at video rate (therefore being easily compatible with such accessories as video recorders or video printers). Tube cameras and CCD cameras are available for video rate operation. CCD cameras can also deliver slow acquisition or high-speed acquisition of images. Scientific, rather than commercial grade, CCD cameras are the variety most suitable for research.

CCD cameras are usually of small size. They have low distortion, no lag, and good linearity of response. These cameras are also more rugged and less susceptible to mishandling than tube cameras. Each pixel of the CCD camera serves as a well for charge storage of the incoming photons for subsequent readout. The depth of these wells relates to the quality of the response. Binning of adjacent pixels by joining them together into ***super pixels*** can be employed to speed readout in a slow-scan CCD camera (2, 37).

An emerging technology that shows promise as the possible future of digital imaging is the active pixel sensor (APS) complementary metal oxide semiconductor (CMOS) ***camera on a chip***. Mass production of CMOS devices is very economical and many facilities that are currently engaged in fabrication of microprocessors, memory, and support chips can be easily converted to produce CMOS optical sensors. Although CCD chips were responsible for the rapid development of video camcorders, the technology has remained trapped as a specialized process that requires custom tooling outside the mainstream of integrated circuit fabrication. Also, the CCD devices require a substantial amount of support circuitry and it is not unusual to find five to six circuit boards in a typical video camcorder.

In the center of the APS CMOS integrated circuit is a large array of optical sensors that are individual photodiode elements covered with dyed filters and arranged in a periodic matrix. A photomicrograph of the entire die of a CMOS chip is illustrated in Figure 28. High magnification views of a single “pixel” element (Figure 28) reveal a group of four photodiodes containing filters based on the primary colors red, green, and blue. Each photodiode is masked by either a red, green, or blue filter in low-end chips, but higher resolution APS CMOS devices often use a teal (blue-green) filter in place of one of the green filters. Together, the four elements illustrated in Figure 28 comprise the light-sensitive portion of the pixel. Two green filter masks are used because visible light has an average wavelength of 550 nanometers, which lies in the green color region. Each pixel element is controlled by a set of three transistors and an amplifier that work together to collect and organize distribution of optical information. The array is interconnected much like memory addresses and data busses on a DRAM chip so that the charge generated by photons striking each individual pixel can be accessed randomly to provide selective sampling of the CMOS sensor.

The individual amplifiers associated with each pixel help reduce noise and distortion levels, but they also induce an artifact known as ***fixed pattern*** noise that arises from small differences in the behavior of individual pixel amplifiers. This is manifested by reproducible patterns of ***speckle*** behavior in the image generated by CMOS active pixel sensor devices. A great deal of research effort has been invested in solving this problem, and the residual

level of noise has been dramatically reduced in CMOS sensors. Another feature of CMOS active pixel sensors is the lack of column streaking due to pixel bloom when shift registers overflow. This problem is serious with the CCDs found in most video camcorders. Another phenomenon, known as ***smear***, which is caused by charge transfer in CCD chips under illumination, is also absent in CMOS active pixel sensor devices.

Assisting the CMOS device is a coprocessor that is matched to the APS CMOS to optimize the handling of image data. Incorporated into the co-processor is a proprietary digital video processor engine that is capable of performing automatic exposure and gain control, white balance, color matrixing, gamma correction, and aperture control. The CMOS sensor and co-processor perform the key functions of image capture, digital video image processing, video compression, and interfacing to the main computer microprocessor.

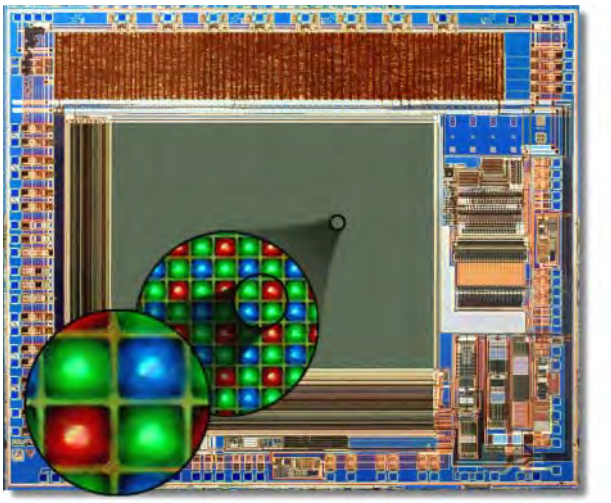

Figure 28. CMOS active pixel sensor used in new camera on a chip technology that is rapidly emerging. The photomicrograph captures the entire integrated circuit surface showing the photodiode array and support circuitry. The insets illustrate progressively higher magnification of a set of pixel elements and a single pixel element composed of four dyed photodiodes.

The primary concerns with CMOS technology are the rather low quality, noisy images that are obtained with respect to similar CCD devices. These are due primarily to process variations that produce a slightly different response in each pixel, which appears in the image as ***snow***. Another problem is that the total amount of chip area that is sensitive to light is less in CMOS devices, thus making them less sensitive to light. These problems will be overcome as process technology advances and it is very possible that CMOS devices will eclipse the CCD as the technology of choice in the very near future.

If you have prized transparencies and negatives collected over a long period of time, many of the better camera stores can take these and put them onto a Kodak Photo CD, which is the same size as an audio CD. The Photo CD can hold up to 100 images that are stored at several levels of resolution. Digital images recorded onto the Photo CD can be displayed on a good monitor by means of a Photo CD player. If you have a computer and a program such as Adobe Photoshop, Corel Photo Paint, or Picture Publisher and a CD drive, you can open the images on your computer screen, manipulate and/or enhance the images and then print the images using a digital printer—all without a darkroom! Kodak, Fuji, Olympus, Tektronix, and Sony market dye sublimation printers that can produce prints virtually indistinguishable from those printed with the usual color enlarger in a darkroom.

35mm negative and positive transparency scanners and flatbed scanners, available from such manufacturers as Nikon, Olympus, Polaroid, Kodak, Agfa, Microtek, Hewlett-Packard, etc., can directly scan transparencies or negatives or prints into your computer for storage or manipulation. Images can be stored on the hard drive of the computer or stored on floppy disks in JPEG or TIFF files. Because floppy disks have storage limited to 1.44 megabytes, many micrographers are now storing images on Zip disks or magneto-optical drive disks; these can hold many images to sizes of 10 megabytes or more. Another popular storage medium, quickly gaining widespread popularity, is the recordable CD-ROM. Magneto-optical disks or CD-ROMs can be given to commercial printers and then printed with stunning color accuracy and resolution.

A photomicrograph is also a photograph. As such, it should not only reveal information about the specimen, it should also do so with attention to the aesthetics of the overall image. Always try to compose photomicrographs with a sense of the balance of the color elements across the image frame. Use diagonals for greater visual impact, and scan the frame for unwanted debris or other artifacts. Select a magnification that will readily reveal the details sought. Remember to keep detailed records to avoid repeating mistakes and to help with review of images that are several years old. Excellent photomicrographs are within the capability of most microscopists, so pay attention to the details and the overall picture will assemble itself.

Acknowledgements

The authors would like to thank the Molecular Expressions (**http://microscopy.fsu.edu**) web design and graphics team for the illustrations in the paper. We would also like to thank George Steares, of Olympus America, Inc., for providing advice and microscopy equipment used in illustration of this manuscript. Assistance from Chris Brandmaier, of Nikon USA, Inc., in providing equipment for reflected light differential interference contrast microscopy is also appreciated. Funding for this research was provided, in part, by the National High Magnetic Field Laboratory (NHMFL), the State of Florida, and the National Science Foundation through cooperative grant No. DMR9016241. We would also like to thank James Ferner, Samuel Spiegel, and Jack Crow for support of the Optical Microscopy program at the NHMFL.

Bibliography

1. B. Herman and J. J. Lemasters (eds.), ***Optical Microscopy: Emerging Methods and Applications***. Academic Press, New York, 1993, 441 pp.
2. S. Inoué and K. R. Spring, ***Video Microscopy: The Fundamentals***. 2e, Plenum Press, New York, 1997, 737 pp.
3. S. Bradbury and B. Bracegirdle, ***Introduction to Light Microscopy***. BIOS Scientific Publishers Ltd., Oxford, UK, 1998, 123 pp.
4. E. M. Slayter and H. S. Slayter, ***Light and Electron Microscopy***. Cambridge University Press, Cambridge, UK, 1992, 312 pp.
5. M. Pluta, ***Advanced Light Microscopy*** (3 vols.). Elsevier, New York, 1989; vol. 1, 464 pp.; vol. 2, 494 pp.; vol. 3, 702 pp.
6. M. Abramowitz, ***Fluorescence Microscopy: The Essentials***. Olympus America, Inc., New York, 1993, 43 pp.
7. B. Herman, ***Fluorescence Microscopy***. 2e, BIOS Scientific Publishers Ltd., Oxford, UK, 1998, 170 pp.
8. F. W. D. Rost, ***Fluorescence Microscopy*** (2 volumes). Cambridge University Press, New York, 1992; vol. 1, 256 pp.; vol.2, 456 pp.
9. G. Sluder and D. E. Wolf (eds.), ***Methods in Cell Biology, Vol. 56: Video Microscopy***. Academic Press, New York, 1998, 327 pp.
10. C. J. R. Sheppard and D. M. Shotton, ***Confocal Laser Scanning Microscopy***. BIOS Scientific Publishers Ltd., Oxford, UK, 1997, 106 pp.
11. S. W. Paddock (ed.), ***Methods in Molecular Biology, Vol. 122: Confocal Microscopy, Methods and Protocols***. Humana Press, Totowa, N. J., 1999, 446 pp.
12. J. B. Pawley (ed.), ***Handbook of Biological Confocal Microscopy***. 2e, Plenum Press, New York, 1995, 632 pp.
13. S. Bradbury, ***The Evolution of the Microscope***. Pergamon Press, New York, 1967, 357 pp.
14. ***Anticipating the Future***. Zeiss Group Microscopes Business Unit, Jena, Germany, 1996, 34 pp.
15. G. Nomarski, ***J. Phys. Radium 16***: 9S-11S (1955).
16. R. Hoffman, ***J. Microscopy 110***: 205-222 (1977).
17. S. Inoué and R. Oldenbourg, in ***Handbook of Optics, Vol. II***. 2e, M. Bass, ed., McGraw-Hill, New York, 1995, pp. 17.1-17.52.
18. M. Abramowitz, ***Contrast Methods in Microscopy: Transmitted Light***. Olympus America, Inc., Melville, New York, 1987, 31 pp.
19. J. G. Delly, ***Photography Through The Microscope***. 9e, Eastman Kodak Co., Rochester, New York, 1988, 104 pp.
20. H. G. Kapitza, ***Microscopy From The Very Beginning***. Carl Zeiss, Oberkochen, Germany, 1994, 40 pp.
21. H. W. Zieler, ***The Optical Performance of the Light Microscope*** (2 vols.). Microscope Publications, Ltd., Chicago, 1972; vol. 1, 102 pp.; vol. 2, 110 pp.
22. J. James and H. J. Tanke, ***Biomedical Light Microscopy***. Kluwer Academic Publishers, Boston, 1991, 192 pp.
23. M. Abramowitz, ***Optics: A Primer***. Olympus America, Inc., Melville, New York, 1984, 22 pp.
24. M. Abramowitz, ***Microscope: Basics and Beyond***. Olympus America, Inc., Melville, New York, 1987, 26 pp.
25. M. Abramowitz, ***Reflected Light Microscopy: An Overview***. Olympus America, Inc., Melville, New York, 1990, 23 pp.
26. R. McLaughlin, ***Special Methods in Light Microscopy***. Microscope Publications, Ltd., Chicago, 1977, 337 pp.
27. A. Tomer, ***Structure of Metals Through Optical Microscopy***. ASM International, Boulder, CO, 1990, 265 pp.
28. G. H. Needham, ***The Practical Use of the Microscope***. Charles C. Thomas, Springfield, IL, 1958, 493 pp.
29. C. P. Shillaber, ***Photomicrography in Theory and Practice***. John Wiley & Sons, Inc., New York, 1944, 773 pp.
30. F. Zernike, ***Physica 9***: 686-693 (1942).
31. F. Zernike, ***Physica 9***: 974-986 (1942).
32. E. A. Wood, ***Crystals and Light: An Introduction to Optical Crystallography***. 2e, Dover Publications, Inc., New York, 1977, 156 pp.
33. R. E. Stoiber and S. A. Morse, ***Crystal Identification with the Polarizing Microscope***. Chapman & Hall, New York, 1994, 336 pp.
34. P. C. Robinson and S. Bradbury, ***Qualitative Polarized-Light Microscopy***. Oxford Science Publications, New York, 1992, 121 pp.
35. A. F. Hallimond, ***The Polarizing Microscope***. 3e, Vickers Instruments, York, UK, 1970, 302 pp.
36. S. Bradbury and P. J. Evennett, ***Contrast Techniques in Light Microscopy***. BIOS Scientific Publishers Ltd., Oxford, UK, 1996, 118 pp.
37. M. Abramowitz, ***Photomicrography: A Practical Guide***. Olympus America, Inc., Melville, New York, 1998, 73 pp.
38. R. P. Loveland, ***Photomicrography: A Comprehensive Treatise*** (2 vols.). John Wiley & Sons, New York, 1970; vol. 1, 526 pp.; vol. 2, 509 pp.
39. ***Photomicrography: Instant Photography Through the Microscope***. Polaroid Corporation, Cambridge, MA, 1995, 72 pp.

Optical Microscopy

Davidson and Abramowitz

The Microscopy

Authors:
Mortimer Abramowitz,
Michael W. Davidson
and al.

http://microscopy.fsu.edu/primer

Contents

Part I

Light Microscopy

Chapter 1

Introduction

Microscopes are instruments designed to produce magnified visual or photographic images of small objects. The microscope must accomplish three tasks: produce a magnified image of the specimen, separate the details in the image, and render the details visible to the human eye or camera. This group of instruments includes not only multiple-lens designs with objectives and condensers, but also very simple single lens devices that are often hand-held, such as a magnifying glass.

The microscope illustrated in Figure 1.1 is a simple compound microscope invented by British microscopist Robert Hooke sometime in the 1660s. This beautifully crafted microscope has an objective lens near the specimen and is focused by turning the body of the microscope to move the objective closer to or farther from the specimen. An eyepiece lens is inserted at the top of the microscope and, in many cases, there is an internal "field lens" within the barrel to increase the size of the viewfield. The microscope in Figure 1.1 is illuminated through the oil lamp and water-filled spherical reservoir, also illustrated in Figure 1.1. Light from the lamp is diffused when it passes through the reservoir and is then focused onto the specimen with a lens attached to the reservoir. This early microscope suffered from chromatic (and spherical) aberration, and all images viewed in white light contained "halos" that were either blue or red in color.

Since so many microscope users rely upon direct observation, it is important to understand the relationship between the microscope and the eye. Our eyes are capable of distinguishing color in the visible portion of the spectrum: from violet to blue to green to yellow to orange to red; the eye cannot perceive ultraviolet or infrared rays. The eye also is able to sense differences in brightness or intensity ranging from black to white and all the gray shades in between. Thus, for an image to be seen by the eye, the image must be presented to the eye in colors of the visible spectrum and/or varying degrees of light intensity. The eye receptors of the retina used for sensing color are the cone cells; the cells for distinguishing levels of intensity, not in color, are the rod cells. These cells are located on the retina at the back of the inside of the eye. The front of the eye (see Figure 1.2), including the iris, the curved cornea, and the lens are respectively the mechanisms for admitting light and focusing it on the retina.

For an image to be seen clearly, it must spread on the retina at a sufficient visual angle. Unless the light falls on non-adjacent rows of retinal cells (a function of magnification and the spreading of the image), we are unable to distinguish closely-lying details as being separate (resolved). Further, there must be sufficient contrast between adjacent details and/or the background to render the magnified, resolved image visible.

FIGURE 1.1: Hooke Microscope, circa 1670

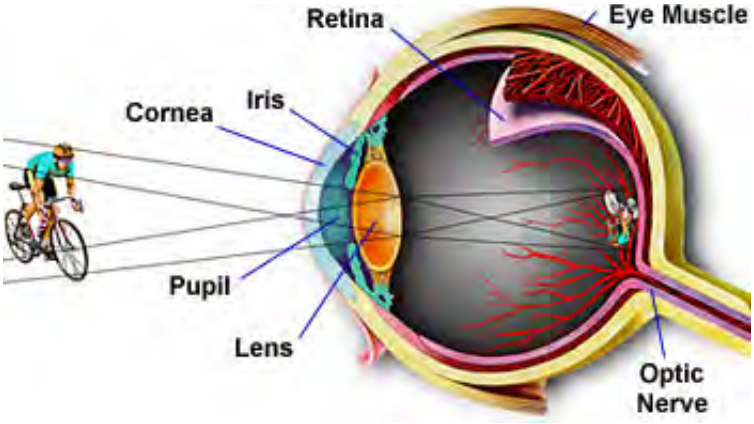

FIGURE 1.2: The Human Eye

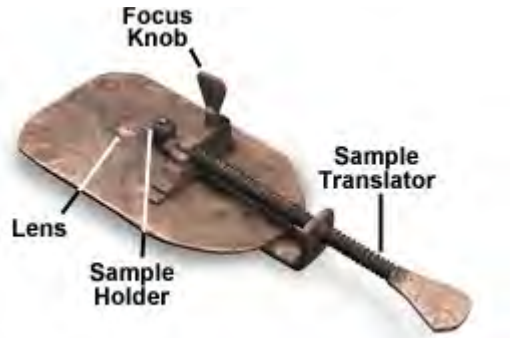

FIGURE 1.3: Von Leeuwenhoek Microscope, circa late 1600s

Because of the limited ability of the eye's lens to change its shape, objects brought very close to the eye cannot have their images brought to focus on the retina. The accepted conventional viewing distance is 10 inches or 25 centimeters.

More than five hundred years ago, simple glass magnifiers were developed. These were convex lenses (thicker in the center than the periphery). The specimen or object could then be focused by use of the magnifier placed between the object and the eye. These "simple microscopes" could spread the image on the retina by magnification through increasing the visual angle on the retina.

The "simple microscope" or magnifying glass reached its highest state of perfection, in the 1600's, in the work of Anton von Leeuwenhoek who was able to see single-celled animals (which he called "animalcules") and even some larger bacteria with a simple microscope similar to the one illustrated in Figure 1.3. The image produced by such a magnifier, held close to the observer's eye, appears as if it were on the same side of the lens as the object itself. Such an image, seen as if it were ten inches from the eye, is known as a virtual image and cannot be captured on film.

Around the beginning of the 1600's, through work attributed to the Janssen brothers (see the microscope in Figure 1.4) in the Netherlands and Galileo in Italy, the compound microscope was developed. In its simplest form, it consisted of two convex lenses aligned in series: an object glass (objective) closer to the object or specimen; and an eyepiece (ocular) closer to the observer's eye (with means of adjusting the position of the specimen and the microscope lenses). The compound microscope achieves a two-stage magnification. The objective projects a magnified image into the body tube of the microscope and the eyepiece further magnifies the image projected by the objective.

Compound microscopes developed during the 17th and 18th centuries were hampered by optical aberration (both chromatic and spherical), a flaw that is worsened by the use of multiple lenses. These microscopes were actually inferior to single lens microscopes of the period because of these artifacts. The images they produced were often blurred and had the colorful halos associated with chromatic aberrations that not only degrade image quality, but also hamper resolution. In the mid 1700's lens makers discovered that by combining two lenses made of glass with different color dispersions, much of the chromatic aberration could be reduced or eliminated. This discovery was first utilized in telescopes, which have much larger lenses than microscopes. It wasn't until the start of the 1800's that chromatically corrected lenses became commonplace in compound microscopes.

The eighteenth and nineteenth centuries witnessed a great improvement in the mechanical and optical quality of compound microscopes. Advances in machine tools allowed more

FIGURE 1.4: Janssen Compound Microscope, circa early 1600

sophisticated parts to be fabricated and, by the mid 1800's, brass was the alloy of choice for the production of high-quality microscopes. A number of British and German microscope manufacturers flourished during this time period. Their microscopes varied widely in design and production quality, but the overall principles defining their optical properties remained relatively constant. The microscope illustrated in Figure 1.5 was manufactured by Hugh Powell and Peter Lealand about 1850. The tripod base provided a sturdy support for the microscope, which many people consider the most advanced of its period.

By the end of the 19th century, there was a high degree of competition among microscope manufacturers and the development and production costs of microscopes became an important factor. Brass, the material of choice for microscope manufacturers, is very expensive and it was a lengthy task to machine, polish, and lacquer microscope bodies and other parts machined from this metal. To cut expenses, microscope manufacturers first started to paint the exterior portion of the microscope body and stand, as well as the stage and other non-moving parts.

During the first quarter of the 20th century, many microscope manufacturers had begun substituting cast iron for brass in microscope frames and stages. Iron was much cheaper and could be not be distinguished from brass when painted black. They also started to electroplate many of the critical brass components such as knobs, objective barrels, nosepieces, eyepieces, and mechanical stage assemblies (illustrated in Figure 1.6). These early 20th century microscopes still subscribed to a common design motif. They were monocular with a substage mirror that was used with an external lamp to illuminate the specimen. A typical microscope of the period is the Zeiss Laboratory microscope pictured in Figure 1.6. This type of microscope is very functional and many are still in use today.

Modern microscopes far exceed the design specifications of those made prior to the mid 1900's. Glass formulations are vastly improved allowing greater correction for optical aberration than ever before, and synthetic anti-glare lens coatings are now very advanced. Integrated circuit technology has allowed manufacturers to produce "smart" microscopes that incorporate microprocessors into the microscope stand. Photomicrography in the late 20th century is easier than ever before with auxiliary attachments that monitor light intensity, calculate exposure based on film speed, and automatically perform complicated tasks such as bracketing, multiple exposure, and time-lapse photography.

The microscope illustrated in Figure 1.7 is an Olympus Provis AX70 research microscope. This microscope represents the latest state-of-the-art design that incorporates mul-

FIGURE 1.5: Powell and Lealand No 1, circa 1850

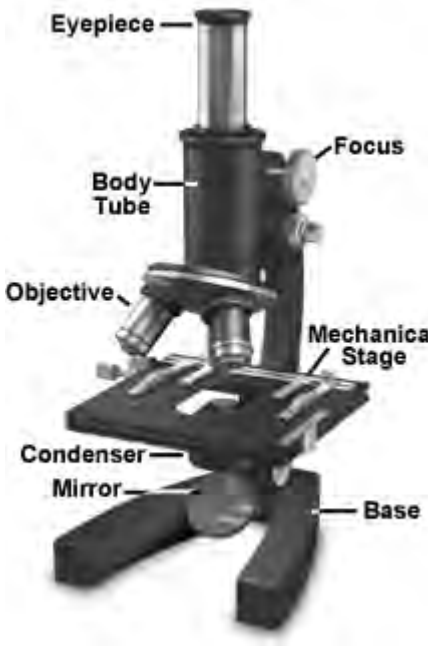

FIGURE 1.6: Zeiss Laboratory Microscope, circa 1930s

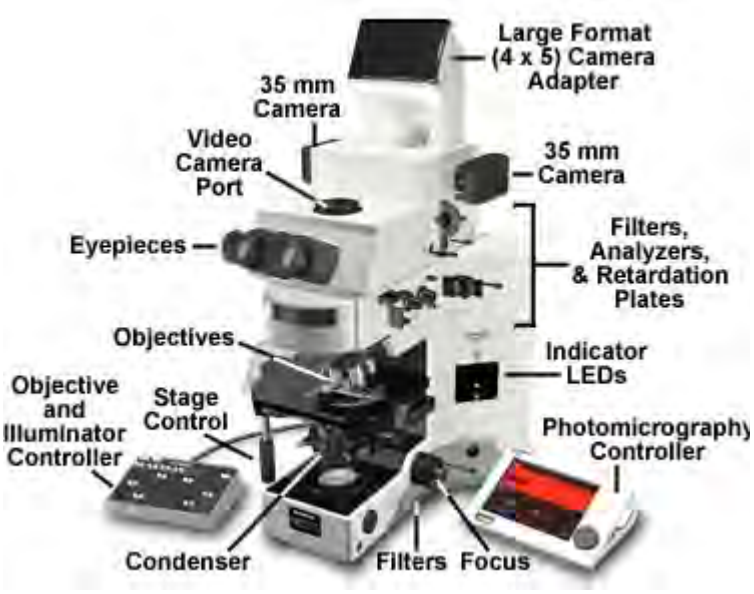

FIGURE 1.7: Olympus Provis AX 70, circa 1998

tiple illuminators (episcopic and diascopic), analyzers and polarizers, DIC prisms, fluorescence attachments, and phase contrast capabilities. The photomicrography system is the ultimate in sophistication and performance featuring spot measurement, automatic exposure control, and zoom magnification for flexible, easy framing. The Y-shaped frame is designed to be user-friendly by offering the maximum in operator comfort and ease of use.

The previous discussion addressed the basic concept of what a microscope is and touched upon an abbreviated history beginning in the 17th century and progressing through modern times. There are a number of additional topics that are of paramount importance towards gaining a complete understanding of microscopes and microscopy. These topics will be discussed in subsequent sections of the primer.

Practically everyone has, at one time or another, viewed the world through an optical microscope. For most people, this experience occurs during biology training in high school or college, although some scientific entrepreneurs have purchased their own microscopes either individually or as part of a science kit. Photography through the microscope, or more commonly, photomicrography, has long been a useful tool to scientists. For many years, the biological and medical sciences have relied heavily on microscopy to solve problems relating to the overall morphological features of specimens as well as a quantitative tool for recording specific optical features and data. In this respect, the optical microscope has proven useful in countless investigations into the mysteries of life.

More recently, microscopy has enjoyed an explosive growth as a tool in the physical and materials sciences as well as the semiconductor industry, due to the need to observe surface features of new high-tech materials and integrated circuits. Microscopy is also becoming an important tool for forensic scientists who are constantly examining hairs, fibers, clothing, blood stains, bullets, and other items associated with crimes. Modern advances in fluorochrome stains and monoclonal antibody techniques have heralded an explosive growth in the use of fluorescence microscopy in both biomedical analysis and cell biology.

The basic differences between biomedical and materials microscopy involves how the microscope projects light onto the sample. In classical biological microscopy, very thin specimens are prepared and the light is passed or transmitted through the sample, focused with the objective and then passed into the eyepieces of the microscope. For observing the surface of integrated circuits (that comprise the internal workings of modern computers) light passed through the objective and is then reflected from the surface of the sample and into the microscope objective. In scientific nomenclature, transmitted and reflected light microscopy are known as diascopic and episcopic illuminated microscopy, respectively. The photomicrographs in our photo galleries are derived from both transmitted and reflected optical microscopic scientific investigations.

One of the most serious problems in microscopy is the poor contrast produced when light is passed through very thin specimens or reflected from surfaces with a high degree of reflectivity. To circumvent this lack of contrast, various optical "tricks" have been perfected by scientists to increase contrast and to provide color variations in specimens. The assortment of techniques in the microscopists bag include: polarized light, phase contrast imaging, differential interference contrast, fluorescence illumination, darkfield illumination, Rheinberg illumination, Hoffman modulation contrast, and the use of various gelatin optical filters. A thorough discussion of these techniques is provided in the Specialized Microscopy Techniques section of this primer.

Chapter 2

The Concept of Magnification

A simple microscope or magnifying glass (lens) produces an image of the object upon which the microscope or magnifying glass is focused. Simple magnifier lenses are bi-convex, meaning they are thicker at the center than at the periphery as illustrated with the magnifier in Figure 2.1. The image is perceived by the eye as if it were at a distance of 10 inches or 25 centimeters (the **reference**, or **traditional** or **conventional** viewing distance).

Since the image appears to be on the same side of the lens as the object, it cannot be projected onto a screen. Such images are termed **virtual images** and they appear upright, not inverted. Figure 2.1 presents an illustration of how a simple magnifying lens operates. The object (in this case the subject is a rose) is being viewed with a simple bi-convex lens. Light reflected from the rose enters the lens in straight lines as illustrated in Figure 2.1. This light is refracted and focused by the lens to produce a virtual image on the retina. The image of the rose is magnified because we perceive the actual size of the object (the rose) to be at infinity because our eyes trace the light rays back in straight lines to the virtual image (Figure 2.1). This is discussed in greater detail below.

When you look into a microscope, you are not looking at the specimen, you are looking at the **image** of the specimen. The image appears to be "floating" in space about 10 millimeters below the top of the observation tube (at the level of the fixed diaphragm of the eyepiece) where the eyepiece is inserted. The image you observe is not tangible; it cannot be grasped. It is a "map" or representation of the specimen in various colors and/or shades of gray from black to white. The expectation is that the image will be an accurate representation of the specimen; accurate as to detail, shape and color/intensity. The implications are that it may well be possible (and is) to produce highly accurate images. Conversely, it may be (and often is) all too easy to degrade an image through improper technique or poor equipment.

To understand how the microscope's lenses function, you should recall some of the basic principles of lens action in image formation. We will now review several different imaging scenarios using a simple bi-convex lens:

- Light from an object that is very far away from the front of a convex lens (we'll assume our "object" is the giraffe illustrated in Figure 2.2) will be brought to a focus at a fixed point behind the lens. This is known as the **focal point** of the lens. We are all familiar with the idea of a "burning glass" which can focus the essentially parallel rays from the sun to burn a hole in piece of paper. The vertical plane in which the focal point lies is the **focal plane**.

  The distance from the center of the convex lens to the focal plane is know as the

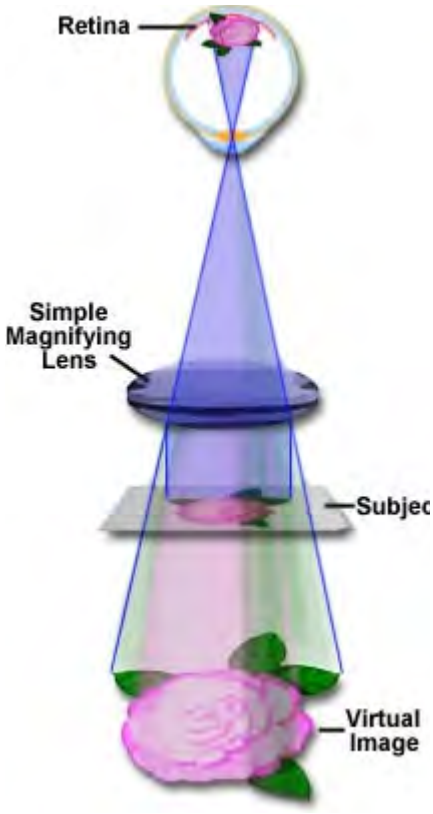

FIGURE 2.1: Magnification with a simple thin lens

FIGURE 2.2: The object is very far away from the lens

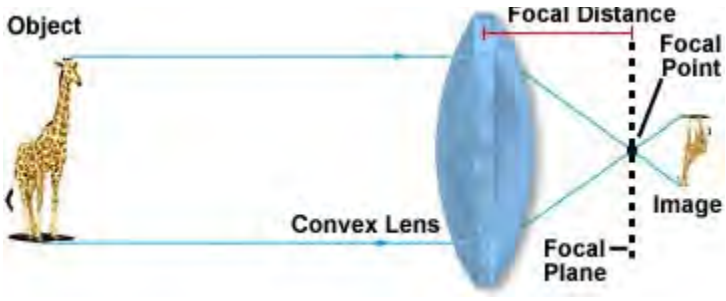

FIGURE 2.3: Inverted real image: the object is brought to more than twice the focal distance, the image is smaller than the object

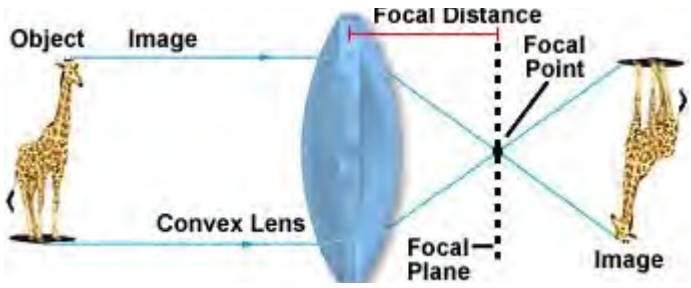

FIGURE 2.4: Inverted real image: the object is brought to twice the focal distance, the image is the same size as the object

focal distance. (For an idealized symmetrical thin convex lens, this distance is the same in front of or behind the lens.) The image of our giraffe now appears at the focal plane (as illustrated in Figure 2.2). The image is smaller than the object (the giraffe); it is inverted and is a real image capable of being captured on film. This is the case for the camera used for ordinary scenic photography.

- The object is now moved closer to the front of the lens but is still more than two focal lengths in front of the lens (this scenario is addressed in Figure 2.3). Now, the image is found further behind the lens. It is larger than the one described above, but is still smaller than the object. The image is inverted, and is a real image. This is the case for ordinary portrait photography.

- The object is brought to twice the focal distance in front of the lens. The image is now two focal lengths behind the lens as illustrated in Figure 2.4. It is the same size as the object; it is real and inverted.

- The object is now situated between one and two focal lengths in front of the lens (shown in Figure 2.5). Now the image is still further away from the back of the lens. This time, the image is magnified and is larger than the object; it is still inverted and it is real. This case describes the functioning of all finite tube length objectives used in microscopy. Such finite tube length objectives project a real, inverted, and magnified image into the body tube of the microscope. This image comes into focus at the plane of the fixed diaphragm in the eyepiece. The distance from the back focal plane of the objective (not necessarily its back lens) to the plane of the fixed diaphragm of the eyepiece is known as the **optical tube length** of the objective.

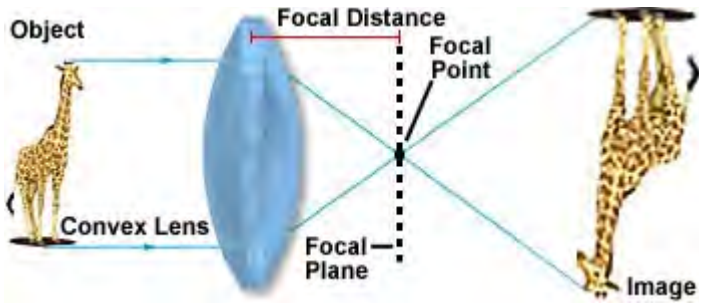

FIGURE 2.5: Inverted real image: the object is situated between one and two focal lengths in front of the lens, the image is bigger than the object

- In the last case, the object is situated at the front focal plane of the convex lens. In this case, the rays of light emerge from the lens in parallel. The image is located on the same side of the lens as the object, and it appears upright (see Figure 2.1). The image is a virtual image and appears as if it were 10 inches from the eye, similar to the functioning of a simple magnifying glass; the magnification factor depends on the curvature of the lens.

The last case listed above describes the functioning of the observation eyepiece of the microscope. The "object" examined by the eyepiece is the magnified, inverted, real image projected by the objective. When the human eye is placed above the eyepiece, the lens and cornea of the eye "look" at this secondarily magnified virtual image and see this virtual image as if it were 10 inches from the eye, near the base of the microscope.

This case also describes the functioning of the now widely used infinity-corrected objectives. For such objectives, the object or specimen is positioned at exactly the front focal plane of the objective. Light from such a lens emerges in parallel rays from every azimuth. In order to bring such rays to focus, the microscope body or the binocular observation head must incorporate a **tube lens** in the light path, between the objective and the eyepiece, designed to bring the image formed by the objective to focus at the plane of the fixed diaphragm of the eyepiece. The magnification of an infinity-corrected objective equals the focal length of the tube lens (for Olympus equipment this is 180mm, Nikon uses a focal length of 200mm; other manufacturers use other focal lengths) divided by the focal length of the objective lens in use. For example, a 10X infinity-corrected objective, in the Olympus series, would have a focal length of 18mm (180mm/10).

An easy way to understand the microscope is by means of a comparison with a slide projector, a device familiar to most of us. Visualize a slide projector turned on its end with the lamp housing resting on a table. The light from the bulb passes through a condensing lens, and then through the transparency, and then through the projection lens onto a screen placed at right angles to the beam of light at a given distance from the projection lens. The real image on this screen emerges inverted (upside down and reversed) and magnified. If we were to take away the screen and instead use a magnifying glass to examine the real image in space, we could further enlarge the image, thus producing another or second-stage magnification.

Now we will describe how a microscope works in somewhat more detail. The first lens of a microscope is the one closest to the object being examined and, for this reason, is called the objective. Light from either an external or internal (within the microscope body) source

is first passed through the substage condenser, which forms a well-defined light cone that is concentrated onto the object (specimen). Light passes through the specimen and into the objective (similar to the projection lens of the projector described above), which then projects a real, inverted, and magnified image of the specimen to a fixed plane within the microscope that is termed the **intermediate** image plane (illustrated in Figure 2.6). The objective has several major functions:

- The objective must gather the light coming from each of the various parts or points of the specimen.
- The objective must have the capacity to reconstitute the light coming from the various points of the specimen into the various corresponding points in the image (Sometimes called anti-points).
- The objective must be constructed so that it will be focused close enough to the specimen so that it will project a magnified, real image up into the body tube.

The intermediate image plane is usually located about 10 millimeters below the top of the microscope body tube at a specific location within the fixed internal diaphragm of the eyepiece. The distance between the back focal plane of the objective and the intermediate image is termed the optical tube length. Note that this value is different from the mechanical tube length of a microscope, which is the distance between the nosepiece (where the objective is mounted) to the top edge of the observation tubes where the eyepieces (oculars) are inserted.

The eyepiece or ocular, which fits into the body tube at the upper end, is the farthest optical component from the specimen. In modern microscopes, the eyepiece is held into place by a shoulder on the top of the microscope observation tube, which keeps it from falling into the tube. The placement of the eyepiece is such that its eye (upper) lens further magnifies the real image projected by the objective. The eye of the observer sees this secondarily magnified image as if it were at a distance of 10 inches (25 centimeters) from the eye; hence this virtual image appears as if it were near the base of the microscope. The distance from the top of the microscope observation tube to the shoulder of the objective (where it fits into the nosepiece) is usually 160 mm in a finite tube length system. This is known as the mechanical tube length as discussed above. The eyepiece has several major functions:

The eyepiece serves to further magnify the real image projected by the objective.

In visual observation, the eyepiece produces a secondarily enlarged virtual image.

In photomicrography, it produces a secondarily enlarged real image projected by the objective. This augmented real image can be projected on the photographic film in a camera or upon a screen held above the eyepiece.

The eyepiece can be fitted with scales, markers or crosshairs (often referred to as graticules or reticles) in such a way that the image of these inserts can be superimposed on the image of the specimen.

The factor that determines the amount of image magnification is the objective magnifying power, which is predetermined during construction of the objective optical elements. Objectives typically have magnifying powers that range from 1:1 (1X) to 100:1 (100X), with the most common powers being 4X (or 5X), 10X, 20X, 40X (or 50X), and 100X. An important feature of microscope objectives is their very short focal lengths that allow increased magnification at a given distance when compared to an ordinary hand lens (illustrated in

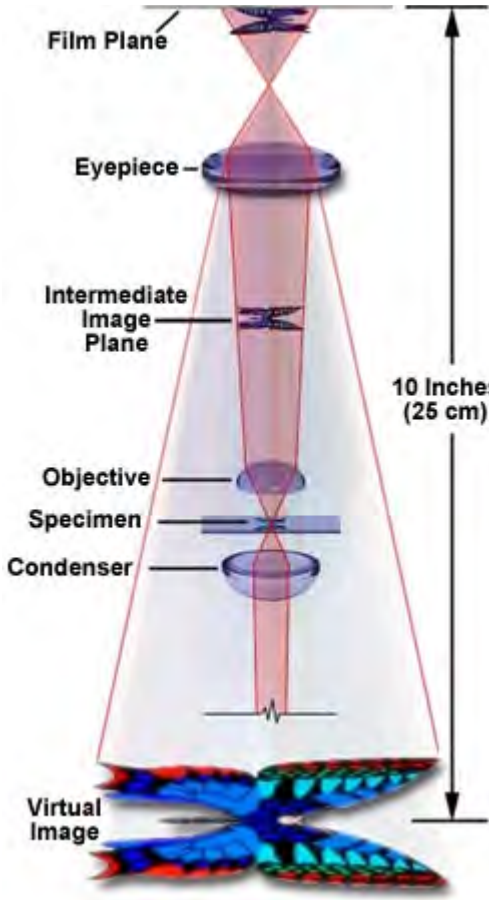

FIGURE 2.6: Image formation in microscopy

Figure 2.1). The primary reason that microscopes are so efficient at magnification is the two-stage enlargement that is achieved over such a short optical path, due to the short focal lengths of the optical components.

Eyepieces, like objectives, are classified in terms of their ability to magnify the intermediate image. Their magnification factors vary between 5X and 30X with the most commonly used eyepieces having a value of 10X–15X. Total visual magnification of the microscope is derived by multiplying the magnification values of the objective and the eyepiece. For instance, using a 5X objective with a 10X eyepiece yields a total visual magnification of 50X and likewise, at the top end of the scale, using a 100X objective with a 30X eyepiece gives a visual magnification of 3000X.

Total magnification is also dependent upon the tube length of the microscope. Most standard fixed tube length microscopes have a tube length of 160, 170, 200, or 210 millimeters with 160 millimeters being the most common for transmitted light biomedical microscopes. Many industrial microscopes, designed for use in the semiconductor industry, have a tube length of 210 millimeters. The objectives and eyepieces of these microscopes have optical properties designed for a specific tube length, and using an objective or eyepiece in a microscope of different tube length will lead to changes in the magnification factor (and may also lead to an increase in optical aberration lens errors). Infinity-corrected microscopes also have eyepieces and objectives that are optically-tuned to the design of the microscope, and these should not be interchanged between microscopes with different infinity tube lengths.

Modern research microscopes are very complex and often have both episcopic and diascopic illuminators built into the microscope housing. Design constrictions in these microscopes preclude limiting the tube length to the physical dimension of 160 millimeters resulting the need to compensate for the added physical size of the microscope body and mechanical tube. This is done by the addition of a set of parallelizing lenses to shorten the apparent mechanical tube length of the microscope. These additional lenses will sometimes introduce an additional magnification factor (usually around 1.25–1.5X) that must be taken into account when calculating both the visual and photomicrographic magnification. This additional magnification factor is referred to as a tube factor in the user manuals provided by most microscope manufacturers. Thus, if a 5X objective is being used with a 15X set of eyepieces, then the total visual magnification becomes 93.75X (using a 1.25X tube factor) or 112.5X (using a 1.5X tube factor).

In addition to the parallelizing lenses used in some microscopes, manufacturers may also provide additional lenses (sometimes called magnification changers) that can be rotated into the optical pathway to increase the magnification factor. This is often done to provide ease in specimen framing for photomicrography. These lenses usually have very small magnification factors ranging from 1.25X up to 2.5X, but use of these lenses may lead to empty magnification, a situation where the image is enlarged, but no additional detail is resolved. This type of error is illustrated in Figure 2.7 with photomicrographs of liquid crystalline DNA. The photomicrograph in Figure 2.7(a) was taken with a 20X plan achromat objective under polarized light with a numerical aperture of 0.40 and photographically enlarged by a factor of 10X. Detail is crisp and focus is sharp in this photomicrograph that reveals many structural details about this hexagonally-packed liquid crystalline polymer. Conversely, the photomicrograph on the right (Figure 2.7(b)) was taken with a 4X plan achromat objective, having a numerical aperture of 0.10 and photographically enlarged by a factor of 50X. This photomicrograph lacks the detail and clarity present in Figure 2.7(a)

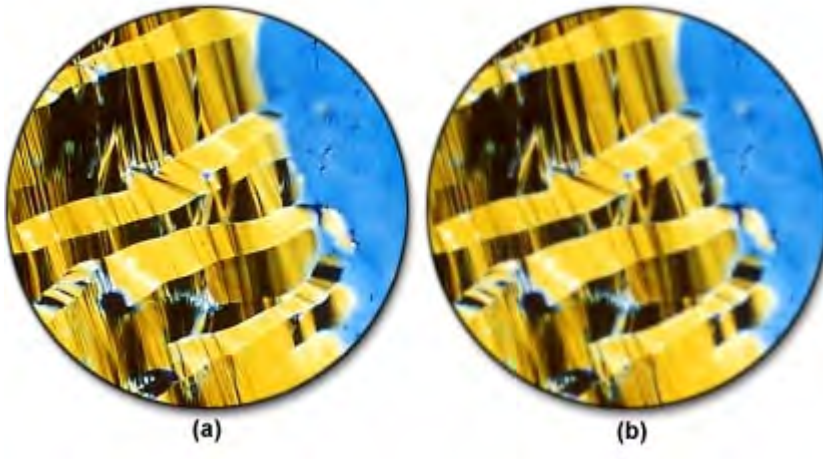

FIGURE 2.7: Empty magnification

and demonstrates a significant lack of resolution caused by the empty magnification factor introduced by the enormous degree of enlargement.

Care should be taken in choosing eyepiece/objective combinations to ensure the optimal magnification of specimen detail without adding unnecessary artifacts. For instance, to achieve a magnification of 250X, the microscopist could choose a 25X eyepiece coupled to a 10X objective. An alternative choice for the same magnification would be a 10X eyepiece with a 25X objective. Because the 25X objective has a higher numerical aperture (approximately 0.65) than does the 10X objective (approximately 0.25), and considering that numerical aperture values define an objective's resolution, it is clear that the latter choice would be the best. If photomicrographs of the same viewfield were made with each objective/eyepiece combination described above, it would be obvious that the 10x eyepiece/25x objective duo would produce photomicrographs that excelled in specimen detail and clarity when compared to the alternative combination.

The range of useful total magnification for an objective/eyepiece combination is defined by the numerical aperture of the system. There is a minimum magnification necessary for the detail present in an image to be resolved, and this value is usually rather arbitrarily set as 500 times the numerical aperture (500 x NA). At the other end of the spectrum, the maximum useful magnification of an image is usually set at 1000 times the numerical aperture (1000 x NA). Magnifications higher than this value will yield no further useful information or finer resolution of image detail, and will usually lead to image degradation, as discussed above. Exceeding the limit of useful magnification causes the image to suffer from the phenomenon of empty magnification (see Figures 2.7 (a) and (b)), where increasing magnification through the eyepiece or intermediate tube lens only causes the image to become more magnified with no corresponding increase in detail resolution. Table 2.2 lists the common objective/eyepiece combinations that lie in the range of useful magnification.

These basic principles underlie the operation and construction of the compound microscope which, unlike a magnifying glass or simple microscope, employs a group of lenses aligned in series. The elaboration of these principles has led to the development, over the past several hundred years, of today's sophisticated instruments. Modern microscopes are often modular with interchangeable parts for different purposes; such microscopes are

TABLE 2.1: Range of Useful Magnification (500-1000 x NA of Objective)

Objective NA	Eyepieces 10x	12.5x	15x	20x	25x
2.5x(0.08)	—	—	—	x	x
4X (0.12)	—	—	x	x	x
10X (0.35)	x	x	x	x	x
25X (0.55)	x	x	x	x	—
40X (0.70)	x	x	x	—	—
60X (0.95)	x	x	x	—	—
100X (1.40)	x	x	—	—	—

x = good combination

TABLE 2.2: Range of Useful Magnification (500-1000 x NA of Objective)

capable of producing images from low to high magnification with remarkable clarity and contrast.

Chapter 3

Microscope Optical Components

Modern compound microscopes are designed to provide a magnified two-dimensional image that can be focused axially in successive focal planes, thus enabling a thorough examination of specimen fine structural detail in both two and three dimensions.

Most microscopes provide a translation mechanism attached to the stage that allows the microscopist to accurately position, orient, and focus the specimen to optimize visualization and recording of images. The intensity of illumination and orientation of light pathways throughout the microscope can be controlled with strategically placed diaphragms, mirrors, prisms, beam splitters, and other optical elements to achieve the desired degree of brightness and contrast in the specimen.

Presented in Figure 3.1 is a typical microscope equipped with a trinocular head and 35–millimeter camera system for recording photomicrographs. Illumination is provided by a tungsten–halogen lamp positioned in the lamphouse, which emits light that first passes through a collector lens and then into an optical pathway in the microscope base. Also stationed in the microscope base is a series of filters that condition the light emitted by the incandescent lamp before it is reflected by a mirror and passed through the field diaphragm and into the substage condenser. The condenser forms a cone of illumination that bathes the specimen, located on the microscope stage, and subsequently enters the objective. Light leaving the objective is diverted by a beam splitter/prism combination either into the eyepieces to form a virtual image, or straight through to the projection lens mounted in the trinocular extension tube, where it can then form a latent image on film housed in the camera system.

The optical components contained within modern microscopes are mounted on a stable, ergonomically designed base that allows rapid exchange, precision centering, and careful alignment between those assemblies that are optically interdependent. Together, the optical and mechanical components of the microscope, including the mounted specimen on a glass micro slide and coverslip, form an optical train with a central axis that traverses the microscope base and stand. The microscope optical train typically consists of an illuminator (including the light source and collector lens), a substage condenser, specimen, objective, eyepiece, and detector, which is either some form of camera or the observer's eye (Table 1). Research-level microscopes also contain one of several light-conditioning devices that are often positioned between the illuminator and condenser, and a complementary detector or filtering device that is inserted between the objective and the eyepiece or camera. The conditioning device(s) and detector work together to modify image contrast as a function of spatial frequency, phase, polarization, absorption, fluorescence, off-axis illumination,

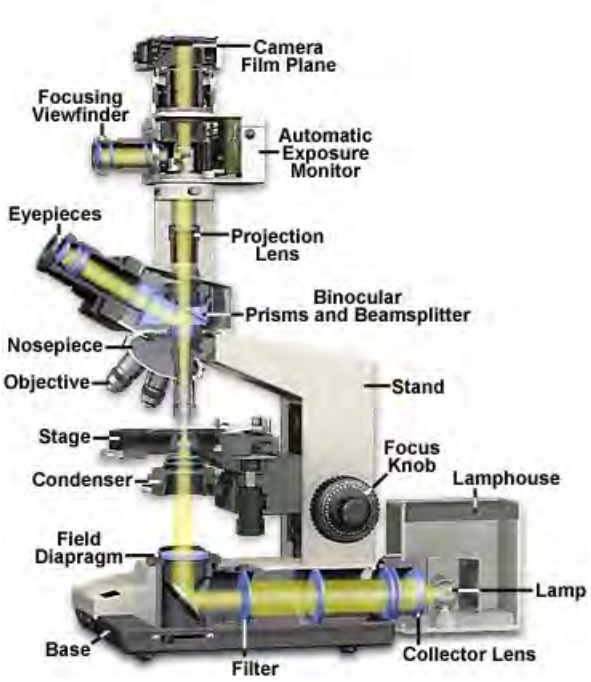

FIGURE 3.1: Modern microscope component configuration

and/or other properties of the specimen and illumination technique. Even without the addition of specific devices to condition illumination and filter image-forming waves, some degree of natural filtering occurs with even the most basic microscope configuration.

Table 1 While some of the microscope optical components act as image-forming elements, others serve to produce various modifications to illumination of the specimen and also have filtering or transforming functions. Components involved in formation of images by the microscope optical train are the collector lens (positioned within or near the illuminator), condenser, objective, eyepiece (or ocular), and the refractive elements of the human eye or the camera lens. Although some of these components are not typically thought of as imaging components, their imaging properties are paramount in determining the final quality of the microscope image.

Fundamental to the understanding of image formation in the microscope is the action of individual lens elements that comprise the components in the optical train. The simplest imaging element is a perfect lens (Figure 3.2), which is an ideally corrected glass element that is free of aberration and focuses light onto a single point. A parallel, paraxial beam of light passes through the converging lens and is focused, by refraction, into a point source located at the focal point of the lens (the point labeled Focus in Figure 3.2). Such lenses are often referred to as positive lenses because they induce a convergent light beam to converge more rapidly, or cause a divergent light beam to diverge less rapidly. A point source of light located at the lens focal point emerges as a paraxial, parallel beam of light as it leaves the lens, moving from right to left in Figure 3.2. The distance between the lens and the focal point is referred to as the focal length of the lens (denoted by the distance f in Figure 3.2).

Optical phenomena are often explained either in terms of quantum theory or wave mechanics, depending upon the particular problem that is being described. In considering the action of lenses, the wave-like properties can often be ignored and light is considered

TABLE 3.1: Microscope Optical Train Components

Microscope Component	*Attributes*
Illuminator	Light Source, Collector Lens, Field Diaphragm, Heat Filters, Light Balancing Filters, Diffuser, Neutral Density Filters
Light Conditioner	Condenser Iris, Darkfield Stop, Aperture Mask, Phase Annulus, Polarizer, Off-Center Slit Aperture, Nomarski Prism, Fluorescence Excitation Filter
Condenser	Numerical Aperture, Focal Length, Aberrations, Light Transmission, Immersion Media, Working Distance
Specimen	Slide Thickness, Cover Glass Thickness, Immersion Media, Absorption, Transmission, Diffraction, Fluorescence, Retardation, Birefringence
Objective	Magnification, Numerical Aperture, Focal Length, Immersion Media, Aberrations, Light Transmission, Optical Transfer Function, Working Distance
Image Filter	Compensator, Analyzer, Nomarski Prism, Objective Iris, Phase Plate, SSEE Filter, Modulator Plate, Light Transmission, Wavelength Selection, Fluorescence Barrier Filter
Eyepiece	Magnification, Aberrations, Field Size, Eye Point
Detector	Human Eye, Photographic Emulsion, Photomultiplier, Photodiode Array, Video Camera

TABLE 3.2: Microscope Optical Train Components

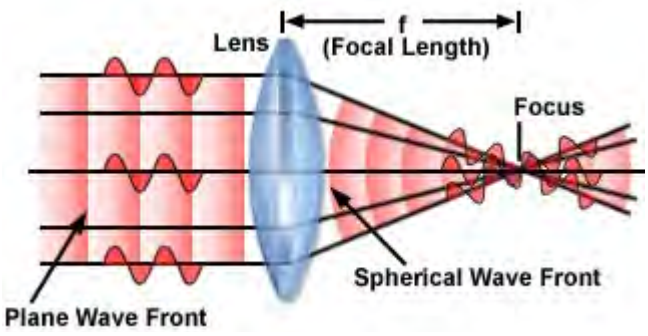

FIGURE 3.2: Wave diagram through a perfect lens

to travel in straight lines often termed rays. Simple ray diagrams are sufficient to explain many important aspects of microscopy including refraction, focal length, magnification, image formation, and diaphragms. In other instances, it is convenient to refer to light waves as being composed of discrete particles (quanta), especially when light is generated by quantum mechanical events or transformed into other forms of energy. This discussion will be restricted to optical lens models utilizing paraxial rays that conform to both the wave-like nature of light and to simple ray diagrams in which light travels from left to right. Paraxial light rays are those traveling very close to the optical axis, resulting in incident and refraction angles that are very small, which when measured in radians, can be considered as equal to their sine values.

In a parallel beam of light, individual monochromatic light waves form a wavetrain having a combination of electric and magnetic vectors vibrating in phase to form a wavefront, which has a vibration orientation perpendicular to the direction of wave propagation. The plane wave is converted to a spherical wave as it passes through the perfect lens, with the front centered at the focal point (Focus) of the lens (Figure 3.2). Light waves arrive at the focal point in phase and interfere constructively with each other at this location. Alternatively, light comprising a spherical wavefront emanating from the focal point of a perfect lens is converted by the lens into a plane wave (proceeding from right to left in Figure 3.2). Each light ray in the plane wave undergoes a different change of direction upon encountering the lens because it arrives at the surface in a slightly different angle of incidence. Upon emerging from the lens, the direction of the light ray also changes. In real systems, the angle of refraction and focal point of a lens or group of lenses is dependent upon the thickness, geometry, refractive index, and dispersion of each component in the system.

The general action of a perfect lens (or lens system) is to convert one spherical wave into another, with the geometrical properties of the lens determining the position of the focal point. As the distance of the light source from the lens is increased, the angle of diverging light rays entering the lens is decreased with a corresponding increase in the radius of the wavefront. If the radius of a spherical wave entering the lens is infinite, the radius of the spherical wave passing through the lens becomes equal to the focal length of the lens. A perfect lens has two focal points, and a plane wave passing through the lens is focused onto one of these points, depending upon whether the light rays enter from the left or right side of the lens.

In situations where the propagation direction of the plane wave does not coincide with the optical axis of the lens, the focal point of the spherical wave produced by the lens is also removed from the axis. Figure 3.3 illustrates the case of a plane wavefront encountering a perfect lens when tilted at an angle (a). The center of the resulting spherical wave is labeled S and lies at a distance d from the axial focal point (labeled Focus in Figure 3.3), but within the same focal plane. The value of d can be expressed as:

$$d = f \sin(a)$$

where f is the focal length of the perfect lens. In terms of geometric optics, f is a value that refers to the radius of an arc centered on S and passing through the center of the lens as if it were a single refracting surface.

An alternative model for investigating a point source of light (S(1)) that does not lie in the focal plane of a lens is illustrated in Figure 3.4. In this figure, the perfect lens is dissected into two individual lens elements (Lens(a) and Lens(b)), such that the point

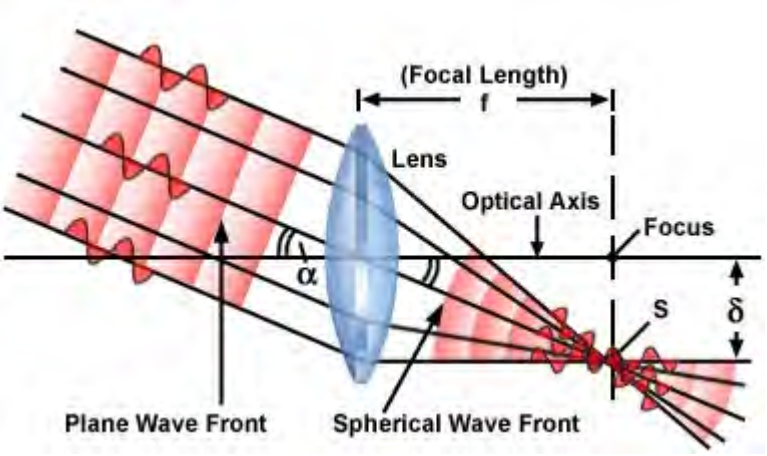

FIGURE 3.3: Oblique wave through a perfect lens

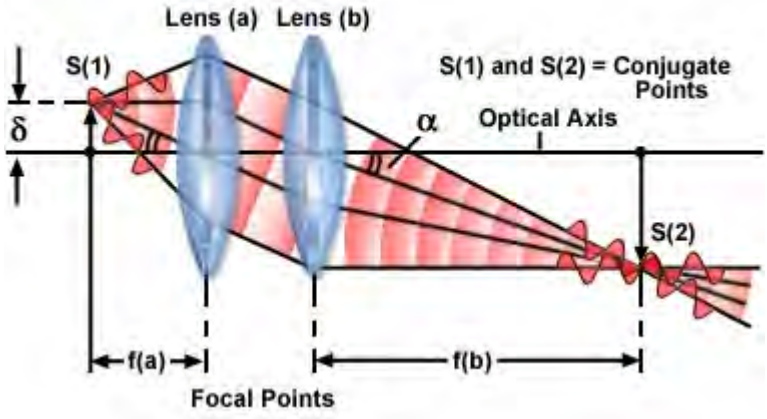

FIGURE 3.4: Oblique wave through a perfect lens system

source of light S(1) is positioned a distance equal to f(a) (the focal length) away from Lens(a). Likewise, the point source S(2) is positioned at a distance of f(b), the focal length of Lens(b). A straight line connecting the centers of Lens(a) and Lens(b) is referred to as the optical axis of the lens system.

In the dual-lens system (Figure 3.4), a spherical wavefront emanating from light source point S(1), and located at a distance d from the optical axis of the lens, is converted by Lens(a) into a plane wave. As it exits from Lens(a), the plane wave is tilted with respect to the lens axis by an angle a. Both d and a are related by the sine equation discussed above, with the value for f being replaced by f(a). After passing through the second lens (Lens(b)), the plane wave is converted back into a spherical wave having a center located at S(2). The result is that the perfect lens L, which equals Lens(a) + Lens(b), focuses light from point S(1) onto point S(2) and also performs the reverse action by focusing light from point S(2) onto point S(1). Focal points having such a relationship in a lens system are commonly referred to as conjugate points.

In the nomenclature of classical optics, the space between light source S(1) and the

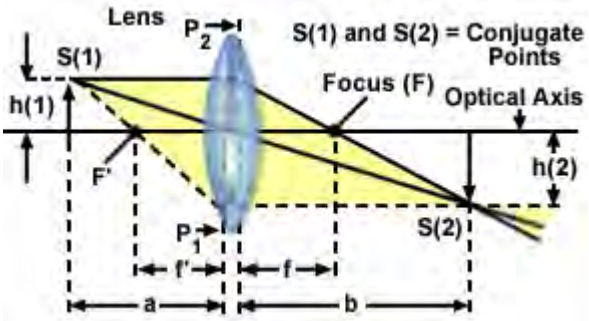

FIGURE 3.5: Oblique wave ray diagram

entrance surface of the first lens is referred to as the object space, while the region between the second lens exit surface and point S(2) is known as the image space. All points involved with primary or secondary light rays are termed objects (or specimens in optical microscopy), while the regions containing light rays concentrated by refraction from the lens are called images. If the light waves intersect, the image is real, whereas if only the projected extensions of refracted light rays intersect, a virtual image is formed by the lens system. A real image can be visualized when projected onto a screen, captured on photographic film emulsion, or organized into a digital array by the photodiode elements of a charge-coupled device (CCD). Conversely, a virtual image requires the assistance of another lens or lens system to be seen by an observer.

If the point S(1) in Figure 3.4 is expanded into a series of points spread throughout the same focal plane, then a perfect lens will focus each point in the series onto a conjugate point in the focal plane of S(2). In the case where a point set of S(1) lies in a plane perpendicular to the optical axis of the lens, then the corresponding conjugate points in set S(2) would also lie in a plane that is perpendicular to the axis. The reverse is also true: the lens will focus every point in the set S(2) onto a conjugate point on the plane or surface of point set S(1). Corresponding planes or surfaces of this type are known as conjugate planes.

An alternative method of representing a train of propagating light waves is illustrated in Figure 3.5 for an oblique light wave. This method relies on applying the laws of geometrical optics to determine the size and location of images formed by a lens or multi-lens system. Two representative light rays, one paraxial and one traveling through the center of the lens (the principal ray), are all that is necessary to establish the parameters of the imaging situation. Many textbooks on Gaussian optics refer to these light rays as characteristic rays, with the principal ray being the one that passes through the center of the entrance and exit pupils, the lens, and any aperture diaphragms present in the optical system. Often, the principal ray is omitted from consideration and the characteristic rays passing through the front and rear focal points of the lens are utilized to define the object and image size and location. In Figure 3.5, the second characteristic ray is illustrated as a yellow-filled dotted line passing through the front focal point (F') of the lens.

The specimen or light source is designated S(1) in Figure 3.5, and is located at distance a to the left of the lens, in the region known as the object space. A single light ray, designated by the dotted line emanating from S(1) and intersecting the optical axis at the object-side focal point (F'), is refracted by both surfaces of the lens and exits parallel to the optical axis. Extensions of the refracted and incident ray intersect at a surface within

the lens located at distance a from the source (S(1)). This surface is known as the first or object-side principal surface, and is designated by P(1) in Figure 3.5. The uppermost light ray, progressing from S(1) in a direction parallel to the optical axis, is refracted by the lens and passes through the image-side focal point (F). Extensions of the refracted and incident ray intersect at the image-side principal surface (noted as P(2) in Figure 3.5) within the lens and positioned at distance b from the image point S(2). Near the vicinity of the lens axis, the surfaces P(1) and P(2) approximate plane surfaces and are known as the principal planes of the lens. The intersections of these planes with the optical axis of the lens (not illustrated) are referred to as the principal points. Simple convex lenses exhibiting bilateral symmetry have principal points that are symmetrical with the lens surfaces. More complex lenses and multiple lens systems often have principal points that coincide with the surface of the lens or even extend outside the glass elements.

Another set of points utilized to define lens parameters are the nodal points, which occur where the extensions of oblique light rays passing through the lens intersect the optical axis. Nodal points are not illustrated in Figure 3.5, but would lie very close to the principal points of the lens. Thus, three pairs of points, the lens focal points (F and F'), principal planes (P(1) and P(2)), and the principal nodes all lie on the lens optical axis. If the location of the focal points and either the principal points or the nodal points is known, then geometrical construction of ray traces to elucidate object and image parameters can be undertaken without considering refraction of light rays at each surface of the lens. The result is that any lens system can be simulated utilizing only the focal points and principal planes by drawing ray traces as if they encounter the first principal plane, travel parallel to the optical axis, and emerge from the second principal plane without refraction.

Note that distance a is greater than the lens front focal length, f' in Figure 3.5. Under these circumstances, an inverted image (S(2)) is then formed in the image space at a distance b to the right of the lens. The length of b is greater than the lens rear focal length, f, which is related to the distances a and b by the classical lens equation:

$$\frac{1}{a} + \frac{1}{b} = \frac{1}{f}$$

The height of image S(2) is denoted by the quantity h(2), and represents an increase in size, resulting from magnification of the object or specimen S(1) positioned at the front of the lens and having a height of h(1). The lateral magnification, M of this simple lens (which approximates a Gaussian thin lens) is expressed by the equation:

$$M = \frac{h(2)}{h(1)} = \frac{b}{a}$$

Because S(1) and S(2) lie in conjugate planes, the image S(2) will be focused at S(1) by the lens. The focal length would then be represented by f' and the magnification (M) inverted to $\frac{1}{\mathrm{M}}$ due to the reduction in size of the image when the reverse situation is considered.

The distance ratio between two image points along the optical axis on the object side of the lens and two conjugate points on the image side is known as the longitudinal or axial magnification. The magnitude of the longitudinal magnification is the square of the lateral magnification for small distances from the image plane.

All of the imaging components in the optical microscope are governed by the basic geometrical relationships described above. This includes the collector lens, condenser, objective, eyepieces (in the projection mode), camera system, and the human eye.

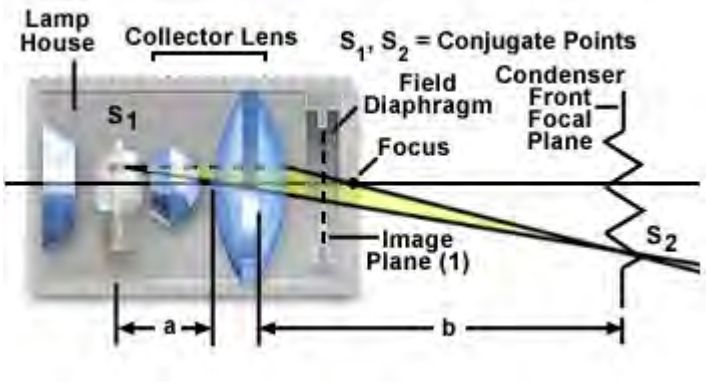

FIGURE 3.6: Collector lens image planes

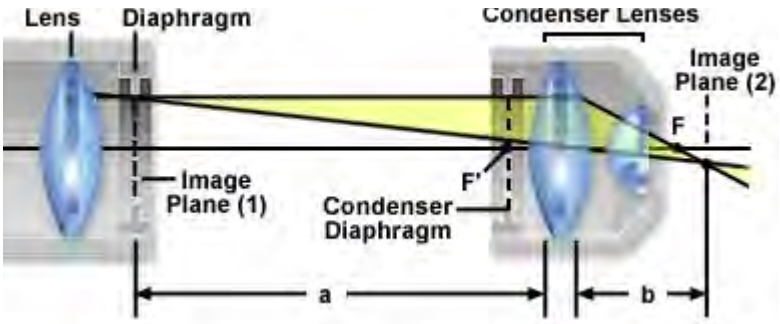

FIGURE 3.7: Image plane of the condenser lens

The first stage of the microscope optical train is the lamphouse, which contains the lamp and collector lens, and is responsible for establishing the primary illumination conditions for the microscope. Illustrated in Figure 3.6 is a schematic diagram of a typical lamp and collector lens configuration. Image sizes and positions are presented according to the conventions introduced in Figure 3.5 for a basic primary lens system. Light emitted by the tungsten–halogen lamp is passed through the collector lens system and the filament is focused onto the front focal plane of the condenser. The first image plane in the microscope optical train (Image Plane (1)) occurs at the position of the field diaphragm.

Point S(1) on the lamp filament is conjugate to point S(2), which is imaged in the focal plane of the condenser aperture diaphragm when the microscope is configured to operate under conditions of Köhler illumination. The distance from S(1) to the first principal plane of the collector lens system is denoted by distance a, and the distance from the condenser iris diaphragm to the image-side principal plane of the collector is given by distance b. The microscope field diaphragm (Figures 3.6 and 3.7) governs the diameter of the light beam emitted by the illumination system before it enters the condenser aperture.

The relationship between conjugate image planes in the condenser lens and the illumination system are illustrated in Figure 3.7. The field diaphragm (Image Plane (1)) is imaged in the same plane as the specimen (Image Plane (2)) when the microscope is configured for Köhler illumination. The front focal plane of the condenser (F') resides in the center of the aperture diaphragm. Lengths a and b represent the respective distances of the field diaphragm (Image Plane (1)) and the specimen plane (Image Plane (2)) from the principal

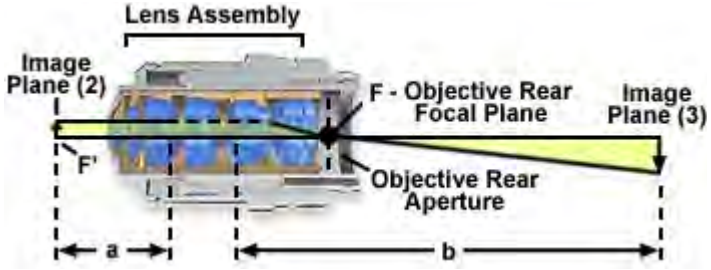

FIGURE 3.8: Objective plane images

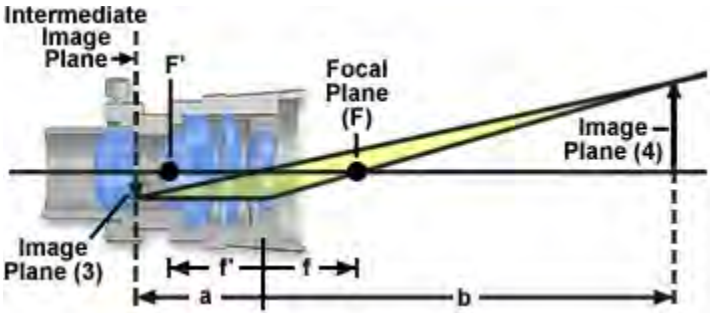

FIGURE 3.9: Eyepiece image planes

planes of the condenser lens elements. Light emitted by the lamphouse and passing through the condenser is formed into a cone of illumination that bathes and subsequently passes through the specimen. Adjustment of the condenser aperture iris diaphragm opening size controls the numerical aperture of this illumination cone.

Image planes of the objective are presented in Figure 3.8, which illustrates a typical objective internal lens system, the specimen plane (Image Plane (2)), and the relative position of the microscope intermediate image (Image Plane (3)). The specimen plane is conjugate to the intermediate image plane, and each are separated from the objective principal planes by distances a and b, respectively. The objective front focal point is designated F', while the rear focal point, which occurs in the plane of the objective rear aperture, is noted as F. Internal lens elements are often complex assemblies consisting of hemispherical and meniscus lenses, lens doublets and triplets, and single lens elements of varying design.

The eyepiece (or ocular) is designed to project either a real or virtual image, depending upon the complex relationship between the intermediate image plane, the eyepiece focal planes, and the internal eyepiece field diaphragm. In addition, the diameter of the fixed eyepiece diaphragm also determines the linear field size observed by the microscopist. This value is termed the field number or field of view number (abbreviated FN) and is often inscribed on the eyepiece housing exterior.

Image planes of the eyepiece, when utilized in projection mode, are presented in Figure 3.9. The principal focal points are F' and F, the front and rear focal points, respectively. The intermediate image plane (Image Plane (3)) is located in the center of the fixed eyepiece field diaphragm, which is placed either before or after the eyepiece field lens, depending upon the design. This image plane is conjugate to Image Plane (4) and is the location into which eyepiece focusing and measuring reticles are inserted. The length a represents

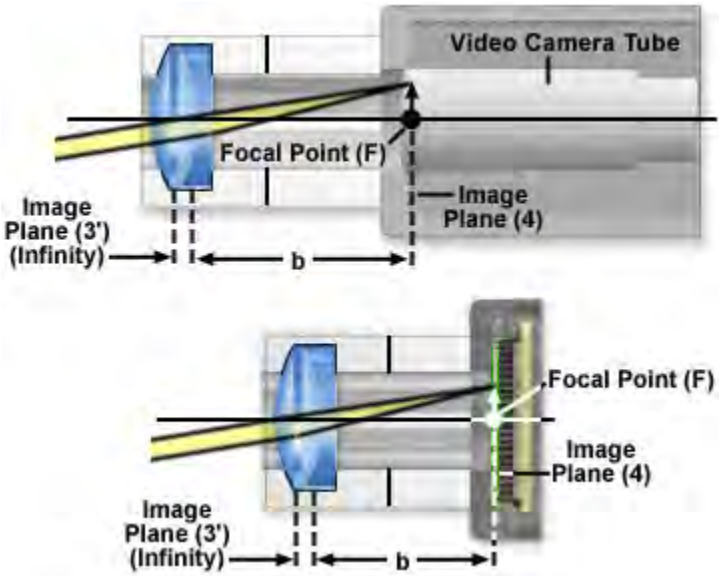

FIGURE 3.10: Video and CCD sensor image planes

the distance from the eyepiece fixed diaphragm to the principal plane of the eyelens (the lens closest to the observer's eye), while b is the distance from the eyelens to Image Plane (4), located on the sensor surface. Because a is greater than the front focal length of the eyelens (f'), the image formed at Image Plane (4) is a real (not virtual) image. The quantity f denotes the distance from the eyelens to the eyepiece rear focal plane (F), and also represents rear focal length of the eyepiece lens system.

Image planes on a video and CCD sensor are presented in Figure 3.10, which illustrates the application of a specialized positive projection lens for imaging onto these sensors. The focal point (F) is located either on the video tube photocathode or the CCD photodiode array surface, depending upon the geometry and other parameters of the detector. If the projection lens is located after the eyepiece in the optical train, then it converges the virtual image (located at Image Plane (3')) onto the sensor surface at Image Plane (4). This image plane is located at distance b from the projection eyelens, which is equal to the focal length of the lens. It should be noted that a conventional film camera system can also be employed in place of a video or CCD sensor, in which case the image plane coincides with the plane of the chemical emulsion layered onto the film base.

When images are examined in the microscope, an intermediate image (see Image Plane (3) in Figure 3.11) is formed by the objective at a distance a, which is slightly closer to the eyepiece than its front focal length (F'). This prevents the formation of a real image after the ocular lens, as was illustrated in Figure 3.9 for the eyepiece operating in projection mode. Together, the eye and eyepiece form an image on the retina (Image Plane (4)) as though the eye were seeing the virtual image.

In situations where distance a is less than the focal length, then the reciprocal equation relating focal length to a and b reveals that b must be less than zero. Therefore, a real image is not formed to the right of the eyepiece in the absence of the eye or a camera. Instead, a virtual image (Image Plane (3')) appears at a distance corresponding to $-b$ (Figure 3.11) to the left of the eyepiece (or b to the right; see Figure 3.5). When observing the image through the eyepiece, the image-forming beam diverging out through the eyelens

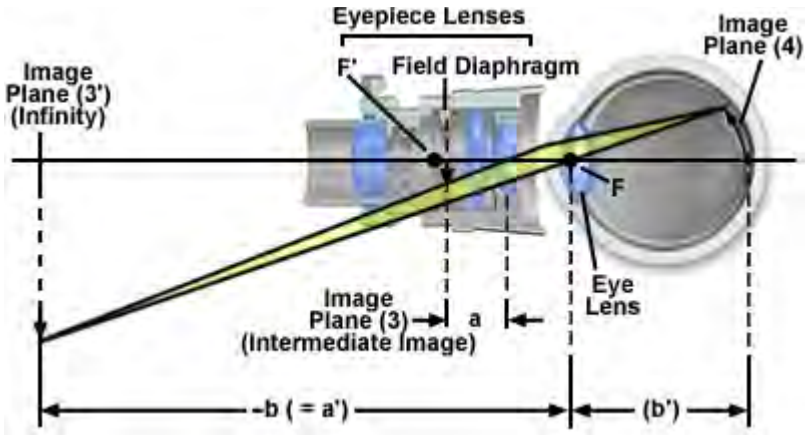

FIGURE 3.11: Formation of the microscope image on the retina

appears to originate from the virtual source (located at Image Plane (3')). Light rays exiting the eyepiece form a cone of illumination that constitutes the exit pupil of the microscope, which is also commonly referred to as the eye point or Ramsden disc. For proper observation of magnified specimens, the microscope exit pupil must coincide with the pupil of the observer's eye.

Image planes 2, 3, 3', and 4 (Figures 3.7–3.11) are related to each other geometrically as illustrated in Figure 3.12. In all of the imaging steps, with the exception of Image Plane (3'), the image is real and inverted (see Figures 3.7– 3.11). When the microscope eyepiece is used for direct viewing (Figure 3.11) rather than for projection (Figure 3.9), the image at Image Plane (3') is not real, but virtual and is not inverted relative to the intermediate image. The human eye will not perceive the image on the retina (Image Plane (4)) as inverted, even though the image is inverted in relation to the intermediate image (Image Plane (3)) and the virtual image (located at Image Plane (3')).

Several of the principal image planes in the microscope occur either in fixed or adjustable apertures or diaphragms, which are essential components of all optical systems. A diaphragm, also referred to as a stop, is an opaque gate or a lens mount with a circular opening (often adjustable) that controls light flow through the microscope. Two basic types of diaphragms are utilized in the microscope: the aperture diaphragm, which adjusts the aperture angles in the microscope, and the field diaphragm that controls the size of the field imaged by the instrument. The primary role of diaphragms in the optical microscope is to prevent light rays with severe aberration and stray light from reaching the image planes, and to ensure a suitable distribution and intensity of light in both the object and image space.

Classical microscope design relies on two apertures and two diaphragms to control passage of light through the microscope. The field diaphragm, positioned in the lamphouse or in the base of the microscope, is an adjustable iris-type diaphragm that determines the size of the illuminating field of light. Positioned at the condenser front focal plane is the condenser aperture, another iris diaphragm that is utilized to adjust the beam size and angle of light rays striking the specimen. The third aperture has a fixed size and is located at the rear focal plane of the objective. This aperture determines the diameter of objective exit pupil and size of the intermediate image, while a conjugate fixed diaphragm in the eyepiece (the eyepiece field diaphragm) determines the size of the viewfield seen by the

microscopist.

The total magnification of the microscope can be determined by considering properties of the objective and eyepieces. Objectives are corrected for a particular projection distance, which is specific to the magnification and is approximately equal to the optical tube length. In a fixed tube length microscope, this projection distance is about 160 millimeters. Therefore, an 8–millimeter focal length objective would have a lateral magnification of about 20x (160/8) with a corresponding longitudinal magnification of 400x (2020).

For visual observation, the eyepiece magnification is assumed to be unity when a specimen (or image) is placed at a distance of 250 millimeters from the eye of the observer. In this regard, an eyepiece having a focal length of 25 millimeters would have a magnification value of 10x (250/25). The total microscope magnification for visual observation is computed by taking the product of the objective and eyepiece magnifications. For the objective and eyepiece just described, the total lateral magnification would be about 200x (10x eyepiece multiplied by the 20x objective). It should be noted that a majority of modern research microscopes are equipped with infinity-corrected objectives that no longer project the intermediate image directly into the intermediate image plane. Light emerging from these objectives is instead focused to infinity, and a second lens, known as a tube lens, forms the image at its focal plane. Wavetrains of light leaving the infinity-focused objective are collimated, allowing introduction of auxiliary components, such as differential interference contrast (DIC) prisms, polarizers, and epi-fluorescence illuminators, into the parallel optical path between the objective and the tube lens with only a minimal effect on focus and aberration corrections.

Magnification of the intermediate image with infinity-corrected optical microscope systems is determined by the ratio of the focal lengths of the tube lens and objective lens. Because the focal length of the tube lens varies between 160 and 250 millimeters (depending upon the manufacturer and model), the focal length of the objective can no longer be assumed to be 160 millimeters divided by its magnification. Thus, an objective having a focal length of 8 millimeters in an infinity-correct microscope with a tube lens focal length of 200 millimeters would have a lateral magnification of 25x (200/8).

Older finite, or fixed tube length, microscopes have a specified distance from the nosepiece opening, where the objective barrel is secured, to the ocular seat in the eyepiece tubes. This distance is referred to as the mechanical tube length of the microscope. The design assumes that when the specimen is placed in focus, it is a few microns further away than the front focal plane of the objective. Finite tube lengths were standardized at 160 millimeters during the nineteenth century by the Royal Microscopical Society (RMS) and enjoyed widespread acceptance for over 100 years. Objectives designed to be used with a microscope having a tube length of 160 millimeters are inscribed with this value on the barrel.

Adding optical accessories into the light path of a fixed tube length microscope increases the effective tube length to a value greater than 160 millimeters. For this reason, addition of a vertical reflected light illuminator, polarizing intermediate stage, or similar attachment can introduce spherical aberration into an otherwise perfectly-corrected optical system. During the period when most microscopes had fixed tube lengths, manufacturers were forced to place additional optical elements into these accessories to re-establish the effective 160–millimeter tube length of the microscope system. The cost of this action was often an increase in magnification and reduced light intensities in resulting images.

For recording images with video microscopy, a photodiode array CCD camera, or clas-

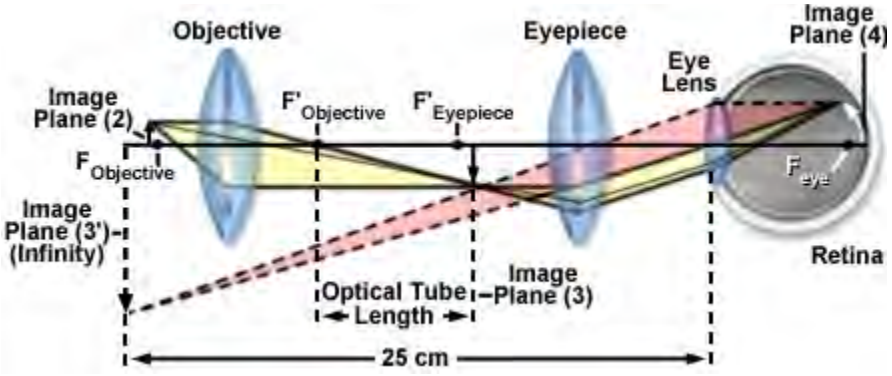

FIGURE 3.12: Conjugate field planes in the optical microscope

sical photomicrography with film cameras, a specialized positive lens is often placed after the eyepiece (see Figure 3.10). Light rays leaving the eyepiece, which is focused to infinity, are converged by the positive lens onto the plane of the photocathode, CCD array, or photographic emulsion. When the magnification of the objective lens is neglected, the lateral magnification of the projection system (M_p) is expressed as:

$$M_p = \frac{f_p}{f_e}$$

where f_p is the focal length of the projection lens and f_e is the eyepiece focal length. In this projection system, the total lateral magnification (M) on the faceplate of the video camera, the CCD photodiode array, or the photographic emulsion is:

$$M = M_o + M_p$$

$$M = \frac{M_o \cdot M_e \cdot f_p}{250 \text{ millimeters}}$$

where M_o is the objective magnification and M_e is the eyepiece lens magnification. If a projection lens is not utilized behind the eyepiece, but rather the eyepiece itself is employed to project the image onto the video image sensor or photographic emulsion, the total lateral magnification becomes:

$$M = \frac{M_o \cdot D_p}{f_e}$$

where D_p is the projection distance from the eyepiece to the image plane. To avoid image distortion, a value of at least 20 to 30 centimeters should be used for D_p, unless a special eyepiece is employed.

Magnifications inscribed on the objective barrel or eyepiece rim by the manufacturer are nominal and must be calibrated with a stage micrometer to obtain the exact value. Measurements of magnification are accomplished by placing the stage micrometer in the specimen plane (on the microscope stage) and imaging the finely ruled lines under identical optical conditions.

In some cases, the camera sensor is placed directly in the intermediate image plane, without the presence of a projection eyepiece and results in an image magnification limited to that produced by the objective. This method is only recommended when the performance of the video system is limited by the absolute amount of light available, because such a

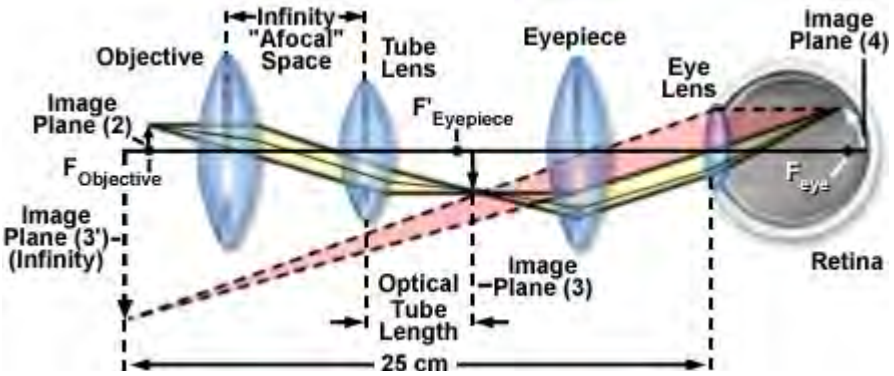

FIGURE 3.13: Infinite–corrected microscope optical pathways

fixed magnification imposes severe limitations on the ability to optimize the quality of the final video image.

In summary, Ray paths through both finite tube length and infinity-corrected microscopes are reviewed and illustrated in Figures 3.12 and 3.13. A finite (fixed tube length) microscope optical train is illustrated in Figure 3.12, which includes the essential optical elements and ray traces defining the relationship between image planes. A specimen located a short distance before the objective front focal plane is imaged through conjugate planes onto the retina of the eye at Image Plane (4). The objective lens projects a real and inverted image of the magnified specimen into the intermediate image plane of the microscope (Image Plane (3)), which is located in the center of the eyepiece field diaphragm at a fixed distance behind the objective. In Figure 3.12, the objective rear focal plane is positioned at a location on the optical axis marked F'(Objective), and the distance between this focal plane and the intermediate image plane represents the optical tube length of the microscope.

The aerial intermediate image is further magnified by the microscope eyepiece and produces an erect image of the specimen on the retina surface, which appears inverted to the microscopist. As discussed above, the magnification factor of the specimen is calculated by considering the distance between the specimen and the objective, and the front focal length of the objective lens system (F(Objective)). The image produced at the intermediate plane is further magnified by a factor of 25 centimeters (called the near distance to the eye) divided by the focal length of the eyepiece. The visual image (virtual) appears to the observer as if it were 10 inches away from the eye.

Most objectives are corrected to work within a narrow range of image distances, and many are designed to work only in specifically corrected optical systems with matching eyepieces. The magnification inscribed on the objective barrel is defined for the tube length of the microscope for which the objective was designed.

Illustrated in Figure 3.13 is the optical train, using ray traces, of an infinity-corrected microscope system. The components of this system are labeled in a similar manner to the finite-tube length system (Figure 3.12) for easy comparison. Here, the magnification of the objective is determined by the focal length of the tube lens. Note the infinity "afocal" space that is defined by parallel light beams in every azimuth between the objective and the tube lens. This is the space used by microscope manufacturers to add accessories such as vertical illuminators, DIC prisms, polarizers, retardation plates, etc., with much simpler designs and with little distortion of the image. The magnification of the objective in the

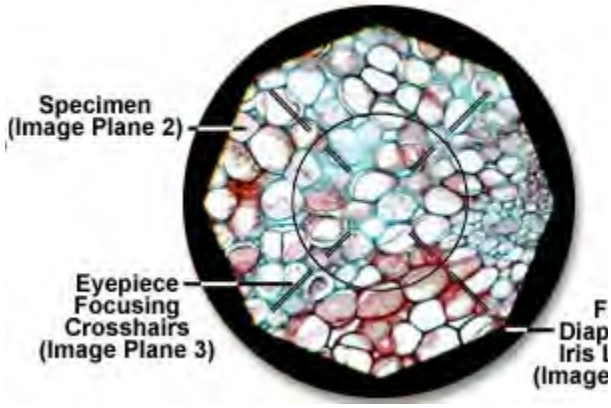

FIGURE 3.14: Optical microscope conjugate planes

infinity-corrected system equals the focal length of the tube lens divided by the focal length of the objective.

In the optical microscope, conjugate planes are imaged into each other and can collectively be observed while examining a specimen in the eyepieces. This concept is illustrated in Figure 3.14 with the image of a stained thin section of plant tissue superimposed on the iris leaves of the field diaphragm and a focusing reticle in the eyepiece intermediate image plane. The field iris diaphragm, adjacent to the lamp collector lens, is imaged sharply into the same plane as the specimen by the microscope condenser. Images of both the field diaphragm and the specimen are formed in the intermediate image plane by the objective and are projected into the fixed field diaphragm of the eyepiece, where the focusing reticle is located. Subsequently, the eyepiece (in conjunction with the observer's eye, located at Image Plane (4)) forms images of all three previous image planes on the sensor surface of an imaging system or the retina of a human eye. The field diaphragm, specimen, intermediate image, and retina all constitute a set of conjugate image planes that appear simultaneously in focus.

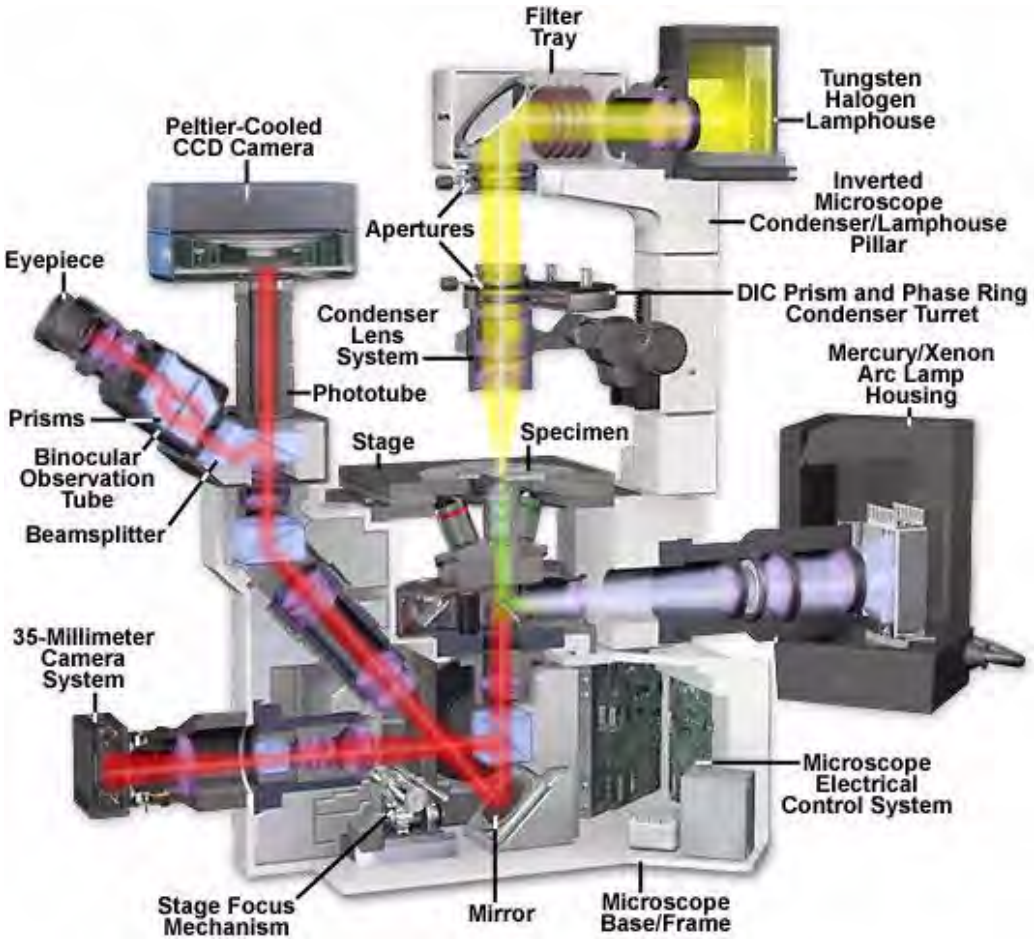

FIGURE 3.15: Olympus IX70 inverted microscope cutaway diagram

Chapter 4

Microscope Illumination

All to frequently, sophisticated and well-equipped microscopes fail to yield excellent images due to incorrect use of the light source, which usually leads to inadequate sample illumination. When optimized, illumination of the specimen should be bright, glare-free, and evenly dispersed in the field of view.

There are numerous light sources available to illuminate microscopes, both for routine observation and critical photomicrography. A most common light source, because of its low cost and long life, is the 50 or 100 watt tungsten halogen lamp as illustrated at the base of the microscope diagram in Figure 2.1, which also details the optical pathways in a typical modern transmitted light microscope. In this figure, the tungsten-halogen lamp emits a continuous spectrum of light centered at 3200 K (when set at a lamp voltage of +9 volts), which is then passed through a collector and field lens before being reflected into the substage condenser and onto the specimen. Image forming light rays are captured by the microscope objective and passed either into the eyepieces or directed by a beam splitter into one of several camera ports. Throughout the optical pathway of the microscope, illumination is directed and focused through a series of diaphragms and lenses as it travels from the source to illuminate the specimen and then into the eyepieces or camera attachment. Alignment of the optical components of a microscope to optimize illumination in modern microscopes is carried out following the rules of Köhler illumination. More details of how both transmitted and reflected light microscopes are aligned for proper Köhler illumination are discussed in our sections on setting up a microscope for transmitted light and reflected light. The optical pathways shown above in Figure 2.1 are typical for a transmitted light microscope and involve a number of lenses, diaphragms, mirrors, and beam splitters to direct light through the microscope.

Tungsten-halogen lamps are relatively bright with a color spectrum centered at 3200 K (when set at approximately +9 volts), but require color conversion filters to raise their color temperature to daylight equivalence. Another popular light source is the 75 to 150 watt xenon lamp because of its very high brightness and long life, a relatively even output across the visual spectrum, and a color temperature which approximates that required by daylight film emulsions. Where very high light intensity is required, tin-halide lamps are often used. In fluorescence microscopy, particular for the purpose of critical photomicrography, 100 watt or 200 watt mercury burners are often employed. In former years, carbon arc lights or zirconium bulbs might have been used, but these sources are seldom seen today. For more information and a detailed discussion of the wide spectrum of lamps available for microscope illumination, visit our section on light sources for microscopy and photomicrography.

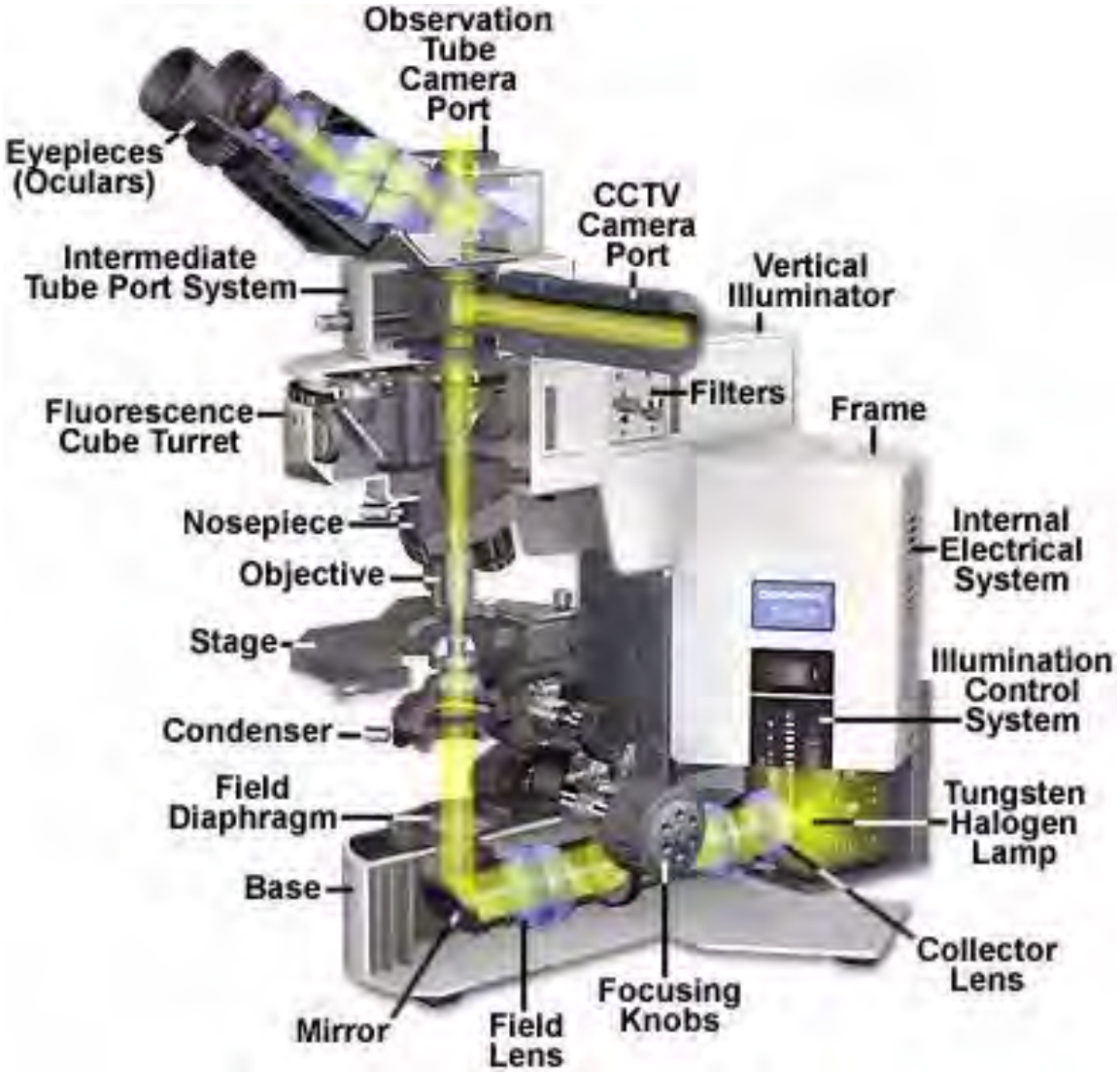

FIGURE 4.1: Microscope Optical pathways

Alignment of the source illumination through optical pathways in reflected light microscopy is also of primary concern, particular with respect to metallography, semiconductor wafer inspection, and the remarkable new progress being made in fluorescence microscopy. Reflected light microscopes are also illuminated with a variety of light sources (as discussed above) and can be adjusted for optimal performance using Köhler illumination. This is discussed in greater detail in our section on configuration of Köhler illumination for reflected light microscopy. Illumination pathways for reflected light microscopy are also the topic of several interactive Java tutorials including the one linked directly below.

In his excellent book "Photography Through the Microscope", John Delly argues that between 80 and 90 percent of all photomicrographs submitted to contests, exhibitions, and scientific publications are victims of improperly aligned optics resulting in poor sample illumination. This is one of the most common problems with microscopy and photomicrography in general, and a surprise examination of the student microscopes in many university laboratories will reveal an abundance of poorly adjusted substage condensers and illumination sources. We suspect that incorrect alignment and adjustment of both the substage condenser and field diaphragm, over the entire range of objectives in a given microscope, are the biggest source of errors in photomicrography.

The necessity for proper illumination cannot be overemphasized. All too often, a $25,000 microscope is reduced to the level of a hand magnifier by improper illumination and alignment, resulting in photomicrographs that are surpassed by those taken with a $2000 microscope under optimum conditions of Köhler illumination. In the companion sections of this primer dealing with the theory of Köhler illumination and its implementation (both for transmitted and reflected light) we discuss critical aspects of microscope configuration and have included a variety of interactive Java tutorials to help students master these important concepts.

4.1 Afocal or Nonfocused Illumination

Illumination systems that do not form an image of the light source at some point in the optical pathway are called afocal or nonfocused illumination. Before the invention of electric bulbs, microscopists were limited in their choice of suitable sources for microscope illumination. During daylight hours, they could point their microscopes (or substage reflector mirrors) towards the sky and use the clouds as a crude diffusion screen to spread illumination evenly across the entire field of view. Instrument makers also ground mirrors to produce concave reflective surfaces in an effort to increase the light intensity in the object plane. Clouds and blue sky are not light sources that lend themselves to being easily imaged within the optical pathway of the microscope, and thus are sources of afocal illumination. Indoor and night work forced early microscopists to rely on artificial sources of illumination which, due to the inherent lower color temperature produced by these sources, rendered specimen colors in different intensities, hues, and tones than were observed under natural daylight. To compensate for this, microscopists have used various types of blue filters to change the apparent color temperature of artificial light to closely match that of natural daylight. However, without forming an image of the light source somewhere within the optical path, these various early methods of illumination still fall into the category of afocal or nonfocused illumination.

Early investigations revealed that when rotating between daylight and artificial light sources, there are (practically speaking) no evident changes in the optical character or re-

solving power of the image, provided the back lens of the objective is completely filled with light. Later, scientists found that the most important requirement is that the numerical aperture of the illumination be at least equal to that of the objective. In the nineteenth century, new illumination sources were developed, and a new "source focused" (later termed critical or Nelsonian illumination) method was developed to improve microscope illumination conditions.

4.2 Critical (or Nelsonian) Illumination

This method of microscope illumination was first developed by British microscopist Edward Nelson using optical principles advanced by Ernst Abbe. Nelsonian illumination was used very successfully by microscopists from the latter part of the nineteenth century until well into the twentieth century. Today, there are still some advocates of critical illumination who continue to use it with microscopes requiring external light sources, or with cheaper student microscopes where photomicrography is not an issue.

Nelsonian illumination relies on using the substage condenser to produce a focused image of the flame from a burning oil lamp (or other homogeneous light source) in the plane of the specimen to achieve a somewhat even illumination condition over the entire viewfield. Homogeneity of the light source is the important aspect when considering this method of illumination. The flame produced by a burning lamp is fairly even and consistent, but other sources such as frosted enlarger bulbs, opal bulbs, or ribbon filaments can also be used for critical illumination. Figure 2.2 illustrates the optical pathways of critical illumination using a hypothetical oil lamp that provides a homogeneous illumination source.

Light emitted from the oil lamp flame must be focused by the substage condenser (see Figure 2.2) so that an image of the flame is produced in the specimen plane at the microslide. In practice, it is often difficult (or impossible) to find focus in the central portion of the flame, so the "edge" of the flame is usually focused with subsequent readjustment of the substage mirror so that the image of the central portion of the flame fills the field of view. The amount of light entering the microscope can be controlled by the field diaphragm, which (if present) is usually attached externally. Enough light must enter the microscope to completely fill the back plane of the objective, and this can be controlled through proper adjustment of the condenser aperture diaphragm. Focusing the light source in the sample plane is precarious and can often yield a grainy, uneven, or speckled background. This can be overcome by slightly defocusing the substage condenser to produce a more uniform background. Nelsonian illumination has largely been supplanted by the far more efficient Khler method of microscope illumination.

4.3 Köhler Illumination

This topic will be discussed in greater detail in another section of the primer, but we will briefly touch upon the major aspects here. In Köhler illumination, an image of the light source is focused at the condenser aperture diaphragm to produce parallel (and unfocused) light through the plane of the specimen or object. A magnified image of the light source below the condenser (at the aperture diaphragm) produces a wide cone of illumination that is required for optimum resolution of the specimen. The size of the condenser aperture diaphragm can be used to control the numerical aperture of the light cone that illuminates

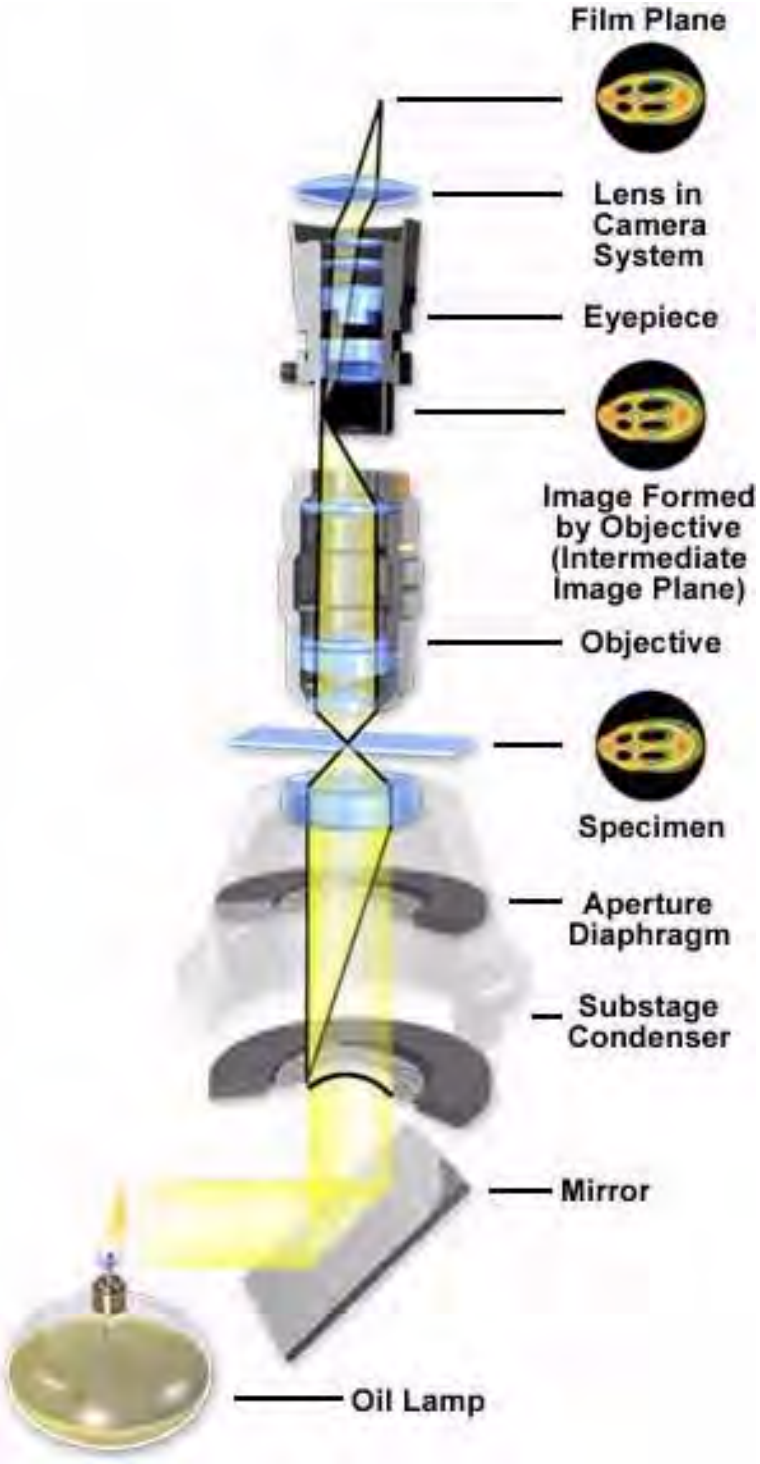

FIGURE 4.2: Nelsonian or critical illumination

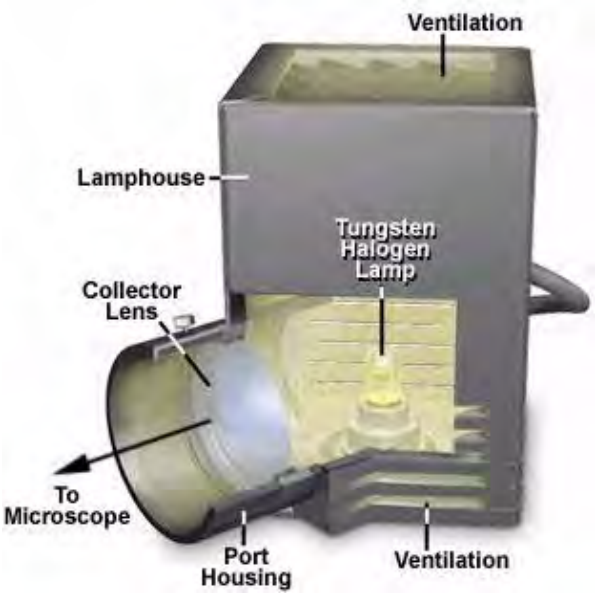

FIGURE 4.3: Tungsten halogen lamphouse

the sample and reduce unwanted stray light and glare. In addition, imaging of dust and other imperfections on the glass surfaces of the condenser is minimized.

Efficient sample illumination is very dependent upon proper alignment of all the optical components in the microscope, including the illumination source. The serious microscopist should become familiar with the adjustment range of each component and should practice aligning these with different samples and objectives. Uneven illumination can have a serious impact on the quality of photomicrographs, causing "hot spots", vignetting, color fringes, poor contrast, and a variety of other undesirable effects. Some of the newest microscopes are equipped with "pre-centered" lamps that do not allow for adjustment, and some even supply condensers that do not have lateral adjustment mechanisms. It is important to ensure that these microscopes were aligned for proper Köhler illumination at the factory before engaging in photomicrography. Carefully read the microscope instruction manual and/or question your factory technical representative for important details about how these microscopes are optimized for illumination.

4.4 Light Sources

Early microscopists relied on oil lamps and natural sunlight to provide an external source of illumination for their primitive (but often remarkably accurate) microscopes. They often employed rather ingenious methods of gathering light, such as reflection from a large white board or scattering of sunlight on a cloudy day. Unfortunately, these methods did not provide reliable illumination and frequently the area of field illumination greatly exceeded the numerical aperture of the objective, causing glare and flooding.

Modern microscopes usually have an integral light source that can be controlled to a relatively high degree. The most common source for today's microscopes is an incandescent tungsten–halogen bulb positioned in a reflective housing that projects light through the collector lens and into the substage condenser. Lamp voltage is controlled through a

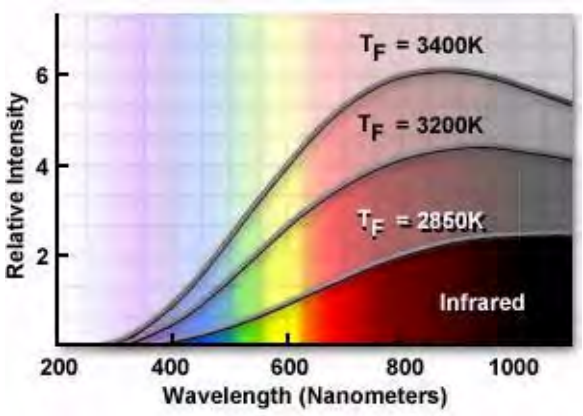

FIGURE 4.4: Tungsten lamp emission spectrum

variable rheostat that is commonly integrated into the microscope stand. A typical illuminator lamp and housing is illustrated in Figure 4.3. The bulb is a tungsten–halogen lamp that operates on a direct current (DC) voltage of 12 volts and produces up to 100 watts of power for illumination. Lamp voltage is controlled by a DC power supply that is often built into the microscope housing, with a voltage control knob that is usually a potentiometer mounted somewhere on the microscope stand. These bulbs generate a large amount of heat during operation, and the housing is provided with several layers of heat sinks to help dissipate excess heat. The position of the lamp is controlled by a series of knobs on the side of the illuminator housing or is pre–centered specifically for the housing. Light from the lamphouse is directed into the microscope base through a collector lens (Figure 4.3), and then frequently through a sintered glass diffuser before being focused on the aperture diaphragm of the condenser.

4.4.1 Incandescent Lamps

Incandescent tungsten–based lamps are the primary illumination source used in modern microscopes, with the exception of those intended for fluorescence microscopy investigations. These lamps are thermal radiators that emit a continuous spectrum of light extending from about 300 nanometers to upward of 1200—1400 nanometers, with a majority of the wavelength intensity centered in the 600—1200 nanometer region as illustrated in Figure 4.4. Their design, construction, and operation is simple consisting of an enclosed glass bulb filled with an inert gas and containing a tungsten wire filament that is energized by a DC electric current. The bulbs produce a tremendous amount of heat and light, but the light accounts for only 5 to 10 percent of their energy output. Tungsten lamps (but not tungsten–halogen) are similar in operation to common household light bulbs and likewise tend to suffer several drawbacks such a decreased intensity with age and a blacking of the inside envelope as evaporated tungsten is slowly deposited. The color temperature and luminance of these lamps varies with the applied voltage, but average values range from about 2200 K to 3400 K. When these lamps are used in photomicrography with color film, the microscopists must use a lamp voltage that produces a color temperature matching that of the film emulsion, usually somewhere in the range between 3150 K and 3250 K. Often, the color temperature must be fine–tuned for photomicrography by inserting filters into the light path that balance the illumination for the color temperature of the film emulsion.

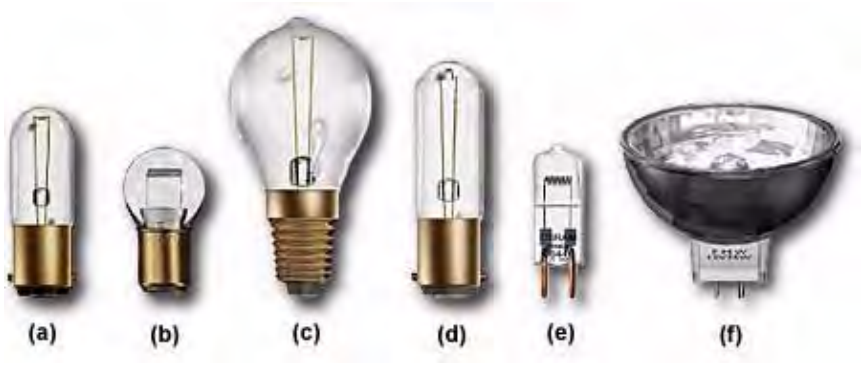

FIGURE 4.5: Incandescent light sources

Tungsten lamps vary widely in their design and the diverse set of models offered by manufacturers feature a variety of envelope shapes, mounting fixtures, and filament arrangements. A typical selection of tungsten lamps used in optical microscopy is illustrated in Figure 4.5. The bulb in Figure 4.5(a) is a 6—12 volt square tungsten filament with a bronze bayonet base that is designed to be used with the end of the cylindrical bulb facing the collector lens. The rounded–envelope bulb illustrated in Figure 4.5(b) also has a bronze bayonet base, but this less–powerful 6 volt bulb can be positioned to project light either sideways or end–on. The bulb in Figure 4.5(c) also has a rounded envelope, but is equipped with an Edison screw–thread base. With an operating voltage between 6 and 30 volts, this bulb is designed to be used end-on.

The bulb illustrated in Figure 4.5(d) is very similar to that in Figure 4.5(a), with the exception of having an extended glass envelope. It is equipped with a brass bayonet base and is a common design used in a number of microscopes built in Eastern Europe. A modern tungsten–halogen lamp (sometimes referred to as a quartz–iodine bulb) is illustrated in Figure 4.5(e). These lamps are now standard equipment on most microscopes manufactured in Japan, the United States, and Western Europe. Tungsten–halogen lamps have compact bulbs that introduce a number of advantages over normal incandescent lamps, most notably their brilliant light, smaller dimension, uniformity of illumination, longer lamp life and greater economy. Unlike tungsten-filament incandescent lamps, tungsten–halogen lamps have halogens added to the filler glass. The halogens (usually iodine) ensure that all vaporized tungsten is returned to the filament and not deposited upon the glass envelope.

CAUTION!

> Tungsten–halogen lamps operate at very high temperatures and may cause serious burn injuries if handled while hot. When replacing these lamps, always allow them to cool for at least 20 minutes before removing them from the lamphouse. Avoid handing the bulb envelope directly because fingerprints left on the envelope will become burned into the glass, often initiating premature lamp failure. Manufacturers package tungsten–halogen lamps in protective plastic bags to avoid handling problems. Use a pair of scissors to cut the bag near the tungsten pins and insert the lamp into its holder while it still remains in the bag. Remove the bag when the lamp is properly positioned in the lamphouse.

The filaments of tungsten–halogen lamps are often very compact arrays mounted in a borosilicate–halide glass (often termed "fused quartz") envelope. Operating voltages for

FIGURE 4.6: Fiber–optics lamphouse

these lamps range from 4—24 volts with power ratings from 20—100 watts. They have very high filament operating temperatures, restricting their use to well-ventilated lamphouses with fan-shaped heat sinks to eliminate the tremendous amount of heat generated by these bulbs. The base is a two-pin style with tungsten lead wires fused to the borosilicate glass envelope. Illumination from tungsten–halogen bulbs is remarkably uniform throughout the bulb life, which can range from 1000—2500 hours. Tungsten–halogen bulbs emit a continuous spectrum of light with a color temperature ranging from 2700—3350 K (depending upon voltage), although there is some decline in the color temperature value as the bulbs begin to age.

The lamp illustrated in Figure 4.5(f) is a tungsten–halogen dichroic reflector that is commonly used in fiber-optics light sources, like the one pictured above in Figure 4.6. The reflector aids in directing the light by allowing most of the infrared radiation generated by these bulbs to pass through the dichroic mirror reflector housing, while reflecting the shorter visible and near-ultraviolet wavelengths. These lamps operate at 6 to 21 volts DC and are usually placed in a lamphouse that provides for control of the operating voltage as well as removal of excess heat through cooling fans. Illuminators using these lamps are often termed "quartz–halogen" fiber optic lamphouses that provide high intensity illumination, but have the downside of producing a significant amount of infrared light in the form of heat. Direct lighting on a specimen will generally result in a high degree of heat absorption by the specimen, and care should be taken to ensure that this does not lead to degradation. The lamphouse illustrated in Figure 4.6 contains lens elements on the ends of the fiber optic tubes that allow the light to be focused onto the specimen.

Also available are other peripheral components such as colored glass filters to produce special effects lighting and polarizers that attach to the lens elements to allow illumination with polarized light. These light sources are often used as auxiliary oblique illumination for reflected light microscopy with compound and stereo microscopes. Specially designed ring illuminators, as depicted in Figure 4.7, can be used to create a bright, 360 cool white, shadow-free even-intensity illumination. They are designed to mount directly to stereo microscope objectives and are useful even with high-magnification and long working distance (1.5 to 10 inches) objectives without light adjustment when refocusing or when zoom features are used. Polarizing units are manufactured for the ring-light guides so that light reflected back into the objective can be polarized. There are also glass and gelatin filter kits that can be used with these lighting attachments.

Microscopes not equipped with an internal source of illumination must resort to external

FIGURE 4.7: Fiber–optic illuminator with ring–light guide

light sources to provide illumination for the sample. A typical external illumination source is illustrated in Figure 4.8. These illuminators may contain a variety of incandescent tungsten lamps including both 6—12 volt DC lamps as well as 120 volt coil-filament lamps that sport power ratings from 25—100 watts.

Direct current-powered versions of the external illumination source depicted in Figure 4.8 often have an external power supply that converts 120 volt wall power into the necessary 6—12 volts DC required by the lamp. These sources also are usually equipped with diffusers to even out the light intensity as well as filters to help with color balance. Some models also provide space for a polarizer so that polarized light microscopy can be conducted with the external lamp. The lamps often have a "field" diaphragm that allows the microscopist to adjust the diameter of the light beam entering the microscope. External light sources focus light onto a substage mirror that must be carefully adjusted to reflect light into the condenser at the proper angle to allow light entering the objective to be "centered" within the optical axis of the microscope.

4.4.2 Arc Lamps

Mercury vapor, xenon and zirconium arc lamps are also useful sources of illumination for specialized forms of microscopy. These lamps are controlled by external power supplies that are designed to meet the electrical requirements of first igniting the lamp, then providing the correct current to maintain constant illumination. Several typical arc lamp designs are illustrated in Figure 4.9. The lamp in Figure 4.9(a) is a mercury vapor lamp equipped with an igniter electrode and the lamp in Figure 4.9(b) is a modern HBO 200 watt mercury short arc lamp powered with alternating current through an external power supply. This and other similar arc lamp power supplies will furnish enough start-up power to ignite the burner (by ionization of the gaseous vapor) and keep it burning with a minimum of flicker.

Arc lamps have an average lifetime of about 200 hours and most external power supplies are equipped with a timer that allows the microscopist to monitor how much time has elapsed. Mercury arc lamps (often referred to as "burners") range in wattage from 50 watts to 200 watts and consist usually of two electrodes sealed under high pressure in a

FIGURE 4.8: External illumination source

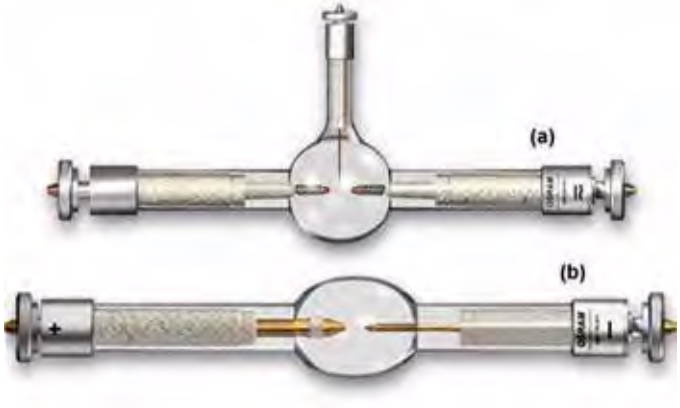

FIGURE 4.9: Arc lamps

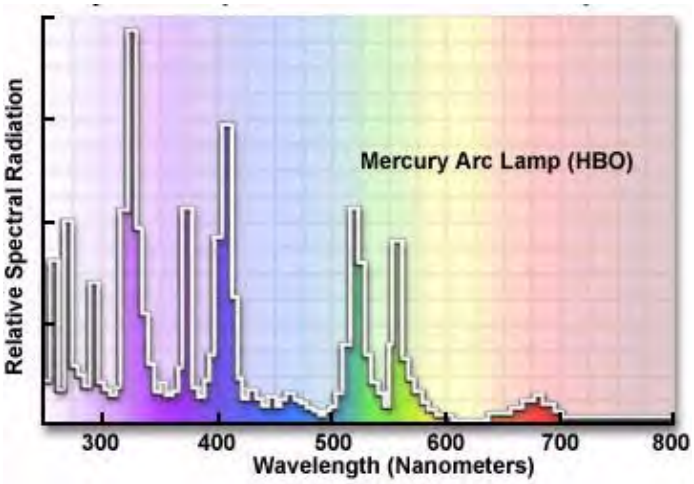

FIGURE 4.10: Mercury arc lamp (HBO)

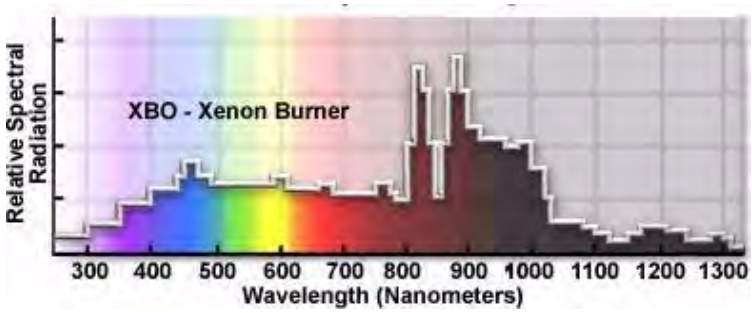

FIGURE 4.11: Xenon arc lamp emission spectrum

quartz glass envelope which also contains mercury. These arc lamps do not provide even intensity across the spectrum from near-ultraviolet to infrared (see Figure 4.10 for the emission spectrum of the mercury arc lamp).

Much of the intensity of the mercury arc lamp is expended in the near-ultraviolet, with peaks of intensity at 313, 334, 365, 406, 435, 546, and 578 nanometers. These lamps are not generally useful for most forms of microscopy (with the exception of fluorescence microscopy), but serve as excellent monochromatic light sources for black and white photomicrography. Using the appropriate filters, the green line at 546 nanometers, the blue line at 435 nanometers, and the near-ultraviolet line at 365 or 406 nanometers can yield excellent monochromatic light in selected wavelength regions. A mercury vapor arc lamp should never be used for brightfield, darkfield, DIC, or polarized color photomicrography because the limited emission spectrum of the lamps will not yield true color renditions of the specimen.

The xenon arc lamps have much more even intensity across the visible spectrum than do the mercury vapor lamps (see Figure 4.11); they do not have the very high spectral intensity peaks that are characteristic of the mercury lamps. Xenon lamps are deficient in the ultraviolet; they expend a large proportion of their intensity in the infrared, and therefore the use of such lamps requires care in control of heat. Short-gap xenon burners are usually more desirable because the size of the arc is such that its light may be much

more readily included within the back aperture of the objective, thus avoiding waste of light intensity.

CAUTION!

Mercury and Xenon arc lamps require caution during operation because of the danger of explosion due to very high internal gas pressures and extreme heat generated during use. Never ignite a lamp outside of its housing or observe the lamp directly when it is burning (this can cause serious eye damage). Neither mercury nor xenon lamps should be handled with bare fingers in order to avoid inadvertent etching of the quartz envelope. Change bulbs only after the lamp has had sufficient time to cool. Store lamps in their shipping containers to avoid accidents.

Always adhere to the safety procedures listed above when installing or changing mercury or xenon arc lamps. Mercury arc lamps, as described above, have a life of about 200 hours; xenon burners several hundreds of hours. Frequent on-off switching reduces lamp life. When the burners reach their rated lifetime, the spectral emissions may change and the quartz envelope weakens.

Zirconium arc lamps are another excellent source for microscope illumination. They provide a very small (almost a point source) beam of light that has a color temperature of about 3200 K. While these lamps do not emit light as bright as the mercury or xenon arc lamps, they do provide a continuous spectrum of light that is suitable for photomicrography using color film.

4.4.3 Laser Light Sources

In recent years, there has been increasing use of lasers, particular the argon–ion laser with powerful emission capability at 488 and 514 nanometers. Laser sources, despite the high cost, have become especially useful in laser scanning confocal microscopy.

There are a number of different types of lasers that each provide a unique emission spectrum. Figure 4.12 illustrates the emission spectra of the two most commonly used lasers in microscopy (fluorescence, confocal, and monochromatic brightfield).

4.4.4 Electronic Flash

A specialized method for photographing moving specimens (especially in darkfield illumination) has been devised using electronic photography flash systems. These flash tubes provide 5500 K illumination in an instantaneous burst that can capture great specimen detail when used with high speed (ISO 400 and above) daylight transparency film. These units must be accompanied by a continuous source of tungsten illumination to ensure framing of the specimen, Köhler illumination, focusing, and alignment of the microscope prior to the flash photomicrography. Flash tubes should be synchronized to the camera shutter of the microscope, and a number of manufacturers provide this equipment as an accessory for photomicrography.

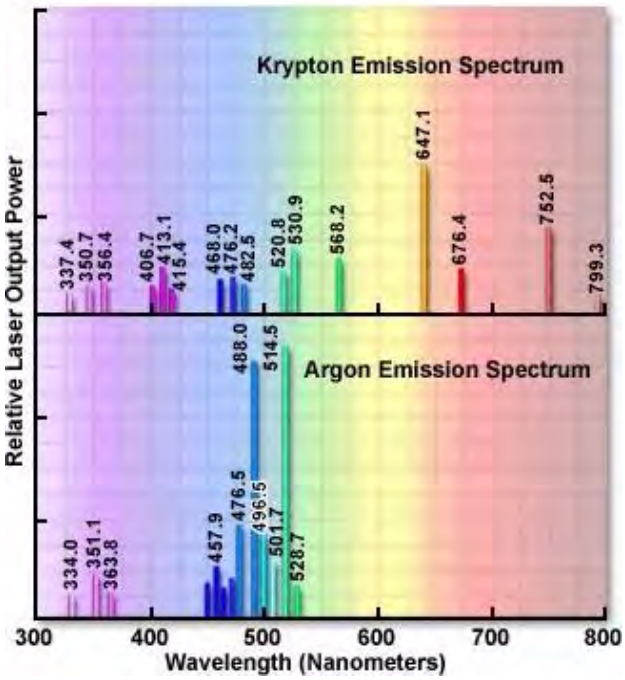

FIGURE 4.12: Laser illumination source emission spectra

Chapter 5

Köhler Illumination

Illumination of the specimen is the most important variable in achieving high-quality images in microscopy and critical photomicrography. Köhler illumination was first introduced in 1893 by August Köhler of the Carl Zeiss corporation as a method of providing the optimum specimen illumination.

This technique is recommended by all manufacturers of modern laboratory microscopes because it can produce specimen illumination that is uniformly bright and free from glare, thus allowing the user to realize the microscope's full potential.

The manufacturers have designed modern microscopes so that the collector lens and any other optical components built into the base of the microscope will project an enlarged and focused image of the lamp filament onto the plane of the aperture diaphragm of a properly positioned substage condenser. Closing or opening the condenser diaphragm controls the angle of the light rays emerging from the condenser and reaching the specimen from all azimuths. Because the light source is not focused at the level of the specimen, the light at specimen level is essentially grainless and extended and does not suffer deterioration from dust and imperfections on the glass surfaces of the condenser. Opening and closing of the condenser aperture diaphragm controls the angle of the light cone reaching the specimen. The setting of the condenser's aperture diaphragm, along with the aperture of the objective, determines the realized numerical aperture of the microscope "system". As the condenser diaphragm is opened, the working numerical aperture of the microscope increases, resulting in greater resolving power and light transmittance. Parallel light rays that pass through and illuminate the specimen are brought to focus at the back focal plane of the objective, where the image of the variable condenser aperture diaphragm and the image of the light source will be seen in focus.

The light pathways illustrated in Figure 5.1 are schematically drawn to represent separate paths taken by the specimen illuminating light rays and the image-forming light rays. This is not a true representation of any real segregation of these pathways, but a diagrammatic representation presented for purposes of visualization and discussion. Figure 5.1(a) shows the ray paths for illuminating light produce a focused image of the lamp filament at the plane of the substage condenser aperture diaphragm, the back focal plane of the objective, and the eyepoint (also called the Ramsden disk) of the eyepiece. These areas that are in common focus are often referred to as conjugate planes, which are critical in achieving proper Köhler illumination. By definition, an object that is in focus at one plane is also in focus at the other conjugate planes of that light path. In each light pathway (both image-forming and illumination), there are four separate planes that together make

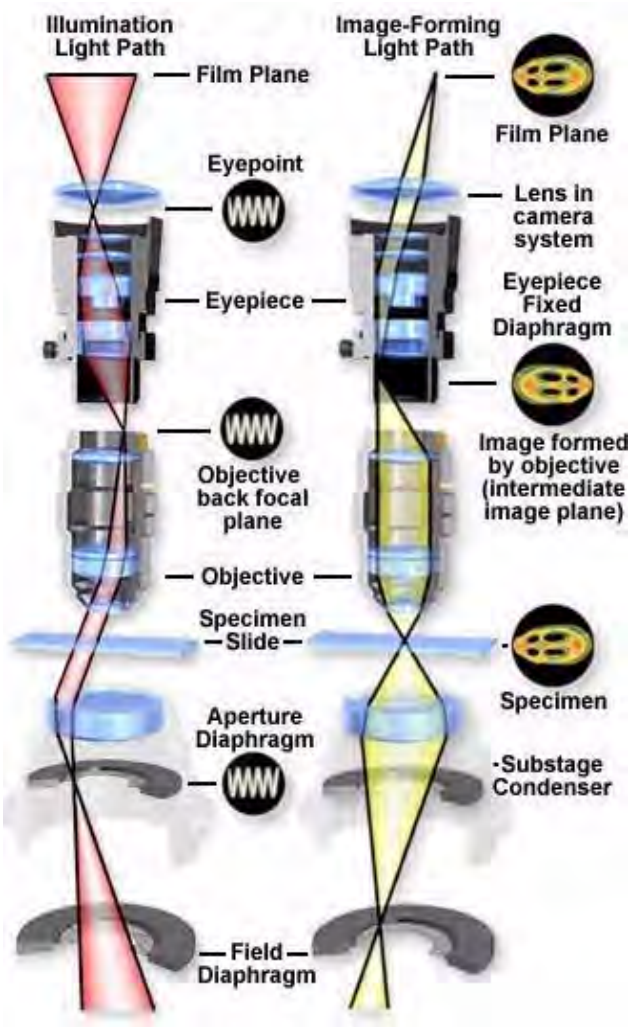

FIGURE 5.1: Köhler illumination

up the conjugate plane set.

Conjugate planes in the path of the illuminating light rays in Köhler illumination (Figure 5.1(a)) include:

- The lamp filament.
- The condenser aperture diaphragm (at the front focal plane of the condenser).
- The back focal plane of the objective.
- The eyepoint (also called the Ramsden disk) of the eyepiece, which is located approximately one-half inch (one centimeter) above the top lens of the eyepiece, at the point where the observer places the front of the eye during observation.

Likewise, the conjugate planes in the image-forming light path in Köhler illumination (Figure 5.1(b)) include:

- The field diaphragm.
- The focused specimen.
- The intermediate image plane (i.e., the plane of the fixed diaphragm of the eyepiece).
- The retina of the eye or the film plane of the camera.

Conjugate focal planes are often useful in troubleshooting a microscope for contaminating dust, fibers, and imperfections in the optical elements. If these artifacts are in sharp focus, it follows that they must reside on or near a surface that is part of the imaging-forming set of conjugate planes. Members of this set include the glass element at the microscope light port, the specimen, the reticle in the eyepiece, and the bottom lens element of the eyepiece. Alternatively, if these contaminants are fuzzy and out of focus, look for them near the illuminating set of elements that share conjugate planes. Suspects in this category are the condenser top lens (where dust and dirt often accumulate), the exposed eyepiece lens element (contaminants from eyelashes), and the objective front lens (usually fingerprint smudges).

Figure 5.2 illustrates a typical microscope setup where the lamp housing (illumination source) is attached to the base and projects light through several lenses and then through the substage condenser after being reflected by a mirror in the microscope base. The light source itself should be precentered or centerable to the optical axis of the microscope. Light emitted from the tungsten-halogen lamp filament first passes through the collector lens located close to the lamp housing, and then through a second lens that is closer to the field diaphragm. Often, a sintered or frosted glass filter is placed between the lamp and the collector lens to diffuse the light and ensure an even intensity of illumination. In practice, the image of the lamp filament is focused onto the front focal plane of the condenser while the diffuser glass is temporarily removed from the light path. The focal length of the collector lens must be carefully matched to the lamp filament dimensions to ensure that a filament image of the appropriate size is projected into the condenser aperture. For proper Köhler illumination, the image of the filament should completely fill the condenser aperture.

The second lens in the light path is called the field lens, which is responsible for bringing the image of the filament into focus at the plane of the substage condenser aperture

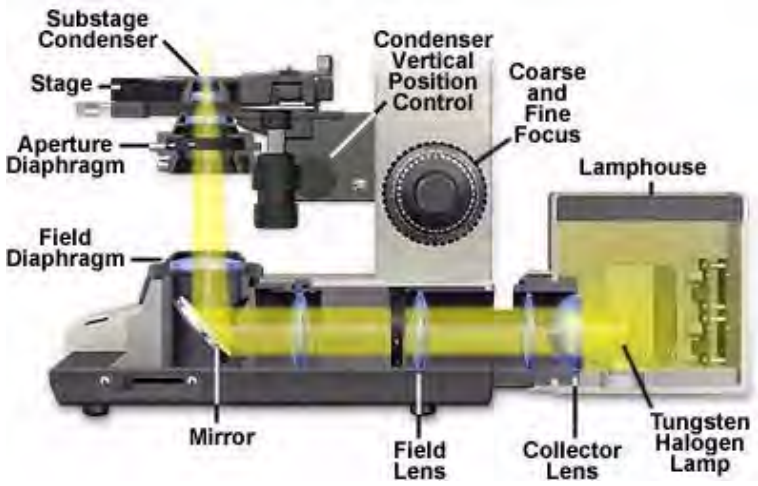

FIGURE 5.2: Microscope illumination system

diaphragm. Focused light leaving the field lens is reflected by a mirror (positioned at a 45-degree angle to the light path) through the field diaphragm and into the substage condenser. The field diaphragm serves as a virtual source of light for the microscope and its image is focused by the condenser onto the specimen plane. Optical designs for the arrangement of these elements may vary by microscope manufacturer, but the field diaphragm should be positioned at a sufficient distance from the field lens to eliminate dust and lens imperfections from being imaged in the plane of the specimen.

The field diaphragm in the base of the microscope controls only the width of the bundle of light rays reaching the condenser–it does not affect the optical resolution, numerical aperture, or the intensity of illumination. Proper adjustment of the field diaphragm (i.e., centered in the optical path and opened so as to lie just outside of the field of view) is important for preventing glare than can reduce contrast in the observed image. The elimination of excess light is particularly important when attempting to image samples with inherently low contrast. When the field diaphragm is opened too far, scattered light originating from the specimen and light reflected at oblique angles from optical surfaces can act to degrade image quality.

The substage condenser is typically mounted directly beneath the microscope stage in a bracket that can be raised or lowered independently of the stage by rotating a knurled knob, as illustrated in Figure 5.2. The aperture diaphragm is opened and closed with either a swinging arm, a lever, or by rotating a collar on the condenser housing. It should be noted that correct adjustment of the substage condenser is probably the most critical aspect of achieving proper Köhler illumination. Unfortunately, however, condenser misalignment and improperly adjusted condenser aperture diaphragms are the main source of image degradation and poor quality photomicrography.

When properly adjusted, light from the condenser will fill the back focal plane of the objective with image-forming light by projecting a cone of light to illuminate the field of view (A thorough discussion of substage condensers is included in another section of the primer). The condenser aperture diaphragm is responsible for controlling the angle of the illuminating light cone and, consequently, the numerical aperture of the condenser. This concept is illustrated in Figure 5.3, where a series of condensers are illustrated with light cones (and numerical apertures) of decreasing size from left to right in the figure.

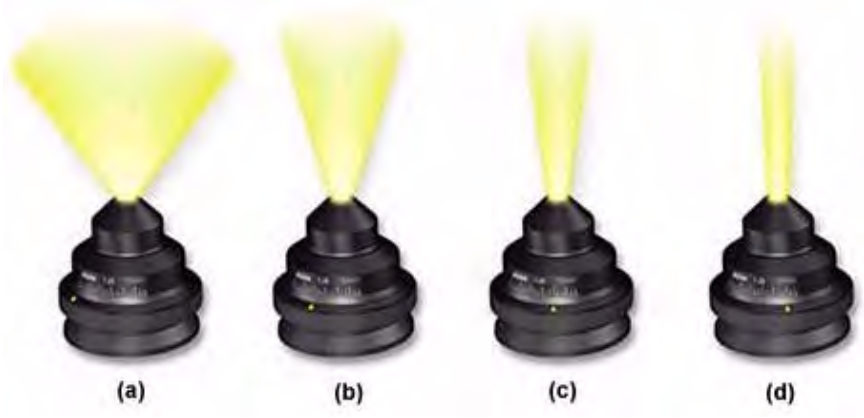

FIGURE 5.3: Condenser illuminating cones

Figure 5.3(a) illustrates a condenser of numerical aperture approximately 1.20, which has a broad light cone allowing imaging of the specimen with high numerical aperture objectives. Figures 5.3(b-d) show how reducing the size of the aperture diaphragm will produce a corresponding decrease in the light cone size and numerical aperture (Figure 5.3(b) NA=0.60; Figure 5.3(c) NA = 0.30; Figure 5.3(d) NA=0.15).

It is important to note, with respect to the size and shape of condenser light cones, that reducing the size of the field diaphragm only serves to slightly decrease the size of the lower portions of the light cones illustrated in Figure 5.3. The angle and numerical aperture of the light cone remains essentially unchanged with reduction in field diaphragm size. Another important concept, often overlooked by novices, is that the intensity of illumination should not be controlled through opening and closing the condenser aperture diaphragm, nor by shifting the condenser axially with respect to the optical center of the microscope. Illumination intensity should only be controlled through the use of neutral density filters placed into the light path or by reducing voltage to the lamp (although the latter is not usually recommended, especially for photomicrography). To ensure the maximum performance of the tungsten-halogen lamp, refer to the manufacturer's instrument manual to determine the optimum lamp voltage (usually 6—10 volts) and use that setting. Brightness of the illumination can then be easily controlled by adding or removing neutral density filters.

The size of the substage condenser aperture diaphragm should not only coincide with the desired numerical aperture, but also the quality of the resulting image should be considered. Generally, the aperture diaphragm should be adjusted to provide sufficient image contrast without being closed to the point of introducing a loss of resolution and detail. Refractive index and inherent specimen contrast are very important in determining the size of the aperture diaphragm. In general, the diaphragm should be set to a position that allows 60 to 90 percent of the entire light disc size (visible in the eye tube after removal of the eyepiece or with a Bertrand lens), although this may vary with extremes in specimen contrast.

The effects of condenser aperture setting on the quality of images captured by photomicrography are illustrated in Figure 5.4. The specimen is a thin section of Tilia (Basswood) stem stained with Fast Green and Eosin and photographed on Fujichrome 64T transparency film using a 40x Planachromat objective (NA = 0.75) and a swing-out top lens achromatic condenser (NA = 0.90). The approximate condenser aperture opening settings are: Fig-

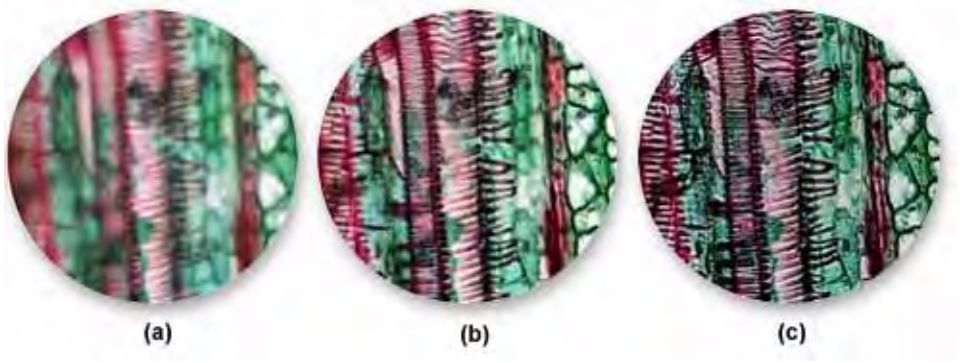

FIGURE 5.4: Condenser aperture size and image quality

ure 5.4(a) - 90 percent (NA = 0.81); Figure 5.4(b) - 60 percent (NA = 0.54); Figure 5.4(c) - 20 percent (NA = 0.18). The tissue section is selectively color stained to reveal fine detail and differentiate sub-cellular components for observation.

In Figure 5.4(a), where the aperture diaphragm is set to a position in which the numerical aperture of the condenser and objective are nearly equal, much of the fine specimen detail is visible, although there remains a considerable amount of scattering and glare. The image is also significantly brighter than its counterparts, which were made with a smaller setting of the aperture diaphragm. Figure 5.4(b) illustrates the Tilia stem at a condenser aperture size that produces a numerical aperture approximately 70 percent that of the objective. Glare is reduced, the image is very sharp, and fine image detail is present without significant diffraction artifacts. For this specimen, the photomicrograph in Figure 5.4(b) represents the optimum setting for the condenser aperture diaphragm. When the diaphragm is closed to the smallest setting at about 25 percent of the objective numerical aperture (Figure 5.4(c)), fine image details become obscured with diffraction artifacts and refraction phenomena. The image also takes on a darker overall cast that produces shifts in the color hues of the specimen.

From the above discussion it is evident that the condenser aperture diaphragm should be set to a position that will provide a compromise mixture of direct and deviated light that depends, to a large degree, on the absorption, diffraction, and refraction characteristics of the specimen. This must be accomplished without overwhelming the image with artifacts that obscure detail and present erroneous enhancement of contrast. The amount of image detail and contrast necessary to produce the best photomicrograph is also dependent upon refractive index, optical characteristics and other specimen-dependent parameters.

When the aperture diaphragm is erroneously closed too far, deviated light begins to obscure direct illuminating rays, resulting in diffraction artifacts that cause visible fringes, banding, and/or pattern formation in photomicrographs. Other problems, such as refraction phenomena, can also produce apparent structures in an image that are not real. Alternatively, opening the condenser aperture too wide causes unwanted glare and light scattering from the specimen and optical surfaces within the microscope. This leads to a significant loss of contrast and washing out of image detail. The correct setting will vary from specimen to specimen, and the experienced microscopist will soon learn to accurately adjust the condenser aperture diaphragm (and numerical aperture of the system) by observing the image without having to view the diaphragm in the back focal plane of the objective. In fact, many microscopists believe that critical reduction of the numerical

TABLE 5.1: Objective numerical aperture and field of view

Objective Designation	Numerical Aperture	Field of View Diameter
Planachromat 1x	0.04	18.0
Planachromat 2x	0.06	9.0
Planachromat 4x	0.10	4.50
Planachromat 5x	0.15	3.60
Planachromat 10x	0.25	1.80
Planachromat 20x	0.40	0.90
Planachromat 40x	0.65	0.45
Planapochromat 50x	0.90	0.36
Planapochromat 60x	0.95	0.30
Planapochromat 100x	1.40	0.18

aperture of the microscope system to optimize image quality is the single most important step in photomicrography.

The illumination system of the microscope, when adjusted for proper Köhler illumination, must satisfy several requirements. The illuminated area of the specimen plane must be at least as large as the field of view for any given objective. Also, the light must be of uniform intensity and the numerical aperture must vary from a maximum (equal to that of the objective) to a minimum value that will depend upon the optical characteristics of the specimen. Table 4.1 contains a list of objective numerical apertures versus the field of view diameter (for an eyepiece of field number 18) for each objective, ranging from very low to very high magnifications.

From the data presented in Table 5.1, it is obvious that the variation in field of view diameters is 100-fold going from the 1x Planachromat to the 100x Planapochromat. This yields an amazing 10,000-fold difference in the area of illumination between the 1x and 100x objectives. Such a wide range of illumination areas requires adjustments to many components in the optical path in order to accommodate all magnifications. These calculations were made assuming an eyepiece field number of 18, but many modern microscopes are equipped with wide field eyepieces having field numbers of 20 or 25. The field of view diameter (as given in column three of Table 5.1) can be recalculated for any eyepiece using the following formula:

$$D = \frac{\text{FN}}{M}$$

where D is the diameter of the field of view, FN is the eyepiece field number, and M is the objective magnification.

Modern microscopes are equipped with specialized substage condensers that have a swing-out lens, which can be removed from the optical path for use with lower power objectives (2x through 5x). This changes the performance of the remaining components in the light path, and some adjustment is necessary to achieve the best illumination conditions. The field diaphragm can no longer be used for alignment and centering of the substage condenser and is now ineffective in limiting the area of the specimen under illumination. Also, much of the unwanted glare once removed by the field diaphragm is reduced because the top lens of the condenser produces a light cone having a much lower numerical aperture, allowing light rays to pass through the specimen at much lower angles. Most importantly,

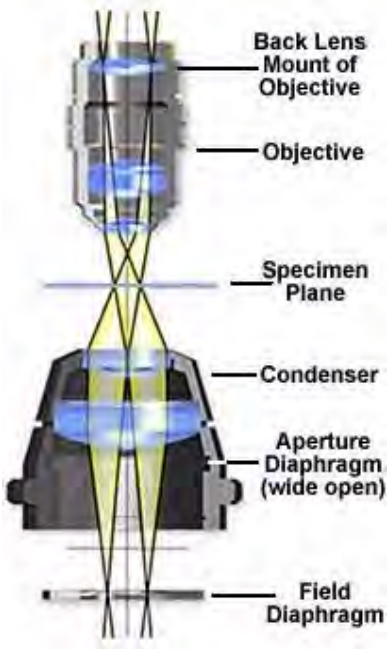

FIGURE 5.5: Low magnification light pathway

the optical conditions for Köhler illumination no longer apply.

Alignment of the microscope optical components and the establishment of Köhler illumination conditions should always be undertaken at a higher (10x) magnification before removing the swing-out condenser lens for work at lower (5x and below) magnifications. The height of the condenser should then not be changed. Condenser performance is radically changed when the swing-out lens is removed. The image of the lamp filament is no longer formed in the aperture diaphragm, which ceases to control the numerical aperture of the condenser and the illumination system. In fact, the aperture diaphragm should be opened completely to avoid vignetting, a gradual fading of light at the edges of the viewfield.

The modified optical pathway for transmitted light in a low power microscope system is illustrated in Figure 5.5. The field diaphragm is now positioned in the correct plane to act as an aperture stop to control the numerical aperture and the size and shape of the light cone for the illuminating and image-forming light rays passing through the condenser. The specimen plane is fully illuminated with equiangular cones (as in Köhler illumination), however the filament is now imaged at back lens mount of the objective instead of the back focal plane.

It is important to note that the image of the field diaphragm is no longer formed in the specimen plane, although the overall intensity of illumination is still uniform within the field of view, provided the lamp condenser lens is slightly diffusing (chemically etched) or frosted.

Contrast adjustment in low magnification microscopy is similar to the procedure using high magnification objectives, as illustrated in Figure 5.4. When the field diaphragm is wide open (greater than 80 percent), specimen details are washed out and a significant amount of scattering and glare is present. Closing the field diaphragm to a position between 50 and 80 percent will yield the best compromise on specimen contrast and depth

of field. Objectives designed for low magnification are significantly simpler in design than their higher magnification counterparts. This is due to the smaller angles of illuminating light cones produced by low magnification condensers, which require objectives of lower numerical aperture.

Measurement graticules, which must be in sharp focus and superimposed on the specimen image, can be inserted into several of the conjugate planes discussed above. The most common eyepiece (ocular) measuring and photomicrography graticules are placed in the intermediate image plane, which is a fixed aperture diaphragm within the eyepiece. It is theoretically possible to also place graticules in the specimen plane or in the plane of the illuminated field diaphragm. Stage micrometers are specialized "graticules" placed on microslides, which are used to calibrate eyepiece graticules and to make specimen measurements. Placing graticules in the plane of the field diaphragm is never done (to our knowledge) and would require a condenser of very high correction for aberration to completely eliminate artifacts and provide a sharp image for measurement.

Both color and neutral density filters are often placed within the optical pathway to reduce light intensity and alter the color characteristics of the illumination. There are several locations within the microscope stand where these filters are usually placed. Some modern laboratory microscopes have a filter holder sandwiched between the lamp housing and collector lens, which serves as an ideal location for these filters. Often, neutral density filters along with color correction filters and a frosted diffusion filter are placed together in this filter holder. Other microscope designs provide a set of filters built internally into the body which can be toggled into the light path by means of a lever. A third common location for filters is a holder mounted on the bottom of the substage condenser, significantly lower than the aperture diaphragm, that will accept gelatin or glass filters.

It is important not to place filters in or near any of the image-forming conjugate planes to avoid dirt or surface imperfections on the filters to be imaged along with the specimen. Some microscopes have an attachment for placing filters near the light port at the base (near the field diaphragm). This placement is probably too close to the field diaphragm, and surface contamination may be either in sharp focus or appear as blurred artifacts superimposed onto the image. It is also not wise to place filters directly on the microscope stage for the same reasons.

5.1 Transmitted Light

Adjustment of a transmitted light microscope for Köhler illumination is a logical and relatively easy process that should be practiced until mastered by all serious students of microscopy. Each time a microscope is turned on, it should be carefully inspected to ensure proper alignment of all optical components, and to guarantee that the lamp is centered and the condenser and field diaphragm are properly adjusted for Köhler illumination.

The microscope illustrated in Figure 5.6 uses an advanced external light source to provide illumination for the microscope. The lamp housing contains both a field diaphragm and collector lens, in addition to a tungsten-halogen bulb. A separate voltage regulator provides an adjustable direct-current voltage source for the lamp that varies between 5 and 12 volts. Modern microscopes usually contain a light source built into the base of the microscope, along with the collector lens and field diaphragm. Adjustment of microscopes with either internal or external light sources for Köhler illumination is similar in theory, however there are certain differences in the procedures that will be described below.

FIGURE 5.6: Trasmitted light microscope with external lamp and camera attachment

An important step in alignment of the microscope, whether it is for Köhler, Nelsonian, or any other strategy for illumination, is alignment of the light source (usually a tungsten-halogen bulb). Many modern microscopes now have pre-centered and pre-focused lamps, but older models still require the light source to be centered and focused by the user. We suggest consulting the owner's manual for instructions about how the lamp is to be centered and for other important information about the illumination source. The following procedures are recommended for aligning both external and internal lamps:

Internal Tungsten-Halogen Lamps

After switching on the lamp of the microscope, fully open both the field diaphragm (usually near the light port of the microscope) and the condenser aperture diaphragm (controlled by a collar or handle on the substage condenser housing).

- Some manufacturers provide a frosted glass filter for diffusing light emitted from the bulb. This filter is usually located in a filter holder adjacent to the lamp housing where it is attached to the body of the microscope. Remove this filter before proceeding with lamp alignment.

- Place a sheet of white paper, frosted glass, Kim-wipe, or lens-cleaning tissue on the microscope port and the image of the filament will be clearly visible as illustrated in Figure 5.7.

- Use the adjustment screws on the lamp housing to rotate the lamp (thus, the filament) in its holder and also to move it back and forth or up and down. Correctly manipulating the combination of lamp housing adjustments should ensure that the lamp

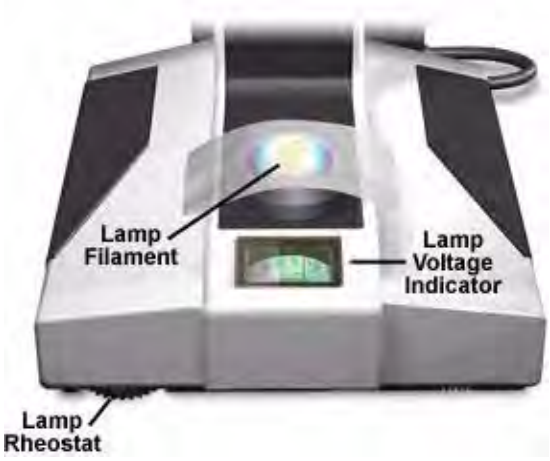

FIGURE 5.7: Centering an internal lamp

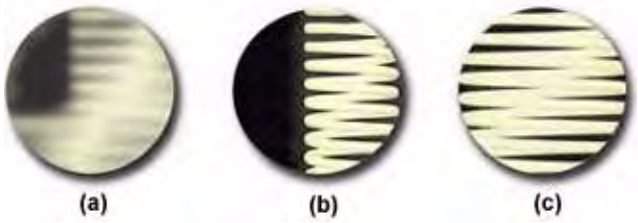

FIGURE 5.8: Lamp filament alignment

filament is centered in the optical pathway and is focused in the aperture diaphragm of the substage condenser.

Figure 5.8 illustrates a typical view of the microscope light port when the filament is made visible using the procedures outlined above. The port on the left in Figure 5.8(a) contains a filament that is severely out of alignment and not positioned properly to focus an image that will completely fill the aperture diaphragm nor the back focal plane of the objective. Using translational adjustments on the lamp housing, the filament is brought into focus (Figure 5.8(b)) and then centered within the light port (Figure 5.8(c)).

External Tungsten and Tungsten-Halogen Lamps

- Most external light sources are older and do not have pre-centered bulbs. The first step in centering an external tungsten-halogen lamp is to project an image of the filament onto a distant sheet of paper, supported by a book or the wall. Use the adjustment screws or knobs to rotate the filament about its own axis and ensure that it is centered within the optical axis of the condenser lens and field diaphragm, which are an integral part of the external illumination source.

- Place the external illuminator about 7-10 inches away from the reflector mirror located on the base of the microscope directly beneath the substage condenser (see Figure 5.6). Many of the mirrors on microscopes designed for external light sources are plano-concave and have one flat (planar) and one concave side. Be certain that the light

FIGURE 5.9: Centering an external lamp

source is reflecting from the flat surface of the mirror when using an external tungsten-halogen light source.

- The lamp filament should be centered in the mirror as illustrated in Figure 5.9. This can be checked in a manner analogous to the internal lamp by placing a piece of tissue paper over the mirror and visualizing where the filament image is projected. Make any adjustments necessary to bring the external illuminator in line with the microscope optical axis. After centering of the filament, the mirror should be positioned to project the reflection into the substage condenser. Check this by placing a piece of tissue paper over the stage opening. The filament should be out of focus, but framed squarely in the center of the stage opening.

5.1.1 Alignment of the Condenser and Field Diaphragm

- Rotate the nosepiece to bring the 10x objective into the light path. Next, place the specimen on the microscope stage and focus the microscope using the coarse and fine focusing knobs. This should be done by slowly raising the microscope stage while viewing the slide until it is very close to (but not touching!) the objective. At this point, the stage will have to be lowered slightly to bring the specimen into focus. This is an important concept which, when carried out properly, will avoid a collision between the objective and the specimen coverslip. Look through the eyepieces and slowly lower the stage, using the fine focus knob, until specimen details come into focus. The specimen should possess ample contrast and provide a sharp and crisp image. A highly stained biological tissue sample is excellent for aligning the microscope in brightfield mode, however optically birefringent samples can also be used when the microscope is equipped for polarized light or differential interference contrast.

- On binocular microscopes, adjust the eye tubes to coincide with your interpupillary distance. The single fused image should be visible through both eyes without significant movement of the head, and viewing should be comfortable. If only one person uses the microscope, this adjustment should not have to be made very often. Many binocular heads have a graded scale (Figure 5.11) that corresponds to the size of the interpupillary distance, allowing the microscopist to quickly adjust the eye tubes without viewing through them (the average interpupillary distance is 65 millimeters).

FIGURE 5.10: Binocular with grade scale

- On modern microscopes, the eye tubes are adjusted in a manner similar to a pair of binoculars. However, on many older models, the eye tubes slide back and forth in a single plane and adjusting them may involve slight changes to the microscope tube length. Regardless of the translation mechanism, the tubes should be positioned at a distance that allows comfortable viewing. Next, rotate the eye lens of the eyepiece that contains the graduated rule or photomicrography until markings on the graticule appear in sharp focus superimposed over a focused specimen. If no graticule is present, rotate the eye lens until the specimen is in focus.

- Diopter adjustment should be made to the eyepieces individually. Some microscopes have a graded scale on each eyepiece that indicates the position of the eyelens with respect to main body of the eyepiece. Other models hold the body of the eyepiece in a fixed position securely in the eye tube with a pin and slot. The first step is to either line up the graded markings on eyepieces equipped with such markings or turn the eye lenses clockwise to the shortest focal length position. Next, focus the specimen with the 10x objective and then rotate the nosepiece until a lower magnification objective (usually the 5x) is above the specimen. At this point, refocus each eye lens individually (do not use the microscope coarse or fine focus mechanisms) until the specimen is in sharp focus. Rotate the 20x objective into the optical path and refocus the microscope with the fine focus knob. Repeat the diopter eye lens adjustments with the 5x objective (again not disturbing the microscope fine focus mechanism), and the microscope should be adjusted to the correct diopter settings. These settings will vary from user to user, so record the position of the eye lenses if the eyepiece has a graded scale for quick return to the proper adjustment.

- Correct diopter adjustment allows for compensation between any differences in the user's left and right eye, so that the entire field of view appears in sharp focus through both eyepieces. This also enables the microscope to remain parfocal through all the different objectives in the nosepiece. Eyepiece diopter adjustment can also offset common vision problems, such as far or near sightedness, allowing the user to view specimens without eyeglasses. However, these eyepiece adjustments will not compensate for astigmatism, forcing users with this eye defect to wear their eyeglasses when examining specimens.

- The next step is to slowly close the field diaphragm (the adjustment is either on the external lamp housing or at the base of the microscope near the light port) to

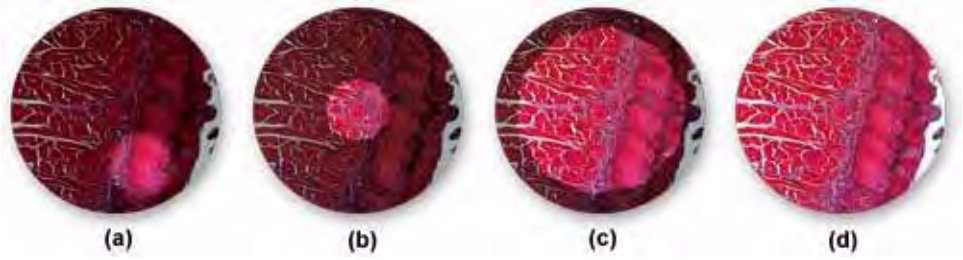

FIGURE 5.11: Field diaphragm alignment

its smallest setting until only a fuzzy outline shows in the viewfield (Figure 5.11(a)). The substage condenser is mounted on a rack that is (usually) controlled by a knurled knob for up and down movement with respect to the stage. Adjust this knob until the leaves of the field diaphragm are in sharp focus on top of the already-focused specimen, and then use the condenser centering screws to move the image of the field diaphragm to the center of the viewfield (and the optical axis of the microscope - Figure 5.11(b)).

- When raising or lowering the condenser to focus the leaves of the field diaphragm, the focused image of the diaphragm may have a red or blue halo surrounding the leaves. This is due to a lack of correction for chromatic aberration in the condenser. A condenser having good correction will yield a very sharp outline of the diaphragm with little or no color. The field diaphragm is now opened until about three-quarters of the viewfield is visible and the condenser is then refocused (Figure 5.11(c)). Check alignment of the condenser and re-adjust if necessary. Now open the field diaphragm until it is just beyond the field of view (for observation), or in the case of photomicrography, just beyond the graticule markings that define the area captured on film. Opening the field diaphragm any farther is unnecessary and will cause excessive glare and a loss of contrast.

- The next step is to remove one of the eyepieces and peer down the tube of the microscope as shown in Figure 5.12(a). As you view down the tube, open and close the condenser aperture diaphragm to see its image at the back focal plane of the objective. If there is a frosted diffuser filter built into the light path in the base of the microscope, an evenly lighted circle of light will be visible. If there is no such filter in the light path, you will instead see an image of the lamp filament as, illustrated in Figure 5.12(b) (a centering or phase telescope inserted in place of the removed eyepiece, or a Bertrand lens will make this adjustment easier to see).

- The purpose of this maneuver is to set the size of the aperture diaphragm to maximize image contrast and to obtain the best possible image of the specimen without introducing a loss of resolution due to refraction and diffraction artifacts. A general rule of thumb is to set the aperture diaphragm between 60 and 90 percent of the size of the entire light disc seen in the eyepiece tube.

In some instances the edge of the partially closed aperture diaphragm is not concentric with the illuminated back focal plane of the objective. This is due either to a misalignment of the substage condenser or the objective, and the manufacturer's instruction manual

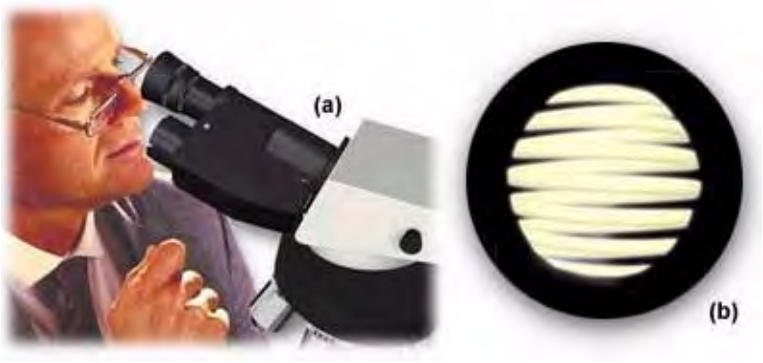

FIGURE 5.12: Observing the objective back focal plane

FIGURE 5.13: Swing–lens condenser

should be consulted for the correct centering regime. Some microscopes are shipped with the aperture diaphragm in a fixed and centered position that is impossible to change in the laboratory. Darkfield and phase contrast condensers usually always will provide a centering mechanism due to the crucial aspect of this step in setting up microscopes for these illumination methods. The condenser aperture should be centered with a 40x or 60x objective to avoid having to re-center the diaphragm with each objective (lower power objectives will almost always fall within acceptable margins using this method).

Now that Köhler illumination has been established with the 10x objective, it must be borne in mind that changing to a higher power objective will require a re-alignment of both the field and aperture diaphragms. For example, if you switch to the 40x objective, you will have to close the field diaphragm somewhat and re-center it (looking at a smaller area of the specimen). Also, the condenser aperture diaphragm should be opened slightly (the 40x objective has a higher numerical aperture than does the 10x objective). Each time an objective is changed, both diaphragms must be adjusted according to the steps outlined above.

The conditions of Köhler illumination do not apply at magnifications using lower power objectives (5x and below). When preparing for low magnification microscopy, first align the microscope and adjust the optical pathway for proper Köhler illumination using the 10x objective. Most modern microscope condensers have a top lens that swings out of the light path for use with objectives of 5x magnification and below, as illustrated in Figure 5.13. Other condenser models have top lenses that can be unscrewed or have a rotating turret

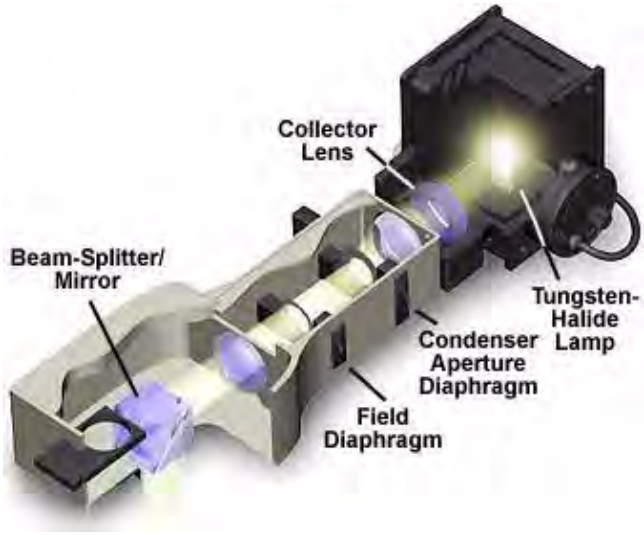

FIGURE 5.14: Reflected–light microscope illuminator

of condenser lenses for use with both low and high magnification objectives.

When the swing-out lens is removed from the optical pathway, condenser performance is radically changed and the aperture diaphragm no longer functions to control the numerical aperture of illuminating light rays. To avoid vignetting, the condenser aperture diaphragm should be opened to its widest setting, and specimen contrast is controlled with the field diaphragm, which now controls the numerical aperture of the illuminating light rays.

By properly adjusting the microscope for Köhler illumination, the specimen will be well-illuminated with even, glare-free light, giving good image resolution and contrast.

5.2 Reflected Light

In brightfield reflected light microscopy, proper use of the two variable diaphragms illustrated in Figure 5.14, the aperture iris diaphragm (closer to the light source) and the field iris diaphragm (closer to the specimen), enable the use of the highly desirable Köhler illumination.

These diaphragms are in the opposite of their respective positions in transmitted light, the aperture diaphragm now being closer to the light source. Such illumination provides bright light evenly dispersed across the plane of the field of view of the focused specimen. Köhler illumination provides glare-free light utilizing the maximum share of the objective's numerical aperture consistent with good contrast and resolution.

It is important to note, that in these reflected light systems, the objective serves a dual function: on the way down as a matching well-corrected condenser properly aligned; on the way up as an image-forming objective in the customary role of an objective projecting the image-carrying rays toward the eyepiece. In a transmitted light system, changing the objective requires an adjustment in the numerical aperture of the condenser to match that of the new objective. However, in reflected light, the objective and condenser numerical apertures change simultaneously with a new objective. Conjugate planes are similar to those described for transmitted light, with images of the light source being formed in the back focal plane of the objective and within the aperture diaphragm iris opening. This

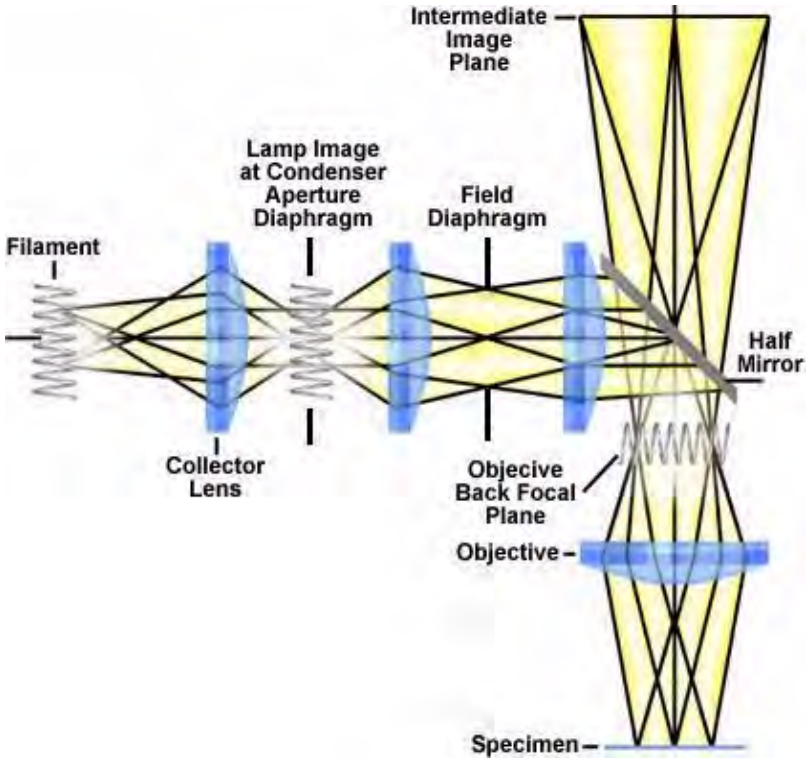

FIGURE 5.15: Köhler illumination for brightfield reflected light

serves to reduce the complexity of establishing the conditions of Köhler illumination in reflected light microscopy.

A function of Köhler illumination (aside from providing evenly dispersed illumination) is to ensure that the objective will be able to deliver excellent resolution and good contrast even if the source of light is a coil filament lamp. The aperture iris diaphragm controls the angle of light striking the specimen from every azimuth in a full cone in brightfield reflected light. The objective's numerical aperture determines the angle of light which can be "captured" as it is reflected from the specimen. Other factors being equal, the higher the numerical aperture, the better the resolution of the objective, i.e. the better the objective is able to clearly separate small details lying close together. The system's vertical illuminator contains the aperture iris diaphragm so that the back of the objective itself does not have to be occluded.

In Köhler illumination, the system is arranged (Figure 5.15) so that the image of the coil filament of the lamp is brought into focus at the plane of the aperture iris diaphragm; it is also in focus at the back focal plane of the objective. Assuming there is no frosted filter in the light path of the illuminator, when an eyepiece is removed, the image of the lamp filament can be seen at the back of the objective. In most systems, the lamp housing exterior has a set of centering screws (Figure 5.16), which enable you to center the lamp filament by moving the filament in a north-south or east-west direction. Also, the closing or opening of the aperture iris diaphragm is observable at the back focal plane of the objective, as described above.

The field iris diaphragm is conjugate (pre-focused) with the focused specimen, the intermediate image plane at the plane of the fixed diaphragm of the eyepiece, and the

FIGURE 5.16: Reflected–light lamp housing

retina of the eye.

Reflected light microscopy is of growing interest, especially in regard to its increasing usefulness in fluorescence microscopy. The rapidly growing semiconductor industry has also led to an increase in the use of reflected light microscopes, which continue to be very useful in classical applications such as metallography, ore petrography, and materials research.

In practice, the specimen is first focused with a medium magnification objective, usually the 10x, and the aperture of the pre-focused field diaphragm is closed until it is visible in the periphery of the viewfield. If the field iris diaphragm is not centered, the centering screws on the vertical illuminator are used to move a partially closed iris opening into the center of the field. The diaphragm is then opened until it just disappears from view or from the area delineated by the film frame in a photomicrography reticle. Next, the lamp filament is centered and focused (if this has not been done at the factory), and the aperture diaphragm is set for the optimum specimen contrast and image quality. These steps are discussed in detail in the sections below.

5.2.1 Adjustment of the Reflected Light Microscope for Köhler Illumination

EYEPIECES AND FIELD DIAPHRAGM

- Choose a sample that has a high degree of reflectivity to maximize the amount of light reflected back into the objective during the initial Köhler illumination configuration steps. An ideal choice is an integrated circuit on highly reflective silicon, a section of highly polished metal, or a smooth metallic thin film. The specimen should possess some degree of detail or texture that can be used to find the focal plane of the specimen.

- Place the reflective specimen on the stage and activate the light source, which is usually a tungsten-halogen bulb positioned in a lamp housing similar to the one illustrated in Figure 5.16. Rotate the nosepiece to position a medium power objective, such as the 10x, facing the specimen. If the bulb is working properly, a small circle of light about 3 millimeters in diameter should be projected by the objective onto the surface of the specimen.

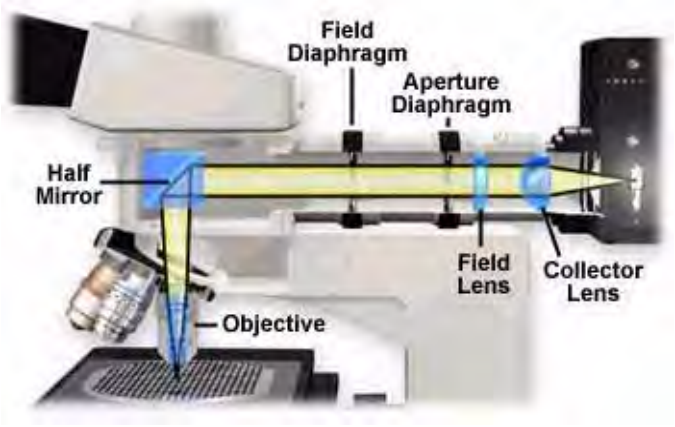

FIGURE 5.17: Reflected–light microscope illuminator

- While watching the objective and the specimen, use the coarse focus knob to raise the stage until it is a couple of millimeters below the front lens of the objective. Be very careful not to drive the specimen into the objective front lens. Next, while observing the specimen through the eyepieces, slowly lower the stage with (at first) the coarse and then the fine focus knob until specimen details come into sharp focus. If the focus point is missed, start over again with slightly less distance between the objective front lens and the specimen. In many instances it is easier to find the correct focus if the specimen is moving while trying to establish focus. Do this by either rotating a circular 360-degree stage or using the mechanical stage knobs to translate the specimen back and forth in the viewfield.

- Adjust the interpupillary distance on binocular microscopes once the specimen is in sharp focus. Diopter adjustments on each of the eyepieces should also be made at this time.

- Many polarizing and differential interference contrast (DIC) microscopes are equipped with circular graduated stages that rotate a full 360 degrees around the optical axis of the microscope. These microscopes are usually equipped with individual adjustments (through set screws in the nosepiece) for each objective to allow the optical axis of the objective to be made concentric with the optical axis of the microscope. It is a good idea to made this adjustment before proceeding.

- The next step is to adjust the field diaphragm, which is the iris diaphragm closest to the front of the microscope as illustrated in Figure 5.17. Sometimes the diaphragm is labeled “F” or “Field” directly on the illuminator housing. Use the lever adjustment to close the field iris diaphragm until you begin to see the leaves in the viewfield. Continue to close the diaphragm to the point where the lever stops and only a small opening is visible in the eyepieces. The specimen and the leaves of the diaphragm should both be in sharp focus, a setting that is usually made at the factory because most modern reflected light microscopes are not equipped to allow adjustment of the axial position of the field diaphragm (it cannot be focused). This is because the objective serves a dual role of also being the condenser, so critical focal planes are preset at the factory to minimize microscope alignment errors. In most instances,

there will be slight differences between the focus and center of the field diaphragm in the various objectives, but this small fluctuation can usually be neglected.

- There is a set of centering knobs located near the field diaphragm that allow the user to center the field diaphragm in the viewfield. Use these knobs to center the field diaphragm image, then slowly open the leaves until the diaphragm image is just outside the field of view. If photomicrography is the prime consideration, the field diaphragm should be opened only wide enough to allow the area outlined in the film frame (inscribed in a photomicrography reticle) to be visible. Changing objectives will not require adjustment of the field diaphragm size setting, because the new objective will also act as the condenser and the relationship will remain the same. This is easily verified by closing the field diaphragm to a pre-determined size in relation to the graticule. After changing the objective, the size of the image in the view field will change but the size relationship between the field diaphragm and the graticule will not.

Filament Alignment and Aperture Adjustment

- Just as with Köhler illumination in transmitted light, adjustment of the ("condenser") aperture diaphragm in reflected light is critical in controlling specimen contrast, reducing diffraction and glare artifacts, and producing the finest image quality. The image of the filament should be in focus and completely fill the aperture diaphragm, similar to the situation with transmitted light.

- The first step is to center and focus the lamp filament. Some modern reflected light microscopes (especially high-end research models) are equipped with a pre-centered tungsten-halogen lamp in a housing that is also fitted with a collector lens and a diffuser screen. There are no adjustments to these systems, but many older epi-illumination systems have lamps that must centered, and adjustment mechanisms are provided for this purpose. The first step is to remove (if possible) the glass diffusion filter that spreads illumination evenly over the view field. Next, use the adjustment knobs (see Figure 5.16) to center the filament while observing the conjugate image in the objective back focal plane. This is done in a manner similar to that for transmitted light microscopes, where the eyepiece is removed and the condenser aperture and filament image are viewed at the back focal plane of the objective through the eye tube.

- When the eyepiece is removed from the eye tube, an image of the lamp filament (in sharp focus) should be visible at the back focal plane of the objective, along with a partially closed aperture diaphragm. This observation is facilitated by using a phase telescope, a Bertrand lens (an accessory usually found on polarized light microscopes) or through an end cap with a pin hole in the center. The latter can be made from an eyepiece plug that is used to protect the microscope's interior during shipment. If the ground glass diffuser screen has not been (or can't be) removed, an evenly illuminated light disk should appear in place of the filament coils. If the filament is not centered, "hot spots" will appear in the light disk, which can be remedied by adjusting the screws on the lamphouse (Figure 5.16). Keep making incremental adjustments until illumination is uniform over the entire light disk.

- The last step is to adjust the opening of the aperture diaphragm, which is usually identified by the letter "A" or the word "Aperture" on the vertical illuminator's exterior. In a transmitted light microscope, the condenser aperture diaphragm must be readjusted each time a new objective of differing numerical aperture is inserted into the light path. This is due to the fact that the objective and condenser are separate entities and changing the objective numerical aperture does not affect the condenser. To compensate, the condenser aperture diaphragm must be opened or closed to provide an illuminating cone of light that matches the numerical aperture of the objective. However, in reflected light microscopy the objective also acts as the condenser (as discussed above, providing both illuminating and image-forming light pathways), and the numerical apertures change accordingly when a new objective is selected.

- Determining the correct setting of the aperture diaphragm is paramount in obtaining images that are free of diffraction artifacts, possess sufficient contrast, and are of the highest quality. Often, this results from a trade-off where a compromise is reached between maximizing image contrast without introducing erroneous artifacts due to refraction and diffraction. As mentioned above, the aperture diaphragm must be reset with each objective change in transmitted light microscopy. However, in reflected light microscopy, the objective and "condenser" change with simultaneous increments in numerical aperture and a single setting can be chosen for the aperture diaphragm. This setting is typically between 60 and 95 percent open, but will vary from specimen to specimen and will depend heavily upon the reflectivity of the specimen. Highly reflective specimens will require a smaller aperture to reduce glare and enhance contrast, but this is best undertaken on a case-by-case basis. The best procedure is to first open the aperture to its widest setting, then slowly close it while viewing the specimen to optimize contrast. In photomicrography, it is often wise to "bracket" a set of micrographs, each with a slightly different aperture size.

The techniques outlined above for brightfield reflected light microscopy also apply to microscopes equipped for crossed polarization, fluorescence, and differential interference contrast (DIC). In fact, the microscope can be adjusted for Köhler illumination while in any of these modes, and often contrast enhancements can be interchanged without the necessity of realigning the microscope illumination.

Chapter 6

Microscope Objectives

6.1 Introduction

Microscope objectives are perhaps the most important components of an optical microscope because they are responsible for primary image formation and play a central role in determining the quality of images that the microscope is capable of producing. Objectives are also instrumental in determining the magnification of a particular specimen and the resolution under which fine specimen detail can be observed in the microscope.

The objective is the most difficult component of an optical microscope to design and assemble, and is the first element that light encounters as it proceeds from the specimen to the image plane. Objectives derive their name from the fact that they are, by proximity, the closest component to the object (specimen) being imaged.

Major microscope manufacturers offer a wide range of objective designs, which feature excellent optical characteristics under a wide spectrum of illumination conditions and provide various degrees of correction for the primary optical aberrations. The objective illustrated in Figure 6.1 is a 250x long working distance apochromat, which contains 14 optical elements that are cemented together into three groups of lens doublets, a lens triplet group, and three individual internal single-element lenses. The objective also has a hemispherical front lens and a meniscus second lens, which work synchronously to assist in capturing light rays at high numerical aperture with a minimum of spherical aberration. Although not present on this objective, many high magnification objectives of similar design

FIGURE 6.1: LWD Plan Infinity-corrected Apochromat Objective

are equipped with a spring-loaded retractable nosecone assembly that protects the front lens elements and the specimen from collision damage. Internal lens elements are carefully oriented and tightly packed into a tubular brass housing that is encapsulated by the objective barrel. Specific objective parameters such as numerical aperture, magnification, optical tube length, degree of aberration correction, and other important characteristics are imprinted or engraved on the external portion of the barrel. Although the objective featured in Figure 6.1 is designed to operate utilizing air as the imaging medium between the objective front lens and specimen, other objectives have front lens elements that allow them to be immersed in water, glycerin, or a specialized hydrocarbon-based oil.

Modern objectives, made up of many glass elements, have reached a high state of quality and performance, with the extent of correction for aberrations and flatness of field determining the usefulness and cost of an objective. Construction techniques and materials used to manufacture objectives have greatly improved over the course of the past 100 years. Today, objectives are designed with the assistance of Computer-Aided-Design (CAD) systems using advanced rare-element glass formulations of uniform composition and quality having highly specific refractive indices. The enhanced performance that is demonstrated using these advanced techniques has allowed manufacturers to produce objectives that are very low in dispersion and corrected for most of the common optical artifacts such as coma, astigmatism, geometrical distortion, field curvature, spherical and chromatic aberration. Not only are microscope objectives now corrected for more aberrations over wider fields, but image flare has been dramatically reduced with a substantial increase in light transmission, yielding images that are remarkably bright, sharp, and crisp.

Three critical design characteristics of the objective set the ultimate resolution limit of the microscope. These include the wavelength of light used to illuminate the specimen, the angular aperture of the light cone captured by the objective, and the refractive index in the object space between the objective front lens and the specimen. Resolution for a diffraction-limited optical microscope can be described as the minimum detectable distance between two closely spaced specimen points:

$$R = \frac{\lambda}{2n(\sin(\theta))}$$

where R is the separation distance, λ is the illumination wavelength, n is the imaging medium refractive index, and θ is one-half of the objective angular aperture. In examining the equation, it becomes apparent that resolution is directly proportional to the illumination wavelength. The human eye responds to the wavelength region between 400 and 700 nanometers, which represents the visible light spectrum that is utilized for a majority of microscope observations. Resolution is also dependent upon the refractive index of the imaging medium and the objective angular aperture. Objectives are designed to image specimens either with air or a medium of higher refractive index between the front lens and the specimen. The field of view is often quite limited, and the front lens element of the objective is placed close to the specimen with which it must lie in optical contact. A gain in resolution by a factor of approximately 1.5 is attained when immersion oil is substituted for air as the imaging medium.

The last, but perhaps most important, factor in determining the resolution of an objective is the angular aperture, which has a practical upper limit of about 72 degrees (with a sine value of 0.95). When combined with refractive index, the product $n(\sin(\theta))$ is known as the numerical aperture (abbreviated NA), and provides a convenient indicator of the resolution for any particular objective. Numerical aperture is generally the most important

design criteria (other than magnification) to consider when selecting a microscope objective. Values range from 0.1 for very low magnification objectives (1x to 4x) to as much as 1.6 for high-performance objectives utilizing specialized immersion oils. As numerical aperture values increase for a series of objectives of the same magnification, we generally observe a greater light-gathering ability and increase in resolution. The microscopist should carefully choose the numerical aperture of an objective to match the magnification produced in the final image. Under the best circumstances, detail that is just resolved should be enlarged sufficiently to be viewed with comfort, but not to the point that empty magnification hampers observation of fine specimen detail.

Just as the brightness of illumination in a microscope is governed by the square of the working numerical aperture of the condenser, the brightness of an image produced by the objective is determined by the square of its numerical aperture. In addition, objective magnification also plays a role in determining image brightness, which is inversely proportional to the square of the lateral magnification. The square of the numerical aperture/magnification ratio expresses the light-gathering power of the objective when utilized with transmitted illumination. Because high numerical aperture objectives are often better corrected for aberration, they also collect more light and produce a brighter, more corrected image that is highly resolved. It should be noted that image brightness decreases rapidly as the magnification increases. In cases where the light level is a limiting factor, choose an objective with the highest numerical aperture, but having the lowest magnification factor capable of producing adequate resolution.

The least expensive (and most common) objectives, employed on a majority of laboratory microscopes, are the achromatic objectives. These objectives are corrected for axial chromatic aberration in two wavelengths (blue and red; about 486 and 656 nanometers, respectively), which are brought into a single common focal point. Furthermore, achromatic objectives are corrected for spherical aberration in the color green (546 nanometers; see Table 6.1). The limited correction of achromatic objectives can lead to substantial artifacts when specimens are examined and imaged with color microscopy and photomicrography. If focus is chosen in the green region of the spectrum, images will have a reddish-magenta halo (often termed residual color). Achromatic objectives yield their best results with light passed through a green filter (often an interference filter) and using black and white film when these objectives are employed for photomicrography. The lack of correction for flatness of field (or field curvature) further hampers achromat objectives. In the past few years, most manufacturers have begun providing flat-field corrections for achromat objectives and have given these corrected objectives the name of planachromats.

The next higher level of correction and cost is found in objectives called fluorites or semi-apochromats (illustrated by center objective in Figure 6.2), named for the mineral fluorite, which was originally used in their construction. Figure 6.2 depicts the three major classes of objectives: The achromats with the least amount of correction, as discussed above; the fluorites (or semi-apochromats) that have additional spherical corrections; and, the apochromats that are the most highly corrected objectives available. The objective positioned on the far left in Figure 6.2 is a 10x achromat, which contains two internal lens doublets and a front lens element. Illustrated in the center of Figure 6.2 is a 10x fluorite objective having several lens groups including two doublets and a triplet, in addition to a hemispherical front lens and a secondary meniscus lens. On the right in Figure 6.2 is a 10x apochromat objective that also contains multiple lens groups and single elements. Although similar in construction to fluorite objectives, the lenses have different thicknesses

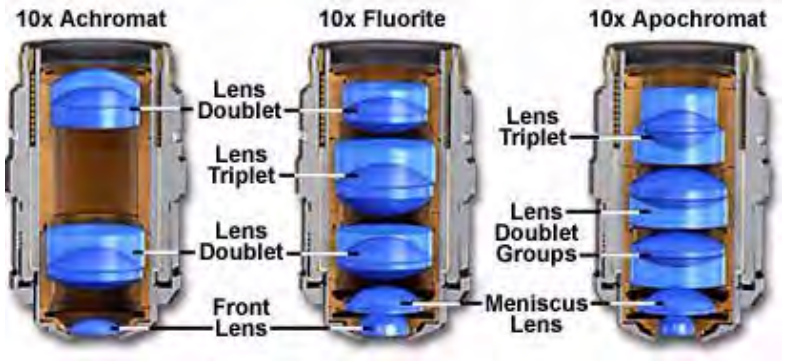

FIGURE 6.2: Common objective optical correction factor

TABLE 6.1: Objective Correction for Optical Aberration

Objective Type	Spherical Aberration	Chromatic Aberration	Field Curvature
Achromat	1 Color	2 Colors	No
Plan Achromat	1 Color	2 Colors	Yes
Fluorite	2-3 Colors	2-3 Colors	No
Plan Fluorite	3-4 Colors	2-4 Colors	Yes
Plan Apochromat	3-4 Colors	4-5 Colors	Yes

and curvatures and are arranged in a configuration that is unique to apochromat objectives.

During assembly of the objective, lenses are first strategically spaced and lap-seated into cell mounts, then packaged into a central sleeve cylinder that is mounted internally within the objective barrel. Individual lenses are seated against a brass shoulder mount with the lens spinning in a precise lathe chuck, followed by burnishing with a thin rim of metal that locks the lens (or lens group) into place. Spherical aberration is corrected by selecting the optimum set of spacers to fit between the lower two lens mounts (the hemispherical and meniscus lens). The objective is parfocalized by translating the entire lens cluster upward or downward within the sleeve with locking nuts so that objectives housed on a multiple nosepiece can be interchanged without losing focus. Adjustment for coma is accomplished with three centering screws that can optimize the position of internal lens groups with respect to the optical axis of the objective.

Fluorite objectives are produced from advanced glass formulations that contain materials such as fluorspar or newer synthetic substitutes. These new formulations allow for greatly improved correction of optical aberration. Similar to the achromats, the fluorite objectives are also corrected chromatically for red and blue light. In addition, the fluorites are also corrected spherically for two or three colors instead of a single color, as are achromats. The superior correction of fluorite objectives compared to achromats enables these objectives to be made with a higher numerical aperture, resulting in brighter images. Fluorite objectives also have better resolving power than achromats and provide a higher degree of contrast, making them better suited than achromats for color photomicrography in white light.

The highest level of correction (and expense) is found in apochromatic objectives, illus-

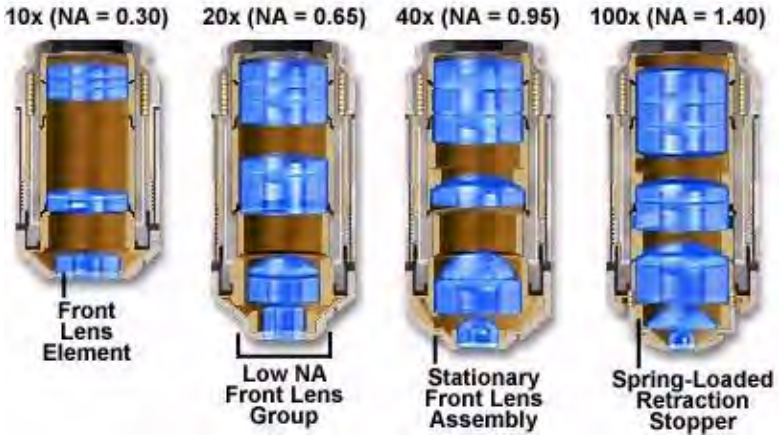

FIGURE 6.3: Apochromat objectives

trated in Figures 6.2 and 6.3. Apochromats represent the most highly corrected microscope lenses currently available, and their high price reflects the sophisticated design and careful assembly required in their manufacture. In Figure 6.3, we compare lens elements in a series of apochromatic objectives ranging from 10x to 100x in magnification. The lower power apochromat objectives (10x and 20x) have a longer working distance and the overall objective length is shorter than in higher power (40x and 100x) apochromat objectives. Traditionally, apochromats are corrected chromatically for three colors (red, green, and blue), almost eliminating chromatic aberration, and are corrected spherically for either two or three wavelengths (see Table 6.1). Apochromatic objectives are the best choice for color photomicrography in white light. Because of their high level of correction, apochromat objectives usually have, for a given magnification, higher numerical apertures than do achromats or fluorites. Many of the newer high-performance fluorite and apochromat objectives are corrected for four (dark blue, blue, green, and red) or more colors chromatically and four colors spherically.

All three types of objectives suffer from pronounced field curvature and project images that are curved rather than flat, an artifact that increases in severity with higher magnification. To overcome this inherent condition arising from curved lens surfaces, optical designers have produced flat-field corrected objectives, which yield images that are in common focus throughout the viewfield. Objectives that have flat-field correction and low distortion are called planachromats, planfluorites, or planapochromats, depending upon their degree of residual aberration. Such correction, although expensive, is quite valuable in digital imaging and conventional photomicrography.

Uncorrected field curvature is the most severe optical aberration that occurs in fluorite (semi-apochromat) and apochromat objectives, and it was tolerated as an unavoidable artifact for many years. During routine use, the viewfield would have to be continuously refocused between the center and the edges to capture all specimen details. The introduction of flat-field (plan) correction to objectives perfected their use for photomicrography and video microscopy, and today these corrections are standard in both general use and high-performance objectives. Correction for field curvature adds a considerable number of lens elements to the objective as illustrated in Figure 6.4 with a simple achromat. The uncorrected achromat on the left in Figure 6.4 contains two lens doublets, in addition to a simple thin-lens front element. In contrast, the corrected plan achromat on the right in

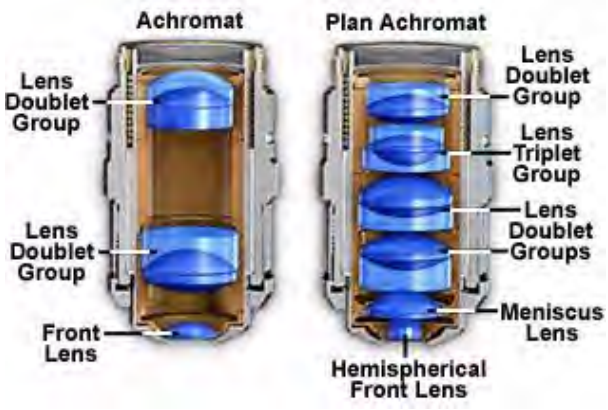

FIGURE 6.4: Objective correction for field curvature

Figure 6.4 contains three lens doublets, a central lens triplet group, and a meniscus lens positioned behind the hemispherical front lens. Plan correction, in this instance, has led to the addition of six lens elements bundled into more sophisticated lens groupings, which dramatically increases the optical complexity of the objective. The significant increase in lens elements for plan correction also occurs with fluorite and apochromat objectives, frequently resulting in an extremely tight fit of lens elements (see Figure 6.1) within the internal objective sleeve. In general, plan objectives corrected for field curvature sacrifice a considerable amount of free working distance, and many of the high-magnification versions have a concave front lens, which can be extremely difficult to clean and maintain.

Older objectives generally have lower numerical apertures, and are subject to an aberration termed chromatic difference of magnification that requires correction by the use of specially designed compensating oculars or eyepieces. This type of correction was prevalent during the reign of fixed tube length microscopes, but is not necessary with modern infinity-corrected objectives and microscopes. In recent years, modern microscope objectives have their correction for chromatic difference of magnification either built into the objectives themselves (Olympus and Nikon) or corrected in the tube lens (Leica and Zeiss).

The intermediate image in an infinity-corrected system appears at the reference focal length (formerly, the optical tube length) behind the tube lens in the optical pathway. This length varies between 160 and 250 millimeters, depending upon design constraints imposed by the manufacturer. The magnification of an infinity-corrected objective is calculated by dividing the reference focal length by the focal length of the objective lens.

In most biological and petrographic applications, a cover glass is utilized in mounting the specimen, both to protect the integrity of the specimen and to provide a clear window for observation. The cover glass acts to converge the light cones originating from each point in the specimen, but also introduces chromatic and spherical aberration (and consequent loss of contrast) that must be corrected by the objective. The degree to which light rays are converged is determined by the refractive index, dispersion, and thickness of the cover glass. Although the refractive index should be relatively constant within a batch of cover glasses, the thickness can vary between 0.13 and 0.22 millimeters. Another concern is the aqueous solvent or excess mounting medium that lies between the specimen and cover glass in wet or thickly mounted preparations. For example, in physiological saline whose refractive index is significantly different from that of the coverslip, the objective must focus through a layer of water only a few microns thick, leading to significant aberrations and a

deviation of the point spread function that is no longer symmetrical above and below the focal plane. These factors add to the effective variations in refractive index and thickness of the coverslip and are very difficult for the microscopist to control.

The imaging medium between the objective front lens and the specimen coverslip is also very important with respect to correction for spherical aberration and coma in the design of lens elements for objectives. Lower power objectives have relatively low numerical apertures and are designed to be used dry with only air as the imaging medium between the objective front lens and the cover glass. The maximum theoretical numerical aperture obtainable with air is 1.0, however in practice it is virtually impossible to produce a dry objective with a numerical aperture above 0.95. The effect of cover glass thickness variation is negligible for dry objectives having numerical apertures less than 0.4, but such deviation becomes significant at numerical apertures exceeding 0.65, where fluctuations as small as 0.01 millimeter can introduce spherical aberration. This poses problems with high-power apochromats, which must use very short working distances in air and contain sensitive corrections for spherical aberration that tend to make it difficult to obtain sharp images.

To remedy this, many high-performance apochromat dry objectives are fitted with correction collars, which allow adjustment to correct for spherical aberration by correcting for variations in cover glass thickness (see Figure 6.5). Optical correction for spherical aberration is produced by rotating the collar, which causes two of the lens element groups in the objective to move either closer together or farther apart. The objective on the left in Figure 6.5 has had the correction collar adjusted for a cover glass thickness of 0.20 mm by bringing the adjustable lens elements very close together. In contrast, the objective on the right in Figure 6.5 has the adjustable lens elements separated by a rather large distance to compensate for very thin cover glasses (0.13 mm). A majority of the correction collar objectives designed for upright transmitted light microscopy have an adjustment range for cover glass thickness variations between 0.10 and 0.23 millimeters. Many of the specialized phase contrast objectives designed for observing tissue culture specimens with an inverted microscope have an even broader compensation range of 0 to 2 millimeters. This allows specimens to be viewed through the bottom of most culture vessels, which often have dramatic thickness fluctuations in this size range. Uncovered specimens, such as blood smears, can also be observed with correction collar objectives when the adjustment is set to 0 to account for the lack of a cover glass.

High numerical aperture dry objectives lacking a correction collar often produce images that are inferior to those of lower numerical aperture objectives where cover glass thickness is of less concern. For this reason, it is often prudent to choose a lower magnification (and numerical aperture) objective in order to obtain superior contrast without the accompanying artifacts introduced by cover glass fluctuations. As an example, a 40x objective having a numerical aperture of 0.65 may be able to produce better images with sharper contrast and clarity than a 60x-0.85 numerical aperture objective, even though the resolving power of the higher magnification objective is theoretically greater.

The standard thickness for cover glasses is 0.17 millimeters, which is designated as a number 1 cover glass. Unfortunately, not all 1 cover glasses are manufactured to this close tolerance (they range from 0.16 to 0.19 millimeters) and many specimens have media between them and the cover glass. Compensation for cover glass thickness can be accomplished by adjusting the mechanical tube length of the microscope, or (as previously discussed) by the utilization of specialized correction collars that change the spacing between critical elements inside the objective barrel. The correction collar is utilized to adjust

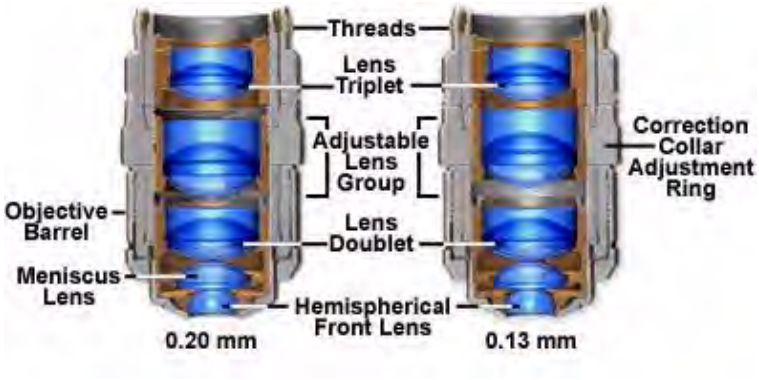

FIGURE 6.5: Correction collar for spherical aberration

for these subtle differences to ensure the optimum objective performance. Proper utilization of objective lenses with correction collars demands that the microscopist is experienced and alert enough to reset the collar using appropriate image criteria. In most cases, focus may shift and the image may wander during adjustment of the correction collar. Use the steps listed below to make small incremental adjustments to an objective's correction collar while observing changes in the specimen image.

- Position the correction collar so that the indicator mark on the objective barrel coincides with the 0.17 millimeter scale mark engraved on the collar housing.
- Place a specimen on the stage and focus the microscope on a small specimen feature.
- Rotate the correction collar very slightly and re-focus the objective to determine if the image has improved or degraded. Due to the fact that most specimen preparations suffer from cover glass/media sandwiches that are too thick, start the rotation experiment by trying larger compensation values (0.18-0.23) first.
- Repeat the previous step to determine if the image is improving or degrading as the correction collar is turned in a single direction.
- If the image has degraded, follow the same steps and rotate the correction collar in the opposite direction (toward lower values) to find the position offering optimum resolution and contrast.

Objective numerical aperture can be dramatically increased by designing the objective to be used with an immersion medium, such as oil, glycerin, or water. By using an immersion medium with a refractive index similar to that of the glass coverslip, image degradation due to thickness variations of the cover glass are practically eliminated whereby rays of wide obliquity no longer undergo refraction and are more readily grasped by the objective. Typical immersion oils have a refractive index of 1.51 and a dispersion similar to that of glass coverslips. Light rays passing through the specimen encounter a homogeneous medium between the coverslip and immersion oil and are not refracted as they enter the lens, but only as they leave its upper surface. It follows that if the specimen is placed at the aplanatic point of the first objective lens, imaging by this portion of the lens system is totally free of spherical aberration.

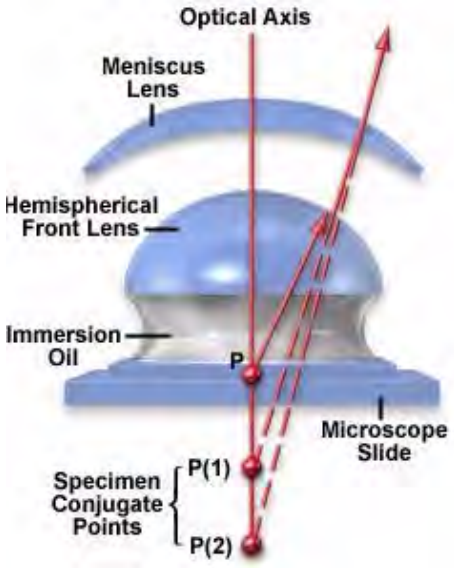

FIGURE 6.6: Oil–immersion microscope objective

The general design of a practical oil immersion objective includes a hemispherical front lens element, followed by a positive meniscus lens and a doublet lens group. Presented in Figure 6.6 are the aplanatic refractions that occur at the first two lens elements in a typical apochromatic oil immersion objective. The specimen is sandwiched between the microscope slide and cover glass at point P, the aplanatic point of the hemispherical lens element. Light rays refracted at the rear of the hemispherical lens appear to proceed from point P(1), which is also the center of curvature for the first surface of the meniscus lens. The refracted light rays enter the meniscus lens along the radius of its first surface and experience no refraction at that surface. At the rear surface of the meniscus lens, light rays are refracted aplanatically, so they appear to diverge from point P(2). Refraction of the light rays at the surfaces of subsequent lens groups in the objective complete the convergence of light rays originating from point P, thus forming the intermediate image.

Properly designed oil immersion objective lenses also correct for chromatic defects that are introduced by the first two lens elements, while introducing a minimum amount of spherical aberration. The fact that the light cone is partially converged before entering the first lens element aids in the control of spherical aberration. It should be noted that employing an oil immersion objective without the application oil between the coverslip and first lens element results in defective images. This due to refraction that occurs at the surface of the front lens, which introduces spherical aberration that cannot be corrected by subsequent lens components within the objective.

The advantages of oil immersion objectives are severely compromised if the wrong immersion fluid is utilized. Microscope manufacturers produce objectives with tight tolerances to refractive index and dispersion, which require matching values in the liquid placed between the cover glass and objective front lens. It is advisable to employ only the oil intended by the objective manufacturer, and to not mix immersion oils between manufacturers to avoid unpleasant artifacts such as crystallization or phase separation.

Objectives that use water and/or glycerin as an imaging medium are also available for applications with living cells in culture or sections of tissue immersed in physiological saline

solution. Plan apochromat water immersion lenses are equipped with correction collars and numerical apertures up to 1.2, slightly less than their oil immersion counterparts. These objectives allow microscopists to focus through up to 200 microns of aqueous media and still retain excellent optical correction. The downside is that high numerical aperture water immersion lenses often cost many thousands of dollars and the image can still degrade when the objective is focused deeply through refractile tissue or cell parts. For more details on water, glycerin, and oil immersion objectives, visit our section on immersion media in the microscopy primer.

There is a wealth of information inscribed on the objective barrel, as discussed in our section on specifications and identification of objectives. Briefly, each objective has inscribed on it the magnification (e.g. 10x, 20x or 40x etc.); the tube length for which the objective was designed to give its finest images (usually 160 millimeters or the Greek infinity symbol); and the thickness of cover glass protecting the specimen, which was assumed to have a constant value by the designer in correcting for spherical aberration (usually 0.17 millimeters). If the objective is designed to operate with a drop of oil between it and the specimen, the objective will be engraved OIL or OEL or HI (homogeneous immersion). In cases where these latter designations are not engraved on the objective, the objective is meant to be used dry, with air between the lowest part of the objective and the specimen. Objectives also always carry the engraving for the numerical aperture (NA) value. This may vary from 0.04 for low power objectives to 1.3 or 1.4 for high power oil-immersion apochromatic objectives. If the objective carries no designation of higher correction, one can usually assume it is an achromatic objective. More highly corrected objectives have inscriptions such as apochromat or apo, plan, FL, fluor, etc. Older objectives often have the focal length (lens-to-image distance) engraved on the barrel, which is a measure of the magnification. In modern microscopes, the objective is designed for a particular optical tube length, so including both the focal length and magnification on the barrel becomes somewhat redundant.

Tables 6.2–6.3 lists working distance and numerical aperture as a function of magnification for the four most common classes of objectives: achromats, planachromats, planfluorites, and planapochromats. Note that dry objectives all have a numerical aperture value of less than 1.0 and only objectives designed for liquid immersion media have a numerical aperture that exceeds this value.

When a manufacturer's set of matched objectives, e.g. all achromatic objectives of various magnifications (a single subset of the objectives listed in Tables 6.2–6.3), are mounted on the nosepiece, they are usually designed to project an image to approximately the same plane in the body tube. Thus, changing objectives by rotating the nosepiece usually requires only minimal use of the fine adjustment knob to re-establish sharp focus. Such a set of objectives is described as being parfocal, a useful convenience and safety feature. Matched sets of objectives are also designed to be parcentric, so that a specimen centered in the field of view for one objective remains centered when the nosepiece is rotated to bring another objective into use.

For many years, objective lenses designed for biological applications from most manufacturers all conformed to an international standard of parfocal distance. Thus, a majority of objectives had a parfocal distance of 45.0 millimeters and were considered interchangeable. With the migration to infinity-corrected tube lengths, a new set of design criteria emerged to correct for aberrations in the objective and tube lenses. Coupled to an increased demand for greater flexibility to accommodate the need for ever-greater working distances

TABLE 6.2: Objective Specifications by Magnification

Magnification	Numerical Aperture	Working Distance (mm)
	Achromat	
4x	0.10	30.00
10x	0.25	6.10
20x	0.40	2.10
40x	0.65	0.65
60x	0.80	0.30
100x (oil)	1.25	0.18
	Plan Achromat	
0.5x	0.02	7.00
1x	0.04	3.20
2x	0.06	7.50
4x	0.10	30.00
10x	0.25	10.50
20x	0.40	1.30
40x	0.65	0.57
50x (oil)	0.90	0.40
100x (oil)	1.25	0.17
40x	0.65	0.48
100x	0.90	0.26
	Plan Fluorite	
4x	0.13	17.10
10x	0.30	16.00
20x	0.50	2.10
40x	0.75	0.72
40x (oil)	1.30	0.2
60x	0.85	0.3
100x (dry)	0.90	0.30
100x (oil)	1.30	0.20
100x (oil with iris)	0.5—1.3	0.20

TABLE 6.3: Objective Specifications by Magnification

Magnification	Numerical Aperture	Working Distance (mm)
	Plan Apochromat	
2x	0.10	8.50
4x	0.20	15.70
10x	0.45	4.00
20x	0.75	1.00
40x	0.95	0.14
40x (oil)	1.00	0.16
60x	0.95	0.15
60x (oil)	1.40	0.21
60x (water immersion)	1.20	0.22
100x (oil)	1.40	0.13
100x (NCG oil)	1.40	0.17

NCG = No Cover Glass

with higher numerical apertures and field sizes, interchangeability between objective lenses from different manufacturers disappeared. This transition is exemplified by the modern Nikon CFI-60 optical system that features "Chrome Free" objectives, tube lenses, and eyepieces. Each component in the CFI-60 system is separately corrected without one being utilized to achieve correction for another. The tube length is set to infinity (parallel light path) using a tube lens, and the parfocal distance has been increased to 60 millimeters. Even the objective mounting thread size has been altered from 20.32 to 25 millimeters to meet new requirements of the optical system.

The field diameter in an optical microscope is expressed by the field-of-view number or simply field number, which is the diameter of the viewfield expressed in millimeters and measured at the intermediate image plane. The field diameter in the object (specimen) plane becomes the field number divided by the magnification of the objective. Although the field number is often limited by the magnification and diameter of the ocular (eyepiece) field diaphragm, there is clearly a limit that is also imposed by the design of the objective. In early microscope objectives, the maximum usable field diameter was limited to about 18 millimeters (or considerably less for high magnification eyepieces), but modern planapochromats and other specialized flat-field objectives often have a usable field that can range between 22 and 28 millimeters or more when combined with wide-field eyepieces. Unfortunately, the maximum useful field number is not generally engraved on the objective barrel and is also not commonly listed in microscope catalogs.

The axial range through which an objective can be focused without any appreciable change in image sharpness is referred to as the depth of field. This value varies radically from low to high numerical aperture objectives, usually decreasing with increasing numerical aperture (see Table 6.4 and Figure 6.7). At high numerical apertures, the depth of field is determined primarily by wave optics, while at lower numerical apertures, the geometrical optical "circle of confusion" dominates. The total depth of field is given by the sum of the wave and geometrical optical depths of field as:

$$d_{tot} = \frac{\lambda n}{\mathrm{NA}^2} + \left(\frac{n}{M \cdot \mathrm{NA}}\right) e$$

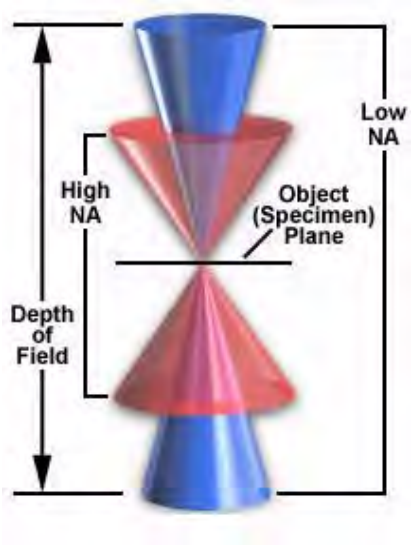

FIGURE 6.7: Depth of field ranges

TABLE 6.4: Depth of Field and Image Depth

Magnification	NA	Depth of Field(mm)	Image Depth(mm)
4x	0.10	15.5	0.13
10x	0.25	8.5	0.80
20x	0.40	5.8	3.8
40x	0.65	1.0	12.8
60x	0.85	0.40	29.8
100x	0.95	0.19	80.0

where l is the wavelength of illumination, n is the refractive index of the imaging medium, NA is the objective numerical aperture, M is the objective lateral magnification, and e is the smallest distance that can be resolved by a detector that is placed in the image plane of the objective. Notice that the diffraction-limited depth of field (the first term on the right-hand side of the equation) shrinks inversely with the square of the numerical aperture, while the lateral limit of resolution is reduced with the first power of the numerical aperture. The result is that axial resolution and the thickness of optical sections are affected by the system numerical aperture much more than is the lateral resolution of the microscope (see Table 6.4).

The clearance distance between the closest surface of the cover glass and the objective front lens is termed the working distance. In situations where the specimen is designed to be imaged without a cover glass, the working distance is measured at the actual surface of the specimen. Generally, working distance decreases in a series of matched objectives as the magnification and numerical aperture increase (see Tables 6.2–6.3). Objectives intended to view specimens with air as the imaging medium should have working distances as long as possible, provided that numerical aperture requirements are satisfied. Immersion objectives, on the other hand, should have shallower working distances in order to contain the immersion liquid between the front lens and the specimen. Many objectives designed with close working distances have a spring-loaded retraction stopper that allows the front

lens assembly to be retracted by pushing it into the objective body and twisting to lock it into place. Such an accessory is convenient when the objective is rotated in the nosepiece so it will not drag immersion oil across the surface of a clean slide. Twisting the retraction stopper in the opposite direction releases the lens assembly for use. In some applications (see below), a long free working distance is indispensable, and special objectives are designed for such use despite the difficulty involved in achieving large numerical apertures and the necessary degree of optical correction.

One of the most significant advances in objective design during recent years is the improvement in antireflection coating technology, which helps to reduce unwanted reflections that occur when light passes through a lens system. Each uncoated air-glass interface can reflect between four and five percent of an incident light beam normal to the surface, resulting in a transmission value of 95-96 percent at normal incidence. Application of a quarter-wavelength thick antireflection coating having the appropriate refractive index can increase this value by three to four percent. As objectives become more sophisticated with an ever-increasing number of lens elements, the need to eliminate internal reflections grows correspondingly. Some modern objective lenses with a high degree of correction can contain as many as 15 lens elements having many air-glass interfaces. If the lenses were uncoated, the reflection losses of axial rays alone would drop transmittance values to around 50 percent. The single-layer lens coatings once utilized to reduce glare and improve transmission have now been supplanted by multilayer coatings that produce transmission values exceeding 99.9 percent in the visible spectral range.

Illustrated in Figure 6.8 is a schematic drawing of light waves reflecting and/or passing through a lens element coated with two antireflection layers. The incident wave strikes the first layer (Layer A in Figure 6.3) at an angle, resulting in part of the light being reflected (R(o)) and part being transmitted through the first layer. Upon encountering the second antireflection layer (Layer B), another portion of the light is reflected at the same angle and interferes with light reflected from the first layer. Some of the remaining light waves continue on to the glass surface where they are again both reflected and transmitted. Light reflected from the glass surface interferes (both constructively and destructively) with light reflected from the antireflection layers. The refractive indices of the antireflection layers vary from that of the glass and the surrounding medium (air). As the light waves pass through the antireflection layers and glass surface, a majority of the light (depending upon the incident angle–usual normal to the lens in optical microscopy) is ultimately transmitted through the glass and focused to form an image.

Magnesium fluoride is one of many materials utilized in thin-layer optical antireflection coatings, but most microscope manufacturers now produce their own proprietary formulations. The general result is a dramatic improvement in contrast and transmission of visible wavelengths with a concurrent destructive interference in harmonically-related frequencies lying outside the transmission band. These specialized coatings can be easily damaged by mis-handling and the microscopist should be aware of this vulnerability. Multilayer antireflection coatings have a slightly greenish tint, as opposed to the purplish tint of single-layer coatings, an observation that can be employed to distinguish between coatings. The surface layer of antireflection coatings used on internal lenses is often much softer than corresponding coatings designed to protect external lens surfaces. Great care should be taken when cleaning optical surfaces that have been coated with thin films, especially if the microscope has been disassembled and the internal lens elements are subject to scrutiny.

The focal length of a lens system is defined as the distance from the lens center to a point

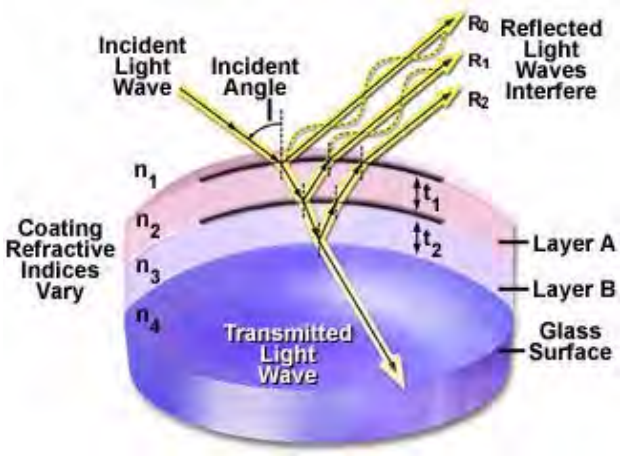

FIGURE 6.8: Geometry of antireflective coatings

where parallel rays are focused on the optical axis (often termed the principal focal point). An imaginary plane perpendicular to the principal focal point is called the focal plane of the lens system. Every lens has two principal focal points for light entering each side, one in front and one at the rear. By convention, the objective focal plane that is nearer to the front lens element is known as the front focal plane and the focal plane located behind the objective is termed the rear focal plane. The actual position of the rear focal plane varies with objective construction, but is generally situated somewhere inside the objective barrel for high magnification objectives. Objectives of lower magnification often have a rear focal plane that is exterior to the barrel, located in the thread area or within the microscope nosepiece.

As light rays pass through an objective, they are restricted by the rear aperture or exit pupil of the objective. The diameter of this aperture varies between 12 millimeters for low magnification objectives down to around 5 millimeters for the highest power apochromatic objectives. Aperture size is extremely critical for epi-illumination applications that rely on the objective to act as both an imaging system and condenser, where the exit pupil also becomes an entrance pupil. The image of the light source must completely fill the objective rear aperture to produce even illumination across the viewfield. If the light source image is smaller than the aperture, the viewfield will experience vignetting from uneven illumination. On the other hand, if the light source image is larger than the rear aperture, some light does not enter the objective and the intensity of illumination is reduced.

In conclusion, the development of high quality microscope objectives was ushered by Ernst Abbe, who first developed apochromatic objectives and compensating oculars during the late 1880s in collaboration with Carl Zeiss and Otto Schott. The next major advance in objective design occurred when Hans Boegehold (Zeiss) constructed the first plan achromat and plan apochromat objectives in the late 1930s. More recently, the development of "Chrome Free" (CF) optics by Zenji Wahimoto (Nikon) and Horst Riesenberg (Zeiss) has led to a new revolution in microscope objective design.

Many of the microscope objectives being produced today offer remarkably low degrees of aberration and other imperfections, provided the appropriate objective is selected and it is utilized properly. Nevertheless, the microscopist needs to be aware that objectives are not made to be perfect from every standpoint, but are designed to meet a certain set

FIGURE 6.9: 60x plan apochromat objective

of specifications depending on intended use, constraints on physical dimensions, and price ranges. Therefore, objectives are made with different degrees of correction for chromatic and spherical aberration, field size and flatness, transmission wavelengths, freedom from fluorescence, birefringence, and other factors contributing to background noise. In addition, they are designed to be used under certain circumscribed conditions, such as with specific tube lengths and tube lenses, type and thickness of immersion media and coverslips, wavelength ranges, field sizes, ocular types, and special condensers. The ultimate goal of the optical microscope is to provide useful magnification that allows minute specimens to be observed in great detail, thus exposing a hidden world of invisible objects that would otherwise remain unseen.

6.2 Specifications and Identification

Identification of the properties of individual objectives is usually very easy because important parameters are often inscribed on the outer housing (or barrel) of the objective itself as illustrated in Figure 6.9. This figure depicts a typical 60x plan apochromat objective, including common engravings that contain all of the specifications necessary to determine what the objective is designed for and the conditions necessary for proper use.

Microscope manufacturers offer a wide range of objective designs to meet the performance needs of specialized imaging methods, to compensate for cover glass thickness variations, and to increase the effective working distance of the objective. Often, the function of a particular objective is not obvious simply by looking at the construction of the objective. Finite microscope objectives are designed to project a diffraction-limited image at a fixed plane (the intermediate image plane), which is dictated by the microscope tube length and located at a pre-specified distance from the rear focal plane of the objective. Microscope objectives are usually designed to be used with a specific group of oculars and/or tube lenses strategically placed to assist in the removal of residual optical errors. As an example, older Nikon and Olympus compensating eyepieces were used with high numerical aperture fluorite and apochromatic objectives to eliminate lateral chromatic aberration and improve flatness of field. Newer microscopes (from Nikon and Olympus) have objectives

that are fully corrected and do not require additional corrections from the eyepieces or tube lenses.

Most manufacturers have now transitioned to infinity-corrected objectives that project emerging rays in parallel bundles from every azimuth to infinity. These objectives require a tube lens in the light path to bring the image into focus at the intermediate image plane. Infinity-corrected and finite-tube length microscope objectives are not interchangeable and must be matched not only to a specific type of microscope, but often to a particular microscope from a single manufacturer. For example, Nikon infinity-corrected objectives are not interchangeable with Olympus infinity-corrected objectives, not only because of tube length differences, but also because the mounting threads are not the same pitch or diameter. Objectives usually contain an inscription denoting the tube focal length as will be discussed.

There is a wealth of information inscribed on the barrel of each objective, which can be broken down into several categories. These include the linear magnification, numerical aperture value, optical corrections, microscope body tube length, the type of medium the objective is designed for, and other critical factors in deciding if the objective will perform as needed. A more detailed discussion of these properties is provided below and in links to other pages dealing with specific issues.

Manufacturer The name of the objective manufacturer is almost always included on the objective. The objective illustrated in Figure 6.9 was made by a fictitious company named Nippon from Japan, but comparable objectives are manufactured by Nikon, Olympus, Zeiss, and Leica, companies who are some of the most respected manufacturers in the microscope business.

Linear Magnification In the case of the apochromatic objective in Figure 6.9, the linear magnification is 60x, although the manufacturers produce objectives ranging in linear magnification from 0.5x to 250x with many sizes in between.

Optical Corrections These are usually listed as Achro and Achromat (achromatic), as Fl, Fluar, Fluor, Neofluar, or Fluotar (fluorite) for better spherical and chromatic corrections, and as Apo (apochromatic) for the highest degree of correction for spherical and chromatic aberrations. Field curvature corrections are abbreviated Plan, Pl, EF, Achroplan, Plan Apo, or Plano. Other common abbreviations are ICS (infinity corrected system) and UIS (universal infinity system), N and NPL (normal field of view plan), Ultrafluar (fluorite objective with glass that is transparent down to 250 nanometers), and CF and CFI (chrome-free; chrome-free infinity). The objective in the illustration (Figure 6.9) is a plan apochromat that enjoys the highest degree of optical correction. See Table 6.2 for a complete list of abbreviations often found inscribed on objective barrels.

Numerical Aperture This is a critical value that indicates the light acceptance angle, which in turn determines the light gathering power, the resolving power, and depth of field of the objective.

Some objectives specifically designed for transmitted light fluorescence and darkfield imaging are equipped with an internal iris diaphragm that allows for adjustment of the effective numerical aperture. Abbreviations inscribed on the barrel for these objectives include I, Iris, and W/Iris. The 60x apochromat objective illustrated above

TABLE 6.5: Specialized Objective Designations

Abbreviation	Type
Achro, Achromat	Achromatic aberration correction
Fluor, Fl, Fluar, Neofluar, Fluotar	Fluorite aberration correction
Apo	Apochromatic aberration correction
Plan, Pl, Achroplan,Plano	Flat Field optical correction
EF, Acroplan	Extended Field (field of view less than Plan)
N, NPL	Normal field of view plan
Plan Apo	Apochromatic and Flat Field correction
UPLAN	Olympus Universal Plan (Brightfield, Darkfield, DIC, and Polarized Light)
LU	Nikon Luminous Universal (Brightfield, Darkfield, DIC, and Polarized Light)
L, LL, LD, LWD	Long Working Distance
ELWD	Extra-Long Working Distance
SLWD	Super-Long Working Distance
ULWD	Ultra-Long Working Distance
Corr W/Corr, CR	Correction Collar
I, Iris, W/Iris	Adjustable numerical aperture (with iris diaphragm)
Oil, Oel	Oil Immersion
Water, WI, Wasser	Water Immersion
HI	Homogeneous Immersion
Gly	Glycerin Immersion
DIC, NIC	Differential or Nomarski Interference Contrast
CF, CFI	Chrome-Free, Chrome-Free Infinity-Corrected (Nikon)
ICS	Infinity Color-Corrected System (Zeiss)
RMS	Royal Microscopical Society objective thread size
M25, M32	Metric 25-mm objective thread; Metric 32-mm objective thread
Phase, PHACO, PC	Phase Contrast
Ph 1, 2, 3, etc.	Phase Condenser Annulus 1, 2, 3, etc.
DL,DM	Phase Contrast: dark low, dark medium

Abbreviation	Type
PLL, PL	Phase Contrast: positive low low, positive low
PM, PH	Phase Contrast: positive medium, positive high contrast (regions with higher refractive index appear darker)
NL, NM, NH	Phase Contrast: negative low, negative medium, negative high contrast (regions with higher refractive index appear lighter)
P, Po, Pol, SF	Strain-Free, Low Birefringence, for polarized light
U, UV, Universal	UV transmitting (down to approximately 340 nm) for UV-excited epifluorescence
M	Metallographic (no coverslip)
NC, NCG	No Coverslip
EPI	Oblique or Epi illumination
TL	Transmitted Light
BBD, HD, B/D	Bright or Dark Field (Hell, Dunkel)
D	Darkfield
H	For use with a heating stage
U, UT	For use with a universal stage
DI, MI, TI	Interferometry, Noncontact, Multiple Beam (Tolanski)

has a numerical aperture of 1.4, one of the highest attainable in modern microscopes using immersion oil as an imaging medium.

Mechanical Tube Length This is the length of the microscope body tube between the nosepiece opening, where the objective is mounted, and the top edge of the observation tubes where the oculars (eyepieces) are inserted. This aspect of microscope design is discussed in more thoroughly in our mechanical tube length section of the primer. Tube length is usually inscribed on the objective as the size in number of millimeters (160, 170, 210, etc.) for fixed lengths, or the infinity symbol (inf) for infinity-corrected tube lengths. The objective illustrated in Figure 6.9 is corrected for a tube length of infinity, although many older objectives will be corrected for tube lengths of either 160 (Nikon, Olympus, Zeiss) or 170 (Leica) millimeters.

Cover Glass Thickness Most transmitted light objectives are designed to image specimens that are covered by a cover glass (or cover slip). The thickness of these small glass plates is now standardized at 0.17 mm for most applications, although there is often some variation in thickness within a batch of coverslips. For this reason, some of the more advanced objectives have a correction collar adjustment of the internal lens elements to compensate for this variation. Abbreviations for the correction collar adjustment include Corr, w/Corr, and CR, although the presence of a movable, knurled collar and graduated scale is also an indicator of this feature.

There are some applications that do not require objectives to be corrected for cover glass thickness. These include objectives designed for reflected light metallurgical specimens, tissue culture, integrated circuit inspection, and many other applications that require observation with no compensation for a cover glass.

Working Distance This is the distance between the objective front lens and the top of the cover glass when the specimen is in focus. In most instances, the working distance of an objective decreases as magnification increases. Working distance values are not included on all objectives and their presence varies depending upon the manufacturer. Common abbreviations are: L, LL, LD, and LWD (long working distance), ELWD (extra-long working distance), SLWD (super-long working distance), and ULWD (ultra-long working distance). Newer objectives often contain the size of working distance (in millimeters) inscribed on the barrel. The objective illustrated in Figure 6.9 has a very short working distance of 0.21 millimeters.

Specialized Optical Properties Microscope objectives often have design parameters that optimize performance under certain conditions. For example, there are special objectives designed for polarized illumination signified by the abbreviations P, Po, POL, or SF (strain-free and/or having all barrel engravings painted red), phase contrast (PH, and/or green barrel engravings), differential interference contrast (DIC), and many other abbreviations for additional applications. A list of several abbreviations, often manufacturer specific, is presented in Table 6.2. The apochromat objective illustrated in Figure 6.9 is optimized for DIC photomicrography and this is indicated on the barrel. The capital H beside the DIC marking indicates that the objective must be used with a specific DIC Wollaston prism optimized for high-magnification applications.

Objective Screw Threads The mounting threads on almost all objectives are sized to

TABLE 6.6: Objective Numerical Aperture and Working Distance

Optical Correction and Magnification	Numerical Aperture	Working Distance(mm)
ACH 10x	0.25	6.10
ACH 20x	0.40	3.00
ACH 40x	0.65	0.45
ACH 60x	0.80	0.23
ACH 100x (Oil)	1.25	0.13
PL 4x	0.10	22.0
PL 10x	0.25	10.5
PL 20x	0.40	1.20
PL 40x	0.65	0.56
PL 100x (Oil)	1.25	0.15
PL FL 4x	0.13	17.0
PL FL 10x	0.30	10.00
PL FL 20x	0.50	1.60
PL FL 40x	0.75	0.51
PL FL 100x (Oil)	1.30	0.10
PL APO 1.25x	0.04	5.1
PL APO 2x	0.06	6.20
PL APO 4x	0.16	13.00
PL APO 10x	0.40	3.10
PL APO 20x	0.70	0.65
PL APO 40x	0.85	0.20
PL APO 60x (Oil)	1.40	1.10
PL APO 100x (Oil)	1.40	0.10

standards of the Royal Microscopical Society (RMS) for universal compatibility. The objective in Figure 6.9 has mounting threads that are 20.32 mm in diameter with a pitch of 0.706, conforming to the RMS standard. This standard is currently used in the production of infinity-corrected objectives by manufacturers Olympus and Zeiss. Nikon and Leica have broken from the standard with the introduction of new infinity-corrected objectives that have a wider mounting thread size, making Leica and Nikon objectives usable only on their own microscopes. Nikon's reasoning is explained in our section describing the Nikon CFI60 200/60/25 Specification for biomedical microscopes. Abbreviations commonly used to denote thread size are: RMS (Royal Microscopical Society objective thread), M25 (metric 25–millimeter objective thread), and M32 (metric 32–millimeter objective thread).

Immersion Medium Most objectives are designed to image specimens with air as the medium between the objective and the cover glass.

To attain higher working numerical apertures, many objectives are designed to image the specimen through another medium that reduces refractive index differences between glass and the imaging medium. High-resolution plan apochromat objectives can achieve numerical apertures up to 1.40 when the immersion medium is special oil with a refractive index of 1.51. Other common immersion media are water and glycerin. Objectives designed for special immersion media usually have a color-coded ring inscribed around the circumference of the objective barrel as listed in Table 6.7 and described below. Common abbreviations are: Oil, Oel (oil immersion), HI (homogeneous immersion), W, Water, Wasser (water immersion), and Gly (glycerol immersion).

Color Codes Microscope manufacturers label their objectives with color codes to help in rapid identification of the magnification and any specialized immersion media requirements. The dark blue color code on the objective illustrated in Figure 6.9 indicates the linear magnification is 60x. This is very helpful when you have a nosepiece turret containing 5 or 6 objectives and you must quickly select a specific magnification. Some specialized objectives have an additional color code that indicates the type of immersion medium necessary to achieve the optimum numerical aperture. Immersion lenses intended for use with oil have a black color ring, and those intended for use with glycerin have an orange ring, as illustrated with the objective on the left in Figure 6.10. Objectives designed to image living organisms in aqueous media are designated water immersion objectives with a white ring, and highly specialized objectives for unusual immersion media are often engraved with a red ring. Table 6.7 lists current magnification and imaging media color codes in use by most manufacturers.

Special Features Objectives often have additional special features that are specific to a particular manufacturer and type of objective. The plan apochromat objective illustrated in Figure 6.9 has a spring-loaded front lens to prevent damage when the objective is accidentally driven onto the surface of a microscope slide.

Other features found on specialized objectives are variable working distance (LWD) and numerical aperture settings that are adjustable by turning the correction collar on the body of the objective as illustrated in Figure 6.10. The plan fluor objective on the left has a variable immersion medium/numerical aperture setting that allows the objective to be used with both air and an alternative liquid immersion medium,

TABLE 6.7: Objective Color Codes

Magnification	Color Code
$\frac{1}{2}$x	No Color Assigned
1x	Black
1.25x	Black
1.5x	Black
2x	Brown (or Orange)
2.5x	Brown (or Orange)
4x	Red
5x	Red
10x	Yellow
16x	Green
20x	Green
25x	Turquoise
32x	Turquoise
40x	Light Blue
50x	Light Blue
60x	Cobalt Blue
63x	Cobalt Blue
100x	White
150x	White
250x	White
Immersion media	**Color Code**
Oil	Black
Glycerol	Orange
Water	White
Special	Red

FIGURE 6.10: Special features

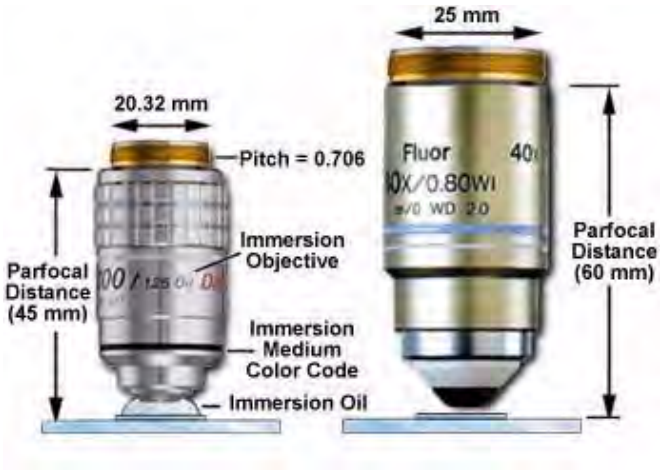

FIGURE 6.11: Parfocal distance

glycerin. The plan apo objective on the right has an adjustable working distance control (termed a "correction collar") that allows the objective to image specimens through glass coverslips of variable thickness. This is especially important in dry objectives with high numerical aperture that are particularly susceptible to spherical and other aberrations that can impair resolution and contrast when used with a cover glass whose thickness differs from the specified design value.

Although not common today, other types of adjustable objectives have been manufactured in the past. Perhaps the most interesting example is the compound "zoom" objective that has a variable magnification, usually from about 4x to 15x. These objectives have a short barrel with poorly designed optics that have significant aberration problems and are not very practical for photomicrography or serious quantitative microscopy.

Parfocal Distance This is another specification that can often vary by manufacturer. Most companies produce objectives that have a 45 millimeter parfocal distance, which is designed to minimize refocusing when magnifications are changed.

The objective depicted on the left in Figure 6.11 has a parfocal distance of 45mm and is labeled with an immersion medium color code in addition to the magnification color code. Parfocal distance is measured from the nosepiece objective mounting hole to the point of focus on the specimen as illustrated in the figure. The objective on the right in Figure 6.11 has a longer parfocal distance of 60 millimeters, which is the result of its being produced to the Nikon CFI60 200/60/25 Specification, again deviating from the practice of other manufacturers such as Olympus and Zeiss, who still produce objectives with a 45mm parfocal distance. Most manufacturers also make their objective nosepieces parcentric, meaning that when a specimen is centered in the field of view for one objective, it remains centered when the nosepiece is rotated to bring another objective into use.

Glass Design The quality of glass formulations has been paramount in the evolution of modern microscope optics, and there are currently several hundred of optical glasses available for the design of microscope objectives. The suitability of glass for the

demanding optical performance of a microscope objective is a function of its physical properties such as refractive index, dispersion, light transmission, contaminant concentrations, residual autofluorescence, and overall homogeneity throughout the mixture. Care must be taken by optical designers to ensure that glass utilized in high-performance objectives has a high transmission in the near-ultraviolet region and also produces high extinction factors for applications such as polarized light or differential interference contrast.

Cements employed in building multiple lens elements usually have a thickness around 5—10 microns, which can be a source of artifacts in groups that have three or more lens elements cemented together. Doublets, triplets, and other multiple lens arrangements can display spurious absorption, transmission, and fluorescence characteristics that will disqualify the lenses for certain applications.

For many years, natural fluorite was commonly used in the manufacture of fluorite (semi-apochromat) and apochromat objectives. Unfortunately, many newly developed fluorescence techniques often rely on ultraviolet excitation at wavelengths significantly below 400 nanometers, which is severely compromised by autofluorescence that occurs from natural organic constituents present in this mineral. Also, the tendency of natural fluorite to exhibit widespread localized regions of crystallinity can seriously degrade performance in polarized light microscopy. Many of these problems are circumvented with new, more advanced materials, such as fluorocrown glass.

Annealing of optical glass for the manufacture of objectives is critical in order to remove stress, improve transmission, and reduce the level of other internal imperfections. Some of the glass formulations intended for apochromat lens construction are slow-cooled and annealed for extended periods, often exceeding six months. True apochromat objectives are manufactured with a combination of natural fluorite and other glasses that have reduced transmission in the near-ultraviolet region.

Extra Low Dispersion (ED) glass was introduced as a major advancement in lens design with optical qualities similar to the mineral fluorite but without its mechanical and optical demerits. This glass has allowed manufacturers to create higher quality objectives with lens elements that have superior optical corrections and performance. Because the chemical and optical properties of many glasses are of a proprietary nature, documentation is difficult or impossible to obtain. For this reason the literature is often vague about the specific properties of glasses utilized in the construction of microscope objectives.

Multilayer Antireflection Coatings One of the most significant advances in objective design during recent years is the improvement in antireflection coating technology, which helps to reduce unwanted reflections (flare and ghosts) that occur when light passes through a lens system, and ensure high-contrast images. Each uncoated air-glass interface can reflect between four and five percent of an incident light beam normal to the surface, resulting in a transmission value of 95-96 percent at normal incidence. Application of a quarter-wavelength thick antireflection coating having the appropriate refractive index can increase this value by three to four percent. As objectives become more sophisticated with an ever-increasing number of lens elements, the need to eliminate internal reflections grows correspondingly. Some modern objective lenses with a high degree of correction can contain as many as 15 lens elements having many air-glass interfaces. If the lenses were uncoated, the reflection losses of

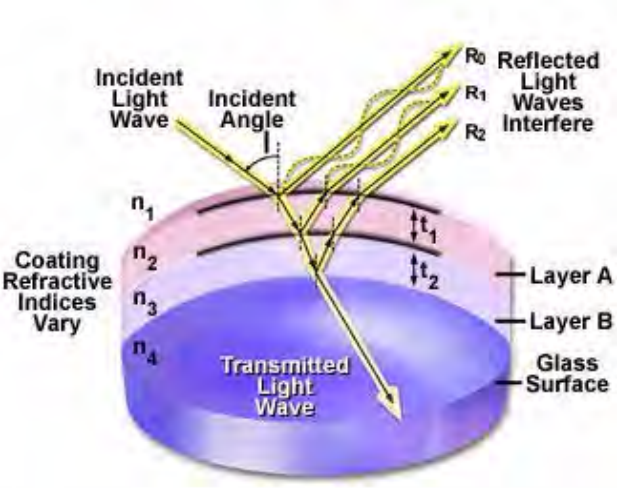

FIGURE 6.12: Geometry of antireflective coatings

axial rays alone would drop transmittance values to around 50 percent. The single-layer lens coatings once utilized to reduce glare and improve transmission have now been supplanted by multilayer coatings that produce transmission values exceeding 99.9 percent in the visible spectral range. These specialized coatings are also used on the phase plates in phase contrast objectives to maximize contrast.

Illustrated in Figure 6.12 is a schematic drawing of light waves reflecting and/or passing through a lens element coated with two antireflection layers. The incident wave strikes the first layer (Layer A in Figure 6.12) at an angle, resulting in part of the light being reflected (R_0) and part being transmitted through the first layer. Upon encountering the second antireflection layer (Layer B), another portion of the light is reflected at the same angle and interferes with light reflected from the first layer. Some of the remaining light waves continue on to the glass surface where they are again both reflected and transmitted. Light reflected from the glass surface interferes (both constructively and destructively) with light reflected from the antireflection layers. The refractive indices of the antireflection layers vary from that of the glass and the surrounding medium (air). As the light waves pass through the antireflection layers and glass surface, a majority of the light (depending upon the incident angle–usual normal to the lens in optical microscopy) is ultimately transmitted through the glass and focused to form an image.

Magnesium fluoride is one of many materials utilized in thin-layer optical antireflection coatings, but most microscope manufacturers now produce their own proprietary formulations. The general result is a dramatic improvement in contrast and transmission of visible wavelengths with a concurrent destructive interference in harmonically-related frequencies lying outside the transmission band. These specialized coatings can be easily damaged by mis-handling and the microscopist should be aware of this vulnerability. Multilayer antireflection coatings have a slightly greenish tint, as opposed to the purplish tint of single-layer coatings, an observation that can be employed to distinguish between coatings. The surface layer of antireflection coatings used on internal lenses is often much softer than corresponding coatings designed to protect external lens surfaces. Great care should be taken when cleaning optical

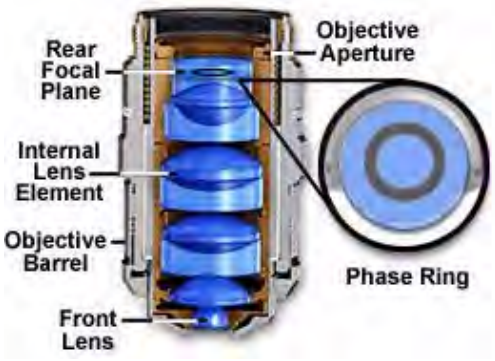

FIGURE 6.13: Phase contrast objective

surfaces that have been coated with thin films, especially if the microscope has been disassembled and the internal lens elements are subject to scrutiny.

From the discussion above it is apparent that objectives are the most important optical element of a compound microscope. It is for this reason that so much effort is invested in making sure that they are well-labeled and suited for the task at hand. We will explore other properties and aspects of microscope objectives in other sections of this tutorial.

6.3 Objectives for Specialized Applications

Perhaps as many as 90 percent of all optical microscopy investigations are conducted utilizing standard achromat or plan achromat objectives, which are the cheapest, most readily available, and already installed on a large base of microscopes around the world. A majority of microscope manufacturers also offer a wide variety of objectives having unique configurations designed to perform specific functions not normally found on common laboratory microscopes.

Standard brightfield objectives, corrected for varying degrees of optical aberration, are the most common and are useful for examining specimens with traditional illumination techniques such as brightfield, darkfield, oblique, and Rheinberg. Several of these methods involve modifications to the substage condenser, but still utilize standard achromat, fluorite, and/or apochromat objectives either with or without flat-field correction. Other, more complex, techniques require specific objective configurations, which often include placement of a detector on or near the rear focal plane. To complicate the issue, the objective rear focal plane usually resides in the center of an internal glass lens element, an area that is not easily accessible to the microscopist.

Objectives designed for phase contrast, Hoffman modulation contrast, and differential interference contrast require the assistance of optical detectors to modify events occurring at the objective rear focal plane. These objectives must be specially constructed to physically place the detecting element at the appropriate focal plane within the objective body. Phase contrast objectives (as discussed below) require the insertion of a phase plate containing neutral density material and/or optical wave retarders at the rear focal plane. In addition, the phase plate must be placed conjugate to a matched annular ring positioned in the substage condenser. Hoffman objectives also require a modulation plate in the objective rear focal plane that is conjugate to a slit plate in the condenser. Dif-

ferential interference contrast objectives generally do not require modification (other than the utilization of strain-free optical elements), but do rely on the action of Wollaston or Nomarski prisms strategically placed to influence optical path differences between sheared light beams at the rear focal plane. Other specialized objectives rely on modified optical elements, insertion of mirrors or oblique reflectors, adjustable apertures, and/or movable elements to perform unique functions. Details concerning the specific requirements of such objectives are discussed in the remainder of this section.

Phase Contrast This is a classical method of introducing contrast into semi-transparent, unstained specimens such as microorganisms and cells in living tissue culture, which has been employed by biologists for the past 50 years. Phase contrast manipulates phase relationships between individual light rays as they are emitted from the specimen and translates them into amplitude or brightness changes that are visible to the microscopist. A special objective is required that is fitted with a darkened circular ring or groove (phase plate) fitted into the glass near the rear focal plane of the objective as illustrated in Figure 6.13. In addition, the condenser must also be modified with special annular openings suited to a particular magnification and objective. Phase contrast objectives are segregated into a number of categories depending upon the construction and neutral density of internal phase rings:

- **DL (Dark-Light)**—DL objectives produce a dark image outline on a light gray background. These objectives are designed to furnish the strongest dark contrast in specimens having major differences in refractive indices. The DL phase contrast objective is the most popular style for examination of cells and other semi-transparent living material and is especially suited for photomicrography and digital imaging.
- **DLL (Dark Lower Contrast)**— Similar to the DL objective, the DLL series allows better images in brightfield and is often used as a "universal" objective in microscope systems that utilize multiple illumination modes such as fluorescence, DIC, brightfield, and darkfield.
- **ADL (Apodized Dark-Light)**— Recently introduced by Nikon, the apodized phase contrast ADL objectives contain a secondary neutral density ring on either side of the phase ring. Addition of the secondary rings assists in reducing unwanted "halo" effects often associated with imaging in phase contrast microscopy.
- **DM (Dark-Medium)**— DM objectives produce a dark image outline on a medium gray background. These objectives are designed to be used for high image contrast with specimens having small phase differences, such as fine fibers, granules, and particles.
- **BM (Bright-Medium)**— Often referred to as negative phase contrast, BM objectives produce a bright image outline on a medium gray background. BM objectives are ideal for visual examination of bacterial flagella, fibrin bundles, minute globules, and blood cell counting.

In order to allow the microscopist to quickly identify phase contrast objectives, many manufacturers inscribe important specifications, such as the magnification, numerical aperture, tube length correction, etc., on the outer barrel in green letters. This serves

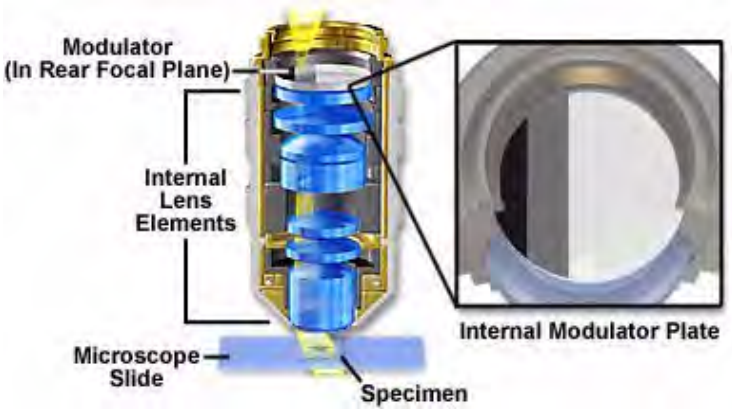

FIGURE 6.14: Hoffman modulation contrast objective

to differentiate phase contrast objectives from ordinary brightfield, polarized, DIC, and fluorescence objectives which either use an alternative color code or the standard black lettering.

Differential Interference Contrast (DIC) Nomarski differential interference contrast is also useful for unstained specimens, but is less effective with birefringent samples and can be used with reflected light for metallography and wafer inspection. DIC objectives are not modified internally, but are designed for use with special magnification-dependent modified Wollaston or Nomarski prisms to produce high-contrast images. These objectives are also useful for brightfield, darkfield and other techniques when the prisms are removed from the optical path. Because DIC microscopy utilizes polarized light, strain must be minimized in objectives designed for this type of application. In the past, only strain-free achromats, planachromats, and some high-performance fluorite objectives were suitable for this task. However, recent improvements in lens design and antireflection coatings now allow utilization of apochromat objectives for DIC observation, photomicrography, and digital imaging. The barrel of objectives intended for use with a DIC prism is usually inscribed with the specific prism (low, medium, high, or 1, 2, 3, etc.) intended to be coupled with the objective.

Hoffman Modulation Contrast Objectives for the Hoffman modulation contrast system are designed to increase visibility and contrast in unstained and living material by detecting optical gradients (or slopes) and converting them into variations of light intensity. Modulation contrast objectives have a unique optical amplitude spatial filter, termed a modulator, inserted into the rear focal plane (see Figure 6.14) of an achromat or planachromat objective (although a higher correction factor can also be utilized). The modulator has three zones of varying neutral density that transmit either one, fifteen, or one hundred percent of the light passing through the objective. Unlike the phase plate in phase contrast objectives, Hoffman modulators are designed not to alter the phase of light passing through any of the zones. When viewed under modulation contrast optics, transparent objects that are essentially invisible in ordinary brightfield microscopy take on an apparent three-dimensional appearance dictated by phase gradients in the specimen. Recent innovations in Hoffman objective design have yielded models that allow the contrast direction to be varied using a

FIGURE 6.15: Polarized light objective color codes

modulator inside the objective. Once adjusted, the contrast direction is maintained over the entire magnification range in a set of matched objectives.

Infrared Microscopy Optical microscopy in the infrared region of the electromagnetic radiation spectrum is often undertaken for the study of materials that are uniformly transparent or opaque in the visible spectrum, but have significant absorption or transmission bands in the 700 nanometer-plus wavelength region. Reflected light is the technique of choice for infrared microscopy, and several specialized catoptric objectives have been designed to capture images with infrared light reflected from opaque specimens.

Although all microscope objectives transmit some degree of the shorter infrared wavelengths, very few are corrected for aberrations in this region and show a marked shift in focus when transcending from visible to infrared light. Most manufacturers offer specialized objectives with reduced numerical apertures that are designed to increase the depth of focus in specimens imaged with infrared light. Oil immersion objectives will not function normally with standard oils and the only suitable immersion fluid that is currently available for infrared microscopy is paraffin oil. The major concern with this type of microscopy is the ability to capture satisfactory photomicrographs using conventional imaging technology. Currently, several film emulsions are available that respond to the infrared spectrum, but electronic detectors are rapidly becoming the imaging device of choice for studies in this wavelength range.

Interference Microscopy Interferometry is applied to the study of microscopic specimens by taking advantage of interference produced when light passing through an object is caused to interfere with a reference beam of light that has followed a somewhat different pathway. Under these circumstances, the opaque surface of a reflected light specimen or transparent specimens are imaged when the path difference between the two light beams is converted into intensity fluctuations. A wide variety of microscope and objective designs have been implemented for interference microscopy, many following the basic principles of the Michelson, Mach–Zehnder, and Jamin interferometers. Manufacturers of industrial microscopes (both reflected and transmitted illumination) often produce specialized objective/microscope combinations that take advantage of the optical interference phenomenon to achieve high-precision measurements.

FIGURE 6.16: Nikon ultraviolet fluorite objective

Polarized Light Unlike most other forms of microscopy, polarized light microscopy produces the best images when a minimum of optical elements are used in the construction of objectives. It is important to ensure that lens elements, optical cements, and antireflection coatings are free of both strain and birefringent materials that might interfere with quantitative assessment of specimen birefringence. Apochromatic objectives, the choice for most forms of microscopy, are generally not utilized for polarized light investigations due to the high number of internal lens elements that often contribute to internal reflections and strain. Most manufacturers produce objectives that are specifically optimized for polarized light and differential interference contrast, with fluorite-class objectives being used most often for these purposes. Objectives optimized for polarized light often have the exterior portion of the barrel painted black, with the specifications inscribed in bright red letters (Figure 6.15).

Ultraviolet Fluor Objectives Epi–fluorescence applications require high numerical aperture objectives in order to capture the maximum amount of light from faintly emitting fluorescent specimens. The ratio of specific specimen fluorescence to the intrinsic background fluorescence becomes a primary concern when imaging single molecule and other low-light fluorescence events. In these situations, auto-fluorescence and/or internal reflection inside the objectives can interfere with imaging small structures and low fluorescence targets.

Fluorescence objectives are designed with quartz and special glasses that have high transmission from the ultraviolet (down to 340 nanometers) through the infrared regions of the electromagnetic radiation spectrum. These objectives are extremely low in autofluorescence in order to optimize the luminous flux emitted as secondary fluorescence by fluorophores attached to specimens. In addition to special lens elements, ultraviolet (UV) fluor objectives utilize specialized optical cements and antireflection coatings that are designed to operate through an extended range of fluorescence excitations throughout the spectrum. Correction for optical aberration and numerical aperture values in UV fluor objectives usually approaches that of apochromats, which contributes to image brightness and enhanced resolution of images generated by these advanced lenses (Figure 6.16). In addition, these objectives are designed with non-fluorescent glass to minimize artifacts arising from auto-fluorescence by internal lens elements. The primary drawback of high-performance fluorescence objectives is that many are not corrected for field curvature, resulting in images that do not have uniform focus throughout the view field. Although this problem is only of secondary concern when imaging weakly fluorescent specimens (es-

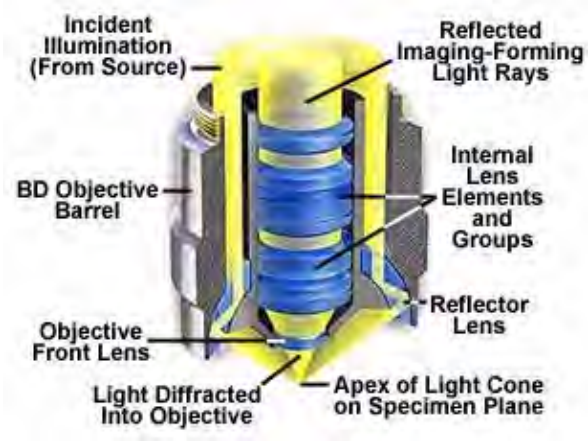

FIGURE 6.17: Reflected light darkfield/brightfield objective

pecially with laser scanning confocal microscopy), it becomes a major issue when the objective is utilized to perform under conventional illumination techniques such as brightfield, darkfield, and differential interference contrast.

Reflected Light Objectives Transmitted light objectives designed to be used with a cover glass are unsuitable for examining reflected light specimens whose surfaces are uncovered. Instead, specialized objectives that are corrected for observation and imaging of specimens without a cover glass are employed for reflected light microscopy. Today, most reflected light microscope objectives are infinity–corrected and are available in a broad spectrum of magnifications ranging from 5x to 200x. These objectives are manufactured in various qualities of chromatic and spherical correction, ranging from simple achromats to planachromats and planapochromats. Most, but not all, are designed to be used "dry" with air in the space between the objective and specimen. Many reflected light objectives are designed to focus at a longer working distance from the specimen than is usual (see below). Such objectives are labeled on the barrel of the objective as LWD (Long Working Distance), ULWD (Ultra-Long Working Distance), and ELWD (Extra-Long Working Distance).

Objectives designed to be used with reflected darkfield illumination have a special construction consisting of a 360-degree hollow chamber surrounding the centrally located lens elements (Figure 6.17). Light from the illuminator passes through the periphery of the objective and is directed at the specimen from every azimuth in oblique rays to form a hollow cone of illumination. This is often accomplished by means of circular mirrors or prisms located at the bottom of the objective's hollow chamber. In this manner, the objective serves as two separate optical systems coupled coaxially such that the outer system functions as a "condenser" and the inner system as a typical objective.

The necessity of a hollow collar surrounding the lens elements in reflected light objectives requires that the diameter of the objective be significantly greater than that of ordinary brightfield objectives. In most cases, a nosepiece-mounting thread diameter larger than the Royal Microscopical Society (RMS) standard is used in reflected light objectives. This requires that reflected light darkfield objectives have a nosepiece with a larger thread size, which is typically referred to as a BD or BF/DF thread

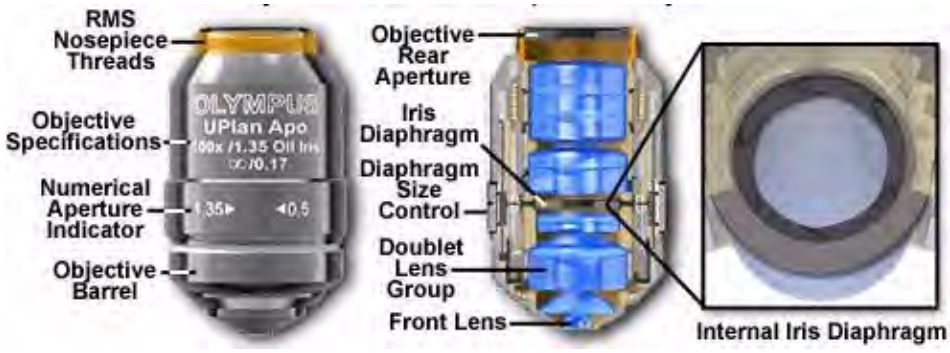

FIGURE 6.18: Adjustable numerical aperture objective

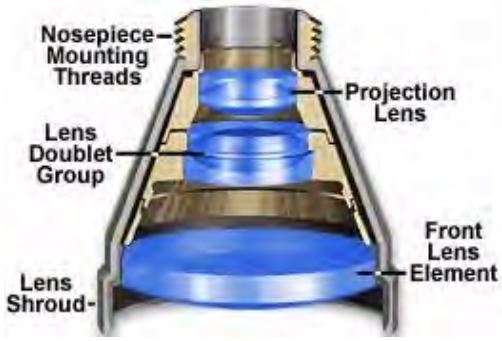

FIGURE 6.19: Nikon ultra–low mag 0.5x objective

size. Most manufacturers offer objective adapters that convert standard RMS thread size nosepieces to BD thread size, allowing the use of these objectives on reflected light microscopes. Care should be taken to ensure that objectives used on BD thread nosepieces will conform to the tube length of the microscope.

Variable Numerical Aperture Objectives Specimens with unusually high fluorescence quantum yields and/or very bright darkfield specimens often induce image flare by light emitted from areas outside the focal plane. To compensate for this artifact, manufacturers offer high numerical aperture objectives that are equipped with an internal iris diaphragm to increase image contrast during photomicrography or digital imaging. Opening or closing the iris diaphragm determines the size of the objective rear aperture yielding a variable numerical aperture range between 0.5 and the objective's upper limit (up to 1.35-1.4 with apochromatic objectives; Figure 6.18). Although iris diaphragms were once utilized in a wide variety of objective designs, modern variable numerical aperture objectives are usually at the high end (60x to 150x) of the magnification range.

Ultra–Low Magnification Objectives Objectives having a magnification factor below 4x are considered to be very low in magnification and may not be compatible with all microscope optical systems. Generally, Köhler illumination is difficult to achieve with low magnification objectives, which often require specialized matching condensers to fill the rear aperture with sufficient illumination. Magnifications down to 0.5x have recently been achieved, but these objectives require special tube lenses and condensers,

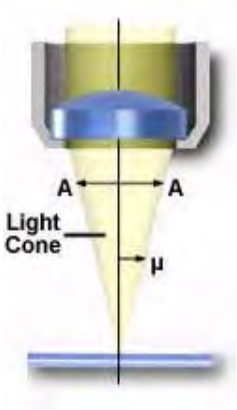

FIGURE 6.20: Angular aperture

making them useful only on the microscopes for which they were designed. Illustrated in Figure 6.19 is a Nikon 0.5x apochromatic objective having a numerical aperture of 0.025. This objective requires a macro slider lens that effectively doubles the focal length to allow the objective to be utilized in Nikon's 200-millimeter tube length infinity-corrected microscopes. This objective, and its matching 1x counterpart, utilize Nikon's MM (Macro/Micro) condenser to ensure uniform illumination across the magnification range between 0.5x and 100x.

Long Working Distance (LWD) These objectives are designed to increase the working distance over that of conventional objectives through the use of special optical elements. The most useful application for LWD objectives is to view living cells in tissue culture through the walls of the thick vessels used to support the cells. Other uses for these objectives are to image samples through thick glass plates (for instance, between two microscope slides), or when micromanipulation of specimens must be conducted while viewing. Reflected light objectives are also produced with long working distances for examination of large specimens that would ordinarily be too bulky to fit within the confines of a normal microscope optical system.

6.4 Numerical Aperture and Resolution

The numerical aperture of a microscope objective is a measure of its ability to gather light and resolve fine specimen detail at a fixed object distance. Image-forming light waves pass through the specimen and enter the objective in an inverted cone as illustrated in Figure 6.20. A longitudinal slice of this cone of light shows the angular aperture, a value that is determined by the focal length of the objective.

The angle mu is one-half the angular aperture (A) and is related to the numerical aperture through the following equation:

$$\mathrm{NA} = n(\sin \mu)$$

where n is the refractive index of the imaging medium between the front lens of the objective and the specimen cover glass, a value that ranges from 1.00 for air to 1.51 for specialized immersion oils. Many authors substitute the variable α for μ in the numerical aperture

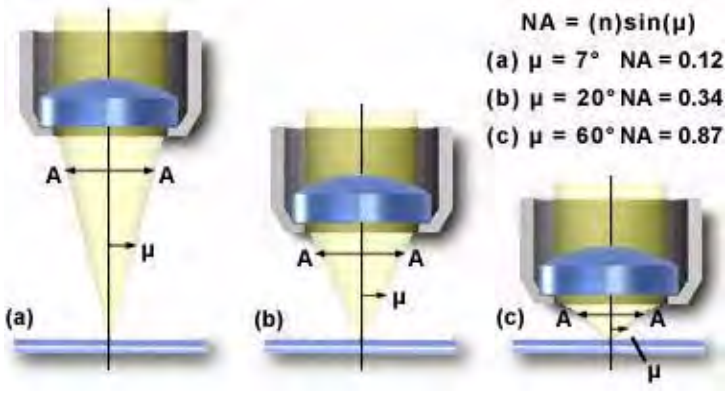

FIGURE 6.21: Angular aperture

equation. From this equation it is obvious that when the imaging medium is air (with a refractive index, n = 1.0), then the numerical aperture is dependent only upon the angle m whose maximum value is 90°. The sin of the angle μ, therefore, has a maximum value of 1.0, which is the theoretical maximum numerical aperture of a lens operating with air as the imaging medium (using "dry" microscope objectives).

In practice, however, it is difficult to achieve numerical aperture values above 0.95 with dry objectives. Figure 6.21 illustrates a series of light cones derived from objectives of varying focal length and numerical aperture. As the light cones change, the angle μ increases from 7° in Figure 6.21(a) to 60° in Figure 6.21(c), with a resulting increase in the numerical aperture from 0.12 to 0.87, nearing the limit when air is the imaging medium.

By examining the numerical aperture equation, it is apparent that refractive index is the limiting factor in achieving numerical apertures greater than 1.0. Therefore, in order to obtain higher working numerical apertures, the refractive index of the medium between the front lens of the objective and the specimen must be increased. Microscope objectives are now available that allow imaging in alternative media such as water (refractive index = 1.33), glycerin (refractive index = 1.47), and immersion oil (refractive index = 1.51). Care should be used with these objectives to prevent unwanted artifacts that will arise when an objective is used with a different immersion medium than it was designed for. We suggest that microscopists never use objectives designed for oil immersion with either glycerin or water, although several newer objectives have recently been introduced that will work with multiple media. You should check with the manufacturer if there are any doubts.

Most objectives in the magnification range between 60x and 100x (and higher) are designed for use with immersion oil. By examining the numerical aperture equation above, we find that the highest theoretical numerical aperture obtainable with immersion oil is 1.51. In practice, however, most oil immersion objectives have a maximum numerical aperture of 1.4, with the most common numerical apertures ranging from 1.0 to 1.35.

The numerical aperture of an objective is also dependent, to a certain degree, upon the amount of correction for optical aberration. Highly corrected objectives tend to have much larger numerical apertures for the respective magnification as illustrated in Table 6.8 below. If we take a series of typical 10x objectives as an example, we see that for flat-field corrected plan objectives, numerical aperture increases correspond to correction for chromatic and spherical aberration: plan achromat, NA=0.25; plan fluorite, NA=0.30; and plan apochromat, NA=0.45.

TABLE 6.8: Objective Numerical Apertures

Magnification	Plan Achromat (NA)	Plan Fluorite (NA)	Plan Apochromat (NA)
0.5x	0.025	n/a	n/a
1x	0.04	n/a	n/a
2x	0.06	n/a	0.10
4x	0.10	0.13	0.20
10x	0.25	0.30	0.45
20x	0.40	0.50	0.75
40x	0.65	0.75	0.95
40x (oil)	n/a	1.30	1.00
60x	0.75	0.85	0.95
60x (oil)	n/a	n/a	1.40
100x (oil)	1.25	1.30	1.40
150x	n/a	n/a	0.90

This feature of increasing numerical aperture across an increasing optical correction factor in a series of objectives of similar magnification holds true throughout the range of magnifications as shown in Table 6.8. Most manufacturers strive to ensure that their objectives have the highest correction and numerical aperture that is possible for each class of objective.

The resolution of a microscope objective is defined as the smallest distance between two points on a specimen that can still be distinguished as two separate entities. Resolution is a somewhat subjective value in microscopy because at high magnification, an image may appear unsharp but still be resolved to the maximum ability of the objective. Numerical aperture determines the resolving power of an objective, but the total resolution of a microscope system is also dependent upon the numerical aperture of the substage condenser. The higher the numerical aperture of the total system, the better the resolution.

Correct alignment of the microscope optical system is also of paramount importance to ensure maximum resolution. The substage condenser must be matched to the objective with respect to numerical aperture and adjustment of the aperture iris diaphragm for accurate light cone formation. The wavelength spectrum of light used to image a specimen is also a determining factor in resolution. Shorter wavelengths are capable of resolving details to a greater degree than are the longer wavelengths. There are several equations that have been derived to express the relationship between numerical aperture, wavelength, and resolution:

$$R = \frac{\lambda}{2NA} \tag{6.1}$$

$$R = \frac{0.61}{NA} \tag{6.2}$$

$$R = \frac{1.22}{NA_{\text{obj}} + NA_{\text{cond}}} \tag{6.3}$$

Where R is resolution (the smallest resolvable distance between two objects), NA equals numerical aperture, λ equals wavelength, NA_{obj} equals the objective numerical aperture, and NA_{cond} is the condenser numerical aperture. These equations are based upon a num-

TABLE 6.9: Resolution and Numerical Aperture by Objective Type

	Objective Type					
	Plan Achromat		Plan Fluorite		Plan Apochromat	
Magnification	NA	Res. (μm)	NA	Res. (μm)	NA	Res. (μm)
4x	0.10	2.75	0.13	2.12	0.20	1.375
10x	0.25	1.10	0.30	0.92	0.45	0.61
20x	0.40	0.69	0.50	0.55	0.75	0.37
40x	0.65	0.42	0.75	0.37	0.95	0.29
60x	0.75	0.37	0.85	0.32	0.95	0.29
100x	1.25	0.22	1.30	0.21	1.40	0.20

ber of factors (including a variety of theoretical calculations made by optical physicists) to account for the behavior of objectives and condensers, and should not be considered an absolute value of any one general physical law. In some instances, such as confocal and fluorescence microscopy, the resolution may actually exceed the limits placed by any one of these three equations. Other factors, such as low specimen contrast and improper illumination may serve to lower resolution and, more often than not, the real-world maximum value of R (about 0.25 μmm using a mid-spectrum wavelength of 550 nanometers) and a numerical aperture of 1.35 to 1.40 are not realized in practice. Table 6.9 provides a list resolution (R) and numerical aperture (NA) by objective magnification and correction.

An important fact to note is that magnification does not appear as a factor in any of these equations, because only numerical aperture and wavelength of the illuminating light determine specimen resolution. As we have mentioned (and can be seen in the equations) the wavelength of light is an important factor in the resolution of a microscope. Shorter wavelengths yield higher resolution (lower values for R) and visa versa. The greatest resolving power in optical microscopy is realized with near-ultraviolet light, the shortest effective imaging wavelength. Near-ultraviolet light is followed by blue, then green, and finally red light in the ability to resolve specimen detail. Under most circumstances, microscopists use white light generated by a tungsten-halogen bulb to illuminate the specimen. The visible light spectrum is centered at about 550 nanometers, the dominant wavelength for green light (our eyes are most sensitive to green light). It is this wavelength that was used to calculate resolution values in Table 6.9. The numerical aperture value is also important in these equations and higher numerical apertures will also produce higher resolution, as is evident in Table 6.9. The effect of the wavelength of light on resolution, at a fixed numerical aperture (0.95), is listed in Table 6.10.

When light from the various points of a specimen passes through the objective and is reconstituted as an image, the various points of the specimen appear in the image as small patterns (not points) known as Airy patterns. This phenomenon is caused by diffraction or scattering of the light as it passes through the minute parts and spaces in the specimen and the circular back aperture of the objective. The central maximum of the Airy patterns is often referred to as an Airy disk, which is defined as the region enclosed by the first minimum of the Airy pattern and contains 84 percent of the luminous energy. These Airy disks consist of small concentric light and dark circles as illustrated in Figure 6.22. This figure shows Airy disks and their intensity distributions as a function of separation distance.

TABLE 6.10: Resolution versus Wavelength

Wavelength (nm)	Resolution (μm)
360	.19
400	.21
450	.24
500	.26
550	.29
600	.32
650	.34
700	.37

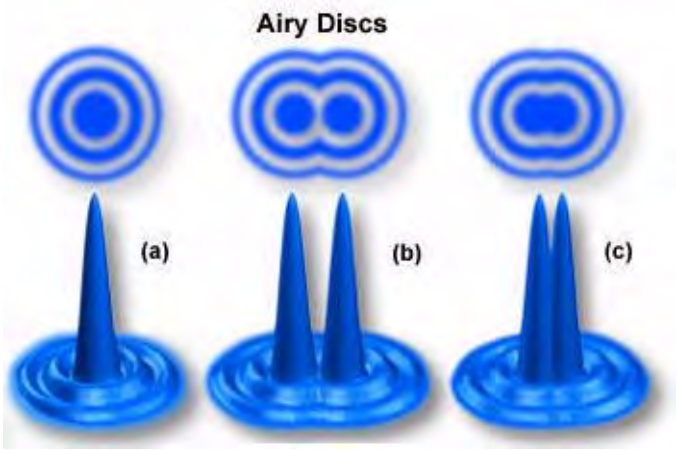

FIGURE 6.22: Intensity distribution

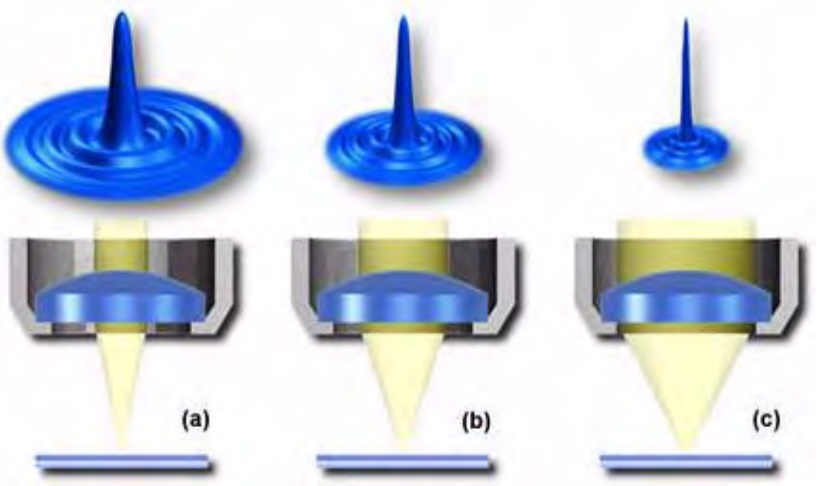

FIGURE 6.23: Numerical aperture and Airy disk

Figure 6.22(a) illustrates a hypothetical Airy disk that essentially consists of a diffraction pattern containing a central maximum (typically termed a zeroth order maximum) surrounded by concentric 1st, 2nd, 3rd, etc., order maxima of sequentially decreasing brightness that make up the intensity distribution. Two Airy disks and their intensity distributions at the limit of optical resolution are illustrated in Figure 6.22(b). In this part of the figure, the separation between the two disks exceeds their radii, and they are resolvable. The limit at which two Airy disks can be resolved into separate entities is often called the Rayleigh criterion. Figure 6.22(c) shows two Airy disks and their intensity distributions in a situation where the center-to-center distance between the zeroth order maxima is less than the width of these maxima, and the two disks are not individually resolvable by the Rayleigh criterion.

The smaller the Airy disks projected by an objective in forming the image, the more detail of the specimen that becomes discernible. Objectives of higher correction (fluorites and apochromats) produce smaller Airy disks than do objectives of lower correction. In a similar manner, objectives that have a higher numerical aperture are also capable of producing smaller Airy disks. This is the primary reason that objectives of high numerical aperture and total correction for optical aberration can distinguish finer detail in the specimen.

Figure 6.23 illustrates the effect of numerical aperture on the size of Airy disks imaged with a series of hypothetical objectives of the same focal length, but differing numerical apertures. With small numerical apertures, the Airy disk size is large, as shown in Figure 6.23(a). As the numerical aperture and light cone angle of an objective increases however, the size of the Airy disk decreases as illustrated in Figure 6.23(b) and Figure 6.23(c). The resulting image at the eyepiece diaphragm level is actually a mosaic of Airy disks which we perceive as light and dark. Where two disks are too close together so that their central spots overlap considerably, the two details represented by these overlapping disks are not resolved or separated and thus appear as one, as illustrated above in Figure 6.22.

An important concept to understand in image formation is the nature of diffracted light rays intercepted by the objective. Only in cases where the higher (1st, 2nd, 3rd, etc.) orders of diffracted rays are captured, can interference work to recreate the image in the

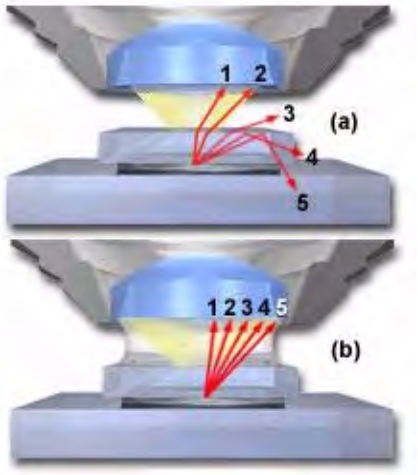

FIGURE 6.24: Oil immersion and numerical aperture

intermediate image plane of the objective. When only the zeroth order rays are captured, it is virtually impossible to reconstitute a recognizable image of the specimen. When 1st order light rays are added to the zeroth order rays, the image becomes more coherent, but it is still lacking in sufficient detail. It is only when higher order rays are recombined, that the image will represent the true architecture of the specimen. This is the basis for the necessity of large numerical apertures (and subsequent smaller Airy disks) to achieve high-resolution images with an optical microscope.

In day-to-day routine observations, most microscopists do not attempt to achieve the highest resolution image possible with their equipment. It is only under specialized circumstances, such as high-magnification brightfield, fluorescence, DIC, and confocal microscopy that we strive to reach the limits of the microscope. In most uses of the microscope, it is not necessary to use objectives of high numerical aperture because the specimen is readily resolved with use of lower numerical aperture objectives. This is particularly important because high numerical aperture and high magnification are accompanied by the disadvantages of very shallow depth of field (this refers to good focus in the area just below or just above the area being examined) and short working distance. Thus, in specimens where resolution is less critical and magnifications can be lower, it is better to use lower magnification objectives of modest numerical aperture in order to yield images with more working distance and more depth of field.

Careful positioning of the substage condenser aperture diaphragm is also critical to the control of numerical aperture and indiscriminate use of this diaphragm can lead to image degradation (as discussed in the section on substage condensers). Other factors, such as contrast and the efficiency of illumination, are also key elements that affect image resolution.

6.5 Immersion Media

The ability of a microscope objective to capture deviated light rays from a specimen is dependent upon both the numerical aperture and the medium through which the light travels.

An objective's numerical aperture is directly proportional to the refractive index of the imaging medium between the coverslip and the front lens, and also to the sin of one-half the angular aperture of the objective. Because $\sin \mu$ cannot be greater than 90 degrees, the maximum possible numerical aperture is determined by the refractive index of the immersion medium. Most microscope objectives use air as the medium through which light rays must pass between the coverslip protecting the sample and front lens of the objective. Objectives of this type are referred to as dry objectives because they are used without liquid imaging media. Air has a refractive index of 1.0003, very close to that of a vacuum and considerably lower than most liquids, including water ($n = 1.33$), glycerin ($n = 1.470$) and common microscope immersion oils (average $n = 1.515$). In practice, the maximum numerical aperture of a dry objective system is limited to 0.95, and greater values can only be achieved using optics designed for immersion media.

The principle of oil immersion is demonstrated in Figure 6.24 where individual light rays are traced through the specimen and either pass into the objective or are refracted in other directions. Figure 6.24(a) illustrates the case of a dry objective with five rays (labeled 1 through 5) shown passing through a sample that is covered with a coverslip. These rays are refracted at the coverslip-air interface and only the two rays closest to the optical axis (rays 1 and 2) of the microscope have the appropriate angle to enter the objective front lens. The third ray is refracted at an angle of about 30 degrees to the coverslip and does not enter the objective. The last two rays (4 and 5) are internally reflected back through the coverslip and, along with the third ray, contribute to internal reflections of light at glass surfaces that tend degrade image resolution. When air is replaced by oil of the same refractive index as glass, shown in Figure 6.24(b), the light rays now pass straight through the glass-oil interface without deviation due to refraction. The numerical aperture is thus increased by the factor of n, the refractive index of oil.

Microscope objectives designed for use with immersion oil have a number of advantages over those that are used dry. Immersion objectives are typically of higher correction (either fluorite or apochromatic) and can have working numerical apertures up to 1.40 when used with immersion oil having the proper dispersion and viscosity. These objectives allow the substage condenser diaphragm to be opened to a greater degree, thus extending the illumination of the specimen and taking advantage of the increased numerical aperture.

A factor that is commonly overlooked when using oil immersion objectives of increased numerical aperture is limitations placed on the system by the substage condenser. In a situation where an oil objective of NA = 1.40 is being used to image a specimen with a substage condenser of smaller numerical aperture (1.0 for example), the lower numerical aperture of the condenser overrides that of the objective and the total NA of the system is limited to 1.0, the numerical aperture of the condenser.

Modern substage condensers often have a high degree of correction (see our section on condensers) with numerical aperture values ranging between 1.0 and 1.40. In order to effectively utilize all the benefits of oil immersion, the interface between the substage condenser front lens and the underside of the microscope slide containing the specimen should be also be immersed in oil. An ideal system is schematically diagramed in Figure 6.25, where immersion oil has been placed at the interfaces between the objective front lens and the specimen slide and also between the front lens of the condenser and the underside of the specimen slide.

This system has been termed a Homogeneous Immersion System and it is the ideal situation to achieve maximum numerical aperture and resolution in an optical microscope.

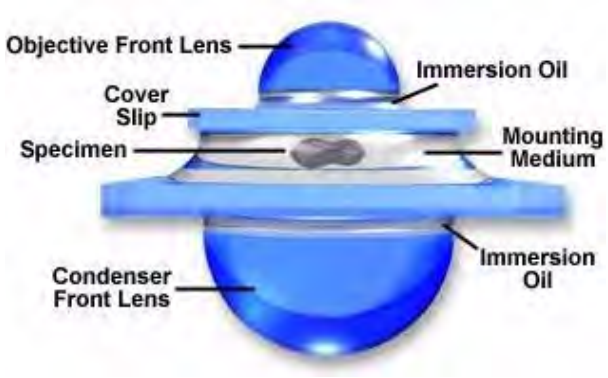

FIGURE 6.25: Homogeneous immersion system

In this case, the refractive index and dispersion of the objective front lens, immersion oil, substage condenser front lens, and the mounting medium are equal or very near equal. In this ideal system, an oblique light ray can pass through the condenser lens and completely through the microscope slide, immersion oil, and mounting medium undeviated by refraction at oil-glass or mounting medium-glass interfaces.

When using high-power achromat oil immersion objectives, it is sometimes permissible to omit the step of oiling the condenser top lens. This is because the condenser aperture diaphragm must often be reduced with lesser-corrected objectives to eliminate artifacts and provide optimum imaging. The reduction in diaphragm size reduces the potential increase in numerical aperture (provided by oiling the condenser lens) so the loss in image quality under these conditions is usually negligible.

There are a variety of commercially available synthetic oils that have been designed to optimize immersion microscopy techniques. Many countries have published their own standards for the necessary qualities of immersion oils and the International Standards Organization has recognized the ISO 8036 standard optical properties for general purpose immersion oils:

$$n_e = 1.5180 \pm 0.0005 \ (n_D = 1.515) \tag{6.4}$$

$$V_e = 44 \pm 3 \ (\text{AbbeNumber} - - - \text{ameasureofdispersion}) \tag{6.5}$$

$$\text{Temperature} = 23 \pm 0.1 \ \text{degrees Centigrade} \tag{6.6}$$

In addition to stringent control of the optical properties, immersion oils must also exhibit suitable physicochemical features such as being non-drying, inert to optical surface coatings, non-fluorescing, chemically inert, non-toxic, and easy to remove. Most microscope manufactures supply a specialized immersion oil with their objectives that is specifically matched to the dispersion properties of the objective. Make sure that any aftermarket oils you purchase meet dispersion criteria matching the objective for which the oil is intended. A number of older commercially-produced immersion oils (particularly those manufactured more than 10 years ago) contained significant amounts of polychlorinated biphenyls. These oils are carcinogenic and should be avoided, however most newer immersion oils are made without this dangerous chemical and are perfectly safe to use. The premier manufacturer of immersion media is Cargille Laboratories, Inc., of Cedar Grove, New Jersey who manufactures five standard types of oils:

TABLE 6.11: Cargille Immersion Oils

Property	Type A	Type B	Type NVH
n_F (Hydrogen F-line)	1.5236	1.5236	1.5227
n_C (Hydrogen C–line)	1.5115	1.5115	1.5118
n_D (Sodium D–line)	1.5150	1.5150	1.5150
n_e (extraordinary)	1.5180	1.5180	1.5176
Mean Dispersion (n_F—n_C)	0.0121	0.0121	0.0109
Abbe Number (V_D)	42.6	42.6	47.2
Temperature Coefficient ($\frac{-dn}{dt}$)	0.00033	0.00033	0.00031
Fluorescence (ultraviolet)	very low	low	low
Viscosity (cSt or mm2/s)	150 (low)	1250 (high)	2100 (v. high)

Normal Light Microscopy The most common immersion oil meeting two viscosity requirements (Types A and B): 150 and 1250 centistokes. These oils can be blended to produce intermediate viscosities.

High Viscosity Oil (Type NVH) Having a viscosity of 21,000 centistokes, this oil is popular for inverted, horizontal, and inclined applications and also for very long working distance objectives and samples that utilize wide condenser gaps.

Fluorescence Microscopy (Type DF) An oil that yields the highest resolution with fluorescence microscopy. This oil produces a background color that is pale green.

Fluorescence Microscopy (Type FF) Improved oil that has essentially no background fluorescence and is crystal clear and non-hydroscopic. This oil is often termed "universal" oil because it can be substituted with confidence for virtually any other immersion oil for fluorescence applications.

Table 6.11 lists the properties of the three most common types of Cargille Laboratories immersion oils.

A primary problem with common immersion oils is their inherently high absorption characteristics in the ultraviolet region of the spectrum (below about 375 nanometers). This does not affect a majority of the visible light optical microscopy done with immersion media, but it can lead to trouble when attempting to image specimens at wavelengths below 400 nanometers. The ultraviolet absorption of glycerin is negligible in the 400-350 nanometer region, so the pure solvent, or a 90:10 mixture with water, could be used for immersion techniques with near ultraviolet microscopy.

Infrared (IR) microscopy is also complicated with artifacts arising from the absorption of immersion materials at wavelengths exceeding 700 nanometers. The only practical media for IR microscopy is paraffin oil, which is also useful for fluorescence immersion microscopy because it has negligible fluorescence at wavelengths down to 350 nanometers.

The immersion media listed in Table 6.12 have a wide spectrum of refractive indices and are useful for a variety of different optical microscopy techniques. Most of the media with refractive indices equal to or lower than that of glass are used in common biological brightfield, phase contrast, DIC, and fluorescence microscopy. Those media with very high refractive indices, such as bromonaphthalene and methylene iodide, are used with specialized objectives to achieve the highest numerical aperture and resolution possible

TABLE 6.12: Common Immersion Media

Material	Refractive Index
Air	1.0003
Water	1.333
Glycerin	1.4695
Paraffin oil	1.480
Cedarwood oil	1.515
Synthetic oil	1.515
Anisole	1.5178
Bromonaphthalene	1.6585
Methylene iodide	1.740

FIGURE 6.26: Aqueous immersion objective

and are also very useful in reflected light microscopy for materials that have very low or varying reflectance.

Modern advances in tissue and cell culture techniques have sparked an interest in being able to image living cells and tissues that are bathed in physiological saline solution. Cellular dynamics inside living tissues are currently being heavily studied with quantitative optical imaging techniques including confocal, differential interference contrast (DIC), and epi-fluorescence microscopy. The average refractive index of living cells is 1.35, very close to that of the surrounding buffered aqueous-saline solution (n = 1.33) that must be present to support ongoing cellular activities. A problem arises when using long working distance dry objectives to visualize cells in aqueous tissue culture due to reflections from the surface of the liquid that will obscure details of the specimen. Likewise, the use of oil immersion objectives to observe living cells is also problematic due to refractive index differences between the aqueous imaging medium and the glass of the objective's front lens.

The objectives illustrated in Figure 6.26 are designed to be used for imaging cells and tissues in buffered saline solution, while providing plenty of room for micromanipulation of the sample during observation. The nose (or dipping cone), housing the front lens elements of the objective is tapered at a 43-degree angle to allow a steep inclination of approach providing easy access to the sample by the manipulator or microelectrodes while keeping the specimen and objective immersed in solution. These objectives also have long working

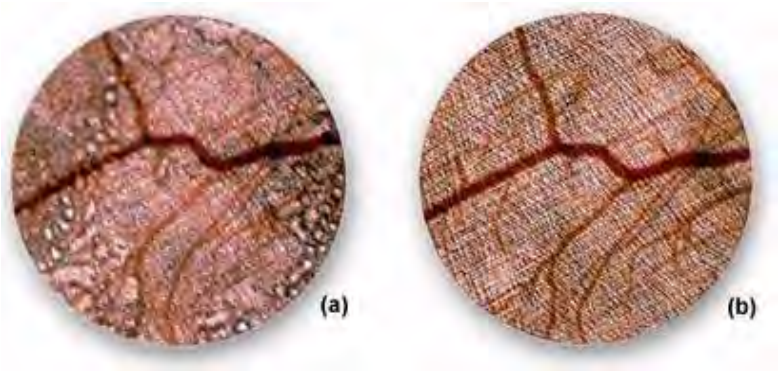

FIGURE 6.27: Rat cremaster muscle in physiologic saline

distances ranging from 2.0 mm (60x Plan Fluorite) to 3.3 mm (10x - 40x Plan Fluorite) that are also useful in allowing additional room for micromanipulation of the sample. Numerical apertures in this series of objectives are comparable (and often slightly higher) to those found in typical dry Plan Fluorites. Objectives of this type are manufactured by all of the major microscope companies including Olympus, Zeiss, Leica, and Nikon, and often the manufacturers provide additional accessories useful in micromanipulation of tissue culture samples and other biological samples.

An excellent demonstration of resolution and enhancement of fine detail seen by water immersion objectives is illustrated in Figure 6.27 with the observation of living rat cremaster muscle in tissue culture.

Figure 6.27(a) is a photomicrograph of the rat tissue taken with a normal dry 4x objective positioned just above the air/water interface. Note the distortion and blurring of the sample that occurs due to reflections from the surface of the water. These effects are eliminated in Figure 6.27(b), which is a photomicrograph of the same viewfield, but using a 4x water immersion objective. This image is considerably sharper and displays a greater resolution of fine detail than that provided by the dry objective.

Another problem with imaging tissue samples is the limited range of resolution and illumination intensity exhibited by oil immersion objectives when examining specimens at high magnification. Immersion objectives typically lose their excellent imaging properties at depths exceeding 10 microns into the sample when it is covered by a coverslip and bathed in aqueous solution. This problem is illustrated in Figure 6.28(a) where ray tracing indicates that a sphere in aqueous media is distorted into an apparently elongated oval when using an oil immersion objective to image the sample through immersion oil having $n = 1.515$.

The same sphere remains spherical when using a water immersion objective, even though the imaging rays must still pass through the glass coverslip with a refractive index equal to 1.515. Water immersion objectives also eliminate spherical aberrations that are often produced when viewing specimens through an aqueous solution. These advanced objectives also have an increased axial resolution that often equals the theoretical limits for the numerical aperture and they produce exceptional contrast, resolution, and provide a higher intensity of illumination.

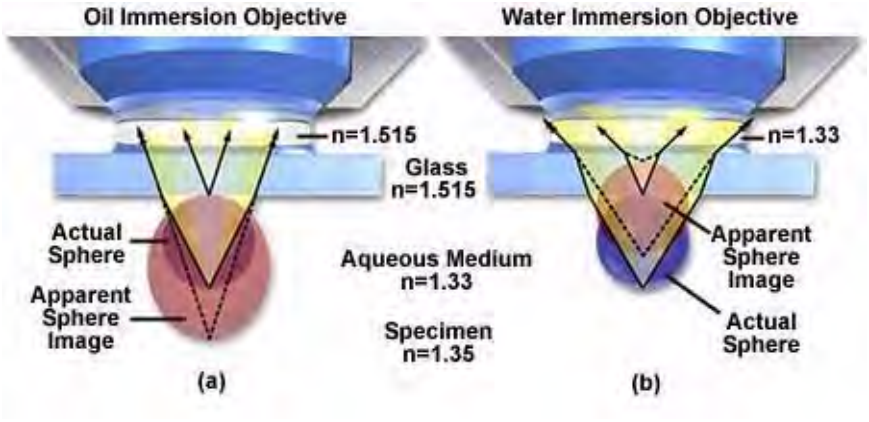

FIGURE 6.28: Distortion in aqueous media

6.5.1 Technical Tips for Oil Immersion Microscopy

The first rule in microscopy is to keep the optical elements completely free of dust, dirt, oil, solvents, and any other contaminants. The microscope should be kept in a low vibration smoke-free room that is clean as possible and has minimal disturbance of the circulated air. Use a dust cover on the microscope when not in use and keep all accessories in air-tight containers. Avoid using corrosive solvents to clean any part of the microscope, and use only diluted soapy water to clean non-optical surfaces. Oil should be used keeping the following techniques and precautions in mind:

- The first step is to locate the sample with a low-power objective and position the microscope slide so that the area of interest is squarely in the central portion of the stage opening. It is often desirable to rotate the immersion objective (without oil) into place to ensure the correct location of the specimen. To achieve optimum results when using the oil immersion technique it is important to also apply oil to the underside of the microscope slide and to the top lens of the substage condenser to form an oil bead between the two, as described below. Most modern microscopes provide a relatively wide oval-shaped opening in the mechanical stage to allow oil to be used in the area between the bottom of the microscope slide and the front lens of the condenser.

- Swing the immersion objective to a position in the nosepiece where it will be the next objective rotated into the optical pathway directly above the specimen. Use a piece of lint-free paper or an eyedropper to place a small droplet of oil directly on the front lens of the immersion objective. Next, place another droplet of oil on the cover glass immediately above the area to be imaged. Many of the newer oil immersion objectives manufactured by Olympus and Nikon use plano-concave front lenses in their immersion objectives, and it is imperative that the step of oiling the objective front lens not be omitted with these objectives. Failure to fill the concave "cavity" in these objectives may result in entrapment of a tiny air bubble resulting in severe flare and image degradation.

- Slowly lower the oil objective into the small pool of oil on the microscope coverslip using the coarse focusing adjustment knob. When the oil-covered objective front lens

makes contact with the oil on the coverslip, a small flash of scattered light will be emitted at the oil junction, indicating that the two oil pools have merged. Be very careful with this step, because racking the objective too close to the coverslip can cause a collision between the two, possibly resulting in damage.

- Bring the specimen slowly into focus using the coarse adjustment until details just begin to become visible, and then switch to the fine adjustment to bring the specimen into proper focus. It is important to remember that the working distance of most fluorite and apochromat objectives is less than one-tenth of a millimeter, resulting in a very narrow range of adjustment of the fine focus knob, so carefully monitor the objective's approach to the oil pool while lowering it with either the coarse or fine adjustment. Although most high-power immersion oil objectives have spring-loaded front ends that can be retracted into the body of the objective, careless use of these objectives can still drive the objective into the specimen slide causing damage.

- An alternative method used by many microscopists is to position the area to be imaged in the center of the microscope's optical path using lower power objectives. Next, the oil immersion objective (without oil) is placed into the optical path and the specimen area of interest is roughly brought into center of the viewfield and focused. This pre-positions all of the components of the system in preparation for the addition of oil. Swing the immersion objective to an adjacent stop on the microscope nosepiece and apply oil both to the objective front lens and specimen as discussed above. Next, quickly rotate the oiled objective into position above the specimen merging the two oil droplets (one on the sample and one on the objective) into a single pool. The specimen is now ready for observation and photomicrography.

For applying oil to the front lens of the substage condenser, use the following considerations:

- Make certain that the mechanical stage of the microscope has an opening of sufficient size to allow scanning of the oiled specimen without spilling oil onto the bottom of the stage. Many advanced research microscopes have a stage insert that is removable for use with oil. Remove the specimen slide from the microscope stage before applying oil to the condenser top lens.

- In a manner similar to oiling an objective, place a drop of oil on the bottom of the microscope slide and apply a similar drop to the front lens of the substage condenser. Make sure that the condenser is slightly lowered in its rack before replacing the microscope slide on the stage. After the slide has been placed on the stage, rack the condenser back to the proper position while carefully observing the oil droplets on the condenser lens and microscope slide. These droplets should merge into one as the condenser is brought into proper position.

- As you scan the surface of an oiled microscope slide, periodically observe the position of the stage with respect to the objective and condenser front lens to assure that there is a continuous bead of oil between these elements and the microscope slide. When scanning over a large area on a microscope slide, it is often necessary to reapply some oil to assure continuity of the imaging medium.

FIGURE 6.29: Mechanical tube length (transmitted light)

Keep The Lenses Clean and Oil-Free

Always strive to make sure that your microscope objective and substage condenser front lenses are kept clean and free of immersion oil. Many manufactures advertise non-drying immersion oils that are reported to have such a high vapor pressure that solvents will not evaporate, leaving crystalline residue on optical surfaces. This may be almost true in some instances, but it is dangerous to gamble with expensive optical equipment. Use a Q-tip or lint-free paper or cloth to gently wipe excess oil from the lenses and microscope slide after experiments are finished. After the oil is removed, use a suitable solvent to remove traces of immersion oil from the lenses. Failure to clean lenses properly may result in small crystallites forming on the coated surfaces when immersion oils either dry or collect dust and other contaminating particles from the atmosphere.

6.6 Mechanical Tube Length

The mechanical tube length of an optical microscope is defined as the distance from the nosepiece opening, where the objective is mounted, to the top edge of the observation tubes where the eyepieces (oculars) are inserted. The drawing in Figure 6.29 illustrates the optical path (the red line) defining the mechanical tube length for a typical transmitted light microscope.

For many years, almost all prominent microscope manufacturers designed their objectives for a finite tube length. The designer proceeded under the assumption that the specimen, at focus, was placed at a distance a "little" further than the front focal plane of the objective. The objective then projects a magnified image of the specimen which converges (is brought into focus) at the level of the eyepiece diaphragm, located ten millimeters below the top edge of the openings of the microscope observation tube–where the

FIGURE 6.30: Reflected light microscope tube length

eyepieces are inserted (see Figures 6.29 and 6.30).

Tube length has now been standardized to the Royal Microscopical Society (RMS) suggestion of 160 millimeters for finite–corrected transmitted light microscopes. Objectives designed for a 160 millimeter finite tube length microscope bear the inscription "160" (mm) on the barrel as outlined in our discussion on objective specifications and identification. The positioning of the ocular and objectives is reversed in metallographs, which are essentially inverted reflected light microscopes as illustrated in figure 6.30. Note that in both the examples depicted in Figures 6.29 and 6.30, the "tube" is not a straight line and the light waves are transmitted from the objectives to the eyepieces (oculars) with mirrored beam splitters. This is the case with most modern microscopes, especially those equipped with trinocular heads for photomicrography.

Some older microscopes have mechanical tube lengths that deviate from the 160 millimeter standard. Microscopes produced by Leitz instruments continued to be manufactured with a 170 millimeter tube length long after the RMS standard had been incorporated by other manufacturers. We caution microscopists who attempt to insert objectives designed for one mechanical tube length into a microscope designed for a different tube length. When objectives and tube lengths are mismatched, image quality often suffers due to the introduction of spherical aberrations because the optical tube length is changed. The optical tube length is defined as the distance between the objective rear focal plane and the intermediate or primary image at the fixed diaphragm of the eyepiece. When this tube length is altered to deviate from design specifications, spherical aberrations are introduced into the microscope and images suffer from deterioration in optical quality. Under circumstances where an objective designed for a 170 millimeter tube length is used in a microscope

with a 160 millimeter tube length, corrections designed into the objective will cause it to under-compensate for aberrations. The opposite is true when 160 millimeter objectives are used in a 170 millimeter tube length microscope.

With a finite tube length microscope system, whenever an accessory such as a polarizing intermediate piece, a DIC Wollaston prism, or a fluorescence illuminator, is placed in the light path between the back of the objective and the eyepiece, the mechanical tube length becomes greater than 160 millimeters. Aberrations may then be introduced when the specimen is refocused. As a result, each such accessory in a finite system must contain optical elements to bring the tube length ostensibly back to 160 millimeters. Often such devices result in a undesirable increase in magnification and lower the overall intensity of the image. There is also the danger of producing "ghost images": the result of converging rays passing through the beam-splitter of a reflected light accessory.

As we have seen from the discussion above, the body tubes in modern microscopes contain a complex assembly of lenses, mirrors, and beam splitters that transmit light from the objective into the eyepieces. Almost all microscope manufacturers are now designing their microscopes to support infinity–corrected objectives. Such objectives project an image of the specimen to infinity (the common description is not quite accurately stated as emerging parallel rays). To make viewing of the image possible, the body tube of the microscope, or in reflected light microscopy the vertical illuminator itself, must contain a tube lens. This lens has, as its main function, the formation of the image at the plane of the eyepiece diaphragm, the so-called intermediate image plane. The eyelens of the eyepiece "looks at" this real, inverted, magnified image and magnifies that image in the usual second stage magnification of the compound microscope.

Infinity–corrected systems are especially valuable because they eliminate "ghost images" (caused by converging light passing through inclined plane glass surfaces) that often accompanied the older forms of instrumentation. Such systems have the advantage of being easier to design and also make possible the insertion of less costly accessories in the "parallel" light path. This advanced new optical system allows microscopes to support complex optical component clusters in the optical pathway between the objective and the lens tube. This is especially useful for techniques such as confocal, polarized, DIC, and epifluorescence microscopy where specialized lens systems must be employed for optimum results.

In modern infinity–corrected systems, the tube lens is a multi-element optic (to prevent introduction of coma or astigmatism even with increased "infinity light path space") built into and sealed in the observation tube. In this design, as many as two intermediate accessories can be accommodated, with no additional optics to correct the image, in the "infinity space" (see Figure 6.31) between the objective and the tube lens. Ghost images are eliminated as discussed above. Accessories are much easier to design; and unwanted extra magnification factors are avoided. The light paths illustrated in Figure 6.31 are diagrammatic representations of an infinity–corrected microscope system. The left-hand side of Figure 6.31 shows the focal points at the front focal plane of the objective and the eyepiece diaphragm plane. The right-hand side illustrates the "infinity space" between the objective and tube lens where intermediate attachments are placed into the light path.

The schematic infinity–corrected systems illustrated in Figure 6.32 indicate how additional optical components can be inserted into the light path. Figure 6.32(a) is a diagrammatic representation of an infinity–corrected system showing a specimen on a microslide being illuminated by a substage condenser. The image-forming light rays pass through the

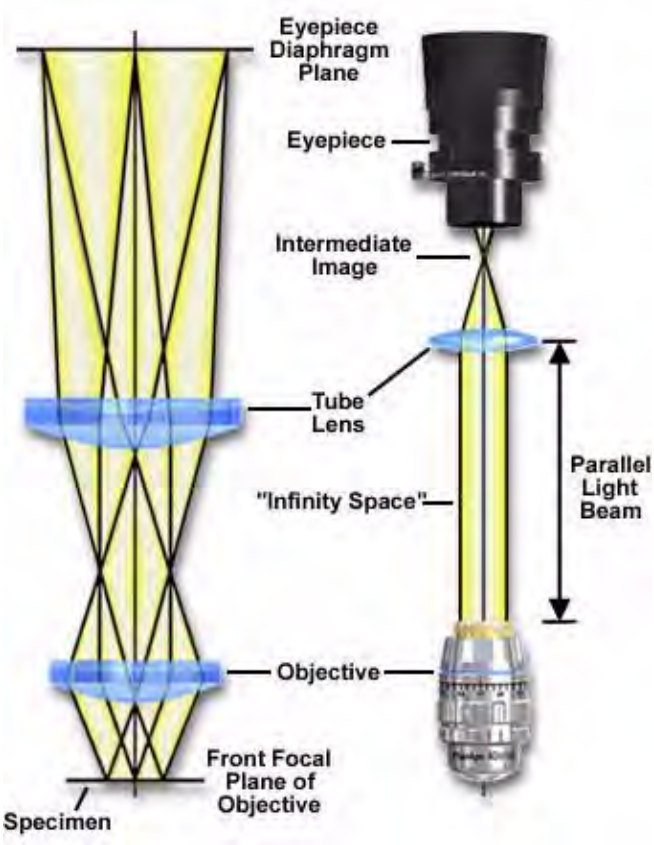

FIGURE 6.31: Infinity–corrected objective system

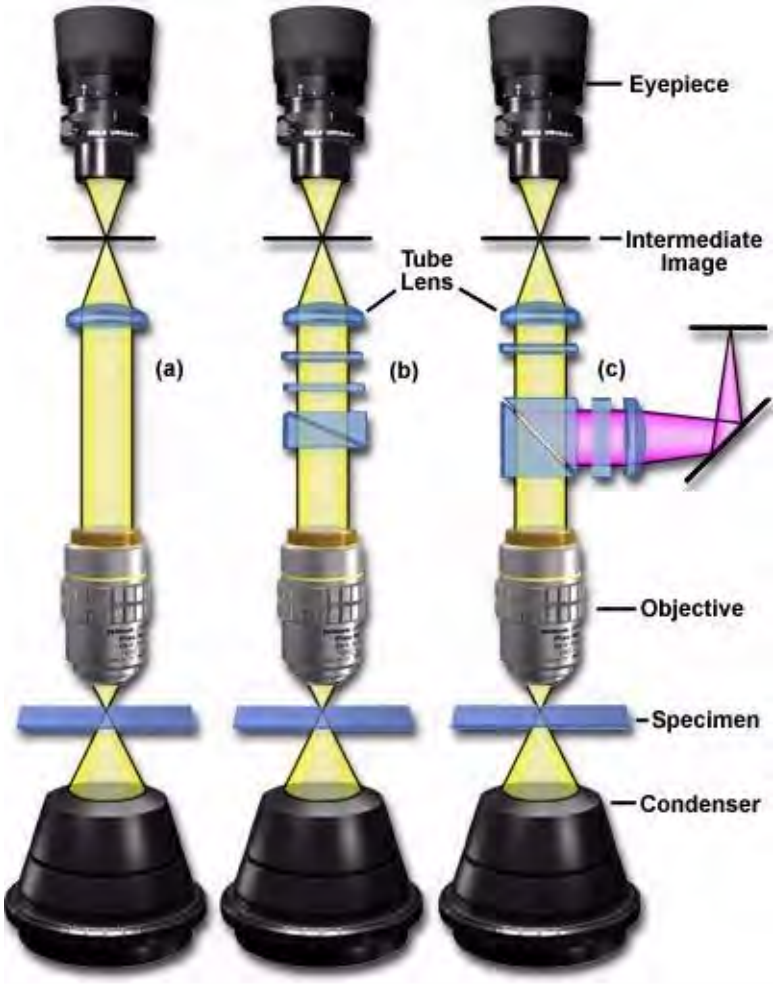

FIGURE 6.32: Infinity–corrected objective system: additional optical components

objective and form a parallel light beam that is focused by the tube lens into the eyepiece. Accessories can be inserted into the parallel light beam without further optical correction as illustrated in Figure 6.32(b), which shows a Wollaston prism and several polarizers inserted into the pathway. Figure 6.32(c) illustrates the insertion of a beam-splitter into the parallel light beam. This beam-splitter diverts light to the external accessory positioned on the right of the parallel beam.

Infinity–corrected objectives come in a wide range of magnifications, from 1.5X to 200X, and in various qualities of chromatic and spherical correctionfrom simple achromats to planachromats and precision planapochromats. Most, but not all, are designed to be used dry, that is with air in the space between the objective and the specimen. The brightfield series have the customary microscope thread for screwing into the nosepiece (see Figure 6.33). The objectives which are used for brightfield/darkfield observation usually have wider diameter threads and require a nosepiece with wider openings for attaching such objectives (these objectives are called Neo, BF/DF, or B/D objectives).

Some reflected light objectives are designed to focus at a longer working distance from the specimen than is usual; such objectives are labeled on the barrel of the objective as LWD (long working distance) or ULWD (ultra-long working distance). The manufacturer

FIGURE 6.33: Infinity–corrected objectives

usually designates the objective series to be used for reflected light Nomarski differential interference contrast studies; e.g., in the case of Olympus, the appropriate series is the MS Plan series for brightfield objectives and the Neo S Plan in the brightfield/darkfield series. Such objectives are sometimes labeled NIC on the objective barrel or designated as strain-reduced.

Infinity–corrected objectives are inscribed with an infinity mark (inf). The magnification yielded by the objective is the quotient of the focal length of the tube lens divided by the focal length of the objective. For example, in the Olympus microscope system with the tube lens having a focal length of 180 millimeters, a 9 millimeter focal length objective will project a 20X magnified image onto the plane of the eyepiece diaphragm. With a tube lens of 180 millimeters, it is possible to design objectives with a magnification as low as 1.25X while still maintaining the parfocalizing distance of 45 millimeters.

6.7 Infinity Optical Systems

Over the past 10 years, the major microscope manufacturers have largely all migrated to the utilization of infinity-corrected optical systems in both research-grade biomedical and industrial microscopes. In these systems, the image distance is set to infinity, and a tube (or telan) lens is strategically placed within the body tube between the objective and the eyepieces (oculars) to produce the intermediate image.

Infinity optical systems allow introduction of auxiliary components, such as differential interference contrast (DIC) prisms, polarizers, and epi-fluorescence illuminators, into the parallel optical path between the objective and the tube lens with only a minimal effect on focus and aberration corrections. Older finite, or fixed tube length, microscopes have a specified distance from the nosepiece opening, where the objective barrel is secured, to the ocular seat in the eyepiece tubes. This distance is referred to as the mechanical tube length of the microscope. The design assumes that when the specimen is placed in focus, it is a few microns further away than the front focal plane of the objective. Finite tube lengths were standardized at 160 millimeters during the nineteenth century by the Royal Microscopical Society (RMS) and enjoyed widespread acceptance for over 100 years. Objectives designed to be used with a microscope having a tube length of 160 millimeters are inscribed with this value on the barrel.

Adding optical accessories into the light path of a fixed tube length microscope increases

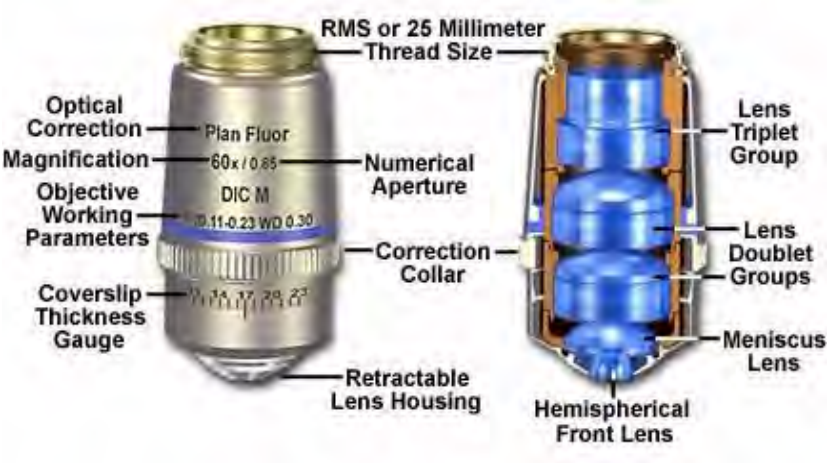

FIGURE 6.34: Infinity–corrected objectives

the effective tube length to a value greater than 160 millimeters. For this reason, addition of a vertical reflected light illuminator, polarizing intermediate stage, or similar attachment can introduce spherical aberration into an otherwise perfectly-corrected optical system. During the period when most microscopes had fixed tube lengths, manufacturers were forced to place additional optical elements into these accessories to re-establish the effective 160-millimeter tube length of the microscope system. The cost of this action was often an increase in magnification and reduced light intensities in resulting images.

Some reflected light systems were also hampered by "ghost images" that occur as a result of converging light rays passing through the beam-splitter. In an attempt to circumvent artifacts brought about by addition of auxiliary optical components, the German microscope manufacturer Reichert originally pioneered the concept of infinity optics. The company started experimenting with infinity-corrected optical systems as early as the 1930s followed later by Leica and Zeiss, but these optics did not become standard equipment with most manufacturers until the 1980s.

The tube length in infinity-corrected microscopes is referred to as the reference focal length and ranges between 160 and 200 millimeters, depending upon the manufacturer (see Table 6.13). Correction for optical aberration in infinity systems is accomplished either through the tube lens or the objective(s). Residual lateral chromatic aberration in infinity objectives can be easily compensated by careful tube lens design, but some manufacturers, including Nikon, choose to correct for spherical and chromatic aberrations in the objective lens itself. This is possible because of the development of proprietary new glass formulas that have extremely low dispersions. Still other manufacturers (notably, Zeiss ICS systems) utilize a combination of corrections in both the tube lens and objectives.

Presented in Table 6.13 are the specifications, including tube lens focal lengths, parfocal distance, and the objective thread type, of infinity-corrected microscopes offered by the major manufacturers. Although both Leica and Nikon use a tube length of 200 millimeters and an objective thread size of 25 millimeters, the objective parfocal distance is significantly greater with the Nikon CFI60 system. Olympus and Zeiss use a shorter tube lens focal length (180 and 165 millimeters, respectively), but both companies have standardized objective thread sizes and adhere to a parfocal length of 45 millimeters.

In a finite optical system of fixed tube length, light passing through the objective

TABLE 6.13: Infinity Optical System Parameters

Manufacturer	Tube Lens Focal Length (mm)	Parfocal Distance (mm)	Thread Type
Leica	200	45	M25
Nikon	200	60	M25
Olympus	180	45	RMS
Zeiss	165	45	RMS

is directed toward the intermediate image plane (located at the front focal plane of the eyepiece) and converges at that point, undergoing constructive and destructive interference to produce an image (Figure 6.35(a)). The situation is quite different for infinity-corrected optical systems where the objective produces a flux of parallel light wavetrains imaged at infinity (often referred to as infinity space; Figure 6.35(b)), which are brought into focus at the intermediate image plane by the tube lens. It should be noted that objectives designed for infinity-corrected microscopes are usually not interchangeable with those intended for a finite (160 or 170 millimeter) optical tube length microscope and vise versa. Infinity lenses suffer from enhanced spherical aberration when used on a finite microscope system due to lack of a tube lens. In some circumstances it is possible, however, to utilize finite objectives on infinity-corrected microscopes, but with some drawbacks. The numerical aperture of finite objectives is compromised when they are used with infinity systems, which leads to reduced resolution. Also, parfocality is lost between finite and infinity objectives when used in the same system. The working distance and magnification of finite objectives will also be decreased when they are used with a microscope having a tube lens.

As mentioned above, the basic optical components of an infinity system are the objective, tube lens, and the eyepieces. As illustrated in Figure 6.35(b), the specimen is located at the front focal plane of the objective, which gathers light transmitted through or reflected from the central portion of the specimen and produces a parallel bundle of rays projected along the optical axis of the microscope toward the tube lens. A portion of the light reaching the objective emanates from the periphery of the specimen, and enters the optical system at oblique angles, advancing diagonally (but still in parallel bundles) toward the tube lens. All of the light gathered by the tube lens is then focused at the intermediate image plane, and subsequently enlarged by the eyepiece.

The objective and tube lens together form a compound objective lens system that produces an intermediate image at a finite distance within the microscope tube. Location of the tube lens with respect to the objective is of primary concern when designing infinity-corrected microscopes. The region between the objective and tube lens (infinity space) provides a path of parallel light rays into which complex optical components can be placed without the introduction of spherical aberration or modification of the objective working distance. In fact, parfocality between different objectives in a matched set can be maintained with infinity-corrected microscopes, even when one or two auxiliary components are added to the optical path. Another major benefit is that accessories can be designed to produce an exact 1x magnification value without altering the alignment between the objective and tube lens. This feature allows comparison of specimens using a combination of several optical techniques, such as phase contrast or DIC with fluorescence (individually or simultaneously). This is possible because optical accessories placed into a set of parallel light waves do not shift the location (either laterally or axially) nor the focal point of the

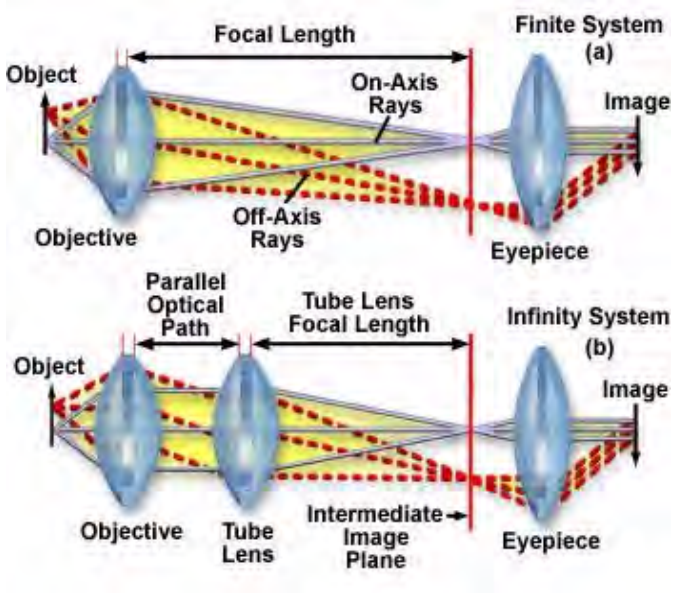

FIGURE 6.35: Finite and infinite optical system

image.

If the tube lens is located very close to the objective, the amount of space available for auxiliary optical components is limited. However, there is an upper limit to the number of optical components that can be situated between the tube lens and the objective within the constraints of modern microscope design. Placing the tube lens too far from the objective reduces the number of peripheral light waves collected by the lens, resulting in images that have darkened or blurred edges, and reducing the performance of the microscope. It should be emphasized that the term infinity optics refers to the production of a flux of parallel right rays after passing through the objective, not that an infinite space is available inside the microscope. To maximize the flexibility of microscope configuration while maintaining high performance, it is necessary to optimize the distance between the objective and tube lens.

The magnification produced by an infinity-corrected objective is calculated by dividing the reference focal length (tube length) by the focal length of the objective. As the focal length of the tube lens is increased, the distance to the intermediate image plane also increases, which results in a longer overall tube length. Tube lengths between 200 and 250 millimeters are considered optimal, because longer focal lengths will produce a smaller off-axis angle for diagonal light rays, reducing system artifacts. Longer tube lengths also increase the flexibility of the system with regard to the design of accessory components.

The advantages of a longer tube lens focal length becomes apparent when comparing systems having a 160-millimeter and a 200-millimeter tube lens focal length (Figure 6.36). Reduction in the off-axis diagonal wave flux angle can approach a significant percentage with the longer focal length optical system. The reduced angle of the oblique light rays produces correspondingly smaller shifts in both on-axis and off-axis rays passing through accessory components (DIC prisms, phase rings, dichroic mirrors, etc.), which improves the efficiency of the microscope. Dramatic enhancement in contrast levels observed with epi-fluorescence illuminators in infinity-corrected systems is attributed to the optical advantage of longer tube lens focal lengths.

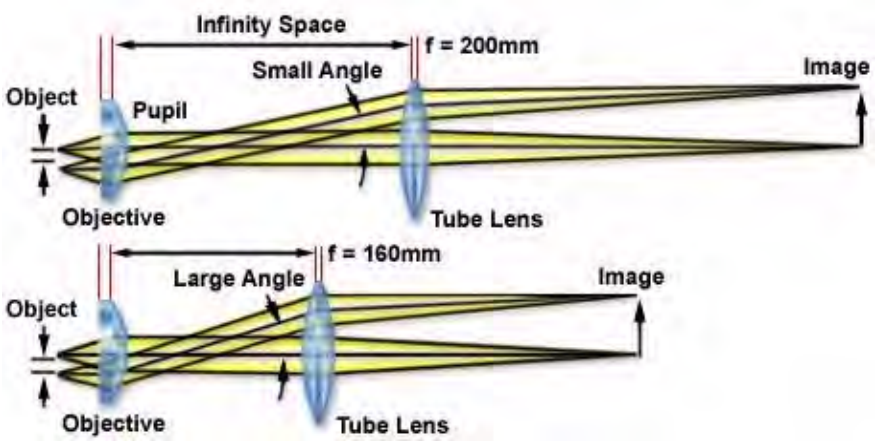

FIGURE 6.36: Off–axis light flux versus tube length in infinity system

The objective focal length must be increased with infinity systems to preserve the same magnification when compared to older fixed tube length systems. A parfocal distance of 45 millimeters was used by all microscope manufacturers for many years with finite tube length systems, but this may be inadequate for high-performance infinity-corrected optics. For instance, a plan apochromatic 60x oil-immersion objective (one of the best performing finite objectives) can have over 10 individual lens elements and groups, resulting in a very tight fit for objectives constrained to a parfocal distance of 45 millimeters. When replaced by an infinity system that is subdivided into a separate objective (with an even greater number of optical elements) and tube lens, the focal length of the tube lens becomes equivalent to approximately 150 millimeters. To meet the full optical potential of the infinity system, the objective parfocal distance must be matched to the tube lens focal length. Thus, for a 200-millimeter focal length, the optimum parfocal distance is 60 millimeters, exceeding the older standardized length by 15 millimeters.

Longer objective focal lengths utilized in infinity optical systems require correspondingly larger working distances to match. Increasing the parfocal distance of the objective is paramount to achieving a significant increase in working distance, especially for lower magnification objectives. For instance, with a 1x objective, the formula used to calculate magnification for infinity-corrected systems dictates that objective focal length should be the same as the tube lens. In a system with a 200-millimeter tube lens focal length, this would necessitate a longer parfocal distance in order to use an objective of this low magnification. Calculations reveal that a magnification as low as 0.5x can be obtained with 200-millimeter tube lens focal lengths, but that shorter focal lengths restrict the minimum objective magnification to values slightly above the 1x range.

Another consideration is the objective pupil diameter, which also must be increased for optimum performance with low-magnification objectives in optical systems having long tube lens focal lengths. The RMS standard objective thread size, 20.32 millimeters, limits the effective pupil diameter and maximum attainable numerical aperture in objectives so equipped. In order to produce higher numerical apertures when long tube lens focal lengths are being utilized, the objective thread size must be increased. The effective exit pupil diameter (D) necessary to achieve a desired numerical aperture is expressed by the formula:

$$D = 2\mathrm{NA} \cdot f$$

where NA is the numerical aperture and f is the objective focal length. Thus, for a 2x apochromatic objective having a focal length of 100 millimeters (utilizing a 200-millimeter focal length tube lens) and a numerical aperture of 0.10, the necessary exit pupil diameter (D) is 20 millimeters. Clearly, a smaller objective thread size limits objective numerical aperture at magnifications lower than 10x when designing infinity optical systems. Increasing the tube length above 200 millimeters requires an even greater objective exit pupil size, making this a limiting factor in the design of infinity-corrected microscopes.

Although all four major microscope manufacturers now offer infinity-corrected microscopes, Nikon is the only one that has made the transition to larger thread sizes, longer working distances, and an increased parfocal range. The company now offers a lineup of over 80 CFI60 objectives having a thread size of 25 millimeters, a parfocal distance of 60 millimeters, and designed to operate in microscopes having a 200-millimeter tube length. The acronym CFI stands for Chromatic aberration-Free (or Chrome Free) Infinity, and these objectives have the longest working distances and largest combinations of magnification at high numerical aperture currently available.

Chapter 7

Eyepieces (Oculars)

Eyepieces work in combination with microscope objectives to further magnify the intermediate image so that specimen details can be observed. Oculars is an alternative name for eyepieces that has been widely used in the literature, but to maintain consistency during this discussion we will refer to all oculars as eyepieces.

Best results in microscopy require that objectives be used in combination with eyepieces that are appropriate to the correction and type of objective. The basic anatomy of a typical modern eyepiece is illustrated in Figure 7.1. Inscriptions on the side of the eyepiece describe its particular characteristics and function.

The eyepieces illustrated in Figure 7.1 are inscribed with UW, which is an abbreviation for the Ultra Wide viewfield. Often eyepieces will also have an H designation, depending upon the manufacturer, to indicate a high-eyepoint focal point that allows microscopists to wear glasses while viewing samples. Other inscriptions often found on eyepieces include WF for Wide-Field; UWF for Ultra Wide-Field; SW and SWF for Super Wide-Field; HE for High Eyepoint; and CF for eyepieces intended for use with CF corrected objectives. Compensating eyepieces are often inscribed with K, C, or comp as well as the magnification. Eyepieces used with flat-field objectives are sometimes labeled Plan-Comp. The eyepiece magnification of the eyepieces in Figure 7.1 is 10x (indicated on the housing), and the inscription A/24 indicates the field number is 24, which refers to the diameter (in millimeters) of the fixed diaphragm in the eyepiece. These eyepieces also have a focus

FIGURE 7.1: Aberration-free 10x eyepiece with diopter adjustment

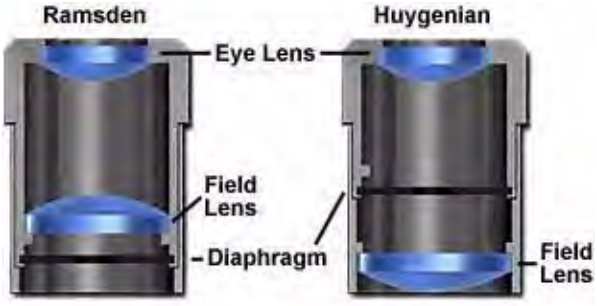

FIGURE 7.2: Simple eyepiece

adjustment and a thumbscrew that allows their position to be fixed. Manufactures now often produce eyepieces having rubber eye-cups that serve both to position the eyes the proper distance from the front lens, and to block room light from reflecting off the lens surface and interfering with the view.

There are two major types of eyepieces that are grouped according to lens and diaphragm arrangement: the negative eyepieces with an internal diaphragm and positive eyepieces that have a diaphragm below the lenses of the eyepiece. Negative eyepieces have two lenses: the upper lens, which is closest to the observer's eye, is called the eye-lens and the lower lens (beneath the diaphragm) is often termed the field lens. In their simplest form, both lenses are plano-convex, with convex sides "facing" the specimen. Approximately midway between these lenses there is a fixed circular opening or internal diaphragm which, by its size, defines the circular field of view that is observed in looking into the microscope. The simplest kind of negative eyepiece, or Huygenian eye-piece (illustrated in Figure 7.2), is found on most routine microscopes fitted with achromatic objectives. Although the Huygenian eye and field lenses are not well corrected, their aberrations tend to cancel each other out. More highly corrected negative eyepieces have two or three lens elements cemented and combined together to make the eye lens. If an unknown eyepiece carries only the magnification inscribed on the housing, it is most likely to be a Huygenian eyepiece, best suited for use with achromatic objectives of 5x-40x magnification.

The other main kind of eyepiece is the positive eyepiece with a diaphragm below its lenses, commonly known as the Ramsden eyepiece, as illustrated in Figure 7.2 (on the left). This eyepiece has an eye lens and field lens that are also plano-convex, but the field lens is mounted with the curved surface facing towards the eye lens. The front focal plane of this eyepiece lies just below the field lens, at the level of the eyepiece diaphragm, making this eyepiece readily adaptable for mounting graticules. To provide better correction, the two lenses of the Ramsden eyepiece may be cemented together.

A modified version of the Ramsden eyepiece is known as the Kellner eyepiece, as illustrated on the left in Figure 7.3. These improved eyepieces contain a doublet of eye-lens elements cemented together and feature a higher eyepoint than either the Ramsden or Huygenian eyepiece as well as a much larger field of view. A modified version of the simple Huygenian eyepiece is also illustrated in Figure 7.3, on the right. While these modified eyepieces perform better than their simple one-lens counterparts, they are still only useful with low-power achromat objectives.

Simple eyepieces such as the Huygenian and Ramsden and their achromatized counterparts will not correct for residual chromatic difference of magnification in the intermediate

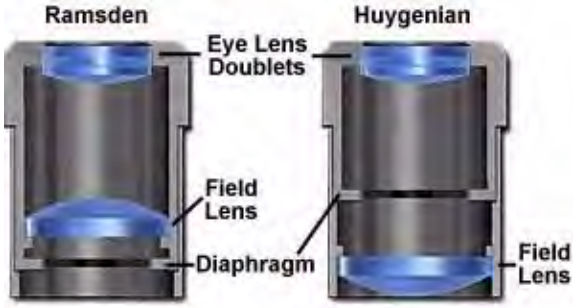

FIGURE 7.3: Corrected simple eyepiece (Kellner design

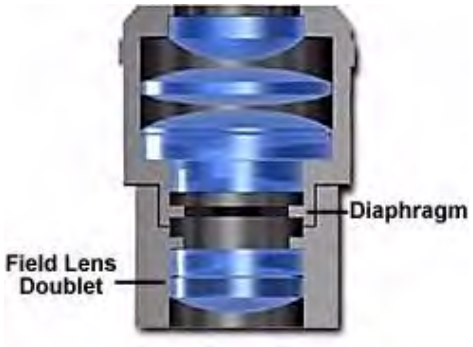

FIGURE 7.4: Periplan eyepiece

image, especially when used in combination with high magnification achromatic objectives as well as any fluorite or apochromatic objectives. To remedy this, manufacturers produce compensating eyepieces that introduce an equal, but opposite, chromatic error in the lens elements. Compensating eyepieces may be either of the positive or negative type, and must be used at all magnifications with fluorite, apochromatic and all variations of plan objectives (they can also be used to advantage with achromatic objectives of 40x and higher). In recent years, modern microscope objectives have their correction for chromatic difference of magnification either built into the objectives themselves (Olympus and Nikon) or corrected in the tube lens (Leica and Zeiss).

Compensating eyepieces play a crucial role in helping to eliminate residual chromatic aberrations inherent in the design of highly corrected objectives. Hence, it is preferable that the microscopist uses the compensating eyepieces designed by a particular manufacturer to accompany that manufacturer's higher-corrected objectives. Use of an incorrect eyepiece with an apochromatic objective designed for a finite (160 or 170 millimeter) tube length application results in dramatically increased contrast with red fringes on the outer diameters and blue fringes on the inner diameters of specimen detail. Additional problems arise from a limited flatness of the viewfield in simple eyepieces, even those corrected with eye-lens doublets.

More advanced eyepiece designs resulted in the Periplan eyepiece that is illustrated in Figure 7.4 above. This eyepiece contains seven lens elements that are cemented into a single doublet, a single triplet, and two individual lenses. Design improvements in periplan eyepieces lead to better correction for residual lateral chromatic aberration, increased flatness of field, and a general overall better performance when used with higher power objectives.

Table 7.1: Properties of Commercial Eyepieces

E. Type	Finder E.			Super Widefield E.	Wide Field E.		
Descriptive Abbreviation	PSWH 10x	PWH 10x	35 SWH 10x	SWH 10xH	CROSS-WH 10x H	WH 15x	WH 10x H
Field Number	26.5	22	26.5	26.5	22	14	22
Diopter Adjustment	-8+2	-8+2	-8+2	-8+2	-8+2	-8+2	
Remarks	$3\frac{1}{4}$x$4\frac{1}{4}$ photo mask	$3\frac{1}{4}$x$4\frac{1}{4}$ photo mask	35mm photo mask	D.C.	D.C. crossline		D.C.
Diameter of Micrometer Graticule	—	—	—	—	—	24	24

E.=eyepiece

D.C.=Diopter correction

Modern microscopes feature vastly improved plan-corrected objectives in which the primary image has much less curvature of field than older objectives. In addition, most microscopes now feature much wider body tubes that have greatly increased the size of intermediate images. To address these new features, manufacturers now produce wide-eyefield eyepieces (illustrated in Figure 7.1) that increase the viewable area of the specimen by as much as 40 percent. Because the strategies of eyepiece-objective correction techniques vary from manufacturer to manufacturer, it is very important (as stated above) to use only eyepieces recommended by a specific manufacturer for use with their objectives.

Our recommendation is to carefully choose the objective first, then purchase an eyepiece that is designed to work in conjunction with the objective. When choosing eyepieces, it is relatively easy to differentiate between simple and more highly compensated eyepieces. Simple eyepieces such as the Ramsden and Huygenian (and their more highly corrected counterparts) will appear to have a blue ring around the edge of the eyepiece diaphragm when viewed through the microscope or held up to a light source. In contrast, more highly corrected compensating eyepieces with have a yellow-red-orange ring around the diaphragm under the same circumstances.

The properties of several common commercially available eyepieces (manufactured by Olympus America, Inc.) are listed according to type in Table 7.1. The three major types of eyepieces listed in Table 7.1 are Finder, Wide Field, and Super Widefield. The terminology used by various manufacturers can be very confusing and careful attention should be paid to their sales brochures and microscope manuals to ensure that the correct eyepieces are being used with a specific objective. In Table 7.1, the abbreviations that designate wide field and super widefield eyepieces are coupled to their correction for high eyepoint, and are WH and SWH, respectively. The magnifications are either 10x or 15x and the Field Numbers (discussed below) range from 14 to 26.5, depending upon the application. The

diopter adjustment is approximately the same for all eyepieces and many also contain either a photomask or micrometer graticule.

Light rays emanating from the eyepiece intersect at the exit pupil or eyepoint, often referred to as the Ramsden disc, where the pupil of the microscopists eye should be placed in order for her to see the entire field of view (usually 8-10 mm from the eye lens). By increasing the magnification of the eyepiece, the eyepoint is drawn closer to the upper surface of the eye lens, making it much more difficult for the microscopist to use, especially if they are wearing eyeglasses. To compensate for this, specially designed high eyepoint eyepieces have been manufactured that feature eyepoint distances approaching 20-25 mm above the surface of the eye lens. These improved eyepieces have larger diameter eye lenses that contain more optical elements and usually feature improved flatness of field. Such eyepieces are often designated with the inscription "H" somewhere on the eyepiece housing, either alone or in combination with other abbreviations, as discussed above. We should mention that high-eyepoint eyepieces are especially useful for microscopists who wear eyeglasses to correct for near or far sightedness, but they do not correct for several other visual defects, such as astigmatism. Today, high eyepoint eyepieces are very popular, even with people who do not wear eyeglasses, because the large eye clearance reduces fatigue and makes viewing images through the microscope much more pleasurable.

At one time, eyepieces were available in a wide spectrum of magnifications ranging from 6.3x to 25x and sometimes even higher for special applications. These eyepieces are very useful for observation and photomicrography with low-power objectives. Unfortunately, with higher power objectives, the problem of empty magnification becomes important when using very high magnification eyepieces and these should be avoided. Today most manufacturers restrict their eyepiece offerings to those in the 10x to 20x range. The diameter of the viewfield in an eyepiece is expressed as a "field-of-view number" or field number (FN), as discussed above. Information about the field number of an eyepiece can yield the real diameter of the object viewfield using the formula:

$$\text{Viewfield Diameter} = \frac{\text{FN}}{M_O \cdot M_T}$$

where FN is the field number in millimeters, M_O is the objective magnification, and M_T is the tube lens magnification factor (if any). Applying this formula to the Super Widefield eyepiece listed in Table 7.1, we arrive at the following for a 40x objective with a tube lens magnification of 1.25: FN $= \frac{26.5}{M_O} = 40xM(T) = 1.25$ a viewfield diameter of 0.53 mm. Table 7.2 lists the viewfield sizes over the common range of objectives that would occur using this eyepiece.

Care should be taken in choosing eyepiece/objective combinations to ensure the optimal magnification of specimen detail without adding unnecessary artifacts. For instance, to achieve a magnification of 250x, the microscopist could choose a 25x eyepiece coupled to a 10x objective. An alternative choice for the same magnification would be a 10x eyepiece with a 25x objective. Because the 25x objective has a higher numerical aperture (approximately 0.65) than does the 10x objective (approximately 0.25), and considering that numerical aperture values define an objective's resolution, it is clear that the latter choice would be the best. If photomicrographs of the same viewfield were made with each objective/eyepiece combination described above, it would be obvious that the 10x eyepiece/25x objective duo would produce photomicrographs that excelled in specimen detail and clarity when compared to the alternative combination.

TABLE 7.2: Viewfield Diameters (SWF 10x Eyepiece)

Magnification	Viewfield Diameter (mm)
1/2x	42.4
1x	21.2
2x	10.6
4x	5.3
10x	2.12
20x	1.06
40x	0.53
50x	0.42
60x	0.35
100x	0.21
150x	0.14
250x	0.085

TABLE 7.3: Range of Useful Magnification (500–1000 x NA of Objective)

	Eyepieces				
Objective NA	10x	12.5x	15x	20x	25x
2.5x (0.08)	—	—	—	x	x
4x (0.12)	—	—	x	x	x
10x (0.35)	—	x	x	x	x
25x (0.55)	x	x	x	x—	
40x (0.70)	x	x	x	—	—
60x (0.95)	x	x	x	—	—
100x (1.42)	x	x	—	—	—

The "range of useful magnification" for an objective/eyepiece combination is defined by the numerical aperture of the system. There is a minimum magnification necessary for the detail present in an image to be resolved, and this value is usually rather arbitrarily set as 500 times the numerical aperture (500 x NA). At the other end of the spectrum, the maximum useful magnification of an image is usually set at 1000 times the numerical aperture (1000 x NA). Magnifications higher than this value will yield no further useful information or finer resolution of image detail, and will usually lead to image degradation. Exceeding the limit of useful magnification causes the image to suffer from the phenomenon of "empty magnification", where increasing magnification through the eyepiece or intermediate tube lens only causes the image to become more magnified with no corresponding increase in detail resolution. Table 7.3 lists the common objective/eyepiece combinations that lie in the range of useful magnification.

Eyepieces can be adapted for measurement purposes by adding a small circular disk-shaped glass graticule (or reticle) at the plane of the field diaphragm of the eyepiece. Graticules usually have markings, such as a measuring rule or grid, etched onto the surface. Because the graticule lies in the same plane as the field diaphragm, it appears in sharp focus superimposed over the image of the specimen. Eyepieces using graticules must contain a focusing mechanism (usually a helical screw or slider) that allows the image of the graticule to be brought into focus. Several typical graticules are illustrated in Figure 7.5 below.

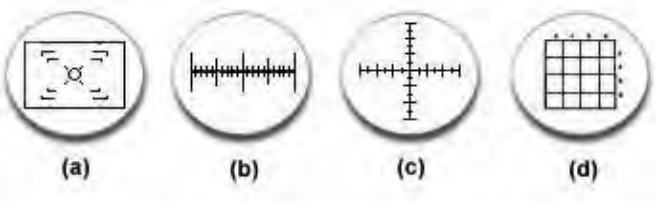

FIGURE 7.5: Measuring graticules

The graticule in Figure 7.5(a) is a common element of eyepieces intended to "frame" viewfields for photomicrography. The small rectangular element circumscribes the area that will be captured on film using 35 mm format. Other film formats (120 mm and 4 x 5 inch) are delineated by sets of "corners" within the larger 35mm rectangle. In the center of the graticule is a series of circles surrounded by four sets of parallel lines arranged in an "X" pattern. These lines are used to focus the graticule and image to be parfocal with the film plane in a camera back attached to the microscope. The graticule in Figure 7.5(b) is a linear micrometer that can be used to measure image distances, and the crossed micrometer in 5(c) is used with polarizing microscopes to locate the alignment of samples with respect to the polarizer and analyzer. The grid illustrated in Figure 7.5(d) is used to partition a section of the viewfield for counting. There are many other variations of eyepiece graticules, and the reader should consult the many manufacturers of microscopes and optical accessories to determine the types and availability of these useful measuring devices.

For highly accurate measurements a Filar Micrometer similar to the one illustrated in Figure 7.6 is used. This micrometer replaces the conventional eyepiece and contains several improvements over conventional graticules. In the filar micrometer, a graticule with a measuring scale (there are many variations in scale types) and a very fine wire is brought into focus with the specimen (Figure 7.6(b)). The wire is mounted so that it can be slowly moved across the viewfield by the calibrated thumbscrew located on the side of the micrometer (Figure 7.6(a)). One complete turn of the thumbscrew (divided into 100 equal divisions) equals the distance between two adjacent graticule marks. By slowly moving the wire from one position on the specimen image to another and taking note of the changes in thumb screw numbers, the microscopist has a much more accurate measurement of distance. Filar micrometers (and other simple graticules) must be calibrated with a stage micrometer for each objective with which it will be used.

Some eyepieces have a movable "pointer" located within the eyepiece and positioned so that it appears as a silhouette in the image plane. This pointer is useful when indicating certain features of a specimen, especially when a microscopist is teaching students about specific features. Most eyepiece pointers can be rotated in a 360 degree angle around the specimen and more advanced versions can translate across the viewfield.

Manufacturers often produce specialized eyepieces, often termed photo eyepieces, that are designed to be used with photomicrography. These eyepieces are usually negative (Huygenian type) and are not capable of being used visually. For this reason, they are typically called projection lenses. A typical projection lens is illustrated in Figure 7.7 below.

Projection lenses must be carefully corrected so that they will produce flat-field images, a definite "must" for accurate photomicrography. They are generally also color-corrected to ensure true reproduction of color in color photomicrography. Magnification factors in pho-

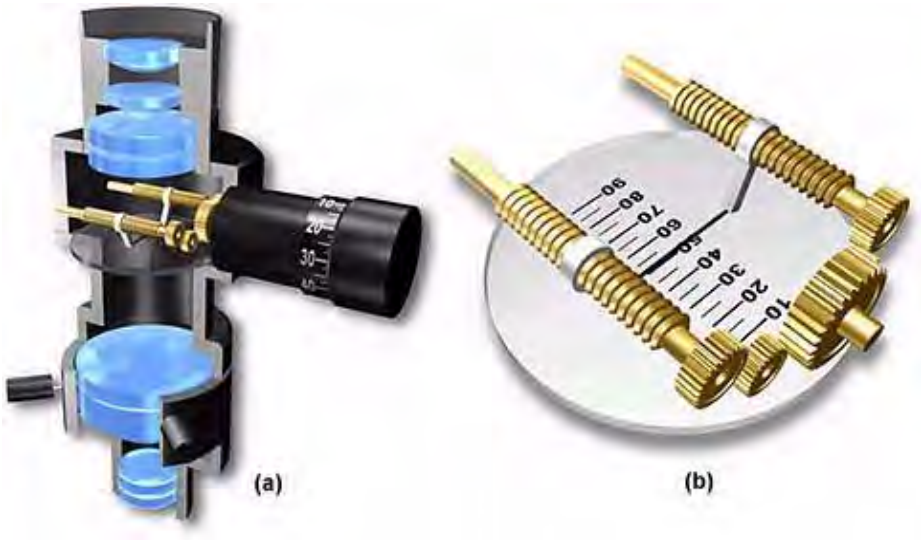

FIGURE 7.6: Filar micrometer

FIGURE 7.7: Photomicrography projection lens

FIGURE 7.8: Focusing telescope

tomicrography projection lenses range from 1x to about 5x, and these can be interchanged to adjust the size of the final image in the photomicrograph.

Camera systems have become an integral part of the microscope and most manufacturers provide photomicrographic attachment cameras as an optional accessory. These advanced camera systems often feature motorized black boxes that store and automatically step through film frame-by-frame as photomicrographs are taken. A common feature of these integral camera systems is a beam-splitter focusing telescopic eyepiece (Figure 7.8) that allows the microscopist to view, focus, and frame samples for photomicrography. This telescope contains a photomicrography graticule, similar to the one illustrated in Figure 7.5(a) that is inscribed with a rectangular element that circumscribes the area captured with 35 mm film, and also corner brackets for larger format films. For convenience in scanning and photographing samples, the microscopist can adjust the telescopic eyepiece so that it is parfocal with the ocular eyepieces to make it easier to frame and take photomicrographs.

Chapter 8

Condensers

The substage condenser gathers light from the microscope light source and concentrates it into a cone of light that illuminates the specimen with uniform intensity over the entire viewfield. It is critical that the condenser light cone be properly adjusted to optimize the intensity and angle of light entering the objective front lens. Each time an objective is changed, a corresponding adjustment must be performed on the substage condenser to provide the proper light cone for the numerical aperture of the new objective.

A simple two-lens Abbe condenser is illustrated in Figure 8.1. In this figure, light from the microscope illumination source passes through the condenser aperture diaphragm, located at the base of the condenser, and is concentrated by internal lens elements, which then project light through the specimen in parallel bundles from every azimuth. The size and numerical aperture of the light cone is determined by adjustment of the aperture diaphragm. After passing through the specimen (on the microscope slide), the light diverges into an inverted cone with the proper angle to fill the front lens of the objective.

Aperture adjustment and proper focusing of the condenser are of critical importance in realizing the full potential of the objective. Specifically, appropriate use of the adjustable aperture iris diaphragm (incorporated into the condenser or just below it) is most important in securing correct illumination, contrast, and depth of field. The opening and closing of this iris diaphragm controls the angle of illuminating rays (and thus the aperture) which pass through the condenser, through the specimen and then into the objective. Condenser height is controlled by a rack and pinion gear system that allows the condenser focus to be adjusted for proper illumination of the specimen. Correct positioning of the condenser with relation to the cone of illumination and focus is critical to quantitative microscopy and optimum photomicrography.

Care must be taken to guarantee that the condenser aperture is opened to the correct position with respect to objective numerical aperture. When the condenser aperture diaphragm is opened too wide, stray light generated by refraction of oblique light rays from the specimen can cause glare and lower the overall contrast. On the other hand, when the aperture is made too small, the illumination cone is insufficient to provide adequate resolution and the image is distorted due to refraction and diffraction from the specimen.

Condensers are divided into classifications of purpose (e.g.: brightfield, darkfield, phase contrast, etc.), and also according to their degree of optical correction. There are four principle types of condensers with respect to correction of optical aberrations, as listed in Table 8.1.

The simplest and least corrected (also the least expensive) condenser is the Abbe con-

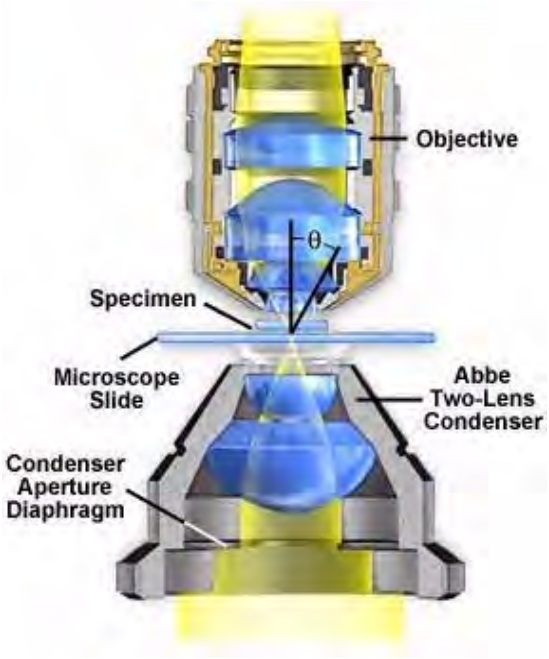

FIGURE 8.1: Abbe condenser optical pathway

TABLE 8.1: Condenser Aberration Corrections

	ABERRATIONS CORRECTED	
Condenser type	Spherical	Chromatic
Abbe	—	—
Aplanatic	x	—
Achromatic	—	x
Aplanatic–achromatic	x	x

FIGURE 8.2: Abbe condenser (NA=1.25)

FIGURE 8.3: Achromatic condenser (NA=0.95)

denser that can have a numerical aperture up to 1.4 in high-end models with three or more internal lens elements. While the Abbe condenser is capable of passing bright light, it is not corrected for either chromatic or spherical optical aberrations. A typical Abbe condenser is illustrated in Figure 8.2. In its simplest form, the Abbe condenser has two optical lens elements that produce an image of the illuminated field diaphragm that is not sharp and is surrounded by blue and red color at the edges.

As a result of no optical correction, the Abbe condenser is suited mainly for routine observation with objectives of modest numerical aperture and magnification. The primary advantages of the Abbe condenser are the wide cone of illumination that the condenser is capable of producing as well as its ability to work with long working distance objectives. Most microscopes are supplied by the manufacturer with an Abbe condenser as the default and these condensers are real workhorses for routine laboratory use.

The next level of condenser correction is split between the aplanatic and achromatic condensers that are corrected exclusively for either spherical (aplanatic) or chromatic (achromatic) optical aberrations. Typical examples of these condensers are illustrated in Figures 8.3 (achromatic) and Figure 8.4 (aplanatic). Achromatic condensers usually contain three to four lens elements and are corrected in two wavelengths (red and blue) for chromatic aberration.

The achromatic condenser illustrated in Figure 8.3 contains four lens elements and has a numerical aperture of 0.95, the highest attainable without requiring immersion oil. This condenser is useful for both routine and critical laboratory analysis with “dry” objectives

FIGURE 8.4: Aplanatic condenser (NA=1.4)

and also for black and white or color photomicrography.

A critical factor in choosing substage condensers is the numerical aperture performance that will be necessary to provide an illumination cone adequate for the objectives. The condenser numerical aperture should be equal to or slightly less than that of the highest objective numerical aperture. Therefore, if the highest magnification objective is an oil-immersion objective with a numerical aperture of 1.40, then the substage condenser should also have an equivalent numerical aperture to maintain the highest system resolution. In this case, immersion oil would have to be applied between the condenser top lens and the underside of the microscope slide to achieve the intended numerical aperture (1.40) and resolution. Failure to use oil will restrict the highest numerical aperture of the system to 1.0, the highest obtainable with air as the imaging medium.

Aplanatic condensers are well corrected for spherical aberration (green wavelengths) but not for chromatic aberration. A typical aplanatic condenser with a numerical aperture of 1.40 is illustrated in Figure 8.4. This condenser features five lens elements and is capable of focusing light in a single plane. Aplanatic condensers are capable of producing excellent black and white photomicrographs when used with green light generated by either a laser source or by use of an interference filter with tungsten-halogen illumination.

The highest level of correction for optical aberration is incorporated in the aplanatic-achromatic condenser. This condenser is well corrected for both chromatic and spherical aberrations and is the condenser of choice for use in critical color photomicrography with white light. A typical aplanatic-achromatic condenser is illustrated in Figure 8.5 (numerical aperture = 1.35). This condenser features eight internal lens elements cemented into two doublets and four single lenses.

Engravings found on the condenser housing include its type (achromatic, aplanatic, etc.), the numerical aperture, and a graded scale that indicates the approximate adjustment (size) of the aperture diaphragm. As we mentioned above, condensers with numerical apertures above 0.95 perform best when a drop of oil is applied to their upper lens in contact with the undersurface of the specimen slide. This ensures that oblique light rays emanating from the condenser are not reflected from underneath the slide, but are directed into the specimen. In practice, this can become tedious and is not commonly done in routine microscopy, but is essential when working at high resolutions and for accurate photomicrography using high-power (and numerical aperture) objectives.

Another important consideration is the thickness of the microscope slide, which is as

FIGURE 8.5: Achromat–aplanar condenser (NA=1.38)

crucial to the condenser as coverslip thickness is to the objective. Most commercial producers offer slides that range in thickness between 0.95 and 1.20 mm with the most common being very close to 1.0 mm. A microscope slide of thickness 1.20 mm is too thick to be used with most high numerical aperture condensers that tend to have a very short working distance. While this does not greatly matter for routine specimen observation, the results can be devastating with precision photomicrography. We recommend that microscope slides be chosen that have a thickness of 1.0 ± 0.05 mm, and that they be thoroughly cleaned prior to use.

When the objective is changed, for example from a 10X to 20X, the aperture diaphragm of the condenser must also be adjusted to provide a new light cone that matches the numerical aperture of the new objective. This is done by turning the knurled knob on the condensers illustrated in Figures 8.2– 8.6. There is a small yellow arrow or index mark located on this knob that indicates the relative size of the aperture when compared to the linear gradation on the condenser housing. Many manufacturers will synchronize this gradation to correspond to the approximate numerical aperture of the condenser. For example, if the microscopist has selected a 10X objective of numerical aperture 0.25, then the arrow would be placed next the value 0.18-0.20 (about 80 percent of the objective numerical aperture) on the gradation inscribed on the condenser housing.

Often, it is not practical to use a single condenser with an entire range of objectives (2X to 100X) due to the broad range of light cones that must be produced to match objective numerical apertures. With low-power objectives in the range 2X to 5X, the illumination cone will have a diameter between 6-10 mm, while the high-power objectives (60X to 100X) need a highly focused light cone only about 0.2-0.4 mm in diameter. With a fixed focal length, it is difficult to achieve this wide range of illumination cones with a single condenser.

In practice, this problem can be solved in several ways. For low power objectives (below 10x), it may be necessary to unscrew the top lens of the condenser in order to fill the field of view with light. Some condensers are produced with a flip-top upper lens to accomplish this more readily, as illustrated in Figure 8.6. Many manufacturers now produce a condenser which flips over completely when used with low power objectives. Other companies may incorporate auxiliary correction lenses in the light path for securing proper illumination with objectives less than 10x. When the condenser is used without its top lens, the aperture iris diaphragm is opened wide and the field diaphragm, now visible at

FIGURE 8.6: Swing-out top lens condenser (NA=1.35)

the back of the objective, serves as if it were the aperture diaphragm. Flip-top condensers are manufactured in a variety of configurations with numerical apertures ranging from 0.65 to 1.35. Those condensers that have a numerical aperture value of 0.95 or less are intended for use with "dry" objectives. However, flip-top condensers that have a numerical aperture greater than 0.95 are intended for use with oil-immersion objectives and they must have a drop of oil placed between the bottom of the microscope slide and the condenser top lens when examining critical samples.

In addition to the common brightfield condensers discussed above, there are a wide variety of specialized models suited to many different applications. Table 8.2 lists a number of different condenser configurations and the intended applications.

From the data in Table 8.2, it is obvious that substage condensers have a great deal of interchangeability among different applications. For instance, the DIC universal achromat/aplanat condenser is useful for brightfield, darkfield, and phase contrast, in addition to the primary DIC application. Other condensers have similar interchangeability. We will deal with various aspects of individual techniques that require modified condensers in our section on Specialized Microscopy Techniques. Please feel free to visit this interesting part of our Website for more specific information about substage condensers.

TABLE 8.2: Substage Condenser Applications

Condenser Type	Brightfield	Darkfield	Phase Contrast	DIC	Polarizing
Achromat/Aplanat NA 1.3	10x—100x				
Achromat Swing-out NA 0.90	4x—100x				
Low-Power NA 0.20	1x—10x				
Phase Contrast Abbe NA 1.25	•	0.65[1]	10x—100x		
Phase Contrast Achromat NA 0.85	•	0.70[1]	4x—100x		
DIC Universal Achromat/Aplanat	•	0.70[1]	10x,100x	20x,40x, 100x	
Darkfield, dry NA 0.80–0.95		4x—40x			
Darkfield, oil NA 1.20—1.43		4x—100x			
Stain-Free Achromat Swing-Out NA 0.90	•				4x—100

([1]): up to NA

Chapter 9

Microscope Stages

All microscopes are designed to include a stage where the specimen (usually mounted onto a glass slide) is placed for observation. Stages are often equipped with a mechanical device that holds the specimen slide in place and can smoothly translate the slide back and forth as well as from side to side. A stage can be classified according to design and functionality. In the simplest case, the plain stage (illustrated in Figure 9.2, on the left) consists of a rectangular or square design containing several clips to hold the specimen slide.

The stage illustrated in Figure 9.1 is a typical rectangular stage with the added feature of a specimen slide translational control device commonly referred to as a mechanical stage. This mechanical stage contains controls for right-handed microscopists that allow the movement of the specimen slide in both the X (right and left) and Y (back and forth) directions so the microscopist can examine the entire microscope slide (secured to the stage with the slide holder). Similar mechanical stages are available with the translational control knobs situated on the left-hand side of the stage for left-handed microscopists. The stage illustrated in Figure 9.1 also contains a rather large opening in the center to allow light from the condenser to pass through the specimen (the stage opening). The stage is also equipped with a locking control that allows the stage to be fixed into position with respect to its rotation around the condenser axis. Graduated locator marks positioned on the mechanical portion of the stage allow the microscopist to note the location of important specimen details, allowing easy return to the area for additional observation or photomicrography.

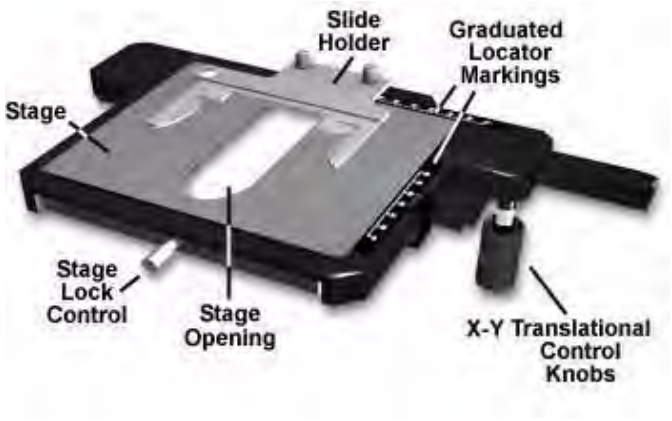

FIGURE 9.1: X–Y traslation mechanical stage

FIGURE 9.2: Simple stage with attachable mechanical stage

A simple (commonly termed "plain") microscope stage is illustrated on the left in Figure 9.2. This stage contains an opening to admit light from the condenser, several mounting holes for a mechanical stage, and two clips that secure the specimen slide in place for observation under increasing magnification (changing of objectives) and for photomicrography. The stage is also equipped with a locking control that can fix the position of the stage. This stage is very useful for quick examination of specimens, but is very difficult to use with higher power objectives (above 20X). At high magnification, small translations of the specimen slide will usually throw the features of interest completely out of the viewfield, and attempting to relocate them can lead to frustration. Auxiliary mechanical stages attached to a simple stage can allow for minute translation of the specimen slide, making it easier for the microscopist to find specific areas on the slide. The mechanical stage attachment illustrated on the right in Figure 9.2 can be easily attached to the simple stage on the left in the same figure. In order to attach this mechanical stage, the specimen clips must first be removed.

Note that the stage opening is much smaller on the stage illustrated in Figure 9.2 when compared to the mechanical stage shown in Figure 9.1. This is because the mechanical portion of the stage in Figure 9.1 encompasses the upper stage plate allowing the gray part of the stage to move with the specimen slide holder in both the X and Y directions. Alternatively, when an auxiliary mechanical stage (similar to the one on the right in Figure 9.2) is attached to the simple stage shown in Figure 9.2, it is only the mechanical slide holder that moves, and the stage itself remains stationary. Locator graduations on the attachable mechanical stage (that help identify specific areas of a specimen) operate in a manner similar to the mechanical stage illustrated in Figure 9.1. Both stages may be rotated with respect to the microscope body to facilitate framing during photomicrography. The stages illustrated in Figures 9.1 and 9.2 are not centerable, but many designs (including some discussed below) are capable of being centered with respect to the optical axis of the microscope.

The circular graduated stage, illustrated on the left in Figure 9.3, is one of the most versatile and useful designs for all types of microscopy and photomicrography. These stages rotate 360°, permitting complete rotation of the samples and great ease in fine-tuning the composition of viewfields for photomicrography. An added feature is the graduations

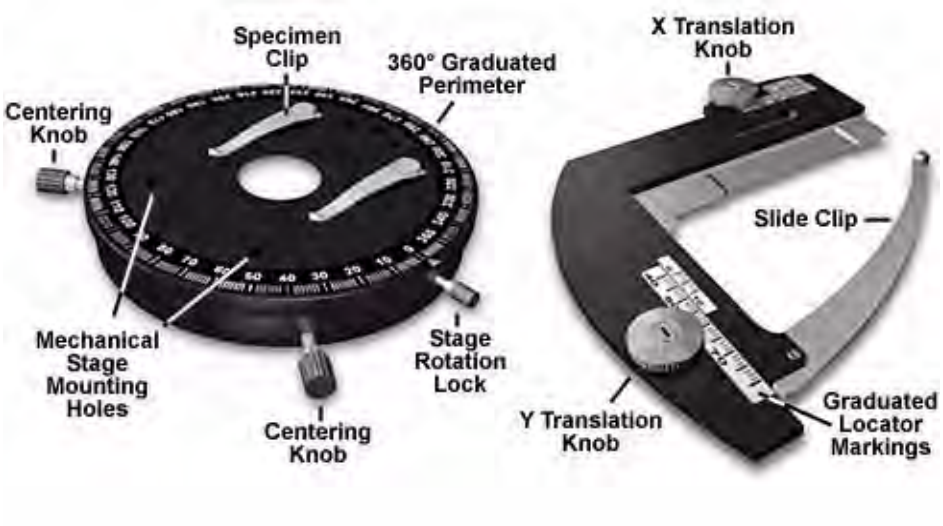

FIGURE 9.3: Circular stage with optional mechanical stage

included on the periphery of the stage, which allow for precise alignment when critical analytical measurements must be undertaken. The stage rotates on ball bearings that provide precision rotation without annoying jerks, bumps, and stalls. Two centering knobs (Figure 9.3) permit the stage to be centered with respect to the optical axis of the microscope. When used with objectives in a centering nosepiece, the microscope can be adjusted to be parcentric, meaning that a specimen centered in the field of view for one objective remains centered when the nosepiece is rotated to bring another objective into use.

An optional mechanical stage attachment (on the right in Figure 9.3) for the circular stage permits accurate translation of samples similar to the mechanical stages discussed above. Most circular stages have pre-drilled mounting holes that allow positioning and firm attachment of the optional mechanical stage. Circular stages also have a locking mechanism (stage rotation lock) that allow them to be locked into a single position. These stages often are equipped with click stops that alert the microscopist at 45° intervals of rotation.

Modern microscope stages are precisely manufactured and very durable. They are cast from either iron or aluminum and machine-finished to accurate tolerances. Translation mechanisms are usually rack-and-pinion styles, machined from aluminum, brass, or (more recently) synthetic polymers. The synthetic gear mechanisms usually are far less durable than their metal counterparts, especially after years of use. These devices should be thoroughly cleaned, lubricated, and tightened for adjustment every several years. Most stages are protected with a very tough non-glossy ceramic coating that resists marks and scratches. The dull surface ensures that stray light is not reflected from the stage into the objective.

9.1 Specialized Microscope Stages

There are a wide variety of microscope stages that are designed for specific purposes. These include stages equipped with auxiliary equipment for manipulating samples during observation, measuring systems that allow precise measurements to be made over very small distances, universal stages that allow measurements over many specimen angles, and other specialized stages that perform a myriad of unique functions. We will discuss some

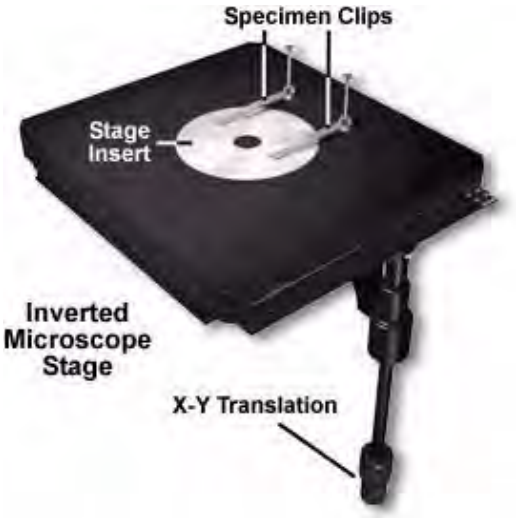

FIGURE 9.4: Inverted microscope stage

of the more common specialized microscope stages below.

9.1.1 Inverted Microscope Stages

Inverted microscopes are configured differently than the standard upright microscope. These microscopes have the objectives placed below the stage and use several different condenser configurations to illuminate the specimen. Tissue culture microscopes have a condenser that is mounted above the stage, while epi-illumination microscopes (metallographs and their relatives) have a substage condenser that preceeds the objectives. In both cases, the stage is slightly modified from standard stages as illustrated in Figure 9.4 below.

The inverted microscope stage is similar in its basic overall design to the mechanical stage illustrated in Figure 9.1. Both stages have translational controls that allow the stage (and specimen) to be moved in both the X and Y directions. The main difference is the large stage opening that accommodates an insert on the inverted microscope stage. The inserts (Figure 9.4) are usually made of stainless steel and have openings of various sizes to allow for large differences in sample size. For instance, with inverted tissue culture microscopes, researchers often must scan large culture flasks to observe the entire population of cells and this is much easier to accomplish when the stage insert has a large opening. Metallography samples are also often quite large and more of their surface can be observed with the specialized inserts. When small specimens are to be observed, an insert with a very small opening (about the size of the one in Figure 9.4) is used to support the sample for observation. Inverted microscope stages do not translate up and down. Focusing is accomplished using a translatable nosepiece that, together with the objectives, moves up and down.

9.2 High-Magnification Measuring Systems

Quantitative microscopy often demands highly accurate measurements of various specimen dimensions. These include measurement of miniature precision parts and semiconductors as

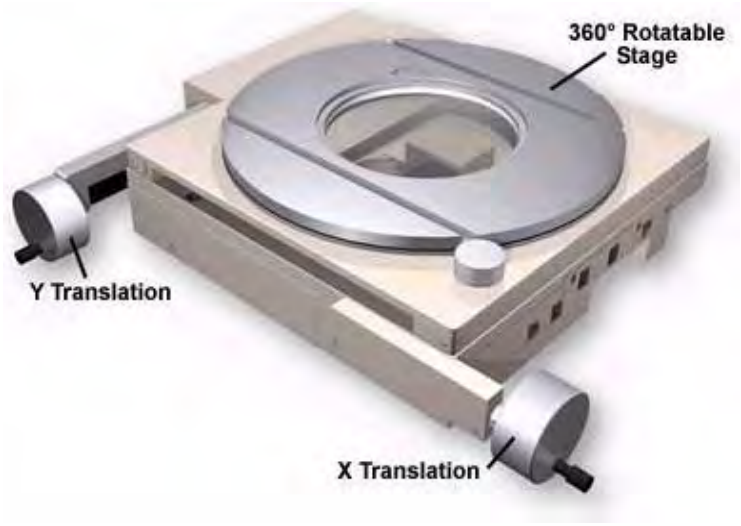

FIGURE 9.5: Precision measurement stage

well as high-precision assembly of magnetic heads and other minute electronic components. Specialized microscopes with precision stages are often used for these purposes. The stage illustrated in Figure 9.5 is an example of a precision microsope stage. It is equipped with a micrometer-style translational apparatus that allows for very accurate and controlled movements of the stage and specimen. The stage is also rotatable over the entire 360 range for total control over the measurements.

Microscopes designed for stages of this type are sometimes equipped with prisms for Erect Image Observation, meaning that the observed image and the specimen both move in the same direction (the opposite is true for most microscopes). The stages are usually accompanied by electronic controllers that give accurate digital readouts of the stage position, and most can be programmed for precise stage movements in a sequence of steps. There are a wide variety of designs for these specialized stages and many aftermarket manufacturers are capable of supplying custom-configured stages built to the customer's specifications.

9.3 Micromanipulators

It is often necessary to manipulate the specimen while it is being observed under the microscope. This is the case in many tissue culture and in vitro fertilization experiments as well as genetic implantation procedures that require close observation of the sample during the experiment. The micromanipulator stage illustrated in Figure 9.6 is an example of the type of equipment necessary to conduct these types of operations.

This specialized stage has two triple-axis hydraulically controlled water micromanipulators that orchestrate specimen handling in a highly accurate manner. In the illustration, a small petri dish containing embryos is being manipulated with the control arms to monitor pH of the solution as well as providing radioactively labeled nutrients to the embryos. These manipulators can be adjusted to perform a wide spectrum of functions ranging from microinjection to electrochemistry experiments. There are a number of manufacturers who supply micromanipulators and accessories that attach to commercial microscopes such as those manufactured by Olympus and Nikon.

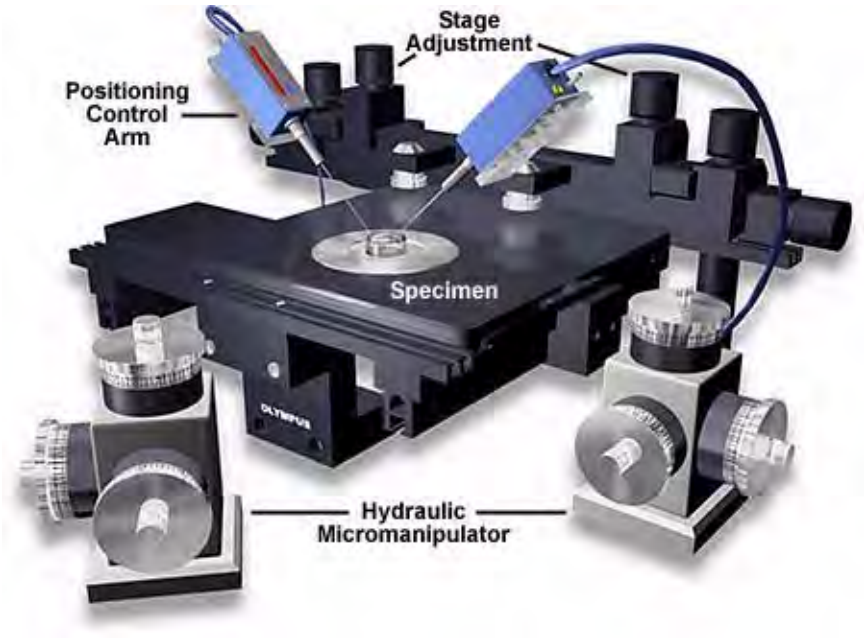

FIGURE 9.6: Micromanipulator system

TABLE 9.1: Universal Stage Objective Specifications

Specifications	U5X	U10X	U20X
Individual Magnification	5X	10X	20X
Numerical Aperture	0.10	0.22	0.33
Working Distance (mm)	5.3	2.9	1.1

9.4 Universal Stage

This unwieldly looking microscope stage permits tilting of a thin specimen at any angle for measuring the optical structure of a birefringent crystal. The universal stage illustrated in Figure 9.7 is an example of this type of stage.

Universal stages are designed to be used with special long working distance (LWD) objectives and very low magnifications usually ranging from 5X to 20X. These stages are graduated on all 4 axes with rotation scales that are distinguished by different color codes. The four rotating centers of the main body all rest on a common point. Two hemispherical lenses are used to sandwich the specimen between their plane surfaces with immersion oil being applied to all contact surfaces.

The universal stage attaches to the circular petrography stage illustrated in Figure 9.3 using screws permanently fixed onto the universal stage. There is a central ring on the microscope stage that must first be removed before installation and centering of the universal stage. The stage contains locking devices that allow the position of the sample to be fixed for viewing and photomicrography. Universal stages are no longer being manufactured by the major microscope producers, but a limited number are still available through distributors and custom aftermarket manufacturers.

FIGURE 9.7: Universal stage

9.5 Others

There are a variety of other specialized microscope stages that we have not covered in this discussion. Rapid growth in the semiconductor arena has led to the design and manufacture of a number of stages utilized to examine and manipulate integrated circuit wafers. Similar microscopes have also been adapted in other areas of integrated circuit manufacture. Many scientists design and build their own custom stages for specific experiments including biomedical investigations, cell manipulation, materials research, and geology.

Chapter 10

Introduction to Reflected Light Microscopy

Reflected light microscopy is often referred to as incident light, epi-illumination, or metallurgical microscopy, and is the method of choice for fluorescence and for imaging specimens that remain opaque even when ground to a thickness of 30 microns.

The range of specimens falling into this category is enormous and includes most metals, ores, ceramics, many polymers, semiconductors (unprocessed silicon, wafers, and integrated circuits), slag, coal, plastics, paint, paper, wood, leather, glass inclusions, and a wide variety of specialized materials. Because light is unable to pass through these specimens, it must be directed onto the surface and eventually returned to the microscope objective by either specular or diffused reflection. As mentioned above, such illumination is most often referred to as episcopic illumination, epi-illumination, or vertical illumination (essentially originating from above), in contrast to diascopic (transmitted) illumination that passes through a specimen.

Today, many microscope manufacturers offer models that permit the user to alternate or simultaneously conduct investigations using both vertical and transmitted illumination. A typical microscope configured for both types of illumination is illustrated in Figure 10.1. The optical pathway for reflected light begins with illuminating rays originating in the lamp housing for reflected light (the upper housing in Figure 10.1 and Figure 10.3). This light next passes through the collector lens and into the vertical illuminator (Figure 10.2) where it is controlled by the aperture and field diaphragms. After passing through the vertical illuminator, the light is then reflected by a beam splitter (a half mirror or elliptically shaped first-surface mirror) through the objective to illuminate the specimen.

Light reflected from the surface of the specimen re-enters the objective and passes into the binocular head where it is directed either to the eyepieces or to a port for photomicrography. Reflected light microscopy is frequently the domain of industrial microscopy, especially in the rapidly growing semiconductor arena, and thus represents a most important segment of microscopical studies.

A typical upright compound reflected light microscope also equipped for transmitted light has two eyepiece viewing tubes (Figure 10.1) and often a trinocular tube head for mounting a conventional or digital/video camera system (not illustrated). Standard equipment eyepieces are usually of 10x magnification, and most microscopes are equipped with a nosepiece capable of holding four to six objectives. The stage is mechanically controlled with a specimen holder that can be translated in the X- and Y- directions and the entire

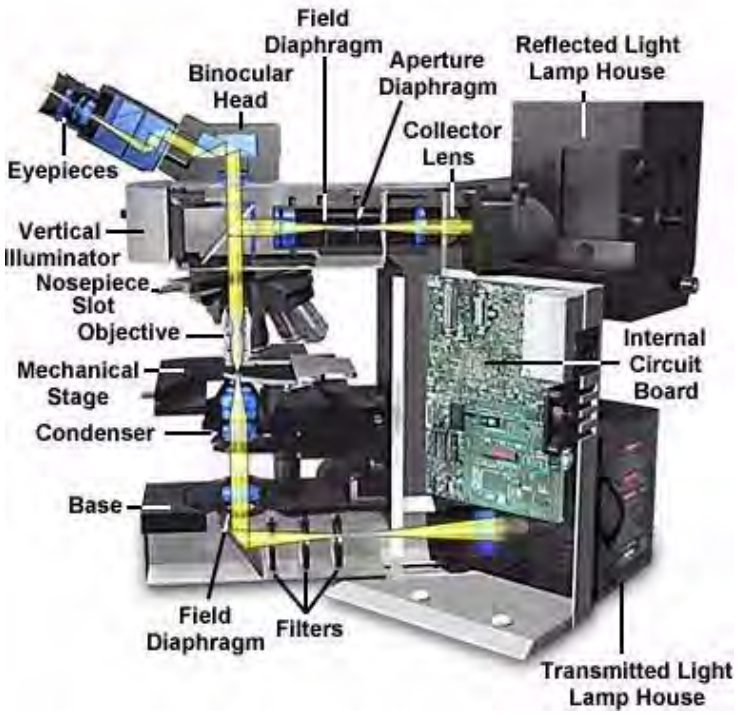

FIGURE 10.1: Reflected/Trasmitted light microscope configuration

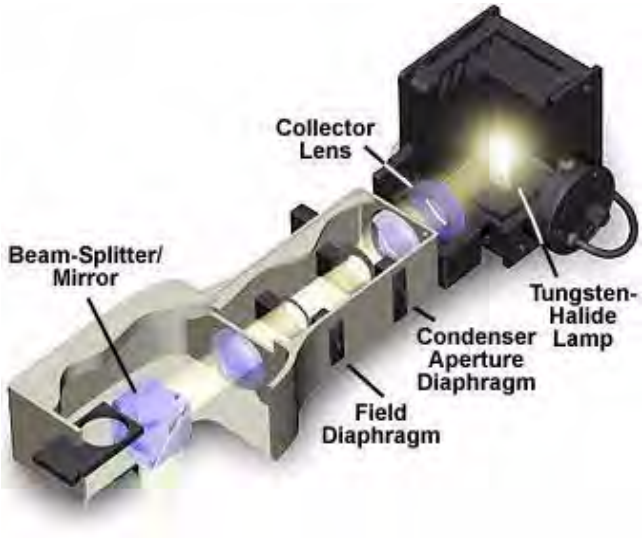

FIGURE 10.2: Reflected light microscopy configuration

FIGURE 10.3: Reflected light lamp housing

stage unit is capable of precise up and down movement with a coarse and fine focusing mechanism.

Built-in light sources range from 20 and 100 watt tungsten-halogen bulbs to higher energy mercury vapor or xenon lamps that are used in fluorescence microscopy. Light passes from the lamphouse through a vertical illuminator interposed above the nosepiece but below the underside of the viewing tube head. The specimen's top surface is upright (usually without a coverslip) on the stage facing the objective, which has been rotated into the microscope's optical axis. The vertical illuminator is horizontally oriented at a 90-degree angle to the optical axis of the microscope and parallel to the table top, with the lamp housing attached to the back of the illuminator. The coarse and fine adjustment knobs raise or lower the stage in large or small increments to bring the specimen into sharp focus.

Another variation of the reflected light microscope is the inverted microscopeof the Le Chatelier design (Figure 10.4). On the inverted stand, the specimen is placed on the stage with its surface of interest facing downward. The primary advantage of this design is that samples can be easily examined when they are far too large to fit into the confines of an upright microscope. Also, only the side facing the objectives need be perfectly flat. The objectives are mounted on a nosepiece under the stage with their front lenses facing upward towards the specimen and focusing is accomplished either by moving the nosepiece or the entire stage up and down.

Inverted microscope stands incorporate the vertical illuminator within the body of the microscope. Many types of objectives can be used with inverted reflected light microscopes, and all modes of reflected light illumination may be possible: brightfield, darkfield, polarized light, differential interference contrast, and fluorescence. Many of the inverted microscopes have built-in 35 millimeter and/or large format cameras or are modular to allow such accessories to be attached. Some of the instruments include a magnification changer for zooming in on the image, contrast filters, and a variety of reticles. Because an inverted microscope is a favorite instrument for metallographers, it is often referred to as a metallograph. Manufacturers are largely migrating to using infinity-corrected optics in reflected light microscopes, but there are still thousands of fixed tube length microscopes in use with objectives corrected for a tube length between 160 and 210 millimeters.

In the vertical illuminator, light travels from the light source, usually a 12 volt 50 or 100

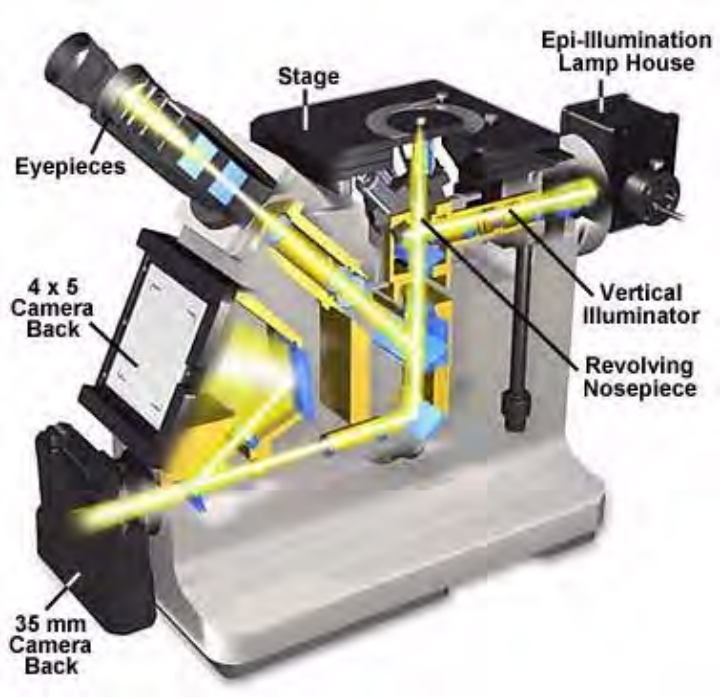

FIGURE 10.4: Inverted reflected light microscopy

watt tungsten halogen lamp, passes through collector lenses, through the variable aperture iris diaphragm opening and through the opening of a variable and centerable pre-focused field iris diaphragm. The light then strikes a partially silvered plane glass reflector, or strikes a fully silvered periphery of a mirror with elliptical opening for darkfield illumination (Figure 10.5). The plane glass reflector is partially silvered on the glass side facing the light source and anti-reflection coated on the glass side facing the observation tube in brightfield reflected illumination. Light is thus deflected downward into the objective. The mirrors are tilted at an angle of 45 degrees to the path of the light travelling along the vertical illuminator.

The light reaches the specimen, which may absorb some of the light and reflect some

FIGURE 10.5: Reflected light mirror blocks

of the light, either in a specular or diffuse manner. Light that is returned upward can be captured by the objective in accordance with the objective's numerical aperture and then passes through the partially silvered mirror (or in darkfield, through the elliptical opening). In the case of infinity-corrected objectives, the light emerges from the objective in parallel (from every azimuth) rays projecting an image of the specimen to infinity. The parallel rays enter the tube lens, which forms the specimen image at the plane of the fixed diaphragm opening in the eyepiece (intermediate image plane). It is important to note, that in these reflected light systems, the objective serves a dual function: on the way down as a matching well-corrected condenser properly aligned; on the way up as an image-forming objective in the customary role of an objective projecting the image-carrying rays toward the eyepiece. Optimal performance is achieved in reflected light illumination when the instrument is adjusted to produce Khler illumination. A function of Khler illumination (aside from providing evenly dispersed illumination) is to ensure that the objective will be able to deliver excellent resolution and good contrast even if the source of light is a coil filament lamp.

Some modern reflected light illuminators are described as universal illuminators because, with several additional accessories and little or no dismantling, the microscope can easily be switched from one mode of reflected light microscopy to another. Often, reflectors can be removed from the light path altogether in order to permit transmitted light observation. Such universal illuminators may include a partially reflecting plane glass surface (the half-mirror) for brightfield, and a fully silvered reflecting surface with an elliptical, centrally located clear opening for darkfield observation. The best-designed vertical illuminators include collector lenses to gather and control the light, an aperture iris diaphragm and a pre-focused, centerable field diaphragm to permit the desirable Khler illumination.

The vertical illuminator (Figure 10.2) should also make provision for the insertion of filters for contrast and photomicrography, polarizers, analyzers, and compensator plates for polarized light and differential interference contrast illumination. In vertical illuminators designed for with infinity-corrected objectives, the illuminator may also include a tube lens. Affixed to the back end of the vertical illuminator is a lamphouse (Figure 10.3), which usually contains a tungsten-halogen lamp. For fluorescence work, the lamphouse can be replaced with a fitting containing a mercury burner. The lamp may be powered by the electronics built into the microscope stand, or in fluorescence, by means of an external transformer or power supply.

In reflected light microscopy, absorption and diffraction of the incident light rays by the specimen often lead to readily discernible variations in the image, from black through various shades of gray, or color if the specimen is colored. Such specimens are known as amplitude specimens and may not require special contrast methods or treatment to make their details visible. Other specimens show so little difference in intensity and/or color that their feature details are extremely difficult to discern and distinguish in brightfield reflected light microscopy. Such specimens behave much like the phase specimens so familiar in transmitted light work, and are suited for darkfield and reflected light differential interference contrast applications.

Part II

Fluorescence Microscope Tecniques

Chapter 11

Introductory Concepts

When specimens, living or non-living, organic or inorganic, absorb and subsequently re-radiate light, we describe the process as photoluminescence. If the light emission persists for up to a few seconds after the excitation light is withdrawn, the phenomenon is known as phosphorescence. Fluorescence, on the other hand, describes light emission which continues only during the absorption of the excitation light. The time interval between absorption of excitation light and emission of re-radiated light in fluorescence is of extraordinarily short duration, usually less than a millionth of a second.

The phenomenon of fluorescence was known by the middle of the 19th century. It was Stokes who made the observation that the mineral fluorspar fluoresces when ultraviolet light is directed upon it; he coined the word "fluorescence". Stokes observed that the fluorescing light is in longer wavelengths than those of the excitation light as illustrated in Figure 11.1 above. In this figure, a photon of ultraviolet radiation (purple) collides with an electron in the atom, exciting and elevating it to a higher energy level. Subsequently, the excited electron relaxes to a lower level and emits light in the form of a lower-energy photon (red) in the visible light region. Figure 11.2 is a diagrammatic representation of the visible light region of electromagnetic radiation, which covers a wavelength range of approximately 400 to 740 nanometers. Surrounding the visible region is higher energy ultraviolet light and lower energy infrared light.

Fluorescence microscopy is an excellent method of studying material which can be made to fluoresce, either in its natural form (primary or autofluorescence) or when treated with chemicals capable of fluorescing (secondary fluorescence). The fluorescence microscope was

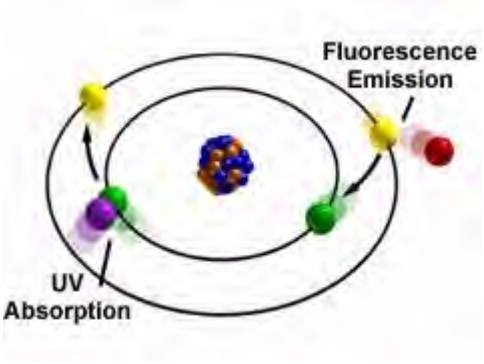

FIGURE 11.1: Stoke's Observation

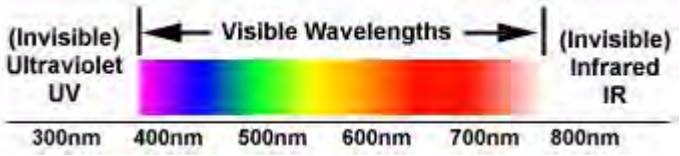

FIGURE 11.2: Spectrum of 'white light'

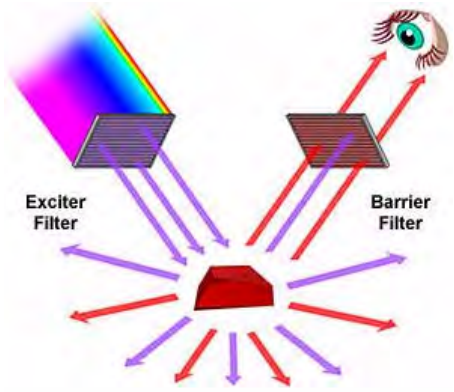

FIGURE 11.3: Example of what happen when a fluorescing sample is observed with a fluorescence microscope

devised in the early part of the 20th century; Köehler, Reichert, and Lehman were among the scientists associated with such development. However, the potential of this instrument was not realized for several decades.

Early investigations showed that many specimens (microminerals, crystals, resins, crude drugs, butter, chlorophyll, vitamins, inorganic compounds, etc.) autofluoresce when irradiated with ultraviolet light. However, it was not until the 1930's that Haitinger and others developed the technique of secondary fluorescence–employing fluorochrome stains to stain specific tissue components, bacteria, or other pathogens which do not autofluoresce. These fluorochrome stains, tagged to specific objects, spurred the use of the fluorescence microscope. The instrument's value was significantly enhanced by the 1950's when Coons and Kaplan demonstrated the localization of antigens in tissues that were stained with a fluorescein (the fluorochrome) tagged antibody.

The basic task of the fluorescence microscope is to permit excitation light to irradiate the specimen and then to separate the much weaker re-radiating fluorescent light from the brighter excitation light. Thus, only the emission light reaches the eye or other detector. The resulting fluorescing areas shine against a dark background with sufficient contrast to permit detection. The darker the background of the non-fluorescing material, the more efficient the instrument.

Figure 11.3 is a graphical representation of what happens when a fluorescing sample is observed with a fluorescence microscope. Ultraviolet (UV) light of a specific wavelength or set of wavelengths is produced by passing light from a UV-emitting source through the exciter filter. The filtered UV light illuminates the specimen, in this case a crystal of fluorspar, which emits fluorescent light when illuminated with ultraviolet light. Visible light emitted from the specimen, red in this case, is then filtered through a barrier filter that does not allow reflected UV light to pass. It should be noted that this is the only

mode of microscopy in which the specimen, subsequent to excitation, gives off its own light. The emitted light re-radiates spherically in all directions, regardless of the direction of the exciting light.

Fluorescence microscopy is a rapidly expanding and invaluable tool of investigation. Its advantages are based upon attributes not as readily available in other optical microscopy techniques. The use of fluorochromes has made it possible to identify cells and sub-microscopic cellular components and entities with a high degree of specificity amidst non-fluorescing material. What is more, the fluorescence microscope can reveal the presence of fluorescing material with exquisite sensitivity. An extremely small number of fluorescing molecules (as few as 50 molecules per cubic micron) can be detected. In a given sample, through the use of multiple staining, different probes will reveal the presence of different target molecules. Although the fluorescence microscope cannot provide spatial resolution below the diffraction limit of the respective objects, the presence of fluorescing molecules below such limits is made visible.

Techniques of fluorescence microscopy can be applied to organic material, formerly living material or to living material (with the use of in vitro or in vivo fluorochromes) or to inorganic material (lately, especially in the investigation of contaminants on semiconductor wafers). There are also a burgeoning number of studies using fluorescent probes to monitor rapidly changing physiological ion concentrations (calcium, magnesium, etc.) and pH values in living cells.

There are specimens that fluoresce when irradiated with shorter wavelength light (primary or autofluorescence). Autofluorescence has been found useful in plant studies, coal petrography, sedimentary rock petrology, and in the semiconductor industry. In the study of animal tissues or pathogens, autofluorescence is often either extremely faint or of such non-specificity as to make autofluorescence of minimal use. Of far greater value for such specimens are the fluorochromes (also called fluorophores) which are excited by irradiating light and whose eventual yield of emitted light is of greater intensity. Such fluorescence is called secondary fluorescence.

Fluorochromes are stains, somewhat similar to the better-known tissue stains, which attach themselves to visible or sub-visible organic matter. These fluorochromes, capable of absorbing and then re-radiating light, are often highly specific in their attachment targeting and have significant yield in absorption-emission ratios. This makes them extremely valuable in biological application. The growth in the use of fluorescent microscopes is closely linked to the development of hundreds of fluorochromes with known intensity curves of excitation and emission and well-understood biological structure targets.

Illustrated in Figure 11.4 are two of the most commonly used fluorochromes in fluorescence microscopy. Fluorescein-isothiocyanate (FITC), the upper molecule in Figure 11.4, is a xanthine derivative with a highly reactive isothiocyanate moiety that is useful for fluorescent labeling of proteins and has been widely used in the fluorescent antibody technique for rapid identification of pathogens. Below the FITC molecule is another fluorochrome, acridine orange (AO) whose DNA-binding and fluorescent properties have been thoroughly studied. AO interacts with DNA in a highly specific manner by intercalation of the acridine nucleus between successive DNA base pairs to actually increase the effective length of the DNA molecule. This type of binding allows AO to be used as a fluorescent probe for cellular DNA. These molecules (and other similar fluorochromes) are highly conjugated aromatic systems whose electronic properties allow for high fluorescence quantum yields. When deciding which label to use for fluorescence microscopy, it should be kept in mind

FIGURE 11.4: Molecular structures of some fluorocromes

that the chosen fluorochrome should have a high likelihood of absorbing the exciting light and should remain attached to the target molecules; the fluorochrome should also be capable of providing a satisfactory yield of emitted fluorescence light. There are hundreds of fluorochromes that have been found useful for microscopy and many of them are listed in our fluorochrome information tables contained in a separate section of the primer.

Chapter 12

Excitation and Emission Fundamentals

Because of their novel electronic configurations, fluorochromes have unique and characteristic spectra for absorption (usually similar to excitation) and emission. These absorption and emission spectra show relative Intensity of Fluorescence, with relative intensity as the vertical axis versus wavelength as the horizontal axis.

For a given fluorochrome, the manufacturers indicate the wavelength for the peak of excitation/fluorescence intensity and the wavelength for the peak of emission/fluorescence intensity. It is important to understand the origin of the graphs/curves showing the excitation and emission spectra for a given fluorochrome.

To determine the Emission spectrum of a given fluorochrome, the dye absorption maximum wavelength (usually the same as the excitation maximum) is found and the fluorochrome is excited at that maximum. The absorption spectrum of a typical fluorochrome is illustrated in Figure 12.1(a) where the relative intensity of absorption is plotted against relative wavelength. A monochromator (a device that allows narrow bands of light wavelengths to pass) is then used to scan the fluorescence emission intensity at successive emission wavelengths. The relative intensity of the fluorescence is measured at the various wavelengths to plot the Emission spectrum as illustrated in Figure 12.1(b). The Excitation spectrum of a given fluorochrome is determined in a similar manner. The emission maximum is chosen and only emission light at that emission wavelength is allowed to pass to the detector. Then excitation is induced–by means of a monochromator–at various excita-

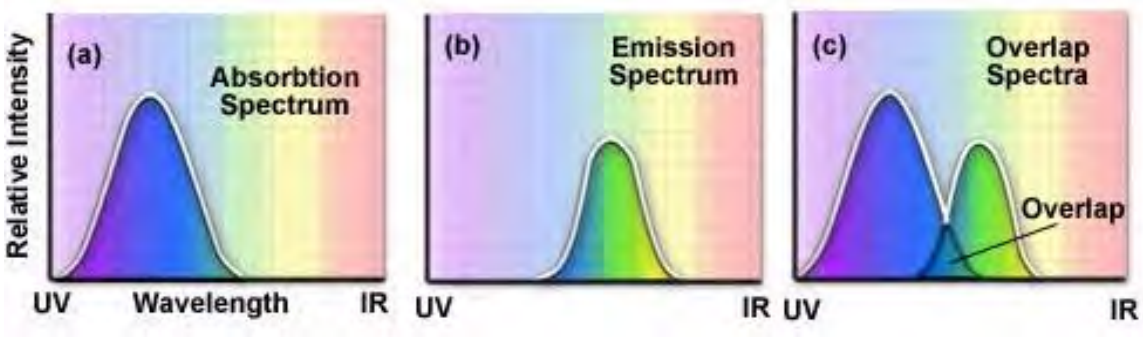

FIGURE 12.1: Absorbtion and Emission Spectra

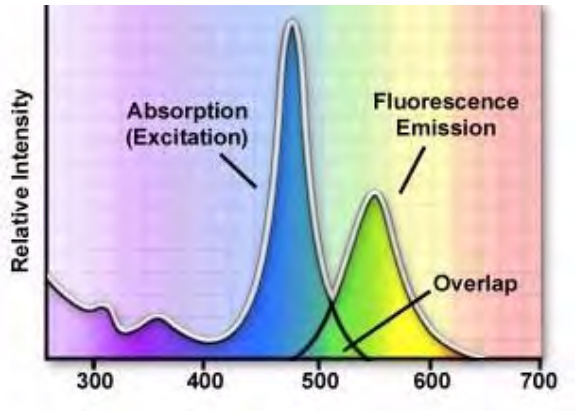

FIGURE 12.2: Typical fluorochrome absorption–emission spectral diagram

tion wavelengths and the intensity of the emitted fluorescence is measured. The result is a graph/curve (illustrated in Figure 12.1(a)) which depicts the relative Fluorescence intensity caused by excitation at the successive excitation wavelengths.

Several observations can be made from a typical excitation/emission set of curves or spectra. There is usually an overlap at the higher wavelength end of the excitation spectrum and the lower wavelength end of the emission spectrum. This overlap of excitation and emission intensities/wavelengths (illustrated in Figure 12.1(c)) must be eliminated, in fluorescence microscopy, by means of appropriate selection of excitation filter, dichromatic beam splitter (in reflected light fluorescence), and barrier filter. Otherwise, the much brighter excitation light overwhelms the weaker emitted light and significantly diminishes specimen contrast.

When electrons go from the excited state to the ground state (see the section below on Molecular Explanation), there is a loss of vibrational energy. As a result, the emission spectrum is shifted to longer wavelengths than the excitation spectrum (wavelength varies inversely to radiation energy). This phenomenon is known as Stokes' Law or Stokes' shift. The greater the Stokes' shift, the easier it is to separate excitation light from emission light. The emission intensity peak is usually lower than the excitation peak; and the emission curve is often a mirror image of the excitation curve, but shifted to longer wavelengths. To achieve maximum fluorescence intensity, the fluorochrome is usually excited at the wavelength at the peak of the excitation curve, and the emission is selected at the peak wavelength (or other wavelengths chosen by the observer) of the emission curve. The selections of excitation wavelengths and emission wavelengths are controlled by appropriate filters. In determining the spectral response of an optical system, technical corrections are required to take into account such factors as glass transmission and detector sensitivity variables for different wavelengths.

A typical fluorochrome absorption-emission spectral diagram is illustrated in Figure 12.2. Note that the curves of fluorescence intensity for absorption (usually similar to the excitation curve for pure compounds) and emission for this typical fluorochrome are somewhat similar in shape. The wavelength shift between excitation and emission has been known since the middle of the nineteenth century (Stokes' Law). Also note that the excitation and emission curves overlap somewhat at the upper end of the excitation and the lower wavelengths of the emission curve.

The separation of excitation and emission wavelengths is achieved by the proper selec-

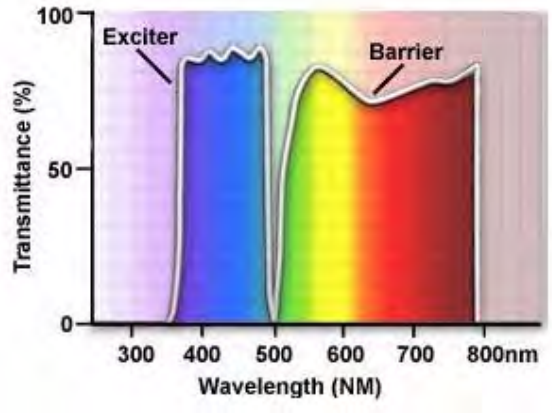

FIGURE 12.3: Exciter and barrier filter spectra

Compound	Solvent	Excitation Wavelength (nm)	Quantum Yield
Acridine Orange	Ethanol	366	0.46
Benzene	Ethanol	248	0.04
Eosin	Water	366	0.16
Fluorescein	Water	366	0.92
Rhodamine–B	Ethanol	535	0.97
Chlorophyl–A	Ethanol	644	0.23

TABLE 12.1: Fluorochrome Fluorescence Quantum Yields

tion of filters to block or pass specific wavelengths of the spectrum as shown in Figure 12.3 below. The design of fluorescence illuminators is based on control of excitation light and emission light by readily changeable filter insertions in the light path on the way toward the specimen and then emanating from the specimen. It is important, in view of low emission intensities, that the light source chosen for excitation be of sufficient brightness so that the relatively weak emission light can be maximized; and that fluorochromes of satisfactory absorption and yield be chosen.

The efficiency with which the fluorochrome absorbs the excitation light is known as the extinction coefficient. The greater the extinction coefficient, the likelier the absorption of light in a given wavelength region (a prerequisite to ensuing fluorescence emission). The yield is referred to as the quantum yield, the ratio of the number of quanta ("packets" of energy) emitted compared to the number of quanta absorbed (usually the yield is between 0.1 and 0.7). Quantum yields below 1 are the result of the loss of energy through non-radiative pathways (e.g. heat or photochemical reaction) rather than the re-radiative pathway of fluorescence. Listed below in Table 1 are fluorescence quantum yields for a group of selected fluorochromes. Notice that some yields are trivial (benzene) while others are very efficient (Fluorescein and Rhodamine-B).

Extinction coefficient, quantum yield, mean luminous intensity of the light source, and fluorescence lifetime are all important factors contributing to the intensity and utility of fluorescence emission.

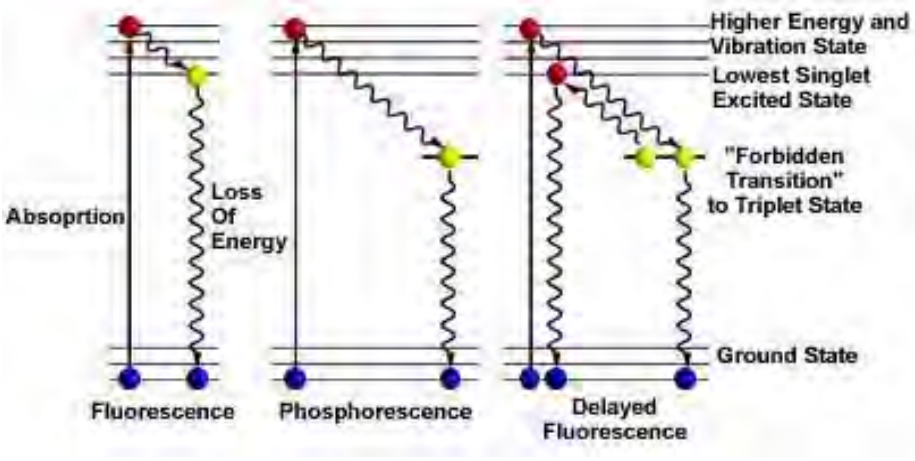

FIGURE 12.4: Energy diagram of fluorescence

12.1 Molecular Explanation

Fluorescence activity is sometimes depicted diagrammatically as shown in Figure 12.4(a) (a so-called Jablonski-type diagram). Prior to excitation, the electron configuration of the molecule is described as being in the ground state. Upon absorbing the excitation light, usually of short wavelengths, electrons may be raised to a higher energy and vibrational excited state; this may take a trillionth of a second (10 to the minus 12th seconds).

In fluorescence, in an interval of approximately a billionth of a second (10 to the minus 9th seconds), the excited electrons may lose some vibrational energy and return to the so-called lowest excited singlet state. From the lowest excited singlet state, the electrons "drop back" to the ground state with simultaneous emission of fluorescent light as illustrated in Figure 12.4(a). The emitted light is always of longer wavelengths than the excitation light (Stokes' Law). If the exciting radiation is halted, the fluorescence ceases.

If the excited electrons, instead of "dropping back" to the lowest singlet state, make a "forbidden transition" to the triplet state and then to the ground state, the emission of radiation may be considerably delayed–up to several seconds or more. This phenomenon is characteristic of phosphorescence as shown in Figure 12.4(b). In some instances, the excited electrons may go from the triplet state to the lowest excited singlet state and then return to the ground state, emitting fluorescent light. This action takes a little longer (about a microsecond or two) than usual fluorescence and is called delayed fluorescence (Figure 12.4(c)). Under some circumstances, e.g. photobleaching or the presence of salts of heavy metals, etc., emitted light may be significantly reduced or halted altogether, as discussed below.

12.2 Fading

There are conditions that may affect the re-radiation of light and thus reduce the intensity of fluorescence. This reduction of emission intensity is generally called fading. Some authors further subdivide fading into quenching and bleaching. Bleaching is irreversible decomposition of the fluorescent molecules because of light intensity in the presence of molecular oxygen. Quenching also results in reduced fluorescence intensity and frequently

Antifade Reagent	Comments	Reference
p–phenylene–diamine	The most effective reagent for FITC. Also effective for Rhodamine.Should be adjusted to 0.1% p-phenylenediamine in glycerol/PBS for use. Reagent blackens when subjected to light exposure so it should be stored in a dark place. Skin contact is extremely dangerous.	G. D. Johnson& G. M. Araujo (1981) J. Immunol. Methods, 43: 349-350
DABCO (1,4–diazabi–cyclo–2,2,2–octane)	Highly effective for FITC. Although its effect is slightly lower than p-phenylenediamine, it is more resistant to light and features a higher level of safety.	G. D. Johnson et. al., (1982) J. Immunol. Methods, 55: 231-242
n–propylgallate	The most effective reagent for Rhodamine, also effective for FITC. Should be adjusted to 1% propylgallate in glycerol/PBS for use.	H. Giloh & J. W. Sedat (1982), Science, 217: 1252-1255
2–mercapto–ethylamine	Used to observe chromosome and DNA specimens stained with propidium iodide, acridine orange, or Chromomysin A3. Should be adjusted to 0.1mM 2-mercaptotheylamine in Tris-EDTA	S. Fujita & T. Minamikawa (1990), Experimental Medicine, 8: 75-82

TABLE 12.2: Widely Used Antifade Reagents

comes about as a result of oxidizing agents or the presence of salts of heavy metals or halogen compounds. Sometimes quenching results from the transfer of energy to other so-called acceptor molecules physically close to the excited fluorophores, a phenomenon known as resonance energy transfer. This particular phenomenon has become the basis for a newer technique of measuring distances far below the lateral resolution of the light microscope. The occurrence of bleaching has led to a technique known as FRAP, or Fluorescence Recovery After Photobleaching. FRAP is based upon bleaching by short laser bursts and subsequent observation of the recovery of fluorescence caused by the diffusion of fluorophores into the bleached area.

To lessen fading in some specimens, it may be advisable to use a neutral density filter in the light path before the light reaches the excitation filter, thus diminishing the excitation light intensity. In other instances, fading effects may be reduced by changing the pH of the mounting medium or by using anti-bleaching agents (several of the more important agents are listed in Table 2). For photomicrography or visual observation, rapidly changing the field of view may also avoid fading effects.

Chapter 13

Fluorescence Component

13.1 Light Sources

In most fluorescence microscopy applications, the number of photons reaching the eye or other detector, such as a video camera or photomultiplier, is usually very low. This is because the quantum yield of most fluorochromes is low (quantum yield is the ratio of the number of quanta emitted by the specimen as compared to the number of quanta absorbed). To generate enough excitation light intensity to furnish emission capable of detection, powerful light sources are needed, usually arc (burner) lamps similar to the example that is presented in Figure 13.1. These lamps are filled with high pressure gases and should be handled with caution.

The most common lamps are the mercury burners, ranging in wattage from 50 watts to 200 watts and the xenon burners ranging from 75 watts to 150 watts. The mercury burner lamp in Figure 13.1 consists of two electrodes sealed under high pressure in a quartz glass envelope which also contains mercury.

These light sources are usually powered by a D.C. power supply furnishing enough start-up power to ignite the burner (by ionization of the gaseous vapor) and to keep it burning with a minimum of flicker. The power supply should have a timer to enable you to keep track of the number of hours the burner has been in use. Arc lamps lose efficiency and are more likely to shatter, if used beyond their rated lifetime. The mercury burners do not provide even intensity across the spectrum from ultraviolet to infrared (See Figure 13.2 for the emission spectrum of the mercury burner). Much of the intensity of the mercury burner is expended in the near ultraviolet, with peaks of intensity at 313, 334, 365, 406, 435, 546, and 578 nanometers. At other wavelengths of visible light, the intensity is steady but not nearly so bright, but still usable for blue excitation. It also should be understood that mere wattage is not the only consideration for determining brightness.

Another important criterion is the size of the arc; the brightness per unit area of the arc encompassed within the back aperture of the objective is a better measure of the useful brightness of the burner. Using the criterion, you will note that of the three mercury burners

FIGURE 13.1: Mercury Arc Lamp

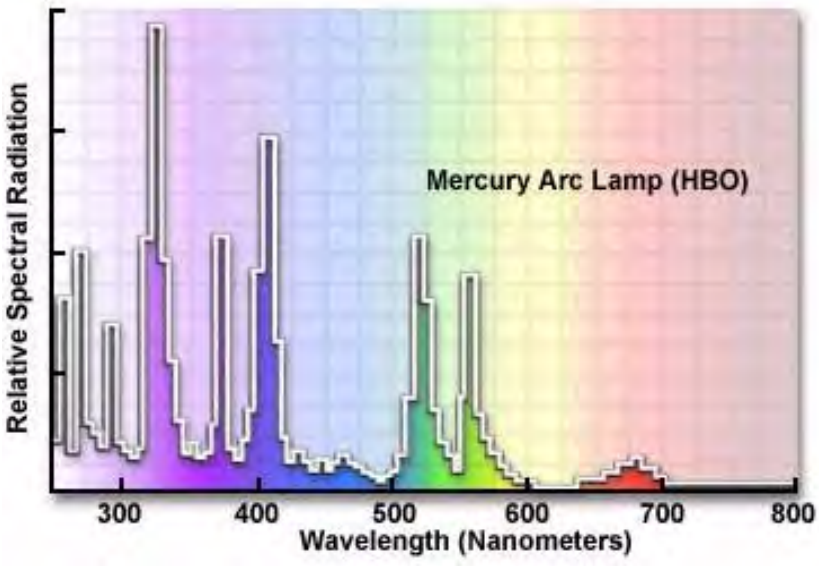

FIGURE 13.2: Mercury Arc Lamp UV and Visible Emission Spectrum

Lamp Type	XBO 150W/1	XBO 75W/2	HBO 200W/2	HBO 100W/2	HBO 50W/3
Current	DC	DC	DC	DC	DC
Rate Power (W)	150	75	200	100	50
Luminous Flux (lumens)	3000	950	10000	2200	1300
Light Intensity (Candela)	300	100	1000	260	150
Avg. Brightness (cd/cm)	15000	40000	40000	170000	90000
Arc Size (w x h in millimeters)	0.50x2.20	0.25x0.50	0.60x2.20	0.25x0.25	0.20x1.35
Life (Hours)	1200	400	400	200	200

TABLE 13.1: Fluorescence Lamp Specifications

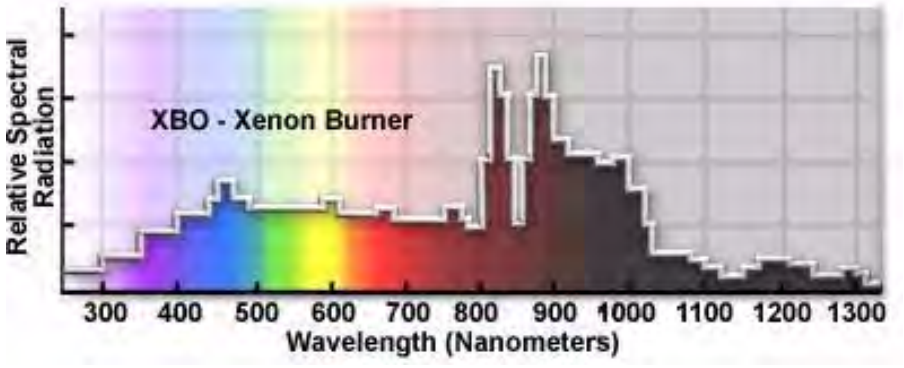

FIGURE 13.3: Xenon Arc Lamp Emission Spectrum

listed in Table 1, the 100 watt burner (other things being equal) is the brightest of the three. Also important in your selection of a burner is whether or not the spectral intensity peaks of the burner's wavelengths match the excitation requirements for the fluorochromes staining the specimen. Whenever an illumination system is being evaluated, it is necessary to consider the entire system including collector lenses and the use of aperture and field diaphragms in securing Köhler illumination.

The xenon burners have much more even intensity across the visible spectrum than do the mercury burners (See Figure 13.3); they do not have the very high spectral intensity peaks that are characteristic of mercury burners. Xenon lamps are deficient in the ultraviolet; they expend a large proportion of their intensity in the intra-red, and therefore the use of such lamps requires care in control of heat. Short-gap xenon burners are usually more desirable because the size of the arc is such that its light may be more readily included within the back aperture of the objective, thus avoiding waste of light intensity.

CAUTION!

> Mercury and Xenon arc lamps require caution during operation because of the danger of explosion due to very high internal gas pressures and extreme heat generated during use. Never ignite a lamp outside of its housing or observe the lamp directly when it is burning (this can cause serious eye damage). Neither mercury nor xenon lamps should be handled with bare fingers in order to avoid inadvertent etching of the quartz envelope. Change bulbs only after the lamp has had sufficient time to cool. Store lamps in their shipping containers to avoid accidents.

Always adhere to the safety procedures listed above when installing or changing mercury or xenon arc lamps. Mercury burners have a life of 200 hours; xenon burners several hundreds of hours. Frequent on-off switching reduces lamp life. When the burners reach their rated lifetime, the spectral emissions may change and the quartz envelope weakens.

Sometimes, tungsten-halogen bulbs are used, especially for blue or green excitation with brightly emitting specimens. Their output is relatively even across the visible spectrum (Figure 13.4); they are deficient in the near-ultraviolet and also have a relatively high proportion of intensity in the infrared. These lamps do not require expensive power supplies for ignition but are powered by low voltage transformers; the bulbs last for thirty to fifty hours when used at their maximum rated voltage. In recent years, there has been increasing

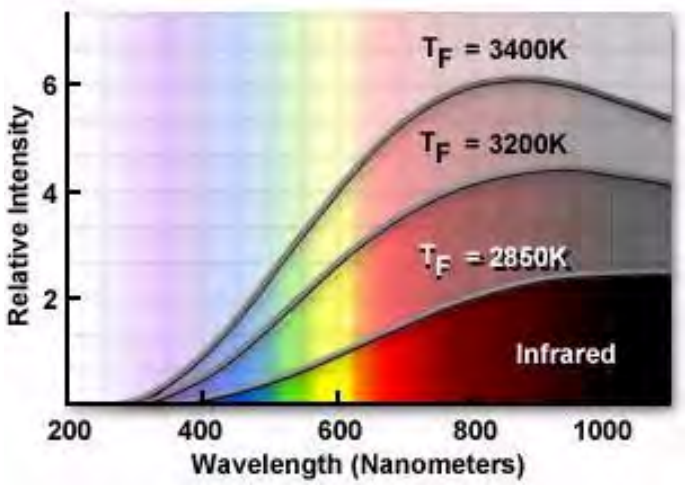

FIGURE 13.4: Tungsten Lamp Emission Spectrum

use of lasers, particularly the argon-ion laser with powerful emission capability at 488 and 514 nanometers. Laser sources, despite the high cost, have become especially useful in laser scanning confocal microscopy. There are a number of different types of lasers that each provide a unique emission spectrum. Figure 13.5 illustrates the emission spectra of the two most commonly used lasers in fluorescence microscopy.

This technique, with its many variations of equipment, has proved to be a powerful tool in rendering very sharp fluorescence images by ingeniously controlling out-of-focus light. This is accomplished through scanning and imaging extremely small, shallow areas successively. The optical sections of the specimen are stored in a computer and reconstituted into the whole image which can then be displayed on a video monitor or printed with a video printer.

13.1.1 Lamp Alignment

Microscope companies may offer an optional centering screen to facilitate the centering of the image of the lamp arc to the back aperture of the objective. This accessory has, at its upper end, the standard Royal Microscopical Society (RMS) thread and can be screwed into the nosepiece. It is placed there and rotated into the light path. The lower face of the accessory has a frosted, orange-colored glass with an inscribed crosshair.

Light coming down from the dichroic mirror strikes the built-in reflector of the centering screen and is reflected onto the crosshairs, as illustrated in Figure 13.6. As you manipulate the lamp condenser knob and the centering screws on the lamp socket, you can move the image so that it is centered to the crosshairs (Figure 13.7(a)). The size of the image of the arc can be made bigger or smaller by manipulating the lamp condenser lever. When you are done with the centering accessory, it can be replaced by a regular objective. If the lamphouse contains a mirror, the mirror position should be adjusted so that the arc image in the mirror is positioned parallel and adjacent to the arc image itself as shown in Figure 13.7(b).

If you do not have a centering screen, the following alternative procedure can be used. Focus the specimen with the 10x objective. Then rotate the nosepiece so that an empty opening on the nosepiece is in the optical path of the microscope. Place a white card on

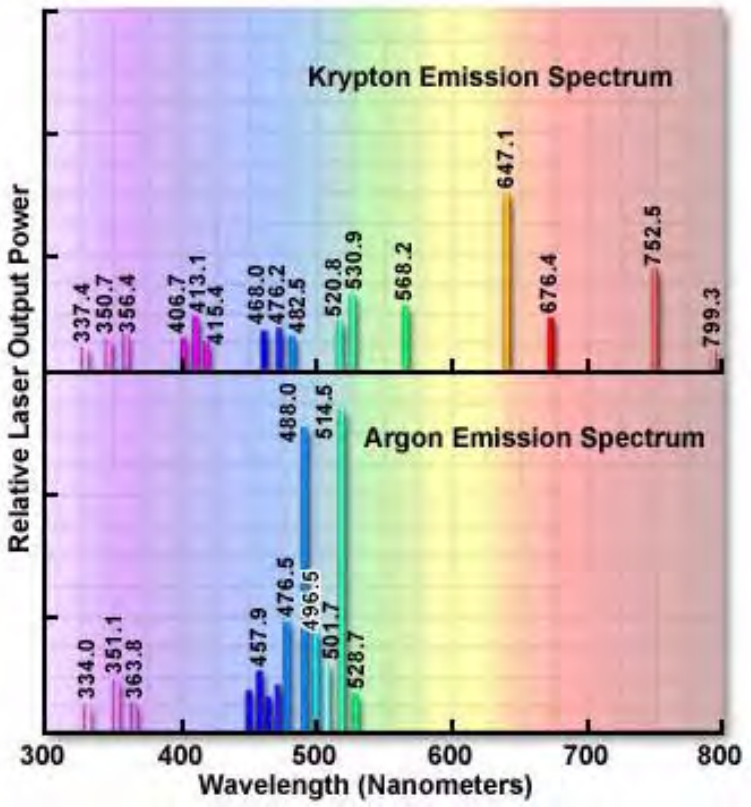

FIGURE 13.5: Laser Illumination Source Emission Spectra

FIGURE 13.6: Light Path

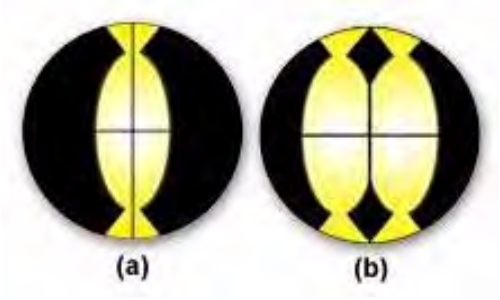

FIGURE 13.7: Adjusted Arc Images

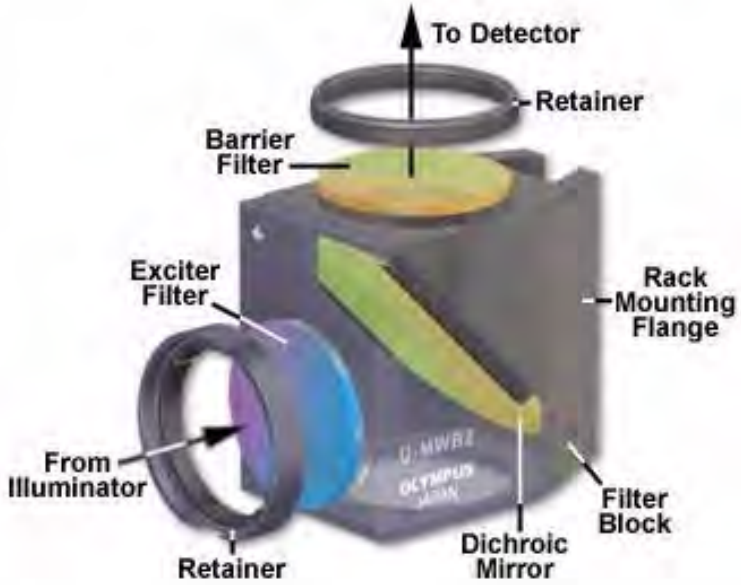

FIGURE 13.8: Fluorescence Interference Filter Block

the stage (in place of the specimen) and you will see the image of the arc projected onto the card. By manipulating the lamp condenser knob and the burner centering screws on the lamphouse, you can center the image of the arc to the optical axis of the microscope.

13.2 Filter Cubes

The terminology applied to fluorescence filters has become a jumble as a result of various initials utilized by different manufacturers to identify their filters. In this discussion, we attempt to make some order of this confusing terminology. Basically there are three categories of filters to be sorted out: exciter filters, barrier filters and dichromatic beam splitters (dichroic mirrors) that are usually combined to produce a filter cube similar to the one illustrated in Figure 13.8. Proper selection of filters is the key to successful fluorescence microscopy.

Exciter filters permit only selected wavelengths from the illuminator to pass through on the way toward the specimen. Barrier filters are filters which are designed to suppress or block (absorb) the excitation wavelengths and permit only selected emission wavelengths to pass toward the eye or other detector. Dichromatic beam splitters (dichroic mirrors) are

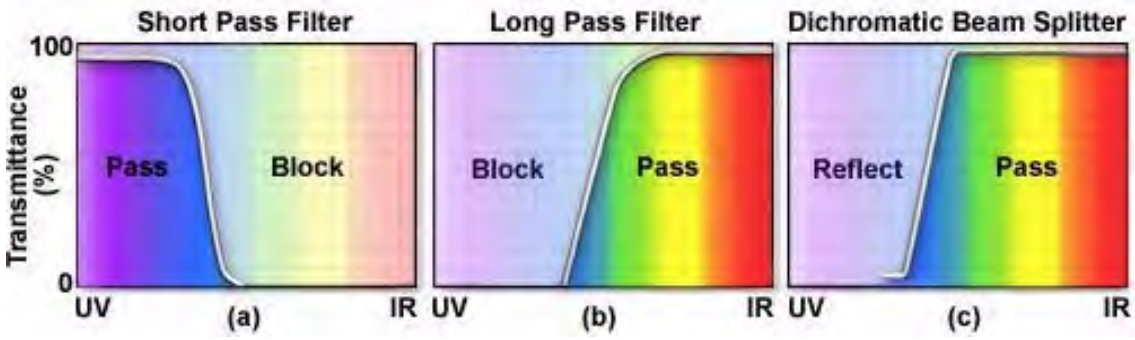

FIGURE 13.9: Fluorescence filter spectra

specialized filters which are designed to efficiently reflect excitation wavelengths and pass emission wavelengths. They are used in reflected light fluorescence illuminators and are positioned in the light path after the exciter filter but before the barrier filter. Dichromatic s are oriented at a 45 degree angle to the light passing through the excitation filter and at a 45 degree angle to the barrier filter as illustrated in Figure 13.8. Filter curves (spectra) show the percentage of transmission (or the logarithm of percentage) as the vertical axis and the wavelengths as the horizontal axis.

Fluorescence filters were formerly almost exclusively made of colored glass or colored gelatin sandwiched between glass. As a result of more sophisticated filter technology, interference filters have been developed that consist of dielectric coatings (of varied refractive indices and reflectivity) on glass. These filters are designed to pass or reject wavelengths of light with great selectivity and high transmission. Most of today's exciter filters are the interference type; some barrier filters are also, for special needs, the interference type. Dichromatic beam splitters are specialized interference filters. Sometimes short pass filters (SP) and long pass (LP) filters are combined to narrow the band of wavelengths passing through such a combination. (Figure 13.10(c))

13.2.1 Exciter Filters

Abbreviations used by manufacturers to denote properties of their filters include: UG (ultraviolet glass) and BG (blue glass), which are glass exciter filters. KP (K is an abbreviation for kurz, short in German) and SP are short pass filters; and EX indicates an exciter filter.

Today, most exciter filters are of the interference type. The transmission curve of a KP or SP filter shows a steep drop at the right-hand side of the curve, as illustrated in Figure 13.9(a). If the exciter filter is labeled with the letter B or BP, it is a band pass filter (Figure 13.10). A BP filter is a filter with wavelength cut-off both to the left and to the right of its curve (see Figures 13.10(a) and 13.10(b)). Numbers associated with these filters may refer to the wavelength of maximum transmission for band pass exciter filters. For SP or KP filters, the number may refer to the wavelength at 50% of the maximum transmission. For band pass filters sometimes the bandwidth, in nanometers, at the 50% level of maximum transmission is stated. Band pass filters are designed to pass only a desired band of the wavelength spectrum; many interference band pass filters pass a narrow band of the spectrum. Some manufacturers label their interference filters with the designation IF. Narrow interference band pass filters are especially helpful if the Stokes' shift is small.

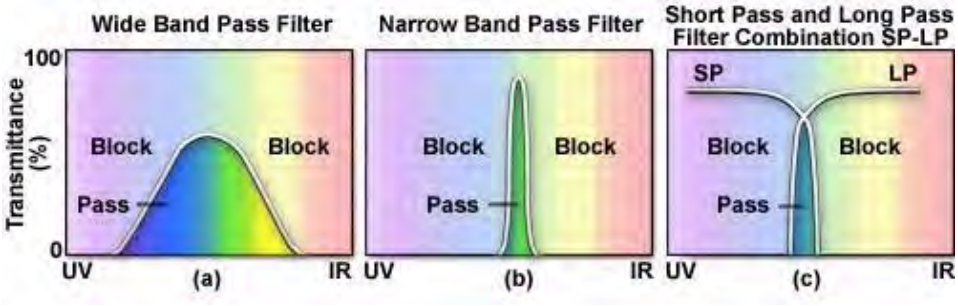

FIGURE 13.10: Barrier Filter Spectra

13.2.2 Barrier Filters

Acronyms or abbreviations for barrier filters include: LP or L for long pass filters, Y or GG for yellow or gelb (german) glass, R or RG for red glass, OG or O for orange glass, K for kante, a German term for edge (filter), and BA for barrier filter.

Barrier filters block (suppress) shorter wavelengths and have high transmission for longer wavelengths. When the filter type is also associated with a number, e.g. BA475, that designation refers to the wavelength (in nanometers) at 50% of its maximum transmission. Curves for barrier filters usually show a sharp edge at the left side, indicating the blocking of wavelengths to the left of that edge (see Figure 13.9(b)). Modern barrier filters are generally the interference type, many of which are band pass with sharp cut-offs at both the left and right sides of the transmission curve, as illustrated below in Figure 13.10.

13.2.3 Dichromatic Beam Splitters

Abbreviations used to describe and identify beam splitters are: CBS for a chromatic beam splitter, DM for a dichroic mirror, TK for "teiler kante", German for edge splitter, FT for "farb teiler", German for color splitter, and RKP for reflection short pass. All of these terms should be considered interchangeable.

These filters are always the interference type. The coatings are designed to have high reflectivity for shorter wavelengths and high transmission for longer wavelengths. Dichromatic beam splitters are oriented at a 45 degree angle to the path of the excitation light entering the cube through the reflected light fluorescence illuminator. Their function is to direct the selected excitation (shorter wavelengths) light through the objective and onto the specimen. They also have the additional functions of passing longer wavelength light to the barrier filter, and reflecting any scattered excitation light back in the direction of the lamphouse. In many of the current reflected light fluorescence illuminators, the exciter filter, the dichroic mirror, and the barrier filter are all incorporated into a single cube as illustrated in Figures 13.8 and 13.13. The illuminator, by means of a slider or rotation device, may incorporate as many as three or four cubes, thus giving the user the option to conveniently work with fluorochromes of various specifications. Alternative exciters and barriers are easily attachable for optimizing the excitation or emission of wavelengths for certain fluorochromes. The standard exciter filters and barrier filters are user-detachable so that custom-made filters can also be fitted into the microscope.

Usually, the lamp housing contains an infrared or heat filter to protect the fluores-

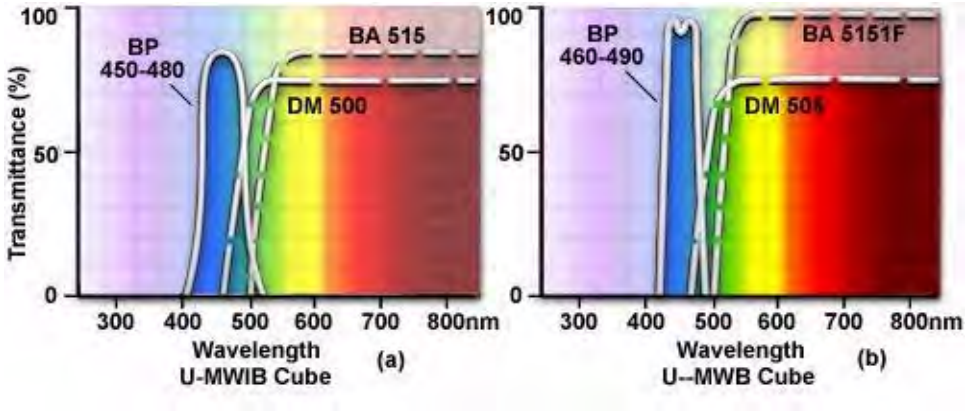

FIGURE 13.11: Blue Cube spectra

cence filters from heat deterioration. Some illuminators may incorporate or accept a red suppression filter (designated BG38) to eliminate reddening of the viewfield background associated with some filter combinations. Also, the illuminator may accept a neutral density filter and/or have a opaque light shutter to reduce or temporarily block the light from reaching the specimen.

It is advisable that you inquire of the manufacturer as to what procedures they use in naming and identifying their particular filters. Samples of such nomenclature use for Olympus fluorescence microscopes are given in our data tables, but you should bear in mind that manufacturers differ in their naming rules. Microscope companies can supply the transmission curves for their exciter and barrier filters and for their dichroic mirrors. As of July, 1998, this information was not available on the Websites of the major manufacturers, but we will supply links when they become available.

13.2.4 Examples of cube

Cubes for Blue Excitation

To understand how a cube functions, let's take, as an example, the commonly-used cube for blue excitation. This cube (using the Olympus designation for the U-URA illuminator) is the U-MWB cube. The U-MWB cube has a band pass 450-480 exciter filter, as illustrated in Figure 13.11(a). This designation means that a high percentage of the excitation light falls between 450 and 480 nanometers in wavelength. The dichroic mirror in this cube is the DM500, so named because 500 nanometers is the wavelength at 50% of the maximum transmission for this mirror. The transmission curve for this mirror shows high transmission above 500 nm, a steep drop in transmission to the left of 500 nanometers, and maximum reflectivity to the left of 500 nanometers but still may have some transmission below 500 nm. The barrier filter in this cube is a BA515, that has a steep slope below 515 nanometers and thus passes little light below 515. The BA515 is a long pass filter which transmits a high percentage of wavelengths above 515 all the way up from green into the far red (Figure 13.11(a)).

If you wish to narrow the excitation band for blue excitation, you might choose the U-MWIB cube. This cube has an interference excitation filter (very sharp slopes on either side of the excitation band) BP460, a dichroic mirror DM505 and a barrier long pass 515IF

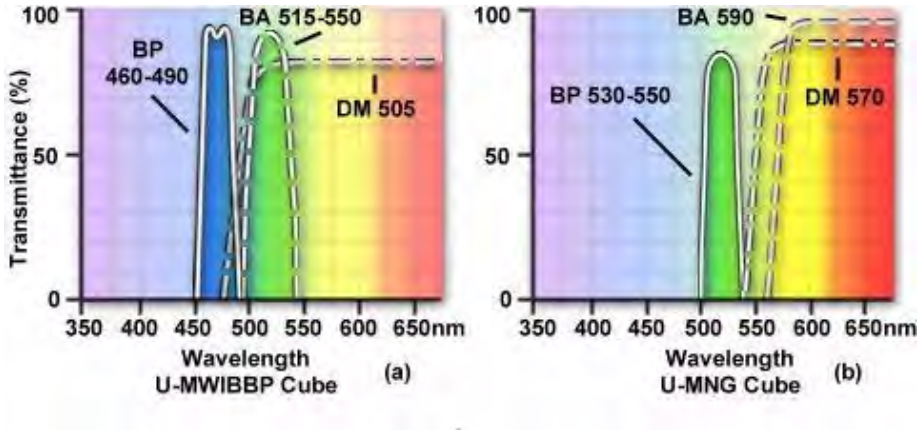

FIGURE 13.12: IGS Cube spectra

(interference barrier filter). The sharp slopes of the exciter and barrier filters do a better job in separation of excitation and emission wavelengths with minimum overlap as illustrated in Figure 13.11(b).

If you wished to do blue excitation but wanted to restrict the emitted wavelengths traversing the barrier filter, to green emission only, you could choose the U-MWIBBP cube. This cube has an identical exciter and dichroic mirror to the U-MWIB cube but, as its barrier filter, it has a band pass BA515-550 (NOT a long pass filter). This barrier filter passes only light in the green wavelengths between 515-550 nm and blocks longer wavelengths above 550 and blocks wavelengths shorter than 515 nm (Figure 13.12(a)).

There are also other cubes for blue excitation, e.g. the U-MNIB and U-MNIBBP cubes that are listed with other U-URA cubes in our fluorescence cube data tables. If none of the microscope manufacturer's cubes fits your needs, you will have to go to an outside commercial manufacturer for custom-made filters and dichroic mirrors. Most microscope manufacturers now produce cubes which have removable exciter and barrier filters and a removable dichroic mirror. The function of the cube is to employ the excitation filter to tailor-make the excitation light reaching the fluorochrome; to ensure maximum reflection of the desired excitation light by the dichroic mirror; and finally to employ the barrier filter to pass the desired emission wavelengths yet block unwanted excitation light or specific unwanted emission wavelengths.

IGS Cube

In addition to the standard fluorescence cubes, manufacturers may offer a cube for immuno-gold staining. This cube, in place of a dichroic mirror, has a standard half-mirror similar to the kind used in metallurgical brightfield reflected light microscopy. In place of an exciter filter, there is positioned a long pass 420 nanometer barrier filter (to block light below 420) and a polarizing filter oriented to pass light vibrating only east-west perpendicularly to the light entering the cube. In place of a barrier filter on the cube, there is another polarizing filter (serving as an analyzer) which allows only light vibrating north-south to the light path to pass to the eye or detector. The analyzer may be placed in a not quite crossed position with respect to the polarizer. The immuno-gold (or silver) stain shows up quite clearly as it adheres to specific targets being studied.

Multiple Staining

FIGURE 13.13: Olympus and Nikon Cubes

Researchers often run into crossover problems when doing multiple fluorochrome staining. For example, in the common double staining using Fluorescein isothiocyanate (FITC) and a Rhodamine conjugate, it may be that the blue excitation light exciting FITC (green emission) will also cause excitation of the Rhodamine conjugate (red emission). For this combination of stains, you might try the U-MWIBBP cube (see the data tables for filter specifications for Olympus U-URA cubes). This cube has a 460-490 nm band-pass excitation filter, which will excite FITC. The barrier filter for this particular cube is NOT a long pass filter but a band pass of 515-550nm which will restrict the emission, reaching the eye or other detector, to the green wavelengths and will block red emission from the Rhodamine.

A second cube, the U-MNG, has a band pass excitation filter 530-550 for green excitation of the Rhodamine conjugate. The barrier filter for the U-MNG cube is a long pass BA590 which will permit the red emission of the Rhodamine to reach the eye or other detector (e.g. film or video) and will block any green emission.

By alternately rotating the U-MWIBBP cube and the U-MNG cube into the light path, you should be able to separate the green emission of FITC and the red emission of Rhodamine in a double stained sample. (Figure 13.12) Similarly, for other combinations of multiple fluorochrome staining, the user must know the excitation-emission spectra for the fluorochromes and the transmission curves for the cubes supplied by the microscope manufacturer.

Fluorescence cube housings from different manufacturers are generally not interchangeable and are restricted for use within specific illuminators provided by the manufacturer. The cubes illustrated in Figure 13.13 show several designs that are currently available from Olympus and Nikon. It should be kept in mind that the individual elements (the exciter filter, barrier filter, and dichroic mirror) from the cubes of one manufacturer may sometimes be adjusted to fit into the cubes of another. This task is left for individual users to determine by trial and error. In some instances, it may be necessary to seek custom-made filters (see data tables for sources) to secure needed excitation wavelengths and/or separation of fluorescence emission wavelengths. Several of the commercial sources now also provide custom-made filters and a dichroic mirror, installed in a single manufacturer-supplied cube, which are capable of handling double or triple fluorochrome stained specimens without crossover problems (e.g., DAPI & FITC, DAPI & FITC & TEXAS RED, pararosaniline & acriflavin, etc.)

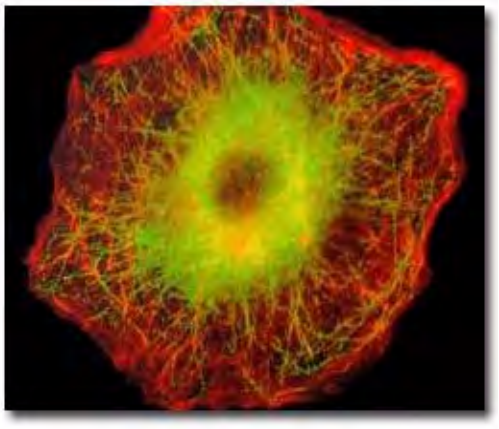

FIGURE 13.14: Multiply-Stained Fluorescence Specimen

The photomicrograph illustrated in Figure 13.14 gives an excellent example of a double-stained specimen imaged using multiple fluorescence filters within a single cube. The sample is stained with FITC (fluorescein isothiocyanate) and Rhodamine-phalloidin to selectively highlight microtubules and actin filaments. The cubes were an Olympus WIBA and WIG combination photographed with a plan fluor 40X objective and the PM30 automatic photomicrography system.

13.3 Illumination

13.3.1 Transmitted Light

The early fluorescence microscope utilized transmitted light illumination (diascopic fluorescence). A primary filter to select the excitation light wavelengths was placed in the light port of the microscope and a secondary barrier filter was positioned above the microscope nosepiece to block residual excitation light and to select emission wavelengths reaching the eye or camera.

The optical pathways illustrated in Figure 13.15(a & b) represent the two most common modes of transmitted light fluorescence. Brightfield fluorescence (Figure 13.15(a)) is similar to standard brightfield microscopy with the addition of a barrier filter after the objective and a dichroic excitation filter before the condenser. The darkfield condenser in Figure 13.15(b) is a very efficient Tiyoda double lens and mirror condenser that projects light onto the sample at oblique angles, preventing excitation wavelengths from directly entering the objective. In this example, the condenser is fitted with an oil front lens and there is immersion oil between the microscope slide and the condenser (for clarity, we have omitted the immersion oil that should reside between the objective and the microscope slide).

In brightfield transmitted light fluorescence, it is difficult to separate the excitation light from the fluorescing light because both kinds of light directly enter the objective. Transmitted light brightfield condensers have largely been replaced by high numerical aperture oil darkfield condensers, like the Tiyoda condenser illustrated in Figure 13.15(b).

The oil darkfield substage condenser directed excitation light at steep angles toward the specimen. Because of the darkfield design, most of the excitation light never enters the objective. As the specimen absorbs excitation light and emits only longer wavelength

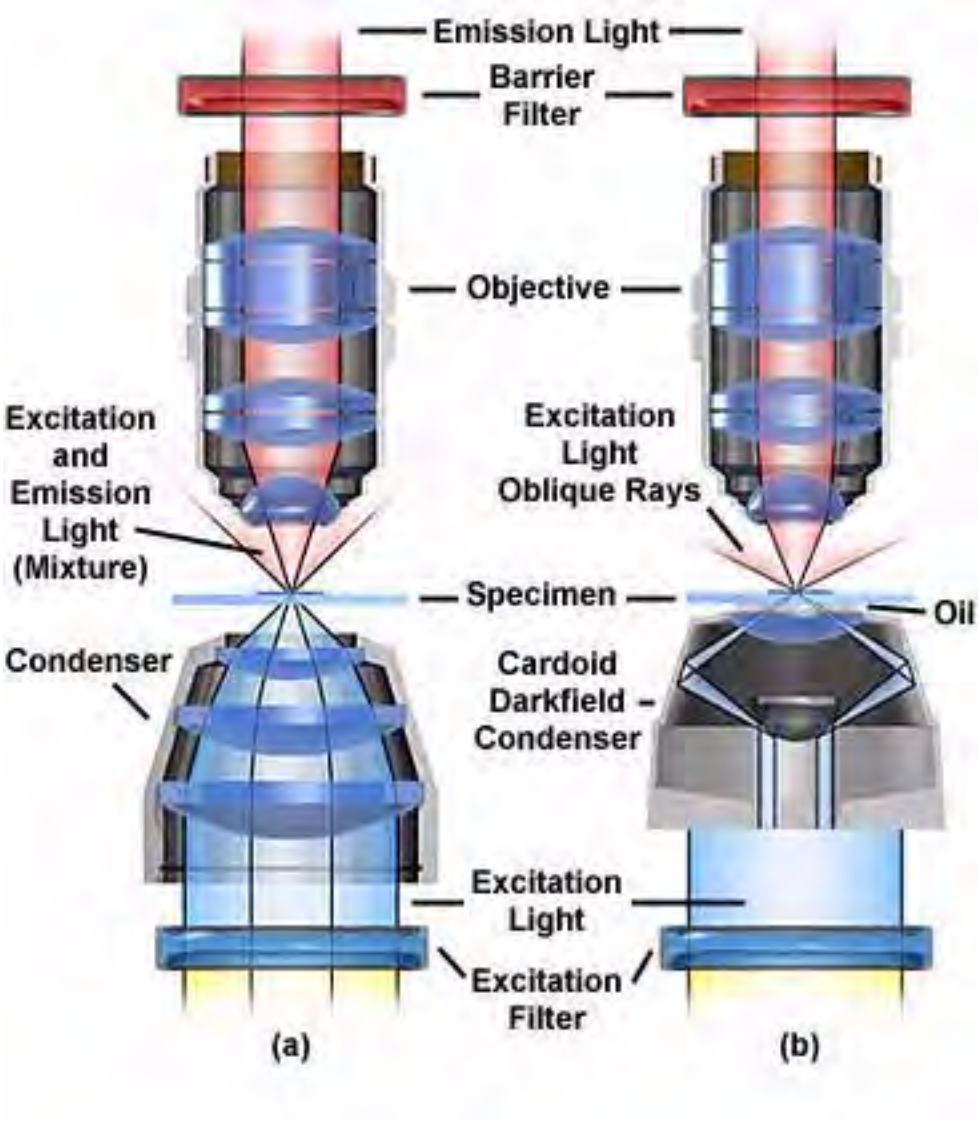

FIGURE 13.15: Transmitted light fluorescence

light, it is the longer wavelength light that gains admittance to the objective and is thus passed through the barrier filter to the eye or other detector. The resulting image shows as a more or less brightly fluorescing object on an otherwise dark background. Any scattered excitation light is blocked by the barrier filter.

Although the equipment for transmitted light darkfield fluorescence is relatively simple, the technique has significant disadvantages. Many users find it difficult to properly align the oiled condenser to the optical axis of the microscope. In addition, the numerical aperture of the higher magnification oil or water immersion objectives has to be reduced by a built-in iris diaphragm (with consequent loss of light intensity and resolution) in order to prevent excitation light from entering the objective directly. Transmitted light darkfield technique also precludes the use of simultaneous fluorescence viewing along with phase microscopy or Nomarski differential interference contrast microscopy. The darkfield method is also very wasteful of light, since the excitation light irradiates much of the specimen outside of the field of view being observed, thus reducing the usability of excitation intensity.

13.3.2 Reflected Light or epi–illumination

The name of J.S. Ploem is almost synonymous with the use of the vertical illuminator for reflected light fluorescence microscopy. Ploem, Brumberg and others were closely associated with the development of dichromatic s (dichroic mirrors) which overcame the light loss problems inherent in the use of ordinary half-mirrors in reflected light microscopy.

Reflected light fluorescence microscopy is overwhelmingly the choice of today's fluorescence workers. This mode of fluorescence microscopy is also known as incident light fluorescence, epi-fluorescence, or episcopic fluorescence. The universal reflected light vertical illuminator is interposed between the observation viewing tubes and the nosepiece carrying the objectives, as illustrated with the Olympus fluorescence microscope in Figure 13.16.

The illuminator is designed to direct light onto the specimen by first passing the light through the microscope objective on the way toward the specimen and then using that same objective to capture the light being emitted by the specimen (diagrammed in Figure 13.18).

This type of illuminator has several advantages: the objective, first serving as a well corrected condenser and then as the image-forming light gatherer, is always in correct alignment relative to each of these functions; most of the unwanted or unused excitation light reaching the specimen travels away from the objective (such " front-face" fluorescence excitation is particularly good with thick specimens); the area being illuminated is restricted to the area being observed; the full numerical aperture of the objective, in Köhler illumination, is utilizable; and, it is possible to combine or alternate reflected light fluorescence with transmitted light phase contrast, Nomarski differential interference contrast (DIC) or Hoffman modulation contrast observation.

The universal reflected light illuminator (see Figure 13.16) has at its far end a universal lamp-house which contains a light source, usually a mercury burner. (Other light sources might be a xenon burner or a halogen bulb.) The light travels along the illuminator parallel to the table top and perpendicular to the optical axis of the microscope. The light passes through collector lenses and a variable, centerable aperture diaphragm and then through a variable, centerable field diaphragm. It is incident upon the excitation filter which selects those excitation wavelengths that are wanted to reach the specimen and blocks the wavelengths not wanted to reach the specimen. The selected wavelengths reach the dichromatic beamsplitting mirror. This mirror is a special type of interference filter

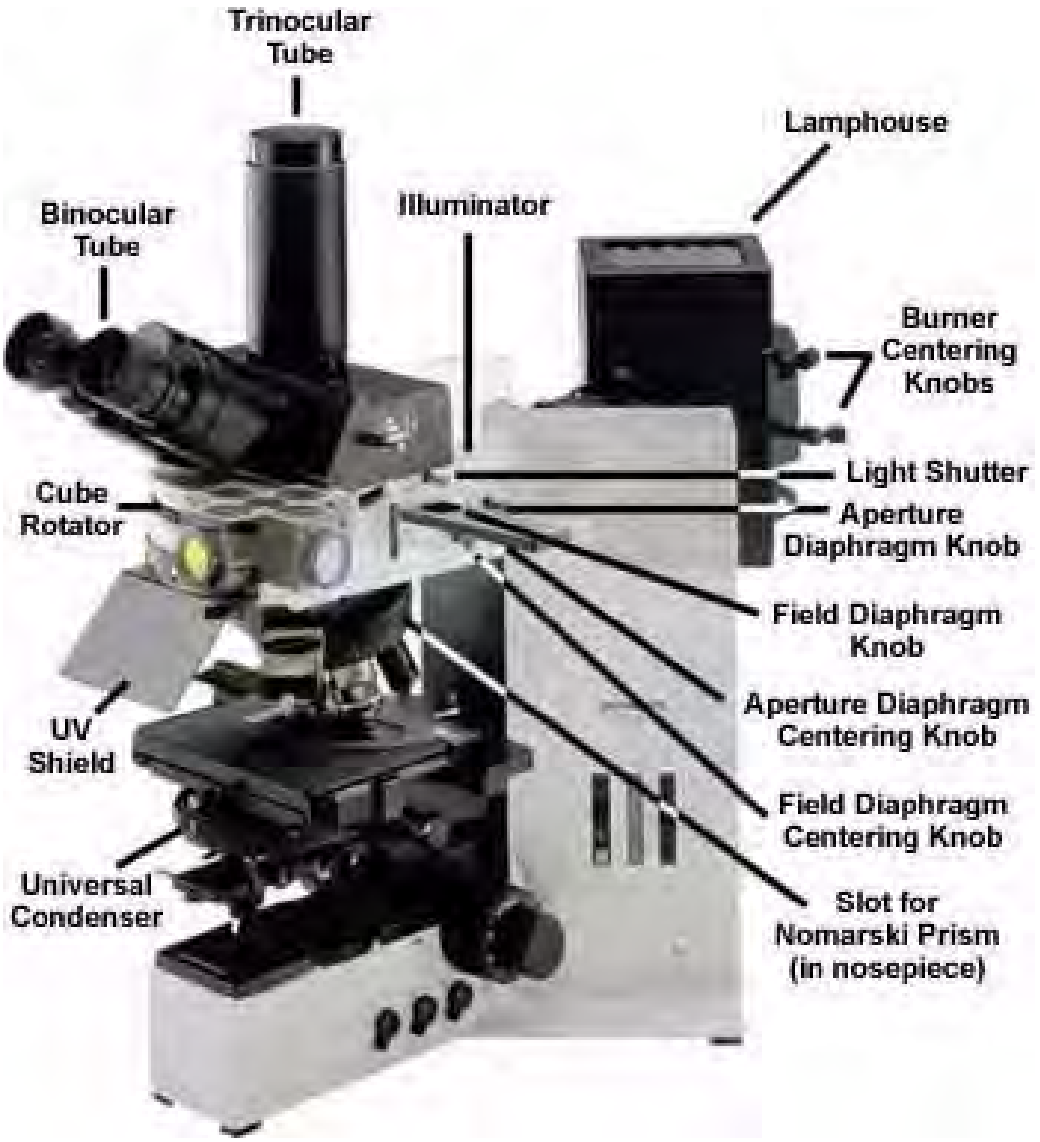

FIGURE 13.16: Olympus fluorescence microscope

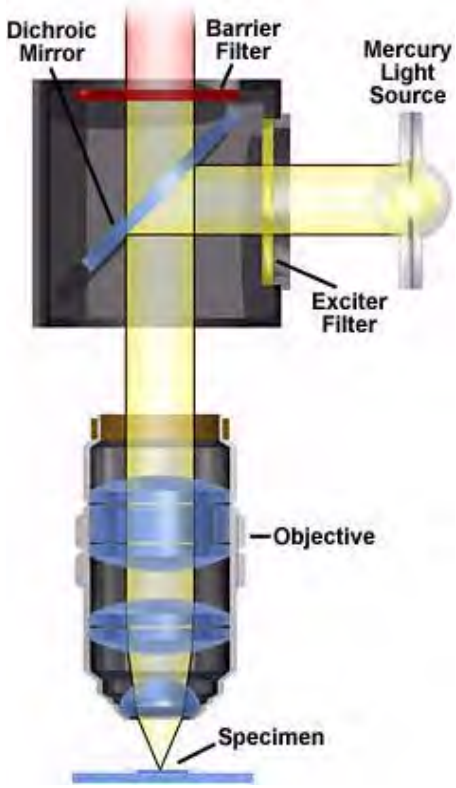

FIGURE 13.17: Epi–illumination

which efficiently reflects shorter wavelength light and efficiently passes longer wavelength light. The dichromatic beam splitter (also sometimes called the dichroic mirror) is tilted at a 45 degree angle to the incoming excitation light and reflects the excitation light at a 90 degree angle directly through the objective and onto the specimen. The fluorescent light emitted by the specimen is gathered by the objective, now serving in its usual image forming function. Since the emitted light consists of longer wavelengths, it is able to pass through the dichroic mirror.

Any scattered excitation light reaching the dichroic mirror is reflected back toward the light source. Before the emitted light can reach the eyepiece, it is incident upon and passes through the barrier or suppression filter. This filter blocks (suppresses) any residual excitation light and passes the desired longer emission wavelengths toward the eyepieces. In most reflected light fluorescence illuminators, the excitation filter, dichroic mirror, and barrier filter are incorporated in a cube, as illustrated in Figure 13.19. The more sophisticated systems accommodate three or four fluorescence cubes (on a revolving turret or on a slider) and permit the user to attach replacement custom made exciters, barrier filters or dichroic mirrors.

The design of the illuminator should permit the user to employ the desirable Köhler Illumination, providing bright and even illumination across the field of view. The corrected condensing lenses of the system make certain that the image of the centerable aperture diaphragm is conjugate with the back aperture of the focused objective. The image of the pre-focused, centerable field diaphragm is conjugate with the focused specimen and the plane of the fixed eyepiece diaphragm.

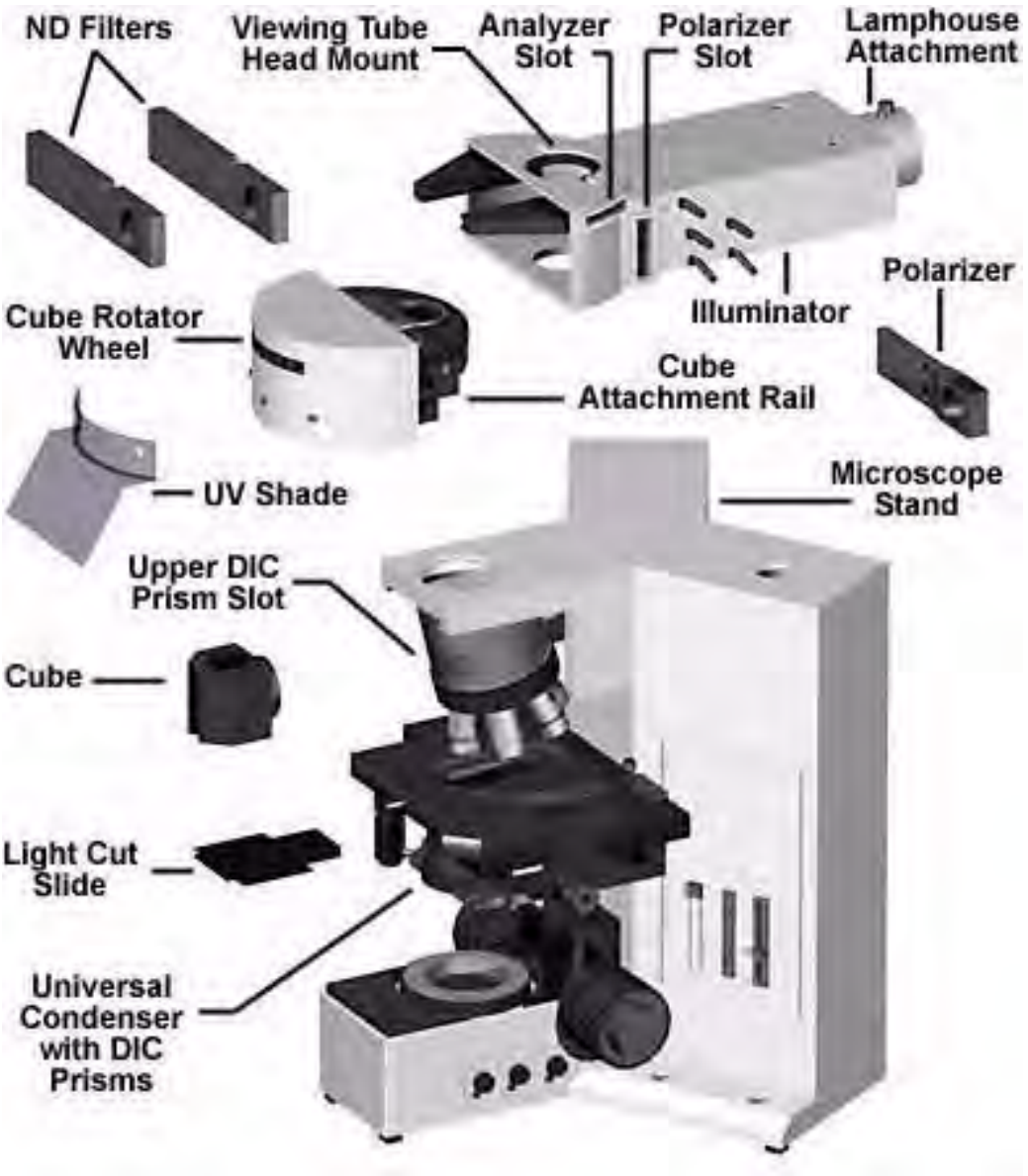

FIGURE 13.18: Epi-illumination microscope components

FIGURE 13.19: Fluorescence cube

The universal illuminator lamphouse should incorporate an infrared filter to block the very long, heat generating wavelengths. Some lamphouses have a built-in red suppression filter (e.g. an BG38), or a slot for such a filter, to eliminate a reddish background seen in the field of view in some applications. The lamphouse itself should not leak harmful ultraviolet wavelengths and, preferably, should incorporate a switch to automatically shut down the lamp if the housing is inadvertently opened during operation. The lamphouse should be sturdy enough to withstand a possible burner explosion during operation. The lamp socket should have lamp centering screws to permit centering the image of the lamp arc or halogen lamp coil to the back aperture of the objective (in Köhler illumination these planes are conjugate).

An ultraviolet protection shield is fitted into the front of the illuminator to protect the user's eyes from any inadvertent leakage of potentially dangerous short wavelength radiation. In the light path, closer to the lamphouse and before the excitation filter, it is desirable to have a light shutter for complete blocking of excitation light. The light shutter thus permits you to block the burner light without switching the burner off; neutral density filters permit reduced intensity to diminish fading in some specimens.

The universal reflected light illuminator can be attached to the standard modular upright microscope; and a similar version is now used with inverted microscope stands. The inverted stands also permit combining or alternating between reflected light fluorescence and the various contrast techniques of transmitted light microscopy.

The vertical illuminator, preferably, should have no magnification factor. Some illuminators have a magnification factor of 1.25X and are so inscribed.

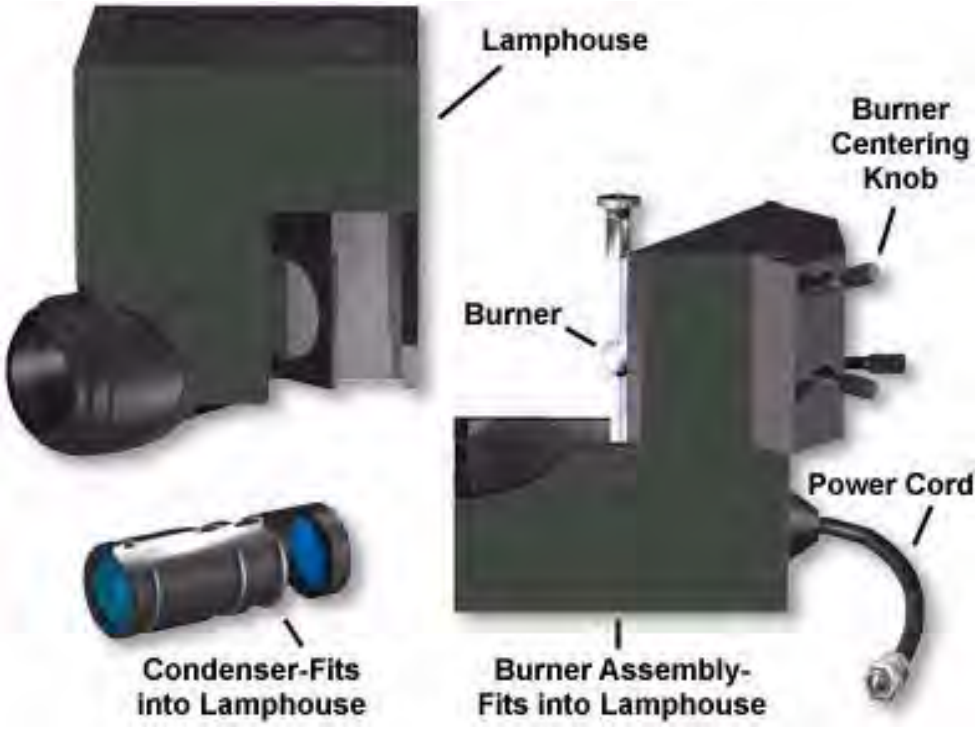

FIGURE 13.20: Illuminator stage

Chapter 14

Fluorescence Optimization and Troubleshooting

A key feature of fluorescence microscopy is its ability to detect fluorescent objects that are sometimes faintly visible or even very bright relative to the dark (often black) background. In order to optimize this feature, image brightness and resolution must be maximized using the principles that will be discussed in this portion of the primer.

14.1 Image Brightness

One of the most important aspects of optimizing image brightness is to ensure that the sample is supplied with sufficient light energy for excitation at the appropriate wavelength for each chromophore attached to the specimen. Equally important is selection of the proper barrier filter to maximize the amount of emitted fluorescence directed to the observation tubes or camera tube. We have assembled a number of tables listing fluorochrome emission and excitation data that will help to accomplish this goal. High-energy light sources such as mercury and xenon burners will provide a large amount of excitation energy in very narrow ranges of near ultraviolet and visible light. When the use of these light sources is coupled to the proper selection of excitation filters that are able to transmit selected wavelengths while blocking those that are undesirable, then the optimal criteria for excitation will be met.

The selection of barrier filters that prevent unwanted wavelengths from entering the observation tubes is a primary concern. The total energy of excitation is far greater than the energy of emission, therefore it is important to choose an efficient barrier filter that will block out unwanted wavelengths while allowing fluorescent emission from the sample to pass. Objectives chosen for fluorescence must be able to transmit light effectively both in the near ultraviolet region and throughout the visible spectrum.

In view of the low emitted light levels, the role of the objective in fluorescence microscopy is crucial because it is the objective's function to gather light from the specimen. The angle of the cone of light accepted by the objective is determined by the numerical aperture (N.A.) of the objective, as illustrated in Figure 1. In transmitted light fluorescence microscopy, the intensity of the light reaching the eye or other detector varies directly as the square of the numerical aperture of the objective and the condenser and inversely as the square of the total magnification.

On the other hand, in reflected light fluorescence, the intensity of the image varies

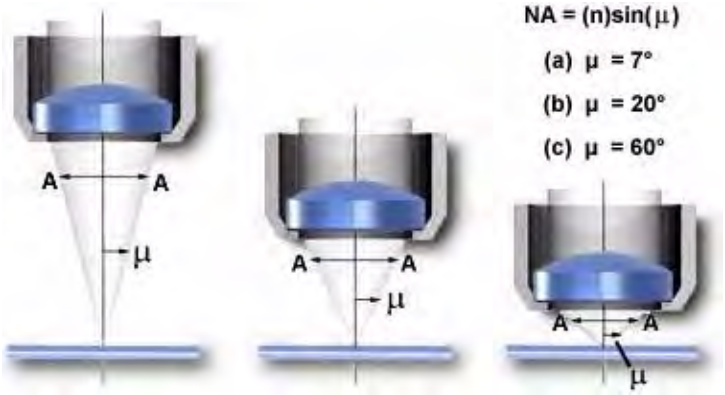

FIGURE 14.1: Angle of cone light accepted by the objective in function of the NA

directly as the fourth power of the numerical aperture of the objective in use, as well as inversely as the square of the numerical total magnification:

$$I = \frac{NA^4}{Mag^2}$$

This difference comes as a result of the objective's initially functioning as a condenser for concentrating light on the specimen, and then as the usual light gatherer for image formation. The implications are clear: high numerical aperture objectives will yield images of much higher intensity than will identical magnification objectives with lower numerical aperture. For example, other things being equal, a 40X objective with an N.A. of 1.0 will yield images more than five times brighter than a 40X objective with a numerical aperture of 0.65. A further implication is that, if possible, the employment of lower magnification visual eyepieces (e.g. 8X magnification) will also increase the brightness of the image as compared to the more commonly used 10X observation eyepieces. Additionally, in reflected light fluorescence, the excitation light is concentrated by the objective (in its function as a condenser) only on the area being observed. As a result the intensity of the excitation light is much higher than in transmitted light darkfield fluorescence where the area being excited does not change as objectives are changed. Also in darkfield, the numerical aperture of the objective must be reduced to below that of the condenser to preserve the darkness of the field of view.

In addition to numerical aperture being an important consideration, it is advisable to have objectives of highest quality chromatic correction since the focusing of the various colors in the same plane will yield sharper images. Further, the better the spherical correction, the sharper the image. Thus, the objectives of choice are planapochromats or planfluorites. These should be designed so that the lens elements and their cements will not themselves autofluoresce when irradiated with light below 400 nanometers in wavelength (light in the near ultraviolet).

When possible, oil-immersion objectives should be employed to minimize the loss of light caused by reflection from the glass slide and coverslip surfaces. Modern microscope manufacturers strive to provide optical elements that are completely free of autofluorescent contaminants, but this aspect should also be taken into consideration as autofluorescence will decrease sample contrast by increasing background brightness.

FIGURE 14.2: 100x Plan apochromat objective with adjusted iris diaphragm

14.2 Image Resolution

The Royal Microscopical Society (RMS) standard thickness for glass coverslips if 0.17mm. There is a slight degree of variation in this number (usually between 0.01mm and 0.03mm) in a statistical sampling of coverslips due to fluctuations in the manufacturing process. High numerical aperture "dry" objectives are the most susceptible to these variations and many are provided with correction collars to allow the microscopist to fine-tune objective correction for cover glass thickness. It is very important to purchase highly accurate coverslips and to make sure that objective correction collars are adjusted optimally. In addition, some manufacturers offer specialized objectives that contain an internal iris diaphragm as illustrated with the 100X apochromat Olympus objective in Figure 2. Glare should be minimized by proper adjustment of the of this iris diaphragm (Figure 2), if the objective in use is so equipped.

When using oil-immersion objectives, blot the front lens with tissue to remove oil after use and make sure that they are cleaned with an appropriate solvent periodically (usually about once a month will suffice). Excess oil left on immersion objectives can pick up dust from the air and reduce image quality and resolution. Also, make sure that the immersion oil is PCB-free, has a very low or non-existent level of autofluorescence, and is applied to the objective-coverslip interface without formation of air bubbles.

The optical path of the microscope should be carefully adjusted to ensure that all components are correctly placed and performing as they are designed. The light source arc should be properly aligned as described in our discussion of light sources for fluorescence microscopy.

14.3 Cleaning Optical Elements

The first rule in fluorescence microscopy (and all other forms of microscopy) is to keep the optical elements completely free of dust, dirt, oil, solvents, and any other contaminants. The microscope should be kept in a low vibration smoke-free room that is clean as possible and has minimal disturbance of the circulated air. Use a dust cover on the microscope when not in use and keep all accessories in air-tight containers. Avoid using corrosive solvents to clean any part of the microscope, and use only diluted soapy water to clean non-optical surfaces. Objectives should be kept clean using the following tips:

- Never drag anything across the lens surface with a high degree of pressure, including lens paper, to avoid the possibility of introducing very fine scratches onto the surface.
- Clean the lens with a solvent designed for optical surfaces or, in an emergency, absolute ethanol. Avoid other solvents because they might react with optical coatings on the glass.
- Dust the lens surface with compressed gas prior to cleaning with a solvent to remove loose particles.
- Soak a Q-tip with lens cleaner or ethanol and very gently wipe it over the lens several times, turning the cotton tip before each pass. Blot excess solvent with lens tissue and allow the lens to dry thoroughly. Repeat this procedure.

Oil-immersion lenses can be cleaned with solvent as described above. Never use oil with an objective that is intended to be used dry, because cleaning a dry objective can be much more difficult than one designed specifically for oil.

14.4 Further Tips and Troubleshooting

In ideal cases, all microscopy should be done in darkened rooms, but this is especially important with fluorescence microscopy. Human eyes have trouble quickly adjusting to the dark and it will be hard to discern a very dim fluorescent specimen immediately after darkening the room. Avoid excessive bleaching of the specimen by blocking the excitation light when not viewing or photographing the specimen. Minimize autofluorescence by thoroughly washing the specimen to remove excess fluorochrome prior to mounting. For other aspects related to general problem-solving and troubleshooting, refer to Tables 14.1–14.2 below.

Photomicrography of fluorescence specimens presents some unique challenges that are unparalleled in optical microscopy. While camera system parameters remain the same, more attention must be paid to exposure details and such artifacts as reciprocity failure that occur as a result of exceedingly long exposure times. There are a number of good books on the subject and the interested reader is referred to our Bibliography, and Web resources sections for further information.

Trouble Cause	Remedy
The bulb is on, but image cannot be seen or is dark.	The shutter knob is closed or an ND filter is in use. Move the shutter to open aperture. Remove ND filter.
The cube is not rotated into the light path correctly.	Rotate the cube into the light path correctly.
The exciter filter and barrier filter are incorrectly combined.	Follow the filter combinations for the fluorochrome.
The aperture iris diaphragm, field iris diaphragm or objective's iris diaphragm opening is not completely opened.	Completely open the aperture iris diaphragm and objective's iris diaphragm openings, and open the field iris diaphragm opening until its image circumscribes the field of view.
A cube unsuitable for the specimen is used.	Change to a suitable cube.
Image is unclear, blurred or has insufficient contrast.	Objectives or filters are dirty. Wipe them clean.
Image is partially obscured or unevenly illuminated.	The objectives are not inserted into the light path correctly. Rotate the revolving nosepiece until it clicks.
The field iris diaphragm opening is closed excessively.	Open the field iris diaphragm as required.
The shutter slider is not pushed in far enough. The mercury burner is not centered correctly, or focus adjustment has not been completed.	Push the shutter slider all the way in. Center the mercury burner or adjust the focus.
Excessive glaring.	Either exciter filter or barrier filter has not been inserted. Insert required filter.

TABLE 14.1: Optical troubleshooting

Trouble Cause	Remedy
Power switch indicator does not light up.	The power cord is connected incorrectly. Connect correctly.
Power switch indicator lights, but mercury burner does not.	Connectors are connected incorrectly. The burner has not been installed. Connect Correctly. Install the burner.
The lamp housing interlock is operating.	Tighten the bulb socket locking screw securely.
Auto ignition is not operating as required.	Turn off the power of the power supply unit. Switch on again. (Repeat as necessary.)
The bulb flickers or is dark.	Insufficient time has elapsed since the burner was turned on. Wait for 10 minutes after turning on the burner.
The bulb life has expired.	Replace the mercury burner if the life meter reads over 200 hours (lamps have lifetimes varying between 100 and 300 hours).

TABLE 14.2: Electrical Troubleshooting

Chapter 15

Fluorescence Photomicrography

Photomicrography under fluorescence illumination conditions presents a unique set of circumstances posing special problems for the microscopist. Exposure times are often exceedingly long (in some instances running from many seconds into several minutes), the specimen's fluorescence may fade during exposure, and totally black backgrounds often inadvertently signal light meters to suggest overexposure.

In addition, fluorescing specimens emit their own light, and particles residing above and below the desired plane of focus often radiate light causing blurring of the image details. Even though fluorescence images may appear to be bright when viewed through the microscope eyepieces (due to the human eye's exquisite sensitivity to light), they usually require lengthy exposure times in order to register a satisfactory image on film. Very long exposures complicate photomicrography of specimens stained with fluorescent dyes by increasing the likelihood of vibration and film reciprocity failure effects causing undesirable color shifts in the image.

While the basic problem with fluorescence photomicrography is often the paucity of light reaching the film, there are a number of steps that can be taken to improve image quality. Microscope objectives utilized for fluorescence should have as high a numerical aperture as possible, with high transmission values for the wavelengths of light being employed in the experiments. Because the light intensity (in reflected light fluorescence) varies as the fourth power of the numerical aperture, these objectives can significantly reduce exposure times in reflected light fluorescence microscopy. Light intensity also varies inversely as the square of the magnification, resulting in brighter images when the total magnification on film is held to a minimum. Reduction of magnification on the film plane is often assisted by the use of low magnification photoeyepieces (or projection lenses). In addition, when using a trinocular head, it is usually desirable to divert all light to the camera rather than have the light split (by means of a) between the viewing eyepieces and the camera. Because the image intensity also varies inversely as the square of the distance to the film plane, microscopes perform better then this distance is kept short. For this reason, and due to widespread availability, most fluorescence microscopy is recorded on 35 millimeter film (as opposed to larger format) when using traditional photomicrography to capture images. Modern low-noise temperature-controlled CCD digital cameras are being increasingly used to replace film as the medium of choice for fluorescence photomicrography.

Low light levels and the fading of fluorescent specimens are two of the primary difficulties to overcome in fluorescence photomicrography. Often, the dynamic nature of fluorescent preparations makes good photomicrography essential to capture a record of events

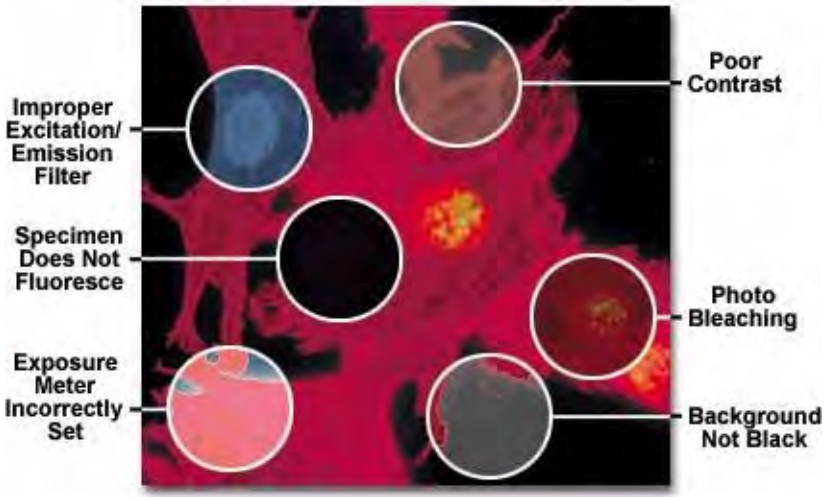

FIGURE 15.1: Troubleshooting fluorescence photomicrography

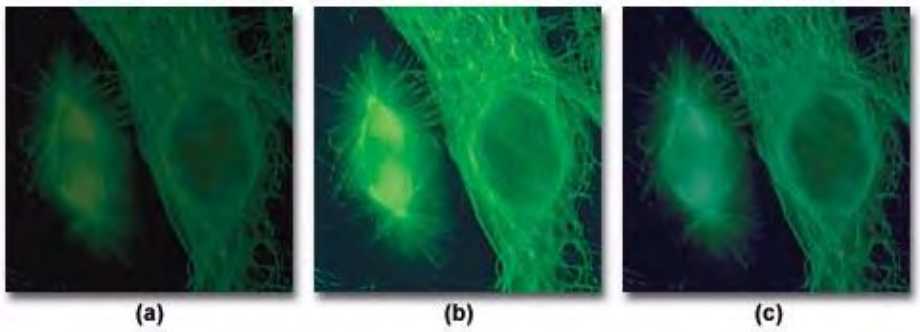

FIGURE 15.2: Photobleaching and photoreciprocity failure in fluorescence photomicrography

occurring with the specimen, and often may reveal details not obvious when examining the specimen through the eyepieces. Long exposures, so commonly used in fluorescence, inevitably lead to reciprocity failure and fading of specimen fluorescence intensity during prolonged irradiation. In fact, fading of specific fluorescent features is often faster than that of the background, leading to a loss of image contrast.

All photographic emulsions (including black & white, color negative, and color transparency films) suffer from an effect known as reciprocity law failure when exposed to light for exceeding long or short time periods. The reciprocity law relates image density to exposure time and light intensity, such that there is a reciprocal relationship between illumination intensity in the microscope and the required exposure time for film. In effect, the law states that exposure time is inversely proportional to light intensity in order to maintain a constant film density. The lower the light intensity, the longer the necessary exposure time required to produce a satisfactory image. This inverse relationship holds true for most films if the proper exposure duration is between 1/500 of a second and 1/2 second.

In fluorescence microscopy, low light levels routinely demand exposures that exceed 1/2 second (often ranging from several seconds to several minutes). The reciprocity relationship no longer holds under these conditions, and the film will require additional exposure time

to yield the proper image density. This phenomenon is called reciprocity failure, a term that only indicates that the linear relationship between exposure time and light intensity no longer holds and does not suggest a failure of the film emulsion in terms of performance.

A side effect of reciprocity law failure is that the already weak specimen fluorescence is further reduced by photobleaching of the specimen, and incorrect color reproduction often occurs due to increased exposure times. The series of images presented in Figure 15.2 are fluorescence photomicrographs illustrating antibody fluorochrome labeling with the popular reagent fluorescein-5-isothiocyanate (FITC) when imaged using an Olympus WIB long-pass fluorescence cube. The cells in the center (Figure 15.2(b)) were photographed using a corrected exposure time adjusted for reciprocity law failure and Kodak Wratten color compensating filters to remove an undesirable color shift. On the left (Figure 15.2(a)), the same viewfield shows the effect of photobleaching, or fading of the fluorescence activity due to prolonged exposure to the illumination source. Color shifts and reduced image intensity resulting from reciprocity law failure are evident in Figure 15.2(c).

Reciprocity failure can often be compensated simply by an increase in exposure time or processing conditions for black & white films, but this is not always the case with color negative and transparency films. Most color films have three color-sensitive dye layers, each of which has a slightly different characteristic curve position and slope resulting in varied responses to the reciprocity effect with the potential to cause undesirable color shifts or casts. Often, both exposure times and color balance filters must be adjusted to compensate for very long or short exposures when using color films.

Utilization of an objective having a very small numerical aperture (for instance, a 40x objective with NA = 0.65 as opposed to the same magnification objective having a NA of 0.85, 0.95, or 1.0) produces an image displaying insufficient brightness, which results in longer exposure times. The numerical aperture is a measure of the objective's light gathering ability, meaning that high numerical aperture objectives can capture a greater amount of the weak fluorescence emission produced by chromophores. Always use the highest available objective numerical aperture when doing fluorescence photomicrography. Using excessive objective and photoeyepiece magnifications will also result in reduced brightness. To compensate for this, always employ the lowest possible magnification photoeyepieces and the highest numerical aperture objectives at a given magnification. For example, a 60x plan apochromat objective having a numerical aperture of 0.95 (brightness index = 22.6) is preferable to a 60x plan fluorite objective of numerical aperture equal to 0.85 (brightness index = 14.5) even though the working distance of the fluorite objective is twice that of the apochromat. Furthermore, since high numerical aperture objectives have a shallower depth of field, their use may avoid contrast-reducing effects of out-of-focus emission from above or below the plane of focus. Likewise, a 2.5x photoeyepiece will provide more illumination than a 3.3x or 5x eyepiece. Laser scanning confocal microscopes are specifically designed to virtually eliminate out-of-focus light and give much clearer fluorescence pictures with somewhat better resolution.

Typical fluorescence applications in fields such as cell biology and medical diagnostics are not only concerned with specimen brightness, but also the ratio of specific specimen fluorescence to the intrinsic background fluorescence. This is particularly important for single-molecule fluorescence events and other low light experiments where autofluorescence and/or internal reflection inside the objective produces vast differences in the ability to image small structures with low fluorescence quantum yields. To maximize the signal-to-noise ratio (intensity of the specimen fluorescence above the background) in objectives designed

Objective Magnification	Numerical Aperture (NA)	Objective Brightness Index
10x	0.25	3.9
10x	0.30	8.1
10x	0.45	41.0
10x	0.50	62.5
20x	0.40	6.4
20x	0.50	15.6
20x	0.75	79.1
40x	0.65	11.1
40x	0.75	19.8
40x	0.95	50.9
40x	1.00	62.5
40x	1.30	178.5
60x	0.85	14.5
60x	0.95	22.6
60x	1.40	106.7
100x	1.25	24.4
100x	1.40	38.4

TABLE 15.1: Objective Brightness Values

for fluorescence microscopy, manufacturers use quartz and other special glass formulations that have high transmission values throughout the spectrum from infrared to the ultraviolet. These objectives are extremely low in autofluorescence and utilize special optical cements and anti-reflection coatings designed to operate through an extended range of fluorescence excitation wavelengths. Higher numerical apertures coupled to advanced glass formulations provide modern fluorescence objectives with the ability to excite specimens at wavelengths down to 340 nanometers with much higher transmission values in order to obtain a brighter fluorescence image.

A comparison of nominal objective brightness values for common magnifications and numerical apertures is presented in Table 15.1. These numbers were calculated according to the following equation:

$$\text{Brightness Index} = \frac{\text{NA}^4}{\text{Magnification}^2} \cdot \text{Transmission Ratio}$$

where NA is the objective numerical aperture and the Transmission Ratio is presumed to be 100,000. From this equation, it is apparent that for the same magnification, image brightness of both the illumination field and secondary fluorescence increases with the numerical aperture of the objective, but also decreases with increasing magnification. The actual numerical aperture and magnification values for a particular objective may vary by as much as 5-10 percent from the nominal values. Brightness transmitted by an objective, as discussed above, is also dependent upon the internal construction parameters, such as the number of glass lens elements, internal reflections and glare, and lens coatings. Often, it is necessary to sacrifice higher optical correction of chromatic aberration found in apochromat objectives for the enhanced image brightness displayed by higher numerical aperture fluorite

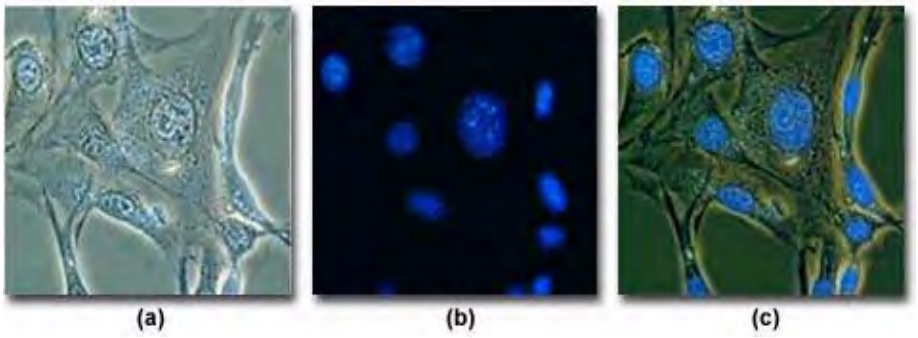

FIGURE 15.3: Combined use of phase contrast and fluorescence illumination

objectives with lesser correction. Use as high a numerical aperture condenser as possible with transmitted light fluorescence to avoid light loss and the accompanying long exposure times. Also when using a substage mirror on older microscopes, purchase a mirror that has an aluminized surface instead of a silvered mirror (silver will reflect ultraviolet light poorly). Often, an oil immersion darkfield condenser may be substituted for standard brightfield condensers for transmitted fluorescence applications. When using immersion oil, apply a non-fluorescent oil between the top lens of the condenser and underside of the microscope slide and between the objective front lens and the coverslip. Oils of this type are readily available from a number of commercial manufacturers.

Photobleaching, or dye photolysis, rapidly degrades fluorescent probes used to stain specimens and should be minimized by exposing the preparation to the lowest illumination levels as is possible. This effect is caused primarily by the photodynamic interaction between the fluorochrome and oxygen, which involves promoting the dye molecule from the singlet ground state to the relatively long-lived triplet excited state by a process termed intersystem crossing. Once the chromophore has been elevated to an excited state, it becomes more chemically reactive and may then participate in irreversible chemical reactions including decomposition, polymerization, oxidation (primarily by singlet oxygen) or reaction with another molecule. Reaction with oxygen will usually cause bleaching of the chromophore, depending upon the intracellular singlet oxygen concentration and the proximity of the chromophore to other internal cellular components such as proteins, lipids, or small molecules. Calculations indicate that singlet oxygen can produce chromophore photolysis over a distance exceeding 500 angstroms.

To minimize the effects of photobleaching, fluorescence microscopy can be combined with other techniques that are non-destructive to the fluorochromes, such as differential interference contrast (DIC), Hoffman modulation contrast (HMC), transmitted darkfield illumination, and phase contrast. The idea is to locate the specific area of interest in a specimen using the non-destructive contrast enhancing technique then, without relocating the specimen, switch the microscope to fluorescence mode. The results of a typical experiment of this type are illustrated in Figures 15.3 and 15.4. Figure 15.3(a) illustrates 3T3 fibroblasts in monolayer tissue culture imaged using phase contrast optics. The cell line was established from a National Institutes of Health line of Swiss mouse embryo cells, which are highly contact inhibited and useful for studies involving sarcoma virus formation and leukemia virus propagation. The photomicrograph in Figure 15.3(b) shows the same viewfield, but this time imaged using fluorescence illumination (a mercury vapor lamp and an Olympus WU filter cube) with cells stained by the fluorochrome 4',6-diamidino-2-phenylindole (DAPI),

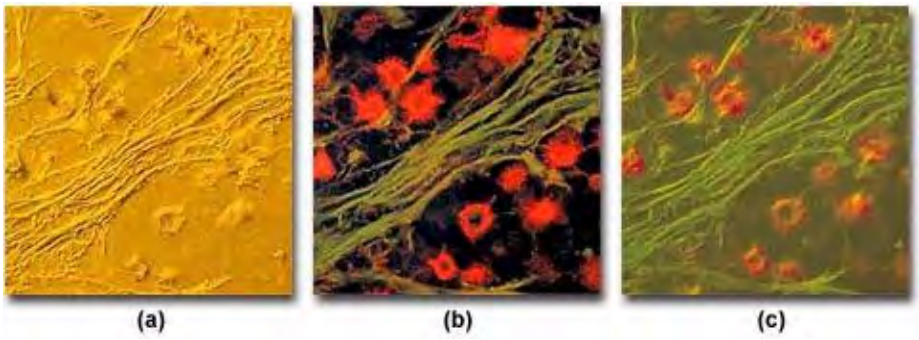

FIGURE 15.4: Combined use of DIC and fluorescence illumination

a nucleic acid specific dye with an emission maximum at 461 nanometers, which is used to selectively stain nuclei and chromatin. Figure 15.3(c) illustrates the two techniques used in combination to produce a beautiful photomicrograph of fluorescent-stained 3T3 cellular nuclei superimposed on a phase contrast image of the fibroblast cell membranes and internal organelles. This image was recorded with a specialized fluorite objective designed with phase rings to permit simultaneous observation of both fluorescence and phase contrast with the same objective.

Another example of combined techniques, this time using differential interference contrast (DIC), is presented in Figure 15.4. Illustrated in Figure 15.4(a) is a thin section of cat brain tissue infected with cryptococcus and imaged using DIC optics and a full-wave retardation plate. Note the pseudo three-dimensional appearance of the photomicrograph. Figure 15.4(b) shows the same viewfield, but imaged with fluorescence illumination and an Olympus WIB filter cube. The cells in Figure 15.4(b) were stained with a combination of fluorescein-5-isothiocyanate (FITC) and Congo red (emission wavelength maxima of 520 and 614 nanometers, respectively). The two techniques are used in combination to produce Figure 15.4(c), which illustrates the infected cat brain tissue in both fluorescence and DIC illumination.

The rate of photobleaching is dependent upon several factors, including the chemical reactivity of the chromophore, the intracellular chemical environment, and the intensity and wavelength of the excitation light. Some fluorescent dyes are readily susceptible to photobleaching while others are relatively insensitive and are stable for much longer periods. In many instances, the specimen may recover from the effects of photobleaching, particularly if it is kept cool and in a dark environment. Photobleaching should be distinguished from another fluorescence artifact termed quenching, which occurs by reduction (or in some cases, enhancement) of fluorescence intensity by competing processes such as temperature, high oxygen concentrations, and molecular aggregation in the presence of salts or halogen compounds. Sometimes quenching results from the transfer of energy to other acceptor molecules residing physically close to the excited fluorochromes, a phenomenon known as resonance energy transfer. This particular phenomenon has become the basis for a newer technique of measuring distances far below the lateral resolution of the light microscope. Impurities in the chromophore may also reduce fluorescence intensity either by photobleaching or quenching.

Photobleaching can be minimized by reducing exposure times (as discussed above) or by lowering the excitation energy (lamp intensity), however these remedies are accompanied by the undesirable effect of reducing the chromophore fluorescence emission energy.

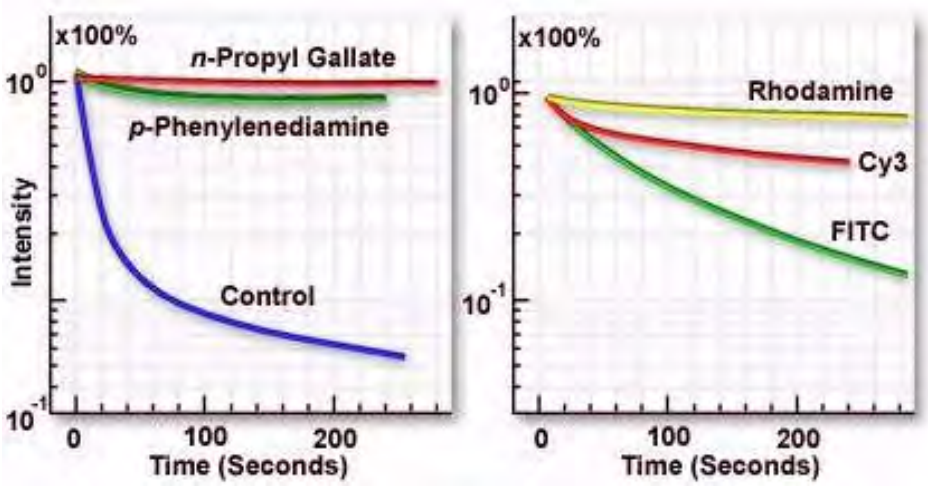

FIGURE 15.5: Inhibition of photobleaching and specimen fading

Neutral density filters can be placed in the light path before the light reaches the excitation filter, thus diminishing the excitation light intensity and reducing fading effects during specimen observation. Many fluorescence microscopes are equipped with a shutter system coupled to neutral density filters that allow excitation light to be reduced in intensity during observation and specimen manipulation, but enable the microscopist to easily switch to full-power illumination for photomicrography. It is also helpful, where possible, to deoxygenate specimens (but not living cells or tissues) and to use specific antifade reagents such as n-propylgallate and other inhibitors, which are commercially available. Chemicals that are capable of quenching singlet oxygen can also be employed to reduce the effects of photobleaching. Examples are 2-mercaptoethylamine, 1,4-diazabicyclo-2,2,2-octane (DABCO), diphenylisobenzofuran, p-phenylenediamine, and the amino acid histidine. Fading effects can also be reduced, in some instances, by changing the pH concentration of the mounting medium.

Figure 15.5(a) illustrates inhibition of the rate of fluorescence fading by several commercially available antifade reagents. The blue curve shows the rapid decline in fluorescence intensity with an untreated specimen, while the green and red curves demonstrate reduction of the fading rate by two antifade reagents of slightly differing efficiency. The specimen is marsupial kidney tissue culture cells (PtK2) stained with either fluorescein-5-isothiocyanate (FITC) or rhodamine phalloidin (both dyes have similar fading properties). Antifade reagents were p-phenylenediamine (green curve) or n-propyl gallate (red curve). Specimen secondary fluorescence fading rates usually differ depending upon the fluorochrome in use, even with observation under identical conditions. The best results can be obtained by selecting a fluorochrome with the lowest fading speed from those available for a particular application. This concept is illustrated in Figure 15.5(b), which compares the difference in marsupial kidney cell fading speed for three fluorochromes: rhodamine (yellow curve), the cyanine dye Cy3 (red curve), and FITC (green curve). Rhodamine, a ubiquitous dye with many applications, displays a very slow fading rate (Figure 15.5(b); yellow curve) under these conditions and is the best fluorochrome for photomicrography using this system.

To further minimize fading, it is advisable to conduct initial observations in one field

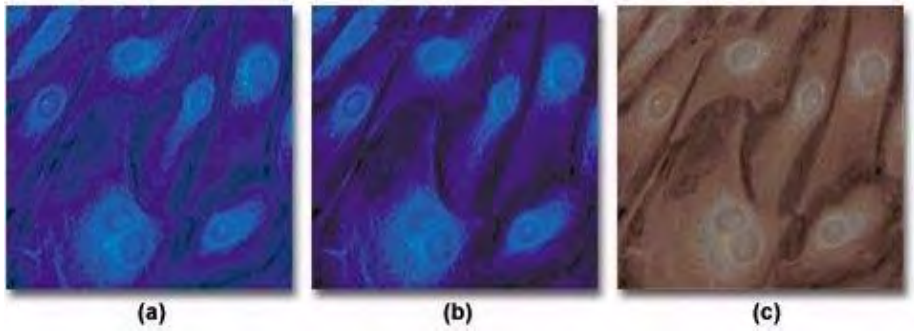

FIGURE 15.6: Filter error in fluorescence photomicrography

within the specimen and then to quickly move to a "fresh" field just prior to taking the exposure. This practice may help to circumvent bleaching and/or fading effects. It is also helpful to do both observation and photomicrography in a partially darkened room environment. Although chemical methods and careful microscopy can reduce photobleaching, the most effective remedy is to increase detection sensitivity (coupled with reduced excitation energy) using a low-light level CCD digital camera designed specifically for fluorescence microscopy.

The occurrence of photobleaching has led to a technique known as FRAP, which is an acronym for Fluorescence Recovery After Photobleaching. This technique is based upon bleaching by short laser bursts and subsequent observation of the recovery of fluorescence caused by the diffusion of fluorochromes into the bleached area.

Barrier filters are designed to absorb specific wavelengths of excitation radiation that are reflected from, or transmitted by, the specimen and to transmit only the chosen visible light fluorescence. The cutoff wavelength range of the barrier filter is critical, because in many instances it must be able to transmit visible wavelengths that are not far in value from the excitation light used to illuminate the specimen. Because film is very sensitive to ultraviolet and visible wavelengths in the 380-450 nanometer region, it is particularly important that the barrier filter block all unwanted wavelengths in this range. To ensure removal of shorter wavelengths, additional ultraviolet blocking filters, such as the Kodak Wratten filter numbers 2A, 2B or 2E, should be added to the optical pathway. All of these filters completely absorb ultraviolet light, but have a slight difference in their absorption of lower wavelength visible blue light. Supplementary ultraviolet filters should be placed before the main barrier filter in the light path in order to block radiation that might induce autofluorescence in the main barrier filter, especially if this filter is yellow, orange, or red in color. If the barrier filter cuts the spectrum at too long a wavelength, specimen fluorescence color will be affected and the intensity of the image may be compromised, especially when only the long-wavelength portions of transmitted fluorescence are passed by the filter.

Color balance errors in fluorescence photomicrography may have a number of origins. The photomicrographs presented in Figure 15.6 illustrate several problems that arise with color degradation from autofluorescence and improper filtration when imaging specimens under fluorescence illumination. The specimen is a monolayer of fibroblast cells grown in tissue culture and stained with 7-amino-4-methylcoumarin-3-acetic acid (AMCA), a bright ultraviolet-excitable dye conjugate with an emission wavelength maximum of 445 nanometers (in the short-wavelength blue region). The optimal excitation wavelength of AMCA is 345 nanometers, which requires an excitation filter that passes a significant

amount of ultraviolet light. Under proper conditions of illumination and filtration, the stained specimen appears with nuclei and cytoplasmic components stained a rich and deep blue color (imaged with an Olympus WU filter cube), as illustrated in Figure 15.6(b). When a barrier filter that passes too much ultraviolet light is used, a blue cast and background color are often present in photomicrographs of the specimen (shown in Figure 15.6(a)), and secondary fluorescence colors are degraded. Placing an auxiliary ultraviolet and/or short blue wavelength barrier filter somewhere in the microscope optical pathway is the method of choice for alleviating this problem.

Fluorochromes used to stain specimens often produce an undesirable amount of short wavelength blue autofluorescence, particularly when staining tissue sections. As mentioned above, this autofluorescence must be absorbed by the barrier filter to avoid degradation of secondary fluorescence emission produced by the fluorochrome-tagged specimen. Kodak Wratten filters 2A and 2E, which absorb short-wavelength blue radiation, are suitable for use in this application. The microscope manufacturers and aftermarket suppliers also offer filters useful in fine-tuning the cutoff range of barrier filters.

Intrinsic autofluorescence in mounting media can also cause the type of problems associated with the photomicrograph illustrated in Figure 15.6(a). Many of the popular permanent mounting media formulations exhibit autofluorescence as an undesirable side effect, and should not be used for quantitative fluorescence work. Instead, temporary mounts made with pure glycerin, glycerin-water mixtures, or fluorescence-free immersion oils should be utilized to prepare specimens. The microscope manufacturers offer specialized objectives that are optically corrected for specimen observation in glycerol. Autofluorescence produced by mounting media is usually pale blue or green in color and will lead to degradation of secondary fluorescence by the specimen. If the barrier filter does not remove superfluous autofluorescence generated by mounting media, sometimes Kodak Wratten color compensating filters can be added to the pathway to alleviate this problem. The pale blue color generated by most media can be removed by using a filter such as the CC20Y (yellow), and pale green fluorescence can be neutralized with a CC20M (magenta) filter. Use of higher density filters (CC30 and above) will often lead to absorption of secondary fluorescence.

Autofluorescence exhibited by cells and tissues in culture can often limit the ability to detect fluorescent probes in stained and fixed preparations. The extent of autofluorescence displayed by fixed tissues will often vary depending upon specimen preparation and the experimental conditions used to detect fluorescence. Flavin coenzymes (FAD and FMN) and reduced pyridine nucleotides (NADH) are the principal sources of autofluorescence in mammalian cells. Secondary fluorescence in fluorochrome-stained plant cells is often masked by autofluorescence from lignins (green autofluorescence) and porphyrins such as chlorophyll (red autofluorescence). This problem can sometimes be overcome with fixed cells and tissues by thorough washing with a 0.1 percent solution of sodium borohydride in phosphate-buffered saline for 30 minutes prior to staining.

When excitation and/or emission filters are not matched to the wavelength absorption and emission spectrum of chromophores used to stain specimens, then secondary fluorescence is usually compromised, as illustrated in Figure 15.6(c). In this example, an improper emission filter having too short of a wavelength cutoff is used to pass secondary fluorescence emitted by the specimen. Because a majority of this fluorescence is centered in the blue region of the spectrum (at 455 nanometers), only muddy reddish long wavelength color tones are passed by the filter. To correct the problem, a new barrier filter should be chosen. Overexposure of color film, along with reciprocity errors, can also cause dramatic

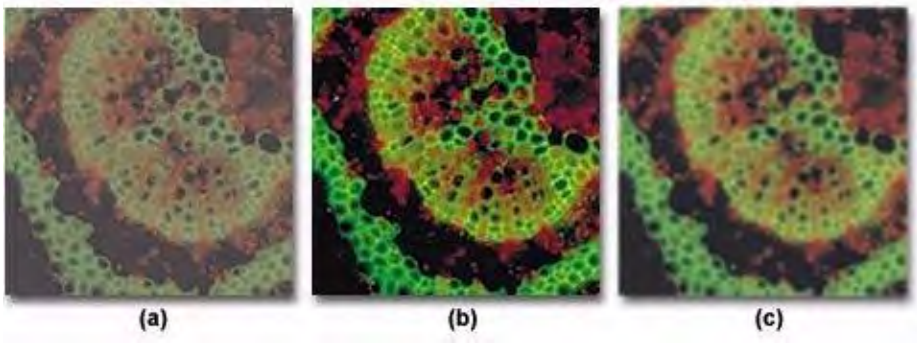

FIGURE 15.7: Contrast error in fluorescence photomicrography

color shifts of secondary fluorescence in final images.

Contrast errors often arise in fluorescence microscopy when the microscope optical train is mis-configured or the wrong filter combinations are utilized. Several of these errors are presented in Figure 15.7, which illustrates poor contrast in secondary fluorescence images caused by improper excitation filter choice and fluorescent immersion oil. The specimen is a cross section of a Japanese maple leaf petiole undergoing autofluorescence and imaged with a 10x fluorite objective using an Olympus WBV filter cube. Under ideal conditions, the image presented in Figure 15.7(b) would be obtained. However, when the excitation filter has too great a bandwidth (allowing unwanted wavelengths to pass), the image loses contrast resulting in the photomicrograph illustrated in Figure 15.7(a). Choosing the correct filter combination requires knowledge of the spectral values of excitation and emission of the chromophore(s) used to stain the specimen. In this case, the excitation filter passes wavelengths up to 550 nanometers, interfering with green secondary fluorescence emitted by the specimen and severely compromising image contrast.

Controlling specimen contrast in fluorescence microscopy requires that all optical components of the microscope be free of autofluorescence, and that they should not scatter light to a significant degree. This includes internal glass lens elements, mirrors, filters, and s. Objectives should provide high image quality while transmitting light with high efficiency down into the near ultraviolet range. Filters must transmit desired wavelengths while blocking others that might interfere with observation of secondary fluorescence. Because excitation light is of far greater intensity than specimen fluorescence, the task of completely removing this light from the fluorescence image is not very easy and requires careful selection of filter combinations that provide a narrow range of excitation wavelengths (usually between 10 and 75 nanometers in bandwidth). When using high numerical aperture immersion objectives, it is critical that the immersion oil be free of contaminants that might exhibit fluorescence. Figure 15.7(c) illustrates an example of poor contrast generated by autofluorescence in immersion oil. Although the use of immersion oil helps to improve image brightness, partially by eliminating the loss of errant light caused by reflection from surfaces (in particular, the coverslip and glass lens elements), fluorescing contaminants that induce autofluorescence mix unwanted wavelengths with secondary fluorescence from the specimen. This has the unfortunate consequence of brightening the background while simultaneously reducing image contrast, both of which are undesirable.

Artifacts in specimen preparation will also produce contrast problems in fluorescence microscopy. Early pioneers in fluorescence often utilized non-specific fluorochromes that

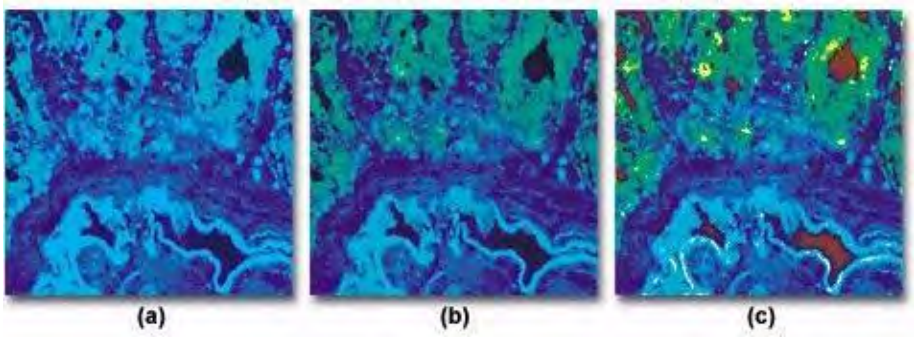

FIGURE 15.8: Autofluorescence and non–specific fluorescence errors in fluorescence photomicrography

produced very bright images due to the fact that the dye molecules were randomly scattered throughout the specimen. Newer fluorescent techniques with improved and highly specific fluorochromes have resulted in specimens exhibiting stained target areas having substantially weaker fluorescence because much less dye is bonded. These newer methods require more careful specimen preparation to avoid unwanted fluorescence artifacts. It is often helpful to pre-stain portions of the specimen with non-fluorescing dyes that compete for binding sites to aid in fluorochrome selectivity. Specimens should be washed thoroughly to remove unbound fluorochrome before placement on acid-cleaned microscope slides made with non-fluorescent glass. Optimization of the fluorochrome environment by addition of chemical additives to minimize photobleaching helps to reduce or eliminate specimen fading. In addition, careful selection of the mounting medium chemical composition and pH is important to obtain the best image from secondary fluorescence. Coverslips and immersion oil should also be non-fluorescent, as discussed above.

Autofluorescence and/or non-specific fluorescence can occur as a result of the inherent properties of the specimen or through errors in staining. Typical errors of this type are illustrated in Figure 15.8(a), which shows a thin section of rat colon tissue stained with a mixture of fluorescein-5-isothiocyanate (FITC) and 4',6-diamidino-2-phenylindole (DAPI). The overall blue cast in the photomicrograph is due to a combination of autofluorescence and non-specific fluorescence due to overstaining with the DAPI fluorochrome. Proper staining with both dyes, followed by thorough washing of the specimen results in the photomicrograph presented in Figure 15.8(b). Errors similar to that illustrated in Figure 15.8(a) are also caused by using too broad an excitation bandwidth, a reversible mistake that can be corrected by use of filters with narrower bandwidths. Alternatively, a combination of excitation filters can be employed to selectively produce a specific set of wavelengths, or barrier filters can be adjusted to pass only longer wavelengths. Figure 15.8(c) illustrates the rat colon thin section when stained properly but now with a light red background caused by lack of a red suppression filter in the optical pathway. This error can be corrected by placing the proper suppression filter in the optical path.

Fluorescence photomicrography also suffers from common problems encountered with other forms of optical microscopy and photomicrography. These include focus errors caused by improper adjustment of the focal distance between the optics and film plane, microscope stand vibration, contamination by dirt and debris, underexposure, overexposure, color balance errors, specular reflections (common with long exposures and overhead room lighting), vignetting, and optical microscope mis-alignment. Examples of these errors are presented

ISO Number	Light Sensitivity	Resolution	Grain Size	Exposure Tolerance
25–50	Low	High	Fine	Wide
100–200	Medium	Medium	Medium	Medium
400+	High	Low	Coarse	Low

TABLE 15.2: Film Properties

in our section entitled Fluorescence Photomicrography Errors with Color Transparency Film in the Photomicrography section of the Molecular Expressions Microscopy Primer.

15.1 Cameras and Film for Fluorescence Photomicrography

Improvements in film technology have produced increased film speeds and resolution improvements, but there are no color films currently available uniquely suited to fluorescence photomicrography. The specific properties of individual color films, including the characteristic curves for individual emulsion layers, properties of coupled dyes, and the spectral response to light used for fluorescence excitation and emission often vary dramatically from film to film and are sometimes difficult to control and reproduce. These problems lead to difficulty in maintaining accurate color rendering and exposure with color photomicrography using film.

Exposure measurement in fluorescence photomicrography is complicated by the fact that the brightness range within a fluorescent specimen is usually much greater than can be accurately recorded on film. Overexposure of the highlights will result in loss of fine detail and color saturation, while underexposure produces very dark images that do not reveal features hidden in shadowed areas. The background, which is usually very dark or black, is not as critical to either over- or underexposure. Three primary methods are utilized to determine exposure when using fluorescence: brightness measurement with a CCD, photodiode, or photomultiplier, continuous measurement during exposure (photomultiplier), and the least desirable method, trial and error. Modern photomicrography systems designed for fluorescence are equipped with the ability to gauge illumination intensity and calculate exposure times based on this reading. For routine fluorescence photomicrography, some cameras have a silicon blue detector cell for determining exposure duration, while others have a photomultiplier metering detector for measuring extremely faint specimens.

It is important to consider several factors in choosing a detector system for fluorescence photomicrography. These include the detector's noise level and the signal-to-noise ratio for the image, spatial and temporal resolution, geometric distortion, linearity, and spectral sensitivity. In determining proper exposure for fluorescing specimens, it is best to use a camera with a CCD or photomultiplier metering system capable of accurate low-light measurement. Spot metering capability is valuable for measuring the area actually fluorescing and not the unwanted metering of the usual dark background surround the fluorescing material. Another technique involves the use of the exposure adjustment control to reduce exposure times that would otherwise be unduly lengthened by measuring the dark background of the field of view. In this respect, Olympus and Nikon offer camera systems that have built-in algorithms for reducing exposure if the camera is set for fluorescence mode. When light is scant (usually most of the time with fluorescence), set the trinocular prism to send all the light up to the film plane to reduce exposure time.

Ideally, a spot meter should be included in the photomicrography system to aid in determining exposure when only a few bright objects are visible on an otherwise dark background. For integrated light measurements made over the entire viewfield without a spot meter, the exposure time should be cut in half or to a fourth of the metered reading (for scattered fluorescing objects on a dark background), much like the situation with darkfield microscopy. If the spot meter light sensor is in a fixed position in the middle of the viewfield, the specimen must first be moved to the center of the field to obtain a suitable area for exposure measurement, then relocated to compose the photomicrograph. High-end camera systems allow translation of the spot meter sensor to enable the microscopist to determine photomicrograph composition prior to exposure measurement. After positioning of the specimen for photomicrography, the spot meter sensor can then be moved to the brightest area in the viewfield for exposure measurement without disturbing the specimen. When using a spot meter, make certain the fluorescent object is large enough to fill the spot and record an accurate exposure reading.

Some photomicrography camera systems provide a permanent assembly that directs a portion of the light to a photometer, which allows light measurement during the actual exposure in order to compensate for fading. This is a convenient method for adjusting exposure times on the fly to avoid photobleaching artifacts, but it has the disadvantage of reducing light intensity directed to the film, necessitating a longer exposure. More advanced computer-aided camera systems are able to compensate for reciprocity failure and fading through a pre-programmed lookup table conveniently stored in the metering system's memory. Automatic correction for reciprocity failure by camera system computers operate by applying the following equation to exposure calculations:

$$T_c = T_m^p$$

where $\mathrm{T_c}$ is the corrected exposure time, $\mathrm{T_m}$ is the metered (uncorrected) time, and p is a constant determined from reciprocity values for individual films housed in the system's lookup table. This system is limited by the amount and type of reciprocity data for films that are added to the lookup table during initial programming of the metering system.

Without an integral exposure metering system, determination of exposure time must be made by trail and error. This method involves making a series of trial exposures at a variety of exposure times, stepped through increments of one-half to a full f-stop (bracketing). After processing the film, the exposure that produces the best result is carefully noted and provides the basis for further photomicrography using the identical microscope configuration. Changes to specimen illumination or microscope setup will necessitate another series of exposure brackets to determine the new optimum exposure time. If only the objective magnification is changed, new exposure times can be calculated from previously recorded bracket data. Many photomicrographers doing fluorescence microscopy bracket their exposures, both over and under by three or more intervals, to make certain that they will secure a correct exposure at one of the settings. Keeping good written records of exposure and associated equipment data can reduce or eliminate the need for future bracketing. When determining exposure using the trial and error method, it is wise to continuously monitor the microscope lamp output for deviations in illumination that occur as the lamp ages. Microscopists using this method of exposure determination often rely on SLR cameras to capture images with fluorescence illumination. With these cameras, movement of the shutter and viewfinder mirror during exposure may cause vibrations that lead to unsharp images. This problem can usually be circumvented by using a remote shutter switch

and/or raising the mirror prior making the exposure. In some cameras, operation of the self-timer releases the mirror, which allows time for vibrations to cease before the exposure is made.

Microscopes equipped specifically for fluorescence illumination often have an illuminated reticle in the system or focusing telescope, which allows the microscopist to visualize a photomicrography grating superimposed over faintly visible specimens positioned against a very dark background. Both Olympus and Nikon provide reticles in their high-end microscopes that offer a choice of crosshair and film frame colors with which to view the specimen. Microscopists can choose between a red or yellow illuminated reticle. The red reticle has the advantage of maintaining the dark adaptation of the observer's eye and provides excellent contrast when viewed over blue and green secondary fluorescence. For red fluorescence and when simultaneous phase contrast or DIC are used, the yellow reticle should be selected to maximize contrast. Some manufacturers offer a focusing telescope with illuminated framing reticle that attaches to the automatic camera housing and allows viewing of the film frame dimensions over the dark background field.

When choosing film for fluorescence photomicrography, the film speed (ASA or ISO rating) is a variable that should be carefully considered. The higher the ISO rating, other things being equal, the less the amount of light necessary to register a satisfactory image on the film. Illumination sources used in fluorescence microscopy require daylight-balanced film emulsions to accurately render specimen secondary fluorescence colors. Most major film manufacturers offer a wide spectrum of daylight films at a variety of ISO ratings in both transparency and color negative formats. Kodak daylight Ektachrome with an ISO of 200 or 400 or Kodachrome 200, both in 35 millimeter size, are positive transparency films that display adequate speed, good color rendition and acceptable resolution. Fujichrome Provia is offered in 400 and 1600 ISO ratings, and is an excellent transparency film in terms of color saturation and resolution. Other manufacturers make comparable transparency films, but we suggest avoiding the use of color negative film if at all possible.

For black & white film, Kodak offers T-Max 400, an excellent fine to medium grain film that is one of the best for fluorescence applications. Several black & white films are available that can be processed with standard color negative chemicals (C41). These include Kodak T-Max 400CN, Kodak Advantix, and Ilford XP-2 Super, all of which are offered in ISO ratings of 400. Keep in mind that faster films allow for much shorter exposure times at the expense of increased grain size. Table 15.2 lists basic film properties for reference.

Contrast, one of the greatest concerns in fluorescence photomicrography, depends not only on microscope configuration, but also upon the physical characteristics of the film chosen, the development process, exposure details, and the specimen itself with respect to the efficiency of staining by the fluorochrome and photobleaching or fading. Color transparency films can be underexposed by one or several f-stops (a bonus when considering reciprocity and fading), then push processed by extending processing time in the first developer to increase contrast and color saturation. Many black & white films can produce variations in contrast that are dependent upon the developer mixing conditions and processing time. Resolution of film in fluorescence photomicrography is determined principally by the optical parameters of the microscope (primarily the objective numerical aperture) and how well it is configured, but is also somewhat dependent upon film characteristics and development methods. In practice however, the film resolution only becomes a factor when the microscope is not performing optimally or the ISO speed is so high that grain becomes a factor.

FIGURE 15.9: Digital camera for fluorescence photomicrography

Recent advances in digital imaging technology have revolutionized capture of photomicrographs using charge-coupled devices (CCDs). When imaging multiply-stained fluorescence specimens, digital cameras provide an excellent solution and are rapidly becoming the medium of choice for many photomicrographers. The price of three-chip integrating color CCD cameras has dropped to an affordable range and, when coupled to a frame-grabber or digital video card and computer, offer an excellent method of collecting, digitizing, editing, and storing fluorescence images.

The weak fluorescence displayed by many specimens necessitates high performance in CCD detector specifications. Currently, the best choice is a back-thinned frame or interline transfer device, which is equipped with heat sinks and/or external reservoirs for cooling. Many of these cameras have a quantum efficiency approaching or exceeding 90 percent and permit the sequential acquisition of several images before readout. Image acquisition cycles run from one to five seconds, depending on the readout rate, video capture parameters, and CCD resolution. A typical CCD camera matching these specifications is the Optronics MagnaFire digital imaging camera system designed for scientific applications. This camera has a SONY ICX085AL 2/3-inch interline transfer CCD with an array size of 1300 x 1030 and a (square) pixel size of 6.7 microns. Camera performance is enhanced with a 60 dB dynamic range and signal-to-noise ratio, a file bit depth of 24, 32, or 48 bit color, a dark current of 4 electrons per pixel/second with a 16,000 electron well depth, and sealed gas Peltier CCD cooling. Color image formation is via multiple dichroic optical glass color filters. Optronics and other manufacturers also offer a wide spectrum of digital cameras (a typical CCD camera is illustrated in Figure 15.9) suited to almost every need in both fluorescence and routine optical microscopy.

The following points summarize important aspects of fluorescence photomicrography.

- Use high numerical aperture objectives equipped with glass or quartz lenses that are transparent to near ultraviolet light. Also use the lowest magnification projection lens possible to limit the total magnification.

- Reflected light fluorescence is preferred to transmitted light fluorescence. If it is not possible to configure the microscope for reflected light, use a transmitted light darkfield condenser.

- Optimize specimen contrast by careful choice of film parameters, proper microscope configuration, and by carefully matching chromophore excitation and secondary fluorescence properties to the proper excitation and barrier filters.
- Remove the trinocular prism from the light path to allow 100 percent of the light to reach the film plane during exposure. Also use 35 millimeter film and avoid larger film formats.
- Choose daylight balanced transparency films for the best rendition of specimen colors, resolution, and contrast. Push process transparency films for enhanced contrast and color saturation.
- The light source must provide high-intensity radiation in very narrow ranges of the spectrum, typically between 10 and 50 nanometers. The best choices are xenon and mercury vapor lamps or lasers tuned to specific wavelengths.
- The microscope optical train, including lenses, mirrors, filters, s, immersion media, microscope slides, and coverslips, should be free of autofluorescing components.
- When not viewing or photographing fluorescence specimens, block the excitation light using the filter slider or shutter in the illuminator to avoid specimen damage by photobleaching.
- Always provide a heat filter between the illuminator and fluorescence filters, which may be damaged by excess heat.
- Monitor the lamp for signs of flicker and replace when illumination intensity becomes uneven. Keep the lamp and vertical illuminator adjusted for proper Köhler illumination.
- Prepare specimens carefully and remove excess chromophores by thorough washing after staining.

In conclusion, the field of fluorescence microscopy is rapidly expanding in many medical and biological research laboratories. The mainstream of fluorescence microscopy has undergone an almost total shift from utilizing transmitted light to incident light, accompanied by the introduction of many new and different fluorochromes. This has been an impetus for spurring many new and varied fluorescence microscopy applications.

Chapter 16

Multiphoton Fluorescence Microscopy

16.1 Introduction

Multiphoton fluorescence microscopy is a powerful research tool that combines the advanced optical techniques of laser scanning microscopy with long wavelength multiphoton fluorescence excitation to capture high-resolution, three-dimensional images of specimens tagged with highly specific fluorophores.

The methodology is particularly useful to cell biologists who endeavor to study dynamic processes in living cells and tissues without inflicting significant, and often lethal, damage to the specimen. Although classical widefield fluorescence microscopy can often provide submicron resolution of biochemical events in living systems, the technique is limited in sensitivity and spatial resolution by background noise caused by secondary fluorescence throughout areas situated above and below the focal plane.

Excitation in multiphoton microscopy occurs only at the focal point of a diffraction-limited microscope, providing the ability to optically section thick biological specimens in order to obtain three-dimensional resolution. Individual optical sections are acquired by raster scanning the specimen in the x-y plane, and a full three-dimensional image is composed by serially scanning the specimen at sequential z positions. Because the position of the focal point can be accurately determined and controlled, multiphoton fluorescence is useful for probing selected regions beneath the specimen surface. The highly localized excitation energy serves to minimize photobleaching of fluorophores attached to the specimen and reduces photodamage, which increases cell viability and the subsequent duration of experiments that investigate the properties of living cells. In addition, the application of near-infrared excitation wavelengths permit deeper penetration into biological materials and reduce the high degree of light scattering that is observed at shorter wavelengths. These advantages enable researchers to conduct experiments on thick living tissue samples, such as brain slices and developing embryos that would be difficult, if not impossible, to image with other microscopy techniques.

Illustrated in Figure 16.1 is a typical configuration used in multiphoton fluorescence microscopy experiments. The microscope is an inverted-style instrument designed to observe living cells in tissue culture and thicker biological specimens bathed in saline solution. For routine non-fluorescence observation, a diascopic lamphouse is positioned above the stage to enable visualization of specimens through conventional techniques such as brightfield, dif-

FIGURE 16.1: Multiphoton excitation fluorescence microscope configuration

ferential interference contrast, phase contrast, and Hoffman modulation contrast. Although not useful in multiphoton applications, a 35-millimeter camera body is attached to the port at the front base of the microscope depicted in Figure 16.1 to capture images taken with conventional illumination. To the right of the microscopy body is a Ti(titanium):Sapphire mode-locked pulsed laser system that is one of the preferred sources for multiphoton excitation due to the high peak intensity but low average power. Control of the laser is accomplished through electronic units situated on top of the laser cabinet, which is joined to a microscope port through either fiber coupling with an optical waveguide or direct coupling with strategically placed relay mirrors. A filtered photomultiplier detection system is attached to another port at the microscope base, as is an x-y raster scanning unit that can rapidly deflect the focused laser beam across the objective field. Digital images collected by the microscope are processed and analyzed by an accompanying computer workstation that can assemble three-dimensional reconstructions from optical sections.

Traditional widefield fluorescence microscopy is plagued by secondary fluorescence occurring away from the focal region, which contributes to flair and a high background noise signal, often obscuring important specimen details. Confocal microscopy circumvents this problem, to a large degree, by rejecting out-of-focus background fluorescence through the use of pinhole apertures, which produce thin (less than a micron) unblurred optical sections from deep within thick specimens. The introduction of multiphoton fluorescence microscopy provides a new alternative to confocal microscopy through selective excitation coupled to a broader range of detection choices. Unlike conventional confocal microscopes, the microscope presented in Figure 16.1 does not require a pinhole near the detector to attain three-dimensional discrimination, dramatically increasing the efficiency of emitted fluorescence signals. In the past, the high cost and complexity of pulsed laser systems required for multiphoton excitation have limited use of the technique, but recently-introduced turnkey lasers and commercial multiphoton systems have made multiphoton fluorescence

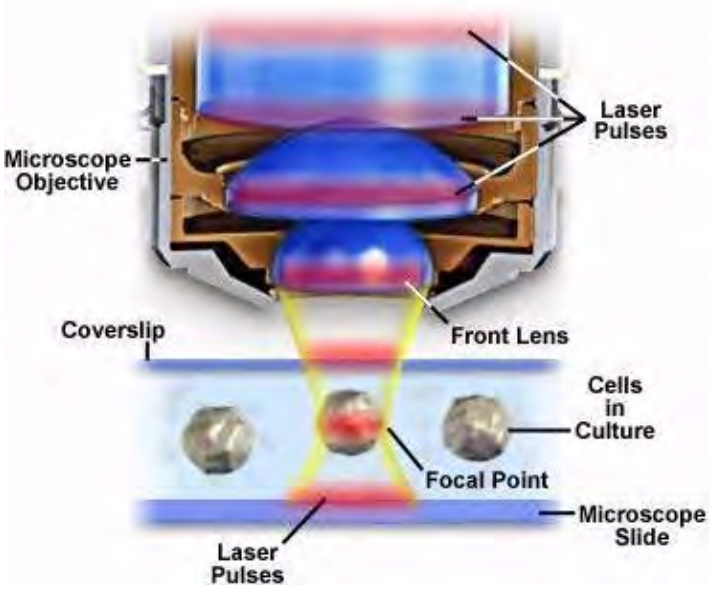

FIGURE 16.2: Multiphoton excitation fluorescence microscopy

microscopy the method of choice for many investigations.

16.2 Two–Photon and Three–Photon Excitation

The basic principles of multiphoton excitation were first described by Maria Göppert–Mayer while conducting her doctoral dissertation research over 70 years ago, but the hypothesis could not be confirmed until the invention of pulsed ruby lasers, about 30 years later. At high photon densities, two photons can be simultaneously absorbed (mediated by a virtual state) by combining their energies to provoke the electronic transition of a fluorophore to the excited state. Because the energy of a photon is inversely proportional to its wavelength, the two photons should have wavelengths about twice that required for single-photon excitation. As an example, two photons having a wavelength of 640 nanometers (red light) can combine to excite an ultraviolet-absorbing fluorophore in the 320-nanometer region (ultraviolet), which will result in secondary fluorescence emission of longer (blue or green) wavelengths. This unique application means that longer wavelengths, extending into the infrared region, can be conveniently utilized to excite chromophores in a single quantum event, which subsequently emit secondary radiation at lower wavelengths.

The requirement of two photons for each excitation event necessitates a rate constant that depends upon the square of the excitation intensity. Although the photons do not have to be of identical wavelength to induce multiphoton excitation, most experimental systems are designed with a single laser source, so the two photons are usually members of a defined population having a narrow wavelength distribution. Unlike the case for single-photon absorption, the probability that a given fluorophore will simultaneously absorb two photons is a function of both the spatial and temporal overlap between the incident photons. Calculations based on the assumption that each fluorophore is exposed to the same laser cross section indicate that photons must arrive within 10(-18) seconds (one attosecond) of each other. The time scale of this overlap period is consistent with the lifetime (10(-17)

seconds or 0.01 femtosecond) of the intermediate virtual state.

High photon densities are necessary in multiphoton fluorescence to ensure a sufficient level of fluorophore excitation. In fact, photon concentration must be approximately a million times that required for an equivalent number of single-photon absorptions. This is accomplished with high-power mode-locked pulsed lasers, which generate a significant amount of power during pulse peaks, but have an average power that is low enough not to damage the specimen. Brief, but intense, pulses emitted by the laser increase the average two-photon absorption probability for a given fluorophore at a constant average incident laser power level. Minimizing the average excitation power level reduces the amount of single photon absorption, which also occurs in the specimen during excitation. It is the single photon excitation events that lead to a majority of the heating and some of the photodamage that occurs during fluorescence experiments.

Typical pulsed laser configurations employ short duty cycles of around 100 femtoseconds (10^{-13} seconds) with a repetition rate of 80 to 100 megahertz for multiphoton fluorescence experiments. This regime permits satisfactory image acquisition without subjecting the specimen to an excessive amount of heat and photodamage. The time scale for each pulse, while often referred to as "ultrashort", is still four to five orders of magnitude longer than the reaction time for two-photon absorption. The population of singlet states in chromophores excited by a two-photon pulse is identical to that obtained during conventional widefield or confocal fluorescence microscopy. Therefore, secondary fluorescence emission after two-photon excitation is indistinguishable from that observed in single-photon experiments. A fluorophore, such as rhodamine, will emit the same broad wavelength range of secondary fluorescence regardless of whether it was excited by a single or two-photon excitation event.

Three-photon excitation is a related non-linear optical absorption event that can occur in a manner similar to two-photon excitation. The difference is that three photons must interact simultaneously with the fluorophore to illicit a transition to the excited singlet state. A benefit of three-photon excitation is that successful absorption requires only a tenfold greater concentration of photons than two-photon absorption, making this technique attractive for some experiments. Three-photon excitation can enhance z-axis resolution to an even greater degree than two-photon absorption. This is due to a smaller cross section for fluorophore excitation caused by the requirement for simultaneous interaction with three individual photons. In practice, a laser emitting infrared light with a wavelength distribution centered at 1050 nanometers is able to excite a fluorophore that absorbs in the ultraviolet region (approximately 350 nanometers, one-third of the excitation wavelength). The same laser can simultaneously excite another fluorophore at half the wavelength (525 nanometers), a useful combination in dual-labeled biological experiments. By utilizing shorter near-infrared wavelengths (down to 720 nanometers), three-photon fluorescence can extend the useful fluorescence imaging range into the deep ultraviolet. Laser wavelengths in the 900 to 700 nanometer range will excite fluorophores that absorb in the 240 to 300 nanometer region, which is virtually inaccessible using conventional microscope optics. The glass used in manufacture of fluorescence objectives has very low transmission for wavelengths below 300 nanometers, but longer wavelength infrared laser radiation can easily pass through to produce three-photon excitation.

Single, dual, and triple photon excitations of a common aromatic amino acid, tryptophan, are schematically illustrated in Figure 16.3. A 4.5 electron volt single photon electronic transition excites tryptophan at 280 nanometers with the subsequent emission

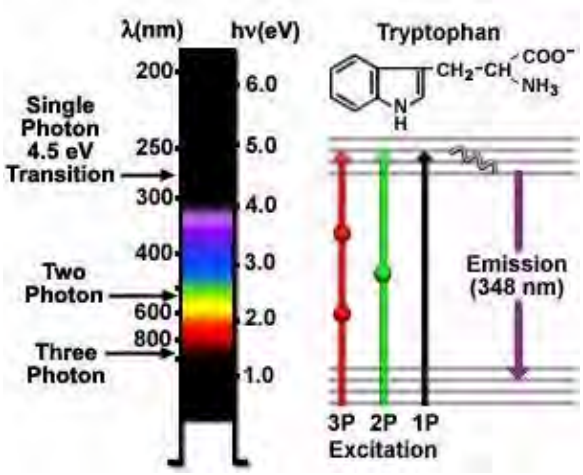

FIGURE 16.3: Tryptophan multiphoton absorption

of secondary fluorescence at 348 nanometers in the ultraviolet region. Excitation by the two-photon mechanism is accomplished with greenish-yellow light centered at 580 nanometers, while three-photon excitation occurs when the amino acid is illuminated with 840-nanometer radiation in the near-infrared region. The transitions are presented in a Jablonski diagram (Figure 16.3), where the virtual state is represented by a sphere for two-photon excitation and by two spheres for three-photon excitation. Tryptophan has much stronger fluorescence with a higher quantum yield than the other aromatic amino acids, and is present only in small quantities in most proteins. These attributes should make multiphoton microscopy an excellent tool for investigations using autofluorescence of tryptophan residues. Even higher order nonlinear phenomena are possible, including four-photon excitation, but these have yet to be applied to biological research.

16.3 Two-Photon Fluorescence Microscopy

The localization of excitation to the region immediately surrounding the focal point in multiphoton microscopy occurs because it is here that the photon density is highest. This advantage arises from the basic physical principle that two-photon absorption by a fluorophore is a function of the square of the excitation intensity. When photons from a pulsed laser source are focused by a high numerical aperture objective, they become more crowded, thus increasing the probability that two or more will interact simultaneously with a single fluorophore. Concentration of photons at the microscope focal point is so critical to multiphoton absorption that this is the only region where appreciable excitation occurs. The concept is presented in Figures 16.2 and 16.4, which illustrate multiphoton excitation on a macroscopic and microscopic level, respectively. Figure 16.2 depicts an exaggerated view of a microscope objective in position to image cultured cells on a microscope slide and coverslip. Red laser pulses traverse the longitudinal axis of the objective and are focused and concentrated onto the cell in the central portion of the figure.

In Figure 16.4, photon crowding and interaction with fluorophores is demonstrated at the microscope focal point. As pulses of red laser light pass through the specimen containing fluorophores (represented as a linear triplet of spheres), the probability of excitation increases as the pulses reach the focal point of the objective. Individual photons are repre-

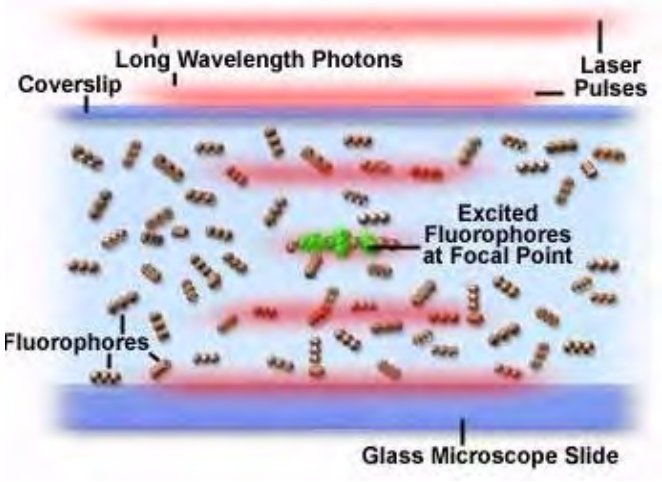

FIGURE 16.4: Fluorophore excitation in multiphoton microscopy

sented as an aggregate segregated into diffuse red lines that define the boundaries of laser pulses. A small group of fluorophore molecules positioned at the center of the focal region in Figure 16.4 have been excited by simultaneous absorption of two photons and are exhibiting green secondary fluorescence. There is nearly a zero probability that chromophores outside the focal plane will absorb two photons, because the photon density is not high enough in this region.

The phenomena of two-photon excitation is possible not only because of the spatial proximity of fluorophores at the microscope focal point, but also because of the temporal overlap of photons contained in sequential laser pulses. As mentioned above, the excitation energy in two-photon absorption occurs in proportion to the square of the photon intensity produced by the laser source. Pulsed laser beam intensity drops as the square of the distance from the focal plane, so the excitation probability of a fluorophore anywhere near the focal region decreases as the fourth power of the fluorophore's distance from the focal plane. The dimensions of the pulsed laser illumination cone are determined by the objective numerical aperture. Thus, the beam intensity decrease away from the focal point is proportional to the diameter of the excitation light cone squared. As the illumination cone expands above and below the focal point, fluorophore excitation probabilities decrease as the fourth power of the cone diameter. For this reason, fluorophore excitation is confined to the immediate region surrounding the focal point, which represents only a very thin optical section of the entire specimen.

Laser pulse durations, which typically range from approximately 100 femtoseconds to 1 picosecond (10^{-13} to 10^{-12} second), are considered ultrashort in macroscopic terms. However, in terms of the time scale for photon absorption events (approximately one thousandth of a femtosecond) the pulses are actually quite long in duration. This limits fluorophore saturation and allows the molecules sufficient time to return to the ground state between pulses before another round of excitation occurs. Pulse repetition rates range from around 80 to 120 megahertz (MHz), which provides high instantaneous peak power for excitation, followed by a dwell time averaging 10 nanoseconds. Because the fluorescence lifetime of a typical fluorophore lasts only a couple of nanoseconds, the population of excited molecules has plenty of time to relax between pulses. The relatively short pulse duty cycle (the pulse duration time divided by the time between pulses) limits the average input laser power to

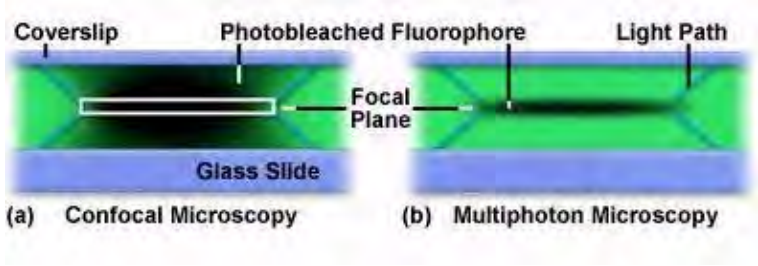

FIGURE 16.5: Excitation photobleaching patterns

less than 10 milliwatts, a value only slightly greater that that routinely employed for laser scanning confocal microscopy.

Limitation of two-photon excitation to the region near the focal plane provides a significant advantage for multiphoton over confocal microscopy. Fluorescence is excited throughout the specimen in confocal microscopy, but secondary fluorescence collected by the detector is restricted to the objective focal plane by the confocal pinhole. This serves to reduce the amount of background noise or fluorescence from other focal planes that add background noise to the data. In contrast, multiphoton microscopy generates fluorescence excitation (and subsequently, fluorescence emission) only at the focal plane, eliminating both the background signal and the necessity of a confocal pinhole. The dramatic difference between excitation modes in confocal and multiphoton microscopy is illustrated in Figure 16.5, which reviews photobleaching profiles for each technique.

Presented in Figure 16.5 are the x-z photobleaching patterns that occur from repeated scanning of a single x-y plane in a formvar polymeric film stained with the fluorophore rhodamine (green stain). On the left (Figure 16.5(a)), is the profile generated by scanning the stained film with a confocal microscope. The white rectangle in the center of the scan represents the focal plane that is passed through the pinhole and imaged by the detector. Diagonal blue lines projecting from the upper and lower corners of the rectangle represent the light path taken by the excitation light beam through the film. As the beam raster scans the film, the fluorescent dye is excited and emits secondary fluorescence. Eventually, photobleaching occurs, which is represented by the dark areas in the focal region. In the film scanned by the confocal microscope (Figure 16.5(a)), the integrated excitation is nearly equal throughout the excitation path, both above and below the focal plane. Conversely, the x-z repetitive scan excitation profile generated by the multiphoton microscope limits excitation and photobleaching to the focal plane (Figure 16.5(b)). Similar to the case for Figure 16.5(a), the diagonal blue lines emanating from the focal plane delineate the path taken by the excitation light to reach the focal plane.

A number of advantages arise from the localized excitation afforded by multiphoton microscopy. Perhaps the most significant is the high degree of three-dimensional resolution that can be achieved with the technique, which is identical to that obtained with an ideal confocal microscope. Also, the lack of absorption from fluorophores positioned outside the focal plane allows more of the excitation light to penetrate through the specimen and reach the plane of focus. The result is a dramatically increased ability of the focused beam to penetrate deep within the specimen, frequently to a depth that can range between two and three times that observed with confocal microscopy.

As was discussed previously, the probability of multiphoton absorption outside the focal region drops as the fourth power of the distance along the optical axis (the z-direction).

When a uniform distribution of fluorophores is subjected to multiphoton excitation with a high numerical aperture objective (1.4), approximately 80 percent of the absorption occurs in a tightly defined space termed the focal volume. The dimensions of this volume are dependent upon objective numerical aperture, but for a typical large aperture fluorescence objective at near-infrared wavelengths, this area is defined by an ellipsoid having a lateral dimension of 0.3 microns in diameter and an axial length of 1 micron.

The significant reduction in the amount of photobleaching (and associated photodamage to cells and tissues) illustrated in Figure 16.5(b) for multiphoton microscopy is substantially less than occurs with confocal microscopy. Photobleaching and photodamage are two of the most important limitations of fluorescence microscopy in the study of living cells, tissues, and other organisms. Excitation of a fluorophore causes promotion of a ground state electron to an excited singlet energy state. During vibrational relaxation from the excited state, there is a probability that intersystem crossing will occur to a triplet state instead of the typical decay back to the singlet ground state. Triplet states are extremely reactive and relatively long-lived, which allows fluorophores in this condition time to react with living cells or to undergo molecular degeneration or rearrangement to a non-fluorescent species. In addition, excited fluorophores in a triplet state can generate singlet oxygen, which will react with a wide variety of functional groups on neighboring biomolecules. Excitation light must penetrate the specimen on all focal planes on the way to the focal point, and most of this light continues to propagate a considerable distance past the focal region. Thus, a population of fluorophores excited throughout the beam path, as is the case in widefield and confocal microscopy, will undergo a considerable amount of photobleaching and produce cell and tissue damage that can be avoided with the multiphoton technique.

Although the exact mechanisms of cell damage induced by exposure to light are poorly understood, it has been established that decreasing photodamage will dramatically extend the viability of biological samples investigated with fluorescence microscopy. Exposure to long-wavelength visible and near-infrared light alone does not appear to affect cell viability, so it is likely that a majority of the damage associated with multiphoton microscopy arises from excitation and is confined to the focal plane.

16.4 Detectors For Multiphoton Microscopy

In multiphoton microscopy, photons emitted through secondary fluorescence originate almost exclusively from the objective focal plane, eliminating the requirement for descanned detection and permitting more flexible detection geometries. This increased versatility can lead to a considerable improvement in fluorescence detection efficiency compared to confocal microscopy. In a system with descanned detection, light collected by the objective is reflected from the surface of a series of scanning mirrors before passing through a pinhole to the detector. While increasing resolution of the image, the confocal pinhole produces a large decrease in detection efficiency and necessitates longer exposure of the specimen to incident illumination, increasing the probability of photodamage and photobleaching.

In some cases it may be desirable to apply modified confocal detection techniques to multiphoton imaging (Figure 16.7). Invading room light can be excluded through the use of a large confocal pinhole, which can produce a slight increase in lateral resolution at the cost of signal collection efficiency. The pinhole also enables the utilization of detectors with small entrance apertures, such as avalanche photodiodes or spectrometers. Utilization of a pinhole for multiphoton imaging should be carefully scrutinized before being implemented.

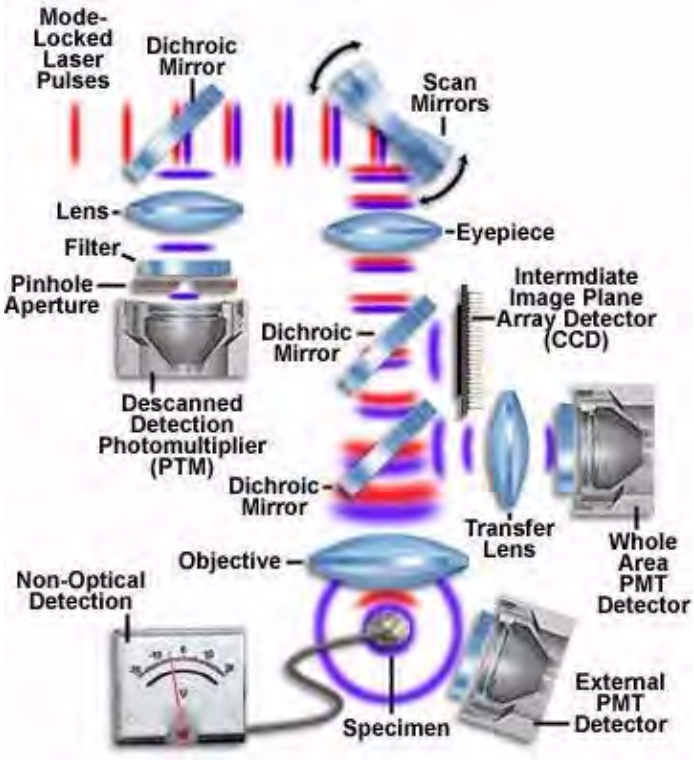

FIGURE 16.6: Detector configuration for multiphoton microscopy

Much of the light emitted by the specimen that can contribute image formation will be blocked by the pinhole. This includes both light that is scattered from locations within the focal plane and light originating from the focus region boundaries. For the same reasons, there will also be a reduction in the amount of fluorescence collected from deep within the specimen. In fact, when confocal pinhole apertures are employed, signal falloff at increasing specimen depths will be similar for multiphoton and confocal imaging. Several detection motifs are presented in Figure 16.7, which illustrates the collection of fluorescence information using photomultiplier tubes (PMTs), a CCD image array detector, and non-optical detection. Photomultipliers are the detectors of choice in multiphoton fluorescence microscopy, because shorter emission wavelengths (ultraviolet and low-wavelength visible) can be captured efficiently with these devices. The main distinction between the various scalar photomultiplier detectors in Figure 16.7 is whether emitted fluorescence is passed back through the scanning mirrors (descanned detection) or relayed through a transfer lens to a detector (PMT) placed in a plane conjugate to the objective rear aperture. A third photomultiplier (labeled the external detector) is shown positioned to the lower right of the specimen, and is designed to capture fluorescence directly from the specimen without passing through any portion of the microscope optical train.

Because of the fact that resolution is defined by the multiphoton excitation process, light emitted by excited fluorophores can be collected without using the objective. In fact, a high numerical aperture condenser will adequately serve the purpose of accumulating secondary fluorescence emission for the detector. In some cases, a photodetector is placed above (or below, depending upon microscope configuration) the specimen in an area removed from the microscope optics (Figure 16.7). This detection scheme enables the utilization of short

wavelength emission that might be hampered or precluded by low transmission through objective lenses. Another strategy is to collect emission directly from the objective with a detector (such as the whole area photomultiplier, as discussed above) placed near a dichroic mirror that reflects light from the rear aperture through a transfer lens. A shorter emission pathway facilitates the number of photons collected, especially when imaging through ten to twenty microns of tissue bathed in saline. Although the latter method can be employed to maximize the fluorescence detection efficiency, it is often vulnerable to contamination by ambient room light.

Photodiode arrays, such as a charge-coupled device (CCD) or complementary metal-oxide semiconductor (CMOS) detector, can also be utilized to collect fluorescence information in multiphoton experiments (Figure 16.7). In this configuration, light emitted by the specimen is again reflected from a dichroic mirror and imaged directly onto the photodiode array surface, which is placed in a plane conjugate to the intermediate image plane. An improvement in lateral resolution can often be obtained with this technique because resolution is determined by the emission wavelength, which is shorter than the excitation wavelength.

Several non-optical detection schemes have the potential to be applied to multiphoton microscopy due to the high degree of spatial localization during excitation. Among these are opto-acoustic detection, used to measure small amounts of absorption, and scanning photochemical detection, which generates images of receptor distributions from ionic current in voltage-clamped cells.

16.5 Resolution in Multiphoton Microscopy

Resolution in multiphoton microscopy does not exceed that achieved with confocal microscopy and, in fact, the utilization of longer wavelengths (red to near-infrared; 700 to 1200 nanometers) results in a larger point spread function for multiphoton excitation. This translates into a slight reduction of both lateral and axial resolution. For example, with an excitation wavelength of 700 nanometers and a 1.3 numerical aperture objective, the observed lateral resolution is approximately 0.2 micrometers with a corresponding axial resolution of 0.6 micrometers. When coupled to the Stoke's shift size, these values can range up to 30 percent larger than the resolution observed with conventional confocal microscopy under identical conditions. In practice, confocal resolution can be degraded by the finite pinhole aperture, chromatic aberration, and imperfect alignment of the optical system, all of which serve to reduce resolution differences between confocal and multiphoton microscopy. From this discussion, it becomes apparent that if structures are not adequately resolved with a confocal microscopy, they will not fare any better (and may be worse) when imaged with multiphoton excitation.

When gathering digital images or counting photons with three-dimensional spatial resolution, it is essential to distinguish between fluorescence emission occurring within the focal volume from that originating in the background. Differentiation between the two signals can be accomplished instrumentally (with confocal or multiphoton instrumentation) or by deconvolution of a three-dimensional data set. The ability to distinguish between fluorescence emission from the focal plane and background fluorescence is defined by the signal-to-background (S/B) ratio, where S is the number or intensity of photons collected from the focal plane and B represents the photons originating from the background (out-of-focus planes). In confocal scanning microscopy, high S/B ratios are generated by rejection

of background signal by the confocal pinhole. However, in multiphoton excitation, S/B ratios are inherently large because there is very little excitation outside the focal plane. Resolution calculations between multiphoton and confocal techniques can be compared by considering an infinitely small pinhole when performing the confocal calculations. For both techniques, the signal-to-background ratio is typically several orders of magnitude larger than for classical widefield fluorescence microscopy.

Another point to consider is that multiphoton excitation enables the utilization of fluorophores with absorption transitions in the low wavelength ultraviolet region. Because confocal microscopy is limited in its ability to excite fluorophores below about 340 nanometers, investigators tend to utilize probes having much longer wavelengths, with correspondingly lower resolutions. In critical situations, resolution in multiphoton microscopy can be enhanced through the restriction of imaging wavelengths via a confocal pinhole, and also by utilizing a spatially resolved detection system such as a CCD photodiode array placed in a scanned image plane.

16.6 Excitation Characteristics of Fluorophores

Fluorophores employed in multiphoton experiments should be subjected to the same scrutiny as those intended for single-photon investigations. The probes should have large absorption cross-sections at convenient wavelengths, high quantum yields, a low photobleaching rate, and the lowest possible degree of chemical and photochemical toxicity. The fluorophores should also be able to withstand high intensity illumination from the laser source without significant degradation. In most cases, investigators have utilized the same common fluorophores for two-photon experiments that are widely applied as markers in widefield and confocal fluorescence microscopy.

The excitation spectrum of common fluorophores is a function of the excitation mode and the wavelength of incident photons. Because of this dependency, the two-photon absorption spectrum can (and often does) differ dramatically from the corresponding single-photon spectrum. Experimentally, a majority of the fluorophores that have been examined are capable of absorbing two-photon excitation at twice the wavelength of their one-photon maximum absorption. In spite of this, there is no fundamental basis for quantitatively predicting the two-photon excitation spectrum of a complex fluorophore simply by examining the single-photon cross section. Significant differences often exist between the single and two-photon excitation spectra for highly conjugated non-symmetrical molecules, which are often exploited in molecular spectroscopy to provide information about the structure of excited states. A good example is the aromatic amino acid derivatives tyrosine and phenylalanine, whose complex two-photon cross-sections are quite different from that displayed by single-photon excitation. In contrast, the two-photon spectrum for tryptophan (Figure 16.2) is very similar to the profile displayed for single-photon excitation.

For quantitative three-dimensional reconstruction and deconvolution experiments, the two-photon absorption spectra of fluorophores should be measured to ensure that excitation wavelengths are centered near peaks in the absorption bands. Although two-photon cross-sections can be calculated, the process is complex at best. Direct experimental measurement of the absorption spectra is the preferred method, however these experiments are difficult due to the small amount of incident power absorbed versus intensity fluctuations in the light source. Thermal lensing and acousto-optical techniques have been employed to determine absorption cross-sections, but perhaps a simpler method is to examine photon emission from

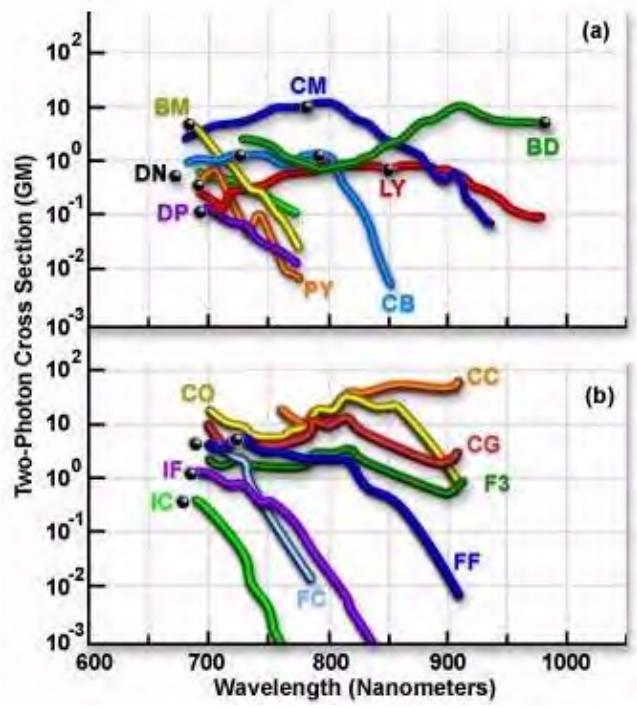

FIGURE 16.7: Two–photon excitation spectra of common fluorophores

fluorophores with known quantum yield. When designing new two-photon experiments, a range of fluorophores should be examined having absorption peaks near the one-half value of the intended excitation wavelength.

Figure 16.7 presents the characteristics of measured two-photon fluorescence excitation spectra for a number of common fluorophores. The data in Figure 16.7 represents two-photon action cross-sections, which is derived by taking the product of the fluorescence emission quantum efficiency and the two-photon absorption cross-section. Spectra were recorded utilizing linearly polarized light emitted by a mode-locked Ti:sapphire laser. In each spectrum, the black dot represents twice the wavelength of the fluorophore's single-photon absorption maximum. Table 16.1 is a key to the two-letter name codes presented beside each spectrum in Figure 16.7. The curves represent the spectral cross-sections of fluorophore two-photon excitation.

Cross-section measurements indicate a trend in which the excitation peak for two-photon absorption is very similar or blue-shifted with respect to the single-photon profile (Figure 16.7). The shorter average wavelengths may be advantageous in coupling fluorophore excitation to the available wavelength range of mode-locked lasers. Another consistent aspect of two-photon absorption spectra is that they are usually much broader than their single-photon counterparts. This eases experimental constraints by increasing the range of wavelengths that are suitable for excitation and enhances the ability to simultaneously excite two fluorophores that have overlapping two-photon cross-sections, but widely separated single-photon spectra. Measurements of three-photon cross-sections indicate that they are, in general, very similar to the corresponding single-photon spectra.

Although absorption spectra often differ for single and two-photon excitation, other fluorescence properties such as lifetime, emission wavelengths, and the rate of intersys-

Fluorophore Name (Abbreviation)	Excitation Wavelength (Nanometers)
(BM) p–bis (o–methylstyryl) benzene	691
(CB) Cascade Blue hydrazide trisodium salt	750
(YL) Lucifer Yellow CH ammonium salt	860
(BD-Bodipy) 4,4–difluoro–1,3,5,7,8–pentamethyl–4–bora–3a, 4a–diazaindacene–2,6–disulfonic acid disodium salt	920
(DP-DAPI not DNA bound) 4',6–diamidino–2–phenylindole dihydrochloride	700
(DN-Dansyl) 5–dimethylaminonaphthalene–1–sulfonyl hydrazine	700
(PY) 1,2–bis–(1–pyrenedecanoyl)–sn–glycero–3–phosphocholine	700
(CM) coumarin 307	776
(IC) indo–1 with Ca++	700
(IF) indo–1 without Ca++	700
(FC) fura–2 with Ca++	700
(FF) fura–2 without Ca++	720
(CG) Calcium Green–1 with Ca++	725
(CO) Calcium Orange with Ca++	800
(CC) Calcium Crimson with Ca++	850
(F3) fluo–3 with Ca++	800

TABLE 16.1: Two-Photon Fluorescence Excitation Spectra of Fluorophores

tem crossing do not appear to be affected. This similarity indicates that the same fluorescence excited states are reached by either linear or nonlinear absorption, and that once the fluorophore has been excited, it will behave the same regardless of the excitation mode. These tenants also hold for three-photon excitation, allowing investigators to utilize well-established ratiometric and spectroscopic methods in a majority of multiphoton experiments.

16.7 Photo and Heat Damage in Multiphoton Excitation

All forms of fluorescence microscopy suffer from photodamage to living cells, the degree of which is dependent upon the excitation wavelength, length of exposure, and the chemical nature of fluorophores utilized as cellular probes. The damage induced by excitation illumination can be segregated into two categories: heat damage and degradation due to chemical reactions. Photochemical side effects caused by biochemical reactions, as a result of fluorophore excitation, are not well understood and vary widely among cell and tissue types. Heat damage, on the other hand, arises principally from two mechanisms that occur because of single-photon absorption by water and by two-photon absorption from fluorophores in the focal region.

In most cells studied (particularly mammalian cells), there is almost no absorption of long wavelength near-infrared excitation radiation by intrinsic fluorophores utilized in multiphoton fluorescence. However, intracellular and intercellular water surrounding cells and tissues can absorb significant amounts of infrared and near-infrared illumination, producing excess heat that is potentially damaging to the viability of biological specimens. On the other hand, when the aqueous biological environment is illuminated with the shorter visible and ultraviolet wavelengths utilized in confocal and widefield fluorescence microscopy, a significant amount of heat is not absorbed by the surrounding water. Heating due to single-photon absorption by water occurs all along the beam path, both above and below the focal plane. Under controlled average multiphoton conditions, the induced temperature increase has been calculated to range between 0.065 and 1.1 degrees Centigrade at 700 and 1000 nanometers, respectively. These calculations are in agreement with heat measurements conducted at 1064 nanometers with optical tweezer laser excitation. In situations where the exciting light beam is held stationary, greater heating can occur, rising rapidly in a logarithmic relationship with time.

Heating due to fluorophore absorption is highly localized to the focal region in multiphoton excitation experiments. Subsequent heat release occurs uniformly within a spherically symmetrical region surrounding the focal volume, and produces no significant amount of heat, even at high fluorophore concentrations.

16.8 Conclusions

Multiphoton fluorescence microscopy is becoming one of the methods of choice for dynamic imaging of living cells and tissues. The technique is particularly useful in biological systems where ultraviolet excitation would not otherwise be possible due the light transmission characteristics of optical systems. In addition, side effects such as photobleaching and photodamage are minimized in multiphoton excitation, and occur only in the immediate region surrounding the focal volume. Although the prediction and measurements of two-photon absorption profiles from common fluorophores are slowly being accomplished, a

significant amount of work in this area is left to be completed. Design of new fluorophores specific for multiphoton excitation remains in the embryonic stages, but some progress along this avenue should be expected over the next few years.

Phototoxicity in cells is a poorly understood phenomenon, but does occur to a large degree in most forms of fluorescence microscopy. The lower quantum energy and lower intrinsic absorption of longer wavelengths utilized in multiphoton microscopy serve to reduce the deleterious effects of light on living cells and tissues, opening the door to new investigations of cellular dynamics. A major impediment to research in multiphoton microscopy is the high cost of equipment, in particular the necessary mode-locked pulsed laser systems that are required for two-photon and three-photon excitation. The two main types of ultrafast laser systems in general use are Ti:sapphire and Nd:YLF lasers, which although are very expensive, do not require water cooling nor have excessive electrical power demands. The wavelength tunability of the Ti:sapphire pulsed laser (700 to 1100 nanometers) renders it far more versatile than the single-wavelength Nd:YLF laser (1047 nanometers), but the convenience of tunability precludes total hands-off operation. As newer, cheaper, and user-friendly lasers are introduced into a competitive market, more commercial multiphoton microscope systems will be introduced at a cheaper price. This availability, coupled to the fact that there are no physical limitations to the implementation of multiphoton fluorescence, will encourage the widespread application of this technique throughout the biological sciences.

Chapter 17

Total Internal Reflection Fluorescence Microscopy

17.1 Introduction and Theoretical Aspects

Conventional widefield and laser scanning confocal fluorescence microscopy are widely employed techniques that rely on illumination of fluorophore-labeled specimens with a broad cone of light. The limited spatial resolution demonstrated by widefield fluorescence microscopy, especially along the optical axis, often renders it difficult to differentiate between individual specimen details that are overpowered by background fluorescence from outside the focal plane.

Confocal microscopes employ a pair of pinhole apertures strategically placed in conjugate planes near the illumination source and detector to produce thin optical sections devoid of background fluorescence. Multiphoton excitation microscopy goes a step further by restricting the illuminated specimen area to an ellipsoid having micron or sub-micron dimensions. Both confocal and multiphoton fluorescence microscopy produce optical sections of similar size. However, multiphoton excitation reduces the amount of secondary fluorescence produced by fluorophores through use of near-infrared long wavelength illumination and restriction of excitation events by the laser source to the objective focal volume.

In contrast, total internal reflection fluorescence microscopy (TIRFM) employs the unique properties of an induced evanescent wave to selectively illuminate and excite fluorophores in a restricted specimen region immediately adjacent to a glass-water (or glass-buffer) interface. The basic concept of TIRFM is simple, requiring only an excitation light beam traveling at a high incident angle through the solid glass coverslip or plastic tissue culture container, where the cells adhere. Refractive index differences between the glass and water phases regulate how light is refracted or reflected at the interface as a function of incident angle. At a specific critical angle, the beam of light is totally reflected from the glass/water interface, rather than passing through and refracting in accordance with Snell's Law. The reflection generates a very thin electromagnetic field (usually less than 200 nanometers) in the aqueous medium, which has an identical frequency to that of the incident light. This field, called the evanescent wave or field, undergoes exponential intensity decay with increasing distance from the surface. The characteristic distance for decay of the evanescent wave intensity is a function of the incident illumination angle, wavelength, and refractive index differences between media on each side of the interface. Fluorophores residing near the glass-liquid surface can be excited by the evanescent field, provided they

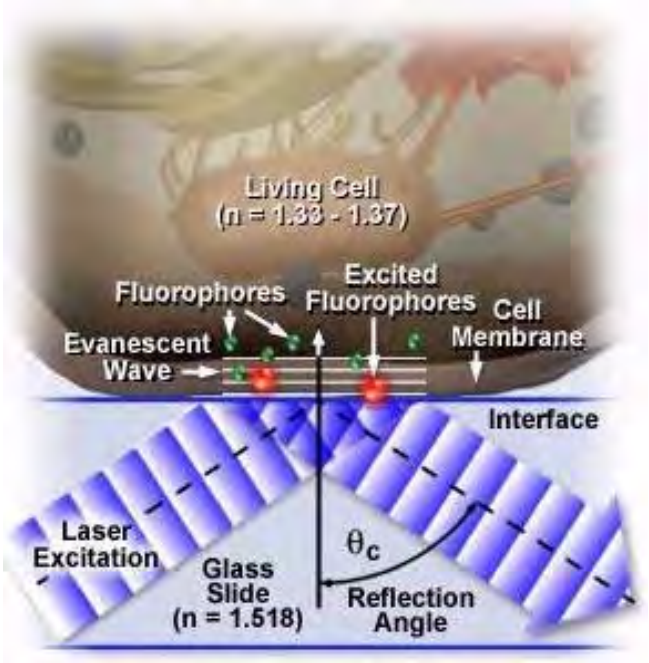

FIGURE 17.1: Total internal reflection fluorescence

have electronic transitions that occur in or very near the wavelength bandwidth of the illuminating light beam. Because of the exponential falloff of evanescent field intensity, fluorophores farther away from the surface avoid being excited, which leads to a dramatic reduction of unwanted secondary fluorescence emission from molecules that are not in the primary focal plane. The effect enables production of high-contrast images of surface events with a significant increase in signal-to-background ratio over classical widefield techniques.

The concept of TIRFM is schematically presented in Figure 17.1, which depicts selective excitation of fluorophores in an tissue culture cell (refractive index, n = 1.33 to 1.37) resting on the surface of a glass slide (refractive index, n = 1.518). Wavefronts from a blue laser excitation source pass through the glass and are reflected from the glass-buffer boundary at a critical angle, q(c), establishing an evanescent wave that travels several hundred nanometers into the cell membrane. Fluorophores in the membrane near the glass interface (small green spheres) are excited by the evanescent wave and subsequently emit secondary fluorescence (red), while those farther away from the interface are not excited.

Total internal reflection fluorescence is employed to investigate the interaction of molecules with surfaces, an area that is of fundamental importance to a wide spectrum of disciplines in cell and molecular biology. Examples are binding and triggering of cells by hormones, neurotransmitters, and antigens; cell adhesion to surfaces; electron transport in the mitochondrial membrane; cytoskeletal and membrane dynamics; cellular secretion events; polymer translation near an interface; single molecule interactions; and surface effects on reaction rates. In a majority of these studies, functionally relevant fluorophores bound to the surface and those in the surrounding medium exist in an equilibrium state. When these molecules are excited and detected with a conventional widefield fluorescence microscope, the resulting fluorescence from those fluorophores bound to the surface is often swamped by the overwhelming fluorescence from a much larger population of non-bound molecules inhabiting the adjacent detection volume. Constraint of the optical field to a refractive

index interface is the basis for all total internal reflection spectroscopy, spectrometry, and microscopy investigations.

Living cells in culture provide an excellent candidate for TIRFM investigations. The technique enables selective visualization of contact regions between individual cells and the substrate, even in specimens where fluorescence from areas outside the surface would obscure important fluorescent information concerning adhesion points. Because illumination is restricted to the interface regions and does not penetrate the specimen bulk, living cells tend to survive longer under fluorescence observation using TIRFM techniques. This feature enables microscopists to increase the length of observations, and to perform time-lapse cinemicrography for extended periods, often ranging for many hours or even one or more days.

TIRFM can also be utilized on featureless non-microscopic specimens to measure fluorophore concentrations as a function of distance from the interface, or to record binding/unbinding equilibria and kinetic rates at a biological surface. Other applications include single molecule fluorescence experiments and model membranes, which have been constructed using the substrate for mechanical support. The technique is also useful for investigating the emission of fluorophores bound to surfaces as a function of molecular dipole orientation. These and other experiments are designed to examine the chemistry and physics of interfaces themselves, and should continue to be the focus of TIRFM studies in many diverse fields.

17.1.1 Theory of Total Internal Reflection

The behavior of a collimated light beam upon refraction or reflection from a plane surface is fundamental to the understanding of TIRFM. Light passing between two media of varying refractive index is either refracted as it enters the second medium or it is reflected at the interface, depending upon the incident angle and the difference in refractive index between the two media. In situations where the light beam is propagating through a medium having a high refractive index and encounters a boundary to a medium of lower refractive index, it is refracted according to Snell's Law:

$$n_1 \cdot \sin\theta_1 = n_2 \cdot \sin\theta_2$$

where n_1 is the higher refractive index medium and n_2 is the medium of lower refractive index. The incident wave is positioned at angle $theta_1$ from the normal, while θ_2 represents the angle of light refracted at the interface into the medium of lesser refractive index. As the incident angle slowly increases (relative to the normal), it reaches a point termed the critical angle where the refraction angle is 90 degrees. At higher incident angles, light is completely reflected at the interface (total internal reflection), and no significant amount is refracted into the bulk phase of the medium having a lower refractive index. In biological investigations involving living tissue culture cells or similar studies of cytoplasmic components, n_1 represents the refractive index of the glass microscope slide or coverslip (n = 1.518), while n_2 is the refractive index of the aqueous buffer solution or internal cellular components (n = 1.33 to 1.37). Therefore, n_1 is greater than n_2, and when θ_1 exceeds the critical angle θ_c, total internal reflection occurs within the glass adjacent to the liquid medium. The critical angle is defined by the equation:

$$n_1 \cdot \sin\theta_c = n_2$$

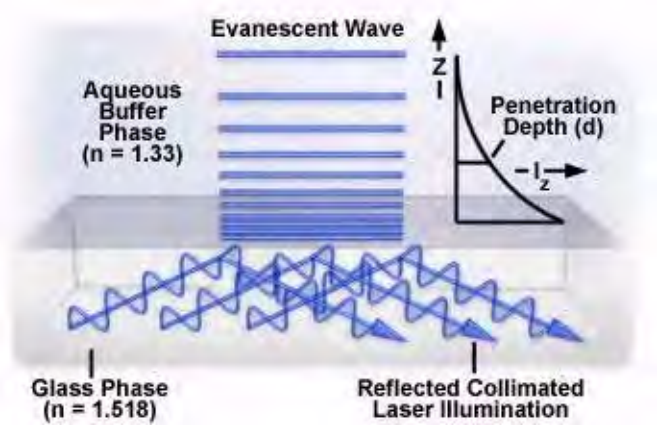

FIGURE 17.2: Evanescent wave exponential intensity decay

or

$$\sin\theta_c = \frac{n_2}{n_1}$$

which is more commonly expressed as:

$$\theta_c = \sin^{-1}\frac{n_2}{n_1} = \sin^{-1} n_{2,1}$$

For angles less than θ_c, a majority of the incident light propagates directly through the interface with a refraction angle measured from the normal as defined by Snell's Law (discussed above). Even in this situation, some of the incident light is reflected back into the glass. However, for all angles greater than the critical angle, total internal reflection is achieved and a vast majority of the light is reflected. A small portion of the reflected light penetrates through the interface, and propagates parallel to the surface in the plane of incidence creating an electromagnetic field in the liquid adjacent to the interface. This field, as described above, is termed the evanescent field and is capable of exciting fluorophores residing in the immediate region near the interface.

The transition from refraction to total internal reflection occurs without any discontinuities, rather than being a sudden new phenomenon appearing at the critical angle. As the incident angle becomes larger, the transmitted (refracted) beam becomes weaker while the reflected beam slowly acquires more intensity. At small incident angles, light waves passing through to the liquid are sinusoidal, with a characteristic period. As the incident angle approaches the critical value, the period becomes longer and refracted rays propagate increasingly parallel to the surface of the interface. When the critical angle is achieved, the period becomes infinite and the refracted light produces wavefronts that are perpendicular (normal) to the surface.

For a light beam having a finite width, the evanescent wave created at the interface can be described as partially emerging from the solid into the liquid medium and traveling for some distance before re-entering the solid phase. This propagation distance, called the Goos-Hänchen shift, can be measured when the beam width is restricted to one or several wavelengths. The size of this shift ranges from a fraction of a wavelength when the incident light is perpendicular to the interface, to infinite at the critical angle, which corresponds to the refracted beam skipping along the surface. Wider beams (those having a width much larger than a few wavelengths) produce an evanescent field whose intensity can be

Distance (nm)	Relative Intensity
1	0.99
10	0.92
100	0.43
1000	0.0002

TABLE 17.1: Fluorescence Intensity versus Penetration Depth

measured in units of energy per unit area per second. The evanescent field intensity decays exponentially (Figure 17.2) with increasing distance from the interface according to the equation:

$$I(z) = I_0 \exp^{-z/d}$$

where I(z) represents the intensity at a perpendicular distance z from the interface and I_0 is the intensity at the interface. The characteristic **penetration depth (d)** at λ_0, the wavelength of incident light in a vacuum, is given by:

$$d = \frac{l(0)}{4\pi\sqrt{n_1^2 \sin^2 - n_2^2}}$$

The penetration depth, which usually ranges between 30 and 300 nanometers, is independent of the incident light polarization direction, and decreases as the reflection angle grows larger. This value is also dependent upon the refractive indices of the media present at the interface and the illumination wavelength. In general, the value of d is on the order of the incident wavelength, or perhaps somewhat smaller. When the incident angle equals the critical value, d goes to infinity, and the wavefronts of refracted light are normal to the surface. Experimental measurements of fluorescent intensity as a function of distance from the interface in a typical TIRF investigation are listed in Table 1 for a set of identical fluorophores.

Evanescent wave intensity at the surface (I_0) is a function of both the incident angle and the polarization components of the light beam. The I_0 intensities observed for polarized vibration vectors can be discussed in terms of a coordinate system arranged to display all three orthogonal directions, as illustrated in Figure 17.3. The plane of incidence (the x-z plane) is defined as being parallel to the exciting light beam with the x-direction parallel and the z-direction perpendicular to the interface surface. The y-direction then becomes normal to the plane of incidence.

Two independent incident light polarization directions, termed **p** and **s**, are possible. These are electric field vectors parallel (p) and perpendicular (s) to the plane of incidence defined by the paths of the incident and reflected light beams. The evanescent electric field vector for the s-polarized incident light is perpendicular (or normal) to the plane of incidence. A non-zero longitudinal component and phase lag manifests the p-polarized incident light, which has an evanescent electric field vector direction that remains in the plane of incidence. The longitudinal component induces the p-polarized light electric field vector to "cartwheel" along the interface and produce elliptical polarization of the evanescent field in the plane of propagation. A spatial period of:

$$\frac{\lambda_0}{n_2 \cdot \sin\theta_2}$$

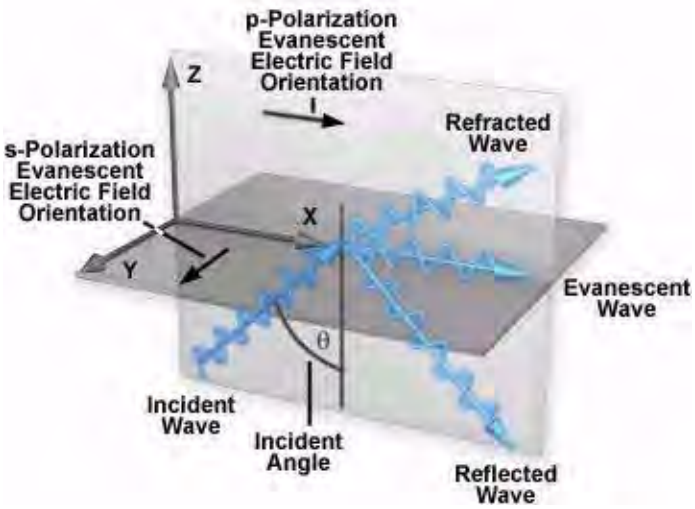

FIGURE 17.3: Evanescent field intensity coordination system

is observed for the p-polarized electric field vectors. The spatial period is not affected by the refractive index or dielectric properties of the resident medium (aqueous buffer or water). Instead, it is determined by the spacing of the incident light wavefronts in the glass medium as they intersect the interface. When the incident angle is reduced from the supercritical range to the critical angle and lower, the longitudinal component disappears and the electric field component in the x-direction simultaneously vanishes.

The evanescent field intensities at the interface (z = 0) for the incident p and s components are complex expressions given by the following series of equations:

$$l_x = \frac{4\cos^2\theta\left(\sin^2\theta - n^2\right)}{(1-n^2)\Big((1+n^2)\sin^2\theta - n^2\Big)} \tag{17.1}$$

$$l_y = \frac{4\cos^2\theta}{1-n^2} \tag{17.2}$$

$$l_z = \frac{4\cos^2\theta\sin^2\theta}{(1-n^2)\Big((1+n^2)\sin^2\theta - n^2\Big)} \tag{17.3}$$

where n represents the refractive index ratio $\frac{n_2}{n_1}$), which is less than unity, and θ is the incident angle. For s-polarized incident light, the total evanescent intensity is equal to the y-component, I(y), while the evanescent intensity for p-polarized incident light is composed of both the x and z components (I(x) and I(z)). As discussed above, the y intensity is linearly polarized, but the x and z intensities are elliptically polarized due to the fact that the electric fields are 90-degrees out of phase with each other.

The p and s evanescent intensities are illustrated in Figure 17.4 as a function of incident angle for transmitted light in the lower refractive index medium when passed through an interface composed of fused quartz ($n_1 = 1.46$) and water or an aqueous buffer solution ($n_2 = 1.33$). These calculations assume a condition of total internal reflection and require a critical angle of 65.7 degrees for the refractive indices listed. Intensity, plotted on the ordinate, is expressed as the ratio of evanescent intensity at the interface (z equals zero) to the incident intensity for each polarization angle. It is interesting to note that the

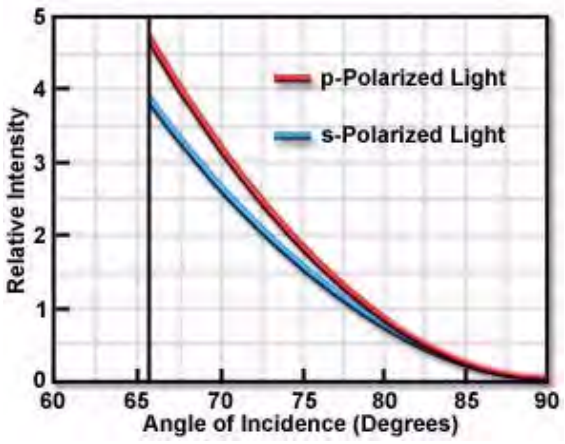

FIGURE 17.4: Polarized light intensity

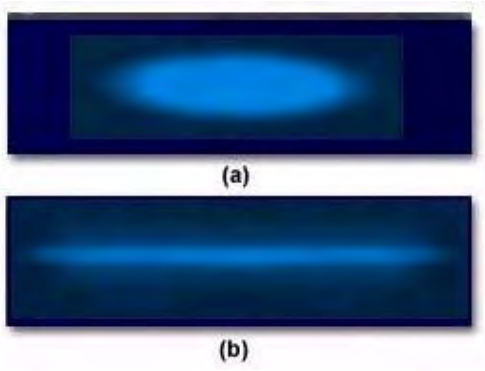

FIGURE 17.5: Incident light beam reflection profiles

evanescent intensities for both polarization orientations exhibit a range between one and five times that of the plane wavefront incident intensity for angles within 15 degrees of the critical angle.

Although not illustrated in Figure 17.4, evanescent intensities of the polarized components can be extended (without breaks) to the subcritical angle region, which is good evidence for the continuity of the transition to total internal reflection. As the incident angle approaches 90 degrees, the evanescent intensities drop almost to zero.

In typical TIRFM experiments, a Gaussian laser beam is focused at a narrow angle of convergence to produce evanescent illumination that resembles an elliptical Gaussian profile, as depicted in Figure 17.5(a). Intensity profiles of a total internal reflection region (2 degrees greater than the critical angle) are presented in the figure, with illumination provided by a Gaussian profile beam emitted by a continuous wave argon-ion laser. The polarization and penetration depth are approximately equal to those exhibited by a single infinite plane wave. To produce the laser reflection profiles presented in Figure 17.5, a glass coverslip surface coated with a thin layer of the chromophore 3,3'-dioctadecylindocarbocyanine (Dil) is illuminated with the argon-ion laser and images were recorded in air through a 10x objective having a numerical aperture of 0.25 and achromatic correction. The beam is slightly defocused at the reflection surface in Figure 17.5(a), but has tight focus in Figure 17.5(b). The long thin stripe exhibited by the focused beam in Figure 17.5(b) is due a

greater convergence angle than the beam in Figure 17.5(a), and a mean angle within a few degrees of the critical angle.

17.1.2 TIRFM with Intermediate Dielectric Layers

Often, the interface in actual TIRFM experiments is not so clearly defined as a simple boundary between the glass coverslip and an aqueous buffer solution. A good example is the case of a biological membrane or lipid bilayer interposed between the glass and buffer solution at the bottom surface of a tissue culture vessel. Another often-utilized example is a metallic thin film coating, which displays some interesting features. These interfaces are described as three-layer systems in which incident light travels from the glass medium ($n_1 = 1.518$) through the intermediate layer (having a refractive index referred to as n_i) toward the lower refractive index aqueous buffer medium ($n_2 = 1.33$).

Among the interesting features of three layer systems is that insertion of the intermediate layer does not hinder total internal reflection, regardless of the layer's refractive index. Instead, the question is whether reflection occurs at the $n_1 - - - n_i$ interface or the $n_i - - - n_2$ interface. Most intermediate layers will be exceedingly thin (10 to 30 nanometers) so the identity of the interface supporting total internal reflection is not important for qualitative studies. The characteristic depth of the evanescent wave is still described by the relationships discussed above, regardless of the refractive index and thickness of the intermediate layer. However, the properties of the intermediate layer will affect the overall penetration distance of the evanescent field, as measured from the surface boundary of the aqueous medium. The evanescent intensity at the interface (z equals zero) is affected by the intermediate layer. Thin layers (around 20 nanometers) of metallic film produce dramatic effects in this regard. The s-polarized evanescent intensity becomes negligible, but the p-polarized intensity is actually enhanced for a very narrow band of incident angles and becomes an order of magnitude brighter just above the critical angle. This "resonance" effect is attributed to excitation of a surface plasmon mode at the metal/water interface. Plots of intensity (not illustrated) versus incident angle yield a peak, which is termed the **surface plasmon angle**. For an aluminum film residing between a glass/water interface, this angle is greater than the critical angle for total internal reflection. Such an illumination enhancement is remarkable when one considers that the thin metallic film is almost opaque.

Among the practical consequences of metallic film effects is that these films can be employed to quench fluorescence within 10 nanometers of the surface, but TIRFM can still selectively excite fluorophores in the 10- to 200-nanometer region above the interface. In addition, it has been noted that a light beam incident (through glass) on a 20-nanometer aluminum film does not require collimation to produce total internal reflection. Light rays incident at the surface plasmon angle will create a strong evanescent wave to excite fluorophores, while the rays having too low or high of an incident angle will produce a negligible field in the buffer layer. This phenomenon may be utilized to allow substitution of uncollimated incident illumination for many TIRFM experiments. In addition, the presence of a metallic film leads to a highly polarized evanescent wave, regardless of the purity of the incident polarization.

Another point to consider is that irregularities in the intermediate layer can induce scattering of the incident light beam, which then propagates in all directions through the medium of lower refractive index (the aqueous buffer layer). Light scattering does not appear to pose a significant experimental problem to specimens such as biological cells in

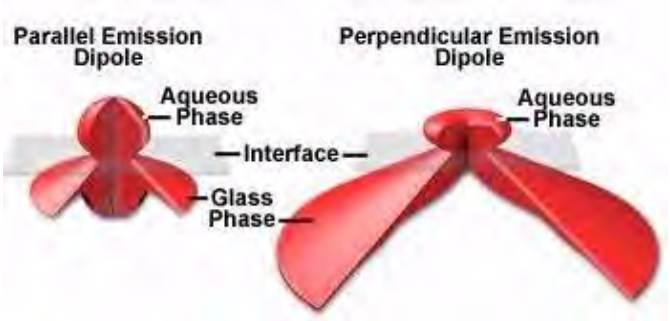

FIGURE 17.6: Anisotropic fluorescence emission intensity

culture. This is due to the fact that excitation of chromophores by scattered light is far less than excitation by the evanescent field, producing a correspondingly smaller contribution to secondary fluorescence emission intensity.

17.1.3 Fluorescence Emission at the Reflection Interface

Fluorophores existing in close proximity to an interface do not emit light isotropically, unlike those dispersed in bulk solution. Instead, secondary fluorescence emission is produced in a complex spatial pattern that is highly dependent upon the orientation of the fluorophore transition dipoles with respect to the interface geometry. Other factors that govern emission parameters are the dielectric properties of the media comprising the interface, which often impose different propagation speeds and directions on light emitted by fluorophores. Also, in many fluorescence microscopy experiments, fluorophores are bound to biological structures or other complex assemblies that impose strict orientational limitations or requirements, and often have association constants exceeding the fluorescence lifetime.

When fluorophores near an interface are modeled as constant power oscillators, the radiated emission intensity in all directions for molecules oriented perpendicular and parallel to the interface are presented in Figure 17.6. In each case, the transition dipole is positioned within the medium of lower refractive index (water or buffer) at a distance z' equal to 80 nanometers from the quartz surface. The fluorophores are assumed to be azimuthally unoriented with the dipole parallel to the surface in Figure 17.6(a) and perpendicular to the surface in Figure 17.6(b). In both cases, the fluorescence emission distribution patterns are complex and highly non-uniform.

In many TIRFM experiments, fluorescence emission is gathered by an objective that is positioned above the specimen on the water/buffer side of the interface. Under these circumstances, even low numerical aperture objectives are capable of capturing a majority of the emission to yield reasonable results from TIRFM experiments. The situation is somewhat different when the objective is placed beneath the glass layer and fluorescence emission is collected after it passes through the glass medium. Because fluorophores are oriented perpendicular to the surface in many cases, the emission patterns require higher numerical apertures for efficient collection of secondary fluorescence (see figure 17.6). Fluorescence emission polarization and lifetimes are also affected by the fluorophore's proximity to the interface. This results in a complex relationship between fluorescence intensity, distance from the interface, and fluorophore orientation, which renders accurate measurements of

these parameters difficult.

17.1.4 Conclusions

An increasing number of important biochemical and cell biology investigations are now being conducted using TIRFM techniques developed over the past few years. The basic theory has been well established and practical implementation of the technique is now within the reach of many laboratories. Configuration of an upright or inverted microscope for TIRFM is relatively easy to accomplish using a laser light source, and several investigators have also demonstrated that these experiments can be conducted with traditional arc-lamp illumination sources, provided additional modifications are made. The technique is compatible with standard epi-fluorescence, brightfield, darkfield, phase contrast, and differential interference contrast illumination modes, and can be utilized to simultaneously record and compare images from several observation methods. This enables investigators to localize fluorescence emission to specific regions within cells, membranes, or macromolecular complexes.

Contact regions between cells and their substrates can also be located by a non-fluorescence technique known as interference reflection microscopy or reflection contrast microscopy, which does not require specific labeling of the cells with fluorophores. However, because of the lack of specific reporter molecules, reflection interference techniques provide no information on biochemical specificities in the contract region and are much less sensitive than TIRFM to changes in contact distance within the critical first 100 nanometers of the surface.

When compared to laser scanning confocal microscopy, TIRFM has several advantages and disadvantages. Confocal microscopy is capable of providing optical sections from virtually any specimen plane instead of being confined to an interface between two media of dissimilar refractive index. In comparison though, the smallest optical sections produced by confocal microscopy are around 600 nanometers, much smaller than the 100-nanometer sections typically seen with TIRFM experiments. Other applications that require restricted illumination (usually to reduce the amount of cell damage) are best done with multiphoton excitation or TIRFM rather than confocal microscopy, which illuminates a relatively large specimen volume. Finally, TIRFM is much more economical to configure because the technique does not require complex scanning galvanometer systems and can be applied to ordinary research-grade laboratory microscopes. Several manufacturers are even addressing the needs of TIRFM investigators by producing high numerical aperture objectives designed specifically for internal reflection experiments.

17.2 Basic Microscope Configuration

A wide spectrum of optical configurations was placed under scrutiny during the early stages of instrument development for total internal reflection fluorescence microscopy investigations (TIRFM). From this effort emerged a number of designs that satisfy the requirements for generating a thin evanescent field at the junction between two materials of differing refractive index.

The majority of these designs centered on inverted microscopes, primarily due to the convenience of adding TIRFM optics above, rather than below, the bulky microscope stage. Upright microscope configurations can also be utilized, especially when this represents the only practical choice for the experimental conditions or the investigator's budget. Observa-

FIGURE 17.7: Anisotropic fluorescence emission intensity

tions of cell-substrate contacts with cells growing in monolayer culture on the bottom of a plastic Petri dish are a good candidate for TIRFM with an upright microscope, especially when water immersion objectives with a dipping cone are employed. Inverted microscopes are more efficient when examining cells or membrane components attached to the upper portion of a sealed specimen chamber or when the objective is utilized both to illuminate and retrieve secondary fluorescence emission from the specimen.

Regardless of the basic microscope design, a majority of the currently utilized TIRFM configurations rely on an added prism to direct laser illumination toward the interface where total internal reflection occurs, which is in the specimen conjugate plane of the microscope. It is also possible to use the microscope objective to simultaneously direct illumination to the interface and capture secondary fluorescence emission produced by excited fluorophores. This discussion reviews many of the basic microscope configurations for TIRFM, and assumes that the example specimen consists of cells in tissue culture labeled with one or more fluorescent dyes and growing in a monolayer attached to a glass coverslip at the total internal reflection interface.

Presented in Figure 17.7 is a typical TIRFM instrument configuration involving an inverted tissue culture microscope, a trapezoidal prism block, external laser illumination, and a photomultiplier/CCD combination detector system. Blue light emitted from the laser first passes through a beam expander and then into a that divides the light between a microscope entrance port and the beam director mirror. After reflecting from the surface of the director mirror, a portion of the light is focused by the focusing lens onto the trapezoidal prism positioned on the microscope stage just above the specimen chamber and objective. The prism directs illumination to the TIRF interface at an angle that is slightly larger than the critical angle for total internal reflection, creating an evanescent field that excites fluorophores in the specimen. Another portion of the light passed by the enters the microscope port, where it can be directed through the optical train to the specimen

for widefield epi-fluorescence excitation. Secondary fluorescence emitted by the specimen is collected by the objective and passed either to the eyepieces, the CCD camera system, or the photomultiplier (PMT). Because the top of the trapezoidal prism is flat, illumination from the tungsten halogen lamphouse can be utilized to observe the specimen in transmitted mode utilizing a variety of contrast enhancing techniques, including differential interference contrast, phase contrast, darkfield, and Hoffman modulation contrast.

When designing TIRFM experiments, the most important factor to consider in the configurational motif is the critical angle of illumination. Ordinary glass coverslips, upon which tissue culture cells are commonly grown, have a refractive index of about 1.52 while the medium surrounding the cells and the interior cellular components have refractive indices ranging from 1.33 to 1.38. Therefore, to obtain total internal refection at the interface between a cell membrane and the coverslip $\frac{n_2}{n_1} = \frac{1.52}{1.38}$), the angle of incidence must be larger than the critical angle of 65 degrees. If the cells are not intact and have been permeabilized, hemolyzed, sonicated, or fixed, then the lower refractive index is that of aqueous buffer ($n_1 = 1.33$) instead of cytoplasm, and the critical incidence angle is reduced to 61 degrees.

In principle, it is possible to employ conventional tungsten halogen or mercury/xenon arc lamps to conduct TIRFM experiments, but a majority of the investigations reported in the literature are performed under laser illumination. The primary reason that lasers are so widely preferred is that laser light is coherent, polarized, and well collimated, so that it can be easily directed into the objective or prism using standard beam expanders, mirrors, and focusing lenses. When the laser source is properly aligned, the total internal reflection interface is illuminated with an area of defined geometry that can be easily adjusted to accommodate experimental variations. High intensity laser sources are also important for experiments that require a significant amount of illumination, such as fluorescence recovery after photobleaching (FRAP) investigations and fluorescence ratio determinations.

The most popular laser sources for TIRMF experiments are the 1 to 3 watt air and water cooled continuous wave argon-ion systems that have strong emission lines at 488 and 514 nanometers, providing the ability to excite a wide spectrum of common fluorophores. Lasers having lines at longer wavelengths, such as helium-neon and krypton-ion gas lasers, can be employed to excite fluorophores that absorb in the 540 nanometer and higher regions. However, virtually any laser with a total visible output in the 0.5 watt or greater range should be adequate. A laser source is generally preferable to an arc lamp for TIRFM, because collimation of the light emitted by the arc lamp results in severe reduction of intensity. However, laser illumination suffers from unavoidable interference fringing on the specimen, which can be somewhat reduced by meticulously cleaning the optical surfaces. For critical experiments, investigators should explore rapid jiggling of the laser beam or at least compute a normalization of sample digital images using a control digital image consisting of a uniform concentration of fluorophores.

17.2.1 Inverted Microscope Configurations

The simplest approach to achieve total internal reflection from a culture chamber on an inverted microscope is direct laser illumination through a glass cube positioned on top of the chamber, as illustrated in Figure 17.8. In general, a fixed-stage microscope (in which the nosepiece/objective combination is translated during focusing) is more convenient than a movable stage microscope. This configuration ensures that the specimen will remain stationary during focusing, requiring only an initial alignment of the laser beam. However,

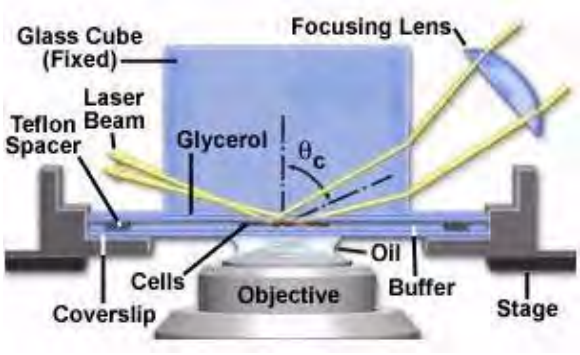

FIGURE 17.8: Basic inverted microscope TIR configuration

moving-stage microscopes are more common and either type can be employed for these experiments.

In all inverted microscope configurations considered here, the buffer-filled sample chamber consists of a lower bare glass coverslip, a 60-micron thick Teflon spacer ring, and the cell adhesion coverslip inverted so the cells face downward towards the microscope objective. An advantage of this design is that cells not bound to the substrate, loose cellular debris, and contaminating protein tend to sediment as an aggregate to the bottom of the chamber without obscuring or adding extraneous fluorescence to the total internal reflection interface.

The upper surface of the cell monolayer-coverslip combination is placed in optical contact with the glass block (or prism) by means of a thin layer of immersion oil or glycerol. The lateral faces of the glass block should be fixed, but the sample must be able to undergo translation in the x and y directions while still maintaining optical contact. The lower coverslip can be oversized and the Teflon spacer is often made with gaps so that the buffer solution bathing the cells can be changed by capillary action with entrance and exit ports (Figures 17.8 and 17.9). Several manufacturers offer tissue culture chambers that are designed specifically for this purpose.

As demonstrated in Figure 17.8, the laser beam first enters a focusing lens positioned obliquely above the microscope stage. The purpose of the lens is to concentrate laser illumination in much the same manner as an objective during epi-illumination, but the lens also serves to narrow the beam width for easier alignment. The focal length of the lens is not critical and can range between 50 and 100 millimeters, but should allow the investigator to easily change the size of the illuminated area over a narrow range. As with other components in the illumination system, the focusing lens should be mounted on an x-y-z translator having one of the axes aligned with the incoming laser beam direction. The translator can be mounted either on the laboratory bench or the microscope stage, but will be easier to align when it is mounted on the stage.

Three primary optical elements control and direct the laser beam size and pathway prior to its entering the focusing lens (see Figure 17.7). These consist of a beam expander to widen the laser light beam as it exits the cavity, a (optional) or mirror, and a beam director to divert the beam into the focusing lens.

Laser beam expanders are widely available from a number of distributors, and are employed to control the width of the beam at the focusing lens. As a consequence, the angle of convergence onto the specimen and the width of the focused spot is then determined by

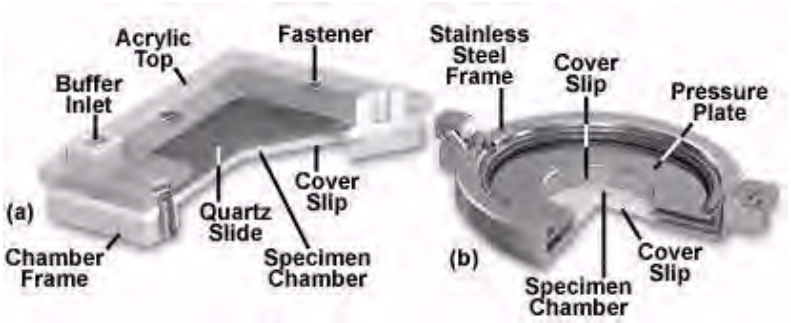

FIGURE 17.9: Tissue culture chambers fot TIR

the focusing lens. Laser light is refracted at a series of angles across the beam profile when it encounters the vertical face of the cube. The resulting geometric aberration produces an elliptically illuminated area at the interface, which is elongated when compared to the expected pattern for a parallel light beam with a Gaussian profile. Beams that are wider when they enter the focusing lens produce a reflection spot having thinner dimensions. Under optimum conditions, a beam half-width approaching a lower limit of 2.5 microns can be attained.

The is a mirror that diverts a horizontal laser beam into a vertical direction (at a 90-degree angle) to elevate it past the height of the microscope stage and glass prism or block. An adjustable optical mount should be utilized to house the so that it can be removed to allow direct entry of laser light into a microscope port for quick and reversible conversion to auxiliary epi-illumination. By using a partially silvered mirror or even a plain glass slide as a , both epi-illumination and total internal reflection can be viewed simultaneously.

A beam director mirror is employed to angle the laser beam from the vertical direction obliquely down toward the focusing lens (see Figure 17.7). The mirror height determines the incidence angle at the total internal reflection surface. In addition to the linear height adjustment, the director mirror should be mounted on a biaxial rotational mount to allow direction of the unfocused laser beam into the prism. If the mirror mount is attached to the stage of a moving-stage microscope (rather than the laboratory bench), the position of the reflection region can be rendered insensitive to changes when focusing the specimen.

When properly aligned, the collimated and focused laser beam enters the glass cube, and is directed by refraction to strike the total internal reflection interface (beneath the cube's lower surface) with an incident angle exceeding the critical minimum. Neither the size nor shape of the cube is vital, and a prism or rectangular glass block can easily be substituted. Equilateral and 45-45-90-degree prisms are standard commercial items and can be purchased from a variety of sources. A prism with a flat top (Figures 17.8 and 17.12), such as the cube described above or a truncated triangle, allows placement of a tungsten halogen lamp and condenser system above the prism. In this configuration, conventional illumination techniques such as brightfield, darkfield, phase contrast, and differential interference contrast can be coupled to TIRFM investigations to assist in determining the spatial location of fluorescence originating at the interface.

To install the prism or glass block, apply a droplet of pure glycerol or immersion oil to the upper surface of the culture chamber and slowly lower the prism onto the oiled surface, thereby spreading the droplet into a thin layer. The contact media (glycerol or oil) serves two purposes: to ensure optical contact between the prism and the specimen chamber,

and to mechanically lubricate the region between the two glass surfaces. As the specimen chamber is laterally translated during scanning, the prism or glass block remains fixed. The incident laser beam should propagate obliquely through the lower portion of the prism, then through the glycerol or oil layer, and finally through the specimen, totally reflecting at the bottom surface of the substrate directly over the optical axis of the microscope. Substrate thickness is not critical, except that thick substrates (those approaching a millimeter or even more) may constrain the laser beam from meeting the bottom surface directly over the microscope's optical axis.

The immersion contact media (oil or glycerol) should be used sparingly, because any excess may accumulate at the lower edges of the prism and interfere with the incident laser illumination when it first enters the glass. Prism size is not critical, but larger prisms may inhibit lateral motion of the specimen, although they will increase the clearance between the immersion media bead and the incident light beam. In general, a prism or glass block with a face area of about a square centimeter is ideal.

The prism employed to couple exciting laser light into the system does not require an exact match in refractive index to the slide or coverslip in which total internal reflection takes place. They may be optically coupled with glycerol, cyclohexanol, or microscope immersion oil, among other optically distinct liquids. Immersion oil has a higher refractive index, which helps to avoid possible total internal reflection at the prism/coupling media interface at low incident angles. However, many brands of immersion oil demonstrate a significant amount of autofluorescence. Another important point is that a truncated prism surface does not require special polishing treatment, but will perform adequately with the smoothness of a standard commercial microscope slide.

Several specimen chamber designs that utilize windows composed of glass slides and/or coverslips are presented in Figure 17.9. On the left (Figure 17.9(a)) is a Tamm chamber devised to provide a thin profile that allows the tissue culture cells to be observed through a thin layer of buffer solution, which permits the use of high numerical aperture objectives having very short focal lengths. A monolayer of cells, grown on the upper glass coverslip (or microscope slide), are separated from the lower coverslip with a thin spacer having a thickness less than 100 micrometers. Access holes enable the cells to be perfused with a variety of solutions to conduct titrations, equilibrium binding experiments, or kinetic analysis of interactions at the cell surfaces. A similar device, the Dvorak-Stotler controlled-environment culture chamber, is illustrated in Figure 17.10(b). This chamber also utilizes coverslips for both the top and bottom windows, but does not have access holes or any mechanism to allow addition of chemicals or changes to the buffer solution.

As depicted in Figure 17.9, the specimen chambers contain the aqueous buffer solution necessary to maintain the cultured cells. This solution is sandwiched between the substrate surface and a glass coverslip, which are separated by a Neoprene or Teflon spacer. Teflon rings are commercially available, having thicknesses ranging upwards from 50 micrometers. The buffer solution depth must be quite thin if high-magnification objectives having large numerical apertures and short working distances are to be employed. In many cases, the downward pressure of the glass prism upon the substrate plate may be adequate to seal the specimen chamber without additional clamping, but many chamber designs (Figure 17.9) include mechanisms to secure the substrate and glass coverslip.

In cases where a prism is employed (as opposed to a glass block) to achieve total internal reflection (see Figure 17.10(a)), the maximum incidence angle is obtained by introducing the laser beam from the horizontal direction. For standard glass (having a refractive index

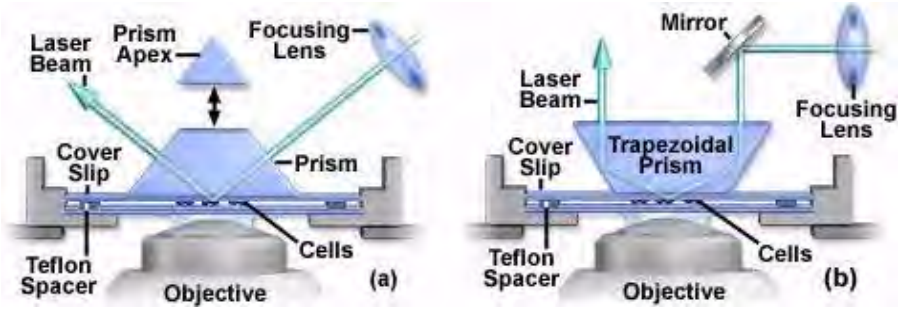

FIGURE 17.10: Inverted microscope TIR prism configuration

of 1.52), the maximum incidence angle is 73 degrees for a right angle prism and 79 degrees for an equilateral prism. Phase contrast and other transmitted light techniques are not compatible with this configuration because the upper surface of the triangular prism is not flat. However, custom truncation and polishing of the prism top (presented as an option in Figure 17.10(a)) produces a surface that can easily pass incident light from above by an inverted microscope condenser system.

When mounted on the microscope condenser unit, a 60-degree trapezoidal prism (Figure 17.10(b)) is the most convenient and reproducible configuration yet developed for TIRFM above the stage on an inverted instrument. The incoming laser beam is vertical, so the total internal reflection area shifts laterally to a very small degree when the prism is raised and relowered during specimen changes. In addition, conventional transmitted light techniques (phase contrast, brightfield, etc.) are compatible with this experimental design. Because the incident angle is fixed at 60 degrees, ordinary optical glass (refractive index of 1.52) is not able to support total internal reflection, and a prism having a high refractive index is required. Prisms fabricated with flint glass (refractive index of 1.64) will meet these specifications, and are commercially available. The beam will then refract away from the normal at an angle of 69 degrees in passing from the prism into the coverslip, thereby exceeding the critical angle at the coverslip/buffer or coverslip/cell interface. A trapezoid with walls ranging between 45 and 60 degrees is ideal, but these units are not readily available and must be manufactured to custom specifications. Unfortunately, 45 or 60-degree trapezoids are also not commercially available, but they can be cheaply produced by truncating and polishing the apex of a commercially available triangular prism.

Presented in Figure 17.11 is a fourth configuration utilizing a parabolic mirror and hemispherical prism to conduct TIRFM experiments with an inverted microscope. In this design, the mirror and prism are positioned so that the laser beam traverses a radius of the prism toward a total internal reflection target area at the focus of the parabolic mirror. Because the light rays enter the prism almost normal to the face at all incidence angles, aberration of the beam profile is reduced compared to that observed with a cube or rectangular prism block. A lateral shift of the vertical incoming laser beam will always focus at the same spot, enabling substantial and convenient changes to the incident light angle. In addition, interference fringes in the evanescent field can be created by splitting the incoming beam into two components, each reflecting at a separate azimuthal position in the parabola, but recombining at the parabolic focal point. The fringe spacing can be varied by adjusting the relative azimuthal positions of the two incident beams, and very high spatial frequencies can be attained. Interference fringes can be employed as an aid

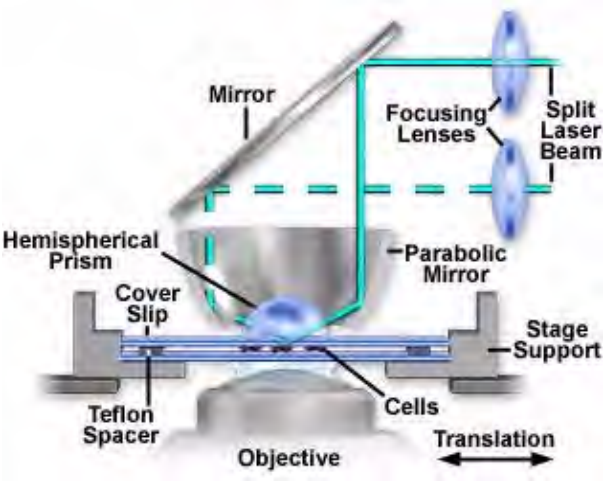

FIGURE 17.11: TIR interference fringe configuration

to focusing on the interface by creating a parallel line interference fringe pattern. This pattern can be observed in fluorescent regions of cell/substrate contact, which confirms the excitation source as the evanescent field (rather than light randomly scattered from the field by cells). Interference patterns are also useful in studies of surface diffusion rates to measure the lateral mobility of membrane components in contact regions. Despite the versatility of this design (Figure 17.11), alignment is very difficult and the system is more sensitive to vibrations.

The inverted microscope TIRFM configurations reviewed here all share some advantages and disadvantages. Among the major advantages are the ability to utilize rather inexpensive optics with ample room on the microscope stage to position the specimen and glass block/prism and supporting optical components. In addition, the prism may be mounted on the condenser holder (housed above the stage on modern inverted microscopes) for ease in raising and lowering, and for auxiliary observation with conventional optical techniques. Finally, these optical arrangements enjoy simplicity in design and are the easiest systems to align for total internal reflection.

Among the chief disadvantages of inverted microscope configurations is the fact that the specimen is not easily accessible from above and conventional illumination is hampered by the prism apex. Also, the shortest working distance objectives may not reach focus across the buffer layer, and image quality with high numerical aperture objectives is reduced due to spherical aberration when viewing specimens through the relatively thick buffer layer.

Alignment of inverted microscope systems with a prism or glass block involves centering the total internal reflection region directly over the objective while the specimen is in sharp focus. The first step is to assemble the specimen chamber and prism combination, then bring the specimen into focus using brightfield illumination (even in cases where the prism apex is present). Next, with the laser-focusing lens removed, direct the beam so that it undergoes total internal reflection over the center of the objective front lens. This can be observed by looking directly (not through the microscope eyepieces) for scattered incident light in the prism, immersion layer, and substrate plate. After re-inserting the focusing lens, adjust its position so that the focused laser beam enters the prism side surface approximately one millimeter above the bottom edge. Directly viewing the beam should reveal three co-linear spots of scattered light at the bottom of the prism: two on the

FIGURE 17.12: Substrate/prism inverted TIF configuration

outside where the beam traverses the immersion layer, and a central spot where the beam undergoes total internal reflection on the specimen. The focusing lens should be adjusted so the middle spot is visible as an elongated cylindrical area. The position and size of the total internal reflection region can be adjusted with the focusing lens translators and by moving the lens longitudinally to optimize the illumination region dimensions.

The shape of the total internal reflection area is dependent upon the orientation of the prism or glass block side surface, where the laser beam enters. If the side is vertical (as in a block or rectangle), the area will be elongated to a degree that is a function of beam convergence. As previously discussed, elongation is due to aberration introduced by the large refraction angle at the first surface of the prism or glass block. On the other hand, if the side surface is angled so the collimated laser beam enters at an angle close to the perpendicular, then the reflection area will resemble a less-elongated conical section, which is expected from slicing a cylindrical beam at an angle.

In all of the optical configurations described above, the illuminated region will remain stationary in the center of the viewfield as the specimen is scanned in the lateral dimensions. However, when the microscope stage is moved during focus, the illuminated region may move laterally as the specimen is focused, depending upon whether the focusing lens and beam director are mounted on the laboratory bench or the microscope stage.

The total internal reflection spot should be focused to a width no larger than the field of view. If the spot is too large, spurious scattering and out-of-focus fluorescence from the immersion oil layer between the prism and coverslip will increase the otherwise low fluorescence background that is possible with TIRFM. Another artifact occurs at incident angles very near the critical minimum, which is manifested by a noticeable shadow cast by the cells along the surface of the interface. This can be avoided by making certain the incidence angle exceeds the critical angle by several degrees.

When the incident angle is near the critical value, it is sometimes difficult to ascertain whether total internal reflection has been achieved. In this case, viewing the resulting fluorescence intensity through the microscope eyepieces can often help the investigator determine if the instrument is properly configured. Fluorescence emission from a TIRF interface is quite distinct from that excited by an incident beam propagating at a subcritical "skimming" angle through the aqueous buffer. Because the evanescent wave (unlike the propagating beam) is far shallower than the objective depth of focus, fluorescence appears to originate from a single plane when excited by total internal reflection. In contrast, epi-illumination (from a subcritical beam) excites fluorophores throughout the bulk of the

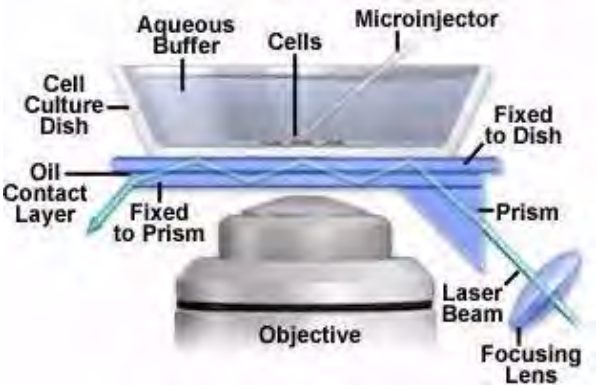

FIGURE 17.13: Inverted TIF substage prism configuration

specimen chamber and secondary fluorescence is observed over a wide range of focal planes.

For local qualitative intensity measurements in total internal reflection experiments, it may be desirable to limit the area from which emission light is gathered. Often the illuminated area is not likely to be very small, but a defined surface area can be obtained with an adjustable diaphragm strategically placed at an image plane in the emission light pathway.

Several additional TIRFM configurations involving inverted microscopes have been employed by investigators. The system illustrated in Figure 17.12 presents an alternative system that fixes the prisms with respect to the specimen instead of the laser beam. Illuminating laser light enters from the right through an entrance prism, and is refracted into the substrate where it propagates toward the microscope's optical axis via multiple internal reflections. Along the way, the multiply reflected beam encounters the specimen (tissue culture cells adhering to the glass coverslip) and illuminates chromophores in the region of the glass/buffer interface. After passing through the specimen and substrate, the reflected beam passes into the exit prism, which directs the light away from the experiment. In this configuration, the illuminated reflection area will move when the specimen is translated.

A more useful configuration that is compatible with simultaneous microinjection or patch clamp experiments is presented in Figure 17.13. In order to provide easy and continuous access from above to a tissue culture bathed in buffer, the prism is deployed below stage level to contact the substrate glass. This configuration, which cannot be employed for all inverted microscopes, suffers from tight geometry because the objective also resides in the immediate area. Like the system illustrated in Figure 17.12, the substage prism initiates multiple total internal reflection in the coverslip, which transfers excitation light as a waveguide from far off-axis to the center of the viewfield.

In the simplest form, a small triangular prism (commercially available) is placed, via immersion oil or glycerol, in optical contact with the bottom of the coverslip containing the cells and buffer solution. The specimen can be translated while the prism remains laterally fixed, although a smear of oil may be left on the lower side of the coverslip that can destroy the first internal reflection (and the experiment). A feasible alternative is to employ an additional intervening coverslip fixed to the prism with optically transparent glue. The sliding motion occurs between the intervening coverslip and the cell coverslip, which are in optical contact and lubricated by a thin layer of immersion oil or glycerol. A major disadvantage of this configuration is that oil or glycerol immersion objectives

FIGURE 17.14: Upright microscope TIR configuration

cannot be used because the immersion medium could destroy the internal reflections prior to formation of the illumination spot. However, air (dry) or water immersion objectives work very well under these circumstances.

17.2.2 Upright Microscope Configuration

A trapezoidal prism, similar to the one illustrated in Figure 17.10(b), can be mounted on the condenser support frame in an upright microscope to observe phenomena at the total internal reflection interface of specimens positioned on the stage (Figure 17.14). The expanded laser beam is introduced into the microscope base using the same port intended for the transmitted light illuminator (which should be removed). A long focal length (approximately 250 millimeters) converging lens placed near the entrance port and mounted on an x-y translator is utilized to focus the incoming laser beam and allow fine-tuning of the lateral position. Collimated laser illumination can then take advantage of the microscope's built-in optical train to direct the beam through the base and vertically upward into the prism. An extra lens positioned just above the microscope base is often useful to translate and focus the total internal reflection spot. This configuration does not offer a great deal of flexibility in adjusting the incidence angle, but a limited range of values can be achieved by employing several trapezoids having differing angular geometries and refractive indices. Images are collected through the cooled scientific CCD digital camera illustrated in Figure 17.11, but a photomultiplier or avalanche photodiode could easily be substituted.

Choice of prism glass is limited by refractive index requirements, with flint glass (refractive index of 1.62) being the preferred formulation. With a 60-degree incidence angle, the refractive index of the prism must be at least 1.53 in order for total internal reflection to occur at the glass/water interface (regardless of the substrate material). This is why flint glass, rather than ordinary optical (crown) glass or fused silica, is the ideal prism material for these experiments.

The illuminating laser light is reflected into the prism by the substage microscope mirror, and refracted through the glass by the angular sides of the prism. Because trapezoidal prisms cut in custom dimensions are not commercially available, the rhombic cross-section is manufactured by truncating and polishing the top of an easily obtainable equilateral triangle prism. The focusing lens is removed for positioning of the laser trajectory, which is adjusted to enter the bottom of the prism off-center where it totally internally reflects at the sloping side and proceeds toward the upper surface at an incidence angle of 60 degrees. When the focusing lens is inserted into the light path, the beam follows the same course but is much thinner and more intense.

The specimen chamber, which may be a plastic culture vessel or Petri dish, is placed on the microscope stage for observation. A small drop of immersion medium (glycerol or oil) is placed on the prism top, and it is brought into optical contact with the lower surface of the culture chamber by raising the substage condenser rack mechanism. The laser beam position is then adjusted by the focusing lens translator to totally internally reflect at the upper surface of the chamber (or substrate) and follow a symmetrical course back down toward the microscope base on the opposite side of the prism. This setup is suitable for many types of substrate, but is particularly well-adapted for viewing cells growing on the bottom of plastic culture dishes. The cells may then be viewed in the same chamber in which they were originally seeded and incubated without any remounting step. Observing the specimen in a upright microscope enables the investigator to simultaneously probe the cells with micropipettes, patch clamps, and injection syringes, provided the objective has a sufficient working distance.

Secondary fluorescence emission may be collected by a dry, oil, or water immersion objective (after decanting most of the buffer) through a coverslip that is suspended above the cell monolayer surface by a spacer. Alternatively, a water immersion objective with a dipping cone can be placed directly into the buffer solution bathing the cells. The upright microscope configuration is very convenient, because specimens may be interchanged easily as they are with standard illumination systems. The position of the TIRF illumination area is also stationary and unaffected by focusing, even on a moving-stage microscope, which accounts for a vast majority of modern upright microscope designs. The chief disadvantage is that the incident illumination angle is not adjustable without switching to another prism with a different slope angle.

An upright system provides high quality images when water immersion objectives are submerged to image cells directly through the buffer solution in an uncovered Petri dish or culture chamber, but the configuration does present several drawbacks. Many of the polymer formulations used in culture vessel construction have some degree of autofluorescence, which may reduce contrast in weakly fluorescent specimens. This effect can be compounded if the immersion-coupling medium is not carefully chosen. Several commercial brands of immersion oil also display autofluorescence at varying levels, and investigators are cautioned to examine both immersion oils and plastic culture vessels for potential fluorescence artifacts before they are used in TIRFM experiments. Different brands of tissue

culture plastic have significant variations in the amount of autofluorescence displayed upon excitation.

The prism, slide, chamber windows, and coverslips can be made with ordinary flint optical glass for most applications, unless shorter penetration depths arising from higher refractive indices are desired. Optical glass does not transmit light below about 310 nanometers and also has a dim autoluminescence with a long decay time, which can be a problem in some photobleaching experiments. The autoluminescence of high quality fused silica (quartz) is much lower. More exotic high refractive index materials, such as sapphire, titanium dioxide, and strontium titanate, do not suffer from high levels of autofluorescence and yield evanescent field penetration depths more than an order of magnitude lower than the illumination wavelength.

17.2.3 Detection of Fluorescence

Unlike confocal and multiphoton microscopy, many TIRFM images can be recorded on film in a manner similar to the classical forms of microscopy that rely heavily on photomicrography (brightfield, darkfield, phase contrast, differential interference contrast, etc.). In some cases, especially when only a few fluorophores are present in the specimen, it is advisable to use more sensitive imaging devices, such as a intensity-enhanced video camera, cooled scientific CCD, avalanche photodiode, or a photomultiplier. Time-lapse cinemicrography is also possible in TIRFM experiments, and the sequence of image frames can be captured with any of the devices mentioned above, the choice of which will depend upon the intensity of secondary fluorescence and the exposure times necessary to acquire images. Richly fluorescent specimens can be recorded on film (singly or in a sequence of frames), but image acquisition with a video or CCD camera is far more convenient with the current hardware readily available to investigators.

A significant amount of versatility is afforded when images are acquired with a photomultiplier tube or avalanche photodiode. Photomultipliers are often employed for spatially unresolved but fast detection and quantitation of fluorescence intensity. Variable apertures and/or image plane diaphragms (discussed above) enable the investigator to selectively capture only portions of the fully available field. This is useful when long sampling intervals at low-light levels are necessary, or when only part of the viewfield is of interest. The photomultiplier spectral characteristics should be considered when choosing a device for image collection, and these should coincide with the emission properties of the fluorophores to be examined.

17.2.4 Conclusions

In general, total internal reflection is more difficult to implement on a microscope that has a moveable stage because focus adjustments require realignment of the laser beam into the focal plane and optical axis of the microscope. When choosing a microscope for TIRFM investigations, pay attention to the mechanical stability and construction motif of the instrument. Inverted or upright microscopes with a heavy frame on an isolation table will enable the investigator to establish a relatively vibration-free environment for the fragile evanescent field. Maintaining a focused laser illumination source within a range of a few microns over long periods is difficult (at best), but can be accomplished when the microscope, laser source, and supporting optical components are secured in proper mounts and firmly fastened to the bench or microscope stage.

A wide range of microscope objective designs are compatible with TIRFM experiments. The only absolute requirement is that the objective have a long enough working distance to observe the interface across a thin gap of buffer solution defined by the spacer thickness. Teflon and Neoprene spacers can be made thinner than any standard objective working distance, while still being much larger than the penetration depth of the evanescent field. This reduces the likelihood of being unable to focus on the interface, but does not compensate for potential aberrations resulting from refractive index variations in the specimen/buffer region. Correction of spherical aberration in most high-magnification objectives is critically dependent upon the specimen being immediately on the far side of a coverslip rather than across an additional thin water layer. The result can be an image lacking in contrast and producing a hazy image even when sharply focused. No general rule for objective specifications can be provided, but water immersion objectives (either dipping or those requiring a coverslip) are probably the best (and most expensive) choice. On the other hand, TIRFM experiments have been successfully conducted with objectives of almost every commercially available numerical aperture and magnification.

During many investigations, it is desirable to switch rapidly between illumination of the interface by total internal reflection and deeper penetration into the bulk of the specimen by classical epi-fluorescence illumination. As an example, a transient process may involve simultaneous, but somewhat different, changes in both the membrane and cytoplasm, both of which must be recorded. Specially designed optoelectronic systems that take advantage of acousto-optic modulators have been described by several investigators. These configurations are computer-controlled and usually contain several modulators that act in synchrony to oscillate illumination between TIRF and epi-fluorescent widefield, while simultaneously collecting data with a photomultiplier or fast-response photodiode device.

The glass surface supporting cell adhesion is often coated with specific substrates for TIRFM investigations. Chemical derivatives of the silicon dioxide surface can yield unique physical and chemical absorption properties that are useful in modulating the formation of model membranes and similar structures. In addition, the covalent attachment of certain specific chemicals is particularly useful in cell biology and biophysics. Cell adhesion can be enhanced by attachment of poly-L-lysine to the glass surface, and hydrophobic surfaces can be created with long-chain hydrocarbons for lipid monolayer absorption. Other useful molecules that can be used to treat the surface for selective specificity include antibodies, antigens, planar phospholipids, and lectins.

Thin layers of aluminum (in the region of 20 nanometers), which can quench fluorescence, can also be applied to the glass surface by standard vacuum evaporation. The deposition thickness can be precisely controlled by completely evaporating a pre-measured constant amount of aluminum. After deposition, the upper surface of the aluminum film spontaneously oxides in the atmosphere to produce a thin layer of aluminum oxide. The oxide-coated film has chemical properties similar to silicon dioxide and can be derivatized by organosilanes in a manner similar to that of glass. The ability of a metal film to almost completely quench fluorescence of those fluorophores within about 10 nanometers allows suppression of the signal from labeled proteins that are nonspecifically absorbed to the substrate. This occurs while permitting fluorescence from the slightly more distant labeled protein adsorbed to an adherent membrane.

Unlike confocal microscopy, which produces optical sections by exclusion of out-of-focus emitted light with a set of image plane pinhole diaphragms, TIRFM is limited to the area within a few hundred nanometers of the glass/buffer interface where total internal reflection

is occurring. Confocal microscopy has a clear advantage in versatility because optical sectioning works at any plane of the specimen and is not restricted to an interface between dissimilar refractive indices. However, TIRFM does have several advantages including a much thinner optical section (around 100 nanometer versus 600 nanometers for confocal), selective illumination of the immediate area adjacent to the interface, and the ability to (relatively inexpensively) adapt existing microscopes to take advantage of the technique.

Part III

Contrast Enhancing techniques

Chapter 18

Contrast in Optical Microscopy

When imaging specimens in the optical microscope, differences in intensity and/or color create image contrast, which allows individual features and details of the specimen to become visible. Contrast is defined as the difference in light intensity between the image and the adjacent background relative to the overall background intensity. In general, a minimum contrast value of 0.02 (2 percent) is needed by the human eye to distinguish differences between the image and its background. For other detectors, such as film, video cameras, or photodetectors (CCD and CMOS devices), the minimum contrast is often a different value. With each detector, the signal–to–noise ratio (noise is all of the light in the optical system devoid of image information) must be large enough to be interpreted in terms of the formation of a coherent image.

Contrast produced in the specimen by the absorption of light, brightness, reflectance, birefringence, light scattering, diffraction, fluorescence, or color variations has been the classical means of imaging specimens in brightfield microscopy. The ability of a detail to stand out against the background or other adjacent details is a measure of specimen contrast. In terms of a simple formula, contrast can be described as :

$$\%\text{Contrast}(C) = 100 \cdot \frac{\text{I}(s) - \text{I}(b)}{\text{I}(b)}$$

Where I(b) is the intensity of the background and I(s) is the specimen intensity. From this equation, it is evident that specimen contrast refers to the relationship between the highest and lowest intensity in the image. The graph shown in Figure 18.1 illustrates the effect of background intensity on contrast. When the background is a very dark gray color (I(b) equals 0.01), a small change in image intensity produces a large change in contrast. By lightening the background to a somewhat lighter gray color (I(b) equals 0.10), small changes in image intensity provide a useful range of contrast. At still lighter background colors (I(b) ¿ 0.20), image contrast is relatively insensitive to background intensity and large changes in I(b) produce only small increases or decreases in image contrast.

Although the optical systems found in modern microscopes may be capable of producing high resolution images at high magnifications, such a capability is worthless without sufficient contrast in the image. Contrast is not an inherent property of the specimen, but is dependent upon interaction of the specimen with light and the efficiency of the optical system coupled to its ability to reliably record this image information with the detector. Control of image contrast in a microscope optical system is dependent upon several factors, primarily the setting of aperture diaphragms, degree of aberration in the optical system,

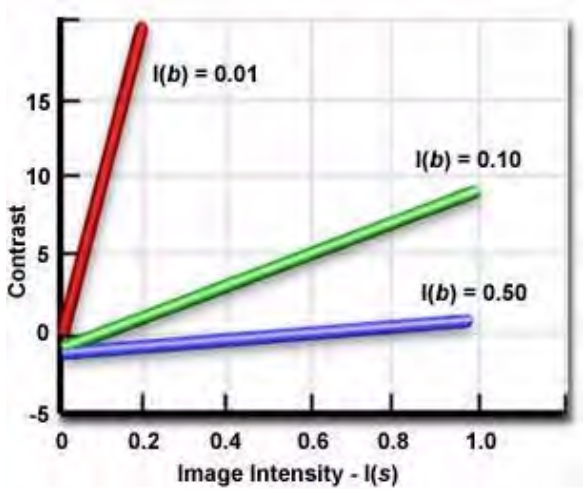

FIGURE 18.1: Background intensity effect on contrast

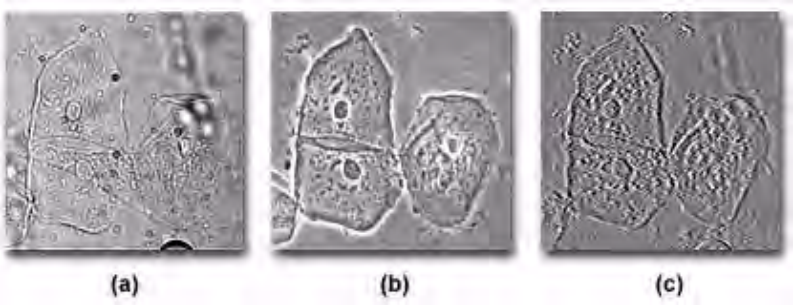

FIGURE 18.2: Transmitted light contrast mode

the optical contrast system employed, the type of specimen, and the optical detector. There are several sites in the microscope that allow adjustment of contrast. These consist of the field aperture, condenser aperture, additional magnification for video detectors, electronic camera gamma, film gamma, printing paper gamma, image processing in real time, as well as specimen staining.

Because the human eye perceives an object by the contrast generated in its image, one can be easily led astray unless there is knowledge of the optical events that occur to produce contrast in the image. Figure 18.2 illustrates three photomicrographs of the same viewfield containing transparent, colorless human cheek cells imaged with an optical microscope under differing contrast modes: brightfield, phase contrast, and Hoffman modulation contrast. It is quite apparent that the three images appear different, and because of these variations, a microscopist might arrive at a different conclusion from each viewfield. The cells illustrated in Figure 18.2(a) were imaged with a microscope operating in brightfield mode with the condenser aperture closed down enough to render the specimen edges visible.

An identical viewfield of the cheek cells using phase contrast optics is shown in Figure 18.2(b). Note the dark inner areas and the bright outer areas surrounding the edges of objects such as the cell membranes and nuclei (called halos, and are artifacts). In this view, it is difficult to specify the edges of the cells and to interpret the cause of the dark

and light areas in the image. The cells also appear quite flat. Finally, the cells illustrated in Figure 18.2(c) were imaged using Hoffman modulation contrast, where one side of the image is dark while its opposite side is bright, leading to the perception of a pseudo three-dimensional object. Each viewfield in Figure 18.2 provides a different specimen image and leads to different interpretations, which can only be deciphered with knowledge about how the microscope created these images.

For many specimens in optical microscopy, especially unstained or living material, contrast is so poor that the specimen remains essentially invisible regardless of the ability of the objective to resolve or clearly separate details. Often, for just such specimens, it is important not to alter them by killing or treatment with chemical dyes or fixatives. This necessity has led microscopists to experiment with contrast enhancing techniques for over a hundred years in an attempt to improve specimen visibility and to bring more detail to the image without altering the specimen itself. It is a common practice to reduce the condenser aperture diaphragm below the recommended size or to lower the substage condenser to increase specimen contrast. Unfortunately, while these maneuvers will indeed increase contrast, they also seriously reduce resolution and sharpness.

It is useful to consider the characteristics of how light and matter interact before discussing methods of controlling contrast in the light microscope. Light responsible for illuminating the specimen may be either spatially coherent, incoherent, or partially coherent. For example, the light beam can be shaped in the form of a slit or annulus, and can be composed of selected wavelengths that vibrate in all directions perpendicular to the direction of propagation or in a single direction due to polarization.

Some specimens are considered amplitude objects because they absorb light partially or completely, and can thus be readily observed using conventional brightfield microscopy. Others that are naturally colored or artificially stained with chemical color dyes can also be clearly imaged with the microscope. These stains or natural colors absorb some part of the white light passing through and transmit or reflect other colors. Often, stains are combined to yield contrasting colors, e.g. blue hematoxylin stain for cell nuclei combined with pink eosin for cytoplasm. It is a common practice to utilize stains on specimens that do not readily absorb light, thus rendering such images visible to the eye.

Other specimens do not absorb light and are referred to as phase objects. Because the human eye can only detect intensity and color differences, the phase changes due to objects must be converted to intensity differences. Phase specimens are characterized by several criteria including their shape (typically round or flat), the density of internal light scattering elements, thickness, and unique chemical or electrical structural properties (collectively grouped as refractive index). Thick specimens may be relatively clear and contain only a few light scattering elements, or they may contain many scattering elements that do not pass light and make the specimen effectively opaque to transmitted illumination. These specimens are often termed reflected light specimens.

When considering optical methods to enhance specimen contrast, it is useful to consider various characteristics of a specimen that can be manipulated to create intensity variations of those characteristics to render them visible. A primary question is which characteristic of the object will be transformed into a different intensity under a unique set of circumstances.

Specimen details and edges that have a size approximating the wavelength of imaging light will diffract or scatter light, provided there is a difference in refractive index between the specimen and its surrounding medium (the surround). Refractive index is defined as the ratio of the speed of light through air or a vacuum divided by the speed of light through

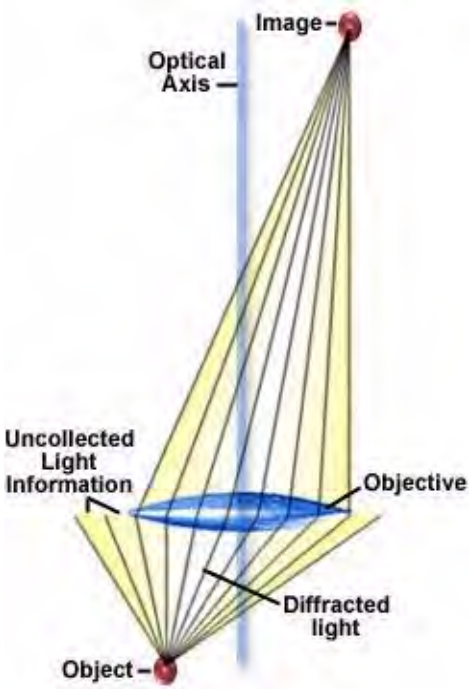

FIGURE 18.3: Diffracted light gathered by an objective

the object. Because the speed of light through any material is less than the speed of light in a vacuum, the refractive index always exceeds a value of 1.0 for specimens examined with a microscope. In order to resolve small distances between objects and to reproduce their shape with reasonable fidelity, a large angle of diffracted light must be captured by the microscope objective.

Diffracted (or deviated) light gathered by the objective must be brought into a sharp focus at the image plane in order to generate specimen detail, as illustrated in Figure 18.3. At the image plane, light waves comprising the diffracted light undergo interference with undiffracted light. The visibility of light after interference is very much dependent upon the coherency of light illuminating the specimen, with visibility increasing proportionally by increasing coherence. In the optical microscope, the condenser aperture diaphragm opening size controls the spatial coherence of light impinging on the specimen. Decreasing the diaphragm opening size yields a greater spatial coherence.

Microscopists have long relied on decreasing the condenser aperture diaphragm opening size to increase visibility of particles and edges in phase specimens. Contrast for amplitude objects can also be improved by proper adjustment of the condenser aperture. Small objects, edges, and particles will diffract light regardless of whether they belong to an amplitude or phase specimen. Only a portion of this diffracted light is captured by the objective (see Figure 18.3) due to numerical aperture limitations of the objective. Remaining diffracted light that is not collected represents image information that is lost. The correct setting for the condenser aperture diaphragm opening size is a tradeoff between enhancement of specimen image contrast and the introduction of diffraction artifacts. These are manifested in a loss of resolution, superimposition of diffraction rings, and other undesirable optical effects originating from regions in the specimen that are not in common focus. As the diffraction limit is approached, image contrast becomes lower as object details become

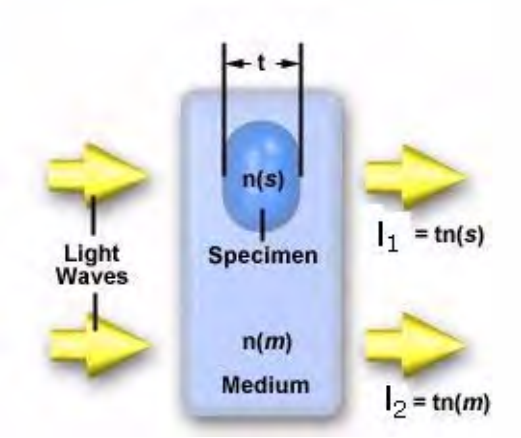

FIGURE 18.4: Optical path difference in phase object

smaller and spatial frequencies become larger.

Inouè and Spring have described the ratio of image contrast to specimen contrast and the phase shift in positions occupied by the actual and idealized sinusoidal image as the optical transfer function (OTF) when plotted as function of spatial frequency. In cases where the distribution of light from the specimen becomes sinusoidal, the modulus of the optical transfer function becomes the modulation transfer function (MTF). As the spatial frequency increases, the modulation transfer function decreases and specimen contrast is reduced.

For each objective, the specific modulation transfer function is dependent upon the objective design and numerical aperture, the mode of contrast generation, wavelength of illuminating light, and the numerical aperture of the substage condenser. The edge of the objective rear focal plane acts as a low pass filter for the diffracted light, which must be focused at the image plane for interference to occur and form the image of the particle or edge. Focusing a microscope brings these diffracted light waves together at the intermediate image plane. The angle of the light wavefront with respect to the specimen determines the degree of difficulty in focusing on the top or bottom of smooth rounded surfaces, which usually contain no diffraction sites. However, the edges of spherical specimens or fibers are easily focused because the edge interface is at a sufficient angle to the wavefront and diffracts light.

When discussing phase specimens, we will define an object as any resolvable portion of the specimen. Many objects will be flat or plate-like as illustrated in Figure 18.4. In this figure, the object has a thickness (t) and a refractive index, n_s. The refractive index of the surrounding medium is n_m.

Light travels through the specimen with an optical path, $l_1 = t \cdot n_s$, and through the surrounding media with an optical path, $l_2 = t \cdot n_m$. The optical path difference (OPD) can be expressed as:

$$OPD = t \cdot n_s - t \cdot n_m = t \cdot (n_s - n_m)$$

With the phase difference being:

$$\delta = \frac{2\pi}{\lambda}(OPD)$$

The optical path difference is the product of two terms: the thickness (t) and the difference in refractive index (n). The OPD can often be quite large even though the thickness of the

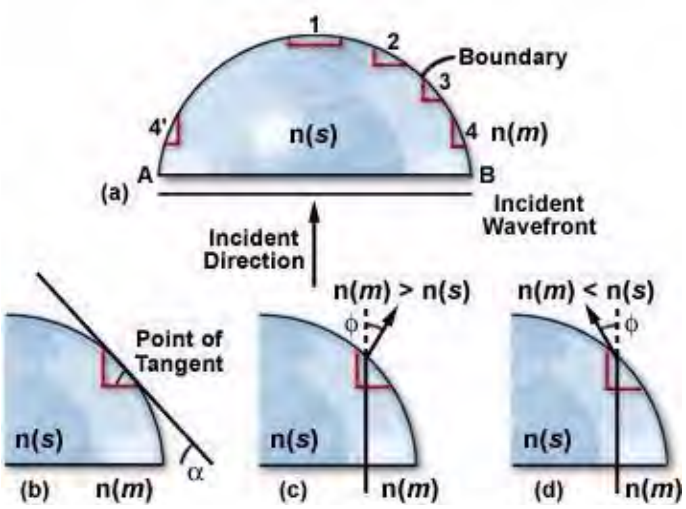

FIGURE 18.5: Continuous optical gradient in phase object

object is quite thin. On the other hand, when the refractive indices of the specimen and the surrounding medium are equal, the OPD is zero even if the specimen thickness is very large. In this case, light traveling through the object is merely delayed (a phase difference) relative to the light passing an equal thickness of the surround. Phase differences are not detectable by the human eye.

The phase contrast microscope is designed to take advantage of phase differences between objects in a specimen and in the surrounding medium. However, it is not simply a phase difference that is necessary, but also diffraction from the specimen must occur for the phase contrast microscope to work.

The most common shape of a phase object is one of continuously changing optical path or density, such as the hemispherical specimen illustrated in Figure 18.5. In this instance, the sides of the phase object can be approximated mathematically by a prism shape, as discussed below. The refractive index of the phase object in Figure 18.5 is designated n(s) and that of the surrounding medium, n(m). Radical geometrical transitions in shape for the phase object occur only at edges A and B (see Figure 18.5(a)). Incident light impacts the object perpendicular to the plane AB, while the plane wavefront is parallel to AB.

The boundary at 1 (the apex of the rounded phase object in Figure 18.5(a)) is essentially parallel to the incident wavefront whereas the boundaries at A and B are perpendicular. Regions 2 through 4 are miniature prisms defined by a tangent to the rounded surface of the phase object (Figure 18.5(b)). The "prism" angle is lesser at region 2 than at region 4, which is opposite to region 4'. At edges A and B diffraction is strongest.

Thus, curved objects are composed of many prisms and opposite sides of the object have prisms oriented in opposite directions. The steepest prisms are at the equator of a spherical object, while prisms with the least slope are located at the top and bottom. These miniature prisms form an optical gradient:

$$\phi = \alpha(n_s - n_m)$$

Where α is the angle of the tangent with respect to the plane wavefront. Notice that the optical gradient is the product of two terms: the angle (α) between the sides that the light passes, and the difference in refractive index $n_s - n_m$. Light that passes through a

prism changes direction by the angle ϕ (see Figure 18.5(c) and 18.5(d)). The change in direction could be large, even though the slope or boundary gradient may be small, if the difference in refractive index is large. If the refractive indices are identical, the light wave passes through the phase object unrefracted. The direction of light exiting the prism is dependent on the relative difference in refractive indices between the phase object n_s and its surrounding medium (n_m; see Figure 18.1(c) and 18.1(d)).

As we have discussed above, rounded phase objects have continuously varying optical gradients, and each individual optical gradient "prism" creates a different angle of light deflection. Figure 18.5(c) illustrates the direction of deflection when the surrounding medium has a refractive index greater than the phase object ($n_m > n_s$), and Figure 18.5(d) shows the direction when the opposite is true ($n_m < n_s$). The angle of deflection, ϕ, is proportional to the tangent angle (α) and the difference in refractive index ($n_s - n_m$), such that:

$$\tan \phi = (n_s - n_m) \cdot \tan \alpha$$

For small angles:

$$\phi = \alpha(n_s - n_m) \text{ (in radians)}$$

To summarize the "prism" effect of optical gradient boundaries, when the refractive index of the phase object exceeds that of the surrounding medium, gradients of equal size on each slope of the object deflect at the same angle. This deflection angle is dependent upon the relative refractive index difference and the geometric tangent angle (a). When the refractive index of the medium (n(m)) is greater than the refractive index of the object (n(s)), the deflection is opposite from when the situation is reversed. When there is no gradient, there is no deflection of light passing through.

Light can interact with a specimen through a variety of mechanisms to generate image contrast. These include reflection from the surface, absorption, refraction, polarization, fluorescence, and diffraction. Contrast can also be increased by physical modification of the microscope optical components and illumination mode as well as manipulation of the final image through photographic or digital electronic techniques. The following discussion highlights various interactions between the specimen and light and reviews some of the optical microscopy techniques that have been developed to enhance specimen contrast.

When incident illumination strikes an opaque surface, it is reflected in a manner that is specific to the terrain of that surface. Very smooth surfaces reflect light at an angle equaling that of the incident light, a mechanism known as specular reflection. Uneven or diffuse surfaces tend to reflect light at all possible angles by a phenomenon known as diffuse reflection, resulting in a reduced amount of light entering the objective. Contrast in reflected light microscopy can be enhanced by careful specimen preparation. Metallographic samples are often etched with reactive liquids and gasses to reveal grain boundaries and/or polished to increase the amount of light reflected into the microscope. Stains, in the form of fluorescent dyes, thin films, and metallic coatings, are also used to introduce contrast in reflected light microscopy specimens. Birefringent specimens can be imaged using polarized reflected light and transparent phase objects are often the subject of observation using techniques such as reflected differential interference contrast, darkfield illumination, and Hoffman modulation contrast.

The human eye is very sensitive to amplitude and wavelength differences in a specimen. For this reason, many specimens are cut into very thin sections (ranging from 1—30 microns in thickness) and stained with chemical dyes to increase contrast and to differentiate between structures residing within the specimen. This technique has been quite commonly

used with biological specimens for several hundred years. Dyes selectively absorb light from one or several wavelengths and pass or reflect all other wavelengths. An example is a blue dye that absorbs all visible light wavelengths with the exception of blue, which is reflected from and transmitted through the specimen. Internal structural elements of a biological specimen are often stained with a mixture of dyes to selectively stain these elements, increasing their contrast against a background of material that is either transparent or stained a different color.

An early and currently used method of increasing contrast of stained specimens utilizes color contrast filters, Wratten lacquered gelatin squares (from Kodak), or interference filters in the light path. For example, if a specimen is stained with a red stain, a green filter will darken the red areas thus increasing contrast. On the other hand, a green filter will lighten any green stained area. Color filters are very valuable aids to specimen contrast, especially when black and white photomicrography is the goal. Green filters are particularly valuable for use with achromat objectives, which are spherically corrected for green light, and phase contrast objectives, which are designed for manipulation of wavelength assuming the use of green light, because phase specimens are usually transparent and lack inherent color.

Anisotropic materials usually exhibit two or more refractive indices and are thus termed birefringent, or doubly refracting. Among the specimens included in this category are minerals, crystals (which exhibit a high degree of structural symmetry), fibers, hairs, and other biological specimens. When light enters a non-optic (an axis other than the optic axis) axis of anisotropic crystals, it is refracted into two rays each polarized with their vibration directions oriented at right angles to one another, and traveling at different velocities. The resulting light waves are polarized and can interfere when recombined in the microscope analyzer to produce images of birefringent specimens that are highly colored and contain a significant amount of contrast.

Living specimens and other phase objects, which often yield poor images when viewed in brightfield illumination, are made clearly visible by optical rather than chemical means when viewed under phase contrast, Hoffman modulation contrast and differential interference contrast illumination. These techniques require special optical components in the microscope, but will usually produce images of sufficient contrast to reveal important details about specimen structure. A more thorough discussion of these contrast enhancing techniques can be found in our Specialized Microscopy Techniques section.

Another simple technique for contrast improvement involves the selection of a mounting medium with a refractive index substantially different from that of the specimen. For example, diatoms can be mounted in a variety of contrast-enhancing mediums such as air or the commercial medium Styrax. The difference in refractive indices improves the contrast of these colorless objects and renders their outlines and markings more visible. The following sections describe many of the more complex techniques used by present-day microscopists to improve specimen contrast.

Table 18.1 presents a summary of the contrast enhancing technique(s) of choice for a variety of specimens and materials that are studied with both transmitted and reflected light microscopy. This table may be used as a rough guide to approach specific imaging problems in optical microscopy.

TABLE 18.1: Contrast–Enhancing Techniques

Specimen Type	Imaging Technique
TRANSMITTED LIGHT	
Transparent Specimens Phase Objects Bacteria, Spermatozoa, Cells in Glass Containers, Protozoa, Mites, Fibers, etc.	Phase Contrast Differential Interference Contrast (DIC) Hoffman Modulation Contrast Oblique Illumination
Light Scattering Objects Diatoms, Fibers, Hairs, Fresh Water Microorganisms, Radiolarians, etc.	Rheinberg Illumination Darkfield Illumination Phase Contrast and DIC
Light Refracting Specimens Colloidal Suspensions powders and minerals Liquids	Phase Contrast Dispersion Staining DIC
Amplitude Specimens Stained Tissue Naturally Colored Specimens Hair and Fibers Insects and Marine Algae	Brightfield Illumination
Fluorescent Specimens Cells in Tissue Culture Fluorochrome-Stained Sections Smears and Spreads	Fluorescence Illumination
Birefringent Specimens Mineral Thin Sections Liquid Crystals Melted and Recrystallized Chemicals Hairs and Fibers Bones and Feathers	Polarized Illumination
REFLECTED LIGHT	
Specular (Reflecting) Surface Thin Films, Mirrors Polished Metallurgical Samples Integrated Circuits	Brightfield Illumination Phase Contrast, DIC Darkfield Illumination
Diffuse (Non-Reflecting)Surface Thin and Thick Films Rocks and Minerals Hairs, Fibers, and Bone Insects	Brightfield Illumination Phase Contrast, DIC Darkfield Illumination
Amplitude Surface Features Dyed Fibers Diffuse Metallic Specimens Composite Materials Polymers	Brightfield Illumination Darkfield Illumination
Birefringent Specimens Mineral Thin Sections Hairs and Fibers Bones and Feathers Single Crystals Oriented Films	Polarized Illumination
Fluorescent Specimens Mounted Cells Fluorochrome-Stained Sections Smears and Spreads	Fluorescence Illumination

Chapter 19

Darkfield Microscopy

Darkfield microscopy is a specialized illumination technique that capitalizes on oblique illumination to enhance contrast in specimens that are not imaged well under normal brightfield illumination conditions.

19.1 Darkfield Illumination

All of us are quite familiar with the appearance and visibility of stars on a dark night, this despite their enormous distances from the earth. Stars can be seen because of the stark contrast between their faint light and the black sky.

Yet stars are shining both night and day; they are invisible during the day because the overwhelming brightness of the sun "blots out" the faint light from the stars rendering them invisible. During a total solar eclipse, the moon moves between the earth and the sun blocking out the light of the sun–the stars can now be seen even though it is daytime; the visibility of the faint star light is enormously enhanced against a dark background.

This principle is applied in darkfield (also called darkground) microscopy, a simple and popular method for making unstained objects clearly visible. Such objects are often have refractive indices very close in value to that of their surroundings and are difficult to image in conventional brightfield microscopy. For instance, many small aquatic organisms have a refractive index ranging from 1.2 to 1.4, resulting in a negligible optical difference from the surrounding aqueous medium. These are ideal candidates for darkfield illumination.

Darkfield illumination requires blocking out of the central light which ordinarily passes through and around (surrounding) the specimen, allowing only oblique rays from every azimuth to "strike" the specimen mounted on the microscope slide. The top lens of a simple Abbe darkfield condenser is spherically concave, allowing light rays emerging from the surface in all azimuths to form an inverted hollow cone of light with an apex centered in the specimen plane. If no specimen is present and the numerical aperture of the condenser is greater than that of the objective, the oblique rays cross and all such rays will miss entering the objective because of their obliquity. The field of view will appear dark.

The darkfield condenser/objective pair illustrated in Figure 19.1 is a high-numerical aperture arrangement that represents darkfield microscopy in its most sophisticated configuration, which will be discussed in detail below. The objective contains an internal iris diaphragm that serves to reduce the numerical aperture of the objective to a value below that of the inverted hollow light cone emitted by the condenser. The cardioid condenser is a reflecting darkfield design that relies on internal mirrors to project an aberration-free

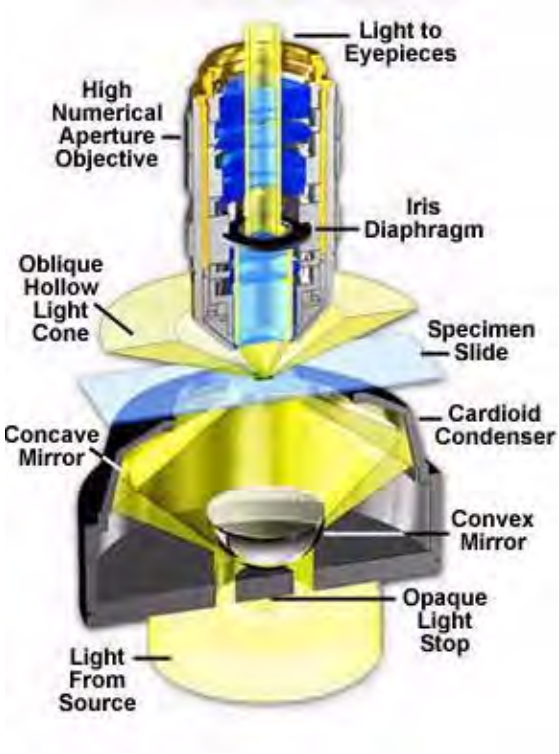

FIGURE 19.1: Cardioid darkfield condenser

cone of light onto the specimen plane.

When a specimen is placed on the slide, especially an unstained, non-light absorbing specimen, the oblique rays cross the specimen and are diffracted, reflected, and/or refracted by optical discontinuities (such as the cell membrane, nucleus, and internal organelles) allowing these faint rays to enter the objective. The specimen can then be seen bright on an otherwise black background. In terms of Fourier optics, darkfield illumination removes the zeroth order (unscattered light) from the diffraction pattern formed at the rear focal plane of the objective. This results in an image formed exclusively from higher order diffraction intensities scattered by the specimen.

The photomicrographs in Figure 19.2 illustrate the effects of darkfield and brightfield illumination on silica skeletons from a small marine protozoan (radiolarian) in a whole mount specimen. In ordinary brightfield, skeletal features of the radiolarian are not well

FIGURE 19.2: Radiolarian in brightfield and darkfield illumination

defined and tend to be washed out in photomicrographs recorded either with traditional film or digitally captured. The photomicrograph in Figure 19.2(a) was taken in brightfield illumination with the condenser aperture diaphragm closed to a point where diffraction artifacts obscure some of the sample detail. This enhances specimen contrast at the expense of image distortion. Under darkfield illumination (Figure 19.2(b)), more detail is present, especially in the upper portion of the organism, and the image acquires an apparent three-dimensional appearance. When a red filter is used in conjunction with a darkfield stop (Figure 19.2(c)), the radiolarian takes on a colorful appearance that is more pleasing, although no additional detail is produced and there is even some reduction in image quality.

Specimens that have smooth reflective surfaces produce images due, in part, to reflection of light into the objective. In situations where the refractive index is different from the surrounding medium or where refractive index gradients occur (as in the edge of a membrane), light is refracted by the specimen. Both instances of reflection and refraction produce relatively small angular changes in the direction of light allowing some to enter the objective. In contrast, some light striking the specimen is also diffracted, producing a 180 degree arc of light that passes through the entire numerical aperture range of the objective. The resolving power of the objective is the same in darkfield illumination as found under brightfield conditions, but the optical character is the image is not as faithfully reproduced (except when the iris diaphragm is used to lower the effective numerical aperture with high-magnification oil immersion objectives.

As in the example of starlight described above, the visibility is greatly enhanced by the contrast between the brightly shining specimen and the dark surround. As discussed above, what has happened in darkfield illumination is that all the ordinarily undeviated rays of the zeroth order have been blocked by the opaque stop. Oblique rays, now diffracted by the specimen and yielding 1st, 2nd, and higher diffracted orders at the back focal plane of the objective, proceed onto the image plane where they interfere with one another to produce an image of the specimen.

Ideal candidates for darkfield illumination include minute living aquatic organisms, diatoms, small insects, bone, fibers, hair, unstained bacteria, yeast, and protozoa. Non-biological specimens include mineral and chemical crystals, colloidal particles, dust-count specimens, and thin sections of polymers and ceramics containing small inclusions, porosity differences, or refractive index gradients. Care should be taken when preparing specimens for darkfield microscopy because features that lie above and below the plane of focus can also scatter light and contribute to image degradation. Specimen thickness and microscope slide thickness are also very important and, in general, a thin specimen is desirable to eliminate the possibility of diffraction artifacts that can interfere with image formation.

The substage condensers illustrated in Figure 19.3 demonstrate the effect of an opaque stop on light pathways through a simple refracting condenser. On the left (Figure 19.3(a)), is a typical Abbe brightfield condenser positioned with the aperture diaphragm opened to maximize the numerical aperture of the light cone. Light from the source passes through the aperture diaphragm and is then refracted through several lens elements to form an inverted cone of light with a numerical aperture of approximately 1.20. When an opaque spider-style light stop (Figure 19.3(b)) is inserted below the completely opened aperture diaphragm, the central light rays are blocked, allowing only peripheral light rays to pass through the lenses to form an inverted oblique hollow cone of light with no change in numerical aperture (1.20). The illuminating hollow light cone is formed by refraction of light at perimeter of the lens elements, where optical correction is often poorest. Even so, this condenser will

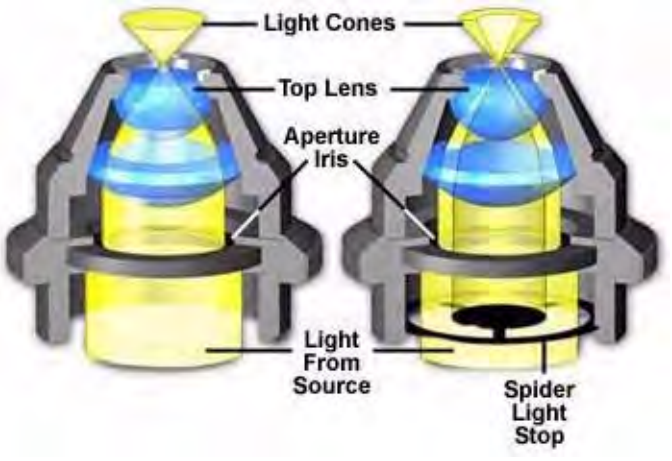

FIGURE 19.3: Abbe darkfield condenser

perform adequately using low magnification objectives, and produces very nice results for qualitative darkfield work. For more exacting quantitative microscopy, it is necessary to use aplanatic condensers (corrected for both chromatic and spherical aberrations), which perform much better by producing images with clearer detail and more reliable features.

In a darkfield microscope, if you were to look at the back of the objective through a Bertrand lens or phase telescope, it would appear filled with light. This faint diffracted light is reconstituted into the visible image at the plane of the eyepiece diaphragm with its contrast reversed, bright image on black background. Since darkfield microscopy eliminates the bright undeviated light, this form of illumination is very wasteful of light and thus demands a high intensity illumination source. Microscope slides must be of the appropriate thickness, approximately one millimeter +/- 0.1 mm. Specimen slides and all optical surfaces in the light path must be scrupulously clean because every dirt speck will be mercilessly bright.

There are several pieces of equipment that are utilized to produce darkfield illumination. The simplest is a "spider stop" placed just under the bottom lens (in the front focal plane) of the substage condenser (Figures 19.3(b) and 19.4(a)). Both the aperture and field diaphragms are opened wide to pass oblique rays. The central opaque stop (you can make one by mounting a coin on a clear glass disk) blocks out the central rays. This device works fairly well, even with the Abbe condenser (Figure 19.3), with the 10x objective up to 40x or higher objectives having a numerical aperture no higher than 0.65. The diameter of the opaque stop should be approximately 16-18 millimeters for a 10x objective of numerical aperture 0.25 to approximately 20-24 millimeters for 20x and 40x objectives of numerical apertures approaching 0.65.

The set of stops illustrated in Figure 19.4(a) vary in size from 8 millimeters to 30 millimeters and provide excellent darkfield opaque stops for virtually any numerical aperture objective (below 0.65). Individual stops can be interchanged simply by removing the screw in the bottom of the support spider and replacing the stop with a new size. The outer size of the spider holder will vary depending upon the housing opening diameter at the bottom of the condenser.

The light stop illustrated in Figure 19.4(b) is an ingenious device that expands and contracts a "reverse iris" diaphragm to increase or decrease the size of the stop using a

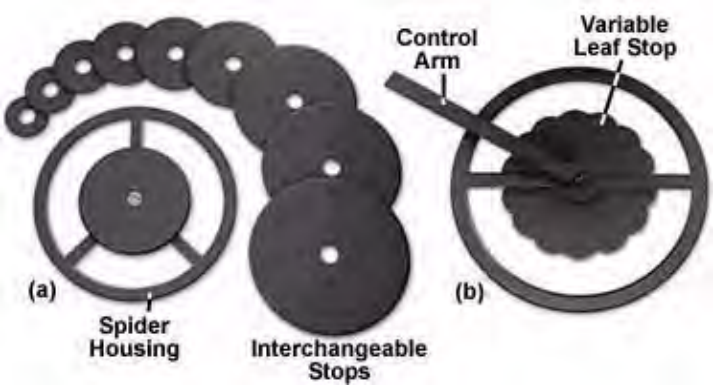

FIGURE 19.4: Stops for darkfield illumination

lever control arm. As this lever is turned, the size of the central leaves changes from about 10 millimeters to 25 millimeters in diameter, creating a larger stop for higher magnification objectives. This type of variable light stop diaphragm eliminates the need for changing light stops each time a higher power objective is inserted into the optical path. It also has the additional advantage of being "tunable" for slight differences in the stop diameter necessary to achieve the best performance while observing the specimen. Although these types of diaphragm light stops are now very rare, they do provide a unique method of achieving highly desirable effects with darkfield illumination.

Almost any brightfield laboratory microscope can be easily converted for use with darkfield illumination. As discussed above, central opaque stops can be fashioned from a small coin, cardboard, plastic, or black paper that can be placed in a filter carrier beneath the condenser (or taped to the condenser bottom with adhesive tape) to block light from entering the front lens of the objective. The diameter of the opaque stop will vary from objective to objective and should be carefully measured by placing a transparent ruler in the substage filter carrier and holding it steady against the bottom of the condenser. Next, determine the opening size by removing an eyepiece and observing the image of the ruler at the back focal plane of the objective using a phase telescope (or by inserting a Bertrand lens). Make certain that both the substage condenser aperture and field diaphragms are opened to their widest position before performing this maneuver. The number of ruler divisions visible in the back focal plane will be equal to the size of the stop necessary to block zeroth order light from entering the objective. Change to the next largest size objective and take another measurement, repeating until stop sizes for all objectives are known.

A guide to approximate opaque stop size versus magnification is given in Table 19.1. The actual size will vary, depending upon several factors including the proximity of the stop with respect to the condenser aperture diaphragm, the numerical aperture of both the objective and condenser, the degree of aberration correction for the condenser, and the field number of the eyepiece. Also important in determining the stop size is the diameter of the condenser back lens, the magnification power of the eyepiece (smaller magnifications require slightly larger stops), and the type of mounting medium. Stop size varies proportionally to the refractive index of the mounting medium: higher refractive index requires a larger stop. A dry mount will also need a smaller stop than an aqueous suspension.

Use scissors or (preferably) a brass cork borer to cut a set of stops matched to all of the objectives, and glue them to a sturdy sheet of clear acetate or glass. The acetate or glass

TABLE 19.1: Approximate Field Stop Diameter Size

Magnification	Numerical Aperture	Stop Size (mm)
1X	0.03	25—30
2x	0.05	8—11
4X	0.10	8—14
10x	0.25	16—18
20X	0.40	18—20
20x	0.65	20—22
40X	0.65	22—24

substrate should be easily mountable onto the underside of the substage condenser, either through a filter holder or by other means, such as adhesive tape. Alignment of the stop can be done by observing it through a Bertrand lens or removing the eyepiece and viewing through a phase telescope while adjusting the condenser centering screws.

19.1.1 Darkfield Microscopy at High Magnifications

For more precise work and blacker backgrounds, you may choose a condenser designed especially for darkfield, i.e. to transmit only oblique rays. There are several varieties: "dry" darkfield condensers with air between the top of the condenser and the underside of the slide–and immersion darkfield condensers which require the use of a drop of immersion oil (some are designed to use water instead) establishing contact between the top of the condenser and the underside of the specimen slide. The immersion darkfield condenser has internal mirrored surfaces and passes rays of great obliquity and free of chromatic aberration, producing the best results and blackest background.

Perhaps the most widely used darkfield condenser is the paraboloid, consisting of a solid piece of glass ground very accurately into the shape of a paraboloid, as illustrated in Figure 19.5(b). Light incident upon the reflecting surface (between the glass and condenser housing in Figure 19.5(b)) of a paraboloid condenser will be focused at the focal point of the reflector. Most paraboloid condensers are cut to ensure that the focal point is slightly beyond the top of the condenser so that parallel light rays will be focused at a position that maximizes illumination of the specimen. The light stop at the bottom of the glass condenser serves to block central rays from reaching the specimen. Light rays that are reflected by the condenser are angled higher than the critical angle of reflection and converge at the principal focus of the condenser. The combination of a glass slide, mounting medium, and immersion oil (between the condenser and the microscope slide) complete the optical homogeneity of the paraboloid shape.

As discussed above, the dry darkfield condenser is useful for objectives with numerical apertures below 0.75 (Figure 19.5(a)), while the paraboloid and cardioid immersion condensers (Figures 19.1 and 19.5(b)) can be used with objectives of very high numerical aperture (up to 1.4). Objectives with a numerical aperture above 1.2 will require some reduction of their working aperture since their maximum numerical aperture may exceed the numerical aperture of the condenser, thus allowing direct light to enter the objective. For this reason, many high numerical aperture objectives designed for use with darkfield as well as brightfield illumination are made with a built-in adjustable iris diaphragm that acts as an aperture stop. This reduction in numerical aperture also limits the resolving

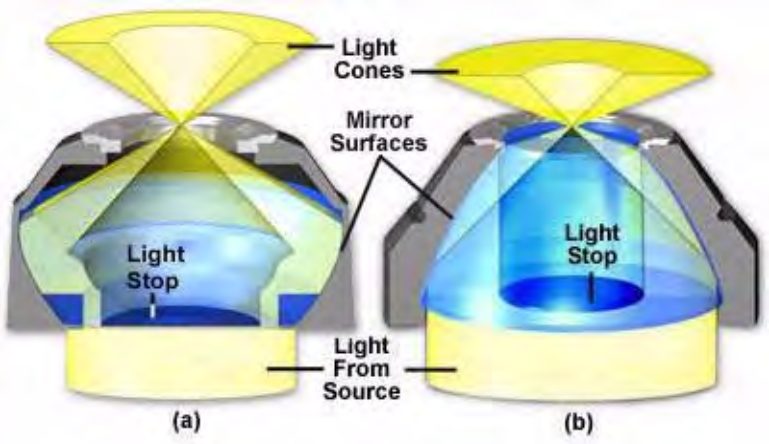

FIGURE 19.5: Reflecting high numerical aperture darkfield condensers

TABLE 19.2: High Numerical Aperture Darkfield Condenser Specifications

Condenser Type	Hollow Cone NA	Objective Max. NA	Number of Reflecting Surfaces	Optical Corrections
Paraboloid	1.00—1.40	0.85	1 Parabolic	Achromatic
Cardioid	1.20—1.30	1.05	1 Spherical 1-/Cardioidal	Achromatic-/Aplanatic
Bicentric	1.20—1.30	1.05	1 Cardioidal-/1 Spherical	Aplanatic
Bispheric	1.20—1.30	1.05	2 Spherical	Aplanatic
Cassegrain	1.40—1.50	1.30	1 Aspheric/1 Spherical	Aplanatic
Spot Ring (Bicentric)	1.40—1.50	1.30	2 Spherical	Aplanatic
Nelson Cassegrain	1.30—1.45	1.20	1 Aspheric/1 Spherical	Aplanatic

power of the objective as well as the intensity of light in the image. Specialized objectives designed exclusively for darkfield work are produced with a maximum numerical aperture close to the lower limit of the numerical aperture of the darkfield condenser. They do not have internal iris diaphragms, however the lens mount diameters are adjusted so at least one internal lens has the optimum diameter to perform as an aperture stop.

Table 19.2 lists several properties of the most common reflecting high numerical aperture darkfield condensers. This table should be used as a guide when selecting condenser/objective combinations for use with high numerical aperture darkfield applications.

The condensers illustrated in Figure 19.5 are designed specifically to produce oblique hollow light cones of high numerical aperture for darkfield illumination. In both instances, the upper surface of the condenser is planar and perpendicular to the optical axis of the microscope. The condenser on the left (Figure 19.5(a)) is designed to be used "dry" with no oil between the condenser and the underside of the microscope slide. In contrast, the paraboloid condenser in Figure 19.5(b) is intended to be "oiled" to the bottom of the

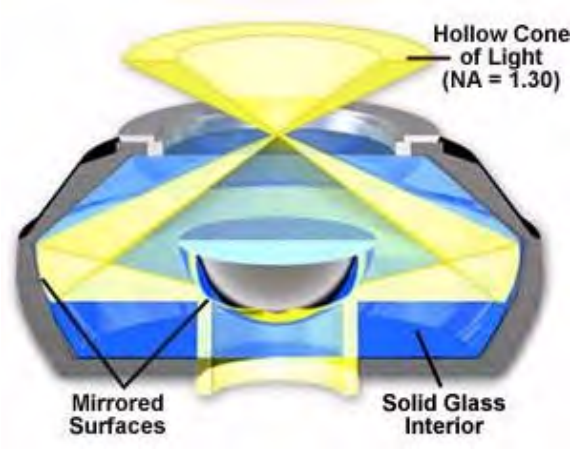

FIGURE 19.6: Bispheric double reflecting condenser

microscope slide, directly underneath the specimen. Omission of immersion oil when using this condenser (or any of the other condensers listed in Table 19.2) will preclude any light from reaching the specimen. The oblique hollow cone of light rays emitted by these condensers cannot emerge from the top lens without oil and will be totally reflected back into the condenser. Light emitted from the illumination source is reflected at the mirrored glass surfaces within the interior of the condensers and exits the top of the condensers at much higher angles of inclination than the critical angle (approximately 41 degrees) at which total reflection occurs for passage of light from glass to air. In the situation of the oiled paraboloid condenser (Figure 19.5(b) and the condensers in Table 19.2) where the refractive index of the condenser glass, immersion oil, and glass slide are equal, light emitted from the condenser passes through the specimen unrefracted by glass-air interfaces.

Reflecting high numerical aperture condensers listed in Table 19.2 cover a wide range of designs used to produce the oblique hollow cone of light necessary for high-magnification darkfield microscopy. The paraboloid darkfield condenser has been discussed in detail above. Another very useful design is the cardioid condenser that is illustrated in Figure 19.1. This condenser design utilizes a mirrored hemisphere in the center of the condenser that serves as both a light stop and a reflector to direct light onto a second reflecting surface shaped to resemble a cardioid of revolution, from which the condenser derives its name. The combination of spherical and cardioid reflecting surfaces produces a condenser that is free from coma and both spherical and chromatic aberration. There are several technical drawbacks to using a condenser of such high numerical aperture. The cardioid condenser is very sensitive to alignment and must be carefully positioned to take advantage of the very sharp cone of illumination, making it the most difficult darkfield condenser to use. In addition, the condenser produces a significant amount of glare, even from the most minute dust particles, and the short focal length may result in poor illumination on objects that exceed a few microns in size or thickness. When choosing microscope slides for quantitative high-magnification darkfield microscopy, make certain to select slides made from a glass mixture that is free of fluorescent impurities.

High numerical aperture reflecting condensers (Figures 19.1, 19.5, 19.6 and Table 19.2) with darkfield illumination provide the method of choice for observing and photographing collections of very small particles or colloidal suspensions, even when the particle diameter is significantly lower than the limit of resolution for the objective. This is due to light

diffracted by the particles, which passes through the objective and becomes visible as bright diffraction disks. Each particle is visible as a minute diffraction disk, provided the lateral distance between adjacent particles is greater than the limit of resolving power of the objective. As illumination intensity is increased, the optical difference between minute diffracting particles and their background increases. Simultaneously, even smaller particles (detectable solely by their ability to scatter light) now diffract enough light to become visible and suspended particles can be seen even when their diameters are smaller than 40 nanometers, which is about one-fifth the 200 nanometer resolution limit with oil immersion objectives of the highest numerical aperture. In biological applications, the movements of living bacterial flagella that average about 20 nanometers in diameter (too small to be seen in brightfield or DIC illumination) can be observed and photographed using high numerical aperture darkfield condensers.

Careful attention should be paid to the details of oiling a high numerical aperture condenser to the bottom of the specimen slide. It is very difficult to avoid introduction of tiny air bubbles into the area between the condenser top lens and the bottom of the microscope slide, and this technique should be practiced to perfection. Air bubbles will cause image flare and distortion, leading to a loss of contrast and overall image degradation. Problems are also encountered when using microscope slides that are either too thick or too thin. Many darkfield condensers contain the range of usable slide thickness inscribed directly on the condenser mount. If the slide is too thick, it is often difficult to focus the condenser without resorting to a higher viscosity immersion oil. On the other hand, slides that are too thin have a tendency to break the oil bond between the condenser and the slide. It is a good idea to purchase precision microscope slides of the correct thickness to avoid any of the problems mentioned above.

A unique situation arises when specimens immersed in aqueous medium are being imaged using a high numerical aperture darkfield condenser. Under these conditions the refractive index of the aqueous solution limits the angle of inclination under which light can pass from the glass microscope slide (n = 1.515) into the water (n = 1.336) surrounding the specimen. The maximum numerical aperture of light passing from glass to water is given by the following equation:

$$\mathrm{NA} = 1.555 \cdot \sin(i) = 1.336 \cdot \sin\left(\frac{\pi}{2}\right) = 1.366$$

Even though reflecting darkfield condensers designed for oil immersion are listed with upper limits of numerical aperture as high as 1.50 (see Table 19.2), light contributing to the illumination of specimens in aqueous media must have a numerical aperture no greater than 1.336, reducing the effective upper limit of darkfield illumination. In the case of specimens immersed in liquids of higher refractive index, the effective upper limit of the numerical aperture of darkfield illumination can approach a maximum of 1.50, although this is difficult to achieve in practice.

High numerical aperture condensers, whether intended for use dry or with oil, must be accurately centered in the optical path of the microscope to realize optimum performance. To achieve this, many darkfield condensers are built with a small circle engraved onto the upper surface to aid in centering the condenser. Centering is performed with a low power (10x-20x) objective by imaging the engraved circle and using the condenser centering screws to ensure the circle (and condenser) are correctly centered in the optical path. For more detailed information about microscope alignment for darkfield illumination, consult our section on darkfield microscope configuration elsewhere in the microscopy primer.

FIGURE 19.7: Stained and unstained specimens in darkfield illumination

In general, objects imaged under proper conditions of darkfield illumination are quite spectacular to see (e.g. try a drop of fresh blood in darkfield). Often specimens containing very low inherent contrast in brightfield microscopy shine brilliantly in darkfield. Such illumination is best for revealing outlines, edges, boundaries, and refractive index gradients. Unfortunately, darkfield illumination is less useful in revealing internal details.

Other types of specimens, including many that are stained, also respond well to illumination under darkfield conditions. Figure 19.7 illustrates darkfield photomicrographs of three types of specimen, all of which produce good contrast in both brightfield and darkfield illumination. Details in the body of the deer tick (Ixodes demmini) shown in Figure 19.7(a) can be washed out in brightfield, unless the condenser aperture is stopped down to maximize contrast. However, in darkfield, most of the specimen detail in the tick becomes visible and can be easily captured on film. The heavily stained helminth trematode (Echinostoma revolutum, Figure 19.7(b)) also reveals considerably more detail when illuminated under darkfield conditions, as does the silkworm trachea and spiracle illustrated in Figure 19.7(c). In addition to the examples presented above, a number of other specimens can also be viewed and photographed under both brightfield and darkfield illumination to achieve the desired effects.

During the first half of the twentieth century, darkfield microscopy had a very strong following and much effort was expended in optimizing darkfield condensers and illuminators. This intense interest slowly began to fade with the emergence of more advanced contrasting-enhancing techniques such as phase contrast, differential interference contrast, and Hoffman modulation contrast. Recently, a renewed in the interest in transmitted darkfield microscopy has arisen due to its advantages when used in combination with fluorescence microscopy.

Darkfield microscopy is still an excellent tool for both biological and medical investigations. It can be effectively used at high magnifications to photograph living bacteria, or at low magnifications to view and photograph cells, tissues, and whole mounts. Marine biologists continue to use darkfield illumination at low powers to observe and record data about fresh and salt water organisms such as algae and plankton.

19.2 Reflected Darkfield Illumination

One of the most effective ways to improve contrast in the reflected light microscope is to utilize darkfield illumination. In reflected darkfield microscopy, an opaque occluding disk

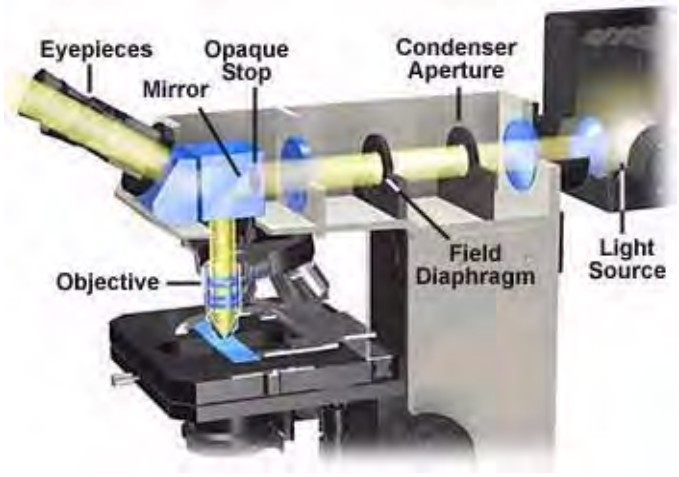

FIGURE 19.8: Reflected light darkfield configuration

is placed in the path of the light traveling through the vertical illuminator so that only the peripheral rays of light reach the deflecting mirror. These rays are reflected by the mirror and pass through a hollow collar surrounding the objective to illuminate the specimen at highly oblique angles.

A typical reflected light microscope with a cut-away drawing of the vertical illuminator is illustrated in Figure 19.8. The illuminator is horizontally oriented, 90 degrees to the optical axis of the microscope and parallel to the table top, with the lamp housing attached to the back of the illuminator. Coarse and fine adjustment knobs raise or lower the stage in large or small increments respectively to bring the specimen into sharp focus. The specimen's top surface is upright on the stage facing the objective, which has been rotated into the microscope's optical axis.

Many modern reflected light illuminators are described as "universal" illuminators because, with several additional accessories and little or no dismantling, the microscopist can easily switch from one mode of reflected light to another. It is even possible to slide the reflectors out of the path altogether in order to perform transmitted light observation. Such universal illuminators may include a partially reflecting plane glass surface (sometimes referred to as a half-mirror) for brightfield, and/or a fully silvered reflecting surface with an elliptical, centrally located clear opening for darkfield observation.

Each of these reflecting devices (housed in mirror blocks or cubes) is tilted at a 45 degree angle facing the light traveling along the vertical illuminator and, simultaneously, at a 45 degree angle to the optical axis of the microscope. Both of the respective mirrors direct the light downward at 90 degrees toward the specimen and also permit the upward-traveling reflected light to pass through to the viewing tubes and eyepieces for observation. The best-designed vertical illuminators include condensing lenses to gather and control the light, an aperture iris diaphragm and a pre-focused, centerable field iris diaphragm to permit the desirable Köhler illumination. Affixed to the back end of the vertical illuminator is a lamphouse containing the light bulb, usually a high-performance tungsten-halogen lamp. For very faint darkfield samples, the lamphouse can be replaced with one containing a mercury burner. The burner lamp may be powered by the electronics built into the microscope stand, or (in simpler models) by means of an external transformer.

Within the vertical illuminator, light emitted by a 50 or 100-watt low voltage-high inten-

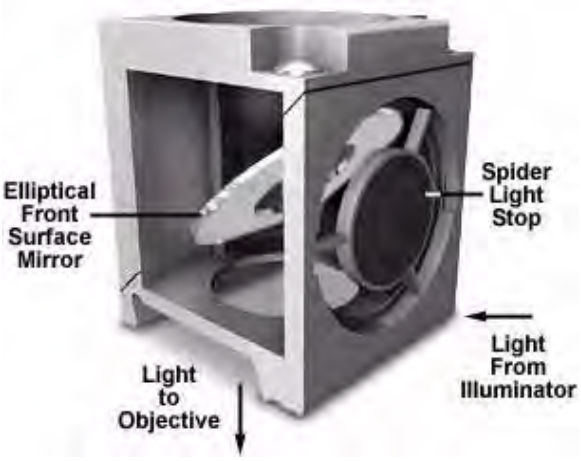

FIGURE 19.9: Reflected light darkfield mirror block

sity tungsten-halogen lamp passes through a collector lens and then through the aperture and field diaphragms before striking the opaque stop in the opening port of the darkfield mirror block located above the objective at the front of the illuminator. The opaque stop blocks the central portion of the light beam allowing only a hollow cylinder of light to pass into the mirror block, as illustrated in Figure 19.9 below. The field and aperture diaphragms are opened to their maximum positions to avoid blocking peripheral rays of light from the source.

Light entering the mirror block is reflected by a special mirror positioned within a tube inside the block. This mirror is oriented at a 45-degree angle to the incident beam and has an elliptically shaped opening surrounded by a fully silvered front surface mirror. Peripheral rays of light reflected from the elliptical mirror are deflected downward, exiting at the bottom of the vertical illuminator. The cylinder of light then travels through the nosepiece before passing into specially constructed objectives known as Neo, BF/DF, or BD objectives (Figure 19.10), depending upon the designation of the manufacturer. These objectives are typically designed with optical corrections necessary for use on specimens lacking a coverslip.

Light from the darkfield mirror block travels down the 360–degree hollow chamber surrounding the centrally located lens elements of the specially constructed BD reflected light objectives, as illustrated in Figure 19.10. This light is directed at the specimen from every azimuth in oblique rays to form a hollow cone of illumination by means of circular mirrors or prisms located at the bottom of the objective's hollow chamber. In this manner, the objective serves as two separate optical systems coupled coaxially such that the outer system functions as a darkfield "condenser" and the inner system as a typical objective.

Today, most darkfield reflected light microscope objectives are infinity-corrected and are available in a broad spectrum of magnifications ranging from 5x to 200x. These objectives are also manufactured in various qualities of chromatic and spherical correction, from simple achromats to planachromats and planapochromats. Most, but not all, are designed to be used "dry" with air in the space between the objective and the specimen. Some reflected light objectives are designed to focus at a longer working distance from the specimen than is usual. Such objectives are labeled on the barrel of the objective as LWD (Long Working Distance), ULWD (Ultra-Long Working Distance), and ELWD (Extra-Long

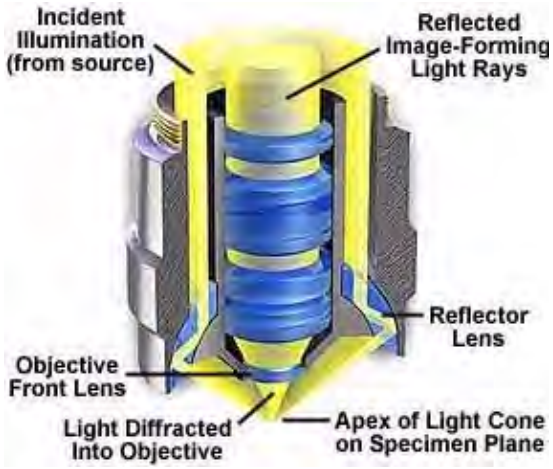

FIGURE 19.10: Reflected light darkfield objective

Working Distance).

Objective design varies depending upon the manufacturer, but the condenser portion may have one of three classical designs. Catoptric reflecting objectives have a single glass lens element positioned at the nose of the objective and rely on reflections from the internal surface of the barrel to focus light onto the specimen. Another important objective design is the dioptric configuration in which a series of prisms are strategically placed in the hollow outer chamber and used to aim and focus light toward the specimen.

The objective illustrated in Figure 19.10 is a catadioptric system, which uses both reflecting and refracting optical elements and surfaces to form the oblique hollow cone of illumination necessary to view the specimen in darkfield mode. A cylinder of light entering the hollow periphery of the objective first encounters a curved lens element that directs light to a mirrored internal surface of the objective lens barrel. Light is reflected from the barrel directly through the glass element and is then reflected from the mirrored internal surface of the outer objective barrel, before being refracted to form the hollow cone of illumination by a second lens element. Light diffracted and refracted by the specimen is then able to enter the front lens of the objective.

The necessity of a hollow collar surrounding the lens elements in reflected light objectives requires that the diameter of the objective be significantly greater than that of ordinary brightfield objectives. In most cases, a nosepiece-mounting thread diameter larger than the Royal Microscopical Society (RMS) standard is used in reflected light objectives. This requires that reflected light darkfield objectives have a nosepiece with a larger thread size, which is typically referred to as a BD or BF/DF thread size. Most manufacturers offer objective adapters that convert standard RMS thread size nosepieces to BD thread size, allowing the use of these objectives on reflected light microscopes. Care should be taken to ensure that objectives used on BD thread nosepieces will conform to the tube length of the microscope.

Table 19.3 lists specifications of a typical series of infinity-corrected Neo planachromat brightfield/darkfield objectives designed for use in reflected light microscopy. Numerical aperture values reach a limit of about 0.90 in this series, which is the practical limitation for “dry” objectives of this design.

In many modern microscope stands, the Neo type objectives, with appropriate modules

TABLE 19.3: Neo D Planachromat Objectives (Infinity-Corrected)

Magnification	Numerical Aperture	Working Distance (mm)
5x	0.10	11.20
10x	0.25	6.00
20x	0.40	1.00
50x	0.75	0.34
80x (dry)	0.90	0.18
100x (dry)	0.90	0.30
150x (dry)	0.90	0.27

TABLE 19.4: Long Working Distance and Apochromat Darkfield Objectives (Infinity-Corrected)

Magnification	Numerical Aperture	Working Distance (mm)
20x (ELWD)	0.40	11.0
50x (ELWD)	0.55	8.2
100x (ELWD)	0.80	2.0
100x (Apo)	0.90	0.40
150x (Apo)	0.90	0.29
200x (Apo)	0.90	0.30

or accessories, can be used for darkfield, brightfield, polarized light, Nomarski differential interference contrast (DIC), and reflected light fluorescence observations.

Specimen geometrical constraints often require specialized objectives to properly image all areas of the specimen. Table 19.4 contains specifications for reflected light darkfield objectives designed to be used at long working distances, and also apochromat objectives that yield superior photomicrographs of specimens at very high magnifications.

Without a specimen on the stage, the field of view in a darkfield reflected light microscope appears black because the oblique rays fall outside the acceptance angle and miss re-entering the objective. When a specimen is placed on the stage, the features of the specimen, including surface irregularities such as grain boundaries, ridges, scratches, depressions or particles, etc., now shine brightly against a black background. The contrast is enormously increased with the result that surface features of the sample, otherwise almost invisible in brightfield, are readily discernible. In fact, many metallurgical and related samples do not require etching or other preparatory procedures in order to produce excellent darkfield images. Color rendition is also spectacular using this method of illumination. The light scattered by specimen detail, which is often obscured in brightfield illumination, is able to enter the objective under darkfield illumination and pass through the central lens elements of the objective eventually to reach the eye or camera.

The photomicrographs illustrated in Figure 19.11 represent a comparison of brightfield and darkfield reflected light images of surface features on the MIPS R10000 microprocessor integrated circuit using BD-type objectives. Bonding wires at the edge of the chip die are very evident in the photomicrographs. The surface of the computer chip is coated with a Passivation layer of silicon nitride that protects electrical components from exposure to the atmosphere. Light reflected and refracted by this layer is responsible for the apparent color in portions of the photomicrographs.

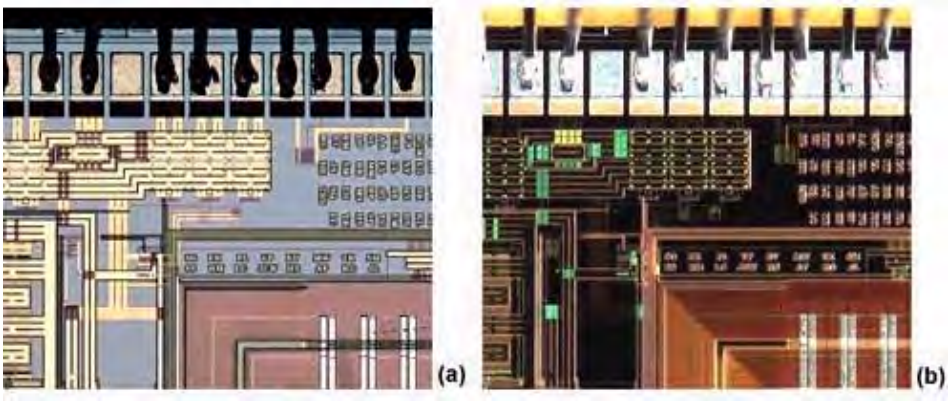

FIGURE 19.11: Brightfield and darkfield reflected light microscopy

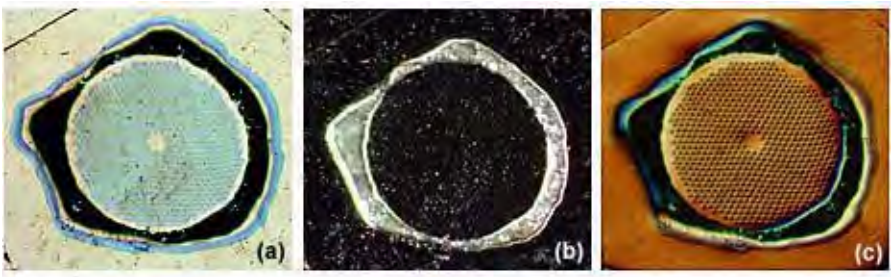

FIGURE 19.12: Niobium—TiN superconducting filament in copper matrix

The brightfield image in Figure 19.11(a) shows that incident light does not reflect from the bonding wires, which appear very dark in the photomicrograph. Initials of the chip designers, which were incorporated onto the chip's surface during the photolithographic fabrication process, appear in the right central portion of both photomicrographs. These initials, along with the bonding wires, reflect oblique light back into the objective, as illustrated in the darkfield photomicrograph in Figure 19.11(b). These two methods of illumination can be successfully used to complement one another during inspection of integrated circuit surfaces.

The photomicrographs in Figure 19.12 serve to further illustrate how different illumination techniques can complement each other when combined with the examination of specimens under darkfield illumination. The specimen is a bundle of niobium-tin superconducting filaments embedded in a copper/bronze matrix that compose a flexible wire used in low-temperature superconducting magnets of high field strength. The photomicrograph in Figure 19.12(a) was taken under brightfield illumination and illustrates the bundle of filaments surrounded by a very dark area and a blue barrier layer that is composed of tantalum. The dark area in Figure 19.12(a) is a layer of residual tin that is left over from a heat treatment step in the construction of the wire bundle. Superconducting filaments and the tantalum barrier are not visible Figure 19.12(b), which is a darkfield photomicrograph of the same area imaged in Figure 19.12(a). However, the residual tin layer reflects light into the objective and appears as a bright metal band surrounding the filaments. Figure 19.12(c) is a photomicrograph of the same viewfield in reflected differential interference contrast. The bronze matrix surrounding the individual filament bundles is very evident,

but the residual tin and tantalum barrier layers are difficult to discern. This series of photomicrographs serves to demonstrate how the techniques of brightfield, darkfield, and differential interference contrast can be used to complement each other and provide a more thorough investigation of the specimen.

The following section reviews the steps in the configuration and alignment of a microscope for reflected (incident) darkfield illumination.

19.2.1 Reflected (Incident) Darkfield Configuration

- Select a sample that has good reflective properties and place it onto the microscope stage. Using the 10x objective, adjust the microscope for reflected light Köhler illumination. Verify that darkfield (Neo, BF/DF, or BD) objectives are inserted into the nosepiece and are ready for use.
- Open the aperture and field iris diaphragms to their maximum positions. After using the microscope in darkfield mode, these diaphragms should always be returned to their normal brightfield positions to avoid a significant loss of specimen contrast with other illumination techniques.
- Insert the darkfield stop into the light path to achieve darkfield illumination. On most modern microscopes, this is accomplished by using a sliding bar that attaches to the darkfield mirror block assembly. There are usually several dtentes that mark the position of the slider (corresponding to a brightfield, darkfield, and florescence mirror block), and these are often designated on the exterior of the microscope body.
- View the sample, which should now be visible under darkfield illumination. If light emitted by the sample is very faint, raise the lamp voltage to increase the intensity of illumination. Also check to ensure the field and aperture diaphragms are opened to their widest settings. Return all microscope settings to the brightfield mode after finishing the darkfield experiments.

Modern reflected light microscopes equipped with accessories for darkfield illumination offer a wide spectrum of innovations. Among these are erect image capability that produces non-reversed letters (especially important in semiconductor technology) when photographed. Other critical features of the specimen are also positioned in the correct orientation in photomicrographs using the erect image technique. The move to infinity-corrected optical systems by most manufacturers helps to eliminate ghost images and astigmatism often generated by the use of half-mirrors, especially when components are added to the optical path.

New infinity-corrected brightfield/darkfield objectives offered by Olympus, Nikon, Zeiss, and Leica offer an increased effective field of view and a wide range of working distances for enhanced optical performance, especially when coupled to ultra-wide viewfield eyepieces. Advanced new illumination systems provide quick and easy changeover between tungsten-halogen and high-energy mercury or xenon light sources to provide optimum illumination for faint darkfield specimens. Also, some reflected light microscopes have internal optical elements that provide built-in zoom magnification to assist focusing and enable intermediate (although empty) magnifications.

Advanced reflected light microscope body designs are also very convenient for multi-format photomicrography. Industrial microscopes from the premier manufacturers are capable of simultaneously mounting 35 millimeter, large-format (4" x 5"), and digital cameras

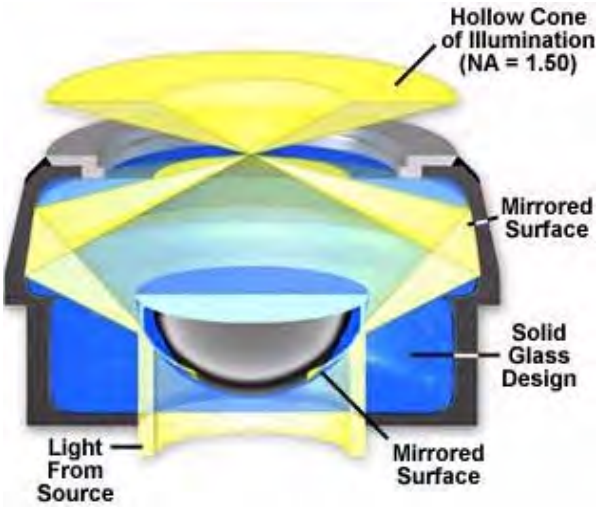

FIGURE 19.13: Spot ring bicentric condenser

to the microscope for greater variability in photomicrography. These advanced systems also offer digital accessories that imprint a micrometer scale, grain scale, exposure information, and/or other notes directly onto the film frame beside the photomicrograph.

Modern advances in reflected light microscopy have been largely driven by the semiconductor industry, materials sciences, and explosive growth in fluorescence microscopy for medical diagnostics and cell sciences. The ability of darkfield illumination to reveal outlines, edges, boundaries, scratches, pinholes and refractive index gradients provides a means to complement other forms of microscopy including brightfield, differential interference contrast, Hoffman modulation contrast, and polarized light techniques. When coupled together, these contrast-enhancing techniques can often lead to new insight about specific details of specimens under study.

19.3 Darkfield Microscope Configuration

The following section reviews the steps in the configuration and alignment of a microscope for both low and high magnification transmitted darkfield illumination.

19.3.1 Low Magnification Transmitted Darkfield Microscope Configuration

- A suitable specimen stained for high contrast is selected and placed on the microscope stage for observation and microscope calibration. The 10x objective is selected and the specimen is brought to sharp focus with brightfield illumination.
- Carefully align the optical elements of the microscope and adjust the light source and diaphragms for proper Köhler illumination using the procedures outlined in our section on Köhler illumination setup with a transmitted light microscope.
- Open both the field and substage condenser aperture iris diaphragms to their full-open positions before proceeding any further. This allows the condenser to operate at its maximum numerical aperture. Choose the appropriate central opaque stop

(usually about a 16-18 millimeter diameter stop for a 10x objective) and place it onto the spider, glass, or acetate stop holder. Next, insert the stop-holder assembly into the optical path of the microscope by either sliding it into a sub-condenser filter holder or taping it into place on the underside of the condenser.

If a condenser designed specifically for darkfield illumination at low magnifications is to be used, insert it into the substage condenser mount at this time.

- Remove the eyepiece and view the rear focal plane of the objective by peering down the eyepiece tube or by inserting a phase telescope (or Bertrand lens). Often a bright disk of light that is partially obscured by the central opaque stop will be visible at the objective rear focal plane. Ideally, the central stop diameter should be slightly larger than the bright disk and mask it completely. If this is not the case, use the substage centering screws to center the condenser so that the bright disk is completely covered by the central stop.

- Replace the eyepiece and place a low-contrast specimen on the stage that is suitable for observation in darkfield illumination. The image of the specimen should be bright on a very dark background, the only artifacts being small particles of dust and smudges on the microscope slide. If the image is too dark, increase the voltage to the tungsten-halogen light source up to its maximum voltage.

- Focusing the condenser is the last step and should receive careful attention, especially when using objectives above 20x magnification. The top lens of the condenser (when used "dry") should almost come into contact with the underside of the microscope slide. When the condenser is positioned too low in the rack, a dark central region surrounded by a bright ring of light is obvious in the viewfield. This is remedied by raising the condenser until a bright circular area of very small diameter is fully illuminated in the central portion of the viewfield.

- The microscope is now ready for observation and photomicrography of specimens under low magnification darkfield illumination.

19.3.2 High Magnification Transmitted Darkfield Microscope Configuration

- In a manner similar to that with low-power darkfield microscope configuration, place a stained specimen on the stage and using the 10x objective, align the microscope for Köhler illumination as described in our section for transmitted light microscopy.

- Use the condenser rack knob to lower and remove the brightfield substage condenser. Insert the reflected light high numerical aperture condenser into the holder, and secure it with the set screw. Slowly raise the condenser until it is less than 2 millimeters from the underside of the specimen slide.

- Select a darkfield specimen and place it onto the microscope stage between the objective and the condenser. The condenser will project a bright ring of light onto the sample that can be used for centering the optical path. Use the condenser translational centering screws to move the ring of light into the center of the viewfield.

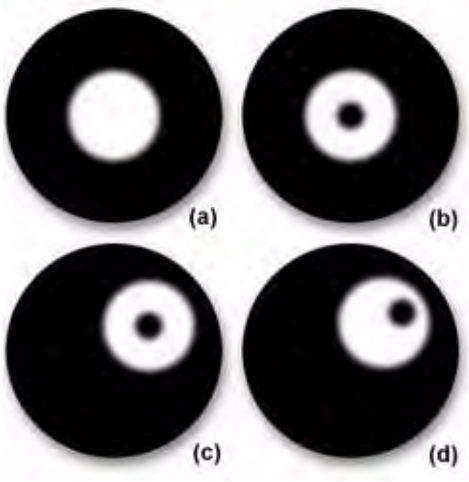

FIGURE 19.14: Centering darkfield condenser

- It is often advantageous to use a low power 10x objective when centering high numerical aperture darkfield condensers. When viewing a specimen with the 10x objective while slowly raising and lowering the condenser, a point will be reached where a bright spot will appear in the field of view as illustrated in Figure 19.14(a). As the condenser is slightly raised or lowered, a dark spot similar to the one shown in Figure 19.14(b) will appear, if the condenser is properly centered. In cases where the condenser is not properly aligned and centered, a typical field of view might look like that shown in Figure 19.14(c), and if the microscope is not properly adjusted for Köhler illumination, the viewfield might appear as it does in Figure 19.14(d). The ideal and correct positioning of the condenser is illustrated in Figure 19.14(a), and the condenser should be adjusted until the field of view appears in this manner.

- High numerical aperture darkfield condensers are designed to be used either "dry" or with immersion oil between the top lens of the condenser and the bottom of the microscope slide. To apply oil to an immersion condenser, remove the microscope slide and slowly rack the condenser down below the mechanical stage and place a drop of oil directly on the front lens. Replace the slide, then slowly raise the condenser until contact is made between the oil droplet and the bottom surface of the slide. Carefully observe the oil contact area to determine if any air bubbles have been introduced into the space between the condenser top lens and the microscope slide. It should be noted that no matter what the magnification of the objective is, if an oil immersion condenser is used without oil, light will not emerge from the condenser.

  Air bubbles will scatter light and should be observable by removing the eyepiece and viewing the back focal plane of the objective with either a phase telescope or Bertrand lens. If no bubbles are present, proceed on to the next step. When bubbles are detected, remove all traces of oil from both the slide and the condenser top lens and repeat the procedure. Make certain both surfaces are clean and completely free of oil, dust, dirt and other contaminating artifacts before re-oiling the condenser.

- Select the objective intended for viewing the specimen and swing it into position above the condenser. If the objective is designed to be used dry, then focus the

specimen and optimize the illumination by adjusting the condenser focus knob. With oil immersion objectives, place a drop of oil on the front lens of the objective before swinging it into place. Slowly move the objective into place and carefully observe the oil contact area between the objective front lens and the microscope slide. A bright flash should occur (from scattered light) the instant oil on the front lens of the objective lens comes into contact with the microscope slide.

Check for air bubbles by observing the back focal plane of the objective with a phase telescope or Bertrand lens. If bubbles are present, swing the objective to the next detent stop on the microscope nosepiece and wipe off excess oil with a piece of lint-free lens tissue. Re-apply oil to the objective front lens and try again. When the oil contact area is free of bubbles, use the condenser rack focus knob to optimize darkfield illumination.

- If the objective has an internal iris diaphragm designed to allow adjustment of the numerical aperture, it should be adjusted at this time (this only applies to oil immersion objectives with a numerical aperture higher than 1.20). Remove the eyepiece and place a phase telescope into the eye tube or use a Bertrand lens to observe the rear focal plane of the objective. If a bright ring of light is seen around a central dark region, the aperture of the objective is too great and must be reduced using the internal iris diaphragm, or an objective of lesser numerical aperture should be chosen. Adjust the iris diaphragm until the ring of light falls out of the viewfield. If a crescent-shaped arc of light is observed, then the condenser is not properly aligned in center of the microscope optical axis. Use the condenser centering screws to align the condenser so that the arc disappears or becomes a complete circle of light.

- Replace the eyepiece and focus the specimen, which should now appear brightly and evenly illuminated upon a dark background. When selecting another objective, repeat the steps above to align the condenser and objective for optimized darkfield microscopy.

Careful attention should always be given to microscope alignment, irrespective of whether the illumination mode is brightfield, darkfield, phase contrast or some other contrast enhancement technique. Time spent in this endeavor will be repaid in excellent performance of the microscope both for routine observation and critical photomicrography.

19.4 Troubleshooting

There are numerous common problems associated with darkfield microscopy and photomicrography. These range from insufficient illumination and condenser mis-alignment to using a field stop of incorrect size. Most darkfield illumination problems are associated with the substage condenser, and this should be the first suspect when things do not work properly. The following problems and solutions should be used as a guide when imaging specimens using this technique.

Problem There is insufficient illumination to make the specimen visible, or the specimen is visible but very faint.

Solution The lamp voltage may be set too low, or the lamp may have insufficient intensity to properly illuminate the specimen. Raise the voltage to a maximum of about 12 volts

(for 12-volt, 100 watt tungsten-halogen bulbs) or replace the light source, if possible, with one of greater intensity. If this does not solve the problem, check the substage condenser to ensure that it is positioned correctly with a field stop of the appropriate size. Also, check the light path for color and/or neutral density filters, polarizers, retardation plates, or any other components that might reduce illumination intensity.

If this problem occurs with high numerical aperture reflecting condensers, check to make certain that the condenser top lens is correctly oiled to the bottom of the microscope slide. If the immersion contact has been broken, re-apply the oil and rack up the condenser until the top lens is completely immersed in oil and in contact with the bottom of the slide.

Problem The viewfield has a dark spot in the center reducing illumination intensity, but objects in the periphery are well-illuminated and appear normal.

Solution The substage condenser is either incorrectly positioned or the light stop is the wrong size for the objective. Carefully rack the condenser up and down while observing the specimen in the viewfield. Check to make certain that both the condenser aperture and field diaphragms are set to the wide open position. If this does not affect the illumination, change the field stop size making it either slightly larger or smaller and then re-check the illumination.

Occasionally this problem arises when microscope slides of excessive thickness (greater than the standard one millimeter) are used. Use a micrometer or a set of dial calipers to determine the thickness of the slide and the slide/coverslip combination. If the slide is too thick, either change to a slide of the correct thickness or check the condenser to determine if it can be adjusted to compensate for slides of varying thickness.

Problem Lamps tend to have a very short lifetime and the bulb interior is sintered with a coating of black evaporated tungsten.

Solution The bulbs have been used at excessive voltage for long periods, which will definitely reduce the life span. Replace the bulb and reduce lamp voltage after observation and/or photomicrography of the specimen.

Problem The image has a brightfield periphery with or without dark regions in the center.

Solution This problem is typical when the substage condenser is incorrectly centered or the field stop is too small. Revert to brightfield and re-establish the conditions of Köhler illumination, then repeat the darkfield procedure, making sure the condenser is centered. If this does not help, increase the size of the field stop until proper darkfield conditions are established.

This problem may also arise when using an objective that has too high a numerical aperture for the darkfield condenser. If there is an internal iris diaphragm in the objective, reduce the iris opening size to determine if too much oblique illumination is entering the front lens of the objective. Also, it may help to increase the size of the field stop or change to a reflected darkfield condenser of higher numerical aperture.

Problem The periphery of the viewfield is bright on one side only.

Solution Check the nosepiece to ensure the objective is correctly positioned in the optical axis of the microscope. There is a detent stop that should produce a positive "click" when the objective is properly positioned. The problem might also occur if the field stop is not correctly centered. Remove the eyepiece and place a phase telescope in the eye tube (or use a Bertrand lens), then use the centering screws to properly align the field stop.

Problem Images of the specimen are not clear and lacking in sufficient contrast and detail.

Solution The specimen might not be suitable for darkfield microscopy. Many stained specimens do not scatter enough light to be clearly imaged under darkfield conditions. Specimen thickness may also be a problem, because very thin specimens are often not imaged well with the oblique light rays emitted from darkfield condensers. Change to brightfield, phase contrast, DIC, or Hoffman Modulation Contrast to determine if this improves specimen contrast.

Problem Bright areas that are out of focus obstruct viewing and/or photomicrography of darkfield specimens.

Solution This is probably due to dust, hair, fibers, and/or dirt contamination of an optical surface somewhere above the condenser. Thoroughly clean the specimen slide with optical-grade tissue or cotton. Occasionally, this problem arises due to contamination on the objective front lens. Carefully loosen the objective from its seat in the nosepiece and slowly turn while observing the specimen through the eyepieces. If the obstruction rotates along with the objective, then it is probably due to dust on the front lens. Remove the objective and moisten the front lens by gently exhaling on it, then clean with lens tissue or a cotton swab wrapped on a long wooden rod. Replace the objective and check to make certain the obstruction has been completely removed.

Problem The background is evenly illuminated but is not completely dark or appears gray in color.

Solution This problem usually occurs when the opaque field stop is too small for the objective. Remove the eyepiece and view the back focal plane of the objective using either a phase telescope or a Bertrand lens without a specimen in the light path. The entire back focal plane should be dark without any rim of bright light appearing around the periphery. If an arc or circle of light is observed in the back focal plane of the objective, change to a slightly larger field stop. Also, reducing the size of the field diaphragm will aid in suppressing glare and producing a jet-black background (be careful not to close this iris aperture diaphragm too much).

Problem The image of the lamp condenser partially fills the viewfield, obscuring details of the specimen.

Solution The slide may be too thin or the condenser may be adjusted too high. Measure the thickness of the microscope slide and check to make certain the oil contact is not broken. If difficulty is encountered keeping the bottom of the slide oiled, try using a thicker slide.

Problem Colors appear in the background, or the background is unevenly lit with a gray cast.

Solution This problem often occurs with whole mounts that are very thick or when too many light-scattering contaminating artifacts are captured in the mounting medium. Close down the field diaphragm and rotate the specimen slide to locate the best orientation, then determine whether the problem has been corrected. The specimen may have to be re-mounted in a thinner mount or the mounting medium may need to be filtered. Carefully clean the entire microscope slide and coverslip with a soft lens tissue or cotton swab.

Problem When viewing aquatic organisms in a aqueous mount, specimens drift constantly in a single direction, making observation and photomicrography difficult.

Solution Convection currents are being created due to slow evaporation at the edges of the coverslip. Place a bead of petroleum jelly or Cytoseal mounting medium around the periphery of the coverslip to seal it firmly onto the microscope slide. Commercial products are available that can be added to the water to slow the movement of these minute organisms, making them easier to photograph.

Problem When viewing the specimen through a 10x objective, there is a oblong spot of light in the center of the viewfield.

Solution The lamp condenser may be incorrectly focused or the diffusion filter may be missing, leading to an image of the lamp filament appearing in the viewfield. Re-focus the condenser and make certain there is a diffusion filter in the light path.

Problem The viewfield has bright spots and there are problems with achieving sharp focus of the specimen.

Solution Small air bubbles may be trapped in the oil between the top of the condenser and the bottom of the microscope slide. Remove the eyepiece (or insert a Bertrand lens) to observe the back focal plane of the objective, where the bubbles will be visible. To remedy, break the oil contact and remove any residual bubbles with a cotton swab. Clean excess oil from the condenser front lens and the microscope slide, then apply a clean drop of oil to the lens. If the problem persists, thoroughly clean all optical surfaces before re-applying the oil.

Problem At high magnifications, colloidal particles display incomplete Newton rings and appear to be unevenly illuminated.

Solution The condenser is probably off-center. Change to a lower power objective and re-center the condenser. Carefully check to determine whether the higher power

objective has a different center, and if so, center the objective to the microscope optical axis.

Chapter 20

Differential Interference Contrast

20.1 Introduction

In the mid–1950s, a French optics theoretician named Georges Nomarski modified the Wollaston prism used for detecting optical gradients in specimens and converting them into intensity differences. Today there are several implementations of this design, which are collectively called differential interference contrast (DIC). Living or stained specimens, which often yield poor images when viewed in brightfield illumination, are made clearly visible by optical rather than chemical means.

In transmitted light DIC, light from the lamp is passed through a polarizer located beneath the substage condenser, in a manner similar to polarized light microscopy. Next in the light path (but still beneath the condenser) is a modified Wollaston prism that splits the entering beam of polarized light into two beams traveling in slightly different directions. The Wollaston prism is composed of two quartz wedges cemented together, from which emerging light rays vibrate at 90 degrees relative to each other with a slight path difference. A different Wollaston prism is needed for each objective of different magnification. Wollaston prisms are usually loaded into a revolving turret on the condenser, which allows the microscopist to rotate the appropriate prism into the light path when changing magnifications.

The plane-polarized light, vibrating only in one direction (East-West) perpendicular to the propagation direction of the light beam, enters the beam-splitting modified Wollaston prism and is split into two rays, vibrating perpendicular to each other. These two rays travel close together but in slightly different directions (see Figure 20.2). The rays intersect at the front focal plane of the condenser, where they pass traveling parallel and extremely close together with a slight path difference, but they are vibrating perpendicular to each other and are therefore unable to cause interference. The distance between the rays, called the shear, is so minute that it is less than the resolving ability of the objective.

The split beams enter and pass through the specimen where their wave paths are altered in accordance with the specimen's varying thickness, slopes, and refractive indices. These variations cause alterations in the wave path of both beams passing through areas of any specimen details lying close together. When the parallel beams enter the objective, they are focused above the rear focal plane where they enter a second modified Wollaston prism that combines the two beams at a defined distance outside of the prism itself. This removes the shear and the original path difference between the beam pairs. As a result of having traversed the specimen, the paths of the parallel beams are not of the same length (optical

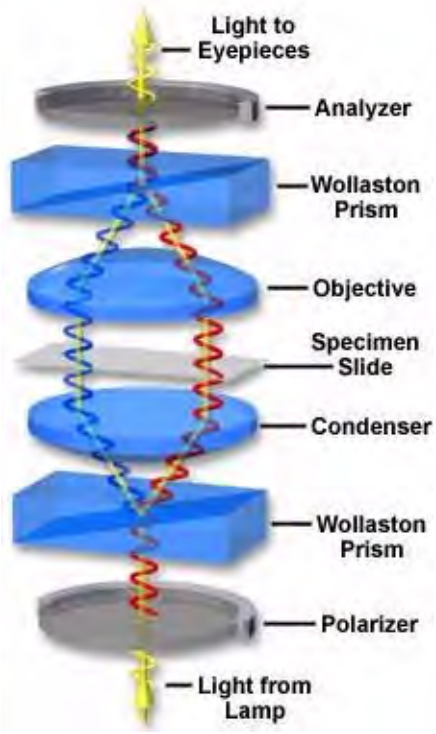

FIGURE 20.1: Schematic DIC configuration

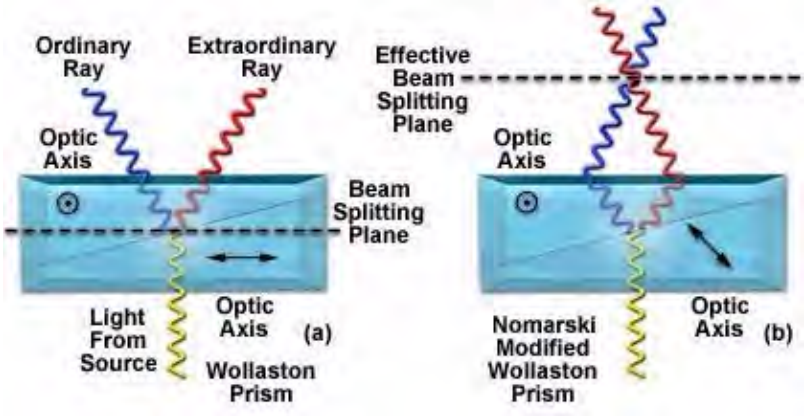

FIGURE 20.2: Wollastone prism for DIC microscopy

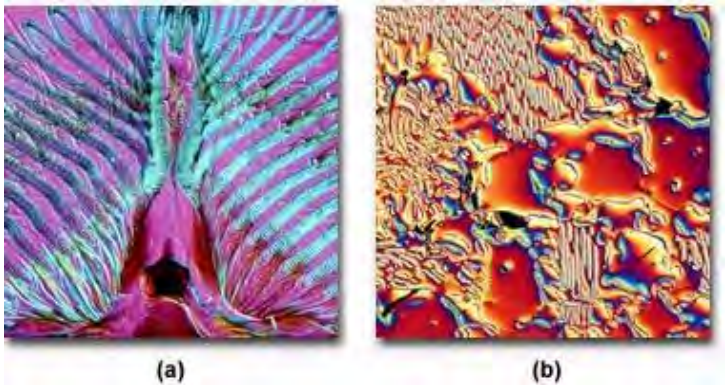

FIGURE 20.3: Trasmitted and reflected DIC photomicrographs

path difference) for differing areas of the specimen.

In order for the beams to interfere, the vibrations of the beams of different path length must be brought into the same plane and axis. This is accomplished by placing a second polarizer (analyzer) above the upper Wollaston beam-combining prism. The light then proceeds toward the eyepiece where it can be observed as differences in intensity and color. The design results in one side of a detail appearing bright (or possibly in color) while the other side appears darker (or another color). This shadow effect bestows a pseudo three-dimensional appearance to the specimen.

In some microscopes, the upper modified Wollaston prism is combined in a single fitting with the analyzer incorporated above it. The upper prism may also be arranged so it can be moved horizontally. This allows for varying optical path differences by moving the prism, providing the user a mechanism to alter the brightness and color of the background and specimen. Because of the prism design and placements, the background will be homogeneous for whatever color has been selected.

The color and/or light intensity effects shown in the image are related especially to the rate of change in refractive index, specimen thickness, or both. Orientation of the specimen can have pronounced effect on the relief-like appearance and often, rotation of the specimen by 180 degrees changes a hill into a valley or visa versa. The three-dimensional appearance is not a representation of the true geometric nature of the specimen, but is an exaggeration based on optical thickness. It is not suitable for accurate measurement of actual heights and depths.

There are numerous advantages in DIC microscopy as compared to phase contrast microscopy. With DIC, it is possible to make fuller use of the numerical aperture of the system and to provide optical staining (color). DIC also allows the microscope to achieve excellent resolution. Use of full objective aperture enables the microscopist to focus on a thin plane section of a thick specimen without confusing images from above or below the plane. Annoying halos, often encountered in phase contrast, are absent in DIC images, and suitable achromat and fluorite objectives can be used for this work.

A downside is that plastic tissue culture vessels and other birefringent specimens yield confusing images in DIC, hence Hoffman modulation contrast is recommended for tissue culture work. Also, high-quality apochromatic objectives are now designed to be suitable for DIC. Figure 20.3 presents transmitted and reflected light DIC photomicrographs of the mouthparts of a blowfly (transmitted DIC; Figure 20.3(a)) and surface defects in a ferro-

FIGURE 20.4: DIC accessories for transmitted light

silicate alloy (reflected DIC; Figure 20.3(b)). Both photomicrographs were made using a retardation plate with a 10x objective.

The equipment needed for DIC microscopy includes a polarizer, a beam-splitting modified Wollaston prism below the condenser, a beam-recombining modified Wollaston prism above the objective, and an analyzer above this upper prism. Individual prisms are required (for each objective) below the condenser (Figure 20.4). For the upper prism, a single prism may serve for all objectives. The upper prism can be moved laterally.

The distance of the placement of the lower prism in relation to the front focal plane of the condenser and the distance of the upper prism from the back focal plane of the objective are quite critical. Manufacturers therefore designate which of their objectives are suitable for their particular DIC apparatus.

The DIC condenser contains four or more prisms, a brightfield opening with aperture diaphragm for regular brightfield work, and/or several light annuli. The light annuli, together with phase objectives, enable the microscopist to make quick comparisons between phase contrast and DIC images. A rotatable polarizer is fitted below the prisms. Use of full objective aperture enables focusing on a thin plane section of a thick specimen without confusing images from above or below the plane that is being focused on; this is called Optical Sectioning. Larger apertures also yield better resolution in optical microscopy.

The color and/or light intensity effects shown in the image are related especially to the rate of change in refractive index, thickness or both in details or adjacent areas of the specimen. The image appears 3-dimensional. This appearance does not represent the true geometric nature of the specimen, but is an exaggeration based on optical thickness, and is not suitable for accurate measurement of actual heights and depths. Optical thickness refers to changes in the light path resulting from change in refractive index or actual thickness or some combination of both of these variables.

As mentioned above, at the gray setting of the movable upper prism, the 3-dimensionality is most marked. Orientation of the specimen can significantly improve the relief-like appearance. Sometimes the rotation of the specimen 180 degrees changes a hill into a valley or vice versa; hence the interpretation of the image must be done with caution. The darker

appearance on one side and the lighter appearance on the other side of a detail greatly improve the visibility by giving a pseudo-relief effect.

To configure a microscope for DIC contrast enhancement, the following steps should be considered:

- Place the DIC condenser into the substage condenser holder of the microscope and fit the DIC Wollaston prism into a slotted nosepiece or in slots behind each objective. Using a 10X objective and the condenser at the brightfield (0) position and polarizer in the light path, set up Köhler illumination with a specimen in place on the stage. Move the specimen out of the light path and remove one of the eyepieces.

- Insert a phase focusing telescope into the eyepiece tube and, while looking at the back focal plane of the objective, rotate the screw of the upper prism until you see a diagonal blackish line appearing at the center of the back of the objective. Now slightly rotate the substage polarizer to make the black line appear as black as possible. This, in effect, is adjusting the polarizer so that it is crossed (at a 90 degree angle) with the analyzer that is situated above the upper prism. Make sure the condenser aperture diaphragm is open to 2/3 to 4/5 of the back lens diameter of the objective.

- Remove the focusing telescope and return the regular eyepiece to the eyetube. Rotate the condenser turret to bring the appropriate lower prism into the light path; this is usually marked by the red or white 10 setting on the turret. Move the specimen back into the light path. Now you may use the knob of the upper prism to translate it back and forth laterally to achieve the desired effect or color. You may also rotate the stage to change the orientation of the specimen to improve the effect.

- Similar steps are taken for each objective being used, making sure the microscope is properly configured for Köhler illumination for each objective in turn by adjusting both the field and aperture diaphragms.

These are numerous advantages in DIC microscopy as compared particularly to phase microscopy:

- It is possible to make fuller use of the numerical aperture of the system because, unlike phase contrast microscopy, there is no substage annulus to restrict the aperture; Köhler illumination is properly utilized.

- There are no confusing halos as may be encountered in phase images.

- Images can be seen in striking color (optical staining) and in 3-dimensional shadowed-like appearance. The visibility of outlines and details is greatly improved, and the photomicrography of these images is striking in color and detail.

- Regular planachromats or achromats (also suitable for ordinary brightfield work) can be used if the manufacturer states that such objectives are designed for their apparatus.

There are several disadvantages or limitations in DIC:

- The equipment for DIC is quite expensive because of the many prisms that are required.

- Birefringent specimens such as those found in many kinds of crystals may not be suitable because of their effect upon polarized light. Similarly, specimen carriers, such as culture vessels, Petri dishes, etc., made of plastic may not be suitable. For such specimens, Hoffman modulation contrast may be a better choice.
- For very thin or scattered specimens, better images may be achieved using phase contrast methods.
- Apochromatic objectives may not be suitable because such objectives themselves may significantly affect polarized light.

Once again, like so many of the contrasting enhancing techniques, we find that manipulation of light at the front focal plane of the condenser and at the rear focal plane of the objective has significant effect upon the appearance of the image that is visualized through the eyepiece.

Chapter 21

Hoffman Modulation Contrast

The Hoffman Modulation Contrast system is designed to increase visibility and contrast in unstained and living material by detecting optical gradients (or slopes) and converting them into variations of light intensity. This technique was invented by Dr. Robert Hoffman in 1975, and employs several accessories that have been adapted to a number of commercial microscopes.

The basic microscope configuration for Hoffman Modulation Contrast is illustrated in Figure 21.1. An optical amplitude spatial filter, termed a "modulator" by Hoffman, is inserted on the back focal plane of an achromat or planachromat objective (although higher correction can also be used). Light intensity passing through this system varies above and below an average value, which by definition, is then said to be modulated. Objectives useful for modulation contrast can cover the entire magnification range of 10x to 100x. The modulator has three zones that are depicted in Figure 21.2: a small, dark zone near the periphery of the back focal plane which transmits only one percent of light (areas marked "D" in Figure 21.2); a narrow gray zone which transmits 15 percent (areas marked "G" in Figure 21.2); and the remaining clear or transparent zone, covering most of the territory at the back of the objective, which transmits 100 percent of the light (areas marked "B" in Figure 21.2). Unlike the phase plate in phase contrast microscopy, the Hoffman modulator is designed not to alter the phase of light passing through any of the zones. When viewed under modulation contrast optics, transparent objects that are essentially invisible in ordinary brightfield microscopy take on an apparent three-dimensional appearance dictated by phase gradients. The modulator does not introduce changes in the phase relationship of light passing through different portions of the modulator, but influences the principal zeroth order maxima. Higher order diffraction maxima are unaffected. Measurements using a Michelson interferometer confirm that the phase changes of light passed through a Hoffman-style modulator varies (if any) by a factor of less than l/20.

Below the stage, a condenser with rotating turret is utilized to hold the remaining components of the Hoffman Modulation Contrast system. The turret condenser has a brightfield opening with an aperture iris diaphragm for regular brightfield microscopy and for alignment and establishing proper conditions of Khler illumination for the microscope. At each of the other turret openings, there is an off-center slit that is partially covered with a small rectangular polarizer. The size of the slit/polarizer combination is different for each objective of different magnification; hence the need for a turret arrangement.

The Hoffman design is such that the slits are located at the front focal plane of the condenser as illustrated in Figures 21.1 and 21.3. When light passes through the off-axis

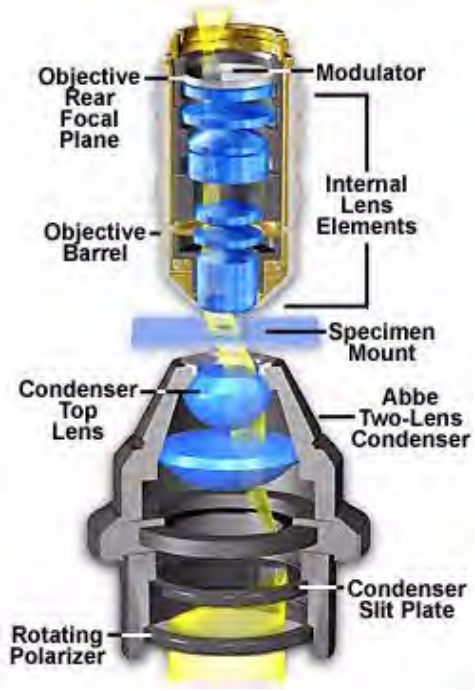

FIGURE 21.1: Hoffman modulation contrast

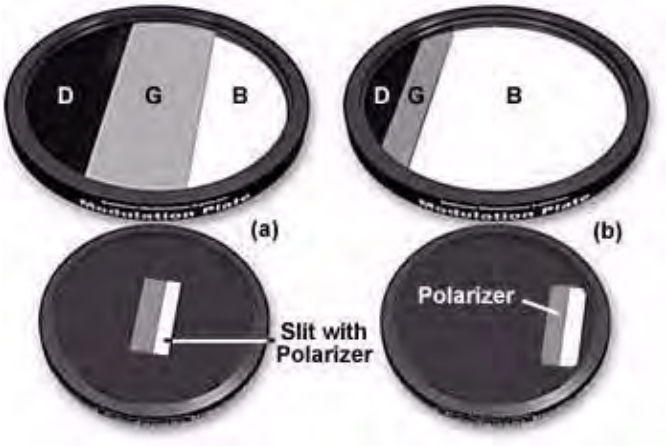

FIGURE 21.2: Modulator and slit designs

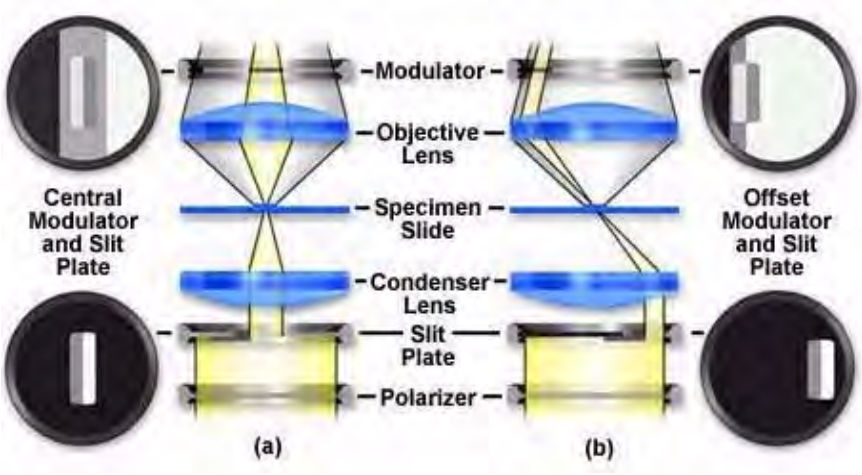

FIGURE 21.3: Principles of Hoffman modulation contrast

slit, it is imaged at the back focal plane of the objective (also termed the Fourier plane) where the modulator has been installed. The front focal plane of the condenser containing the off-axis slit plate is optically conjugate to the modulator in objective back focal plane. Image intensity is proportional to the first derivative of the optical density in the specimen, and is controlled by the zeroth order of the phase gradient diffraction pattern.

The principles of modulation contrast provide for at least two basic modulator-slit plate configurations that are illustrated in Figures 21.2 and 21.3. Drawings of the modulator plates shown in Figure 21.2 are exaggerated and increased in size for the purposes of this discussion. The arrangement on the left in Figures 21.2 and 21.3 (Figure 21.2(a) and Figure 21.3(a)) is a symmetrical system where both the modulator gray stripe and the slit are placed in the optical axis (center) of the microscope. Resolution in this system is limited to Resolution $= \frac{\lambda}{\mathrm{NA}}$ where NA is the numerical aperture of the objective and l equals the wavelength average of the imaging light source. The dark (one percent transmittance) and light or transparent (100 percent transmittance) zones are identical in size, while the gray (15 percent transmittance) zone is in the form of a narrow stripe that is 10 percent of the diameter of the exit pupil of the objective. The other arrangement (Figures 21.2(b) and 3(b)) is asymmetrical or offset, where the dark area of the modulator lies outside the exit pupil of the objective. The resolution in this system is much improved and approaches: Resolution $= \frac{\lambda}{2\mathrm{NA}}$ where values for NA and λ are the same as described above. It is obvious that resolution in the offset system (Figure 21.3(b)) is almost twice as good as in the central (Figure 21.3(a)) system. The transparent (clear) zone in the offset system fills almost 90 percent of the diameter of the objective exit pupil with the gray and dark zones filling the other 10 percent.

Below the condenser, a circular polarizer is placed on the light exit port of the microscope (note that both polarizers are below the specimen). The rotation of this polarizer can control the effective width of the slit opening. For example, a "crossing" of both polarizers at 90 degrees to each other results in "narrowing" the slit so that its image falls within the gray area of the modulator, as illustrated in Figure 21.3. The part of the slit controlled by the polarizer registers on the bright area of the modulator. As the polarizer is rotated, contrast can be varied for best effect. A very narrow slit produces images that are very high in contrast with a moderate degree of coherence. Optical section imaging is also

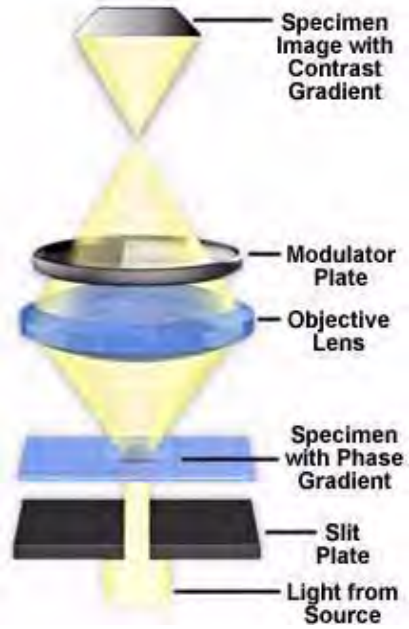

FIGURE 21.4: Modulation contrast light paths

optimized when the slit is adjusted to its narrowest position. When the circular polarizer is oriented with its vibration direction parallel to that of the polarizer in the slit, the effective slit width is at a maximum. This reduces overall image contrast and coherence, but yields much better images of thicker objects where large differences in refractive index exist.

Early designs of the modulation contrast system did not utilize the slit polarizer or the circular polarizer on the microscope light port, and relied on a single-sized slit as illustrated in Figure 21.4 for a symmetrical configuration. In this figure, light from the source passes through a fixed-aperture slit (termed a "slit–plate" in the figure) and then through a specimen containing phase gradients. These gradients deflect light, according to the direction of the gradient, into either the clear or dark zones of the symmetrical modulator that is positioned in the rear focal plane of the objective. The resulting image displays a simple contrast gradient that is dictated by the positioning and slope of phase gradients in the sample.

In modern advanced modulation contrast systems, both the modulator and the slit are offset from the optical axis of the microscope. This arrangement permits fuller use of the numerical aperture of the objective and results in good resolution and details. Shapes and details are rendered in shadowed, pseudo three-dimensional appearance. These appear brighter on one side, gray in the central portion, and darker on the other side, against a gray background. The modulator converts optical phase gradients in details (steepness, slope, rate of change in refractive index, or thickness in specimen details) into changes in intensity of various areas of the image at the plane of the eyepiece diaphragm. Resulting images have an apparent three-dimensional appearance with directional sensitivity to optical gradients.

Opposite gradients result in deflection of the slit image to either the very dark part of the modulator or the bright section of the modulator, as illustrated in Figure 21.5. In this figure, a hypothetical specimen containing both positive and negative phase (thickness) gradients and a flat (non-gradient) area is imaged using modulation contrast optical components.

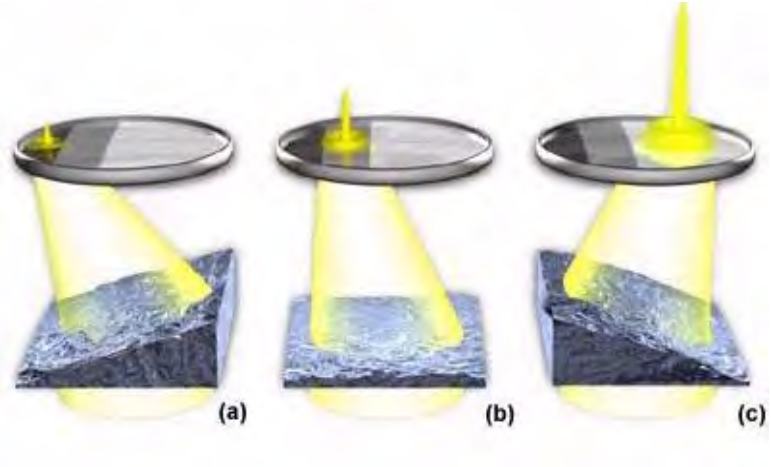

FIGURE 21.5: Imaging phase gradients

The negative gradient depicted in Figure 21.5(a) deflects light into the dark area of the modulator, where it is attenuated to approximately one percent of its former value. Likewise in Figure 21.5(c), light deflected by a positive gradient into the clear area of the modulator is not attenuated, and 100 percent of this light is transmitted into the intermediate image plane. Any non-gradient part of the specimen (Figure 21.5(b)) and also the background (surround) register on the gray part of the modulator, where about 15 percent of the light is transmitted into the intermediate image plane. The result is that the intensity of the image area from one side of the gradient is dark. Intensity from the opposite side of the gradient yields a bright image area, and the non-gradient areas appear gray on the image, as does the background.

The contrast (related to variations in intensity) of the dark and bright areas against the gray gives a shadowed pseudo-relief effect. This is typical of modulation contrast imaging. Rotation of the polarizer alters the contrast achieved and the orientation of the specimen on the stage (with respect to the polarizer and offset slit) may dramatically improve or degrade contrast.

Since the modulator affects the image of the slit according to how the specimen's details shift the image of the slit (and thus results in altering light intensities), it is described as an amplitude filter. Hoffman and others have demonstrated that phase gradients in the specimen, like spatial frequencies, are distributed over the entire exit pupil of the objective. The optical transmission intensity distribution of the modulator will provide satisfactory images of a wide variety of objects that produce phase gradients including: all types of cells and tissues (both live, stained, and unstained), and surface details of crystals, transparent polymers, glasses and other similar materials. Reflected light modulation contrast microscopy is also useful for imaging grain boundaries in opaque and metallurgical specimens and surface details of complex integrated circuits and other electronic materials.

There are numerous advantages as well as limitations to modulation contrast. Some of the advantages include fuller use of the numerical aperture of the objective yielding excellent resolution of details along with good specimen contrast and visibility. Although many standard modulation contrast objectives are achromats or planachromats, it is also possible to use objectives with a higher degree of correction for optical aberration, as discussed above. Many major microscope manufacturers now offer modulation contrast

objectives in fluorite-correction grades, and apochromats can be obtained by special order. Older objectives can often be retrofitted with a modulator made by Modulation Optics, Inc., the company founded by Dr. Robert Hoffman specifically to build aftermarket and custom systems.

In addition to the advantages of using higher numerical apertures with modulation contrast, it is also possible to do "optical sectioning" with this technique. Sectioning allows the microscopist to focus on a single thin plane of the specimen without interference from confusing images arising in areas above or below the plane that is being focused on. The depth of a specimen is measured in a direction parallel to the optical axis of the microscope. Focusing the image establishes the correct specimen-to-image distance, allowing interference of the diffracted waves to occur at a pre-determined plane (the image plane) positioned at a fixed distance from the eyepiece. This enables diffracting objects that occur at different depth levels in the specimen to be viewed separately, provided there is sufficient contrast. The entire depth of a specimen can be optically sectioned by sequentially focusing on each succeeding plane. In this system, depth of field is defined as the distance from one level to the next where imaging of distinct detail occurs, and is controlled by the numerical aperture of the objective. Higher numerical aperture objectives exhibit very shallow depths of field and the opposite holds for objectives of lower numerical aperture. The overall capability of an objective to isolate and focus on a specific optical section diminishes as the optical homogeneity of the specimen decreases.

Images appear shadowed or pseudo three-dimensional, enhancing visibility because of differences in contrast on either side of a detail. There are no halos exhibited in the image, unlike the images produced with phase contrast optics. Modulation contrast converts phase gradient information into amplitude differences that are very different from the phase relationship variations (and optical path differences) produced by a phase contrast microscope. Use of the dark and gray zones in the modulator produce images that contain varying shades of gray and are devoid of color. It is possible to introduce color into modulation contrast images by producing modulators that have the gray and dark zones substituted for colored zones of equal transmittance values. In this case, resulting images from the phase gradient are rendered in colors with similar gradients having the same tint. Currently, we are unaware of any commercial source of modulation filters that contain colored zones.

Achromats or planachromats are the most widely utilized objectives for modulation contrast microscopy because they can yield good images since color is not involved. Using these objectives with a green filter (placed under the polarizer) will further improve the image because achromats are spherically corrected for green light. Objectives of higher correction, including fluorites and apochromats, can also be used for modulation contrast microscopy, but the added expense is often not worth the improvement in image quality, except at very high magnifications.

The cost of the modulation contrast accessories is considerably below that of differential interference contrast (DIC) equipment. Although both techniques require turret condensers with components matched to each objective, DIC-equipped microscopes also contain a polarizer below the condenser and an analyzer that is placed before the intermediate image plane in the optical path (above the objectives). The presence of a crossed polarization system, necessary for DIC microscopy, diminishes its effectiveness with samples that react to polarized light.

Birefringent objects (rock thin sections, crystals, bone, etc.), that can confuse images in DIC, can be examined since the specimen is not situated between the two polarizers.

Further, specimens can be contained in plastic or glass vessels without deterioration of the image because of polarization effects since such vessels are also above both polarizers, not between them. This allows the Hoffman system to be far more useful than DIC in the examination and photomicrography of cell, tissue, and organ culture performed in plastic containers.

When the condenser is set at the brightfield position, objectives with a modulator installed can also be used for regular brightfield work. Because the modulator is off-axis, little deterioration of the image results. Objectives (but not the slit-plate condenser) equipped with a modulator can also be used for fluorescence and darkfield work, but these objectives should be avoided when attempting DIC microscopy. The modulation contrast system has been used very successfully with polarized light microscopy to enhance the detection of both optical gradients and birefringency in the specimen. In this application, a non-polarized slit is used and the polarized light configuration should be parallel polarizers (although crossed polarizers will also produce good results, albeit with diminished illumination). An objective modified for modulation contrast is very useful using ordinary polarized illumination without a slit plate in the condenser.

There are also several disadvantages and limitations of the Hoffman Modulation Contrast system. Images must be viewed with caution because different observers can "see" a "hill" in the image as a "valley" or vice versa as the pseudo three-dimensional image is observed through the eyepiece. The system is most sensitive to gradients perpendicular to the length of the slit, resulting in the requirement for some degree of skill in orientation of the specimen for best effect.

The cost of modification of each objective and the condenser openings must be added to the basic cost of these accessories themselves. Complex, high numerical aperture, multi-element objectives are difficult or too expensive to modify. In recent years, Robert Hoffman's company, Modulation Optics of Greenvale, New York (a wholly owned subsidiary of Slant Fin Corporation), has been producing modified objectives and condensers. Modulation Optics specializes in modifying objectives produced by the leading microscope manufacturers. Some objectives are easily modified, while some are difficult or impossible to modify for the modulation optics specification. However, any objective can be used with one of the company's intermediate tube systems, including a broad range that spans macro camera lenses to 100x microscope objectives. Also included in this category are objectives designed to image specimens either dry or with immersion media (oil, water, and glycerin), single and multiple wavelength objectives, reflected and transmitted light objectives, and objectives corrected for either infinity or a finite tube length. Modulation Optics designs and manufactures their own condenser systems to satisfy a wide range of numerical aperture and working distance combinations.

Non-absorbing specimens are not rendered in color, with the exception of those observed using a special modulator containing semi-transparent colored filters in place of the gray and dark zones. Specimens that naturally absorb specific wavelengths or lightly stained are rendered in color as well as those observed with the combination of modulation contrast and fluorescence or with the combination of modulation contrast and polarized light.

21.1 Configuration for Hoffman Modulation Contrast

- Attach the pertinent modulation contrast-enabled objectives to the nosepiece of the microscope, and install the turret condenser containing the appropriate slit plates. If

the microscope is equipped for differential interference contrast (DIC) or polarizing microscopy, remove all polarizers, retardation plates, and Wollaston or Nomarski prisms from the optical path.

- Place a stained specimen (preferably a tissue thin section) on the stage and, using the 10x objective (with a modulator installed), align the microscope for proper Khler illumination, outlined in our section on Anatomy of the Microscope. The modulation contrast slit plate should be removed from the condenser for this operation. If the turret condenser has a position for brightfield illumination with an aperture diaphragm, rotate the turret to select this condenser.

- View the modulator plate in the back focal plane of the objective, using a Bertrand lens (common on polarized light microscopes), a phase telescope, or by simply removing an eyepiece and peering down the eye tube. Make certain that the sample is removed from the optical path or that it is moved to a clear area on the microscope slide.

- Select the slit aperture plate that corresponds to the 10x objective by moving the appropriate condenser (from the turret) into the optical path. There should be a set of adjustment screws or a lever that allows rotation and translation of the illuminating slit plate within the condenser.

- Place the circular polarizing filter on the microscope light port beneath the condenser. Rotate this filter while observing the slit image through the Bertrand lens (or phase telescope) and observe that the angle of rotation influences the amount of light (brightness) passing through the polarizer portion of the slit.

- Translate the image of the slit so that the opened portion lacking a polarizer is superimposed over the gray region of the modulator plate as illustrated in Figure 21.3(b). The portion of the slit containing the polarizing material should be imaged in the clear portion of the modulator just to the right of the gray region. Rotate the circular polarizing filter and observe how the region of the slit containing the polarizing material appears and disappears. When the vibration plane of the circular polarizer is aligned perpendicular to the vibration plane of polarizer in the slit, the slit size if minimized and maximum contrast is obtained.

- Remove the Bertrand lens or phase telescope and replace the eyepiece in the eye tube of the microscope. Place a specimen candidate on the stage and focus with the 10x objective.

- Readjust the condenser position by refocusing the field diaphragm to achieve a sharp focus. Open the field iris diaphragm until it is just outside the field of view.

- The image is now ready for observation or photomicrography with modulation contrast. Rotate the specimen and/or the circular polarizer at the base of the microscope to achieve optimum contrast. These settings will vary from specimen to specimen.

- Repeat the above steps each time a different magnification is selected for viewing the specimen in modulation contrast.

Once again, we find that manipulation of light at the front focal plane of the condenser (by means of an offset slit) and manipulation of light at the back focal plane of the objective (offset modulator) can have a significant effect upon the image presented in the eyepieces.

21.2 Troubleshooting Hoffman Modulation Contrast

Proper alignment of the illuminating slit is critical in achieving the optimum results with Hoffman Modulation Contrast microscopy. The following problems and solutions are often encountered when imaging specimens using this technique.

Problem The image is very low in contrast and is difficult to visualize and/or produces flat photomicrographs also lacking is sufficient contrast.

Solution This problem can arise from incorrect alignment of the illuminating slit, or when the contrast control polarizer is missing or rotated out of position. Use a Bertrand lens or a phase telescope to re–align the slit while observing its image at the rear focal plane of the condenser. Make certain that the contrast control polarizer is aligned with the vibration direction perpendicular to the polarizer in the slit opening. This is accomplished by rotating the polarizer while observing the slit with the phase telescope. When properly positioned, the image of the slit should appear superimposed over the gray area of the modulator.

Problem Illumination of the specimen is uneven and the image appears to have dark and/or light overtones.

Solution This problem may arise for several reasons:

- *the wrong slit plate is being used with the objective*
  Rotate the turret condenser until the matching slit plate is in place in the optical axis. Repeat the illuminating slit alignment procedure with a Bertrand lens or phase telescope.
- *the image of the illuminating slit is not properly aligned and superimposed on the gray area of the modulator*
  Use a Bertrand lens or a phase telescope to adjust the image of the illuminating slit plate making sure it is properly superimposed on the gray area of the modulator.
- *the overall microscope illumination is not properly adjusted*
  Adjust the microscope for Köhler illumination using a brightfield condenser with an adjustable aperture diaphragm.

Problem The illuminating slit can not be imaged on the gray region of the modulator plate.

Solution In most cases, the wrong illuminating slit plate is being used in the substage condenser. Make sure the slit plate is matched to the objective and realign the microscope with a Bertrand lens or phase telescope.

Problem When imaging the back focal plane of the objective, the dark and gray zones are not present in the modulator.

Solution The wrong objective is being used. Carefully remove the objective and hold it up to a bright light source and peer through the rear lens. The modulator plate should be visible, if it is present and properly aligned in the objective. If not, change to an objective that contains a modulator plate.

Chapter 22

Introduction to Phase Contrast

The search was still on in the 1930's to find a way of using both direct and diffracted light from all azimuths to yield good contrast images of unstained objects that do not absorb light. Research by Frits Zernike during this period uncovered phase and amplitude differences between zeroth order and deviated light that can be altered to produce favorable conditions for interference and contrast enhancement.

Unstained specimens that do not absorb light are called phase objects because they slightly alter the phase of the light diffracted by the specimen, usually by retarding such light approximately 1/4 wavelength as compared to the undeviated direct light passing through or around the specimen unaffected. Unfortunately, our eyes as well as camera film, are unable to detect these phase differences. To reiterate, the human eye is sensitive only to the colors of the visible spectrum (variations in light frequency) or to differing levels of light intensity (variations in wave amplitude).

In phase specimens, the direct zeroth order light passes through or around the specimen undeviated. However, the light diffracted by the specimen is not reduced in amplitude as it is in a light-absorbing object, but is slowed by the specimen because of the specimen's refractive index or thickness (or both). This diffracted light, lagging behind by approximately 1/4 wavelength, arrives at the image plane out of step (also termed out of phase) with the undeviated light but, in interference, essentially undiminished in intensity. The result is that the image at the eyepiece level is so lacking in contrast as to make the details almost invisible.

Zernike succeeded in devising a method–now known as Phase Contrast microscopy–for making unstained, phase objects yield contrast images as if they were amplitude objects. Amplitude objects show excellent contrast when the diffracted and direct light are out of step (display a phase difference) by 1/2 of a wavelength. Zernike's method was to speed up the direct light by 1/4 wavelength so that the difference in wavelength between the direct and deviated light for a phase specimen would now be 1/2 wavelength. As a result, the direct and diffracted light arriving at the image level of the eyepiece would be able to produce destructive interference (see the section on image formation for absorbing objects previously described). Such a procedure results in the details of the image appearing darker against a lighter background. This is called dark or positive phase contrast. A schematic illustration of the basic phase contrast microscope configuration is illustrated in Figure 22.1.

Another possible course, much less often used, is to arrange to slow down the direct light by 1/4 wavelength so that the diffracted light and the direct light arrive at the eyepiece in step and can interfere constructively. This arrangement results in a bright image of the

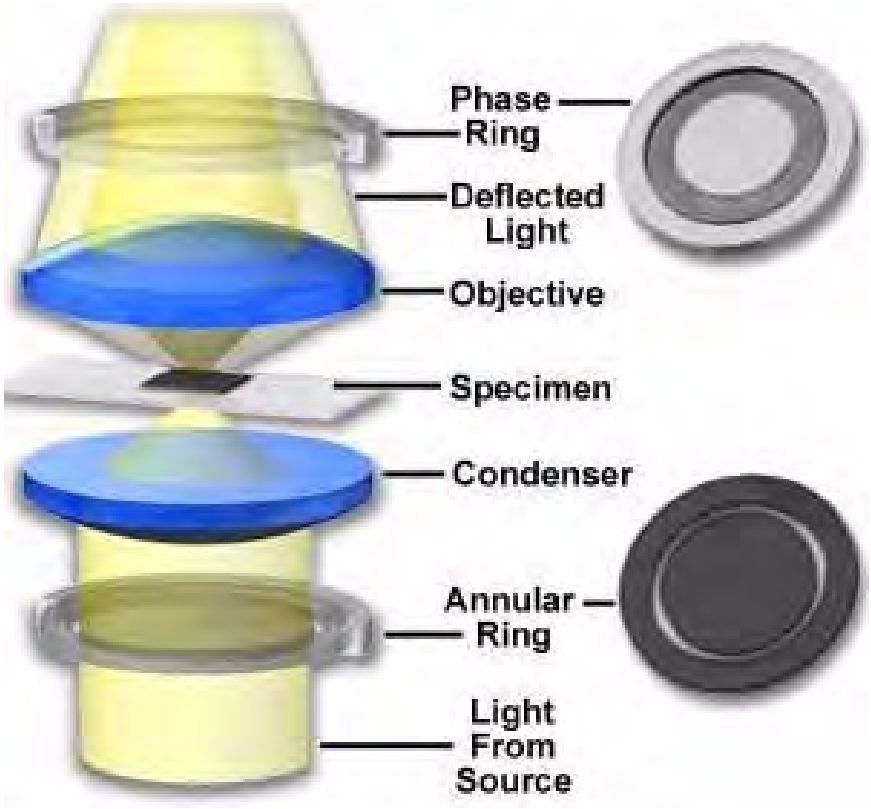

FIGURE 22.1: Phase contrast light pathways

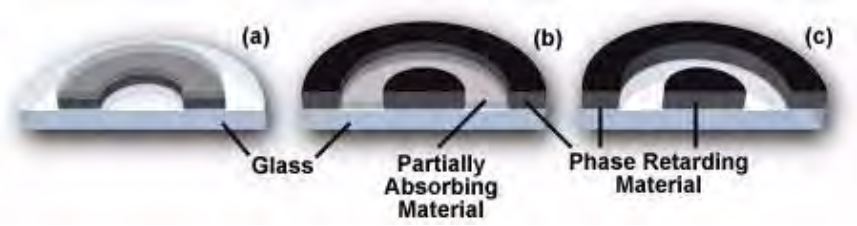

FIGURE 22.2: Annular phase plates

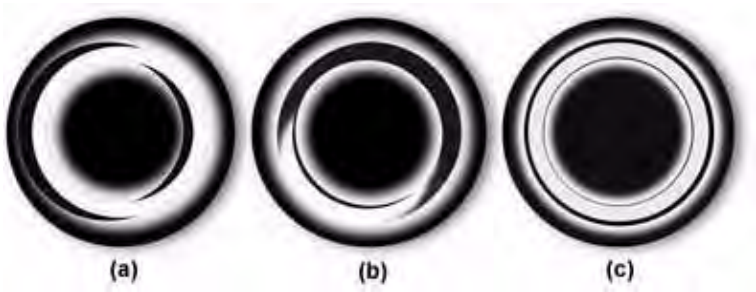

FIGURE 22.3: Phase plate and light annulus alignment

details of the specimen on a darker background, and is called negative or bright contrast.

Phase contrast microscopy was very successful and ultimately gained widespread application, resulting in Zernike's award of the prestigeous Nobel prize in physics in 1953. The phase contrast technique has hailed as the greatest advance in microscopy in a century. Phase contrast, by "converting" phase specimens such as living material into amplitude specimens, allowed scientists to see details in unstained and/or living objects with a clarity and resolution never before achieved.

The Zernike method involves the separation of the direct zeroth order light from the diffracted light at the rear focal plane of the objective. To do this, a ring annulus is placed in position directly under the lower lens of the condenser at the front focal plane of the condenser, conjugate to the objective rear focal plane. As the hollow cone of light from the annulus passes through the specimen undeviated, it arrives at the rear focal plane of the objective in the shape of a ring of light. The fainter light diffracted by the specimen is spread over the entire rear focal plane of the objective.

If this combination were allowed, as is, to proceed to the image plane of the eyepiece, the diffracted light would be approximately 1/4 wavelength behind the direct light. At the image plane, the phase of the diffracted light would be out of phase with the direct light, but the amplitude of their interference would be almost the same as that of the direct light. This would result in very little specimen contrast.

To speed up the direct undeviated zeroth order light, a phase plate is installed with a ring shaped phase shifter attached to it at the rear focal plane of the objective. The narrow area of the phase plate is optically thinner than the rest of the plate. As a result, undeviated light passing through the phase ring travels a shorter distance in traversing the glass of the objective than does the diffracted light.

Now, when the direct undeviated light and the diffracted light proceed to the image plane, they are 1/2 wavelength out of phase with each other. The diffracted and direct light can now interfere destructively so that the details of the specimen appear dark against

a lighter background (just as they do for an absorbing or amplitude specimen). This is a description of what takes place in positive or dark phase contrast.

If the ring phase-shifter area of the phase plate were to be made thicker than the rest of the plate, direct light is slowed by 1/4 wavelength. In this case, the zeroth order light arrives at the image plane in step (or in phase) with the diffracted light, and constructive interference takes place. The image would appear bright on a darker background. The image appears bright on a darker background. This type of phase contrast is described as negative or bright contrast.

Because the undeviated light of the zeroth order is much brighter than the faint diffracted light, a thin absorptive transparent metallic layer is deposited on the ring to bring the direct and diffracted light into better balance of intensity in order to increase contrast. Also, because the speeding up or slowing down of the direct light is calculated on a 1/4 wavelength of green light, the phase image will appear best when a green filter is placed in the light path (a green interference filter is preferable). Such a green filter also helps achromatic objectives produce their best images, since achromats are spherically corrected for green light.

The accessories needed for phase contrast work are a substage phase contrast condenser equipped with annuli and a set of phase contrast objectives, each of which has a phase plate installed. The condenser usually has a brightfield position with an aperture diaphragm and a rotating turret of annuli (each phase objective of different magnification requires an annulus of increasing diameter as the magnification of the objective increases). Each phase objective has a darkened ring on its back lens. Such objectives can also be used for ordinary brightfield transmitted light work with only a slight reduction in image quality.

The phase outfit, as supplied by the manufacturer, usually includes a green filter and a phase telescope. The latter is used to enable the microscopist to alight the condenser annulus to superimpose it onto the ring of the phase plate. A set of centering screws in the substage condenser allows manipulation of the annulus to align it while observing the back focal plane of the objective with the phase telescope (or through a Bertrand lens).

To set up a phase microscope (cheek lining cells are a readily available test material), focus the specimen with the 10X phase objective. Next, configure the microscope for Köhler illumination using the brightfield (0) position of the condenser. This critical step is to assure the proper alignment of the microscope's objective, condenser, and field diaphragm. After the microscope is properly aligned, open up the condenser aperture diaphragm and swing the turret of the condenser into the 10 position (this usually automatically opens the aperture diaphragm). Place the green filter in the light path, and remove one of the eyepieces. Insert the phase telescope and, while observing the back of the objective, use the Annulus Centering Screws to center the annulus to the ring of the plate. A Bertrand lens or a pinhole eyepiece, if available, will allow a view of the back focal plane of the objective. Centering the phase annulus is often easier to do if the specimen is temporarily removed from the light path. After alignment of the phase ring with the annulus, reinsert the eyepiece and place the specimen back into its proper place on the microscope stage in the optical path.

Repeat the same procedure for each objective, making sure that the turret is rotated so the appropriate phase annulus is positioned to match the objective magnification. Some manufacturers provide individual push-in, centering, annuli that can be inserted into the lower part of the common Abbe condenser. Such inexpensive, simple devices do well with the 10X, 20X, and 40X phase objectives, but the condenser can receive only one at a time.

Phase microscopy continues to be a widely used and important tool, particularly for the microscopist studying living and/or unstained material, such as cells and tissues in culture. The method is also currently used simultaneously with reflected light fluorescence to reveal areas of a specimen that do not fluoresce. Phase microscopy techniques are particularly useful with specimens that are thin and scattered in the field of view.

There are some limitations of phase contrast microscopy:

- Phase images are usually surrounded by halos around the outlines of details. Such halos are optical artifacts, which sometimes obscure the boundaries of details.
- The phase annuli do limit the working numerical aperture of the optical system to a certain degree, thus reducing resolution.
- Phase contrast does not work well with thick specimens because of shifts in phase occur from areas slightly below or slightly above the plane that is in focus. Such phase shifts confuse the image and distort image detail.
- Phase images appear gray if white light is used and green if a green filter is used. In the past, many microscopists restricted their film to black and white when performing photomicrography on phase specimens. Today, many color films reproduce black, white, and grayscales very effectively, especially the tungsten-balanced transparency films from Fuji, Kodak, and Agfa.

Phase microscopy is another exemplification of how the manipulation of light at the substage condenser lower lens level and at the objective rear focal plane level has significant effect upon the image that is observed through the eyepiece.

22.1 Apodized Phase Contrast

Differences in light absorption are often negligible between the various intracellular components and plasma membranes in living cells, rendering them barely visible when observed through the microscope utilizing the classical technique of brightfield illumination. Phase contrast microscopy takes advantage of minute refractive index differences within cellular components and between unstained cells and their surrounding aqueous medium to produce contrast in these and similar transparent specimens.

Light passing through a ring aperture or annulus, mounted in the substage condenser front focal plane, is used to illuminate the specimen in phase contrast microscopy (Figure 22.4). As the hollow cone of light emanating from the phase annulus encounters the transparent specimen, it is either diffracted by subcellular components and the membrane or passes through undeviated. Light that passes through the specimen undeviated arrives at the rear focal plane of the objective in the shape of a ring, whereas the fainter light diffracted by the specimen is spread over the entire surface of the focal plane. A small phase shift measuring approximately one quarter wavelength relative to the direct light is induced in the light diffracted by the specimen.

The phase differences of the direct light from the background and the diffracted light from the specimen cause the two beams to interfere with each other at the intermediate image plane. This is achieved by adding or subtracting a quarter wave shift to the direct light by means of a semi-transparent phase plate strategically placed in a plane that is conjugate (the objective rear focal plane) to the annulus in the condenser (the condenser

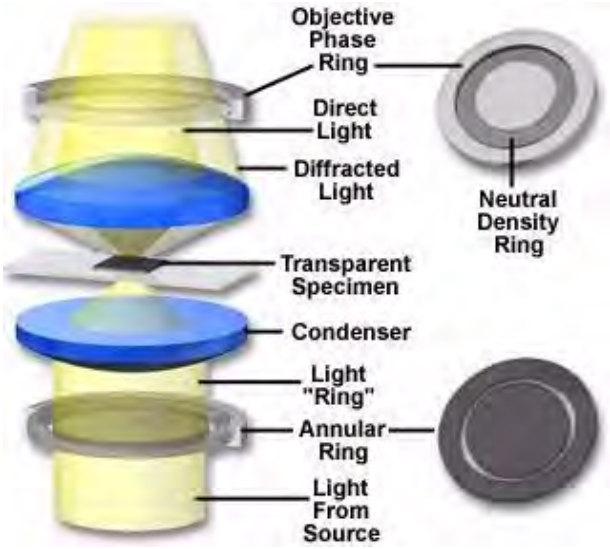

FIGURE 22.4: Phase contrast light pathways

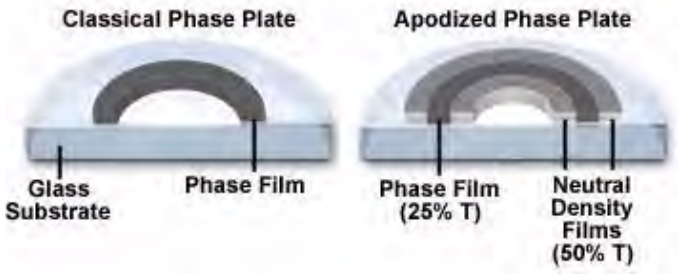

FIGURE 22.5: Apodized phase plate configuration

front focal plane). The direct background light is attenuated by a neutral density thin film applied to the phase ring in the objective. At the intermediate image plane, an interference pattern results, which produces intensities proportional to the phase shift induced by the specimen.

An unfortunate artifact in phase contrast microscopy is the halo effect, which results in spurious bright areas around phase objects or reverse contrast in images. This effect is especially prevalent with specimens that induce large phase shifts. Reducing the halo artifact was once thought to be a difficult theoretical problem, but recent advances in objective phase ring configuration have resulted in a new technique termed apodized phase contrast (Figure 22.5), which allows structures of phase objects having large phase differences to be viewed and photographed with outstanding clarity and definition of detail.

Presented in Figure 22.5 are a conventional (or classical) and an apodized phase plate positioned at an angle to the viewer and sectioned through the center for ease of illustration. The classical phase plate on the left, which is positioned at the objective rear focal plane, has a thin ring of neutral density material (termed a phase film) applied to the surface. The purpose of the film is to retard the phase of direct light passing through the specimen by one quarter wavelength to allow constructive and destructive interference with diffracted light at the intermediate image plane. On the right in Figure 22.5 is an illustration of an

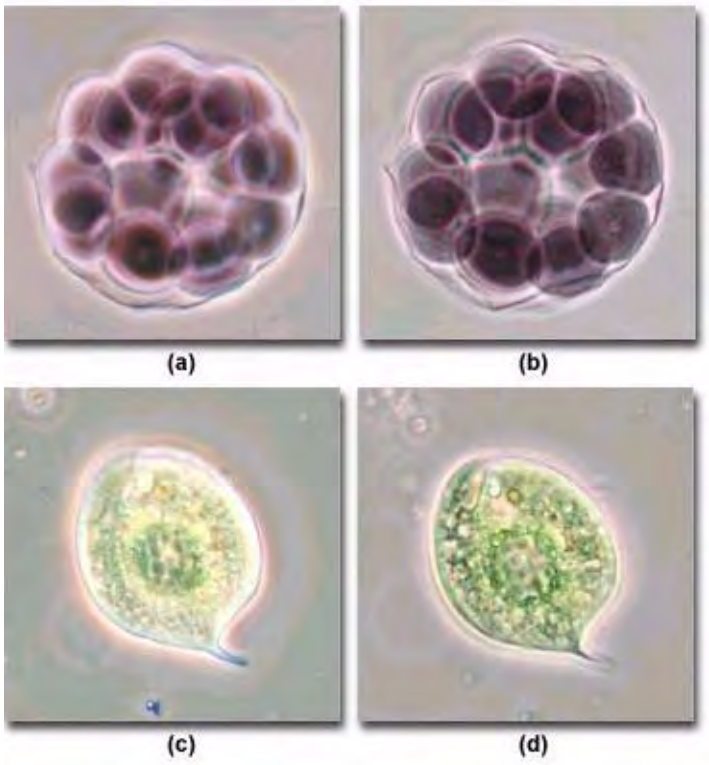

FIGURE 22.6: Halo reduction in apodized phase contrast

apodized phase plate. Surrounding the phase film in this plate are two concentric areas of semi-transparent neutral density material, which reduce the intensity of light diffracted from the specimen at small angles.

The effect of apodized phase plates on images seen in the microscope is illustrated in Figure 22.6 for two specimens. Figure 22.6(a) is a photomicrograph of a starfish embryo taken with a Nikon Eclipse E600 microscope operating in standard phase contrast mode. The objective used was a long working distance (LWD) Ph1 DL (dark-light) designed to produce a dark image outline on a light gray background. This type of objective is the most popular type for routine phase contrast examination of cells and other living material, because it produces the strongest dark contrast in objects having major differences in refractive indices. Note the halo surrounding the outer periphery of the embryo and the lack of contrast and image detail present in the central portion of the cell mass. A significant improvement in contrast is observed with the use of a corresponding objective having apodized phase plates, as illustrated in Figure 22.6(b). In this figure, the starfish embryo has a dramatically reduced halo around the periphery and exhibits sharper edges with enhanced internal specimen detail and apparent depth of field.

A similar pair of photomicrographs is illustrated in Figures 22.6(c) and 22.6(d), using a live euglena specimen. Euglenas are a member of the protozoan order Euglenida, a remarkable group of single-celled creatures, many of which exhibit characteristics of both plants and animals. Figure 22.6(c) presents a classical phase contrast image taken of the euglena specimen using a DL phase objective. Internal specimen details have a vague contrast and the outer cellular membrane is surrounded by a substantial halo. When the same specimen is imaged using apodized phase optics (Figure 22.6(d)), the halo size is

reduced and internal specimen features are more highly resolved.

22.1.1 Apodized Phase Contrast Theory

The refractive index (n) of most phase objects, especially living cells, ranges between 1.36 and 1.37 when illuminated with light having an average wavelength centered in the visible region of the spectrum (550 nm). For specimens that have a spherical geometry, the phase difference between the specimen and the surrounding medium increases as the specimen thickness grows larger, resulting in a smaller diffraction angle for light deviated by the specimen. Assuming a spherical specimen, the maximum phase difference (δ) and diameter (d) are related by the following equation:

$$\delta = \frac{2\pi}{\lambda}(n' - n)d$$

where λ is the wavelength of light in a vacuum (or in air), n' is the refractive index of the specimen, and n is the refractive index of the surrounding medium (usually a buffered aqueous solution). It is evident from the equation that increasing the specimen diameter (d) will illicit a correspondingly larger phase difference (δ) in the illumination wavefront, provided the refractive indices of the specimen and media remain constant.

Now, we will consider the diffraction pattern produced by a circular aperture of diameter d. In the ideal case, when the objective is aberration-free and provides a uniform circular aperture, two adjacent points are just resolved when the centers of their Airy disks are separated by a distance r, the central Airy disk radius. The quantity r is determined by the equation:

$$r = 0.61\frac{\lambda}{n \cdot \sin(\theta)}$$

where λ is the wavelength of light with air as the immersion medium and q is the angle of diffraction (aperture angle). For this discussion, we assume that the aperture diameter d equals the resolution distance r, and can then state:

$$r = d = 0.61\frac{\lambda}{n \cdot \sin(\theta)}$$

$$\sin(\theta) = 2\pi \cdot (n' - n)\frac{0.61}{nd}$$

If the diffraction angle (θ) is small, then there is an inverse relationship between the term θ and the phase difference (δ):

$$\theta \propto \frac{1}{\delta}$$

In order to examine the diffracted and undeviated light intensity at the intermediate image plane, we must first consider the physical aspects of the illuminating wavefronts. If the illuminating wavefront is a uniform plane wave, then the incident wavefront $\phi(0)$ and the wavefront after passing through a phase object (specimen; $\phi(1)$) can be described by the following equations:

$$\begin{aligned} \phi(0) &= \sin(\omega \cdot t) \\ \phi(1) &= \sin(\omega \cdot t + \delta) \end{aligned}$$

where ω is the angular frequency of the illuminating wavefront, t is time, and δ is the relative phase difference between the wavefronts passing through the specimen or through the surrounding media. In most cases the value for δ is small, so that equation reduces to:

$$\phi(1) = \sin(\omega \cdot t) + \delta \cos(\omega \cdot t) \tag{22.1}$$

The first term in this equation describes the incident light wave and represents the undiffracted or direct light passing through and around the specimen, while the second term indicates the sum of the light diffracted by the specimen. In most cases, the diffracted light has a quarter wave phase difference with respect to the direct light, and an amplitude that is proportional to the phase difference caused by the specimen. Taking into account the addition (or subtraction) of one quarter wavelength from the direct portion of the light through the utilization of an appropriate zonal phase shift plate at the objective rear focal plane, equation 22.1 reduces to:

$$\phi(1) = (1 + \delta) \cos(\omega \cdot t)$$

To arrive at the intensity (I) of the wave at the intermediate image plane, we can take the square of this equation and integrate to remove the time dependency:

$$I = (1 + \delta)^2$$

The image intensity is proportional to $(1 + \delta)^2$ because the integral of the squared cosine is a constant. Thus, the relationship between the diffraction angle, the amplitude of light diffracted by the specimen, and the phase difference have been established. From the last equation, it is obvious that the intensity of light at the intermediate image plane is proportional to the sum of the amplitudes of the direct and diffracted light. It should be noted that the diffracted light intensity varies with field position, while direct light is uniform across the image plane.

22.1.2 Apodized Phase Plates

In practice, halo reduction and an increase in specimen contrast can be obtained by the utilization of selective amplitude filters located adjacent to the phase film in the phase plates built into the objective at the rear focal plane. These amplitude filters consist of neutral density filter thin films applied to the phase plate surrounding the phase film as illustrated in Figure 22.5. The transmittance of the phase shift ring in the classical phase plate is approximately 25 percent, while the pair of adjacent rings surrounding the phase shift ring in the apodized plate have a neutral density with 50 percent transmittance. The width of the phase film in both plates is the same. These values are consistent with the transmittance values of phase shifting thin films applied to standard plates in phase contrast microscopes.

The necessary width of the surrounding neutral density films can be calculated by the diffraction angle (θ), discussed in equations (2) through (7). This value is somewhat specimen-dependent, but commercial apodized phase objectives available from Nikon are fabricated assuming an object (specimen) diameter of approximately 10 microns, a typical value for biological cells used in tissue culture experiments.

Basic principles of the apodized phase contrast technique are presented in Figure 22.7, which illustrates the effects of both small and large specimens. The relationship between

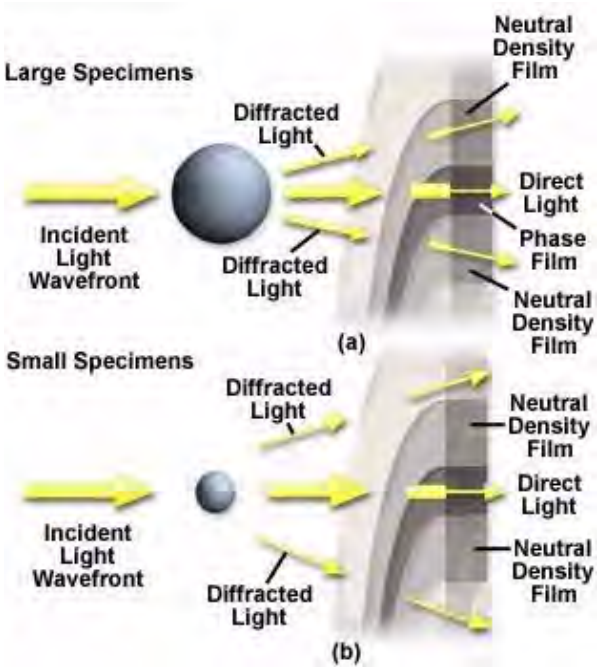

FIGURE 22.7: Diffraction angles in apodized phase plate

the phase difference in specimens of various sizes heavily influences the attenuation effects of apodized phase plates. A generous portion of the light diffracted by larger specimens (greater than or equal to 10 microns in diameter; Figure 22.7(a)) passes through the neutral density absorption rings and will be attenuated, thus reducing the intensity. On the other hand, for specimens that are smaller than 10 microns in diameter, such as nucleoli, plasma membranes, and cytoplasmic granules, diffracted light will pass on the outer periphery of the neutral density filter rings because of the large diffraction angle. In this case, the amplitude of diffracted light will not be attenuated by the transparent portion of the phase plate, rendering specimen details in high contrast (but with associated halos).

The apodization technique has been used successfully with other optical configurations to reduce the intensity of direct light at the aperture. In any diffraction-limited imaging system, the point spread function usually has side-lobes or side-rings of significant intensity. These artifacts can be of considerable concern in systems designed to resolve a weak light point-source that is positioned adjacent to a stronger point-source. The term apodize is derived from the Greek word meaning "to remove the feet". In optical terms, the "feet" are considered to be the side–lobes or side-rings in a diffraction-limited imaging system. A similar technique, commonly employed in digital imaging, is known by the term windowing.

In general terms, apodization of an optical system requires the introduction of amplitude attenuation (or in some cases, enhancement) to light passing through the exit pupil. The amount of attenuation is usually negligible in the center of the pupil, but increases with radius and becomes greatest at the edges of the pupil near the aperture. In other words, the edges of an image at the aperture can be "softened" by the introduction of a light-attenuating mask. Because diffraction at an abrupt aperture results in edge waves originating at the rim, the softening effect helps to spread the apparent origin of the diffracted waves over a broader area. This results in a suppression of the ringing effects induced by the edge waves.

Apodization has classically been utilized to provide a tapering of transmittance near the edges of light traveling through the exit pupil of an optical system in order to suppress the intensity of side-lobes surrounding the point spread function. In recent years, however, apodization has been applied to other systems and used to describe any introduction of absorption into the exit pupil, regardless of whether the side-lobes are suppressed or accentuated.

In conclusion, the utilization of apodized phase contrast optics results in dramatically improved images, which have reduced halos and high contrast in minute specimen detail. In most cases, subcellular features (such as nucleoli) can be clearly distinguished as having dark contrast with apodized objectives, but these same features have bright halos or are imaged as bright spots using conventional phase contrast optics. With the apodized optics, contrast is reversed due to the large amplitude of diffracted light relative to that of the direct light passing through the specimen.

The contrast of the image from a phase object can be altered by modulating the transmittance and size of the annular neutral density zones surrounding the central phase film. If these zones are produced with a gradient of transmittance, then object contrast can be more closely controlled for a large variety of specimen sizes.

Chapter 23

Polarized Light Microscopy

23.1 Introduction

Although much neglected and undervalued as an investigative tool, polarized light microscopy (Figure 1) provides all the benefits of brightfield microscopy and yet offers a wealth of information, which is simply not available with any other optical microscopy technique.

As well as providing information on absorption color and boundaries between minerals of differing refractive indices obtainable in brightfield microscopy, polarized light microscopy can distinguish between isotropic and anisotropic materials. The technique exploits optical properties of anisotropy to reveal detailed information about the structure and composition of materials, which are invaluable for identification and diagnostic purposes.

Isotropic materials, which include gases, liquids, unstressed glasses and cubic crystals, demonstrate the same optical properties in all directions. They have only one refractive index and no restriction on the vibration direction of light passing through them. Anisotropic materials, in contrast, which include 90 percent of all solid substances, have optical properties that vary with the orientation of incident light with the crystallographic axes. They demonstrate a range of refractive indices depending both on the propagation direction of light through the substance and on the vibrational plane coordinates. More importantly, anisotropic materials act as beam splitters and divide light rays into two parts (as illustrated in Figure 1). The technique of polarizing microscopy exploits the interference of the split light rays, as they are re-united along the same optical path to extract information about these materials.

Polarized light microscopy is perhaps best known for its geological applications–primarily for the study of minerals in rock thin sections, but it can also be used to study many other materials. These include both natural and industrial minerals whether refined, extracted or manufactured, composites such as cements, ceramics, mineral fibers and polymers, and crystalline or highly ordered biological molecules such as DNA, starch, wood and urea. The technique can be used both qualitatively and quantitatively and is an outstanding tool for materials science, geology, chemistry, biology, metallurgy and even medicine.

While an understanding of the analytical techniques of polarized microscopy may be perhaps more demanding than other forms of microscopy, it is well worth pursuing, simply for the enhanced information that can be obtained over brightfield imaging. An awareness of the principles of polarizing microscopy is also essential for the effective interpretation of differential interference contrast (DIC) microscopy.

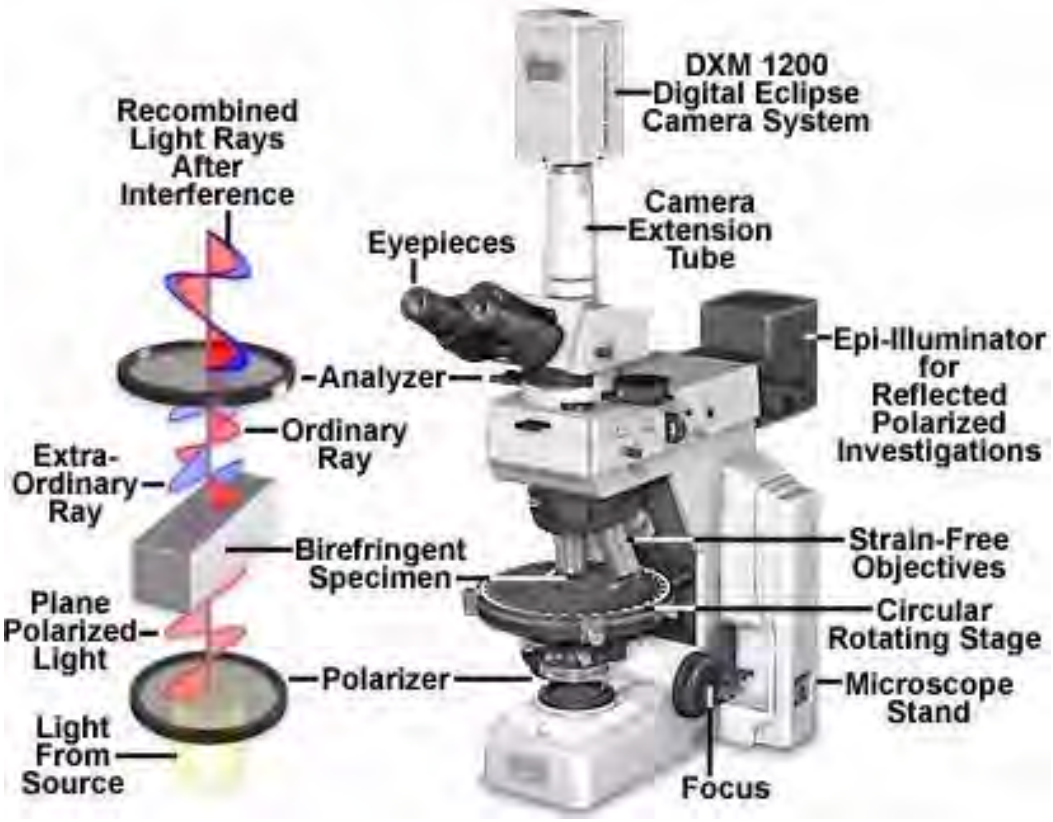

FIGURE 23.1: Polarized light microscopy configuration

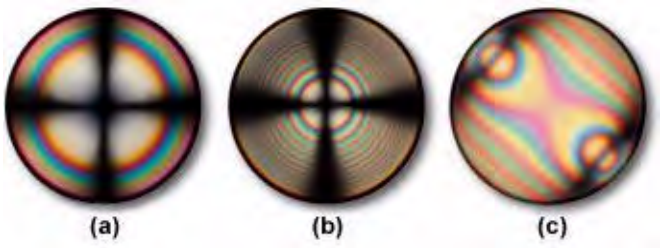

FIGURE 23.2: Conoscopic interference pattern

23.1.1 Polarized Light

The wave model of light describes light waves vibrating at right angles to the direction of travel of light with all vibration directions being equally probable. This is "common" light. In plane-polarized light there is only one vibration direction (Figure 1). The human eye-brain system has no sensitivity to the vibration directions of light, and plane-polarized light can only be detected by an intensity or color effect, for example, by reduced glare when wearing polarized sun glasses.

The most widely used material is Polaroid^{TM} film. Invented by Land in 1932, Polaroid film consists of long chain polymers, treated with light absorbing dyes, and stretched so that the chains are aligned. Light vibrating parallel with the chains is absorbed while light perpendicular to the chains is transmitted.

There are two polarizing filters in a polarizing microscope - the polarizer and analyzer (see Figure 1). The polarizer is situated below the specimen stage usually with its permitted vibration direction fixed in the left-to-right, East-West direction, although this is usually rotatable through 360 degrees. The analyzer, usually aligned North-South but again rotatable on some microscopes, is sited above the objectives and can be moved in and out of the light path as required. When both the analyzer and polarizer are in the optical path, their permitted vibration directions are positioned at right angles to each other. In this configuration, the polarizer and analyzer are said to be crossed, with no light passing through the system and a dark field of view present in the eyepieces.

The polarizer and analyzer are the essential components of the polarizing microscope - but other desirable features include:

- A rotating specimen stage to facilitate orientation studies with centration of the objectives and stage with the microscope optical axis to make the center of rotation coincide with the center of the field of view.
- Strain free objectives stress in assembly can produce optical effects under polarized light, a factor that could complicate observations.
- An eyepiece fitted with a cross wire graticule to mark the center of the field of view. Often, the cross wire graticule is substituted for a photomicrography graticule that assists in focusing the specimen and composing images with a set of frames bounding the area of the viewfield to be captured either digitally or onto film.
- A Bertrand lens to enable easy examination of the objective rear focal plane, to allow accurate adjustment of the illuminating aperture diaphragm and to view interference figures, as presented in Figure 2.
- A slot to allow the insertion of compensators/retardation plates between the polarizers, which are used to enhance optical path differences in the specimen. In most modern microscope designs, this slot is placed either in the microscope nosepiece or an intermediate tube positioned between the body and eyepiece tubes. Compensation plates inserted into the slot are then situated between the specimen and the analyzer.

Polarizing microscopy can be used both with reflected and transmitted light. Reflected light is useful for the study of opaque materials such as mineral oxides and sulphides, metals and silicon wafers (Figure 3). Reflected light techniques require a dedicated set of objectives that have not been corrected for viewing through the coverslip, and those for polarizing work should, again, be stress free.

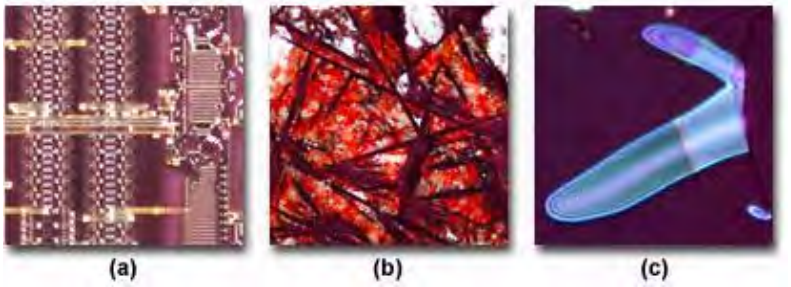

FIGURE 23.3: Reflected polarized light microscopy

Illustrated in Figure 3 is a series of reflected polarized light photomicrographs of typical specimens imaged utilizing this technique. On the left (Figure 3(a)) is a digital image revealing surface features of a microprocessor integrated circuit. Birefringent elements employed in the fabrication of the circuit are clearly visible in the image, which displays a portion of the chip's arithmetic logic unit. The polished surface of a ceramic superconducting tape (Yttrium-1,2,3) is presented in Figure 3(b), which shows birefringent crystalline areas with interference colors interspersed in a matrix of isotropic binder. Metallic thin films are also visible with reflected polarized light. Figure 3(c) illustrates blisters that form imperfections in an otherwise confluent thin film of copper (about 0.1 micron thick) sandwiched over a nickel/sodium chloride substrate to form a metallic superlattice assembly.

Careful specimen preparation is essential for good results. The method chosen will depend on the type of material studied. In geological applications the standard thickness for rock thin sections is 25—30 micrometers. Specimens can be ground down with diamond impregnated wheels and then hand finished to the correct thickness using abrasive powders of successively decreasing grit size. Softer materials can be prepared in a manner similar to biological samples using a microtome. Slices between one and 40 micrometers thick are used for transmitted light observations. These should be strain-free and free from any knife marks. Specimens are mounted between the slide and the coverslip using a mounting medium whose composition will depend on the chemical and physical nature of the specimen. This is particularly significant in the study of synthetic polymers where some media can chemically react with and cause structural changes to the material being studied.

23.1.2 Making Use of Anisotropy

Different levels of information can be obtained in plane-polarized light (analyzer out of the optical path) or with crossed polarizers (analyzer inserted into the optical path). Observations in plane-polarized light reveal details of the optical relief of the specimen, which is manifested in the "visibility" of boundaries, and increases with the increase of refractive index across them. Differences in the refractive indices of the mounting adhesive and the specimen determine the extent to which light is scattered as it emerges from the uneven specimen surface. Materials with high relief, which appear to stand out from the image, have refractive indices, which are appreciably different from that of the mountant. Immersion refractometry is used to measure substances having unknown refractive indices by comparison with oils of known refractive index.

Examinations of transparent or translucent materials in plane-polarized light will be

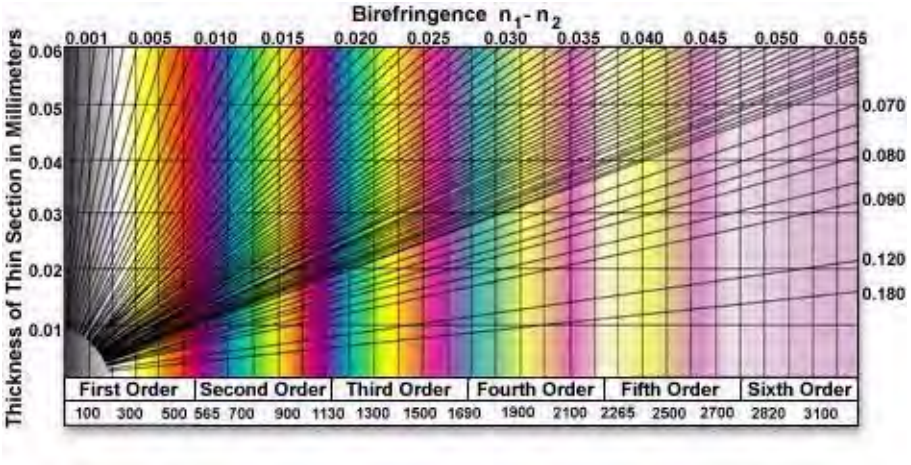

FIGURE 23.4: Michel—Levy interference color chart

similar to those seen in natural light until the specimen is rotated about the optical axis of the microscope. Then observers may see changes in the brightness and/or the color of the material being examined. This pleochroism, that is, variation of absorption color with vibration direction of the light, depends on the orientation of the material in the light path and is a characteristic of anisotropic materials only. An example of a material showing pleochroism is crocidolite, more commonly known as blue asbestos. This effect helps in its identification.

Polarization colors result from the interference of the two components of light split by the anisotropic specimen and may be regarded as white light minus those colors that are interfering destructively. Figure 2 illustrates conoscopic images of uniaxial and biaxial crystals observed at the objective rear focal plane. Interference patterns are formed by light rays traveling along different axes of the crystal being observed. Uniaxial crystals (Figures 2(a) and 2(b)) display an interference pattern consisting of two intersecting black bars (termed isogyres) that form a Maltese cross-like pattern. When illuminated with white (polarized) light, birefringent specimens produce circular distributions of interference colors (Figure 2), with the inner circles, called isochromes, consisting of increasingly lower order colors (see the Michel-Levy interference color chart, Figure 4). A common center for both the black cross and the isochromes is termed the melatope, which denotes the origin of the light rays traveling along the optical axis of the crystal. Biaxial crystals display two melatopes (Figure 2(c)) and a far more complex pattern of interference rings.

The two components of light travel at different speeds through the specimen and have different refractive indices, or refringences. Birefringence is the numerical difference between these refringences. The faster beam emerges first from the specimen with an optical path difference (OPD), which may be regarded as a "winning margin" over the slower one. The analyzer recombines only components of the two beams traveling in the same direction and vibrating in the same plane. The polarizer ensures that the two beams have the same amplitude at the time of recombination for maximum contrast.

There is constructive and destructive interference of light in the analyzer, depending on the OPD on the specimen and the wavelength of the light, which can be determined from the order of polarization color(s). This relies on the properties of the specimen, including the thickness difference between the refractive index and the birefringence of the two beams,

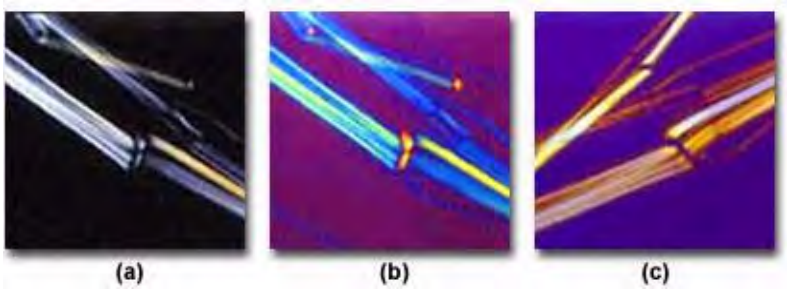

FIGURE 23.5: Chrysolite Asbestos fiber in polarized light

which has a maximum value dependent on the specimen and on the direction of travel of light through the specimen. Optical path differences can be used to extract valuable "tilt" information from the specimen.

Superimposed on the polarization color information is an intensity component. As the specimen is rotated relative to the polarizers, the intensity of the polarization colors varies cyclically, from zero (extinction) up to a maximum after 45 degrees and back down to zero after a 90—degree rotation. That is why a rotating stage and centration are provided, which are critical on a polarizing microscope. Centration of the objective and stage ensures that the center of the stage rotation coincides with the center of the field of view, a great convenience, as anyone who has tried to manage without it will know.

Whenever the specimen is in extinction, the permitted vibration directions of light passing through are parallel with those of either the polarizer or analyzer. This can be related to geometrical features of the specimen, such as fiber length, film extrusion direction, and crystal faces. In crossed polarizers, isotropic materials can be easily distinguished from anisotropic materials as they remain permanently in extinction (remain dark) when the stage is rotated through 360 degrees.

To help in the identification of fast and slow beams, or to improve contrast when polarization colors are of low order, such as dark grey, accessory plates can be inserted in the optical path. These will cause color changes in the specimen, which can be interpreted with the help of a polarization color chart (Michel—Levy chart; see Figure 4). These charts show the polarization colors provided by optical path differences from 0 to 1800—3100 nanometers together with birefringence and thickness values. The wave plate produces its own optical path difference. When the light passes first through the specimen and then the accessory plate, the OPDs of the wave plate and the specimen are either added together or subtracted from one another in the way that "winning margins" of two races run in succession are calculated. They are added when the slow vibration directions of the specimen and accessory plate are parallel, and subtracted when the fast vibration direction of the specimen coincides with the slow vibration direction of the accessory plate. If the slow and fast directions are known for the accessory plate (they are usually marked on the mount of commercially available plates), then those of the specimen can be deduced. Since these directions are characteristic for different media, they are well worth finding out and are essential for orientation and stress studies.

The strengths of polarizing microscopy can best be illustrated by examining particular case studies and their associated images. All images illustrated in this section were recorded with a Nikon Eclipse E600 microscope equipped with polarizing accessories, a research grade microscope designed for analytical investigations.

FIGURE 23.6: Phyllite thin section in polarized light

23.1.3 Identification of Asbestos Fibers

Asbestos is a generic name for a group of naturally occurring mineral fibers, which have been widely used, for example, in insulating materials, brake pads and to reinforce concrete. They can be harmful to health when inhaled and it is important that their presence in the environment be easily identified. Samples are commonly screened using scanning electron microscopy and x-ray microanalysis, but polarizing microscopy provides a quicker and easier alternative that can be utilized to distinguish between asbestos and other fibers and between the major types asbestos –chrysotile, crocidolite and amosite. From a health care point of view, it is believed that the amphibole asbestos varieties (crocidolite and amosite) are more harmful than the serpentine, chrysotile.

Plane–polarized light provides information about gross fiber morphology, color, pleochroism and refractive index. Glass fibers will be unaffected by rotation under plane-polarized light while asbestos fibers will display some pleochroism. Chrysotile asbestos fibrils may appear crinkled, like permed or damaged hair, under plane-polarized light, whereas crocidolite and amosite asbestos are straight or slightly curved. Chrysotile has a refractive index of about 1.550, amosite 1.692 and crocidolite, 1.695.

With the use of crossed polars it is possible to deduce the permitted vibration direction of the light as it passes through the specimen, and with the whole wave plate, a determination of the slow and fast vibration directions (Figure 5). Under crossed polars, chrysotile shows pale interference colors - low order whites (Figure 5(a)). When a full wave plate is added (530-560 nanometers), the colors are transformed. Aligned Northeast-Southwest, the wave plate is additive and gives blue and yellow in the fiber (Figure 5(b)). When aligned Northwest-Southeast (Figure 5(c)) the plate is subtracting to give a paler yellow fiber with no blue. From this it is possible to deduce that the slow vibration direction is parallel with the long axis of the fiber. Amosite is similar in this respect.

Crocidolite displays blue colors, pleochroism and murky brown polarization colors and has its fast vibration direction parallel with its length. In summary, identification of the three asbestos fiber types depends on shape, refractive indices, pleochroism, birefringence, and fast and slow vibration directions.

23.1.4 Uncovering the History of Rock Formation

Phyllite An examination of geological thin sections using polarizing microscopy, as well as providing information on component minerals, can reveal a great deal about how the rock was formed. Phyllite, a metamorphic rock, clearly shows the alignment of crystals under the effects of heat and stress. Small-scale folds are visible in the plane-

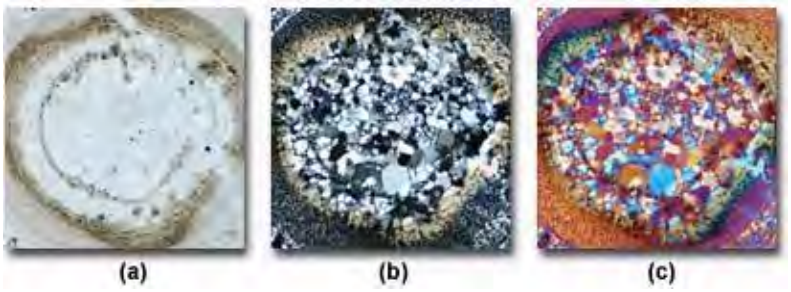

FIGURE 23.7: Oolite thin section in polarized light

polarized image (Figure 6(a)) and more clearly defined under crossed polars (Figure 6(b)) with and without the wave plate. The crossed polars image reveals that there are several minerals present–quartz in grey and whites and micas in higher order colors. The alignment of the micas is clearly apparent. Addition of the wave plate (Figure 6(c)) improves contrast for clear definition in the image.

Oolite Oolite, a light gray rock composed of siliceous oolites cemented in compact silica, is formed in the sea. The mineral's name is derived from its structural similarity to fish roe - caviar! It forms in the sea when sand grains are rolled by gentle currents over beds of calcium carbonate or other minerals. These minerals build up around the sand grains and subsequent cementation transforms the grains into coherent rock. The thin sections show the original quartz nuclei (Figure 7(a-c)) on which the build up of carbonate mineral occurred.

In plane–polarized light (Figure 7(a)), the quartz is virtually invisible having the same refractive index as the cement, while the carbonate mineral with a different refractive index shows high contrast. The crossed polarizer image (Figure 7(b)) shows quartz grains in grays and whites and the calcium carbonate in the characteristic biscuit colored, high order whites. The groups of quartz grains in some of the cores reveal that these are polycrystalline and are metamorphic quartzite particles. When a full-wave retardation plate is inserted into the optical path (Figure 7(c)), optical path differences become apparent in the specimen, and contrast is enhanced.

Natural and Synthetic Polymers During the solidification of polymer melts there may be some organization of the polymer chains, a process that is often dependent upon the annealing conditions. When nucleation occurs, the synthetic polymer chains often arrange themselves tangentially and the solidified regions grow radially. These can be seen in crossed polarized illumination as white regions with the black extinction crosses. When these spherulites impinge, their boundaries become polygonal. This can be clearly seen in crossed polars but not under plane-polarized light.

The addition of the whole wave plate (Figure 8(a)) confirms the tangential arrangement of the polymer chains. The banding occurring in these spherulites indicates slow cooling of the melt allowing the polymer chains to grow out in spirals. This information on thermal history is almost impossible to collect by any other technique. Nucleation in polymer melts can take place as the result of accidental contamination or contact with a nucleating surface and can lead to substantial weakening of the product. Identification of nucleation can be a valuable aid for quality control.

FIGURE 23.8: Natural and synthetic polymers in polarized light

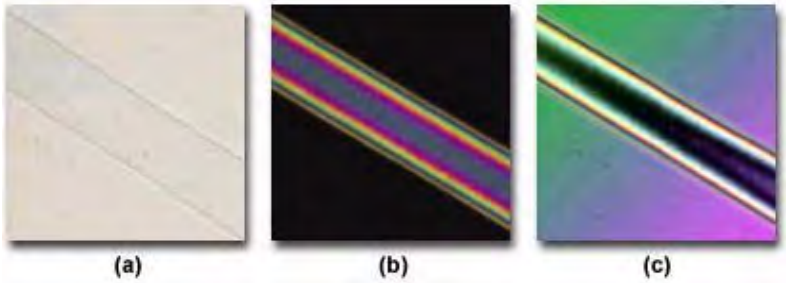

FIGURE 23.9: Nylon fiber in polarized light

Other polymers may not be birefringent (evidenced by the polycarbonate specimen illustrated in Figure 8(b)), and do not display substantial secondary or tertiary structure. In other cases, both biological and synthetic polymers can undergo a series of lyotropic or thermotropic liquid crystalline phase transitions, which can often be observed and recorded in a polarized light microscope. Figure 8(c) illustrates a birefringent columnar-hexatic liquid crystalline phase exhibited by DNA at very high concentrations (exceeding 300 milligrams/milliliter).

Nylon Fibers Observations under plane–polarized light (Figure 9(a)) reveal refractive index differences between the fiber and the mountant and the presence of opacifying titanium dioxide particles. The image under crossed polars (Figure 9(b)) shows third order polarization colors and their distribution across the fibers indicates that this is a cylindrical and not a lobate fiber useful in predicting mechanical strength. The use of the quartz wedge (Figure 9(c)) enables the determination of optical path differences for birefringence measurements.

In summary, polarizing microscopy provides a vast amount of information about the composition and three-dimensional structure of a variety of samples. Virtually unlimited in its scope, the technique can reveal information about thermal history and the stresses and strains to which a specimen was subjected during formation. Useful in manufacturing and research, polarizing microscopy is a relatively inexpensive and accessible investigative and quality control tool, which can provide information unavailable with any other technique.

FIGURE 23.10: Monocular polarized light microscope

23.2 Microscope Configuration

The polarized light microscope is designed to observe and photograph specimens that are visible primarily due to their optically anisotropic character. In order to accomplish this task, the microscope must be equipped with both a polarizer, positioned in the light path somewhere before the specimen, and an analyzer (a second polarizer), placed in the optical pathway between the objective rear aperture and the observation tubes or camera port.

Image contrast arises from the interaction of plane-polarized light with a birefringent (or doubly-refracting) specimen to produce two individual wave components that are each polarized in mutually perpendicular planes. The velocities of these components are different and vary with the propagation direction through the specimen. After exiting the specimen, the light components become out of phase with each other, but are recombined with constructive and destructive interference when they pass through the analyzer.

When an anisotropic specimen is brought into focus and rotated through 360 degrees on a circular polarized light microscope stage, it will sequentially appear bright and dark (extinct), depending upon the rotation position. When the specimen long axis is oriented at a 45–degree angle to the polarizer axis, the maximum degree of brightness will be achieved, and the greatest degree of extinction will be observed when the two axes coincide. During rotation over a range of 360 degrees, specimen visibility will oscillate between bright and dark four times, in 90–degree increments. This is due to the fact that when polarized light impacts the birefringent specimen with a vibration direction parallel to the optical axis, the illumination vibrations will coincide with the principal axis of the specimen and it will appear isotropic (dark or extinct). If the specimen orientation is altered by 45 degrees, incident light rays will be resolved by the specimen into ordinary and extraordinary components, which are then united in the analyzer to yield interference patterns. Because

interference only occurs when polarized light rays have an identical vibration direction, the maximum birefringence is observed when the angle between the specimen principal plane and the illumination permitted vibrational direction overlap. Interference between the recombining white light rays in the analyzer vibration plane often produces a spectrum of color, which is due to residual complementary colors arising from destructive interference of white light. The colors observed under illumination with white light in the microscope eyepiece can be utilized to quantitatively draw conclusions about path differences and specimen thickness values when the refractive indices of the specimen are known.

Polarized light microscopy is utilized to distinguish between singly refracting (optically isotropic) and doubly refracting (optically anisotropic) media. Anisotropic substances, such as uniaxial or biaxial crystals, oriented polymers, or liquid crystals, generate interference effects in the polarized light microscope, which result in differences of color and intensity in the image as seen through the eyepieces and captured on film, or as a digital image. This technique is useful for orientation studies of doubly refracting media that are aligned in a crystalline lattice or oriented through long-chain molecular interactions in natural and synthetic polymers and related materials. Also investigated in polarized light are stresses in transparent singly refracting media (for example, glass) and the identification and characterization of a wide spectrum of anisotropic substances through their refractive index and birefringence.

The microscope illustrated in Figure 23.10 is equipped with all of the standard accessories for examination of birefringent specimens under polarized light. Although similar to the common brightfield microscope, the polarized light microscope contains additional components that are unique to instruments of this class. These include the polarizer and analyzer, strain-free objectives and condenser, a circular graduated stage capable of 360-degree rotation, and an opening in the microscope body or intermediate tube for a full-wave retardation plate, quartz wedge, Berek compensator, or quarter-wavelength plate. The monocular microscope presented in Figure 23.10 is designed with a straight observation tube and also contains a 360-degree rotatable analyzer with a swing-out Bertrand lens, allowing both conoscopic and orthoscopic examination of birefringent specimens. The objectives (4x, 10, and 40x) are housed in mounts equipped with an individual centering device, and the circular stage has a diameter of 140 millimeters with a clamping screw and an attachable mechanical stage. Removal of the polarizer and analyzer (while other components remain in place) from the light path renders the instrument equal to a typical brightfield microscope with respect to the optical characteristics. Polarized light is a contrast-enhancing technique that improves the quality of the image obtained with birefringent materials when compared to other techniques such as darkfield and brightfield illumination, differential interference contrast, phase contrast, Hoffman modulation contrast, and fluorescence.

Typical modern polarized (and brightfield) microscopes (Figure 23.11) have a lamphouse, which contains a 50 to 100-watt high-energy tungsten-halogen lamp, attached to the base of the microscope. A transformer providing direct current (DC) voltage to the lamp is usually built directly into the microscope base and is controlled by a potentiometer positioned near the lamp switch in bottom of the base (the lamp voltage control). Between the lamphouse and the microscope base is a filter cassette that positions removable color correction, heat, and neutral density filters in the optical pathway. Also built into the microscope base is a collector lens, the field iris aperture diaphragm, and a first surface reflecting mirror that directs light through a port placed directly beneath the condenser in

FIGURE 23.11: Modern polarized light microscope

the central optical pathway of the microscope. These components control the size, intensity, and distribution of light in the illumination field. The entire base system is designed to be vibration free and to provide the optimum light source for Köhler illumination. In general, the modern microscope illumination system is capable of providing controlled light to produce an even, intensely illuminated field of view, even though the lamp emits only an inhomogeneous spectrum of visible, infrared, and near-ultraviolet radiation.

In some polarized light microscopes, the illuminator is replaced by a plano-concave substage mirror (Figure 23.10). Almost any external light source can directed at the mirror, which is angled towards the polarizer positioned beneath the condenser aperture. This configuration is useful when an external source of monochromatic light, such as a sodium vapor lamp, is required. Because the illumination intensity is not limited by a permanent tungsten-halogen lamp, the microscope can be readily adapted to high intensity light sources in order to observe weakly birefringent specimens.

23.2.1 Polarizers

Polarized light microscopy was first introduced during the nineteenth century, but instead of employing transmission-polarizing materials, light was polarized by reflection from a stack of glass plates set at a 57–degree angle to the plane of incidence. Later, more advanced instruments relied on a crystal of doubly refracting material (such as calcite) specially cut and cemented together to form a prism. A beam of white unpolarized light entering a crystal of this type is separated into two components that are polarized in mutually perpendicular directions. One of these light rays is termed the ordinary ray, while the other is called the extraordinary ray. The ordinary ray is refracted to a greater degree in the birefringent crystal and impacts the cemented surface at the angle of total internal

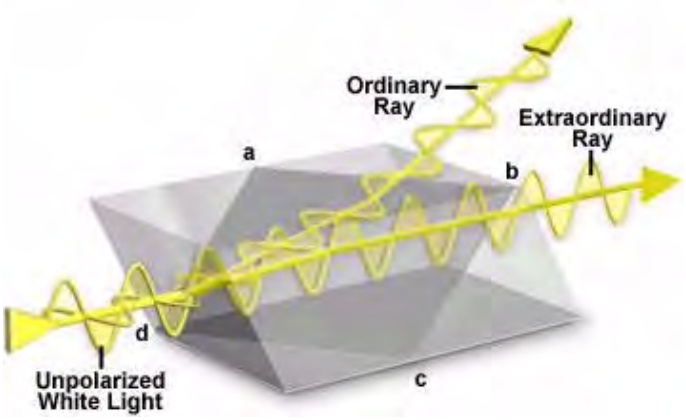

FIGURE 23.12: Nicol polarizing prism

reflection. As a result, this ray is reflected out of the prism and eliminated by absorption in the optical mount. The extraordinary ray traverses the prism and emerges as a beam of linearly polarized light that is passed directly through the condenser and to the specimen (positioned on the microscope stage). Several versions of this polarizing device (which was also employed as the analyzer) were available, and these were usually named after their designers. The most common polarizing prism (illustrated in Figure 23.12) was named after William Nicol, who first cleaved and cemented together two crystals of Iceland spar with Canada balsam in 1829. Nicol prisms were first used to measure the polarization angle of birefringent compounds, leading to new developments in the understanding of interactions between polarized light and crystalline substances.

Presented in Figure 23.12 is an illustration of the construction of a typical Nicol prism. A crystal of doubly refracting (birefringent) material, usually calcite, is cut along the plane labeled a-b-c-d and the two halves are then cemented together to reproduce the original crystal shape. A beam of unpolarized white light enters the crystal from the left and is split into two components that are polarized in mutually perpendicular directions. One of these beams (labeled the ordinary ray) is refracted to a greater degree and impacts the cemented boundary at an angle that results in its total reflection out of the prism through the uppermost crystal face. The other beam (extraordinary ray) is refracted to a lesser degree and passes through the prism to exit as a plane-polarized beam of light.

Other prism configurations were suggested and constructed during the nineteenth and early twentieth centuries, but are currently no longer utilized for producing polarized light in most applications. Nicol prisms are very expensive and bulky, and have a very limited aperture, which restricts their use at high magnifications. Instead, polarized light is now most commonly produced by absorption of light having a set of specific vibration directions in a dichroic medium. Certain natural minerals, such as tourmaline, possess this property, but synthetic films invented by Dr. Edwin H. Land in 1932 soon overtook all other materials as the medium of choice for production of plane-polarized light. Tiny crystallites of iodoquinine sulphate, oriented in the same direction, are embedded in a transparent polymeric film to prevent migration and reorientation of the crystals. Land developed sheets containing polarizing films that were marketed under the trade name of Polaroid®, which has become the accepted generic term for these sheets. Any device capable of selecting plane-polarized light from natural (unpolarized) white light is now referred to as a polar

FIGURE 23.13: Analyzer intermediate tube

or polarizer, a name first introduced in 1948 by A. F. Hallimond. Today, polarizers are widely used in liquid crystal displays (LCDs), sunglasses, photography, microscopy, and for a myriad of scientific and medical purposes.

Light exiting the port in the microscope base is first passed through a neutral linear Polaroid HN-type polarizer to create plane-polarized light having a vibration vector that is confined to a single plane. H-films are produced by stretching a sheet of polyvinyl alcohol to align the long-chain polymeric molecules, which are subsequently impregnated with iodine. These films are less effective polarizing devices than a calcite prism, but do not restrict numerical aperture. Typically, a pair of crossed polarizing H-films transmits between 0.01 percent and 40 percent of the incident light, depending upon the film thickness.

On most microscopes, the polarizer is located either on the light port or in a filter holder directly beneath the condenser. The microscope illustrated in Figure 23.11 has a rotating polarizer assembly that fits snugly onto the light port in the base. The polarizer can be rotated through a 360-degree angle and locked into a single position by means of a small knurled locking screw, but is generally oriented in an East-West direction by convention. Other microscopes typically have the polarizer attached to the substage condenser assembly housing through a mount that may or may not allow rotation of the polarizer. Some polarizers are held into place with a detent that allows rotation in fixed increments of 45 degrees. Polarizers should be removable from the light path, with a pivot or similar device, to allow maximum brightfield intensity when the microscope is used in this mode.

Light diffracted, refracted, and transmitted by the specimen converges at the back focal plane of the objective and is then directed to an intermediate tube (illustrated in Figure 23.13), which houses another polarizer, often termed the "analyzer". The analyzer is another HN-type neutral linear Polaroid polarizing filter positioned with the direction of light vibration oriented at a 90-degree angle with respect to the polarizer beneath the condenser. By convention, the vibration direction of the polarizer is set to the East-West (abbreviated E-W position). The same convention dictates that the analyzer is oriented with the vibration direction in the North-South (abbreviated N-S) orientation, at a 90-degree angle to the vibration direction of the polarizer.

The analyzer is positioned after the specimen, either in a slot above the objective or in an intermediate tube between the nosepiece and the observation tubes. Older polarized light microscopes may have an analyzer that is fitted into the eyepiece, either near the eyelens or somewhere before the intermediate image plane (Figure 23.10). It is not wise to place

polarizers in a conjugate image plane, because scratches, imperfections, dirt, and debris on the surface can be imaged along with the specimen. Simple polarized light microscopes generally have a fixed analyzer, but more elaborate instruments may have the capability to rotate the analyzer in a 360–degree rotation about the optical axis and to remove it from the light path with a slider mechanism. Analyzers of this type are usually fitted with a scale of degrees and some form of locking clamp.

Before using a polarized light microscope, the operator should remove any birefringent specimens from the stage and check to ensure the polarizer is secured in the standard position (often indicated by a click stop), and that the light intensity is minimal when the analyzer is set to the zero mark on the graduated scale. When properly configured, the vibration direction of the analyzer is North-South when the polarizer vibration plane is oriented in an East-West direction (this orientation is now standardized). If the polarizer and analyzer are both capable of rotation, it is possible that they may be crossed (with light intensity at a minimum when minus a specimen) even through their permitted vibration directions are not East-West and North-South, respectively. This situation may be rectified by moving the polarizer to its zero degree click stop (or rotation angle), followed by re-setting the analyzer to this reference point. It is essential that the polarizer and analyzer have vibration planes oriented in the proper directions when retardation and/or compensation plates are inserted into the optical path for measurement purposes.

In older microscopes that are not equipped with graduated markings for the polarizer and analyzer positions, it is possible to use the properties of a known birefringent specimen to adjust the orientation of the polarizer and analyzer. Recrystallized urea is excellent for this purpose, because the chemical forms long dendritic crystallites that have permitted vibration directions that are both parallel and perpendicular to the long crystal axis. A small quantity (about 5 milligrams) of the purified chemical can be sandwiched between a microscope slide and cover glass, then carefully heated with a Bunsen burner or hot plate until the crystals melt. Once liquefied, the cover glass can be pressed onto the slide to minimize the thickness of the urea sandwich, which is then allowed to cool. After recrystallization, the slide is placed on a polarized light microscope stage and the long axes of the crystals oriented East-West using the crosshairs in the eyepiece reticle as a reference. The polarizer and analyzer are then rotated as a pair until both the crystal and background are equally dark.

23.2.2 Condensers for Polarized Light Microscopy

Basic substage condenser construction in a polarized light microscope is no different from an ordinary condenser used in brightfield microscopy. In all forms of microscopy, the degree of condenser optical correction should be consistent with that of the objectives. Typical laboratory polarizing microscopes have an achromat, strain-free condenser with a numerical aperture range between 0.90 and 1.35, and a swing-out lens element that will provide even illumination at very low (2x to 4x) magnifications (illustrated in Figure 23.14). Removal of the swing lens alters the focal length of the condenser to enable illumination of a much larger specimen area and to allow the larger field of view provided by low magnification objectives to be evenly illuminated. This is ideal for polarized light microscopy where low magnifications are used to view crystals and other birefringent materials in the orthoscopic mode.

When interference patterns are to be studied, the swing lens can quickly be brought into the optical path and a high numerical aperture objective selected for use in conoscopic

FIGURE 23.14: Swing-out top lens condenser (NA=1.35)

observation. It is important that the numerical aperture of the condenser is high enough to provide adequate illumination for viewing conoscopic images. Failure to insert the top condenser lens when utilizing high magnification objectives will result in poor illumination conditions and may lead to photomicrographs or digital images that have an uneven background. Also, because the cone of illumination and condenser numerical aperture are reduced without the top lens, resolution of the microscope will be compromised, resulting in a loss of fine specimen detail.

The condenser aperture diaphragm controls the angle of the illumination cone that passes through the microscope optical train. Reducing the opening size of this iris diaphragm decreases the cone angle and increases the contrast of images observed through the eyepieces. It should be noted, however, that the condenser aperture diaphragm is not intended as a mechanism to adjust the intensity of illumination, which should be controlled by the voltage supplied to the lamp. Some polarized light microscopes are equipped with a fixed condenser (no swing-lens) that is designed to provide a compromise between the requirements for conoscopic and orthoscopic illumination. Variation in the degree of illumination convergence can be accomplished by adjusting the condenser aperture diaphragm or by raising or lowering the condenser (although the latter technique is not recommended for critical examinations).

23.2.3 Rotating Circular Stages

Early polarized light microscopes utilized fixed stages, with the polarizer and analyzer mechanically linked to rotate in synchrony around the optical axis. Although this configuration was cumbersome by today's standards, it had the advantage of not requiring coincidence between the stage axis and the optical axis of the microscope. Modern polarized light microscopes are often equipped with specially designed 360-degree rotatable circular stages, similar to the one shown in Figure 23.15, which ease the task of performing orientation studies in polarized light. The circular stage illustrated in Figure 23.15 features a goniometer divided into 1-degree increments, and has two verniers (not shown) placed 90 degrees apart, with click (detent or pawl) stops positioned at 45-degree steps. Use of a precision ball bearing movement ensures extremely fine control over the verniers, which allow the microscopist to read angles of rotation with an accuracy near 0.1 degree. A clamp is used to secure the stage so specimens can be positioned at a fixed angle with respect to the polarizer and analyzer.

The most critical aspect of the circular stage alignment on a polarizing microscope is

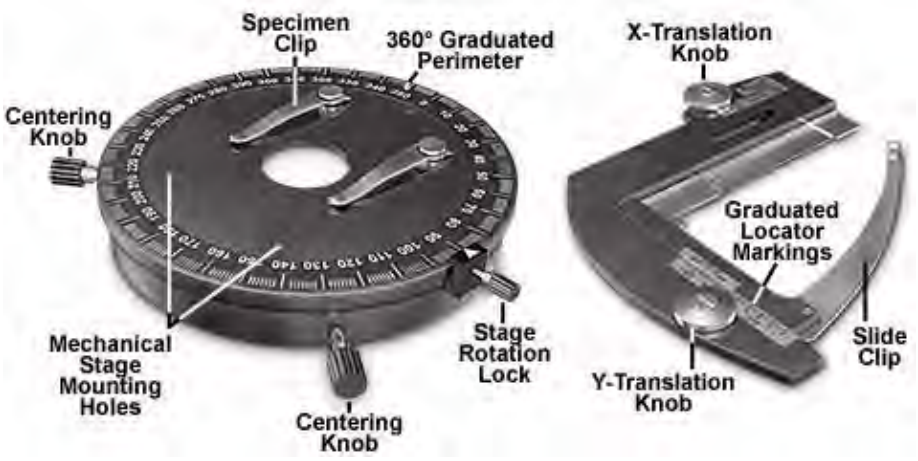

FIGURE 23.15: Circular stage with optical mechanical translation attachment

to ensure that the stage is centered within the viewfield and the optical axis of the microscope. This is accomplished with the two centering knobs located on the front of the stage illustrated in Figure 23.15. The first step in the alignment process is to center the microscope objectives with respect to the condenser, the field of view, and the optical axis of the microscope. A pair of small setscrews in the nosepiece of most research-grade polarizing microscopes allows centering of individual objectives by means of an Allen wrench. Each objective should be independently centered to the optical axis, according to the manufacturer's suggestions, while observing a specimen on the circular stage. Some microscopes provide for individual objective centration, while other centration systems operate on the nosepiece as a unit. After the objectives are centered, the stage should be centered in the viewfield, which will coincide with the optical axis of the microscope. When the stage is properly centered, a specific specimen detail placed in the center of a cross hair reticle should not be displaced more than 0.01 millimeter from the microscope optical axis after a full 360-degree rotation of the stage. In general, microscopes are designed to allow adjustment of either the stage or the objectives to coincide with the optical axis, but not both. Some designs have objectives that are in fixed position in the nosepiece with an adjustable circular stage, while others lock the stage into position and allow centration of the objectives.

Errors in centration of the rotating circular stage can lead to aggravation when examining birefringent specimens with a polarized light microscope. If the center of stage rotation does not coincide with the center of the field view, a feature being examined may disappear when the stage is rotated. As objective magnification increases (leading to a much smaller field of view), the discrepancy between the field of view center and the axis of rotation becomes greater. At the highest magnifications (60x and 100x), even minute errors in centration can lead to huge differences in specimen placement as the stage is rotated.

The circular microscope stage shown on the left in Figure 23.15 contains a pair of spring clips intended to secure the specimen during observation with the microscope. An optional mechanical stage intended for use on the circular stage is illustrated on the right in Figure 23.15. This stage is a low-profile model that has a cross-travel motion of about 25 x 25 millimeters, with a graduated vernier to log specific locations on the specimen. The mechanical stage is fastened to pre-drilled holes on the circular stage and the specimen is

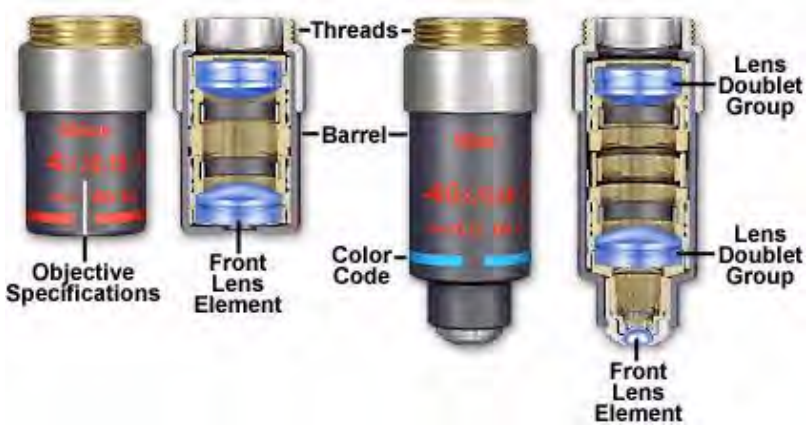

FIGURE 23.16: Strain–free objective for polarized light microscopy

translated with two rack-and-pinion gear sets controlled by the x- and y-translational knobs. Use of a mechanical stage allows precise positioning of the specimen, but the protruding translation knobs often interfere with free rotation of objectives and can even collide with them.

In the past, several manufacturers offered a universal attachment for circular polarized microscope stages. This accessory allows a mineral thin section to be secured between two glass hemispheres and rotated about several axes in order to precisely orient selected grains in the optical path. The universal stage is employed to observe selected optical, crystallographic, and textural features that yield clues to the structure of semi-crystalline specimens. Another stage that is sometimes of utility in measuring birefringence and refractive index is the spindle stage adapter, which is also mounted directly onto the circular stage. Specimen grains are secured to the spindle tip, which is positioned on a base plate that allows the spindle to pivot around a horizontal axis while holding the grain immersed in oil between a glass window and a coverslip. Although these stages are presently difficult to obtain, they can prove invaluable to quantitative polarized light microscopy investigations.

23.2.4 Objectives for Polarized Light Microscopy

Optical correction of polarized light objectives can be achromatic, plan achromatic, or plan fluorite. Apochromatic objectives from older fixed tube length microscopes should be avoided because it is difficult to remove all residual stress and strain from the numerous lens elements and tight mounts. Recently however, advances in objective design for infinity-corrected microscopes have yielded high-quality strain-free apochromatic objectives that are useful for differential interference contrast or examination of birefringent specimens with crossed polarized illumination. The average numerical aperture of 20x and 40x polarized light objectives is usually 10 to 25 percent higher than those for ordinary microscopes because observations of conoscopic interference patterns require high numerical apertures. Objectives designed for polarized light microscopy must be stress and strain-free. Most manufacturers thoroughly test objectives designed for use on polarized microscopes, selecting only those that pass the rigorous tests.

Unwanted birefringence in microscope objectives can arise primarily by two mechanisms. The first is “natural” birefringence, which is an artifact of the inherent anisotropic character of glasses, crystals and other materials used to make the lenses. To circumvent this

problem, manufacturers choose strain-free optical glass or isotropic crystals to construct lens elements. The second type is "strain" birefringence, which occurs when multiple lenses are cemented together and mounted in close proximity with tightly fitting frames. Strain birefringence can also occur as a result of damage to the objective due to dropping or rough handling.

Those objectives that pass the stress test are marked P or POL, and are usually labeled with red engraved letters. Several manufacturers also use a flat black or dark gray barrel (with or without red letters) for quick identification of strain-free polarized light objectives (illustrated in Figure 23.16). When both the objectives and the condenser are stress and strain-free, the microscope viewfield background appears a deep solid black when observed through the eyepieces without a specimen between crossed polarizers. Any stress in these optical components can give rise to an appreciable degree of anisotropic character, termed internal birefringence. This results in a contribution to specimen interference effects by the microscope optical system itself, and can often make interpretation of images very difficult. Evidence for stress and/or strain in the optical system can be obtained by the presence a blue, gray, or brownish background when observing specimens that ordinarily would have a black background.

A pair of typical objectives designed exclusively for polarized light microscopy is presented in Figure 23.16. The objective barrels are painted flat black and are decorated with red lettering to indicate specific capabilities of the objectives and to designate their strain-free condition for polarized light. Cut-away diagrams of the objectives reveal internal lens elements, which are corrected for chromatic and spherical aberration. The objective on the left is a low-power 4x objective designed to view birefringent specimens at lower magnifications. The front lens element is larger than the 40x objective on the right because illumination requirements for the increased field of view enjoyed by lower power objectives. Polarized light objectives range in magnification from about 2x to 100x, with the most common being 4x, 10x, 20, and 40x, a selection that serves a majority of purposes for specimen examination in both orthoscopic and conoscopic modes.

23.2.5 Retardation and Accessory Plates

Almost all polarized light microscopes are equipped with a slot in the body tube above the nosepiece and between the polarizer and analyzer. The purpose of this slot is to house an accessory or retardation plate in a specific orientation with respect to the polarizer and analyzer vibration directions. Originally, the slot was oriented with its long axis directed Northeast-Southwest as observed from the eyepieces, but more recent microscopes have the direction changed to Southeast-Northwest. In older microscopes, the slot dimensions were 10 x 3 millimeters, but the size has now been standardized to 20 x 6 millimeters. When the accessory/retardation plates are not inserted into the body tube, a cover is often fitted to prevent dust from entering the microscope through the slots.

Retardation plates are composed of optically anisotropic quartz, mica, or gypsum minerals ground to a precise thickness and mounted between two windows having flat (plane) faces. These plates produce a specific optical path length difference (OPD) of mutually perpendicular plane-polarized light waves when inserted diagonally in the microscope between crossed polarizers. The three most common retardation plates produce optical path length differences of an entire wavelength (ranging between 530 and 570 nanometers), a quarter wavelength (137—150 nanometers), or a variable path length obtained by utilizing a wedge-shaped design that covers a wide spectrum of wavelengths (up to six orders or

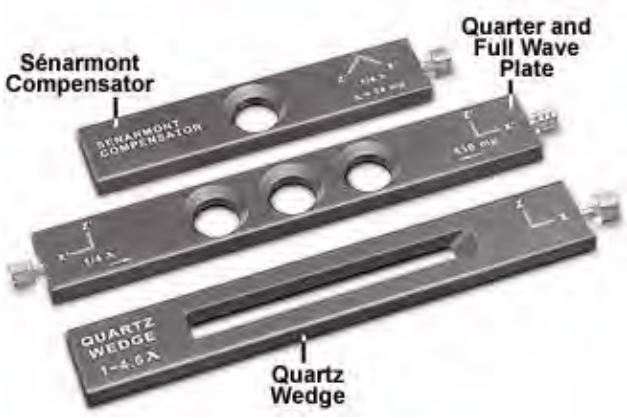

FIGURE 23.17: Polarized light compensators

about 3000 nanometers).

The quartz wedge is the simplest example of a compensator, which is utilized to vary the optical path length difference to match that of the specimen, either by the degree of insertion into the optical axis or in some other manner. A whole-wave plate is often referred to as a sensitive tint or first-order red plate, because it produces the interference color having a tint similar to the first-order red seen in the Michel-Levy chart. Older compensators were made by cleaving gypsum to the appropriate thickness to achieve the first-order red color, and may be marked gypsum plate, Gips, Gyps, one λ, or $\Delta = 530$ nm on the frame housing. If the plate originated in Germany, it will probably be labeled Rot I. Quarter wave plates (sometimes referred to as a mica plate) are usually fashioned from quartz or muscovite crystals sandwiched between two glass windows, just as the first-order plates. Depending upon the manufacturer, quarter wave plates may be marked Mica, Glimmer, 1/4 λ, or $\Delta = 147$ nm. First-order red and quarter wavelength plates are usually mounted in long rectangular frames that slide the plate through the compensator slot and into the optical pathway. Late model microscopes combine these plates into a single framework that has three openings: one for the first-order red plate, one for the quarter wave plate, and a central opening without a plate for use with plane-polarized light without compensators. In addition, these plate frames have knobs at each end that are larger than the slot dimensions to ensure the plates cannot be dropped, borrowed, or stolen.

A primary consideration when using compensation plates is to establish the direction of the slow permitted vibration vector. By convention, this direction will be Northeast-Southwest, in the image, and will be marked slow, z', or g, but it is also possible that the slow axis will not be marked at all on the frame. A convenient method of ascertaining the slow vibration axis of retardation or compensating plates is to employ the plate to observe birefringent crystals (such as urea) where the long axis of the crystal is parallel to the Northeast-Southwest direction of the plate. If the there is an addition to the optical path difference when the retardation plate is inserted (when the color moves up the Michel-Levy scale), then the slow vibration direction of the plate also travels parallel to the long axis. Alternatively, if there is a difference (subtraction) between the optical paths, then the slow axis of the retardation plate is perpendicular to the long axis of the framework.

The most common compensators are the quarter wave, full wave, and quartz wedge plates. Other compensators that are available from various manufacturers are listed in

TABLE 23.1: Characteristics of Compensation Plates

Plate Type	Optical Path Difference (OPD - Nanometers)	Comments
Quarter Wavelength	140	Gray Interference Tint
Full Wave	540—570	First–Order Red and Sensitive Tint
Quartz Wedge	0—3000	Graduated Scale over Six Orders
Babinet	0—3000	Twin Opposed Quartz Wedges
Wright	0—3000	Combination Quartz Wedge
Soleil	0—3000	Twin Quartz Wedges and Parallel Plate
Brace–Köhler	0—3000	Combination Mica Wedges
Sénarmont	0—540 (or 570)	Elliptical Polarization with Rotating Analyzer
Elliptic	0—540 (or 570)	Rotating Plate on Vertical Axis
Berek	0—2800	Tilting Calcite Plate
Ehringhaus	0—2800	Twin Rotating Quartz Plates

Table 1, along with their optical path difference range and abbreviated comments. The Babinet, Wright, and Soleil wedge compensators are variations on the standard quartz wedge plate. In the quartz wedge, the zero reading coincides with the thin end of the wedge, which is often lost when grinding the plate during manufacture. To overcome this difficulty, the Babinet compensator was designed with two quartz wedges superposed and having mutually perpendicular crystallographic axes. The result is the zeroth band being located at the center of the wedge where the path differences in the negative and positive wedges exactly compensate each other, to produce a full wavelength range on either side. In contrast, the Wright wedge is mounted over a parallel compensating plate composed of either quartz or gypsum, which reduces the path difference throughout the wedge equal to the parallel plate contribution. Soleil compensators are a modified form of the Babinet design, consisting of a pair of quartz wedges and a parallel plate. Phase differences due to the compensator are controlled by changing the relative displacement of the wedges. The Brace-Köhler compensator enables precise measurements of exceedingly small retardation values found in weakly birefringent organic specimens and low-strain glasses. Snarmont and elliptic compensators take advantage of elliptical polarization, by employing a rotating analyzer (Snarmont) or with a quartz plate that rotates about a vertical axis (elliptic). The Berek compensator consists of a calcite plate cut normal to the optical axis that is tilted about the horizontal axis by means of a calibrated micrometer drum to enable precise measurements of retardation. Twin quartz plates are substituted for calcite in the Ehringhaus compensator, which operates in a manner similar to the Berek compensator. The Berek, and Ehringhaus compensators are standard tools for fiber analysis with polarized light microscopy.

23.2.6 The Bertrand Lens

Advanced polarized light microscopes are often equipped with a Bertrand lens (sometimes referred to as an Amici-Bertrand lens) positioned on a movable sliding or tilting mount that is located between the analyzer and the eyepieces. In some cases, there is also a provision for focusing the Bertrand lens. When coupled to the eyepiece, the Bertrand lens provides a system that focuses on the objective rear focal plane, allowing the microscopist to observe illumination alignment, condenser aperture size, and conoscopic polarized light images. In Köhler illumination, an image of the lamp filament is formed in the objective rear focal plane, together with the image of the condenser aperture, so the Bertrand lens is often utilized to adjusting the illuminating (condenser) aperture diaphragm for optimum specimen contrast. The primary function in polarized light microscopy, however, is to view interference figures (conoscopic images). These images appear in the objective rear focal plane when an optically anisotropic specimen is viewed between crossed polarizers using a high numerical aperture objective/condenser combination.

Older polarized light microscopes may have a provision for centration of the Bertrand lens to allow the center of the objective rear aperture to coincide with the intersection of the eyepiece crosshairs. Some of the older microscopes also have an iris diaphragm positioned near the intermediate image plane or Bertrand lens, which can be adjusted (reduced in size) to improve the clarity of interference figures obtained from small crystals when the microscope is operated in conoscopic mode. If the diaphragm is not opened again after conoscopic observations, the field of view is restricted when the microscope is returned to orthoscopic viewing mode. This diaphragm, if present, is operated by a lever or knurled ring mounted either in the microscope body tube or the viewing head (near or

FIGURE 23.18: Binocular microscope observation tube with Bertrand Lens

within the intermediate image plane; Figure 23.18). Later model microscopes often mount the Bertrand lens in a turret along with lenses that change the image magnification factor. Adjustment is made with a small knob that is labeled B or Ph for the Bertrand lens position, and 0 or some other number for the magnification lens. A Bertrand lens can also serve as a telescope for configuring phase contrast objectives by providing a magnified image of the objective rear focal plane with the phase rings superimposed over the condenser phase plate annulus.

23.2.7 Eyepieces (Oculars)

Early polarized light microscopes, like their brightfield counterparts, were often equipped with monocular observation tubes and a single eyepiece. Coupled to a reflecting substage mirror for illumination, these microscopes did not provide adequate illumination to visualize and photograph very weakly birefringent specimens. Although low-cost student microscopes are still equipped with monocular viewing heads, a majority of modern research-grade polarized light microscopes have binocular or trinocular observation tube systems. The eye tubes are usually adjustable for a range of interocular distances to accommodate the interpupillary separation of the microscopist (usually between 55 and 75 millimeters).

Many polarized light microscopes are equipped with an eyepiece diopter adjustment, which should be made to each of the eyepieces individually. Some microscopes have a graded scale on each eyepiece that indicates the position of the eyelens with respect to main body of the eyepiece. Other models hold the body of the eyepiece in a fixed position securely in the eye tube with a pin and slot. The first step in diopter adjustment is to either line up the graded markings (Figure 23.19) on eyepieces equipped with such markings or turn the eye lenses clockwise to the shortest focal length position. Next, focus the specimen with the 10x objective and then rotate the nosepiece until a lower magnification objective (usually the 5x) is above the specimen. At this point, refocus each eye lens individually (do not use the microscope coarse or fine focus mechanisms) until the specimen is in sharp focus. Rotate the 20x objective into the optical path and refocus the microscope with the fine focus knob. Repeat the diopter eye lens adjustments with the 5x objective (again not disturbing the microscope fine focus mechanism), and the microscope should be adjusted to the correct diopter settings. These settings will vary from user to user, so record the

FIGURE 23.19: 10x eyepiece with diopter adjustment and cross hair reticle

position of the eye lenses if the eyepiece has a graded scale for quick return to the proper adjustment.

Best results in polarized light microscopy require that objectives be used in combination with eyepieces that are appropriate to the optical correction and type of objective. Microscopes with a fixed tube length often have eyepieces (termed compensating eyepieces) that help to correct for chromatic difference of magnification when coupled to objectives designed specifically for that purpose. Newer microscopes with infinity-corrected optical systems often correct aberrations in the objectives themselves or in the tube lens. Inscriptions on the side of the eyepiece describe its particular characteristics and function, including the magnification, field number, and whether the eyepiece is designed for viewing at a high eyepoint.

Modern microscopes feature vastly improved plan-corrected objectives in which the primary image has much less curvature of field than older objectives. In addition, most polarized light microscopes now feature much wider body tubes that have greatly increased the size of intermediate images. To address these new features, manufacturers now produce wide-eyefield eyepieces that increase the viewable area of the specimen by as much as 40 percent. Because the strategies of eyepiece-objective correction techniques vary from manufacturer to manufacturer, it is very important to use only eyepieces recommended by a specific manufacturer for use with their objectives.

Care should be taken in choosing eyepiece/objective combinations to ensure the optimal magnification of specimen detail without adding unnecessary artifacts. For instance, to achieve a magnification of 200x, the microscopist could choose a 20x eyepiece coupled to a 10x objective. An alternative choice for the same magnification would be a 10x eyepiece with a 20x objective. Because the 20x objective has a higher numerical aperture (approximately 0.45 to 0.55) than does the 10x objective (approximately 0.25), and considering that numerical aperture values define an objective's resolution, it is clear that the latter choice would be the best. If photomicrographs or digital images of the same viewfield were made with each objective/eyepiece combination described above, it would be obvious that the 10x eyepiece/20x objective duo would produce images that excelled in specimen detail and clarity when compared to the alternative combination.

Eyepieces designed for polarized light microscopy are usually equipped with a crosshair reticle (or graticule) that locates the center of the field of view (Figure 23.19). A pin or slot system, described above, is often utilized to couple the eyepiece to a specific orientation in the observation tube so that the crosshairs may be quickly located and brought into a North-South and East-West direction with respect to the microscopist's view. These eyepieces can

be adapted for measurement purposes by exchanging the small circular disk-shaped glass reticle with crosshairs for a reticle having a measuring rule or grid etched into the surface. Because the reticle lies in the same plane as specimen and the field diaphragm, it appears in sharp focus superimposed over the image of the specimen. Eyepieces using reticles must contain a focusing mechanism (usually a helical screw or slider) that allows the image of the reticle to be brought into focus. Each objective must be individually calibrated to the ruled reticle by comparison with a stage micrometer, which is a microscope slide containing an etched millimeter scale. The calibration is conducted by focusing the microscope on the stage micrometer and determining how many millimeters is represented by each division on the ocular reticle rule.

Many modern microscopes are designed with inclined observation tubes in an effort to position the eyepieces at an ergonomically reasonable height above the laboratory bench. The result is a convenient viewing angle that allows the stage to remain horizontal, but these designs require several prisms to be interpolated into the optical path. Depending upon the glass utilized in manufacture, the prisms may produce considerable depolarization effects, which are offset by inclusion of high-order retardation plates in the observation tube optical system.

23.2.8 Adjusting the Polarized Light Microscope

Crossing the polarizers in a microscope should be accomplished when the objectives, condenser, and eyepieces have been removed from the optical path. If the analyzer is restricted to a fixed position, then it is a simple matter to rotate the polarizer while peering through the eye tubes until maximum extinction is achieved. For microscopes equipped with a rotating analyzer, fixing the polarizer into position, either through a graduated goniometer or click–stop, allows the operator to rotate the analyzer until minimum intensity is obtained. If markings are not provided on either the analyzer or polarizer, the microscopist should remember that simply crossing the polarizers in order to obtain minimum intensity in not sufficient. It is necessary to restrict the permitted vibration directions of the polarizer in the North-South orientation, and the analyzer in the East-West direction.

As described above, a thin preparation of well-shaped prismatic urea crystallites can be oriented either North-South or East-West by reference to the crosshairs in the eyepiece. Then, the polarizers can be rotated as a pair in order to obtain the minimum intensity of background and crystal in combination. If both polarizers can be rotated, this procedure may yield either a North-South or an East-West setting for the polarizer. The former orientation is preferred because it can be set by comparison with a polarizer whose vibration direction is known.

The condenser can focused and centered by reducing the size of the illuminated field diaphragm (located in front of the collector lens), then translating the condenser so that the image of the diaphragm edge is sharp when observed through the eyepieces. Next, the field diaphragm should be centered in the viewfield by using the condenser adjusting thumbscrews mounted on the substage housing that secures the condenser. After the diaphragm (and condenser) is centered, the leaves may be opened until the entire field of view is illuminated.

The lamp filament should be focused into the front focal plane of the condenser (a requirement of Köhler illumination) by altering the focus of the collector lens so that the tungsten helices are visible. The condenser front focal plane lies in or near the plane of the illuminating aperture (condenser) diaphragm. Because the rear focal plane of the objective

is in a plane conjugate to the condenser, it is possible to observe the filament image by removing the eyepiece or inserting the Bertrand lens. When viewing interference fringes in conoscopic mode, it is often convenient to employ a section of opal glass or a frosted filter near the lamp collector lens in order to diffuse the filament image in the objective rear focal plane.

In order to match the objective numerical aperture, the condenser aperture diaphragm must be adjusted while observing the objective rear focal plane. Again, the Bertrand lens provides a convenient mechanism of observing the relationship between the condenser illuminating aperture and the objective aperture. For most studies in polarized light, the diameter of the condenser aperture should be set to about 90 percent of the objective numerical aperture.

Although it is not essential, centering the rotating stage is very convenient if measurements are to be conducted or specimens rotated through large angles. The simplest method is to locate a small specimen feature (as a marker) and move the feature into the center of the rotation axis of the stage. This location may not coincide with the viewfield center, as defined by the eyepiece crosshairs. Using the centration knobs or keys near the stage, the marker feature can be translated (through trial and error) until its center of rotation coincides with the viewfield center. Some polarized light microscopes allow independent centering of the objectives in the nosepiece. If so, this task should be accomplished prior to attempting stage centration.

23.2.9 Conclusions

Microscopes dedicated for use with polarized light are very sophisticated instruments having components specifically designed to minimize strain and provide sharp, crisp, and clear images of birefringent specimens. For simple qualitative work, a standard microscope can be converted for polarized light studies. Typically, a small circle of Polaroid film is introduced into the filter tray or beneath the substage condenser, and a second piece is fitted in a cap above the eyepiece or within the housing where the observation tubes connect to the microscope body. Using the maximal darkening of the viewfield as a criterion, the substage polarizer is rotated until the field of view is darkest without a specimen present on the microscope stage.

Ensuring that the polarizer and analyzer have permitted vibration directions that are North-South and East-West is more difficult. If the orientation of one of the Polaroid films is known, then it can be inserted into the optical path in the correct orientation. It is then a simple matter to rotate the other polarizer (or analyzer) until the field of view achieves a maximum degree of darkness. Adding retardation plates to this setup is somewhat more difficult, because the "plates" must be located between the polarizer and analyzer, which are themselves often placed in tenuous locations. Several manufacturers sell thin films of retardation material, available in quarter and full wavelengths, but quartz wedges are difficult to simulate with thin films. The most convenient location for retardation films is above the objective (in the nosepiece), or before the analyzer in either the upper body housing or an eyepiece cap. Orientation of the retardation film should await polarizer and analyzer orientation efforts, because the film slow axis must be oriented at a 45-degree angle with respect to the polarizer (and analyzer) vibration direction.

A majority of standard microscopes lack a Bertrand lens, but a phase telescope may be substituted to observe conoscopic images appearing in the objective rear focal plane on microscopes retrofitted with thin film polarizers. There is no easy method to reproduce the

360-degree rotation of a circular polarized light microscopy stage. However, with practice, it is possible to achieve dexterity in rotating the slide itself while keeping the feature of interest within the viewfield.

Polarized light microscopy is often utilized by geologists for the study of naturally occurring minerals and rocks in thin section, and to mineralogists and ceramicists in both research and industrial environments. The technique is also heavily employed by scientists who study the various phase transitions and textures exhibited by liquid crystalline compounds, and polymer technologists often make significant use of information provided by the polarized light microscope. Forensic scientists take advantage of polarized techniques in the analysis of fibers, hairs, and other particles that are discovered at crime scenes. Recently, the advantages of polarized light have been utilized to explore biological processes, such as mitotic spindle formation, chromosome condensation, and organization of macromolecular assemblies such as collagen, amyloid, myelinated axons, muscle, cartilage, and bone.

Chapter 24

Rheinberg Illumination

Rheinberg illumination, a form of optical staining, was initially demonstrated by the British microscopist Julius Rheinberg to the Royal Microscopical Society and the Quekett Club (England) over a hundred years ago. This technique is a striking variation of low to medium power darkfield illumination using colored gelatin or glass filters to provide rich color to both the specimen and background.

The Rheinberg technique can be compared to the more familiar darkfield illumination. In darkfield microscopy, the substage condenser is arranged so that the rays of light from the lamp, coming through the condenser, will pass through the specimen only at very oblique angles. The central area of the cone of light traversing the condenser is occluded by means of an opaque stop, large enough in diameter so as to prevent light from directly entering the microscope objective. In more sophisticated darkfield condensers–paraboloid, cardioid, Cassegrain, or Leuchtbild–the occlusion of the direct light and the utilization of oblique rays only are achieved by use of specially designed mirror surfaces.

In darkfield illumination, the objective's numerical aperture is chosen (or reduced via an objective iris or funnel stop) so that light from the condenser cannot enter the objective directly. The only light that does enter the objective is light reflected, refracted, or diffracted by the specimen when the oblique rays from the condenser "strike" the specimen. The specimen then appears bright on an otherwise black field; hence the name darkfield illumination. The stark contrast of a bright object on a black field increases the visibility of already-resolved detail. A darkfield condenser can be approximated with the illustration in Figure 24.1 when the green central filter is substituted with an opaque stop, and the red oblique illumination filter is removed, allowing unfiltered white light to pass through.

In Rheinberg illumination (illustrated in Figure 24.1), which is related to darkfield, several kinds and shapes of filters are used. The oblique or outer light rays coming through a wide-open bright-field condenser pass through an annular (doughnut-shaped) filter of one or more colors (shown as the red filter in Figure 24.1 and the annular filters in Figure 24.2); the central rays of light pass through another spot-shaped filter fitting into the circular opening of the annular-shaped filter as shown for several combinations in Figure 24.2. The objective is used at full aperture. In this particular case, the specimen would appear as either red on a green background (Figure 24.2(a)), yellow on a blue background (Figure 24.2(b)), or green on a red background (Figure 24.2(c)).

The Rheinberg filters are prepared, or manufactured, in the form of transparent, annular colored rings with a circular opening in the center as depicted in Figure 24.3. In commercial versions of these filters, an accompanying set of transparent colored spots or

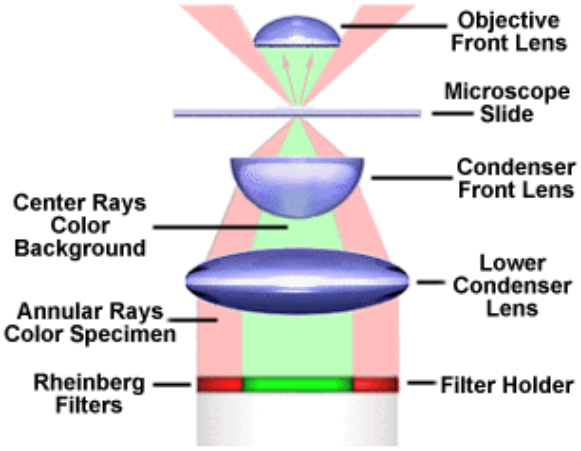

FIGURE 24.1: Rheinberg illumination

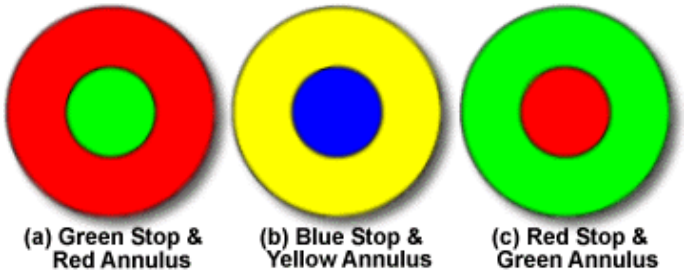

FIGURE 24.2: Rheinberg illumination filters

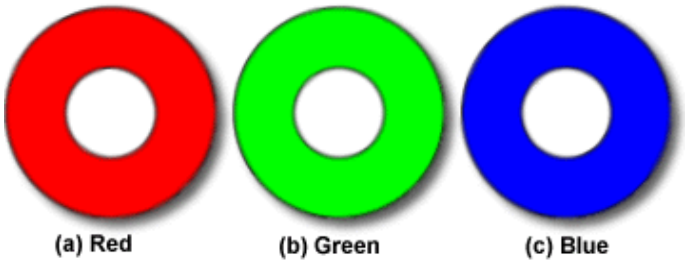

FIGURE 24.3: Annular Rheinberg filter rings

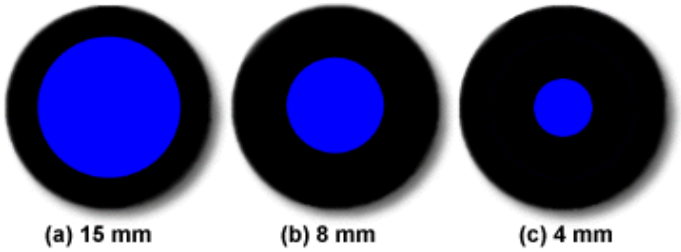

FIGURE 24.4: Central stops for Rheinberg illumination

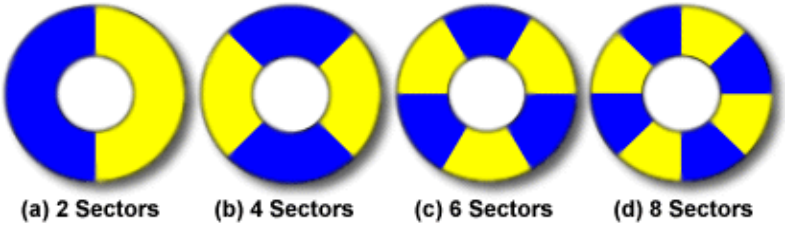

FIGURE 24.5: Alternative sector annular filters

"central filters" is made to fit snugly into the openings of the annular rings (Figure 24.4). The diameter of the central filter can be varied (to modulate background illumination intensity) by increasing the size of the narrow black rings that separate the filter from the outer ring (Figure 24.4(a–c)). Effective combinations include: red ring, violet central filter; yellow-orange ring, blue central filter, and so forth. Other visually effective images are produced by using a clear uncolored ring with a colored central filter. For example, a clear ring with a red central filter will produce white or colorless images on a red background.

In effect, the outer ring "becomes" the color of the specimen and the central filter "becomes" the color of the background. The outer ring can also be divided into alternating sectors of color as illustrated in Figure 24.5. The sector filters are especially effective in the study of warp-proof fabrics, crystal faces, diatoms, and wood sections where the length-width dimensions are displayed in contrasting colors.

For years, some microscope manufacturers sold Rheinberg filters in colored gels (similar to Kodak Wratten filters) that were precut to fit the substage filter ring of their microscopes. The annular rings had outside diameters of 31-35 millimeters and central filters usually had a diameter of 15-18 millimeters for use with a 10x - 0.25 NA objective. These filters can also be readily fabricated in the laboratory using either Kodak Wratten filters or colored filters that are widely available at scientific supply houses and optical component distributors. Gelatin filters can be prepared by cutting the central filter with a cork-borer of the proper diameter, and the annular rings can be prepared by carefully drawing a circle on the filter paper and cutting it out with a pair of scissors. In our laboratory, the support machinists have constructed a brass die that cuts annular filter circles that are the same diameter as our Rheinberg filter holder. This die can quickly stamp very smooth circles from sheets of acetate or gelatin colored filters. The center of the annular filter can be cut with the same cork-borer used to prepare the central filter.

Sometimes, it is difficult to provide a solid housing for the central filter within the annular filter when these are both made of very thin acetate or gelatin filters. In this case,

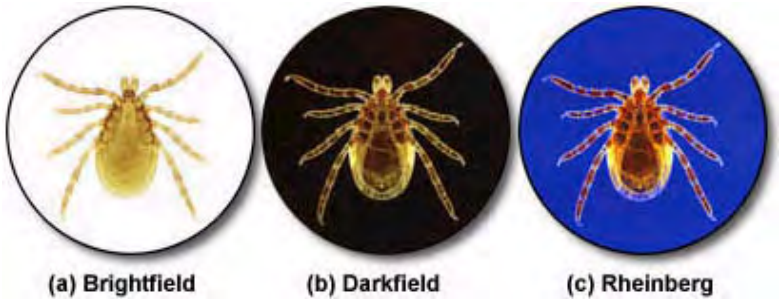

FIGURE 24.6: Specimen examples

you can just tape the central filter over the center of the annular filter with double-sided tape, but remember that the central filter and annular filter colors will add, so use a very dark filter for the central filter. The central filter, in general, should be much darker than the annular filter to allow the specimen highlights to be in sharp contrast to the background. We often place two or three pieces of the same color central filters in a stack to adjust the transmittance of light through the central filter. Rheinberg filters can also be made using glass filters and this is very convenient when the substage condenser is fitted with a housing for these filters. In this case, it is best to simply tape the central filter onto the center of the glass filter. For those interested in making their own filters, a more complete discussion is presented in Needham's Practical Use of the Microscope, listed in our bibliography.

We have compared brightfield, darkfield, and Rheinberg illumination techniques using photomicrographs of a Deer tick (Ixodes dammini) in Figure 24.6. The first photomicrograph (a) illustrates the tick under brightfield illumination. The image is lacking in contrast and many details are hard to resolve. Figure 24.6(b) shows the same tick under darkfield illumination, where more contrast and detail are present and many of the features on the tick are apparent. Rheinberg illumination (Figure 24.6(c)) of the tick using a blue central filter and a yellow annular ring (see Figure 24.2(b)) cause an increased contrast effect, similar to darkfield, but with a pleasant blue background. In this example, the darkfield and Rheinberg illumination techniques yield remarkably better photomicrographs than does brightfield.

During the late 1930s, Carl Zeiss manufactured a special condenser, the Mikropolychromar, designed to produce beautiful Rheinberg images. This condenser is long out of production and is now virtually unobtainable, but it consisted of an aplanatic condenser under which there were three separately controlled diaphragms. The outermost diaphragm controlled the diameter of the field, and two smaller diaphragms controlled the light passing through the central disk. Annular transparent rings of various colors were part of the set. Accompanying these was a set of transparent glass central disks which fitted neatly into the central opening of the annular ring. This ingenious condenser has been used by one of the authors (M. Abramowitz) to produce striking photomicrographs at various magnifications, some of which have appeared in the publications Omni, Time-Life, Scientific American, and National Wildlife.

Rheinberg illumination is suitable for objectives ranging from 2x to 100x. However, in order to clearly separate the inner and outer colors, opaque metal or paper rings should be placed around the central filter. For example, the opaque rings might have an outside diameter of 15-18 millimeters for a 10x objective, and an outside diameter of 22 millimeters might be best for a 60x oil immersion objective. It is a good idea to experiment using central

filters like the ones illustrated in Figure 24.4 to achieve the best results with Rheinberg illumination.

For studying fibers, protozoa, textiles, insects, wood sections, crystal, or other unstained low-contrast subjects, microscopists should consider adding Rheinberg illumination to their library of contrast techniques. It will be possible to view and photograph specimens yielding images that are visually enhanced, as well as aesthetically beautiful.

One final note from the authors: It is strongly suggested to the microscope manufacturers and/or independent accessory manufacturers that they produce Rheinberg condensers and filters for use by microscopists. The necessary components would be very inexpensive to produce and would greatly aid microscopists in setting up their microscopes for Rheinberg Illumination.

Part IV

Digital Imaging

Chapter 25

Electronic Imaging Detectors

Electronic Imaging Detectors Over the past several years, the rapidly growing field of fluorescence microscopy has evolved from a dependence on traditional photomicrography using emulsion-based film to one in which electronic images are the output of choice. The imaging device is one of the most critical components in fluorescence microscopy because it determines at what level specimen fluorescence may be detected, the relevant structures resolved, and/or the dynamics of a process visualized and recorded.

The range of light detection methods and the wide variety of imaging devices currently available to the microscopist make the selection process difficult and often confusing. This discussion is intended to aid in understanding the basics of light detection and to provide a guide for selecting a suitable detector for specific applications in fluorescence microscopy. Illustrated in Figure 25.1 is an epi-fluorescence microscope equipped with a state-of-the-art megapixel digital imaging camera system with Peltier cooling designed to image specimens over a wide exposure range in 24-bit color at low light levels. Detectors of this type as well as other alternatives are reviewed in the following paragraphs.

25.1 Detector Characterization Parameters

Electronic imaging sensor performance may be described by a number of variables including: spectral sensitivity, quantum efficiency, spatial resolution, uniformity, the signal/noise ratio, dynamic range, and response speed. Each of these specifications is discussed in detail in our section reviewing Concepts in Digital Imaging Technology, but a brief description is included here for convenience. Spectral sensitivity refers to the detector signal as a function of the wavelength of the incident light. This parameter is often expressed in terms of the quantum efficiency (QE), a measure of the detector's ability to produce an electronic charge from the percentage of incident photons that are detected. The limiting spatial resolution is commonly determined from the minimum separation required for discrimination between two high contrast objects, for instance, white points or lines on a black background. Contrast is an important factor in resolution because high contrast objects (e.g. black and white lines) are more readily resolved than low contrast objects (e.g. adjacent gray lines).

More informative measures of the spatial resolution of an electronic detector are the modulation transfer function (MTF) and the contrast transfer function (CTF), both of which demonstrate the magnitude of the detector response as a function of spatial frequency. The CTF is determined from the detector response to a series of black and white bars that become progressively narrower and closer together. Each pair of bars is essentially a square

FIGURE 25.1: Fluorescence microscope with digital camera

wave with 100 percent contrast. The MTF is an expression describing the reduction in contrast of a sinusoidal signal (60% contrast sine waves) as a function of spatial frequency. The limiting resolution of an electronic detector is the smallest target size that is detectable above the noise threshold, a concept that is often referred to as the frequency of limiting resolution, which is the spatial frequency for which the MTF falls to a value of 3 percent, corresponding to the limit of visible detection.

The uniformity of electronic detectors encompasses several variables: gain variations across the sensor, regional differences both in noise and sampling efficiency (often termed shading), and spatial variation in the efficiency of light collection or transmission. Electronic detectors are often compared by their signal/noise ratio (designated S/N), a measure of the variation of a signal that indicates the confidence with which the magnitude of the signal can be estimated. Visible light has an inherent noise component arising from the stochastic nature of the photon flux, which is equal to the square root of the signal. Noise also derives from a variety of other sources such as the output amplifier (read noise), and in electronic devices can often be reduced by lowering the operating temperature. Noise arising in electronic devices in the absence of light is termed dark current or dark noise, which is thermally sensitive, increasing as a function of the detector temperature.

Intrascene dynamic range is derived from the maximum and minimum intensities that can be simultaneously detected in the same field of view. This quantity represents the range of intensities that can be accommodated when detector gain, integration time, lens aperture, or other variables are adjusted for differing fields of view. The terms dynamic range and signal/noise should not be confused. Dynamic range is often calculated as the maximum signal that can be accumulated divided by the noise associated with reading that signal. The response speed of an electronic detector is described by its lag, representing the fraction of the previous image that carries over into the next one after a prescribed time interval has elapsed.

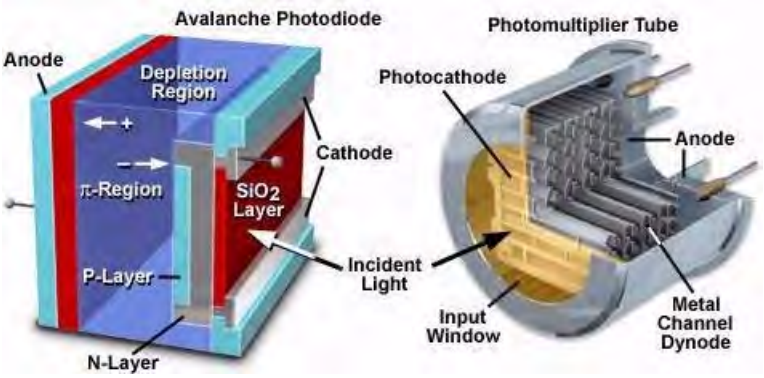

FIGURE 25.2: Electronic light detector

25.2 Electronic Detection of Light

Two examples of commonly used light detectors lacking spatial discrimination are the photomultiplier tube and the photodiode (illustrated in Figure 25.2). Both devices employ a photosensitive surface that captures incident photons and generates electronic charges that are sensed and amplified. Photomultiplier tubes (PMTs) are widely used in confocal microscopes and high-end automatic exposure bodies for film cameras as well as in spectrometers. These devices respond when photons impinge on a photocathode and liberate electrons that are accelerated toward an electron multiplier composed of a series of curved plates, known as dynodes.

Light entering the input window of a PMT strikes the photocathode, which utilizes the energy of the incident photons to release electrons with a peak quantum efficiency that has recently been improved to about 40 percent (see the GaAsP curve in Figure 25.3). The photocathode active area can range in size from a few millimeters to a half meter in diameter, depending upon the application.

The output from the metal channel dynode chain is a current proportional to the number of photons striking the photocathode and to the voltage drops along the dynode channel. Spectral sensitivity depends on the chemical composition of the photocathode; the best devices often incorporate gallium-arsenide and are sensitive to ultraviolet, visible, and infrared light in the wavelength range from 300 to 850 nanometers (Figure 25.3). PMT photocathodes are not uniformly sensitive and typically the photons are spread over the entire entrance window rather than concentrating into one region. Because PMTs do not store charge and respond to changes in input light fluxes within a few nanoseconds, they can be used for the detection and recording of extremely fast events. These devices typically generate low noise values (and dark current) resulting in a huge dynamic range over which electrical current output still accurately reflects the photon flux. The large gain exhibited by these devices is obtained without sacrificing bandwidth, which can range from 100 to 1500 MHz with a very high signal/noise ratio in scientific grade PMTs.

The spectral sensitivity curves for three electronic detectors illustrating quantum efficiency as a function of the illumination wavelength is presented in Figure 25.3. Two of the curves (the lower curves in Figure 25.3) were generated with PMTs having photocathode compositions utilizing either gallium-arsenide-phosphide (Ga-AS-P) or gallium-arsenide (Ga-As) alloys, while the third curve represents the response of a silicon photodiode with a ultraviolet-transparent window.

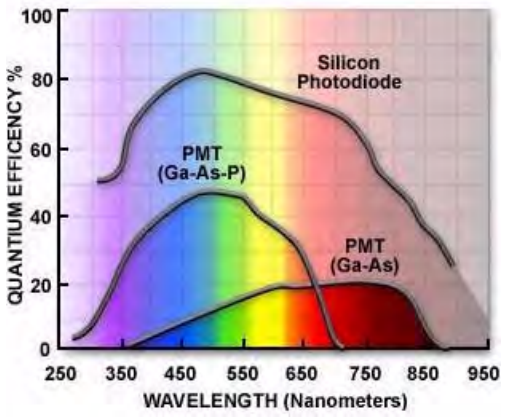

FIGURE 25.3: Electronic detector spectral sensitivities

Silicon photodiodes also respond rapidly to light by the generation of a current, but they do so without the huge gain that accompanies electron multiplication by the PMT. Photodiodes have a relatively flat response over the entire visible spectrum (Figure 25.3) with high quantum efficiency that ranges from 80 to 90 percent. Uniformity of the photosensitive surface is excellent and the dynamic range and response speed of these devices are among the highest of any light detector. However, silicon diodes produce a considerable amount of noise, (much of it thermal) resulting in relatively poor S/N under photon-limited conditions, such as are common in fluorescence microscopy. Photodiodes that incorporate limited gain have been developed (avalanche photodiodes, illustrated in Figure 25.2) and been utilized in some confocal and wide-field fluorescence microscopes. Although they have up to 300-fold gain, they exhibit significant dark noise even when cooled to 0°C.

25.3 Area detectors

These devices are generally divided into two categories: tube-type and solid state detectors. The vidicon tube camera (illustrated in Figure 25.4) is a tube-type detector in which the photosensitive surface is "read out" by a scanning electron beam. In vidicons, the photosensitive surface stores charge rather than liberating electrons as in a photocathode. Photons captured by the photosensor alter its electrical resistance at their site of impact, and the current of the scanning beam flows more readily through these sites generating a signal. Because vidicon tube sensors have been largely supplanted by modern solid-state detectors and are of interest only due to historical significance, they will not be considered in any further detail.

Solid-state detectors consist of a dense matrix of photodiodes incorporating charge storage regions. Several variations on the basic concept are commercially available including the popular charge-coupled device (CCD), the charge-injection device (CID), and the complimentary-metal-oxide-semiconductor detector (CMOS). In each of these detectors, a silicon diode photosensor (often denoted a pixel) is coupled to a charge storage region that is, in turn, connected to an amplifier that reads out the quantity of accumulated charge. In the CID and CMOS detectors, each individual photosensor has an amplifier associated with it and the combined signal from a row of amplifiers is output in parallel. Although techniques for charge storage by silicon photodetectors were known for many years before

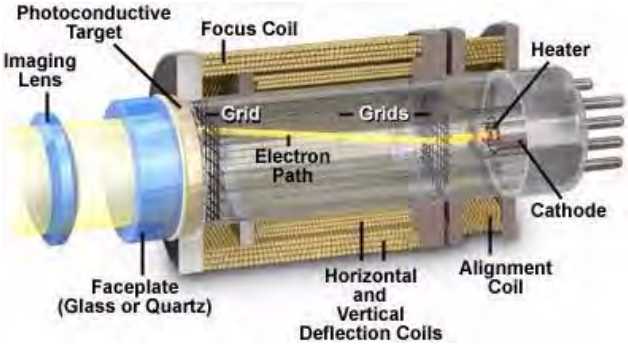

FIGURE 25.4: Vidicon camera tube

the development of the CCD, a suitable mechanism for the systematic read out of this stored charge needed to be devised before the device became a reality. In a CCD, there is typically only one amplifier at the corner of the entire array, and the stored charge is sequentially transferred through the parallel registers to a linear serial register and then to an output node adjacent to the read-out amplifier.

Because the CCD is presently the most widely used detector for fluorescence microscopy, we will consider its performance in more detail. Distinctions will be made, where appropriate, between the two classes of CCD cameras: consumer-grade and scientific-grade. It is important to point out that although all electronic detectors are analog devices that generate electrical currents or charges, cameras with an internal digitizer have recently been denoted digital cameras because they do not have an analog signal output.

Some CCD cameras used in scientific applications are operated at room temperature while others are cooled to reduce dark current (a 20C decrease in temperature reduces the dark current of the CCD ten-fold). Because the charge storage wells do not fill with thermally-generated dark noise during the integration period, longer exposures are possible. Cooled cameras for scientific use are often designated slow-scan because their frame rate is less than that of a standard video camera.

A video-rate camera reads the stored charge and outputs a video field every 16.7 milliseconds to conform to the recommended standards (denoted RS-170 or RS-330) in which 30 video frames are produced per second with each frame consisting of two interlaced fields (the European standard format requires 50 fields per second with a field every 20 milliseconds). Video exploits the lag in our visual system by generating images at a rate faster than the critical flicker frequency, the video refresh frequency in which flicker is no longer perceived by the human eye. Each video field, containing 50 percent of the information in an entire frame, is obtained in sequence with the result that there is a 16.7 millisecond time difference between successive odd or even scan lines in the complete image. If the output of a video-rate camera is stopped and light is allowed to fall on the CCD for a prolonged period, the first two video fields produced contain all of the information accumulated during the integration period.

Interlacing of two video fields to produce a complete video frame was a clever solution to the engineering problem resulting from the bandwidth limitations of the electronics and signal transmission and reception components available at the time of the development of television. Now much higher frequency amplifiers and associated electronics permit the production, storage, and subsequent display at frame rates of up to 1000/second without the need to interlace scan lines. Such progressive-scan cameras produce a continuous scan

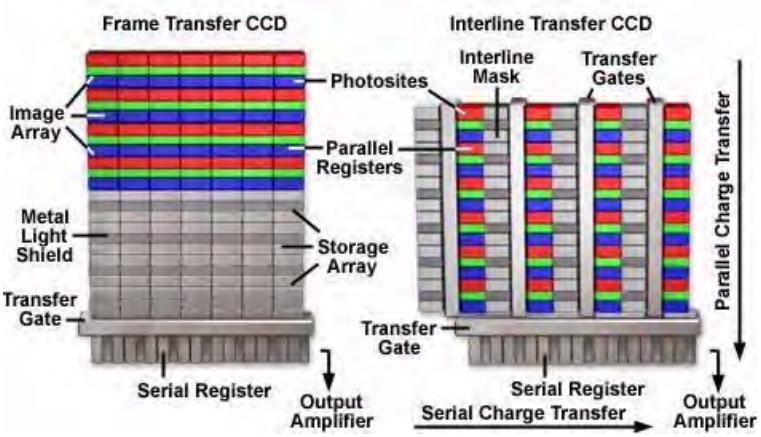

FIGURE 25.5: Charged couple device architecture

from the top to the bottom of the image. This does not mean that the top lines were obtained before the bottom ones; rather, the devices first integrate the photon flux over the entire sensor and then rapidly displace the accumulated charge to a charge storage and transfer region that is protected from further illumination.

Two CCD designs are commonly used to achieve such rapid transfers: the interline-transfer CCD and the frame-transfer CCD, which are diagrammatically illustrated in Figure 25.5. The interline-transfer CCD incorporates charge transfer channels (termed "interline masks" in Figure 25.5) immediately adjacent to each photodiode so that the accumulated charge can be efficiently and rapidly shifted into the channels after image acquisition has been completed. Interline-transfer CCDs can be electronically shuttered by altering the voltages at the photodiode so that the generated charges are injected into the substrate rather than shifted to the transfer channels. These devices also include an electron "drain" to prevent blooming and are usually equipped with microlens arrays to increase the photodiode fill factor and quantum efficiency.

The frame-transfer CCD uses a two-part sensor in which one-half of the parallel array is used as a storage region and is protected from light by a light-tight mask. Incoming photons are allowed to fall on the uncovered portion of the array and the accumulated charge is then rapidly shifted into the masked storage region for charge transfer to the serial output register. While the signal is being integrated on the light-sensitive portion of the sensor, the stored charge is read out. A disadvantage of this architecture is charge smearing during the transfer from the light-sensitive to the masked regions of the CCD, but this can often be compensated.

The spectral sensitivity of the CCD differs from that of a simple silicon photodiode detector because the CCD surface has channels used for charge transfer that are shielded by polysilicon gate electrodes. These structures absorb the shorter wavelengths and reduce the blue sensitivity of the device. A typical spectral sensitivity curve for a consumer or scientific-grade CCD is illustrated in Figure 25.6 (Standard CCD) where it should be noted that the peak quantum efficiency of 40 percent is markedly below that of a individual silicon photodiode. Recently, the transparency of the channels has been increased with substantial improvement in blue-green sensitivity of some scientific-grade CCDs (Blue Plus curve in Figure 25.6). The losses due to the channels are completely eliminated in the back-illuminated CCD. In this design, light falls onto the back of the CCD in a region that has

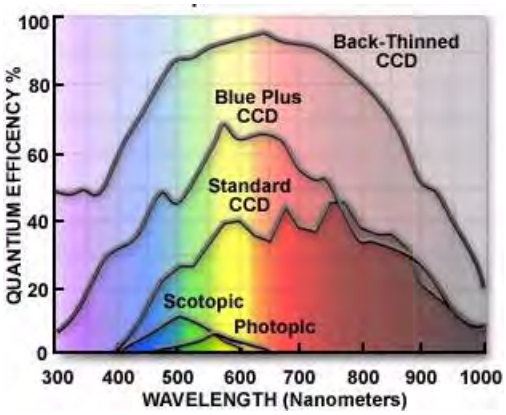

FIGURE 25.6: CCD spectral sensitivities

been thinned by etching until it is transparent (a thickness corresponding to about 10-15 microns). The resultant spectral sensitivity curve, also shown in Figure 25.6 (Back-Thinned CCD), illustrates the high quantum efficiency that can be realized with this configuration. However, back-thinning results in a delicate, relatively expensive sensor that, to date, has only been employed in high-end scientific-grade CCD cameras.

The resolution of a CCD is a function of the number of photodiodes and their size relative to the projected image. CCD arrays of 1000 x 1000 sensors are now commonplace in scientific-grade video cameras. The trend in consumer and scientific-grade CCD manufacture is for the sensor size to decrease, and cameras with photodiodes as small as 4 x 4 microns are currently available in the consumer market. A typical MTF curve for a CCD camera with 6.7-micron pixels is shown in Figure 25.7. The spatial frequency of 60-percent contrast sine waves projected onto the sensor surface is plotted on the abscissa and the resultant modulation percentage on the ordinate. The limiting resolution is normally defined as the 3 percent modulation level.

Adequate resolution of an object can only be achieved if at least two samples are made for each resolvable unit (many investigators prefer three samples per resolvable unit to ensure sufficient sampling). In the case of the epi-fluorescence microscope, the resolvable unit from the Abbe diffraction limit at a wavelength of 550 nanometers using a 1.4 numerical aperture lens is 0.21 microns. If a 100x objective is employed, the projected size of a diffraction-limited spot on the face of the CCD would be 21 microns. A sensor size of 10.5 x 10.5 microns would just allow the optical and electronic resolution to be matched, with a 7 x 7 micron sensor size preferred. Although small sensors in a CCD improve spatial resolution, they also limit the dynamic range of the device. Table 25.1 provides suggested sensor pixel size for commonly used objectives in fluorescence microscopy.

The charge storage capacity of a CCD is proportional to the size of the individual photodiode, such that the maximum number of electrons stored is about 1000 times the cross sectional area of each photodiode. Thus, a CCD with 7 x 7 micron photodiodes should have a maximum charge storage capacity (a full-well capacity) of 49,000 electrons or holes. A hole is the region of the silicon from which the electron came and constitutes an equally valid and usable measure of detected photons. The term "electrons" will be used predominantly throughout this discussion even though many CCDs read out the number of holes generated rather than electrons. Because CCDs do not have inherent gain, one electron-hole pair is accumulated for each detected photon. The dynamic range of a CCD

Objective (Numerical Aperture)	Resolution Limit (μm)	Projected Size on CCD (μm)	Required Pixel Size (μm)
4x (0.20)	1.5	5.8	2.9
10x (0.45)	0.64	6.4	3.2
20x (0.75)	0.39	7.7	3.9
40x (0.85)	0.34	13.6	6.8
40x (1.30)	0.22	8.9	4.5
60x (0.95)	0.31	18.3	9.2
60x (1.40)	0.21	12.4	6.2
100x (0.90)	0.32	32.0	16.0
100x (1.25)	0.23	23.0	11.5
100x (1.40)	0.21	21.0	10.5

TABLE 25.1: Pixel Size Requirements for Maximum Optical Resolution in Fluorescence Microscopy

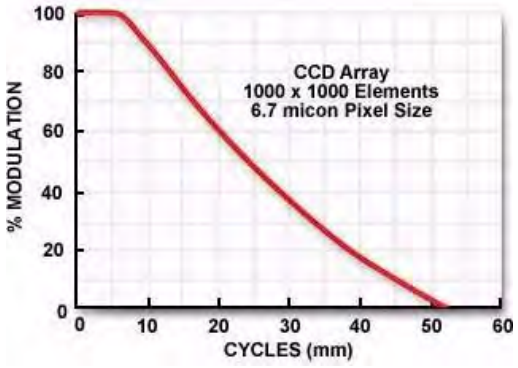

FIGURE 25.7: Modulation transfer function

is typically defined as the full-well capacity divided by the camera noise. The camera noise is the sum, in quadrature, of the dark and read-out noise. Recent improvements in CCD design have greatly diminished dark charge to negligible levels and reduced read-out noise to about 10 electrons per pixel. Even room temperature cameras may have such a low dark signal that it can be ignored for integration periods of 10 seconds or less. Cooling further reduces the dark signal and permits much longer integration periods, up to several hours, without significant dark charge accumulation. Thus, the dynamic range of a 49,000 electron full-well capacity CCD with 10 electrons of read-out noise and negligible dark noise is about 4900, corresponding to a 12-bit dynamic range (4096 gray-scale levels).

A CCD with a 49,000 electron full-well capacity has a maximum achievable signal/noise of about 220 (the square root of 49,000). Of course, camera noise would add, in quadrature, to the photon statistical noise and reduce the maximum S/N below this value. A simple estimate of the S/N of any homogeneous region in an image may be made from the average intensity of the region of interest divided by the standard deviation of the intensities of that region.

Cameras for consumer use often have a rectangular format CCD with an aspect ratio of 4:3. That means that the height of the image will be 3/4 of the width to conform with video standards based on our landscape view of the world. Indeed, the newest generation

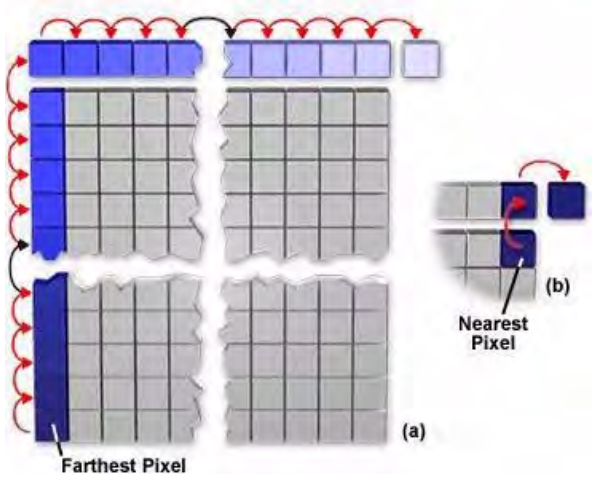

FIGURE 25.8: Charge transfer efficiency in CCDs

of consumer-grade products designed for HDTV employ a 16:9 aspect ratio. Scientific imaging, on the other hand, is best conducted with a square image made up of square pixels as they are better suited to digital image processing.

CCD sensor uniformity is generally very good, with less than 10 percent variation in gain between photodiodes. However, shading may be introduced into the image from a CCD camera because of inefficiencies in charge transfer. The operation of a CCD requires that each packet of charge underlying a photodiode be transferred to the read-out amplifier. This transfer is accomplished by a series of parallel and serial shifts that displace rows of charge along the chip toward a single corner containing the read-out amplifier. If the read-out amplifier is in the upper right-hand corner of a 1000 x 1000 sensor CCD, the charge from the photosensor nearest to that corner will have to be shifted only once upward into the serial shift register (a parallel shift) and once rightward (a serial shift) to reach the amplifier. On the other hand, the charge from the photodiode in the lower left hand corner will have to be shifted upward 1000 times and rightward 1000 times to be read out. If the transfer efficiency is 99.9 percent for each shift, only 13.5 percent of the charge accumulated by the lower left photodiode would remain after the requisite 2000 shifts. This charge loss would make the lower left corner much darker than the upper right and would also tend to blur or smear that region of the image because of spillover by charges from adjacent photodiodes. The concept is illustrated schematically in Figure 25.8 using blue colored pixels to represent integrated charge density. The pixel in the lower left hand corner of the CCD (farthest pixel - dark blue) is shown slowly losing color intensity as the charge is transferred first in parallel to the serial shift register, then serially to the output node. A pixel closer to the node (the upper right-hand "nearest" pixel) is also illustrated in dark blue and undergoes only a two-step jump to yield an accumulated charge transfer efficiency of 99.8 percent at the output node.

Slow-scan CCD cameras increase charge transfer efficiency by cooling the CCD and slowing the transfer rate. The high speed charge transfer required in video-rate CCD cameras necessitates a different strategy. In these cameras, the read-out amplifier gain is adjusted to compensate for the charge lost from each row by sampling extra pixels outside of the image area. The additional gain required for the lower rows inevitably increases the noise in the highly corrected regions of the sensor.

Some control over the read-out rate as well as the size of the pixel that constitutes a sensor is permitted by slow-scan CCD cameras. Video-rate CCD cameras are simpler and do not allow such control. Slowing the read-out usually reduces the amplifier noise associated with reading the charge, a beneficial situation when the photon flux is very low and the signal can be produced relatively slowly (in a second or two rather than in 33 milliseconds). Scientific-grade CCD cameras usually offer two or more read-out rates so that speed may be traded off against noise.

The size of a pixel in a scientific-grade CCD may be increased by binning, a process in which the charge from a cluster of adjacent photodiodes is pooled and treated as if it came from a larger detector. In binning, several shifts of charge to the serial register and output node storage regions occur before read out. The extent of binning depends on how many shifts occur before the stored charge is read, with the only limitation being the charge storage capacity of the serial register (usually twice that of a single photodiode) or of the output node (usually three times that of a photodiode). The maximum charge storage capacity of the serial register and output node are not a concern in most fluorescence microscopy applications because binning is employed when light levels are very low and few photons are detected. Binning enables the investigator to trade spatial resolution for sensitivity.

There are a variety of scientific CCDs available on the market that feature a wide range of array and individual pixel sizes. Several of the most popular CCDs found in digital imaging cameras used in microscopy are listed in Table 25.2. Currently, the most popular CCD is the Sony ICX205AK interline-transfer progressive scan chip that supports a high frame readout rate of 30 frames/second. This CCD has a 1360 x 1024 active pixel array producing an 8 millimeter image size using 4.65 x 4.65 micron square pixels. The chip also features high sensitivity, low dark current, low smear, excellent antiblooming characteristics, and a continuous variable speed shutter.

Slow-scan CCD cameras also allow region-of-interest read-out. This means that a selected portion of the image can be displayed and the remainder of the accumulated charge discarded. The framing rate generally increases with reduction in the size of the detected area. For example, a CCD with a sensor size of 1000 x 1000 and an output rate of ten frames/second can produce 100 frames/second if the read-out region is reduced to 100 x 100 diodes. By trading off field-of-view and framing rate, an investigator can adjust to a far wider range of experimental circumstances than would be possible with a fixed framing rate video camera.

25.4 Low-Light-Level Imaging of Fluorescence

Because of the problems of photodestruction of fluorochromes in the presence of oxygen ("photobleaching") and limitations on the numbers of fluorochromes that can be involved a single region, a variety of sensitive electronic detectors are used in fluorescence microscopy. Only about 5-10 percent of the emitted light from an excited fluorochrome is collected and transferred to the sensor in a typical epi-fluorescence microscope. There are two approaches to capturing as much of this limited light flux as possible: integration by a slow-scan CCD, as previously described, or image intensification and capture on a video-rate or progressive-scan CCD camera. The general finding is that a cooled, slow-scan CCD camera always produces a higher S/N than an intensified CCD, provided sufficient integration time is available.

TABLE 25.2: CCD Specifications

Manufacturer and Model	Format	Pixel Size (μm)	Array Size(mm)
Kodak KAF–2001CE	1732 x 1172	13 x 13	22.5 x 15.2
Kodak KAF–3000CE	2016 x 1512	9 x 9	18.1 x 13.6
Kodak KAF–3040CE	2144 x 1432	6.8 x 6.8	14.6 x 9.7
Kodak KAF–6302CE	3052 x 2016	9 x 9	27.5 x 18.1
Kodak KAI–4000	2048 x 2048	7.4 x 7.4	15.16 x 15.16
Sony ICX205AK	1392 x 1040	4.65 x 4.65	7.6 x 6.2
SITe ST–002A	2048 x 4096	15 x 15	30.72 x 30.72
Marconi CCD 42–90	4608 x 2048	13.5 x 13.5	27.6 x 62.2
Marconi CCD 48–20	1028 x 1033	13 x 13	13.3 x 13.3
Philips FTF3020–C	3072 x 2048	12 x 12	36.8 x 24.6
Philips FT18	1024 x 1024	7.5 x 7.5	7.68 x 7.68

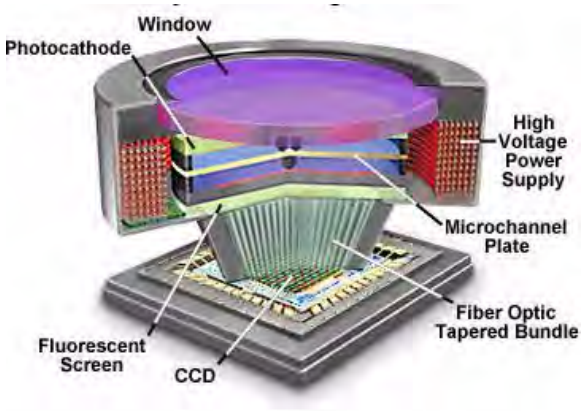

FIGURE 25.9: Proximity–focused image intensifier

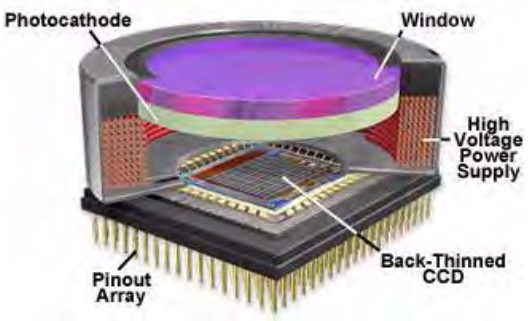

FIGURE 25.10: Electron–bombarded back–thinned CCD

Image intensifiers (see the examples in Figures 25.9 through 25.11) were developed for military use to enhance our night vision. They have an input photocathode followed by a micro-channel plate electron multiplier and a phosphorescent output screen. The photocathode in the latest generation of these devices, while similar to that in photomultiplier tubes, has a higher quantum efficiency (up to 50 percent) in the blue-green end of the spectrum. The gain of the micro-channel plate is adjustable over a wide range with a typical maximum of about 80,000 (a detected photon at the input leads to a pulse of 80,000 photons from the phosphor screen). The phosphor matches the spectral sensitivity of the eye and is often not ideal for a CCD. Resolution of an intensified CCD depends on both the intensifier and the CCD, but is usually limited by the intensifier microchannel plate geometry to about 75 percent of that of the CCD alone. The latest generation of image intensifiers (denoted blue-plus Gen III or sometimes Gen IV; Figure 25.9) employ smaller microchannels (6 micron diameter) and better packing geometry than in previous models with a resultant substantial increase in resolution and elimination of the chicken-wire fixed-pattern noise that plagued earlier devices.

Image intensifiers have a reduced intrascene dynamic range compared to a slow-scan CCD camera and it is difficult to obtain more than a 256-fold intensity range (8 bits) from an intensified CCD camera. Intensifier gain may be rapidly and reproducibly changed to accommodate variations in scene brightness, thereby increasing the interscene dynamic range. Indeed, since image intensifiers can be rapidly gated (turned off or on in a few nanoseconds), relatively bright objects can be visualized by a reduction in the "on" time. A gated, variable gain intensified CCD camera is commercially available with a 12 order of magnitude dynamic range. Gated, intensified CCD cameras are required for most time-resolved fluorescence microscopy applications because the detector must be turned on and off in nanoseconds or its gain rapidly modulated in synchrony with the light source.

Thermal noise from the photocathode as well as electron multiplication noise from the microchannel plate reduce the S/N in an intensified CCD camera to below that of a slow-scan CCD. The contribution of these components to the noise created by the statistical nature of the photon flux depends on the gain of the device and the temperature of the photocathode. Generally, a reduction of the gain of the intensification stage is employed to limit the noise although intensified CCD cameras are available with a cooled photocathode.

Intensified CCD cameras have a very fast response limited by the time constant of the output phosphor and often the CCD camera read out is the slowest step in image acquisition. Because of the low light fluxes emanating from the fluorochromes bound to or within

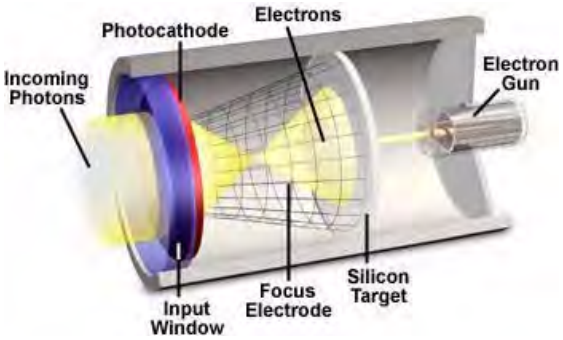

FIGURE 25.11: Silicon intensifier target tube

living cells, intensified CCD cameras are frequently employed to study dynamic events and for ratio imaging of ion-sensitive fluorochromes. The simultaneous or near-simultaneous acquisition of two images at different excitation or emission wavelengths is required for ratio imaging and intensified CCD cameras have the requisite speed and sensitivity.

A hybrid of the image intensifier and the CCD camera is the recently introduced, electron-bombarded CCD (EBCCD; Figure 25.10). In this device, photons are detected by a photocathode similar to that in an image intensifier. The released electrons are accelerated across a gap and impact on the back side of a CCD. These energetic electrons generate multiple charges in the CCD resulting in a modest gain of a few hundred. The advantages of this device over a cooled, slow-scan CCD are the additional gain and accompanying speed; the main disadvantages are the lower quantum efficiency of the photocathode and diminished dynamic range. Compared to an intensified CCD, the electron bombarded CCD usually has higher spatial resolution and a better S/N at moderate light levels, but the limited gain adjustment range and modest low-light-level detection capability make the electron-bombarded CCD the solid-state equivalent of the outmoded SIT (silicon intensifier target; Figure 25.11) camera.

25.5 Electronic versus Visual Detection

How does the human eye compare with electronic detectors? Figure 25.6 illustrates spectral sensitivity curves for the eye, corresponding to photopic and scotopic vision, arising from the cones and rods (Figure 25.12), respectively. Peak sensitivity is in the green (photopic at 555 nanometers and scotopic at 507 nanometers) with a maximum quantum efficiency of 3 percent for photopic vision and 10 percent for scotopic. Our spatial resolution is not uniform because the cones are not evenly distributed. The highest density occurs in the fovea where the distance between cones is about 1.5 microns, giving us a 5 to 6 micron limiting spatial resolution on the retina. Under achromatic (black and white) constant illumination conditions, visual intrascene dynamic range is only about 50-fold (6 bits). Our visual pigment, rhodopsin, exhibits little thermal noise, and the minimum detectable signal after dark adaptation is about 100 to 150 photons at the pupil or about 10 to 15 photons at the retina. The signal/noise for the eye at the visual detection limit is about 3:1. Lag is about 20 milliseconds at high light levels and about 100 milliseconds in dim illumination.

It is obvious that, compared to our eyes, a scientific-grade CCD camera has a broader

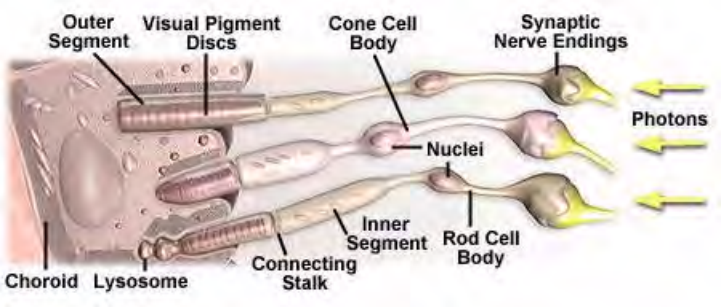

FIGURE 25.12: Rode and cone photoreceptors in human eyes

spectral sensitivity, much higher quantum efficiency, greater integration capability, more uniformity, better intrascene dynamic range (more "bits"), comparable or higher signal/noise, but lower spatial resolution. When matched against our visual system, low-light-level cameras have a much wider spectral range, less lag and far greater sensitivity and resolution under photon-limited conditions.

25.6 Choosing the Appropriate Camera

No single detector will meet all requirements in fluorescence microscopy and the investigator is often forced into a compromise. In addition, the choice is made difficult because the slow-scan cameras are getting faster and the video-rate cameras are often cooled.

When time is the critical parameter, intensified cameras are often the only choice. If the event under investigation is rapid but can be precisely triggered, a slow-scan CCD operating in a burst or high-speed mode may be suitable. However, when the event is not readily predictable and the specimen must be monitored continuously at low incident light flux, the intensified CCD is the detector of choice. For this reason single molecule fluorescence studies have often employed intensified CCD cameras.

When time is available for image integration, a slow-scan CCD camera will usually outperform an intensified camera in all areas, in large part due to its higher quantum efficiency and lower noise. Cooling always improves camera performance although the difference may not be noticeable when the integration time is a few seconds or less and the digitization level is 10 to 12 bits or less. For applications involving digital deconvolution, the detector of choice is a cooled, scientific-grade, slow-scan camera capable of producing a high resolution, 14 to 16 bit image. However, some of the latest CCDs have such small pixels that the integration period must be limited to avoid saturation of the wells and, as a result, the dynamic range and peak S/N may be no better than those of an intensified CCD.

Two types of color CCD cameras are used for scientific applications: a single CCD with a wavelength selection filter or a three sensor (three chip) camera. Both use filters to produce red, green and blue versions of the field-of-view. The single sensor camera utilizes an adherent filter, filter wheel or liquid-crystal tunable filter to acquire the red, green, and blue images. When a tunable filter or filter wheel are used, three images must be obtained in sequence. The three sensor camera has a beam splitting prism and trim filters that enable each sensor to image the appropriate color and to acquire all three images simultaneously. Invariably, color cameras are less sensitive than their monochrome counterparts because of

the additional beam-splitting and wavelength selection components. In some applications, particularly immunofluorescence, the loss of sensitivity is offset by being able to capture multiple wavelengths simultaneously. In addition, some color cameras achieve a higher resolution by employing a piezo-controlled translocation mechanism to offset the CCD slightly, thereby increasing the sampling frequency.

Recent improvements in the performance of CMOS cameras herald a potentially important future role for these devices in fluorescence microscopy. CMOS cameras have an amplifier and digitizer associated with each photodiode in an integrated on-chip format. The individual amplifiers associated with each pixel help reduce noise and distortion levels, but they also induce an artifact known as "fixed pattern noise" that arises from switching and sampling artifacts of individual pixel amplifiers. This is manifested by reproducible patterns of "mottle" behavior in the image generated by CMOS active pixel sensor devices. A great deal of research effort has been invested in solving this problem, and the residual level of noise has recently been dramatically reduced in CMOS sensors. The result is a cheap, compact, versatile detector combining the virtues of silicon detection without the problems of charge transfer. CMOS sensors allow gain manipulation of individual photodiodes, region-of-interest read-out, high speed sampling, electronic shuttering and exposure control. They have extraordinary dynamic range as well as an ideal format for the computer interface. It is likely that they will replace CCD cameras in a number of scientific applications in the near future.

Chapter 26

Charge Coupled Devices

26.1 Anatomy of a Charge-Coupled Device

Charge-coupled devices (CCDs) are silicon-based integrated circuits consisting of a dense matrix of photodiodes that operate by converting light energy in the form of photons into an electronic charge. Electrons generated by the interaction of photons with silicon atoms are stored in a potential well and can subsequently be transferred across the chip through registers and output to an amplifier. The schematic diagram illustrated in Figure 26.1 shows various components that comprise the anatomy of a typical CCD.

CCDs were invented in the late 1960's by research scientists at Bell Laboratories, who initially conceived the idea as a new type of memory circuit for computers. Later studies indicated that the device, because of its ability to transfer charge and the photoelectric interaction with light, would also be useful for other applications such as signal processing and imaging. Early hopes of a new memory device have all but disappeared, but the CCD is emerging as one of the leading candidates for an all-purpose electronic imaging detector, capable of replacing film in the emerging field of digital photomicrography.

Fabricated on silicon wafers much like integrated circuits, CCDs are processed in a series of complex photolithographic steps that involve etching, ion implantation, thin film deposition, metallization, and passivation to define various functions within the device. The silicon substrate is electrically doped to form p-type silicon, a material in which the main carriers are positively charged electron holes. Multiple dies, each capable of yielding a working device, are fabricated on each wafer before being cut with a diamond saw, tested, and packaged into a ceramic or polymer casing with a glass or quartz window through which light can pass to illuminate the photodiode array on the CCD surface.

When a ultraviolet, visible, or infrared photon strikes a silicon atom resting in or near a CCD photodiode, it will usually produce a free electron and a "hole" created by the temporary absence of the electron in the silicon crystalline lattice. The free electron is then collected in a potential well (located deep within the silicon in an area known as the depletion layer), while the hole is forced away from the well and eventually is displaced into the silicon substrate. Individual photodiodes are isolated electrically from their neighbors by a channel stop, which is formed by diffusing boron ions through a mask into the p-type silicon substrate.

The principal architectural feature of a CCD is a vast array of serial shift registers constructed with a vertically stacked conductive layer of doped polysilicon separated from a silicon semiconductor substrate by an insulating thin film of silicon dioxide (see Figure 26.2).

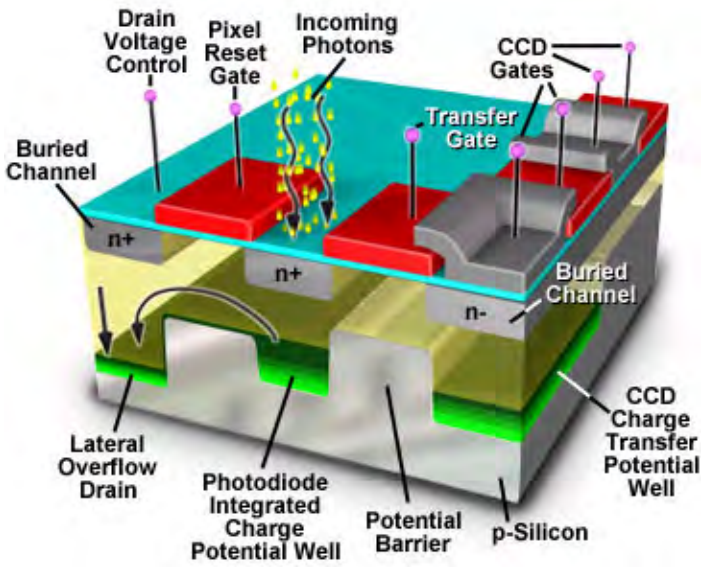

FIGURE 26.1: Anatomy of a CCD

After electrons have been collected within each photodiode of the array, a voltage potential is applied to the polysilicon electrode layers (termed gates) to change the electrostatic potential of the underlying silicon. The silicon substrate positioned directly beneath the gate electrode then becomes a potential well capable of collecting locally-generated electrons created by the incident light. Neighboring gates help to confine electrons within the potential well by forming zones of higher potentials, termed barriers, surrounding the well. By modulating the voltage applied to polysilicon gates, they can be biased to either form a potential well or a barrier to the integrated charge collected by the photodiode.

The most common CCD designs have a series of gate elements that subdivide each pixel into thirds by three potential wells oriented in a horizontal row. Each photodiode potential well is capable of holding a number of electrons that determines the upper limit of the dynamic range of the CCD. After being illuminated by incoming photons during a period termed integration, potential wells in the CCD photodiode array become filled with electrons produced in the depletion layer of the silicon substrate. Measurement of this stored charge is accomplished by a combination of serial and parallel transfers of the accumulated charge to a single output node at the edge of the chip. The speed of parallel charge transfer is usually sufficient to be accomplished during the period of charge integration for the next image.

After being collected in the potential wells, electrons are shifted in parallel, one row at a time, by a signal generated from the vertical shift register clock. The electrons are transferred across each photodiode in a multi-step process (ranging from two to four steps). This shift is accomplished by changing the potential of the holding well negative, while simultaneously increasing the bias of the next electrode to a positive value. The vertical shift register clock operates in cycles to change the voltages on alternate electrodes of the vertical gates in order to move the accumulated charge across the CCD. Figure 26.1 illustrates a photodiode potential well adjacent to a transfer gate positioned within a row of CCD gates.

After traversing the array of parallel shift register gates, the charge eventually reaches

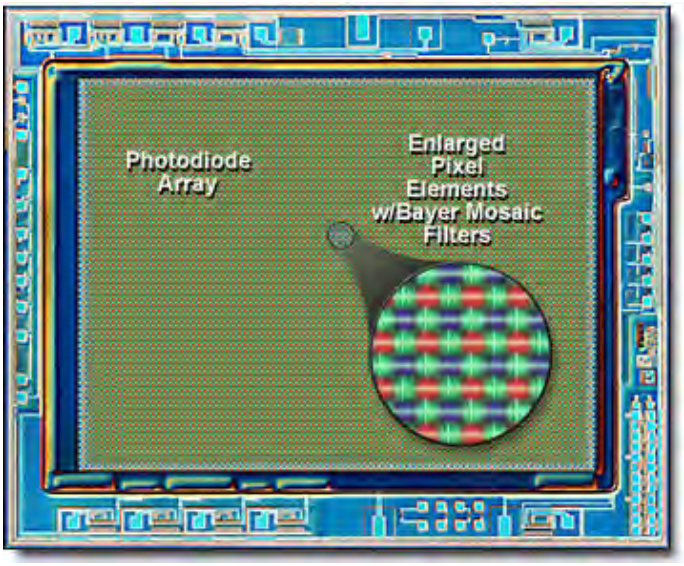

FIGURE 26.2: CCD photodiode array integrated circuit

a specialized row of gates known as the serial shift register. Here, the packets of electrons representing each pixel are shifted horizontally in sequence, under the control of a horizontal shift register clock, toward an output amplifier and off the chip. The entire contents of the horizontal shift register are transferred to the output node prior to being loaded with the next row of charge packets from the parallel register. In the output amplifier, electron packets register the amount of charge produced by successive photodiodes from left to right in a single row starting with the first row and proceeding to the last. This produces an analog raster scan of the photo-generated charge from the entire two-dimensional array of photodiode sensor elements.

26.2 Pixel Binning

Pixel binning is a clocking scheme used to combine the charge collected by several adjacent CCD pixels, and is designed to reduce noise and improve the signal-to-noise ratio and frame rate of digital cameras. The binning process is performed by on-chip CCD clock timing circuitry that assumes control of the serial and parallel shift registers prior to amplification of the CCD analog signal.

To help illustrate the pixel binning process, refer to Figure 26.3, which reviews an example of 2x2 binning. A schematic drawing of a 4x4 parallel shift register pixel array is illustrated in Figure 26.3(a), along with a four-gate serial shift register and summing pixel or well (also termed an output node). Illuminating photons impact the CCD photodiodes, creating a pool of electrons that accumulates in each pixel, shown in Figure 26.3(b) as a cluster of four blue-shaded squares in the upper right hand corner of the parallel shift register. The number of electrons that each pixel can accommodate is termed the well depth and ranges from about 30,000 to 350,000, depending upon the CCD specifications. Dynamic range of a CCD is directly proportional to the well depth. Incident light levels and exposure time determine the number of electrons collected at each photogate or pixel site. After exposure of the CCD to one illumination cycle is completed, the electrons are

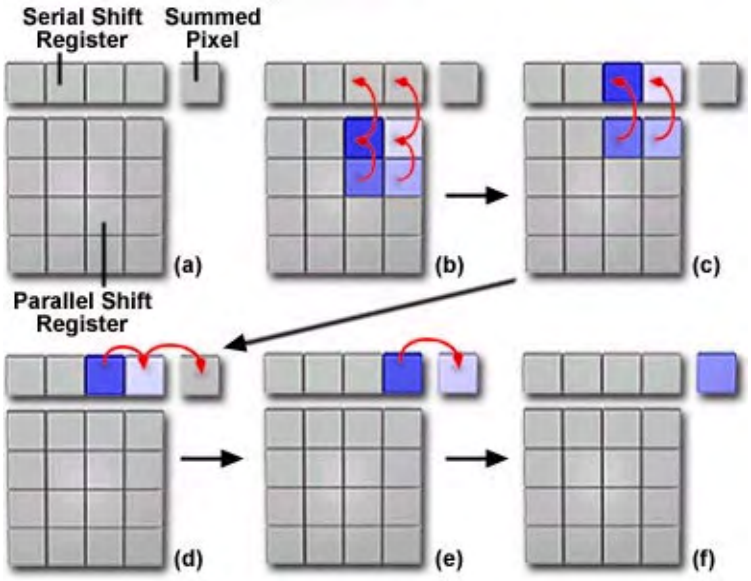

FIGURE 26.3: Pixel binning

transferred through the parallel and serial shift registers to a output amplifier and then digitized by an analog-to-digital (A/D) converter circuit. Binning can be used to increase focusing accuracy by reducing the time necessary for image acquisition, while providing greater sensitivity to lower out-of-focus light levels.

To illustrate this process, Figure 26.3(b) shows each integrated pixel in the parallel register stepping by an increment of one gate to yield the arrangement shown in Figure 26.3(c). Here, the electrons from two pixels remain in the parallel shift register, while those from the other two have been transferred to the serial shift register. Another step (Figure 26.3(c)), shifts the remaining electrons in the parallel shift register to fill the adjacent gate elements in the serial register (Figure 26.3(d)). The final steps involve shifting of charge from the serial register, two pixels at a time, to the summing pixel (Figure 26.3(d) and 26.3(e)). Figure 26.3(f) illustrates the combined charge of four pixels in the summing well awaiting transfer to the output amplifier, where the signal will be converted to a voltage and then transferred to other integrated circuits for further amplification and digitization. The process continues until the entire array has been read out. In this example, the area of four adjacent pixels has been combined into one larger pixel, sometimes referred to as a super pixel. The signal-to-noise ratio has been increased by a factor of four, but the image resolution is cut by 50 percent.

Binning array sizes are controlled by the CCD clock, bias voltages, and video processing signal timing, and are usually adjustable from 2 x 2 pixels to a maximum that can include almost the entire CCD array. However, in the binning mode, both the serial shift register and output node will accumulate a significantly larger charge than in normal operation and must contain sufficient electron charge capacity to prevent saturation. Typical CCD serial registers have twice the charge capacity as the parallel registers, and the output nodes usually contain 50- to 100-percent more charge capacity than do the shift registers. As an example, the Kodak KAF full-frame CCD image sensors have a parallel array of 9-micron pixels, each with a capacity of 120,000 electrons. The KAF serial registers have an electron capacity twice that of the parallel registers (240,000 electrons), while the output node has

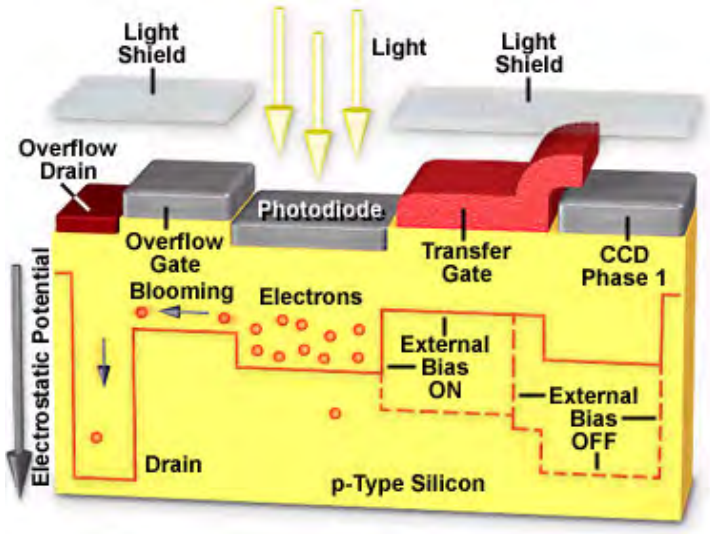

FIGURE 26.4: Lateral overflow drain to prevent blooming

a capacity of 330,000 electrons.

The primary benefit of pixel binning is to improve the signal-to-noise ratio in low light conditions at the expense of spatial resolution. Summation of many charge packets reduces the read noise level and produces an improvement in signal equal to the binning factor (4x in the example above). Dark current noise is not reduced by binning and may only be overcome by cooling the CCD to low temperatures. Binning is useful in a variety of applications, especially where fast throughput times (frame rates) are desired at the expense of resolution.

26.3 CCD Blooming

Under conditions where a CCD is exposed to very high intensity illumination, it is possible to exhaust the storage capacity of the CCD wells, a condition known as blooming. When this occurs, excess charge will overflow into adjacent CCD photodiode wells resulting in a corrupted image near the blooming site.

The size of a pixel charge accumulation well is determined by the photodiode area, which is filled with electrons in a linear relationship dependent on the amount of light incident upon the photodiode. As the pixel well nears the saturation limit (becomes filled with electronic charge), this linear relationship fails and the pixel's response to additional illumination decreases, causing degradation of the signal. The point at which the photometric response to illumination deviates from linearity is termed a linear full well, and is usually the size of the signal necessary to satisfy the dynamic range of the analog-to-digital converter. Prior to saturation, random noise (determined by the square root of the signal) is reduced by a condition known as noise clipping.

When saturated, additional charge generated by light on the photodiode spills over to adjacent pixel wells, which will also become saturated and report erroneously high illumination levels. Because pixel wells can integrate more charge than they can effectively transfer, saturation occurs when the maximum well-transfer capacity is reached. Under conditions where the entire photodiode array is saturated, or during periods of extensive

serial and parallel shift register binning, the output node may also become saturated and cause the output sequence to collapse, resulting in total signal loss. Blooming is manifested by white streaks that totally wash out any details of the image.

In many cases, blooming can be minimized by decreasing charge integration time, but this remedy is not always successful so additional mechanisms to drain excess charge have been developed. Clocking schemes have also been devised to control pixel blooming during integration. The most common clocking approach involves alternate switching of clock-voltage phases to force excess charge into the barrier region nested between the CCD silicon substrate and oxide layer, where it is recombined with electron "holes" in the crystalline silicon lattice. Clock voltage switching selectively bleeds off excess charge without compromising image information in pixels that are not yet saturated. This technique has been termed clocked anti-blooming, and is useful in low-light level scientific applications, such as fluorescence microscopy, but suffers from reduced efficiency at high frame rates.

A more common anti-blooming technique involves "overflow" drain structures that are incorporated into the CCD during fabrication. Two of the most common drain structures are the vertical overflow drain (VOD) and the lateral overflow drain (LOD). Drains enable integration time to be controlled independently of charge readout, which allows them to serve as an electronic exposure or shutter mechanism to limit pixel saturation and provide a more reliable shuttering method than is currently possible with mechanical devices.

During CCD fabrication, a new gate is established adjacent to the photodiode called the pixel reset gate or the overflow gate (see Figure 26.4). This gate allows excess charge to be shunted from the photodiode to a common drain without affecting the CCD signal. Figure 26.4 illustrates a typical lateral overflow drain structure that manufacturers incorporate into high-performance CCD architectures. Excess charge collected by the photodiode is allowed to spill (via the overflow gate) into the drain, which is a reversed-biased diode that removes the charge to ground. Many CCD designs incorporate lateral drains that run the length of the parallel shift register and are shared by all pixel gates. In contrast, vertical overflow drains are positioned in the charge accumulation site and have an electrostatic potential barrier that is limited to allow excess charge to overflow directly into the silicon substrate. The primary drawback of the lateral overflow gate is a reduced quantum efficiency manifested in a reduced charge handling capacity, which leads to a less sensitive photo response.

26.4 Dynamic Range

The dynamic range of a CCD is typically specified as the maximum achievable signal divided by the camera noise, where the signal strength is determined by the full-well capacity and noise is the sum of dark and read noises. As the dynamic range of a device is increased, the ability to quantitatively detect differences between the dimmest and brightest intensities in an image (intrascene performance) is improved. The interscene dynamic range represents the spectrum of intensities that can be accommodated when detector gain, integration time, lens aperture, and other variables are adjusted for differing fields of view.

Photodiode size determines, in part, the size of the depletion wells–larger diodes having greater full-well capacity compared to camera noise. Typical diode sizes in modern CCDs utilized in photomicrography range from 4.5 to 24 microns with corresponding well capacities of 20,000 to 600,000 electrons. Read noise is a combination of all noise generated during readout of the device. This includes noise from input clocking and fixed pattern,

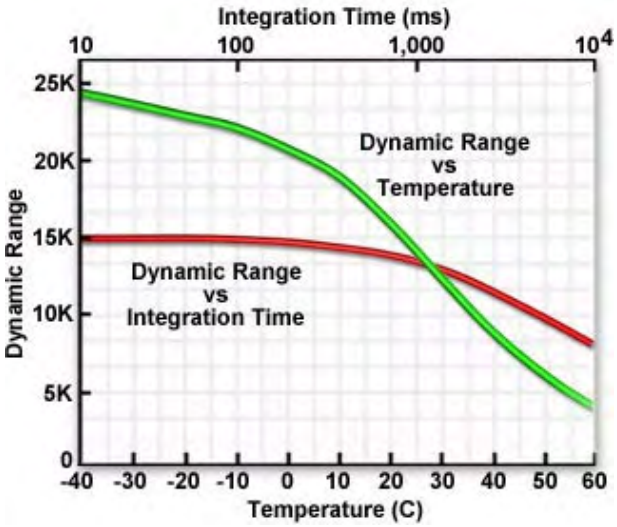

FIGURE 26.5: Variables affecting dynamic ranges

along with reset transistor noise and amplifier output noise. Read noise is usually specified in the performance data sheets that accompany a CCD sensor, with typical values ranging from 10–20 electrons/pixel in high quality chips operated at room temperature, and dropping to 2–5 electrons/pixel in Peltier-cooled CCDs for scientific imaging applications. The dynamic range is expressed in decibel units according to the following equation:

$$\text{Dynamic Range} = 20 \cdot \log \frac{N_{\text{sat}}}{N_{\text{noise}}}$$

where N_{sat} is the linear full well capacity stated in the number of electrons and N_{noise} is the total value of the read and dark noise, also expressed as the number of electrons. In a high-performance cooled CCD camera, the well capacity is proportional to the size of the individual photodiode, such that the maximum number of electrons stored is about 1000 times the cross sectional area of each photodiode. Thus, a CCD with 6.7x6.7 micron photodiodes should have a maximum charge storage capacity (a full-well capacity) of about 44,900 electrons (or holes). At a typical readout rate of 1 MHz, the read noise for this CCD is about 10 electrons/pixel, which yields a dynamic range of 44,900/10 or 4,490. In order to utilize the full range of grayscale levels available with this dynamic range, the camera should have a 12-bit analog-to-digital (A/D) converter capable of resolving 4096 gray levels. Controlling the size of the read and dark noise is a critical factor in maintaining a high dynamic range in these devices.

Higher performance cooled CCD sensors designed with low noise output amplifiers and suitable for use in slow-scan imaging of photomicrographs often have lower read noise and an extended dynamic range. As an example, the Marconi Applied Technologies CCD39-01 sensor is a back-illuminated, frame-transfer CCD having a square pixel size of 24 microns with a split output register allowing the utilization of quad output amplifiers. The full well capacity of this device can reach a level 300,000 electrons. Coupled with a readout noise root-mean-square (rms) level of three electrons at 20 kilohertz (when cooled), the CCD39-01 is capable of yielding a dynamic range of approximately 100,000:1. To fully utilize the potential of this CCD, a 17-bit A/D converter having 131,072 grayscale levels

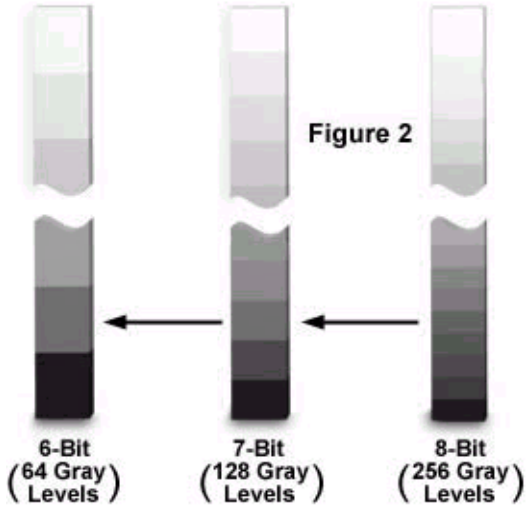

FIGURE 26.6: Bit depth in binary images

should be employed (although a 16-bit A/D converter having 65,536 grayscale levels would also suffice).

The dynamic range of a particular CCD is dependent upon several variables. Dark current is strongly influenced by temperature (Figure 26.5), doubling every 8 to 10 degrees Centigrade. At higher temperatures, dark current is dominant, while at lower temperatures, dynamic range is determined by the noise of the output amplifier. The amount of dark charge collected in each pixel is dependent not only on the device temperature, but also on the integration time and the storage time before readout. The noise level is also proportional to the bandwidth of the read-out amplifier, which is influenced by pixel transfer rate and is thus affected by the clock frequency. As the clocking frequency is increased, the number of dark current and shot noise electrons is correspondingly decreased and less bandwidth is required by the output amplifier and video-processing electronics. Integration time also affects the dynamic range of a CCD, as illustrated in Figure 26.5. An increase in the total integration time produces an increase in dark current and a subsequent decrease in dynamic range, but this effect only comes into play at integration times exceeding 5 minutes.

Bit depth refers to the binary range of possible grayscale values utilized by the A/D converter to translate analog image information into discrete digital values capable of being read and analyzed by a computer. For example, the most popular 8-bit A/D converters have a binary range of 28 or 256 possible values (Figure 26.6), while a 12-bit converter has a range of 212 (4,096 values), and a 16-bit converter has 216, or 65,536 possible values. The bit depth of the A/D converter determines the size of the gray scale increments, with higher bit depths corresponding to a greater range of useful image information available from the camera. Better results are obtained when the signal is sampled at a level that is well beneath the limit suggested by the readout noise. For instance, if the Marconi CCD39-01 is used with signal averaging, an 18-bit (262,144 grayscale levels) A/D converter might be used to sample data at 1 part in 262,144. However, the noise level statistics for this device indicate that image data cannot be accurately measured to greater than 1 part in 100,000 without signal averaging. Clearly, a 16-, 17-, or 18-bit A/D converter will produce better results when coupled to the Marconi CCD39-01 chip. In contrast, Fujichrome Velvia, a

TABLE 26.1: Dynamic Range of Charge-Coupled Devices

Bit Depth	Grayscale Levels	Dynamic Range (Db)
1	2	6 dB
2	4	12 dB
3	8	18 dB
4	16	24 dB
5	32	30 dB
6	64	36 dB
7	128	42 dB
8	256	48 dB
9	512	54 dB
10	1,024	60 dB
11	2,048	66 dB
12	4,096	72 dB
13	8,192	78 dB
14	16,384	84 dB
16	65,536	96 dB
18	262,144	108 dB
20	1,048,576	120 dB

fine-grained color transparency film, has been demonstrated to produce less than 10-stops (1024 grayscale levels) of dynamic range.

Table 1 presents the relationship between the number of bits used to store digital information, the numerical equivalent in grayscale levels, and the corresponding value in decibels (one bit equals approximately 6 dB). As illustrated in the table, if a 0.72 volt video signal were digitized by an A/D converter with 1-bit accuracy, the signal would be represented by two values, binary 0 or 1 with voltage values of 0 and 0.72 volts. Most digitizers found in digital cameras used in photomicrography employ 8 bit A/D converters, which have 256 discrete grayscale levels (between 0 and 255), to represent the voltage amplitudes. A maximum signal of 0.72 volts would then be subdivided into 256 steps, each step having a value of 2.9 millivolts.

The number of grayscale levels that must be generated in order to achieve acceptable visual quality should be enough that the steps between individual gray values are not discernible to the human eye. The "just noticeable difference" in intensity of a gray-level image for the average human eye is about two percent under ideal viewing conditions. At most, the eye can distinguish about 50 discrete shades of gray within the intensity range of a video monitor, suggesting that the minimum dynamic range of an image should lie between 6 and 7 bits (64 and 128 grayscale levels; Figure 26.6).

Digital images should have at least 8-bit resolution to avoid producing visually obvious gray-level steps in the enhanced image when contrast is increased during image processing. The effect of reducing the number of grayscale levels on the appearance of photomicrographs can be seen in Figure 26.7, which shows a black & white (originally 8-bit) image of stained thin section of Solanum tuberosum (potato) that is displayed at different resolutions ranging from 6-bit (Figure 26.7(a)), down to 5-bit (Figure 26.7(b)), 4-bit (Figure 26.7(c)), and 3-bit (Figure 26.7(d)).

Improved digital cameras with CCDs capable of 12-bit resolution allow investigators to

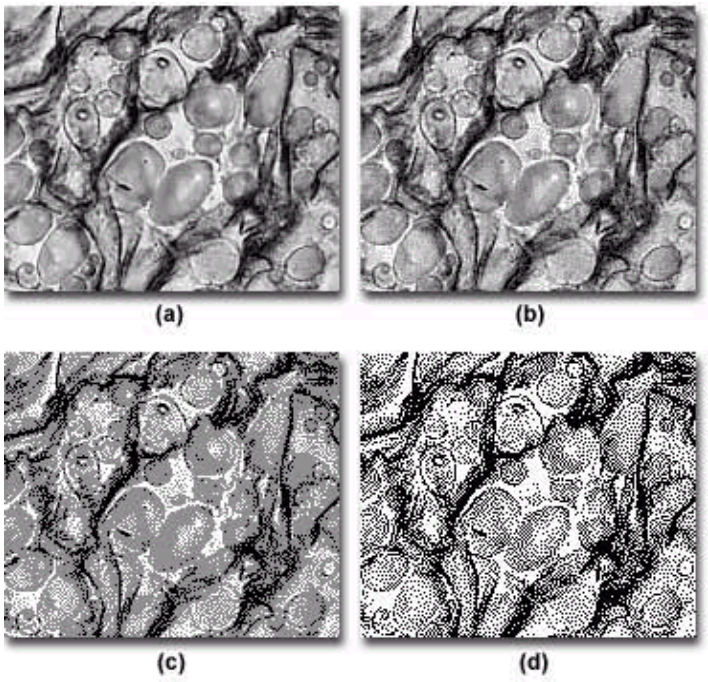

FIGURE 26.7: Grayscale resolution and image appearance

display images with a greater latitude than is possible with 8-bit images. This is possible because the appropriate software can render the necessary shades of gray from a larger palette (4,096 grayscale levels) for display on computer monitors, which typically present images in 256 shades of gray. In contrast, an 8-bit digital image is restricted to a palette of 256 grayscale levels that were originally captured by the digital camera. As the magnification is increased during image processing, the software can choose the most accurate grayscales to reproduce portions of the enlarged image without changing the original data. This is especially important when examining shadowed areas where the depth of the 12-bit digital image allows the investigator to visualize subtle details that would not be present in an 8-bit image.

The accuracy required for digital conversion of analog video signals is dependent upon the difference between a digital gray-level step and the rms noise in the camera output. CCD cameras with an internal A/D converter produce a digital data stream that does not need to be resampled and digitized in the computer. These cameras are capable of producing digital data with up to 18-bit resolution (262,144 grayscales) in high-end models, and are not constrained to the 0.72-volt signal limitation of RS-170 video systems and utilize a wider analog voltage range in their A/D converters. The major advantage of the large digital range exhibited by CCD cameras lies in the signal-to-noise improvements in the displayed 8-bit image and in the wide linear dynamic range over which signals can be digitized.

26.5 Electron–Bombarded Charge–Coupled Devices

The electron-bombarded charge-coupled device (EBCCD) is a hybrid of the image intensifier and the CCD camera, which has just been recently introduced. In this device, photons are detected by a photocathode similar to that in an image intensifier. The released elec-

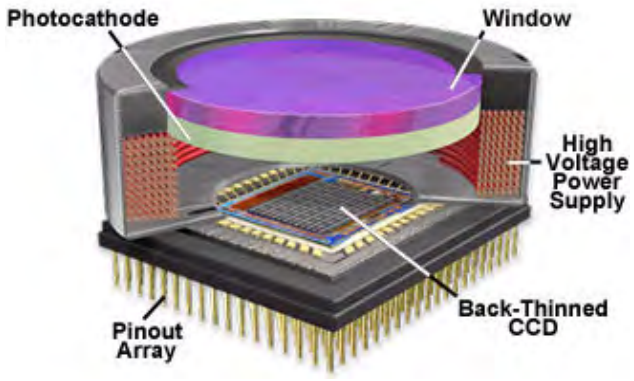

FIGURE 26.8: Electron bombarded back-thinned CCD

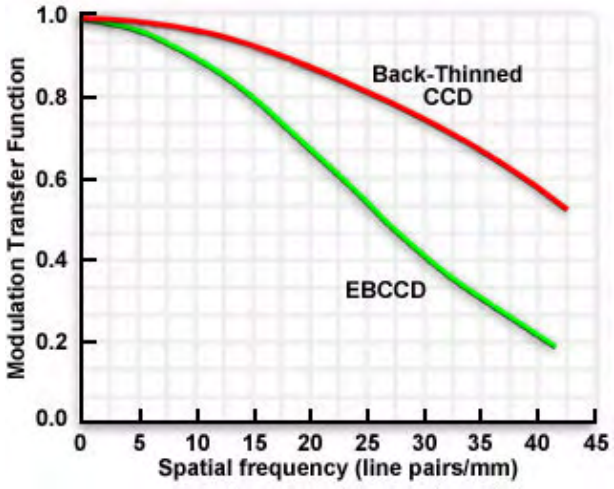

FIGURE 26.9: Modulation transfer function of EBCCDs

trons are accelerated across a gap and impact on the back side of a back-thinned CCD.

These energetic electrons generate multiple charges in the CCD resulting in a modest gain of a few hundred. Figure 26.8 illustates the design of an electron-bombarded CCD in which photoelectrons, accelerated by a high voltage gradient (1.5—2.0 kilovolts), impact directly onto a back-thinned CCD operating at video rate.

The advantages of this device over a cooled, slow-scan CCD are the additional gain and accompanying speed. EBCCDs also demonstrate no significant geometrical distortion or shading, relatively low noise (40 electrons/pixel) because of design improvements in CCD read-out, on-chip integration capability, and the option for a variety of read-out rates and fomats such as binning and subsampling. The main disadvantages are the lower quantum efficiency of the photocathode (30 percent) compared to that of an unmodified back-thinned CCD (80 to 90 percent) and a significant degradation in the modulation transfer function compared to that of the back-thinned CCD alone (see Figure 26.9).

Limitation of the dynamic range of the EBCCD is also a consequence of the increased gain. This occurs because each photoelectron generates approximately 300 electron/hole pairs causing the wells fill 300 times faster than in an ordinary CCD. The result is that

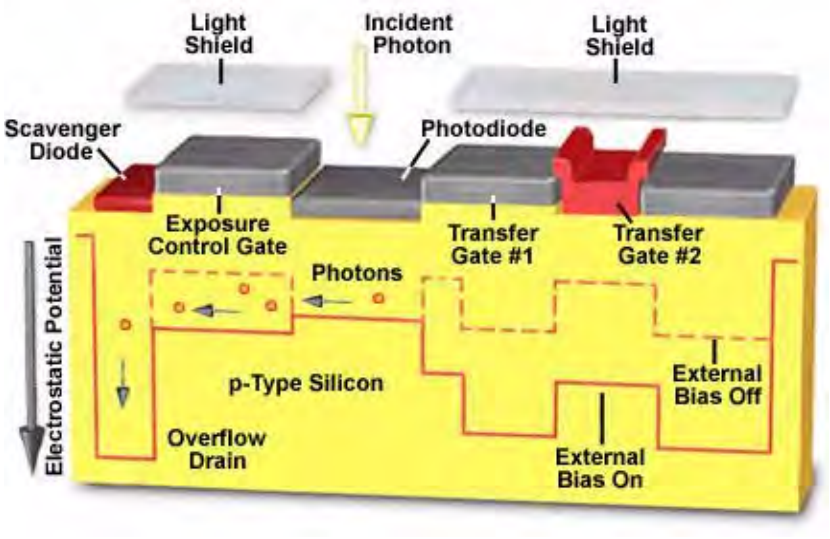

FIGURE 26.10: CCD electronic shutters

a CCD having a full-well capacity of 150,000 electrons is completely filled by only 500 photons.

Compared to an intensified CCD, the electron-bombarded CCD usually has higher spatial resolution and a better signal-to-noise ratio at moderate light levels, but the limited gain adjustment range and modest low-light-level detection capability make the EBCCD the solid-state equivalent of the outmoded silicon intensifier target (SIT) camera.

26.6 Electronic Shutters

Electronic shutters are employed in charge-coupled devices (CCDs) to control integration time (exposure) of the photodiode array and reduce blooming, overexposure, and smear when capturing moving objects using time-lapse or full motion video in the microscope.

Presented in Figure 26.10 is a diagrammatic illustration of a CCD pixel that is equipped with an electronic shutter exposure control gate. The shutter is used to vary the integration time by draining all charge from a photodiode potential well for a fraction of the total integration time. Electronic shutters usually operate in stepped increments, decreasing the collected illumination (exposure time) by 50 percent for each step.

Integration of electrons in the photodiode potential well is controlled by the exposure control gate, which will shunt electrons to the scavenger diode when biased to the "on" state by the CCD clock circuitry. In some CCD configurations, the electronic shutter can be used to balance the color response of the red, green, and blue channels.

Shutters allow all light sensitive photodiodes to be simultaneously erased without affecting darkened shift registers, thus controlling the time period between flushing the photodiodes and the start of the readout process. The exposure rate of an electronic shutter can vary between 1/60th and 1/16,000 second, depending upon CCD architecture.

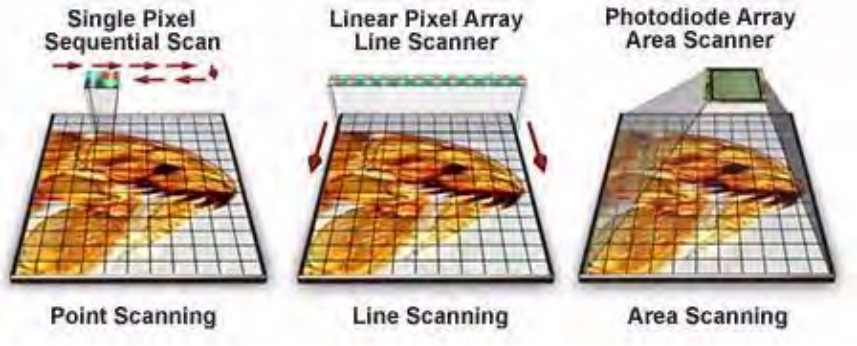

FIGURE 26.11: CCD scanning formats

26.7 CCD Scanning Formats

Charge-coupled device (CCD) digital imaging sensors are capable of acquiring images in one of three formats: point scanning, line scanning, and area scanning. Each of these formats has specific applications in digital photography and scanning of documents and images.

The simplest digital scanning technique utilizes a single pixel-cell detector to scan an image sequentially throughout a series of X and Y coordinates. CCD detectors of this type are relatively inexpensive and provide a uniform measurement from one scan site to another. The major disadvantage of this type of system is the repeated number of digital exposures necessary to compose an entire image and the mechanical complexity of the camera X-Y translation mechanism. Registration errors can also degrade images produced in this manner, although complex algorithms can often be employed to overcome this handicap.

A linear array of single-cell CCD detectors can be used to linearly scan along a single axis to produce a digital image, dramatically improving performance over that of the sequential scan format. Scanning takes place in a single direction where each line of information is captured, stored, and amplified before stepping to the next. This type of mechanism is commonly used in desktop flatbed scanners. In systems with colored filters placed over the photodiode elements, an image can be captured in a single pass, eliminating registration problems caused by three-pass systems. The size of the CCD scanning element is limited by a number of factors including wafer size, fabrication complexity, and mechanical restrictions on the stepper mechanism. In many cases, several linear CCD elements are positioned in series to increase the overall length of the scanning detector.

Linear CCD scanners (Figure 26.11) provide a higher rate of image acquisition when compared to single cell detectors, and they are also capable of producing high resolution images with less sophisticated scanning mechanics. Image resolution is restricted by pixel spacing and size, and scan times are usually on the order of seconds to minutes, making these devices largely unsuitable for camera applications.

The most sophisticated digital scanning technique (area scanning; see Figure 26.11) uses two-dimensional pixel array detectors, which allow an entire image to be captured with a single exposure. This method eliminates movement of the image sensor and the need for costly mechanical translation devices. Area scanners provide the fastest image acquisition frame rates with a high degree of registration accuracy between pixels, making them the ideal detection devices for digital cameras. Drawbacks include a limitation of resolution and a lower signal-to-noise performance when compared to the devices described above.

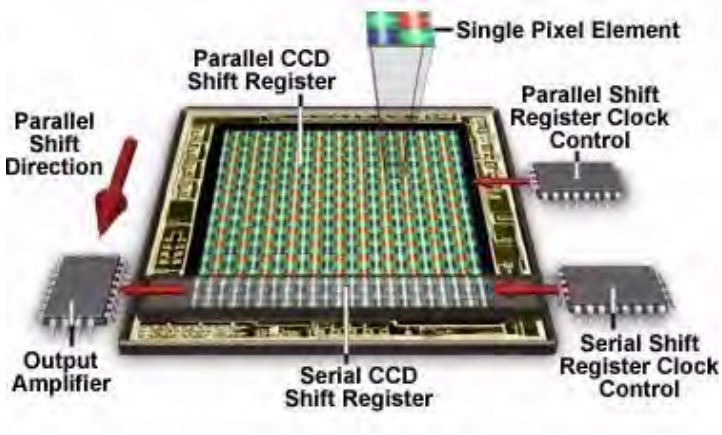

FIGURE 26.12: Full-frame CCD architecture

Device cost is generally higher because of lower yields from the semiconductor fabrication techniques used to produce such complex chips.

26.8 Full-Frame CCD Architecture

Full-frame charge-coupled devices (CCDs) feature high-density pixel arrays capable of producing digital images with the highest resolution currently available. This popular CCD architecture has been widely adopted due to the simple design, reliability, and ease of fabrication.

The pixel array illustrated in the full-frame CCD drawing presented in Figure 26.12 consists of a parallel shift register, onto which images are optically projected by means of a camera lens or microscope optical train. In this configuration, all of the photodiodes in the pixel array collectively act as the image plane and are available for detecting photons during the exposure period. A miniature portion of the total image is contained in each pixel element, which consists of four photodiodes masked with red, green, and blue colored filters. The image presented in the upper portion of Figure 26.12 is an actual high-magnification photomicrograph of a single pixel element.

After photons composing the image have been collected by the pixel elements and converted into electrical potential, the CCD undergoes readout by shifting rows of image information in a parallel fashion, one row at a time, to the serial shift register (illustrated as a series of gray-scale elements at the bottom of the pixel array). The serial register then sequentially shifts each row of image information to an output amplifier as a serial data stream. All integrated charge must be clocked out of the serial register before the next parallel line of image data can be transferred to the horizontal array. The entire process is repeated until all rows of image data have been directed to the output amplifier and off the chip to a analog-to-digital signal converter integrated circuit. Reconstruction of the image in a digital format yields the final photograph or photomicrograph.

Full-frame CCD architecture has what is termed a 100 percent fill factor, meaning that the entire pixel array is used to detect incoming photons during exposure to the object being imaged. Full-frame pixel array sizes are often based upon powers of 2 (512x512, 768x768, or 1024x1024 pixels) to simplify memory mapping of the array and image processing algorithms. CCDs of this type typically have square pixel dimensions to avoid image distortion

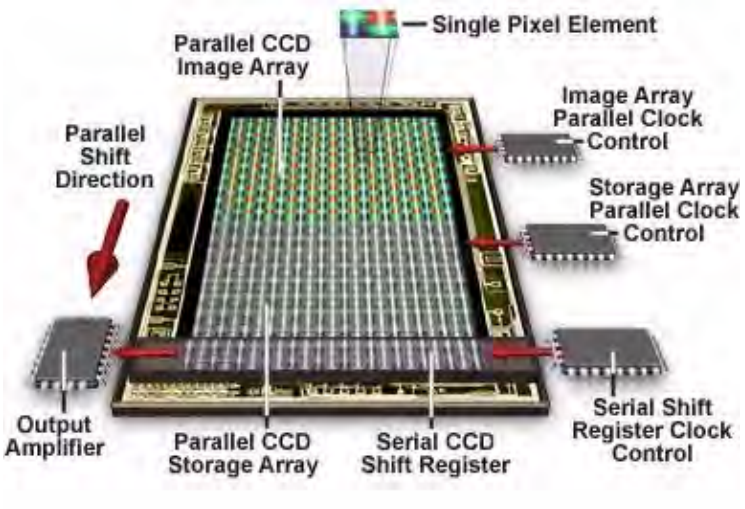

FIGURE 26.13: Frame-transfer CCD architecture

and are fabricated with pixel sizes ranging from 7 to 24 microns in arrays containing up to 6 million pixels. Due to the fact that the pixel array is used for both image detection and readout, a mechanical shutter or synchronized strobe illumination scheme must be used to prevent smearing for most exposure periods. Smear occurs when the photodiodes are continuously illuminated during parallel register readout, and will be oriented in the direction of charge transport through the parallel array. In Fluroescence microscopy, where image integration time greatly exceeds the register readout rate, smear may become insignificant.

Image data transfer rates are limited by the output amplifier bandwidth and the conversion speed of the analog-to-digital converter. Readout rates can be dramatically increased by subdividing the pixel array into smaller, but identical sub-arrays, which can then be read simultaneously. Image reconstruction is then performed by an external video processor circuit that collects, decodes, and reformats the original image.

Both frontside and backside illumination schemes have been successfully utilized with full-frame CCD architecture, although devices illuminated from the back typically provide a higher quantum transfer yield. Incoming photons are converted to electrical charge (integrated) with greater efficiency because light enters the CCD silicon substrate from the rear, circumventing the necessity to pass through semiconductor gate areas that blanket the light-sensitive photodiodes. Recently, new CCD technologies have been introduced that apply materials such as indium tin oxide to gate fabrication in an effort to render the gates more sensitive to light, helping to raise the quantum efficiency and eliminating the need for backside illumination.

26.9 Frame-Transfer CCD Architecture

Frame-Transfer charged coupled image sensors have an architecture similar to that of full-frame CCDs. These devices have a parallel shift register that is divided into two separate and almost identical areas, termed the Image and Storage arrays.

The image array consists of a light-sensitive photodiode register, which acts as the image plane and collects incoming photons projected onto the CCD surface by the camera or microscope lenses. After image data has been collected and converted into electrical

potential by the image array, the data is then quickly shifted in a parallel transfer to the storage array for readout by the serial shift register. Transfer time from the image-integrating array to the shielded storage array is dependent upon the pixel array sizes, but is typically on the order of 500 microseconds or less. The storage array is not light sensitive in most frame-transfer CCD designs, however some arrays are not equipped with an integral light shield. Arrays of the this design are capable of being operated in either full-frame or frame-transfer modes. With the use of a mechanical shutter, a frame-transfer CCD can be used to quickly capture two sequential images, a useful feature in fluorescence microscopy and other applications that require simultaneous acquisition of images generated at different emission and/or excitation wavelengths.

As presented in Figure 26.13, the storage array is illustrated as a large area of gray-scale "pixels" that have been covered with an opaque metal mask or light shield to prevent any potential interaction with incoming photons. A miniature portion of the total image is contained in each pixel element, which consists of four photodiodes masked with red, green, and blue colored filters. The image presented in the upper right-hand corner of Figure 26.13 is an actual high-magnification photomicrograph of a single pixel element. Like the full-frame architecture, the frame-transfer CCD undergoes readout by shifting rows of image information in a parallel fashion, one row at a time, to the serial shift register. The serial register then sequentially shifts each row of image information to an output amplifier as a serial data stream. The entire process is repeated until all rows of image data are transferred off the chip, first to a signal output amplifier and then to an analog-to-digital signal converter integrated circuit. Reconstruction of the image in a digital format yields the final photograph or photomicrograph.

During the period in which the parallel storage array is being read, the image array is busy integrating charge for the next image frame. A major advantage of this architecture is the ability of the frame-transfer device to operate without a shutter or synchronized strobe, allowing for an increase in device speed and faster frame rates. Frame-transfer CCDs suffer from several drawbacks including image "smear", which occurs because integration and dump to the storage array occur simultaneously. Smear artifacts are limited to the time necessary for transfer of image integration data to the storage array. Frame-transfer devices are also more costly to produce because twice the silicon area is required to implement the architecture, resulting in lower image resolution and higher cost.

26.10 Interline Transfer CCD Architecture

Interline charge-coupled device architecture is designed to compensate for many of the shortcomings of frame-transfer CCDs. These devices are composed of a hybrid structure incorporating a separate photodiode and an associated parallel readout CCD storage region into each pixel element. The functions of these two regions are isolated by a metallic mask structure placed over the light shielded parallel readout CCD elements.

Masked regions of the pixels are positioned alongside the photodiode elements in an alternating parallel array traversing the length of the CCD's vertical axis. Photodiodes in the array comprise the image plane and collect incoming photons projected onto the CCD surface by the camera or microscope lenses. After image data has been collected and converted into electrical potential by the image array, the data is then quickly shifted in a parallel transfer to the adjacent CCD storage area of each pixel element. The storage portion of the pixel element is illustrated as a cluster of gray-scale elements covered with an

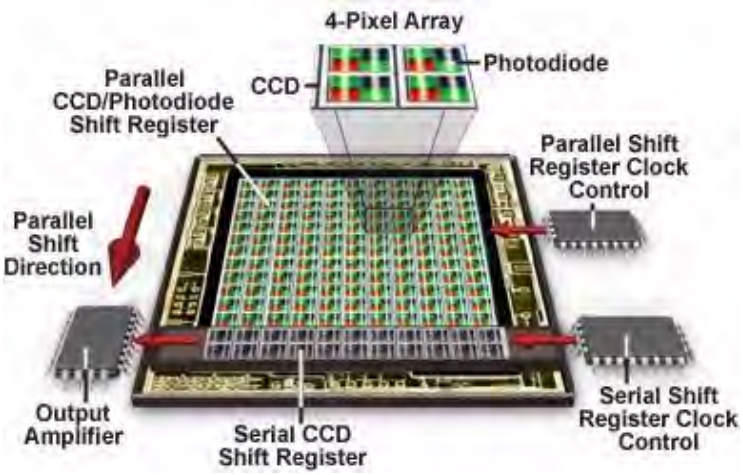

FIGURE 26.14: Interline transfer CCD architecture

opaque mask adjacent to the red, green, and blue photodiode elements in each CCD. These pixel elements combine to form vertical columns that run from the serial shift register to the top of the array grid. An enlarged view of a four-pixel array containing both photodiode and CCD elements appears in the upper portion of Figure 26.14.

Like the full-frame and frame-transfer architectures, interline transfer CCDs undergo readout by shifting rows of image information in a parallel fashion, one row at a time, to the serial shift register. The serial register then sequentially shifts each row of image information to an output amplifier as a serial data stream. The entire process is repeated until all rows of image data are transferred to the output amplifier and off the chip to a analog-to-digital signal converter integrated circuit. Reconstruction of the image in a digital format yields the final photograph or photomicrograph.

During the period in which the parallel storage array is being read, the image array is busy integrating charge for the next image frame, similar to the operation of the frame-transfer CCD. A major advantage of this architecture is the ability of the interline transfer device to operate without a shutter or synchronized strobe, allowing for an increase in device speed and faster frame rates. Image "smear", a common problem with frame-transfer CCDs, is also reduced with interline CCD architecture because of the rapid speed (only one or a few microseconds) in which image transfer occurs. Drawbacks include a higher unit cost to produce chips with the more complex architecture, and a lower sensitivity due to a decrease in photosensitive area present at each pixel site. This shortcoming can be partially overcome by incorporation of microlenses (or lenslets) on the photodiode array complex to increase the amount of light entering each element. Interline devices with microlens enhancement typically increase the optical fill factor from approximately 20-25 percent to over 75 percent, dramatically improving the net quantum efficiency of the device in the visible light wavelength region.

Interline transfer CCDs experience sampling errors that are increased due to the reduced aperture size. In addition, a portion of the incident light can leak into CCD vertical registers, especially in brightfield applications where microscope lamp intensity is undiminished by the specimen. Some interline CCD designs experience image "lag" as a result of charge transfer time constant delays associated with transfer of charge from photodiodes to the CCD storage areas. This transfer delay results in a residual charge being left in the

photodiodes that is added to the next frame, resulting in an "after-image" artifact. Newer hole-accumulation charge-coupled devices are capable of complete transfer, thus eliminating image lag.

Chapter 27

Microlens Arrays

Microlens arrays (also referred to as microlenticular arrays or lenslet arrays) are used to increase the optical fill factor in CCDs, such as interline-transfer devices, that suffer from reduced aperture due to metal shielding. These tiny lens systems serve to focus and concentrate light onto the photodiode surface instead of allowing it to fall on non-photosensitive areas of the device, where it is lost from the imaging information collected by the CCD.

A typical lenslet placement scheme is illustrated in Figure 27.1, where a tiny optical lens is strategically placed over the dye layer and metal light shield of a photodiode. The lenslets are either grown in parallel arrays during the CCD fabrication process or manufactured out of a material such as quartz and placed on the array surface during packaging. Each lenslet is a high quality optical surface containing refractive elements ranging in size from several hundred to around 10 microns in diameter, depending upon the application. Lens quality is so good that microlenses are physically equivalent to an ordinary single-element lens.

Addition of microlens arrays to CCD photodiodes can increase the optical fill factor by up to three times that realized without the tiny optical components. Increasing the fill factor yields a corresponding increase in the sensitivity of the photosite. Microlens arrays provide a substantial increase in performance of interline-transfer CCD imaging arrays that have lateral overflow drains and a sizeable amount of shielded pixel space. These devices typically suffer from reduced optical fill factors because of reduced active pixel area compared to total pixel size.

Illustrated in Figure 27.2 is a schematic diagram of an interline-transfer CCD pixel

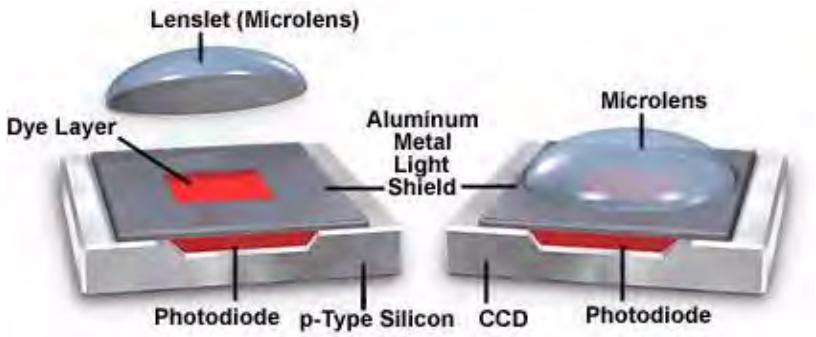

FIGURE 27.1: Microlens or lenslet arrays

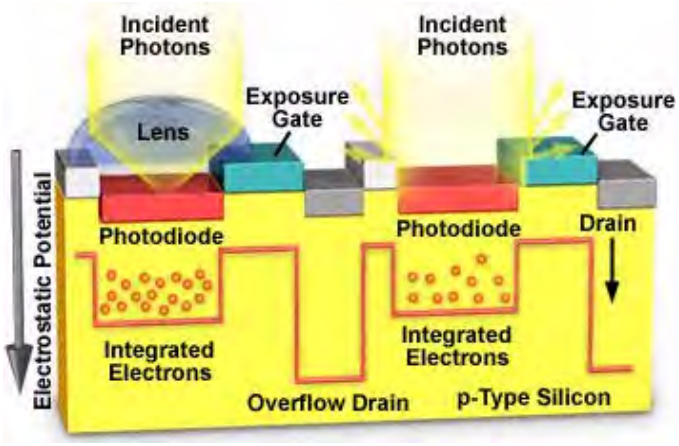

FIGURE 27.2: Microlens array architecture

pair, one equipped with a microlens to concentrate light into the photodiode, while the other must absorb incident light rays without the benefit of optical assistance from a microlens. Incident photons that strike the microlens are directed into the photodiode by refraction through the glass or polymer comprising the microlens. The photodiode without a microlens collects a significantly lower portion of incoming photons, because those that impact on shielded areas (the exposure gate and neighboring structures) are not useful in charge integration. The optical fill factor of interline CCDs can be reduced to less than 20 percent by shielded vertical transfer shift registers. With the microlens array, the fill factor can approach 100 percent, depending upon manufacturing parameters.

Organization of the cone of light reaching the microlens surface depends upon the optical characteristics of the microscope or camera lens used to direct light to the CCD. Also, polysilicon gate thickness heavily influences the ability to collect light by the photodiode positioned beneath the gate structure. Microlens arrays are fabricated using reflow techniques on resist layers to achieve numerical apertures ranging from 0.15 to 0.4 with short focal lengths and corresponding lens diameters of 20 to 800 microns. The fill factor of a microlens array is strongly dependent upon the manufacturing process used to create the array. Glass lenses of somewhat lower (0.05 to 0.2) numerical aperture are also utilized. Lower numerical aperture microlenses have fewer optical aberrations with significantly longer focal lengths.

Disadvantages encountered with microlenses are far outweighed by increased sensitivity of devices having these optical components in place. One of the primary difficulties occurs when light rays from the outer portions of a pixel are focused onto an adjacent lens (and subsequently onto the detector photodiode) resulting in mis-registration. In addition, when detector pixel size reaches the diffraction limit of the microlenses, the pixels become overfilled leading to inaccurate measurements. As photodiodes become smaller, the problems associated with producing quality microlenses increase. Higher quality microlenses are needed to produce images on these arrays, but spherical aberration then becomes a problem. Adding microlenses to CCDs increases the number of processing steps, and the uniformity of the lens array is a variable that can often cause problems during fabrication.

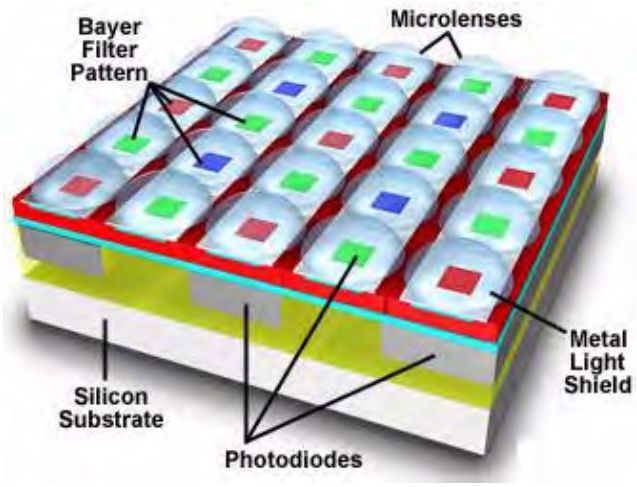

FIGURE 27.3: Microlens array on photodiodes

Chapter 28

Other devices

28.1 Avalanche Photodiodes

An avalanche photodiode is a silicon-based semiconductor containing a pn junction consisting of a positively doped p region and a negatively doped n region sandwiching an area of neutral charge termed the depletion region. These diodes provide gain by the generation of electron-hole pairs from an energetic electron that creates an "avalanche" of electrons in the substrate.

Presented in Figure 28.1 is an illustration of a typical avalanche photodiode. Photons entering the diode first pass through the silicon dioxide layer and then through the n and p layers before entering the depletion region where they excite free electrons and holes, which then migrate to the cathode and anode, respectively. When a semiconductor diode has a reverse bias (voltage) applied and the crystal junction between the p and n layers is illuminated, then a current will flow in proportion to the number of photons incident upon the junction.

Avalanche diodes are very similar in design to the silicon p-i-n diode, however the depletion layer in an avalanche photodiode is relatively thin, resulting in a very steep localized electrical field across the narrow junction. In operation, very high reverse-bias voltages (up to 2500 volts) are applied across the device. As the bias voltage is increased, electrons generated in the p layer continue to increase in energy as they undergo multiple

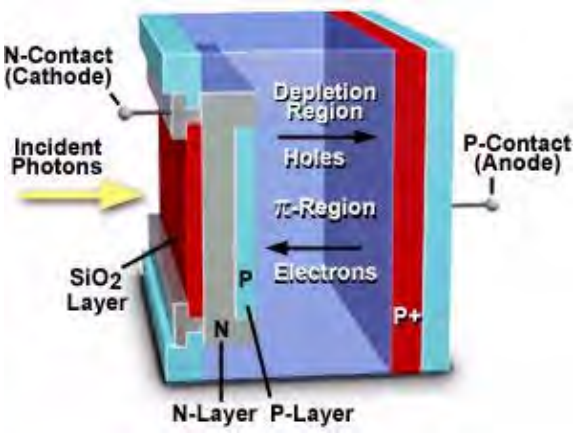

FIGURE 28.1: Avalanche photodiodes

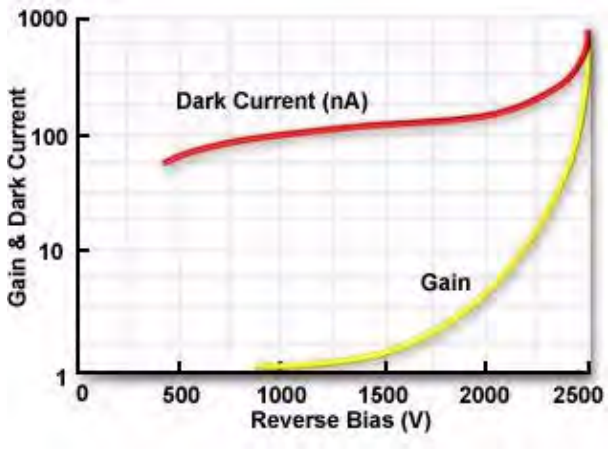

FIGURE 28.2: Avalanche photodiodes gain and dark current

collisions with the crystalline silicon lattice. This "avalanche" of electrons eventually results in electron multiplication that is analogous to the process occurring in one of the dynodes of a photomultiplier tube.

Avalanche photodiodes are capable of modest gain (500-1000), but exhibit substantial dark current, which increases markedly as the bias voltage is increased (see Figure 28.1). They are compact and immune to magnetic fields, require low currents, are difficult to overload, and have a high quantum efficiency that can reach 90 percent. Avalanche photodiodes are now being used in place of photomultiplier tubes for many low-light-level applications.

28.2 Photomultiplier Tubes

A photomultiplier tube, useful for light detection of very weak signals, is a photoemissive device in which the absorption of a photon results in the emission of an electron. These detectors work by amplifying the electrons generated by a photocathode exposed to a photon flux.

Photomultipliers acquire light through a glass or quartz window that covers a photosensitive surface, called a photocathode, which then releases electrons that are multiplied by electrodes known as metal channel dynodes. At the end of the dynode chain is an anode or collection electrode. Over a very large range, the current flowing from the anode to ground is directly proportional to the photoelectron flux generated by the photocathode.

The spectral response, quantum efficiency, sensitivity, and dark current of a photomultiplier tube are determined by the composition of the photocathode. The best photocathodes capable of responding to visible light are less than 30 percent quantum efficient, meaning that 70 percent of the photons impacting on the photocathode do not produce a photoelectron and are therefore not detected. Photocathode thickness is an important variable that must be monitored to ensure the proper response from absorbed photons. If the photocathode is too thick, more photons will be absorbed but fewer electrons will be emitted from the back surface, but if it is too thin, too many photons will pass through without being absorbed. The photomultiplier used in this tutorial is a side-on design, which uses an opaque and relatively thick photocathode. Photoelectrons are ejected from the front face of the photocathode and angled toward the first dynode.

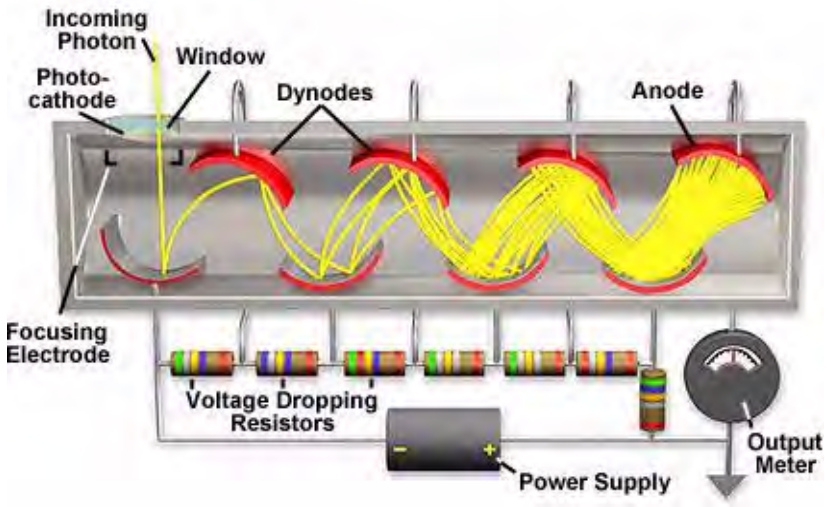

FIGURE 28.3: Photomultiplier tube

Electrons emitted by the photocathode are accelerated toward the dynode chain, which may contain up to 14 elements. Focusing electrodes are usually present to ensure that photoelectrons emitted near the edges of the photocathode will be likely to land on the first dynode. Upon impacting the first dynode, a photoelectron will invoke the release of additional electron that are accelerated toward the next dynode, and so on. The surface composition and geometry of the dynodes determines their ability to serve as electron multipliers. Because gain varies with the voltage across the dynodes and the total number of dynodes, electron gains of 10 million (Figure 28.3) are possible if 12-14 dynode stages are employed.

Photomultipliers produce a signal even in the absence of light due to dark current arising from thermal emissions of electrons from the photocathode, leakage current between dynodes, as well as stray high-energy radiation. Electronic noise also contributes to the dark current and is often included in the dark-current value.

Channel photomultipliers represent a new design that incorporates a unique detector having a semitransparent photocathode deposited onto the inner surface of the entrance window. Photoelectrons released by the photocathode enter a narrow and curved semiconductive channel that performs the same functions as a classical dynode chain. Each time an electron impacts the inner wall of the channel, multiple secondary electrons are emitted. These ejected photoelectrons have trajectories angled at the next bend in the channel wall (simulating a dynode chain), which in turn emits a larger quantity of electrons angled at the next bend in the channel. The effect occurs repeatedly, leading to an avalanche effect, with a gain exceeding 100 million. Advantages of this design are lower dark current (picoamp range) and an increase in dynamic range.

Confocal microscopes, spectrophotometers, and many high-end automatic camera exposure bodies utilize photomultipliers to gauge light intensity. Spectral sensitivity of the photomultiplier depends on the chemical composition of the photocathode with the best devices having gallium-arsenide elements, which are sensitive from 300 to 800 nanometers. Photomultiplier photocathodes are not uniformly sensitive and typically the photons are spread over the entire entrance window rather than on one region. Because photomultipliers do not store charge and respond to changes in input light fluxes within a few nanoseconds,

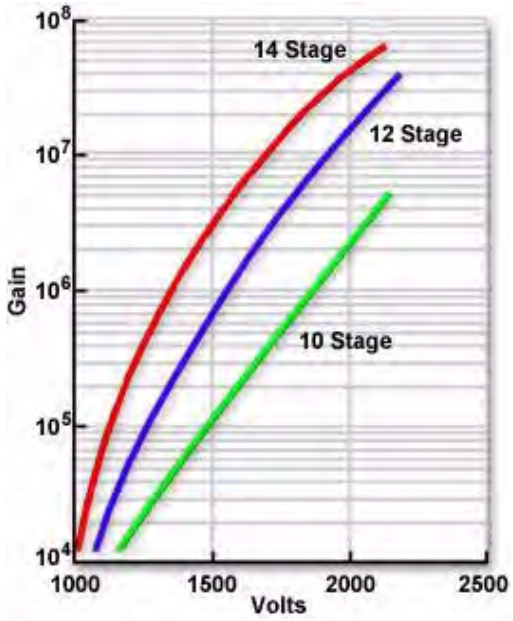

FIGURE 28.4: Dynode number vs PMT gain

they can be used for the detection and recording of extremely fast events. Finally, the signal to noise ratio is very high in scientific grade photomultipliers because the dark current is extremely low (it can be further reduced by cooling) and the gain may be greater than one million.

28.3 Proximity-Focused Image Intensifiers

Image intensifiers were developed for military use to enhance our night vision and are often referred to as wafer tubes or proximity-focused intensifiers. They have a flat photocathode separated by a small gap on the input side of a micro-channel plate (MCP) electron multiplier and a phosphorescent output screen on the reverse side of the MCP.

Substantial voltages are present across the small gaps between the photocathode, the phosphorescent output screen, and the MCP, which require careful construction of the devices to ensure they are free from contamination and can maintain high internal vacuums. Proximity-focused intensifiers are free from geometrical distortion or shading because the photoelectrons follow short, direct paths between the cathode, output screen, and the MCP rather than being focused by electrodes. Input and output windows are typically around 18 millimeters in diameter and consist of either a multialkali or bialkali photocathode (Gen II intensifiers) or a gallium arsenide photocathode (Gen III and Gen IV devices) and a P20 output phosphor. The overall photon gain of these devices averages about 10,000, which is calculated according to the equation:

$$\text{Gain} = \text{QE} \cdot G(\text{mcp}) \cdot V(p) \cdot E(p)$$

where QE is the photocathode quantum efficiency (0.1 to 0.5 electrons/photon), G(mcp) is the microchannel plate gain (averaging between 500-1000), V(p) is the voltage between the MCP and the output phosphor (around 2500-5000 volts), and E(p) is the electron-to-light conversion efficiency of the phosphor (0.08-0.2 photons/electron). When the voltage

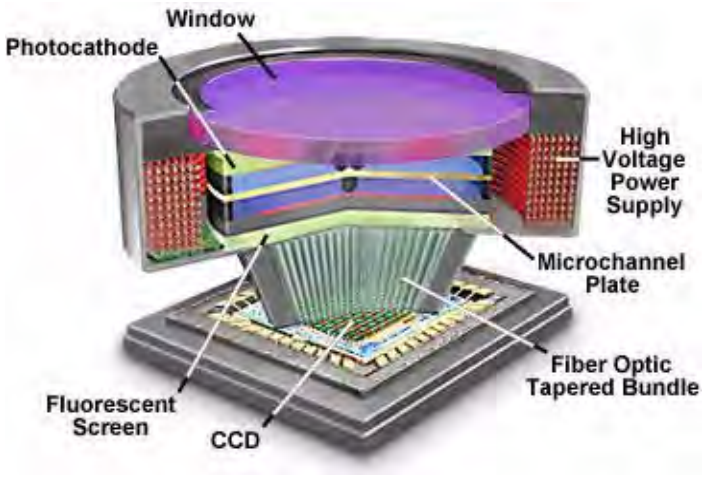

FIGURE 28.5: Proximity-Focused Image Intensifiers

drop between the MCP and the output phosphor decreases below 2500 volts, the phosphor becomes unresponsive.

The photocathode in the latest generation of these devices, while similar to that in photomultiplier tubes, has a higher quantum efficiency (up to 50 percent) in the blue-green end of the spectrum. The gain of the micro-channel plate is adjustable over a wide range with a typical maximum of about 80,000 (a detected photon at the input leads to a pulse of 80,000 photons from the phosphor screen). The phosphor matches the spectral sensitivity of the eye and is often not ideal for a CCD. Resolution of an intensified CCD depends on both the intensifier and the CCD, but is usually limited by the intensifier microchannel plate geometry to about 75 percent of that of the CCD alone. The latest generation of image intensifiers (denoted blue-plus Gen III or sometimes Gen IV; Figure 28.5) employ smaller microchannels (6 micron diameter) and better packing geometry than in previous models with a resultant substantial increase in resolution and elimination of the chicken-wire fixed-pattern noise that plagued earlier devices. The broad spectral sensitivity and high quantum efficiency (Figure 28.5) of the "high blue" GaAs and gallium arsenide phosphide (GaAsP) photocathodes are ideally suited to applications in fluorescence or low-light-level microscopy.

Image intensifiers have a reduced intrascene dynamic range compared to a slow-scan CCD camera and it is difficult to obtain more than a 256-fold intensity range (8 bits) from an intensified CCD camera. Intensifier gain may be rapidly and reproducibly changed to accommodate variations in scene brightness, thereby increasing the interscene dynamic range. Indeed, since image intensifiers can be rapidly gated (turned off or on in a few nanoseconds), relatively bright objects can be visualized by a reduction in the "on" time. A gated, variable gain intensified CCD camera is commercially available with a 12 order of magnitude dynamic range. Gated, intensified CCD cameras are required for most time-resolved fluorescence microscopy applications because the detector must be turned on and off in nanoseconds or its gain rapidly modulated in synchrony with the light source.

Thermal noise from the photocathode as well as electron multiplication noise from the microchannel plate reduce the signal-to-noise ratio in an intensified CCD camera to below that of a slow-scan CCD. The contribution of these components to the noise created by the statistical nature of the photon flux depends on the gain of the device and the temperature

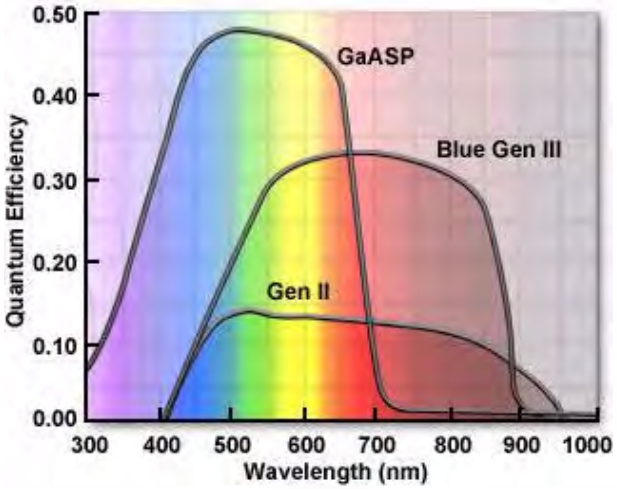

FIGURE 28.6: Photocathode quantum efficiencies

of the photocathode. Generally, a reduction of the gain of the intensification stage is employed to limit the noise although intensified CCD cameras are available with a cooled photocathode.

Intensified CCD cameras have a very fast response limited by the time constant of the output phosphor and often the CCD camera read out is the slowest step in image acquisition. Because of the low light fluxes emanating from the fluorochromes bound to or within living cells, intensified CCD cameras are frequently employed to study dynamic events and for ratio imaging of ion-sensitive fluorochromes. The simultaneous or near-simultaneous acquisition of two images at different excitation or emission wavelengths is required for ratio imaging and intensified CCD cameras have the requisite speed and sensitivity.

Two of the most popular approaches for relaying the output of an image intensifier to a video-rate camera (vidicon or CCD) are using an optical relay lens coupling or a fiber-optic coupling. Relay lenses are designed to capture light from the intensifier output window with minimal geometrical distortion or spherical aberration and project as much of the image as possible onto the video pickup device. The efficiency of a relay lens is given by the equation:

$$\text{Efficiency} = \frac{T}{4f^2 \cdot (1 + M^2)}$$

where T is the lens transmission (around 0.9), M is the magnification (ranging between 0.5x and 2x), and f is the lens f-number (1.0 to 2.8). An ideal 1:1 relay lens with 100 percent transmission and an f-number of 1.0 will give a maximum transfer efficiency of only around 12 percent. When the input window of the video sensor (CCD array size) is smaller than the intensifier output window, the relay lens is required to demagnify the image to match the format of the sensor. Coupling efficiency increases proportionally with demagnification according to the efficiency equation given above. If the intensifier has sufficient gain and output luminance, the losses in the relay lenses may not adversely affect overall performance. Optical relay lenses work well with Gen II inverter tubes and some Gen III (or Gen IV) tubes coupled to Newvicon tube or CCD detectors because the high gain and high screen luminance of these intensifiers help to offset the inefficiency of the relay lenses.

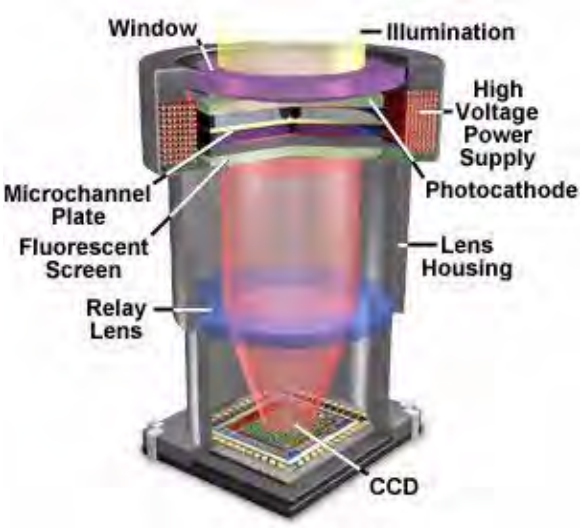

FIGURE 28.7: Image intensifier with Relay lens

The optimum method for coupling Proximity-focused image intensifiers to CCD sensors is through a fiber-optic taper (Figure 28.4). This approach achieves a coupling efficiency between 40 and 80 percent with matching formats, but requires a high degree of skill in bonding the fiber-optic taper to both devices. Maximum efficiency and minimal fixed-pattern noise are achieved when the CCD front window is removed and the fiber-optic taper is machined to fit directly onto the diode array surface. High resolution, artifact-free images require precision quality tapers having a small fiber diameter (between 2 and 3 microns) with very few missing or broken fibers and low fixed-pattern noise.

Use of optical relay lenses allows for convenient interchange of the video camera, CCD, and/or intensifier tube, and provides electrical isolation of the sensitive video camera input from the high voltages and high-frequency electrical interference present on the output of the image intensifier. Bonding fiber-optic tapers to the CCD surface is relatively permanent, and CCD failure can lead to loss of an expensive image intensifier and fiber-optic taper. To alleviate this problem, improvements in nonpermanent, optically matched, silicon bonding materials make it possible to disassemble fiber-optic coupled systems without destruction.

28.4 Sequential Three-Pass Color CCD Imaging

Three-pass sequential color CCD imaging systems employ a rotating color wheel to capture three successive exposures in order to obtain the desired RGB (red, green, and blue) color characteristics of a digital image. The major advantage of this technique is the ability to fully utilize the entire pixel array of a CCD imaging chip, by using one pass for each color.

Silicon based charge-coupled devices lack the ability to distinguish color information presented to the pixel elements by incoming photons. Even though electromagnetic radiation of varying energy passes through the devices to a depth determined by the wavelength, the interaction that produces free elections and holes is not color sensitive. A typical sequential color imaging system design is illustrated in Figure 28.8, which shows the red filter being used to pass illuminating light waves from the microscope optics to the CCD surface.

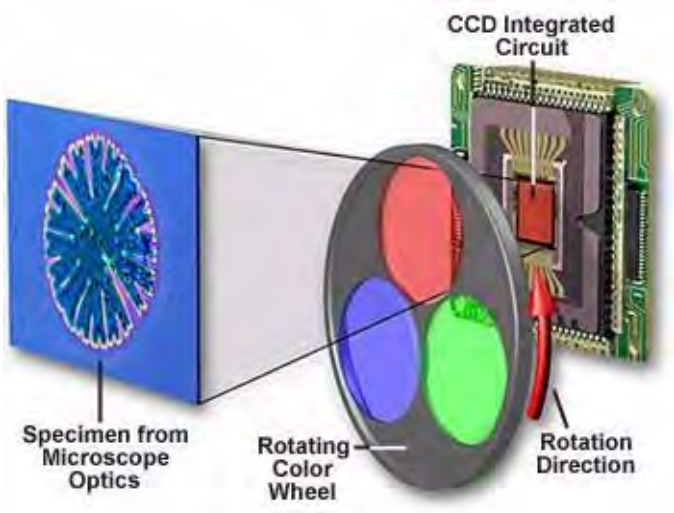

FIGURE 28.8: Sequential Three-Pass Color CCD Imaging

The primary advantage of this technique is the ability to achieve the highest resolution capable of the device, which equals the size of the CCD array.

After all of the image information has been captured in three individual passes, it is recombined off-chip and processed in a manner similar to that of other CCD architectures. The major disadvantage of this system is the relatively long exposure times necessary to accumulate three individual color arrays, which requires an almost stationary subject and vibration-free operation of the rotating color wheel mechanical components. This technique is being slowly phased out as single-shot CCD cameras with higher resolutions become commonplace. However, a number of applications now incorporate a rapidly switchable liquid crystal array screen that can be used to capture the three colors in milliseconds, thus speeding the throughput of the device and reducing the risk of mechanically-induced vibration.

Chapter 29

Quantum Efficiency

The quantum efficiency of a charge-coupled device (CCD) is a property of the photovoltaic response defined as the number of electron-hole pairs created and successfully read out by the device for each incoming photon. This property is especially important for low-light imaging applications such as fluorescence microscopy where emission photon wavelengths are often in the 375-550 nanometer range and have a relatively high absorption coefficient in silicon. Standard CCDs, which are illuminated in the front of the device through the gate electrodes and oxide coatings, are more sensitive to green and red wavelengths in the region between 550 and 900 nanometers.

The spectral sensitivity of the CCD differs from that of a simple silicon photodiode detector because the CCD surface has channels used for charge transfer that are shielded by polysilicon gate electrodes, thin films of silicon dioxide, and a silicon nitride passivation layer. These structures, used to transfer the charge from the imaging area and to protect the CCD from humidity and electrostatic discharge, absorb the shorter wavelengths (450 nanometers and lower), reducing the blue sensitivity of the device. Polysilicon transmittance starts to decrease below 600 nanometers and the material becomes essentially opaque to photons at 400 nanometers, but absorption depends upon gate thickness and interference effects of light passing through thin films on the CCD surface. Interline-transfer CCDs have photodiodes that deviate from standard polysilicon gate structure, a factor that reduces interference effects and produces a more ideal and uniform spectral response. These devices are also usually equipped with vertical antibloom drains that produce a reduced response to longer wavelength photons. As photons above 700 nanometers penetrate deep into the silicon substrate close to the buried drain, they have a greater chance of liberating electrons that will diffuse into the drain and be instantly removed. Quantum efficiency is also dependent upon gate voltage, with lower voltages producing small depletion regions and visa versa.

Traditional film emulsions are hypersensitive to the blue region of the visible light spectrum, in contrast to the response displayed by CCDs, a feature that often results in color differences between images captured on film and those recorded with a CCD. As pixel geometry's grow smaller, the blue light absorption problem increases as the blue response of the sensor decreases rapidly with pixel size.

A typical spectral sensitivity curve for a standard CCD is illustrated in Figure **??** (Standard CCD) where it should be noted that the peak quantum efficiency of 40 percent is markedly below that of a individual silicon photodiode. Ripples in the spectrum occur because of interference effects from thin films on the CCD surface. Recently, transparency

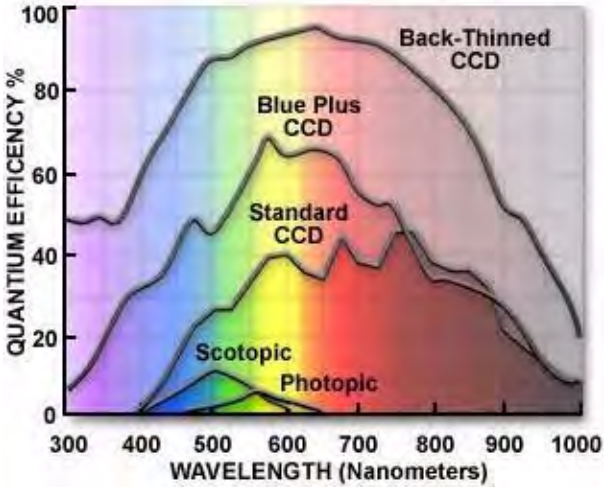

FIGURE 29.1: CCD spectral sensitivities

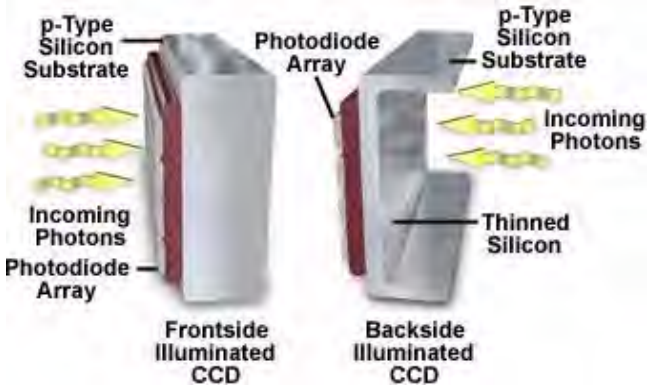

FIGURE 29.2: Frontside and backside illuminated CCDs

of the channels has been increased with substantial improvement in blue-green sensitivity of some scientific-grade CCDs (Blue Plus curve in Figure **??**) through the use of pioneering gate materials and proprietary phosphor coatings. Coatings of this type (Lumogen) are deposited directly onto the array surface and emit light in the 500 to 580 nanometer region when excited by short wavelength (120 to 450 nanometer) high-energy ultraviolet and visible light. Phosphors embedded within the coating produce a secondary fluorescence that is emitted in all directions, with only those photons entering the array being absorbed to yield a quantum efficiency of approximately 15 to 20 percent. The coatings are transparent to visible light, so they do not affect photon absorption at wavelengths exceeding 450 nanometers, producing an apparent spectral response range of almost 1000 nanometers (120 to 1100 nanometers).

For comparison, Figure **??** also illustrates spectral sensitivity curves for the human eye, corresponding to photopic and scotopic vision, arising from the cones and rods, respectively. Peak sensitivity is in the green (photopic at 555 nanometers and scotopic at 507 nanometers) with a maximum quantum efficiency of 3 percent for photopic vision and 10 percent for scotopic. From this data it is obvious that compared to our eyes, a scientific-grade CCD camera has a broader spectral sensitivity with a much higher quantum efficiency.

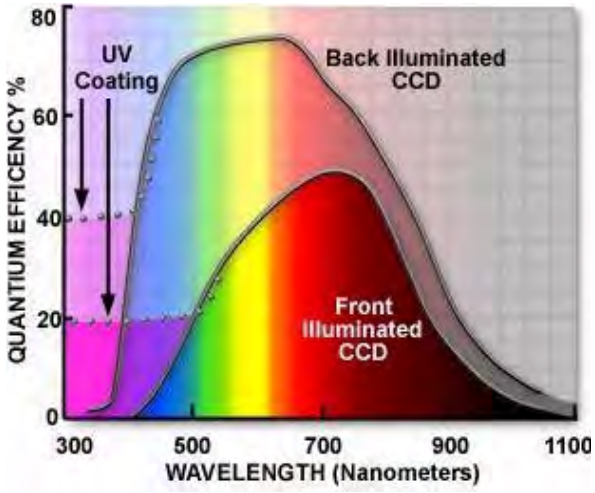

FIGURE 29.3: Quantum efficiency for frontside and backside illuminated CCDs

The losses due to gate channel structures are completely eliminated in the back-illuminated CCD. In this design, light falls onto the back of the CCD in a region that has been thinned by etching until it is transparent (a thickness corresponding to about 10-15 microns). The resultant spectral sensitivity curve, also shown in Figures **??** and **??** (Back-Thinned and Back-Illuminated CCD), illustrates the high quantum efficiency that can be realized with this configuration. However, back-thinning results in a delicate, relatively expensive sensor that, to date, has only been employed in high-end scientific-grade CCD cameras.

Anti-reflection coatings are used in back-thinned CCDs to increase quantum efficiency, but it is not possible to produce coatings that are effective across the entire visible range. Coatings that increase spectral response in the longer wavelengths often produce a corresponding decrease in absorption of lower wavelength photons, so research is ongoing to produce anti-reflection coatings that are effective across the entire visible light spectrum.

The photovoltaic effect, where light energy in the form of photons is converted into electronic potential, is dependent upon a wide spectrum of conditions. When visible and infrared photons in the 400 to 1100 nanometer range collide with a silicon atom positioned within the substrate of a CCD, electrons are excited from the valence band to the conduction band due to a reaction between the photons and silicon orbital electrons. A number of factors determine the amount of electronic charge generated by a quanta of light energy, including the absorption coefficient, photon recombination lifetime, diffusion length, and the chemical and physical nature of overlying materials on the CCD surface. The absorption coefficient of photons in silicon is wavelength dependent, with long-wavelength (greater than 800 nanometers) photons penetrating deeper into the silicon substrate than those having shorter wavelengths.

In cases where the photon energy is greater than the band gap energy, an electron has a high probability of being excited into the conduction band, thus becoming mobile. This interaction is also known as the photoelectric effect, and is dependent upon a critical wavelength above which photons have insufficient energy to excite or promote an electron positioned in the valence band and produce an electron-hole pair. When photons exceed the critical wavelength (usually beyond 1100 nanometers), band gap energy is greater than the intrinsic photon energy, and photons pass completely through the silicon substrate.

TABLE 29.1: Photon Absorption Depth

Wavelength (Nm)	Penetration Depth (μm)
400	0.19
450	1.0
500	2.3
550	3.3
600	5.0
650	7.6
700	8.5
750	16
800	23
850	46
900	62
950	150
1000	470
1050	1500
1100	7600

Table 1 lists the depth (in microns) at which 90 percent of incident photons are absorbed by a typical CCD.

Most of the photons with a wavelength between 450 and 700 nanometers are absorbed either in the depletion region or within the bulk material (silicon) of a CCD substrate. Those absorbed into the depletion region will have a quantum efficiency approaching 100 percent, whereas photons entering the substrate liberate electrons that experience a three-dimensional random walk and either recombine with holes or diffuse into the depletion region. For those electrons that have negligible diffusion lengths, the quantum efficiency is very low, but those with high diffusion lengths eventually reach a charge well.

Most CCD arrays utilized in digital cameras designed for scientific applications are sealed within a protected environment to reduce artifacts, improve response, and prolong CCD life. Incoming photons often must pass through a glass or quartz window to reach the pixel array and enter the silicon substrate. Reflection losses at the window surface occur at all photon wavelengths, and transmittance of photons through glass (but not quartz) decreases dramatically for wavelengths below 400 nanometers. Scientific CCD sensors are designed for applications requiring high sensitivity and use quartz coatings to decrease reflection across all wavelengths.

Appendix A

Image Formation

In the optical microscope, when light from the microscope lamp passes through the condenser and then through the specimen (assuming the specimen is a light absorbing specimen), some of the light passes both around and through the specimen undisturbed in its path. Such light is called direct light or undeviated light. The background light (often called the surround) passing around the specimen is also undeviated light. On the other hand, some of the light passing through the specimen is deviated when it encounters parts of the specimen.

Such deviated light (as you will subsequently learn, called diffracted light) is rendered one-half wavelength or 180 degrees out of step (more commonly, out of phase) with the direct light that has passed through undeviated. The one-half wavelength out of phase caused by the specimen itself enables this light to cause destructive interference with the direct light when both arrive at the intermediate image plane at the diaphragm of the eyepiece. The eye lens of the eyepiece further magnifies this image which finally is projected onto the retina or the camera film.

What has happened is that the direct or undeviated light is projected by the objective and spread evenly across the entire image plane at the diaphragm of the eyepiece. The light diffracted by the specimen is brought to focus at various localized places on the same image plane, as illustrated in Figure A.2; and there the diffracted light causes destructive interference, and reduces intensity resulting in more or less dark areas. These patterns of light and dark are what we recognize as an image of the specimen. Since our eyes are sensitive to variations in brightness, the image then becomes a more or less faithful reconstitution of the original specimen.

To help you understand the basic principles, it is suggested that you try the following exercise and use as your "specimen" an object of known structure, such as a stage micrometer or similar grating of closely spaced dark lines. To proceed, place the finely ruled grating on the microscope stage and bring it into focus using first a 10X and then the 40X objective. Remove the eyepiece and, in its place, insert a phase telescope so that you can focus on the back focal plane of the objective. If you close down the condenser diaphragm most of the way, you will see a bright white central spot of light which is the image of the aperture diaphragm. To the right and left of the central spot, you will see a series of spectra, each colored blue on the part closest to the central spot and colored red on the part of the spectrum farthest from the central bright spot (as illustrated in Figure A.3). The intensity of these colored spectra decreases according to how far the spectrum is from the central spot.

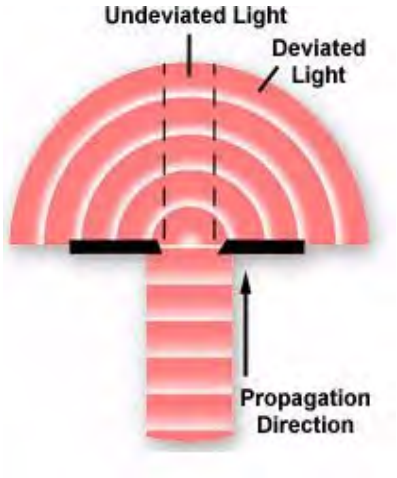

FIGURE A.1: Undeviated/deviated light

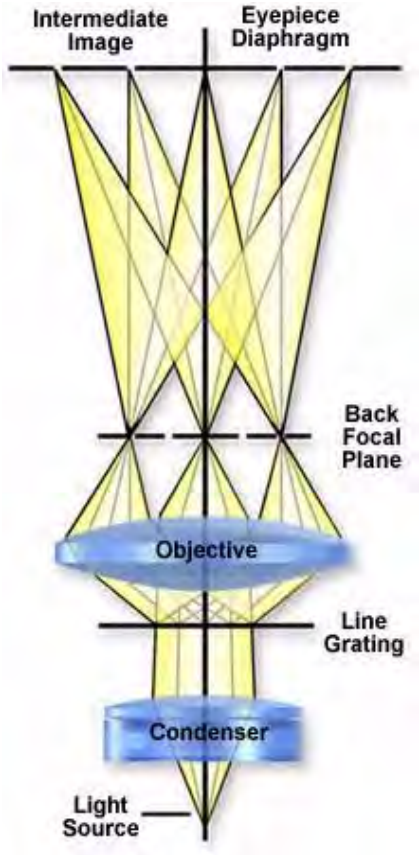

FIGURE A.2: Light path in the microscope

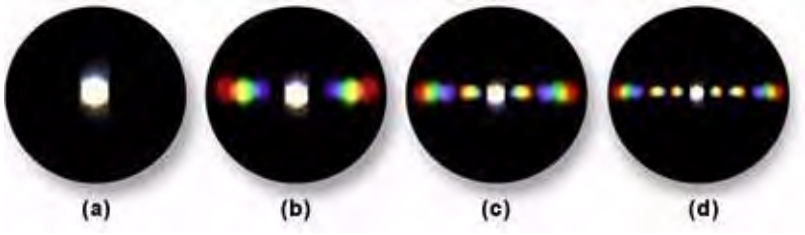

FIGURE A.3: Line grating diffraction patterns

Those spectra nearer the periphery of the objective are dimmer than those to the central spot. This is illustrated in Figure A.3 using three different magnifications. In Figure A.3(b), the diffraction pattern at the back focal plane of a 10X objective shows two diffraction spectra. If you remove the grating from the stage, as illustrated in Figure A.3(a), these spectra disappear and only the central image of the aperture diaphragm remains. If you put back the grating, the spectra reappear. Note that the spaces between the colored spectra appear dark. If you examine the grating with the 10x objective, you will observe that only one pair of spectra can be seen, one to the left of the central spot, one to the right. If you examine the line grating with a 60x objective (as shown in Figure A.3(d), assuming it has a higher numerical aperture than your 40x), you will observe more spectra to the right and left than you were able to see with the 40x (Figure A.3(c)) in place.

Since the colored spectra disappear when the grating is removed, it can be assumed that it is the specimen itself that is affecting the light passing through, thus producing the colored spectra. Further, if you close down the aperture diaphragm, you will observe that objectives of higher numerical aperture "grasp" more of these colored spectra than do objectives of lower numerical aperture. The crucial importance of these two statements for understanding image formation will become clear in the ensuing paragraphs.

The central spot of light (image of the condenser aperture diaphragm) represents the direct or undeviated light passing through the specimen or around the specimen undisturbed (illustrated in Figure A.4(b)). It is called the 0th or zeroth order. The fainter colored images of the aperture diaphragm on each side of the zeroth order are called the 1st, 2nd, 3rd, 4th, etc. orders respectively, as represented by the simulated diffraction pattern in Figure A.4(a) that would be observed at the rear focal plane of a 40X objective. All the "captured" orders represent, in this case, the diffraction pattern of the line grating as seen at the back focal plane of the objective.

The fainter colored diffracted images of the aperture diaphragm are caused by light deviated or diffracted, spread out in fan shape, at each of the openings of the line grating (Figure A.4(b)). The blue wavelengths are diffracted at a lesser angle than the green wavelengths, which are at a lesser angle than the red wavelengths.

At the back focal plane of the objective, the blue wavelengths from each slit interfere constructively to produce the blue area of the diffracted image of each spectrum or order; similarly for the red and green areas (Figure A.4(a)). Where the diffracted wavelengths are 1/2 wave out of step for each of these colors, the waves destructively interfere. Hence the dark areas between the spectra or orders. At the position of the zeroth order, all wavelengths from each slit add constructively; this produces the bright white light you see as the zeroth order at the center of the back focal plane of the objective (Figures A.3 and A.4).

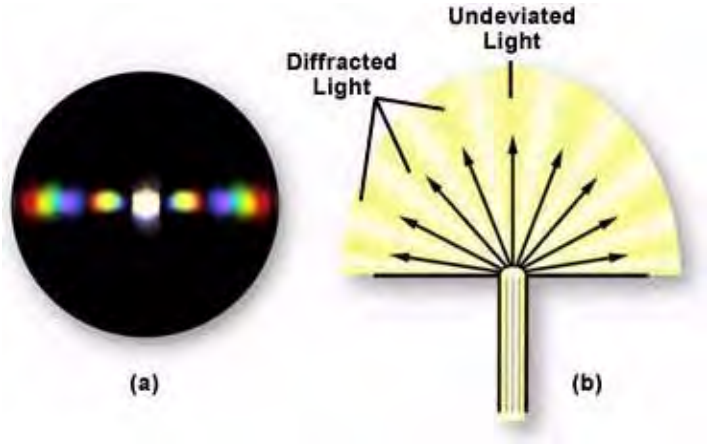

FIGURE A.4: Diffracetd light

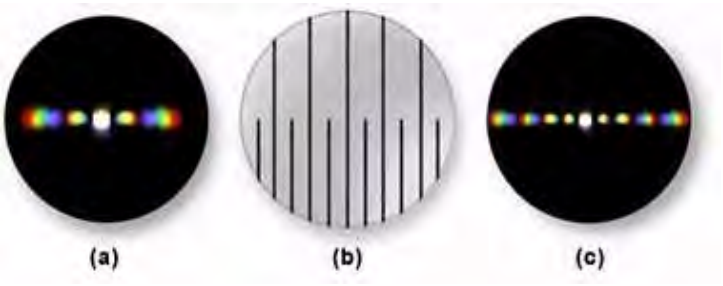

FIGURE A.5: Diffraction patterns of narrow and wide slits

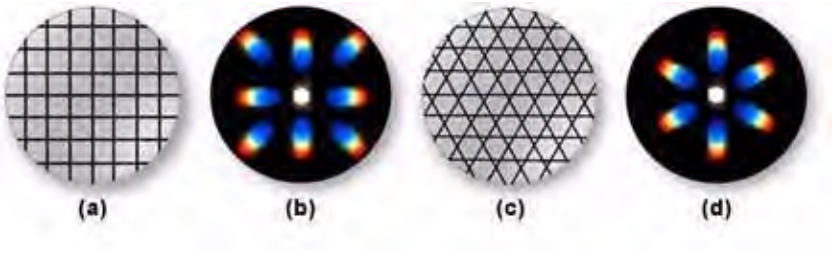

FIGURE A.6: Complex grid diffraction pattern

The closer the spacing of a line grating, the fewer the spectra that will be "captured" by a given objective, as illustrated in Figure A.5. The diffraction pattern illustrated in Figure A.5(a) was captured by a 40x objective imaging the lower portion the line grating in Figure A.5(b), where the slits are closer together. In Figure A.5(c), the objective is focused on the upper portion of the line grating (Figure A.5(b)), and more spectra are captured by the objective. The direct light and the light from the diffracted orders continue on, being focused by the objective, to the intermediate image plane at the diaphragm of the eyepiece. Here the direct and diffracted light rays interfere and are thus reconstituted into the real, inverted image that is "seen" by the eye lens of the eyepiece and further magnified. This is illustrated in Figure A.6 with two types of diffraction gratings. The square grid illustrated in Figure A.6(a) represents the orthoscopic image of the grid (i.e. the usual specimen image) as seen through the full aperture of the objective, while the diffraction pattern derived from this grid is shown as a conoscopic image that would be seen at the back focal plane of the objective. Likewise, the orthoscopic image of a hexagonally arranged grid (Figure A.6(c)) produces a corresponding hexagonally arranged conoscopic image of first order diffraction patterns (Figure A.6(d)).

Microscope specimens can be considered as complex gratings with details and openings of various sizes. This concept of image formation was largely developed by Ernst Abbe, the famous German microscopist and optics theoretician of the 19th century. According to Abbe (his theories are widely accepted at the present time), the details of a specimen will be resolved, if the objective "captures" the 0th order of the light and at least the 1st order too; or any two orders. The greater the number of diffracted orders that gain admittance to the objective, the more accurately the image will represent the original object.

Further, if a medium of higher refractive index than air (such as immersion oil) is used in the space between the front lens of the objective and the top of the coverslip (as shown in Figure A.7(a)), the angle of the diffracted orders is reduced and the fans of diffracted light are compressed. As a result, an oil immersion objective can "capture" more diffracted orders and yield better resolution than a dry objective (Figure A.7(b)).

Moreover, since blue light is diffracted at a lesser angle than either green light or red light, a lens of a given aperture may capture more orders of light when the light is blue. These two principles explain the classic Rayleigh equation often cited for resolution:

$$d = 1.22\frac{\lambda}{2\mathrm{NA}}$$

where d is the space between two adjacent particles (still allowing the particles to be perceived as separate), is the wavelength, and NA is the numerical aperture of the objective.

The greater the number of the higher diffracted orders admitted to the objective, the smaller the details of the specimen that can be clearly separated (resolved). Hence the

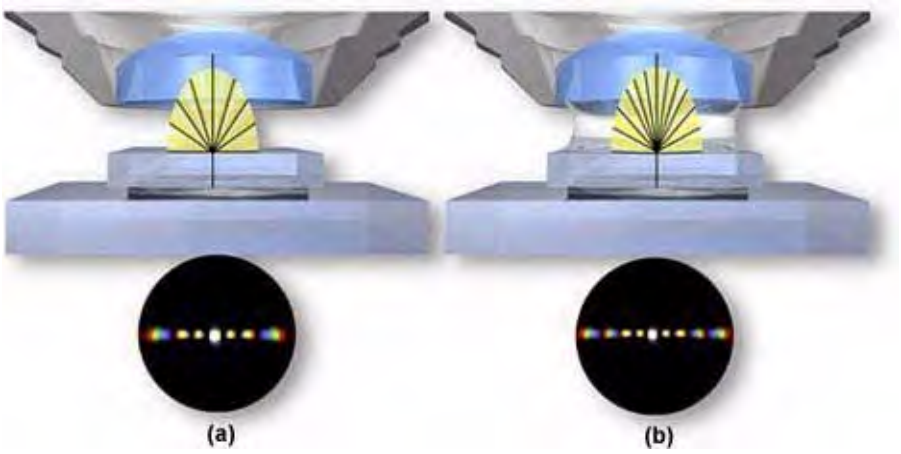

FIGURE A.7: Dry/immersion objective

FIGURE A.8: Aperture diaphragm and diffracted orders

value of high numerical aperture for such specimens. Likewise, the shorter the wavelength of visible light used, the better the resolution. These ideas explain why high numerical aperture, apochromatic lenses can separate extremely small details in blue light.

If you were to block out the outermost diffracted orders by placing an opaque mask at the rear of the objective, you could reduce the resolution of the lines of the grating, or any other detailed object, or "destroy" the resolution altogether so that the specimen would not be visible. Hence the usual caution not to close down the condenser aperture diaphragm below the suggested 2/3-4/5 of the objective's aperture.

Failure of the objective to "grasp" any of the diffracted orders results in an unresolved image (as shown in Figure A.8(a)). Since, in a specimen with very minute details, the diffraction fans are spread at a very large angle, a high numerical aperture objective is needed to "capture" them. Likewise, since the diffraction fans are compressed in immersion oil or in water, objectives designed for such use can give better resolution than dry objectives. Diffraction patterns obtained from objectives of varying resolution are illustrated in Figure A.8. The image on the left in Figure A.8 has no resolution because there are no higher diffracted orders captured by the objective. The patterns in Figures A.8(b) and (c) show an increasing number of diffracted orders indicating better resolution of the specimen as more orders are grabbed by the objective.

If alternate diffracted orders are blocked out (still assuming the grating as our specimen), the number of lines in grating would appear doubled (a spurious resolution). The important caveat is that actions introduced at the rear aperture of the objective can have significant effect upon the eventual image produced.

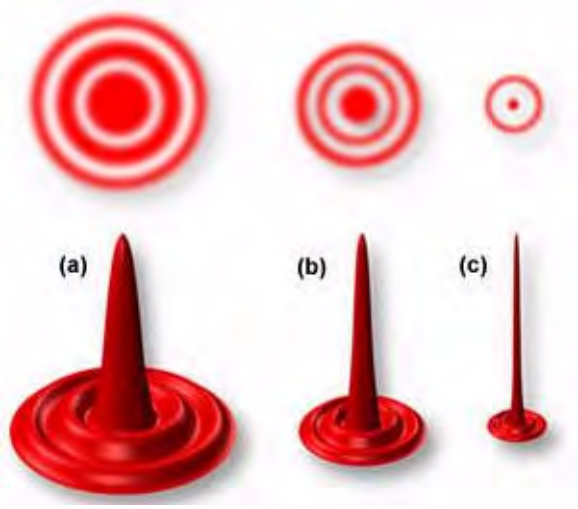

FIGURE A.9: Circular aperture Airy disk patterns

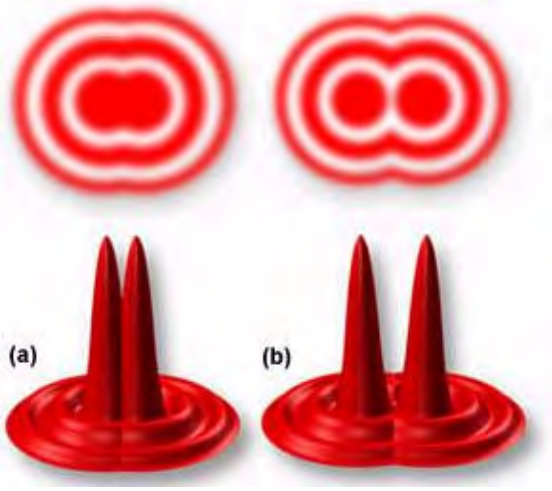

FIGURE A.10: Airy disk and resolution

For small details in a specimen (rather than a grating), the objective projects the direct and diffracted light onto the image plane of the eyepiece diaphragm in the form of small, circular diffraction disks known as Airy disks (as illustrated in Figure A.9). High numerical aperture objectives "capture" more of the diffracted orders and produce smaller size disks than do low numerical aperture objectives. In Figure A.9, Airy disk size is shown steadily decreasing from Figure A.9(a) through Figure A.9(c). The larger disk sizes in Figures A.9(a) and (b) are produced by objectives with lower numerical aperture, while the very sharp Airy disk in Figure A.9(c) is produced by an objective of very high numerical aperture.

The resulting image at the eyepiece diaphragm level is actually a mosaic of Airy disks which you perceive as light and dark. Where two disks are too close together so that their central black spots overlap considerably, the two details represented by these overlapping disks are not resolved or separated and thus appear as one (illustrated in Figure A.10(a)).

The basic principle is that the combination of direct and diffracted light (or the manipulation of direct or diffracted light) is critically important in image formation. The key

places for such manipulation are the back focal plane of the objective and the front focal plane of the substage condenser. This principle is fundamental to most of the contrast improvement methods in optical microscopy; it is of particular importance at high magnification of small details close in size to the wavelength of light. Abbe was a pioneer in developing these concepts to explain image formation of absorbing or so-called amplitude specimens. In the 1930's, F. Zernike, a Dutch physicist, extended these principles when he devised and explained phase microscopy.

Appendix B

Optical Aberrations

An ideal microscope objective produces a symmetrical diffraction limited image of an Airy pattern from an infinitely small object point. The image plane is generally located at a fixed distance from the objective front lens in a medium of defined refractive index. Microscope objectives offered by the leading manufacturers have remarkably low degrees of aberrations and other imperfections, provided the appropriate objective is selected for the task and the objective is utilized properly in accordance with the manufacturer's recommendations. It should be emphasized that objective lenses are not made to be perfect from every standpoint, but are designed to meet certain specifications depending on their intended use, constraints on physical dimensions, and price ranges.

Objectives are made with differing degrees of optical correction for both monochromatic (spherical, astigmatism, coma, distortion) and polychromatic aberrations, field size and flatness, transmission wavelengths, freedom from fluorescence, birefringence and other factors contributing to background noise. Depending upon the degree of correction, objectives are generally classified as achromats, fluorites, and apochromats, with a plan designation added to lenses with low curvature of field and distortion. This section addresses some of the more common optical aberrations that are commonly found (and often corrected) in microscope objectives.

B.1 Optical Aberrations

Lens errors in modern optical microscopy are an unfortunate problem caused by artifacts arising from the interaction of light with glass lenses. There are two primary causes of non-ideal lens action: Geometrical or Spherical aberrations are related to the spherical nature of the lens and approximations used to obtain the Gaussian lens equation; and Chromatic aberrations, which arise from variations in the refractive indices of the wide range of frequencies found in visible light.

In general, the effects of optical aberrations are to induce faults in the features of an image being observed through a microscope. Chromatic aberration in the substage condenser is illustrated in Figure B.1, where blue fringing at the edge of the field diaphragm image is due to chromatic aberration. These artifacts were first addressed in the eighteenth century when physicist John Dollond discovered that chromatic aberrations would be reduced or corrected by using a combination of two different types of glass in the fabrication of lenses. Later, during the nineteenth century, achromatic objectives with high numerical aperture were developed, although there were still geometrical problems with the lenses.

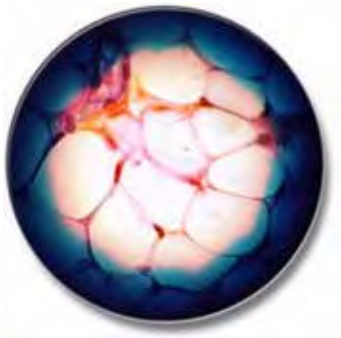

FIGURE B.1: Substage condenser chromatic aberration

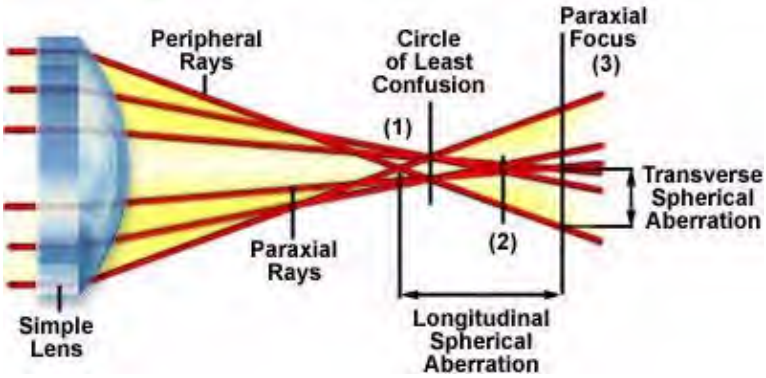

FIGURE B.2: Longitudinal and transverse spherical aberration

Modern glass formulations and antireflective coatings coupled to advanced grinding and manufacturing techniques have all but eliminated most aberrations from today's microscope objectives, although careful attention must still be paid to these effects, especially when conducting quantitative high-magnification video microscopy and photomicrography.

B.1.1 Spherical Aberration

These artifacts occur when light waves passing through the periphery of a lens are not brought into focus with those passing through the center as illustrated in Figure B.2. Waves passing near the center of the lens are refracted only slightly, whereas waves passing near the periphery are refracted to a greater degree resulting in the production of different focal points along the optical axis. This is one of the most serious resolution artifacts because the image of the specimen is spread out rather than being in sharp focus.

Figure B.2 illustrates an exaggerated view of three hypothetical monochromatic light rays passing through a convex lens. Refraction of the peripheral rays is greatest followed by those in the middle and then the rays in the center. The larger refraction by the outermost rays results in a focal point (drawn as focal point 1) that occurs in front of the focal points produced by rays passing closer to the center of the lens (focal points 2 and 3). Most of this discrepancy in focal points arises from approximations of the equivalency of sine and tangent values of respective angles made to the Gaussian lens equation for a spherical

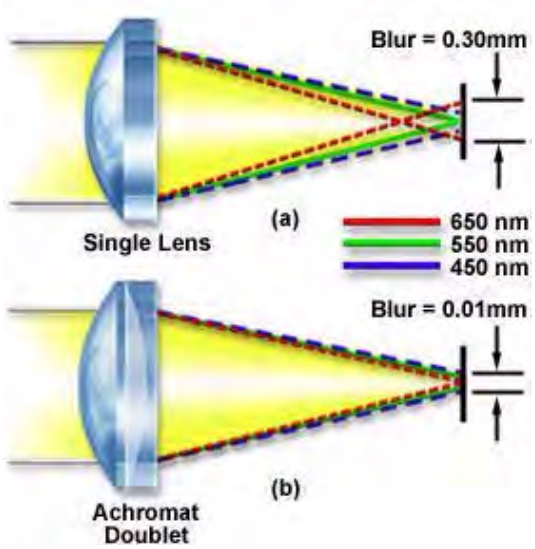

FIGURE B.3: Axial chromatic aberration

refracting surface:

$$\frac{n}{s} + \frac{n'}{s'} = \frac{n' - n}{r}$$

where n and n' represent the refractive index of air and the glass comprising the lens, respectively, s and s' are the object and image distance, and r is the radius of curvature of the lens. This expression determines the relative locations of images formed by the curved surface of a lens having radius r sandwiched between media of refractive indices n and n'. A refinement of this equation is often referred to as a higher-order (first, second, or third) correction by including terms in the cube of the aperture angle resulting in a more refined calculation.

Spherical aberrations are very important in terms of the resolution of the lens because they affect the coincident imaging of points along the optical axis and degrade the performance of the lens, which will seriously affect specimen sharpness and clarity. These lens defects can be reduced by limiting the outer edges of the lens from exposure to light using diaphragms and also by utilizing aspherical lens surfaces within the system. The highest-quality modern microscope objectives address spherical aberrations in a number of ways including special lens-grinding techniques, improved glass formulations, and better control of optical pathways.

B.1.2 Chromatic Aberrations

This type of optical defect is a result of the fact that white light is composed of numerous wavelengths. When white light passes through a convex lens, the component wavelengths are refracted according to their frequency. Blue light is refracted to the greatest extent followed by green and red light, a phenomenon commonly referred to as dispersion. The inability of the lens to bring all of the colors into a common focus results in a slightly different image size and focal point for each predominant wavelength group. This leads to colored fringes surrounding the image as illustrated in Figure B.3 below:

where we have greatly exaggerated the differences in the refractive properties of white light component wavelengths. This is described as the dispersion of the refractive indices

of the components of white light. Refractive index is the ratio of the speed of light in a vacuum as compared to its speed in a medium such as glass. For all practical purposes, the speed of light in air is virtually identical to the speed of light in a vacuum. As can be seen in Figure B.3, each wavelength forms its own independent focal point on the optical axis of the lens, an effect called axial or longitudinal chromatic aberration. The net result of this lens error is that the image of a point, in white light, is ringed with color. For example, if you were to focus at the "blue plane", the image point would be ringed with light of other colors, with red on the outside of the ring. Similarly, if you were to focus a point at the "red plane", the image point would be ringed with green and blue.

Chromatic aberration is very common with single thin lenses produced using the classical lens-maker's formula that relates the specimen and image distances for paraxial rays. For a single thin lens fabricated with a material having refractive index n and radii of curvature r_1 and r_2, we can write the following equation:

$$\frac{1}{s} + \frac{1}{s'} = (n-1)\left(\frac{1}{r_1} - \frac{1}{r_2}\right)$$

where s and s' are defined as the object and image distance, respectively. In the case of a spherical lens, the focal length (f) is defined as the image distance for parallel incoming rays:

$$\frac{1}{f} = \frac{1}{s} + \frac{1}{s'}$$

The focal length f varies with the wavelength of light as illustrated in Figure B.3. This variation can be partially corrected by using two lenses with different optical properties that are cemented together. Lens corrections were first attempted in the latter part of the 18th century when Dollond, Lister and others devised ways to reduce longitudinal chromatic aberration. By combining crown glass and flint glass (each type has a different dispersion of refractive index), they succeeded in bringing the blue rays and the red rays to a common focus, near but not identical with the green rays. This combination is termed a lens doublet where each lens has a different refractive index and dispersive properties. Lens doublets are also known as achromatic lenses or achromats for short, derived from the Greek terms "a" meaning without and "chroma" meaning color. This simple form of correction allows the image points at 486 nanometers in the blue region and 656 nanometers in the red region to now coincide. This is the most widely used lens and is commonly found on laboratory microscopes. Objectives which do not carry a special inscription stating otherwise are likely to be achromats. Achromats are satisfactory objectives for routine laboratory use, but since they are not corrected for all colors, a colorless specimen detail is likely to show, in white light, a pale green color at best focus (the so-called secondary spectrum). A simple achromat lens is illustrated in Figure B.4 below.

As can be seen in this figure, the proper combination of lens thickness, curvature, refractive index, and dispersion allows the doublet to reduce chromatic aberration by bringing two of the wavelength groups into a common focal plane. If fluorspar is introduced into the glass formulation used to fabricate the lens, then the three colors red, green, and blue can be brought into a single focal point resulting in a negligible amount of chromatic aberration. These lenses are known as apochromatic lenses and they are used to build very high-quality chromatic aberration-free microscope objectives. Modern microscopes utilize this concept and today it is common to find optical lens triplets (Figure B.5) made with three lens elements cemented together, especially in the higher-quality objectives. For chromatic aberration correction, a typical 10x achromat microscope objective is built with two

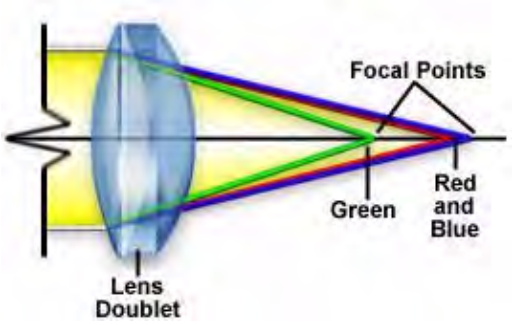

FIGURE B.4: Achromat doublet

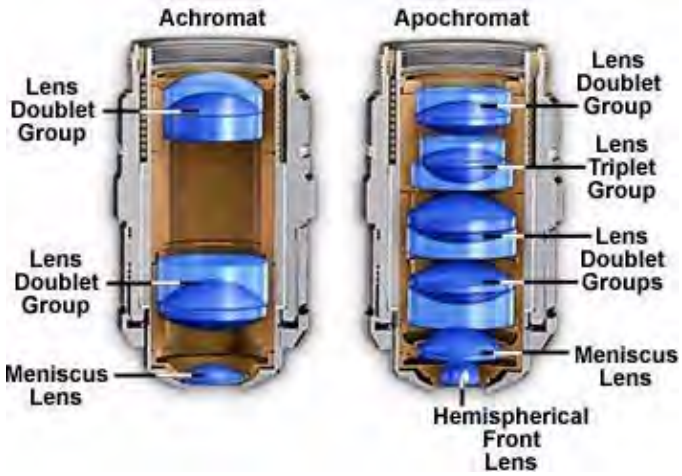

FIGURE B.5: Achromatic and apochromatic objective correction

lens doublets, as illustrated in Figure B.5, on the left. The apochromat objective illustrated on the right in Figure B.5 contains two lens doublets and a lens triplet for advanced correction of both chromatic and spherical aberrations.

The famous German lens maker Ernst Abbe was the first to succeed in making apochromatic objectives in the late 19th century. Since Abbe, for design reasons at the time, did not accomplish all chromatic correction in the objectives themselves, he chose to complete some of the correction via the eyepiece; hence the term compensating eyepieces.

In addition to longitudinal (or axial) chromatic aberration correction, microscope objectives also exhibit another chromatic defect. Even when all three main colors are brought to identical focal planes axially (as in fluorite and apochromat objectives), the point images of details near the periphery of the field of view are not the same size. This occurs because off-axis ray fluxes are dispersed, causing the component wavelengths to form images at different heights on the image plane. For example, the blue image of a detail is slightly larger than the green image or the red image in white light, resulting in color ringing of specimen details at the outer regions of the field of view. Thus, the dependence of axial focal length on wavelength produces a dependence of the transverse magnification on wavelength as well. This defect is known as lateral chromatic aberration or chromatic difference of magnification. When illuminated with white light, a lens with lateral chromatic aberration will produce a series of overlapping images varying in both size and color.

In microscopes having a finite tube length, it is the compensating eyepiece, with chromatic difference of magnification just the opposite of that of the objective, which is utilized to correct for lateral chromatic aberration. Because this defect is also found in higher magnification achromats, compensating eyepieces are frequently used for such objectives, too. Indeed, many manufacturers design their achromats with a standard lateral chromatic error and use compensating eyepieces for all their objectives. Such eyepieces often carry the inscription K or C or Compens. As a result, compensating eyepieces have built-in lateral chromatic error and are not, in themselves, perfectly corrected. In 1976, Nikon introduced CF optics, which correct for lateral chromatic aberration without assistance from the eyepiece. Newer infinity-corrected microscopes deal with this issue by introducing a fixed amount of lateral chromatic aberration into the tube lens used to form the intermediate image with light emanating from the objective.

It is interesting to note that the human eye has a substantial amount of chromatic aberration. Fortunately, we are able to compensate for this artifact when the brain processes images, but it is possible to demonstrate the aberration using a small purple dot on a piece of paper. When held close to the eye, the purple dot will appear blue at the center surrounded by a red halo. As the paper is moved farther away, the dot will appear red surrounded by a blue halo.

Although microscope manufacturers expend a considerable amount of resources to produce objectives free of spherical aberration, it is possible for the user to inadvertently introduce this artifact into a well-corrected optical system. By utilizing the wrong mounting medium (such as live tissue or cells in aqueous environments) with an oil immersion objective or by introducing similar refractive index mismatches, microscopists can often produce spherical aberration artifacts in an otherwise healthy microscope. Also, when using high magnification, high numerical aperture dry objectives, the correct thickness of the cover glass (suggested 0.17 mm) is critical; hence the inclusion of a correction collar on such objectives to enable adjustment for incorrect cover glass thickness as shown in Figure B.6 below. The objective on the left has been adjusted for a cover glass thickness of 0.20mm by bringing the lens elements of the correction collar closer together. By moving the lens elements far apart on the other extreme (the objective on the right in Figure B.6), the objective is corrected for a cover glass thickness of 0.13mm. Similarly, the insertion of accessories in the light path of finite tube length objectives may introduce aberrations when the specimen is refocused, unless such accessories have been properly designed with additional optics.

Different quality objectives differ in how well they bring the various colors to common focus and same size across the field of view. Between the achromatic and apochromatic type correction, there are also objectives known as semi-apochromats or, rather confusingly, as fluorites. The fluorites cost less but are almost as well-corrected as the apochromats; as a result, they are usually also well-suited for photomicrography in white light.

B.1.3 Other Geometrical Aberrations

These include a variety of effects including astigmatism, field curvature, and comatic aberrations that are easily corrected with proper lens fabrication. The topic of field curvature has already been discussed in detail in a previous section. Comatic aberrations are similar to spherical aberrations, but they are only encountered with off-axis objects and are most severe when the microscope is out of alignment. In this instance, the image of a point is asymmetrical, resulting in a comet-like (hence, the term coma) shape. Coma is often

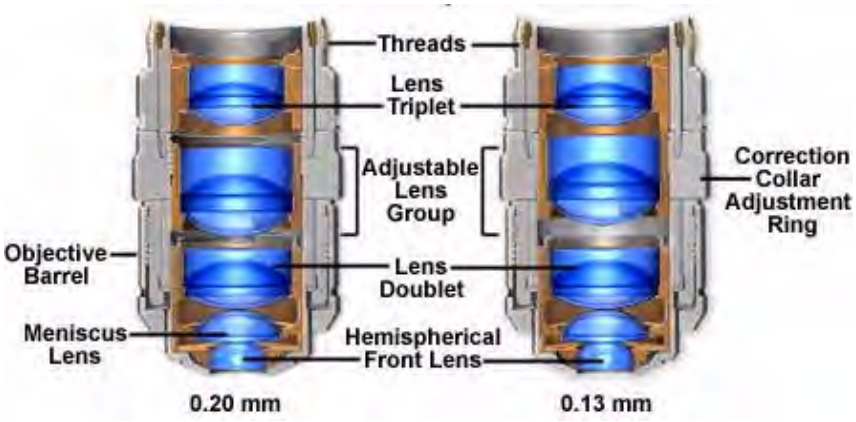

FIGURE B.6: Correction collars for spherical aberrations

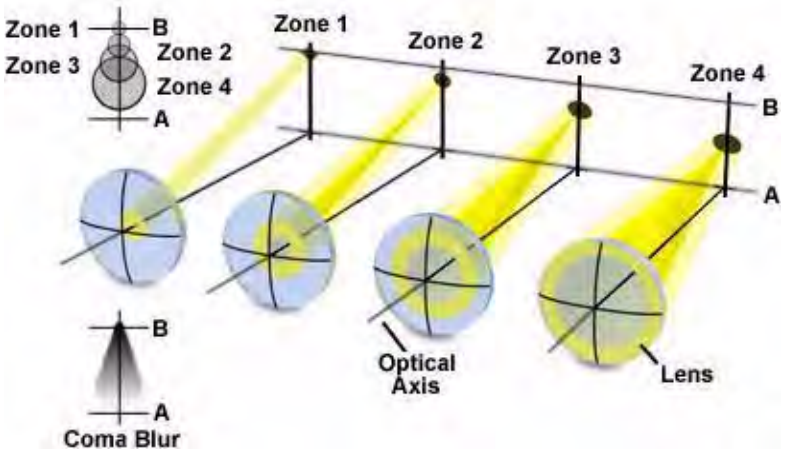

FIGURE B.7: Off-axis comatic aberration

considered the most problematic aberration due to the asymmetry it produces in images. It is also one of the easiest aberrations to demonstrate. On a bright, sunny day, use a magnifying glass to focus an image of the sun on the sidewalk and slightly tilt the glass with respect to the principal rays from the sun. The sun's image, when projected onto the concrete, will then elongate into a comet-like shape that is characteristic of comatic aberration.

The distinct shape displayed by images with comatic aberration is a result of refraction differences by light rays passing through the various lens zones as the incident angle increases. The severity of comatic aberration is a function of thin lens shape, which in the extreme, causes meridional rays passing through the periphery of the lens to arrive at the image plane closer to the axis than do rays passing nearer the axis and closer to the principal ray (see Figure B.7). In this case the peripheral rays produce the smallest image and the coma aberration sign is said to be negative. In contrast, when the peripheral rays are focused further down the axis and produce a much larger image, the aberration is termed positive. The "comet" shape may have its "tail" pointing toward the center of the field of view or away depending upon whether the comatic aberration has a positive or negative value.

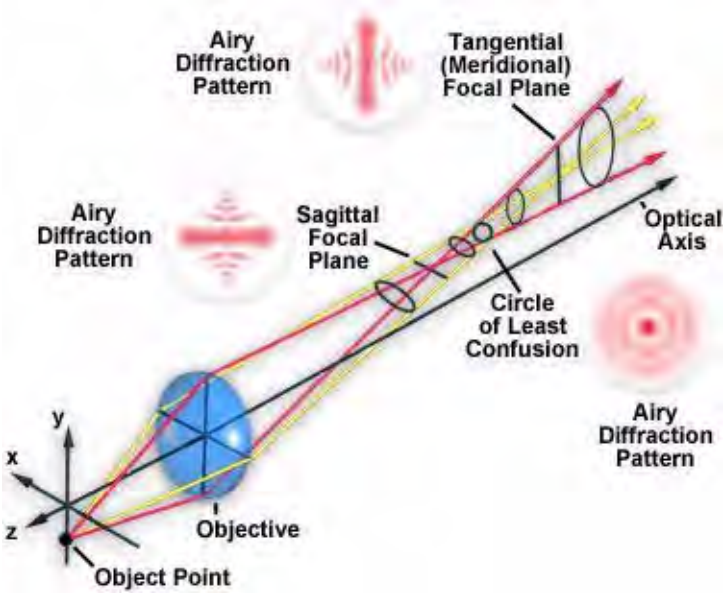

FIGURE B.8: Astigmatism aberration

Comatic aberrations are usually corrected with spherical aberrations or by designing lens elements of various shapes to eliminate this error. Objectives that are designed to yield excellent images for wide field-of-view eyepieces, have to be corrected for coma and astigmatism using a specially-designed multi-element optic in the tube lens to avoid these artifacts at the periphery of the field of view.

Astigmatism aberrations are similar to comatic aberrations, however these artifacts are not as sensitive to aperture size and depend more strongly on the oblique angle of the light beam. The aberration is manifested by the off-axis image of a specimen point appearing as a line or ellipse instead of a point. Depending on the angle of the off-axis rays entering the lens, the line image may be oriented in either of two different directions (Figure B.8), tangentially (meridionally) or sagittally (equatorially). The intensity ratio of the unit image will diminish, with definition, detail, and contrast being lost as the distance from the center is increased.

Astigmatism errors are usually corrected by design of the objectives to provide precise spacing of individual lens elements as well as appropriate lens shapes and indices of refraction. The correction of astigmatism is often accomplished in conjunction with the correction of field curvature aberrations.

From our discussion on optical aberrations, it should be clear that there are a number of factors that influence the performance of optical elements within the microscope. While there has been tremendous progress in the correction of these artifacts in recent years, designers still find it very difficult to completely remove or suppress all of the complicating optical problems associated with microscopy.

B.2 Field Curvature

Curvature of field in optical microscopy is an aberration that is familiar to most experienced microscopists. This artifact is the natural result of using lenses that have curved surfaces.

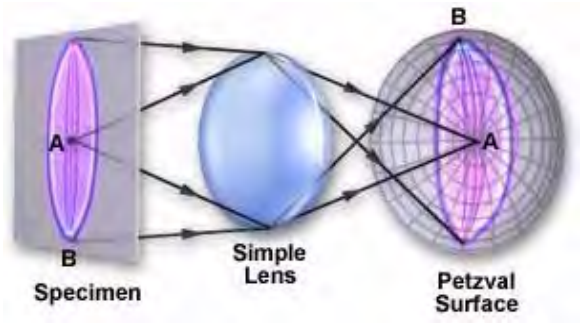

FIGURE B.9: Curvature of field

When visible light is focused through a curved lens, the image plane produced by the lens will be curved as illustrated in Figure B.9. Notice that there are two curved planes that we have labeled A and B.

The image can be focused over the range between A and B to produce either a sharp focus on the edges or in the center. When the image is viewed in the eyepieces (oculars) of a microscope, it either appears sharp and crisp in the center or on the edges of the viewfield but not both. Normally, this is not a serious problem when the microscopist is routinely scanning samples to observe their various features. It is a simple matter to use the fine focus knob to correct small deficiencies in specimen focus. However, for photomicrography, field curvature can be a serious problem, especially when a portion of the photomicrograph is out of focus.

This concept is illustrated in Figure B.10 using photomicrographs of a stained thin section of an elephant toe bone. The upper image (a) in Figure B.10 shows the thin section with only the edges in focus. Notice that the central portion of the image is very blurred and it is not possible to distinguish any minor structural details present in the specimen. The bottom image (c) in Figure B.10 shows the section with the central portion of the viewfield in focus and the edges blurred. This would be the focus that a microscopist would be forced to use for photomicrography with optics in this state. Figure B.10 (b) illustrates the case of an objective that has been corrected for curvature of field aberrations. This objective is the obvious choice for optimum results in photomicrography.

As we have mentioned before, curvature of field can be tolerated when just scanning samples, but it is disastrous when one is trying to produce quality photomicrographs. In the early days of microscopy before corrected lenses were enjoying widespread use, photomicrographers would often restrict the area recorded on film to the focused central area of the view field, thus obscuring the blurred edges. This can be easily accomplished by inserting a projection lens in the phototube to reduce the amount of viewfield available for the camera. Another method is to use a bellows extension on the camera to increase the camera film distance until only the central portion of the viewfield is visible.

Modern microscopes deal with field curvature by correcting this aberration using specially designed flat-field objectives. These specially-corrected objectives have been named plan or plano and are the most common type of objective in use today. Plan objectives are also corrected for other optical artifacts such as spherical and chromatic aberrations. In the case of a plan objective that also has been mostly corrected for chromatic aberration, the objective is referred to as a plan achromat. This is also the case for fluorite and apochromatic objectives, which have the modified names: plan fluorite and plan apochromat.

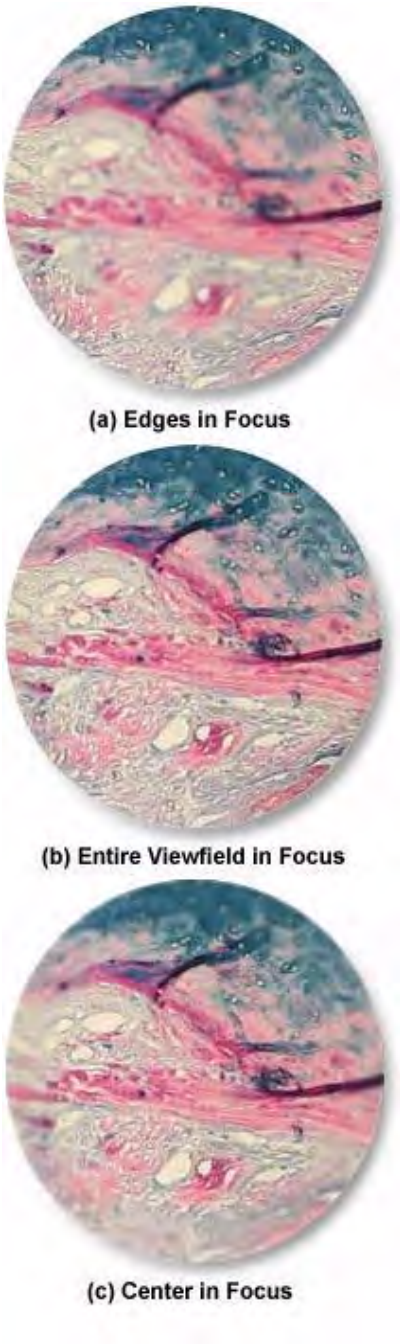

FIGURE B.10: Effect of curvature

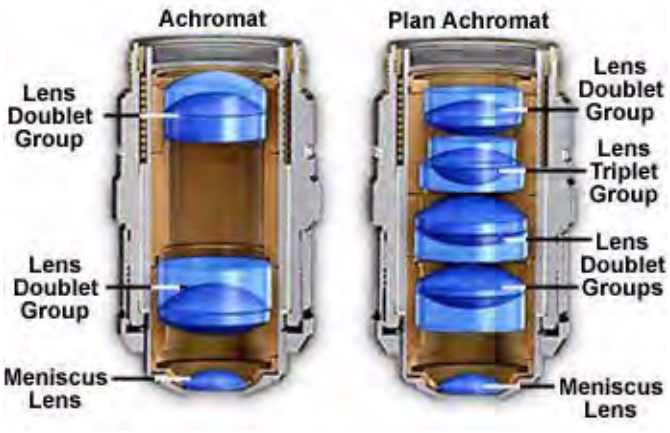

FIGURE B.11: Objective correction fo a field curvature

Adding field curvature lens corrections to an objective that has already been corrected for optical aberrations can often add a significant number of lens elements to the objective. For example, the typical achromat objective has two lens doublets and a hemispherical lens, making of total of five lens elements, as shown on the left-hand side of Figure B.11. In contrast, a comparable plan achromat objective has three doublets and three single lenses for a total of nine lens elements, making it considerably more difficult to fabricate. Cutaway diagrams illustrating both of these objectives are presented in Figure B.11. As we have seen, the number of lens elements increases as lenses are corrected for spherical errors as well as chromatic and field curvature aberrations. Unfortunately, as the number of lens elements increases so does the cost of the objective.

Sophisticated plan apochromatic objectives that correct for spherical, chromatic, and field curvature aberrations can contain as many as eighteen to twenty separate lens elements, making these objectives the most expensive and difficult to manufacture. Plan apochromatic objectives can cost upward of $3,000 to $4,000 each for high-magnification units that also have a high numerical aperture. For most photomicrography applications, however, it is not absolutely necessary to have the best correction, although this is heavily dependent upon the specimen and the desired magnification range. When cost is important (when isn't it?), it is often wise to select more modestly priced plan fluorite objectives that have a high degree of correction, especially the more modern versions. These objectives provide crisp and sharp images with minimal field curvature, and will be sufficient for over 90 percent of photomicrography applications.

Field curvature is very seldom totally eliminated, but it is often difficult to detect edge curvature with most plan-corrected objectives and it does not show up in photomicrographs. This artifact is more severe at low magnifications and can be a real problem with stereo microscopes. Manufacturers have struggled for years to eliminate field curvature in the large objectives found in stereo microscopes. In the past ten years companies like Nikon, Olympus, Zeiss, and Leica have made great strides in the quality of optics used to build stereo microscopes and, while the artifacts and aberrations have not been totally eliminated, the high-end models are now capable of producing superb photomicrographs.

Appendix C

Introduction to Modulation Transfer Function

The resolution and performance of an optical microscope can be characterized by a quantity known as the modulation transfer function (MTF), which is a measurement of the microscope's ability to transfer contrast from the specimen to the intermediate image plane at a specific resolution. Computation of the modulation transfer function is a mechanism that is often utilized by optical manufacturers to incorporate resolution and contrast data into a single specification.

The modulation transfer function is useful for characterizing not only traditional optical systems, but also photonic systems such as analog and digital video cameras, image intensifiers, and film scanners. This concept is derived from standard conventions utilized in electrical engineering that relate the degree of modulation of an output signal to a function of the signal frequency. In optical microscopy, signal frequency can be equated to a periodicity observed in the specimen, ranging from a metal line grating evaporated onto a microscope slide or repeating structures in a diatom frustule to subcellular particles observed in living tissue culture cells.

The number of spacings per unit interval in a specimen is referred to as the spatial frequency, which is usually expressed in quantitative terms of the periodic spacings (spatial period) found in the specimen. A common reference unit for spatial frequency is the number of line pairs per millimeter. As an example, a continuous series of black and white line pairs with a spatial period measuring 1 micrometer per pair would repeat 1000 times every millimeter and therefore have a corresponding spatial frequency of 1000 lines per millimeter.

Another important concept is the *optical transfer function* (OTF), which represents the ratio of image contrast to specimen contrast when plotted as a function of spatial frequency, taking into account the phase shift between positions occupied by the actual and ideal image. In general terms, the optical transfer function can be described as:

$$OTF = MTF \exp^{i\phi(f)}$$

in which the imaginary term represents the *phase transfer function* (PTF), or the change in phase position as a function of spatial frequency. Therefore, the optical transfer function is a spatial frequency-dependent complex variable whose modulus is the modulation transfer function, and whose phase is described by the phase transfer function. If the phase transfer function is linear with frequency, it represents a simple lateral displacement of the image as would be observed with an aberration such as geometric distortion. However, if the phase

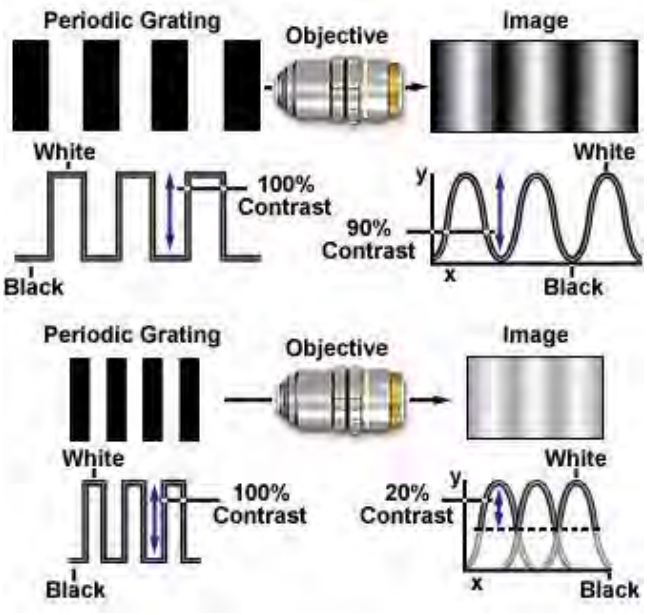

FIGURE C.1: Modulation and contrast transfer function

transfer function is nonlinear, it can adversely affect image quality. In the most dramatic example, a phase shift of 180 degrees produces a reversal of image contrast, where light and dark patterns are inverted.

A perfect optical system would have a modulation transfer function of unity at all spatial frequencies, while simultaneously having a phase transfer factor of zero. In cases where the image produced by the microscope (or other optical system) is sinusoidal and there is no significant phase shift, the modulus of the optical transfer function reverts to the modulation transfer function.

In situations where the specimen is a periodic line grating composed of alternating black and white lines of equal width (square waves), a graph relating the percentage of specimen contrast transferred to the image is known as the *contrast transfer function* (CTF). Most specimens display a composition of sinusoidally varying intensities having differing spatial frequencies instead of distinct sharp profiles in the form of square waves. In this case, a graph relating output as a fraction of input intensity versus signal (spatial) frequency is analogous to the modulation transfer function. As the spatial frequency approaches very large values, the square wave response resembles that of a sinusoid, yielding graphs of the contrast transfer function and the modulation transfer function that are virtually identical.

The effect of increasing spatial frequency on image contrast in a diffraction-limited optical microscope is illustrated in Figure C.1. A periodic line grating consisting of alternating white and black rectangular bars (representing 100 percent contrast) is presented at two spatial frequencies on the left-hand side of the figure. The resulting image produced in the microscope is shown on the right side of each objective, and appears as a sinusoidal intensity that has reduced contrast, which is plotted in the graph below the image in terms of a relative percentage of the object contrast. One hundred percent contrast represents regular white and black repeating bars, while zero percent contrast is manifested by gray bars that blend into a gray background of the same intensity. After the contrast value reaches zero, the image becomes a uniform shade of gray, and remains as such for all higher

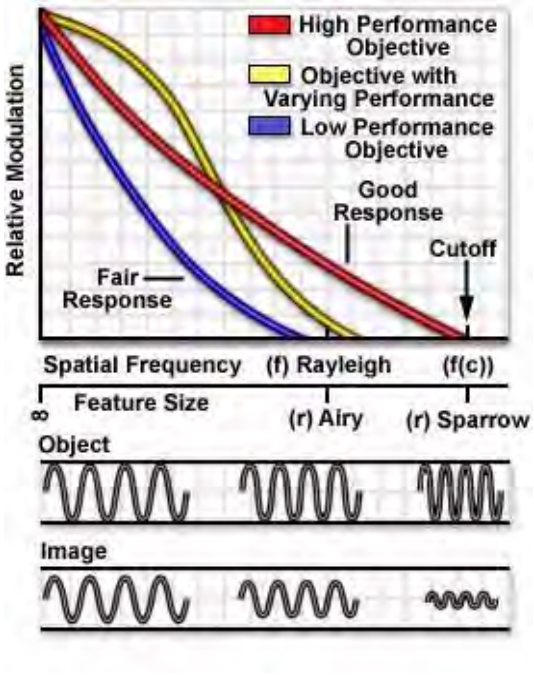

FIGURE C.2: Modulation transfer function

spatial frequencies.

When the input is a high contrast square wave, such as the periodic grating target illustrated in Figure C.1, transfer of contrast is determined by the contrast transfer function. A majority of specimens observed in the microscope, however, do not display such a regular periodicity and consist of "square waves" that are sinusoidal to varying degrees at the submicron level. In this case, the modulation transfer function is utilized to calculate transfer of contrast from the specimen to the image produced by the microscope.

Modulation of the output signal, the intensity of light waves forming an image of the specimen, corresponds to the formation of image contrast in microscopy. Therefore, a measurement of the MTF for a particular optical microscope can be obtained from the contrast generated by periodic lines or spacings present in a specimen that result from sinusoidal intensities in the image that vary as a function of spatial frequency. If a specimen having a spatial period of 1 micron (the distance between alternating absorbing and transparent line pairs) is imaged at high numerical aperture (1.40) with a matched objective/condenser pair using immersion oil, the individual line pairs would be clearly resolved in the microscope. The image would not be a faithful reproduction of the line pair pattern, but would instead have a moderate degree of contrast between the dark and light bars (Figure C.1). Decreasing the distance between the line pairs to a spatial period of 0.5 microns (spatial frequency equal to 2000 lines per millimeter) would further reduce contrast in the final image, but increasing the spatial period to 2 microns (spatial frequency equal to 500 lines per millimeter) would produce a corresponding increase in image contrast.

The limit of resolution with an optical microscope is reached when the spatial frequency approaches 5000 lines per millimeter (spatial period equal to 0.2 microns), using an illumination wavelength of 500 nanometers at high numerical aperture (1.4). At this point, contrast would be barely detectable and the image would appear a neutral shade of gray.

In real specimens, the amount of contrast observed in a microscope depends upon the size, brightness, and color of the image, but the human eye ceases to detect periodicity at contrast levels below about three to five percent for closely spaced stripes and may not reach the 0.2-micron limit of resolution.

When a specimen is observed in an optical microscope, the resulting image will be somewhat degraded due to aberrations and diffraction phenomena, in addition to minute assembly and alignment errors in the optics. In the image, bright highlights will not appear as bright as they do in the specimen, and dark or shadowed areas will not be as black as those observed in the original patterns. The specimen contrast or modulation (M) can be defined as:

$$M = \frac{I_{\max} - I_{\min}}{I_{\max} + I_{\min}}$$

where I_{max} is the maximum intensity displayed by a repeating structure and I_{min} is the minimum intensity found in the same specimen. By convention, the modulation transfer function is normalized to unity at zero spatial frequency. Modulation is typically less in the image than in the specimen and there is often a slight phase displacement of the image relative to the specimen. By comparing several specimens having differing spatial frequencies, it can be determined that both image modulation and phase shifts will vary as a function of spatial frequency. By definition, the modulation transfer function (MTF) is described by the equation:

$$\text{MTF} = \frac{\text{Image Modulation}}{\text{Object Modulation}}$$

This quantity, as discussed above, is an expression of the contrast alteration observed in the image of a sinusoidal object as a function of spatial frequency. In addition, there is a position or phase shift of the sinusoid that is dependent upon spatial frequency in both the horizontal and vertical coordinates. A good example occurs in video microscopy where the raster scanning process produces slightly different responses resulting in a variation between the horizontal and vertical modulation transfer functions.

The phase response from an ideal imaging system demonstrates a linear dependence on spatial frequency, with a position shift that is independent of the frequency and normalized to zero at zero spatial frequency. In the ideal system, all sinusoidal image components are displaced by the same amount, resulting in a net position shift for the image without degradation of image quality. When the phase response deviates from ideal linear behavior, then some components will be shifted to a greater degree than others resulting in image degradation. This is especially critical in electronic video systems, which often possess less than ideal phase characteristics that can lead to noticeable loss of image quality. Fortunately, an ideal aberration-free optical system having a circular aperture and a centered optical axis (such as a high-performance microscope) will produce a phase transfer function that has a value of zero for all spatial frequencies in all directions. In this case, phase shifts occur exclusively for off-axis rays and only the modulation transfer function need be considered.

A perfect aberration–free optical system is termed diffraction limited, because the effects of light diffraction at the pupils limit the spatial frequency response and establish the limits of resolution. Presented in Figure C.2 is a graph relating the modulation transfer function of a repeating specimen imaged with incoherent illumination by visible light with several different diffraction-limited microscope objectives having a circular pupil. In this case, objective quality affects the modulation response as a function of spatial frequency. Higher

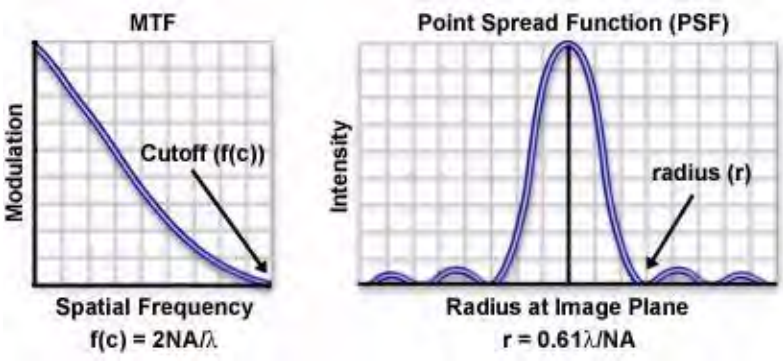

FIGURE C.3: Fourier relationship between MTF and PSF

quality objectives (red line in Figure C.2) exhibit greater performance than those of a lower quality (yellow line), and are able to transfer contrast more effectively at higher spatial frequencies. The objective represented by the yellow curve has the highest performance at low spatial frequencies, but falls short of the high numerical aperture objective at larger frequencies. Beneath the graph is a representation of relative feature size versus spatial frequency with respect to the Rayleigh criteria and Sparrow limit. Also presented is a series of sine waves representing a specimen (object) and the resulting image produced in a typical microscope as the frequency of the sinusoid increases.

When there are no significant aberrations present in an optical system, the modulation transfer function is related to the size of the diffraction pattern, which is a function of the system numerical aperture and wavelength of illumination. In quantitative terms, the modulation transfer function for an optical system with a uniformly illuminated circular aperture can be expressed as:

$$\mathrm{MTF} = 2\frac{\phi - \cos\phi \cdot \sin\phi}{\pi}$$

where

$$\phi = \cos^{-1}\left(\frac{\lambda \cdot \nu}{2\mathrm{NA}}\right)$$

In these equations, ν is the frequency in cycles per millimeter, λ is the wavelength of illumination, and NA is the numerical aperture. At low spatial frequencies, image contrast is the highest, but falls to zero as the spatial frequency is increased beyond a certain point (drawn in Figure C.2 as a reduction in amplitude produced in the image). The cutoff (f_c) is the spatial frequency at which contrast reaches zero and can be expressed by the equation:

$$f_c = \frac{2\mathrm{NA}}{\lambda}$$

It is interesting to note that this equation expresses (in terms of spatial frequency) the fact that resolution increases with both numerical aperture and shorter wavelengths.

The modulation transfer function is also related to the point spread function, which is the image of a point source of light (commonly referred to as the Airy disk) from the specimen projected by the microscope objective onto the intermediate image plane. Optical aberrations and numerical aperture variations affect the distribution of light intensity observed at the image plane, and thus influence the shape of the point spread function. Also

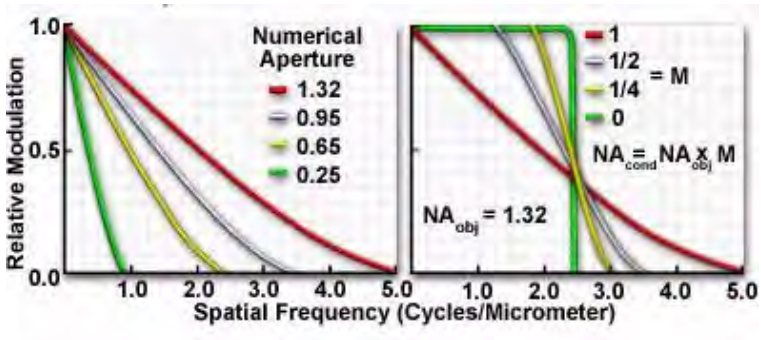

FIGURE C.4: Numerical aperture effect on modulation transfer function

note that the sum of the point spread functions produced by a specimen in a diffraction-limited microscope comprises the diffraction pattern produced at the image plane.

The highest spatial frequencies that can be imaged by a microscope objective are proportional to the numerical aperture and are based on the distribution size of the point spread function. Objectives with low numerical apertures produce point spread functions that have a wider intensity distribution at the image plane than those formed by objectives with higher numerical apertures. At the limit of resolution, adjacent Airy disks or point spread functions start to overlap, obscuring the ability to distinguish between individual intensities. Narrower intensity distributions (at higher numerical apertures) can approach each other more closely and still be resolved by the microscope. This implies that a narrow point spread function corresponds to a high spatial frequency. In fact, the optical transfer function, a measure of spatial frequency response for an optical system, is the mathematical Fourier transform of the point spread function.

The relationship between the modulation transfer function and the point spread function for a diffraction-limited optical microscope is illustrated in Figure C.3. As discussed above, the limiting cutoff frequency (f_c) of the modulation transfer function is directly proportional to the objective numerical aperture and inversely proportional to the illumination wavelength. The radius of the first dark concentric ring surrounding the central intensity peak of a point spread function (or Airy disk) is expressed by the equation:

$$r = 0.61\frac{\lambda}{\mathrm{NA}}$$

which is more commonly referred to as the Rayleigh criterion, or the resolution limit of the microscope. Because r is inversely proportional to numerical aperture and directly proportional to the illuminating wavelength, it follows that r and f_c are also inversely proportional, a fundamental property of Fourier transforms (the width of a function is inversely proportional to the width of its transform).

Individual objectives in a microscope display a specific modulation transfer function (or optical transfer function) that depends on numerical aperture, objective design, illumination wavelength, and the mode of contrast generation. When the numerical aperture of the condenser is equal to or greater than that of the objective, the spatial frequency cutoff value decreases with decreasing objective numerical aperture (Figure C.4(a)). Holding the objective numerical aperture value constant and varying the condenser numerical aperture results in progressively lower cutoff values with decreasing condenser numerical aperture (Figure C.4(b)).

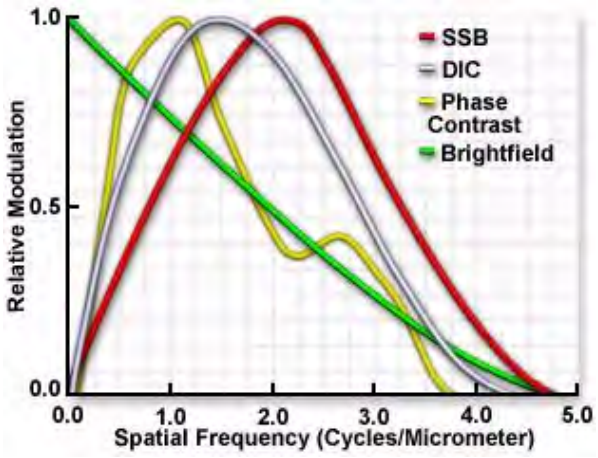

FIGURE C.5: Contrast enhancing technique MTFs

Utilization of contrast enhancing techniques such as phase contrast and differential interference contrast (DIC) results in unique modulation transfer functions that display curves markedly different from those observed in brightfield illumination using the objective's full numerical aperture (Figure C.5). For example, the narrow illumination produced by phase rings in phase contrast microscopy produces a modulation transfer function curve that oscillates above and below the brightfield curve, while the curves generated by DIC objectives vary with the angle between the specimen period and the shear direction of the Wollaston or Nomarski prisms. Also illustrated in Figure C.5 is the curve produced by a single-sideband edge enhancement microscope (developed by Dr. Gordon W. Ellis), which yields images of superior contrast at high spatial frequencies.

In practice, the performance of a microscope objective or other lens system is often determined by tracing a large number of light rays emitted by a point source in a uniformly distributed array over the vignetted entrance pupil of the objective. After passing through the exit pupil and being distributed over the image plane, the ray intersections are used to plot a spot diagram of the light points at the image plane. In most cases, several hundred rays are utilized to construct a spot diagram, which may take into account optical aberrations if the spacings of light rays are so adjusted. The resulting spot diagram is then regarded as a point spread function and is converted into a graph of the modulation transfer function versus spatial frequency by means of a Fourier transform.

Direct measurements of the modulation transfer function are conducted by utilizing specific test pattern targets consisting of high-contrast periodic line gratings having a series of spacings that usually range from one or several millimeters down to 0.1 micrometer, as illustrated in Figure C.8. These targets allow evaluation of microscope objective diffraction patterns, both in and out of focus, in a variety of contrast enhancing modes. Detector arrays are utilized to measure the distribution of light in the image plane by summation of the point spread functions, and a Fourier transform algorithm applied to the data to determine the modulation transfer function.

The target presented in Figure C.6(a) is designed specifically for testing the horizontal modulation transfer function of a macro imaging system such as a telescope, binoculars, video system, camera, or digital video recorder. It is composed of sinusoidal patterns having a spatial frequency range between 0.2 and 80 line pairs per millimeter with a grayscale

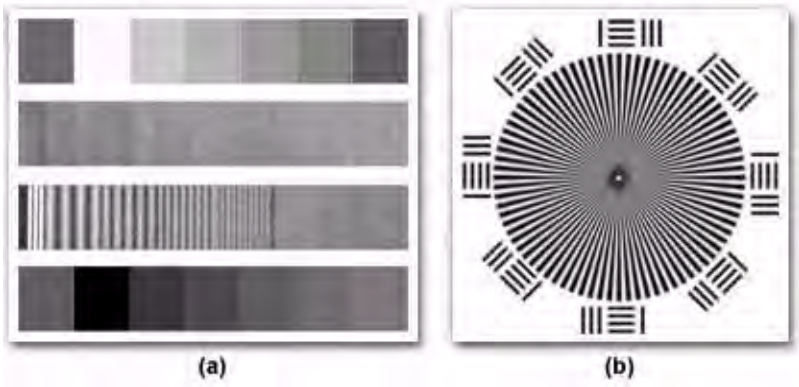

FIGURE C.6: Sinusoidal and star targets

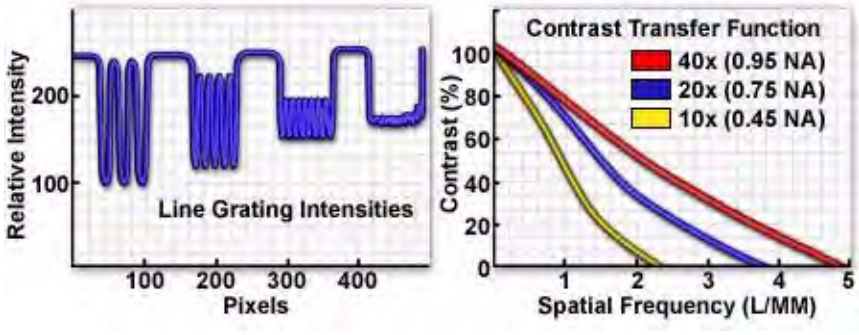

FIGURE C.7: Siemens star target intensity scan and CTF

optical density range varying between 0.2 and 1.2 and an 80 percent modulation of the sine waves. This type of target relays image quality information over a wide range of frequencies and contains on-target references for denoting the contrast levels of the sinusoidal frequencies. In video microscopy, microscopic test targets of sinusoidal targets are not readily available, so the contrast transfer function of a video detector coupled to the microscope is often determined rather than the modulation transfer function.

In systems that have a circular aperture (such as an optical microscope), the modulation and/or contrast transfer function is often computed or measured with star and bar targets similar to the one illustrated in Figure C.6(b). Targets of this type have both radial and tangential patterns that are orthogonal to each other and are also useful for detecting focus errors and aberrations such as astigmatism. Variations of the basic star target design contain paired lines and dots that allow determination of objective diffraction patterns both in and out of focus and are useful for measurements conducted in brightfield, reflection contrast, or epifluorescence illumination modes. The wedge and bar spacing period ranges from 0.1 micrometer to tens of microns with spatial frequencies between 0.2 and 25 line pairs per millimeter. Radial modulation transfer targets are ideal for high-resolution measurements using photographic film or analog sensors, but the horizontal and vertical pixelated nature of CCD detectors benefits from analysis utilizing targets that are geometrically consistent with the pixel rows and columns of the imaging device.

A typical intensity scan made from a star target measured with a high numerical aperture apochromatic objective operating in transmitted light mode is presented in Fig-

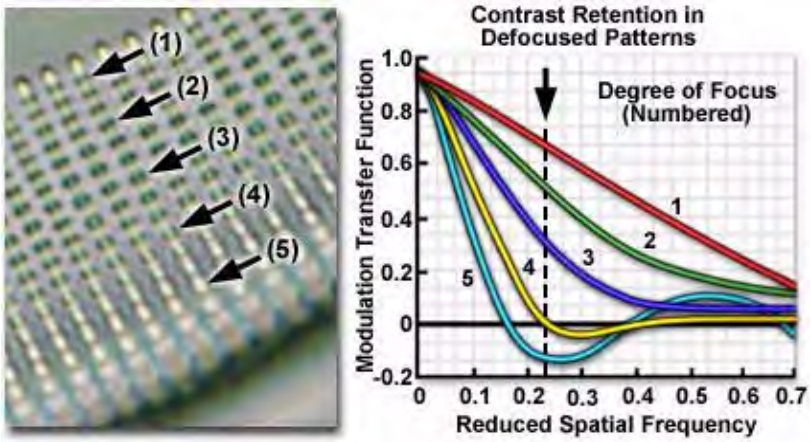

FIGURE C.8: Contrast inversion with defocus

ure C.7(a). Intensity values were averaged over the dimension parallel to the target grating lines. When these types of data are collected for a variety of objectives at varying numerical aperture and plotted as percent contrast versus spatial frequency, a graph similar to that illustrated in Figure C.7(b) is obtained. Contrast transfer approaches 100 percent at very low spatial frequencies (wide spacing periods) and gradually drops with increasing spatial frequency. As spatial frequencies reach the Abbe limit (the imaging wavelength divided by twice the objective numerical aperture), contrast values are generally too low to detect individual spacings in the line grating.

In some instances, the modulation transfer function of an optical microscope can actually be less than zero. This occurs in an otherwise functional system when performance is degraded due to defocus, aberrations, and/or manufacturing errors. Often, the modulation transfer function will oscillate above and below zero as the microscope is racked through the point of best focus on a specimen having features with high spatial frequency. When the transfer function dips below zero, the image undergoes a phase reversal in which dark features become bright and vice versa.

This phenomenon is illustrated in Figure C.8(a) for the periodic knobs imaged from the curved surface of a diatom frustule. As the microscope focus is changed, the knobs undergo inversion of contrast, producing a ripple effect in the relative modulation (compare knobs (1) through (5) in Figure C.8(a)). Increasing the degree of defocus will produce a corresponding increase in the oscillations observed with a modulation transfer function plot, with contrast reversals affecting increasingly larger features in the image. As the specimen plane is defocused, contrast drops rapidly for microscopic feature having high spatial frequencies and more slowly for those with low frequencies. It is often useful to measure contrast at a particular spatial frequency and then follow contrast as a function of distance on either side of the image plane. This analysis is sometimes termed the through-focus transfer function and is a measure of the depth of focus for a particular objective.

The relationship between spatial frequency and the modulation transfer function for the diatom is illustrated in Figure C.8(b). The graph represents a series of varying focus levels where the measured MTF is plotted against spatial frequency (number of sinusoidal features per unit distance). A drop in relative modulation values with defocus at fixed

spatial frequencies is obvious in the figure, as well as the contrast reversal at focus levels 4 and 5 where the reduced spatial frequency drops into negative values of the MTF. Curve number 1 represents the diatom frustule in focus, and curves 2 through 5 present the results with successively increasing levels of defocus. The dotted line corresponds to the approximate spatial frequency of the knobs illustrated in Figure C.8(a). Contrast is at a minimum where the dotted line crosses curve 4 and is reversed where curve 5 dips below zero on the y-axis.

All optical systems and supporting components including microscopes, digital and analog video systems, video capture boards, cables, computer monitors, photographic film emulsions, and the human eye each have a characteristic modulation transfer function. In the case of analog and digital electronic imaging detectors, the reciprocal relationship discussed above between spatial resolution and frequency response is valid. In this case, however, the point spread function is replaced by the time response to a very short electrical impulse, and the optical transfer function is replaced by the imaging system's response to the sinusoidal electrical signal with respect to amplitude and phase. Electronic systems lack the symmetry of optical systems, which introduces non-linear phase effects into the function. Regardless of these differences, the underlying concepts are similar between electronic and optical systems, and this allows optical microscopes coupled to digital (or analog) imaging equipment to be analyzed within a common framework.

The modulation transfer function of an optical system that contains a cascading series of components (microscope, digital video camera, video capture board, computer monitor, etc.) can be calculated by multiplying the individual MTF's of each component. By conducting a careful analysis of the combined system modulation transfer functions, a prediction about performance of the system can be obtained. In the same manner, the system phase response can be obtained by adding the phase transfer functions of individual components (Note: phase transfer functions are summed while modulation transfer functions are multiplied). Together, the modulation and phase transfer functions define the optical transfer function of the system. It is important to point out that the contrast transfer function does not have the same mathematical properties as the modulation transfer function and cannot be obtained simply by multiplying the CTF of individual components.

In a cascaded series of devices that work together to produce an image, contrast is lost in certain frequency regions at each step, generally at the higher end of the spatial frequency range. In this regard, each detector or image processing function can also be used to cut off or boost the modulation transfer function at certain frequencies. At each stage, noise introduced by image transfer and processing is also a function of spatial frequency. Therefore, fine-tuning the response for optimum image contrast and system performance is dependent not only upon the type of image information desired, but also the frequency dependence of noise levels in the image. In addition, because the modulation transfer function of a detector is wavelength-dependent, it must be determined under carefully defined conditions of illumination.

The modulation transfer function has not yet been established for several contrast enhancing modes commonly utilized in optical microscopy (such as polarized light), which await more highly perfected theories of image formation and appropriate test patterns (or specimens) to determine, by experiment, the MTF values.

Appendix D

Polarization and birefringence

D.1 Polarization of Light

Natural sunlight and almost every other form of artificial illumination transmits light waves whose electric field vectors vibrate in all perpendicular planes with respect to the direction of propagation. When the electric field vectors are restricted to a single plane by filtration, then the light is said to be polarized with respect to the direction of propagation and all waves vibrate in the same plane.

This concept is illustrated in Figure D.1 below. In this example, the incident light electric field vectors are vibrating perpendicular to the direction of propagation in an equal distribution of all planes before encountering the first polarizer. The polarizers illustrated above are actually filters containing long-chain polymer molecules that are oriented in a single direction. Only the incident light that is vibrating in the same plane as the oriented polymer molecules is absorbed, while light vibrating at right angles to the plane is passed through the first polarizing filter. In Figure D.1, polarizer 1 is oriented vertically to the incident beam so it will pass only the waves that are vertical in the incident beam. The wave passing through polarizer 1 is subsequently blocked by polarizer 2 because the second polarizer is oriented horizontally with respect to the electric field vector in the light wave. The concept of using two polarizers oriented at right angles with respect to each other is commonly termed crossed polarization and is fundamental to the practice of polarized light

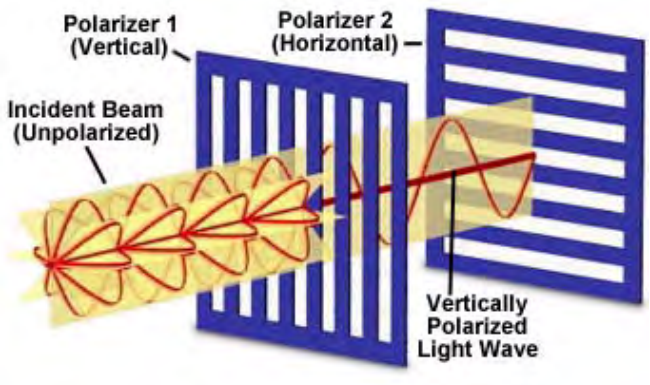

FIGURE D.1: 10x eyepiece with diopter adjustment and cross hair reticle

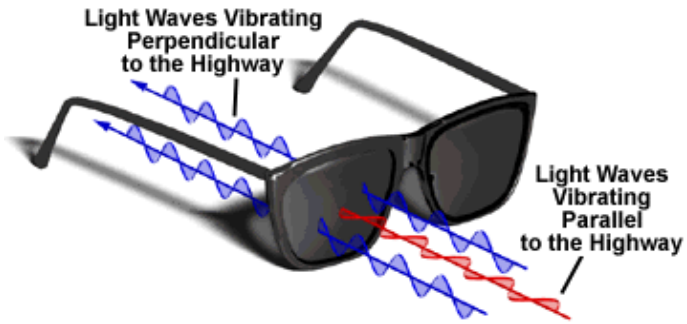

FIGURE D.2: Polarized sunglasses

microscopy.

Unpolarized incident light (natural sunlight, for example) is polarized to a certain degree when it is reflected from an insulating surface like water or a highway. In this case, light waves that have the electric field vectors parallel to the surface are reflected to a greater degree than those with different orientations. The optical properties of the insulating surface determine the exact amount of reflected light that is polarized. Mirrors are not good polarizers, although many transparent materials will be very good polarizers, but only if the incident light angle is within certain limits. In this case, the particular angle inducing maximum polarization is known as the *Brewster angle* given by the expression:

$$n = \frac{\sin\theta(i)}{\sin\theta(r)} = \frac{\sin\theta(i)}{\sin\theta(90-i)} = \tan\theta(i)$$

where n is the refractive index of the medium, $\theta(i)$ is the angle of incidence, and $\theta(r)$ is the angle of refraction.

This type of polarized light is often termed glare and can be easily demonstrated by viewing the distant part of a highway on a sunny day. Light reflected by the flat surface of a highway is partially polarized with the electric field vectors vibrating in a direction that is parallel to the ground. This light can be blocked by polarizing filters oriented in a vertical direction as illustrated below in Figure D.2 with a pair of polarized sunglasses.

The lenses of the sunglasses have polarizing filters that are oriented vertically with respect to the frames. In the Figure D.2 above, the blue light waves have their electric field vectors oriented in the same direction as the polarizing lenses and, thus, are passed through. In contrast, the red light wave is perpendicular to the filters and is blocked by the lenses. Polarizing sunglasses are very useful when driving in the sun or at the beach where sunlight is reflected from the surface of the road or water leading to glare that can be almost blinding.

One of the most common uses of polarization today is the liquid crystal display (LCD) used in numerous applications including wrist watches, computer screens, timers, clocks, and many others. These devices are based upon the interaction of rod-like liquid crystalline molecules with an electric field and polarized light waves. The liquid crystalline phase exists in a ground state that is termed cholesteric where the molecules are oriented in layers where each successive layer is slightly twisted to form a spiral pattern. When polarized light waves interact with the liquid crystalline phase the wave is "twisted" by an angle of approximately 90 degrees with respect to the incident wave. This angle is a function of the helical pitch of

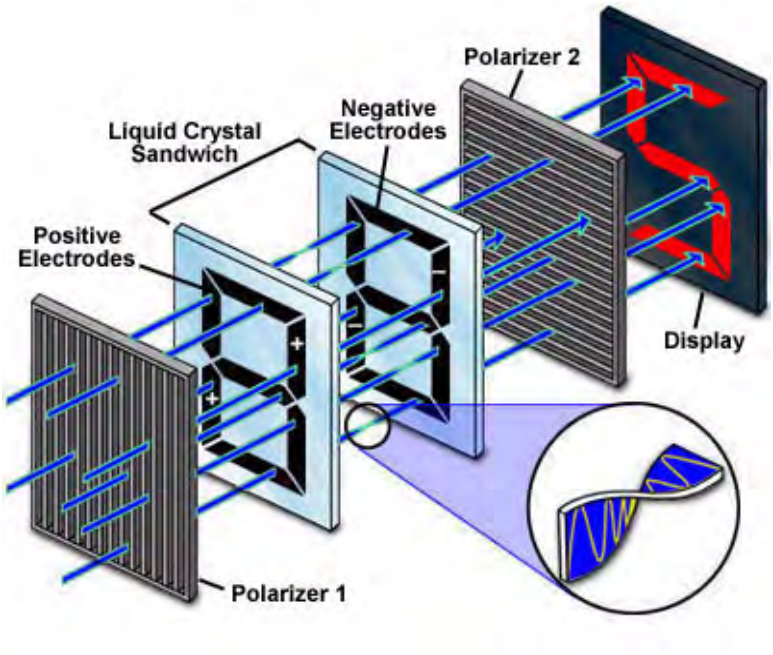

FIGURE D.3: Seven–segment liquid crystal display (LCD)

the cholesteric liquid crystalline phase, which is dependent upon the chemical composition of the molecules (it can be fine-tuned by small changes to the molecules).

An excellent example of the basic application of liquid crystals to display devices can be found in the seven-segment LCD numerical display (Figure D.3). Here, the liquid crystalline phase is sandwiched between two glass plates that have electrodes attached similar to those depicted in the illustration below. In figure D.3, the glass plates are drawn with seven black electrodes that can be individually charged (these electrodes are transparent to light in real devices). Light passing through polarizer 1 is polarized in the vertical direction and, when no current is applied to the electrodes, the liquid crystalline phase induces a 90 degree "twist" of the light and it can pass through polarizer 2, which is polarized horizontally and is perpendicular to polarizer 1. This light can then form one of the seven segments on the display.

When current is applied to the electrodes, the liquid crystalline phase aligns with the current and loses the cholesteric spiral pattern. Light passing through a charged electrode is not twisted and is blocked by polarizer 2. By coordinating the voltage on the seven positive and negative electrodes, the display is capable of rendering the numbers 0 through 9. In this example the upper right and lower left electrodes are charged and block light passing through them, allowing formation of the number "2".

Polarization of light is very useful in many aspects of optical microscopy. The microscope configuration uses crossed polarizers where the first polarizer (termed: the polarizer) is placed below the sample in the light path and the second polarizer (termed: the analyzer) is placed above the sample, between the objective and the eyepieces. With no sample on the microscope stage, the light polarized by the polarizer is blocked by the analyzer and no light is visible. When samples that are birefringent are viewed on the stage between crossed polarizers, the microscopist can visualize aspects of the samples through light rotated by the sample and then able to pass through the analyzer. The details of polarized

light microscopy are thoroughly discussed in our microscopy section of this primer.

D.2 Optical Birefringence

Many transparent solids are optically isotropic, meaning that the index of refraction is equal in all directions throughout the crystalline lattice. Examples of isotropic solids are glass, table salt (sodium chloride, illustrated in Figure D.4(a)), many polymers, and a wide variety of both organic and inorganic compounds.

The simplest crystalline lattice structure is cubic, as illustrated by the molecular model of sodium chloride in Figure D.4(a), in which all of the sodium and chloride ions are arranged with uniform spacing along three mutually perpendicular axes. Each chloride ion is surrounded by (and electrostatically bonded to) six individual sodium ions and visa versa for the sodium ions. The lattice structure illustrated in Figure D.4(b) represents the mineral calcite (calcium carbonate), which consists of calcium and carbonate ions. Calcite has an anisotropic crystalline lattice that interacts with light in a totally different manner than isotropic crystals. The polymer illustrated in Figure D.4(c) is amorphous and devoid of any recognizable crystalline structure. Polymers often possess some degree of crystalline order and may or may not be optically transparent.

Crystals are classified as being either isotropic or anisotropic depending upon their optical behavior and whether or not their crystallographic axes are equivalent. All isotropic crystals have equivalent axes that interact with light in a similar manner, regardless of the crystal orientation with respect to incident light waves. Light entering an isotropic crystal is refracted at a constant angle and passes through the crystal at a single velocity without being polarized by interaction with the electronic components of the crystalline lattice.

Anisotropic crystals, on the other hand, have crystallographically distinct axes and interact with light in a manner that is dependent upon the orientation of the crystalline lattice with respect to the incident light. When light enters the optical axis of anisotropic crystals, it acts in a manner similar to interaction with isotropic crystals and passes through at a single velocity. However, when light enters a non-equivalent axis, it is refracted into two rays each polarized with the vibration directions oriented at right angles to one another, and traveling at different velocities. This phenomenon is termed “double” or “bi” refraction and is seen to a greater or lesser degree in all anisotropic crystals.

Perhaps the most dramatic demonstration of double refraction occurs with calcium carbonate (calcite) crystals as illustrated in Figure D.5. The rhombohedral cleavage block of calcite in Figure D.5 produces two images when it is placed over the blue pencil. One of the images appears as you normally would expect when viewing an object through clear glass or an isotropic crystal. The other pencil image appears displaced, due to the nature of doubly-refracted light. When anisotropic crystals refract light, the resulting rays are polarized and travel at different velocities as discussed above. One of the rays travels with the same velocity in every direction through the crystal and is termed the ordinary ray. The other ray travels with a velocity that is dependent upon the propagation direction within the crystal. This light ray is termed the extraordinary ray. The distance of separation between the ordinary and extraordinary ray increases with increasing crystal thickness. The two independent refractive indices of anisotropic crystals are quantified in terms of their birefringence, a measure of the difference in refractive index. Thus, the birefringence (B, often termed δ, or Δ) of a crystal is defined as:

$$B = |n_{\text{high}} - n_{\text{low}}|$$

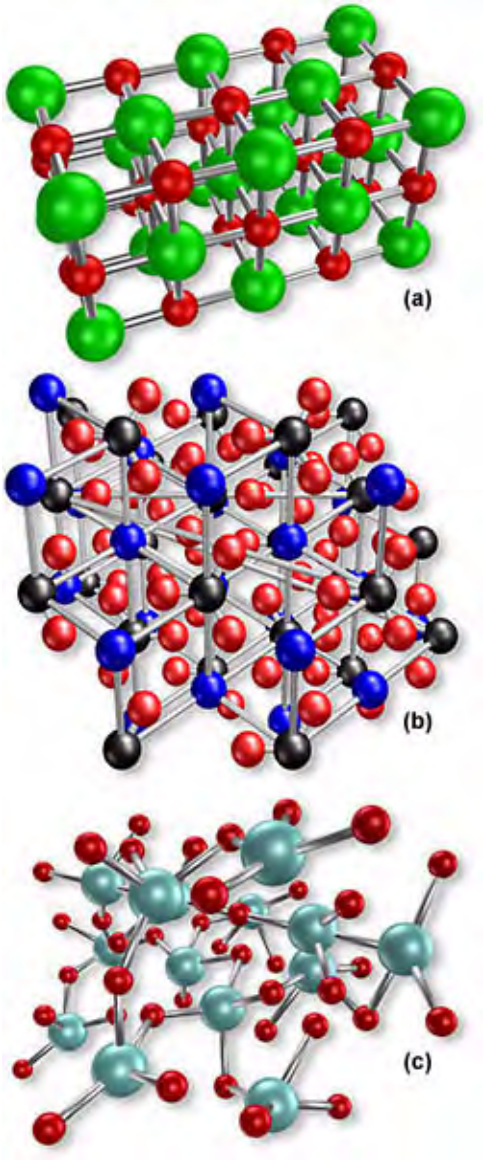

FIGURE D.4: Examples of lattice

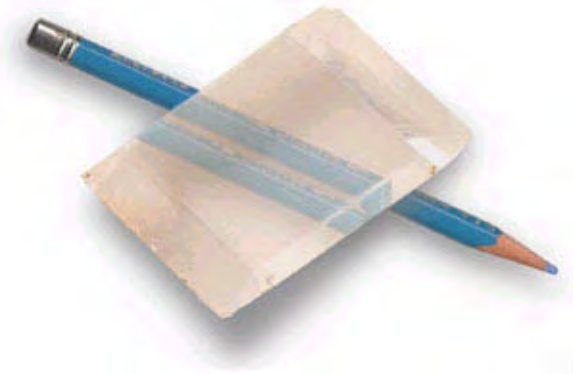

FIGURE D.5: Calcite crystal birefringence

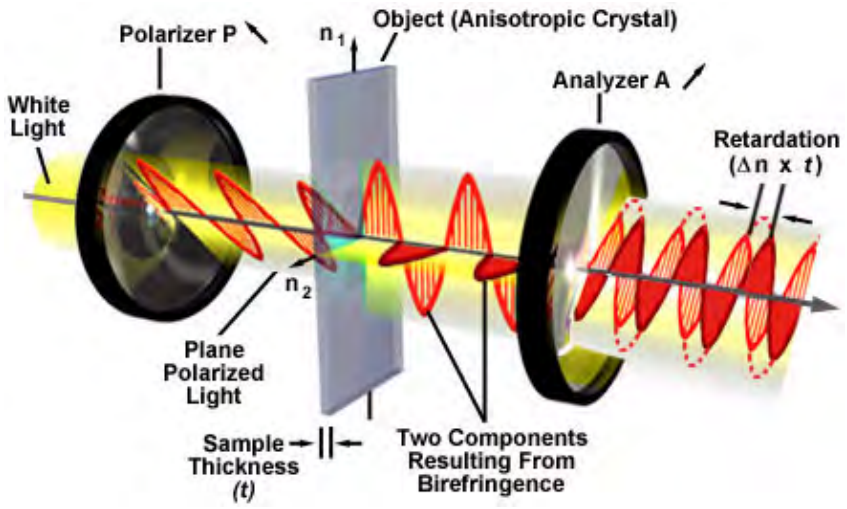

FIGURE D.6: Birefringence crystal between crossed polarizers

where n_{high} is the largest refractive index and n_{low} is the smallest. This expression holds true for any part or fragment of an anisotropic crystal with the exception of light waves propagated along the optical axis of the crystal. As we mentioned above, light that is doubly refracted through anisotropic crystals is polarized with the vibration directions of the polarized ordinary and extraordinary light waves being oriented perpendicular to each other. We can now examine how anisotropic crystals behave under polarized illumination in a polarizing microscope. Figure D.6 illustrates a birefringent crystal placed between two polarizers whose vibration directions are perpendicular to each other (and oriented according to the arrows next to the polarizer and analyzer labels).

White light entering the polarizer on the left is polarized with an orientation in the direction indicated by the arrow (next to the polarizer label) and is arbitrarily represented by a "red" sinusoidal light wave. Next, the polarized light enters the anisotropic crystal where it is refracted and divided into two separate components vibrating parallel to the crystallographic axes and perpendicular to each other (arbitrarily, the "blue" and "red" light waves). The polarized light waves then pass through the analyzer (whose polarization position is indicated by the arrow next to the analyzer label), which passes only those components of the light waves that are parallel to the polarization direction of the analyzer. The retardation of one ray with respect to another is indicated by $\Delta n \cdot t$, the difference in speed between the ordinary and extraordinary rays refracted by the anisotropic crystal.

Let us now examine more closely how birefringent anisotropic crystals interact with polarized light in an optical microscope. Our subject material is a hypothetical tetragonal crystal having an optical axis oriented parallel to the long axis of the crystal. Light entering the crystal from the polarizer will be traveling perpendicular to the optical (long) axis of the crystal. Figure D.7 illustrates the crystal as it would appear in the eyepieces of a microscope under crossed-polarized illumination. In each part of Figure D.7, the axis of the microscope polarizer is indicated by a P and is oriented in an East-West direction. The axis of the microscope analyzer is indicated by an A and is oriented in a North-South direction. These axes are perpendicular to each other and result in a totally dark field when viewed through the eyepieces without insertion of birefringent crystals. Figure D.7(a) illustrates an anisotropic birefringent crystal that has the long (optical) axis oriented parallel to the

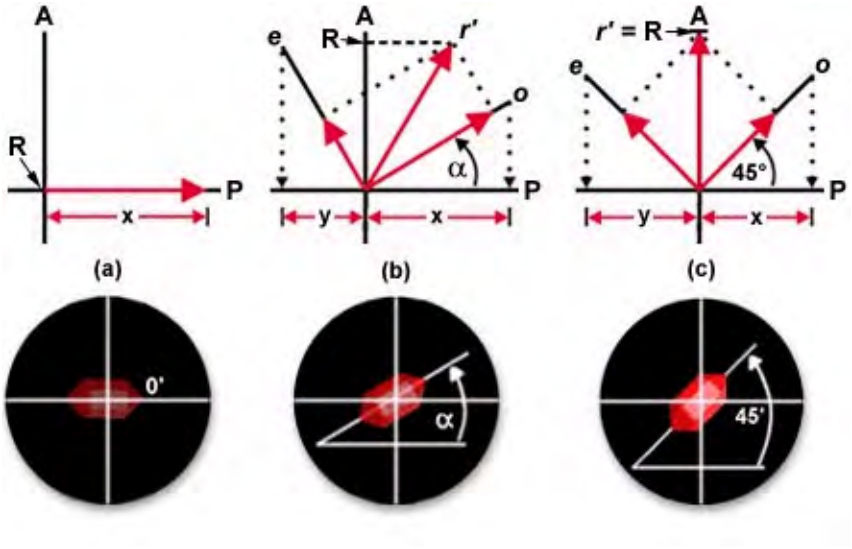

FIGURE D.7: Anisotropic birefringence

direction of the polarizer.

In this case, light passing through the polarizer, and subsequently through the crystal, is vibrating in a plane that is parallel to the direction of the polarizer. There is no contribution from light passing through the analyzer (because of the single direction of light vibration – parallel to the polarizer) resulting in the crystal being very dark and almost invisible. In Figure D.7(a) the crystal is not totally extinct (as it would be between crossed polarizers) but passes a small portion of red light. This was done for illustration purposes only to allow visitors to note the position of the crystal.

Microscopists classically refer to this orientation as being a position of extinction for the crystal. This observation is important in determining the refractive indices of anisotropic materials with a polarizing microscope. By removing the analyzer in a crossed polarizing microscope, the single permitted direction of vibration of light passing through the polarizer interacts with only one electrical component in the birefringent material (crystal). This allows segregation of a single refractive index for measurement. The remaining refractive index of the material can then be measured by rotation of the polarizer by 90 degrees.

The situation is very different in Figure D.7(b), where the long (optical) axis of the crystal is now positioned at an angle (α) with respect to the polarizer. In this case a portion of the light received through the polarizer is passed on to the analyzer. To quantitate the amount of light passing through the analyzer, we can apply simple vector analysis to solve the problem. The first step is to find the contributions from the polarizer to o and e (see Figure D.7(b)—these are arbitrary designations for the ordinary (o) ray and extraordinary (e) ray similar to the method described by Foster). This is accomplished by dropping projections of the vectors onto the axis of the polarizer. This method assumes the arbitrary value of 1 for both o and e, which are proportional to the actual intensities of the ordinary and extraordinary ray. The contributions from the polarizer for o and e are illustrated with red arrows designated by x and y on the polarizer axis (P) in Figure D.7(b). These lengths are then measured on the vectors o and e (also shown as red arrows on the vectors) to produce the resultant r', which is projected onto the analyzer axis (A) as the absolute value R. As we discussed above, the value of R on the analyzer axis is proportional to

the amount of light passing through the analyzer. This indicates that some light from the polarizer passes through the analyzer and the birefringent crystal displays some order of brightness.

The maximum brightness for a the birefringent material is shown when the long (optical) axis of the crystal is oriented at a 45 degree angle to both the polarizer and analyzer, as illustrated in Figure D.7(c). Dropping the projections of the vectors o and e onto the polarizer axis (P) determines the contributions of the polarizer to these vectors. When these projections are then measured on the vectors (again with red arrows on the vectors) and completing the rectangle to compute the resultant value r', we find the maximum possible contribution to light passed through to the analyzer in this system. This method will work for the orientation of any crystal with respect to the polarizer and analyzer axis because o and e are always at right angles to each other, with the only difference being the orientation of o and e with respect to the crystal axes.

Now we will consider the phase relationship and velocity differences between the ordinary and extraordinary rays after they pass through a birefringent crystal. These rays are oriented so that they are vibrating at right angles to each other. Each ray will encounter a slightly different electrical environment (refractive index) as it enters the crystal and this will affect the velocity at which ray passes through the crystal. Because of the difference in refractive indices, one ray will pass through the crystal at a slower rate than the other ray. In other words, the velocity of the slower ray will be retarded with respect to the faster ray. This retardation (Γ) can be quantified using the following equation:

$$\Gamma = t \cdot |n_{\text{high}} - n_{\text{low}}|$$

Where t is the thickness of the birefringent crystal (or material). Factors contributing to the value of retardation are the magnitude of the difference in refractive indices for the environments seen by the ordinary and extraordinary rays and also the sample thickness. Obviously, the greater the difference in either refractive indices or thickness, the greater the degree of retardation. Early observations made on the mineral calcite indicated that thicker calcite crystals caused greater differences in splitting of the images seen through the crystals illustrated in Figure D.5. This agrees with the equation above that states retardation will increase with crystal (or sample) thickness.

When the ordinary and extraordinary rays emerge from the birefringent crystal, they are still vibrating at right angles with respect to one another. However, the components of these waves that pass through the analyzer are vibrating in the same plane as illustrated in Figure D.6 above. Because one wave is retarded with respect to the other, interference (either constructive or destructive) occurs between the waves as they pass through the analyzer. The net result is that some birefringent samples acquire a spectrum of color when observed in white light through crossed polarizers. This will be discussed in greater detail in the section on Polarized Light Microscopy.

Quantitation of the colors seen in birefringent samples is commonly provided by means of the Michel-Levy chart illustrated in Figure D.8 above. As is evident from this graph, the polarization colors seen in the microscope can be correlated with the actual retardation, thickness, and birefringence of the sample. The chart is simple to use with birefringent samples if you know two of the three variables. When the sample is placed between crossed polarizers in the microscope and rotated to a position of maximum brightness, the color produced by the sample can be traced down on the retardation axis to find the wavelength difference between the ordinary and extraordinary ray of the sample. Alternatively, by

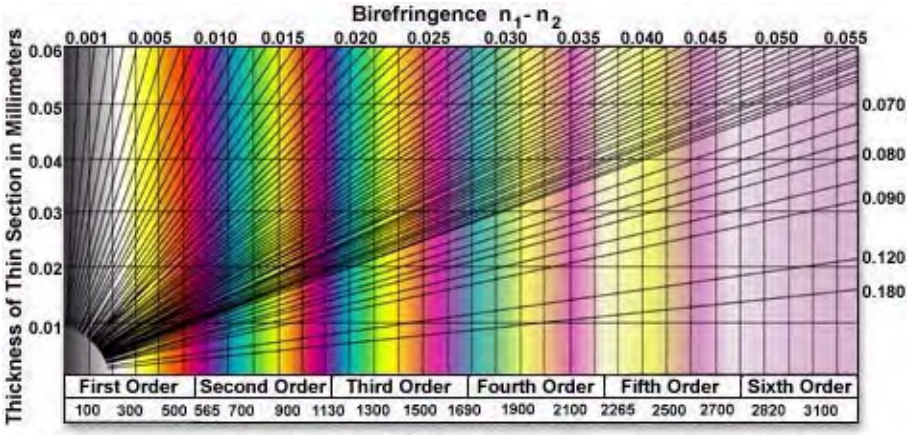

FIGURE D.8: Michel–Levy chart

measuring the refractive indices of the sample and calculating their difference (the birefringence (B), you can find the color of the sample from the birefringence values along the top of the chart. By extrapolating the angled lines back to the ordinate, you can also calculate the thickness of the sample.

The bottom section of the Michel-Levy chart marks the orders of retardation in multiples of approximately 550 nanometers. The area between zero and 550 nanometers is known as the first order of the polarization colors, and the magenta color that occurs in the 550 nanometer region is often called first-order red. Colors between 550 and 1100 nanometers are termed second-order colors and so on up the chart. The black color at the beginning of the chart is called zero-order black. Most Michel-Levy charts plot higher-order colors up to the fifth or sixth order.

The most sensitive area of the chart is first-order red (550 nanometers), because even a slight change in retardation causes the color to shift dramatically either up to cyan or down to yellow. Many microscope manufacturers take advantage of this sensitivity by providing a full-wave retardation plate or first-order red compensator with their polarizing microscopes to assist scientists in determining the properties of birefringent materials.

Appendix E

Fluorescence Microscopy Combination Methods

To minimize the effects of photobleaching, fluorescence microscopy can be combined with other techniques that are non-destructive to the fluorochrome, such as differential interference contrast (DIC), Hoffman modulation contrast (HMC), transmitted darkfield illumination, and phase contrast.

E.1 Fluorescence with Differential Interference Contrast

The idea is to locate a specific area of interest in a specimen using the non-destructive contrast enhancing technique then, without relocating the specimen, switch the microscope to fluorescence mode. The results of a typical experiment of this type are illustrated in Figure **??**. Figure **??**(a) illustrates a rat retina optic ganglion tissue thin section imaged using differential interference contrast. The photomicrograph in Figure **??**(b) shows the same viewfield, but this time imaged using fluorescence illumination (a mercury vapor lamp and an Olympus WU filter cube) with cells stained by the fluorochrome fast blue, a diazonium salt that specifically stains phospholipids in the myelin sheath. Figure **??**(c) illustrates the two techniques used in combination to produce a beautiful photomicrograph of fluorescent-stained optic ganglion lipid tissue superimposed on a differential interference contrast image of the retina. This image was recorded with a specialized fluorite objective designed to permit simultaneous observation of both fluorescence and differential interference contrast with the same objective.

The microscope configuration typically utilized to simultaneously image specimens using both differential interference contrast (DIC) and fluorescence illumination is illustrated in Figure **??**. DIC is conducted using transmitted light provided by a tungsten-halogen lamp positioned in a lamphouse attached to the microscope base. Light passing through the field diaphragm is reflected by a mirror into the substage condenser and through a Wollaston prism located at the front focal plane of the condenser.

Light diffracted by the specimen is first passed through a second Wollaston prism positioned near the objective rear focal plane before interfering at the intermediate image plane with light passing through the specimen undiffracted. Simultaneously, ultraviolet light emitted by a mercury burner is passed through an exciter filter, then reflected by a dichroic mirror onto the specimen from above. Secondary fluorescence emitted by the chromophore attached to the stained specimen is captured by the objective and passed

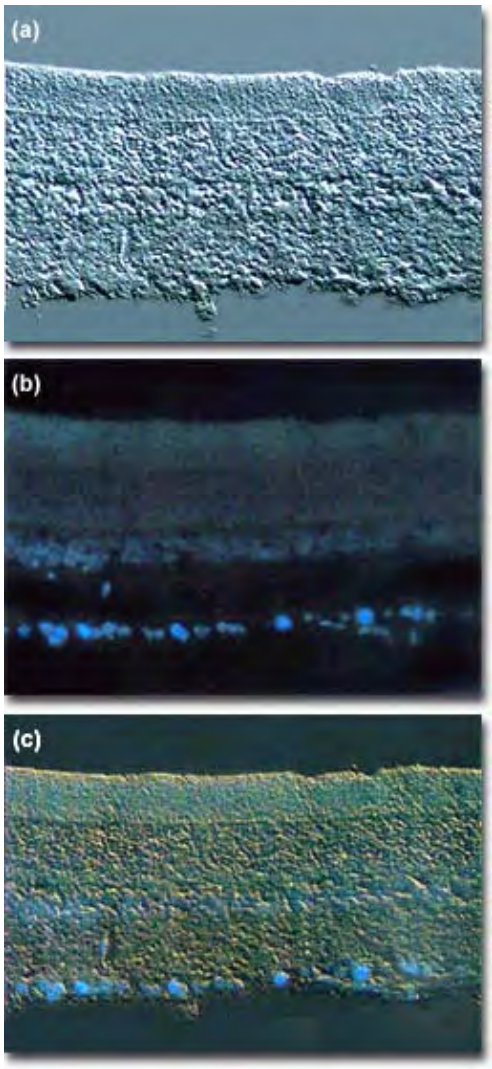

FIGURE E.1: Fluorescence with DIC

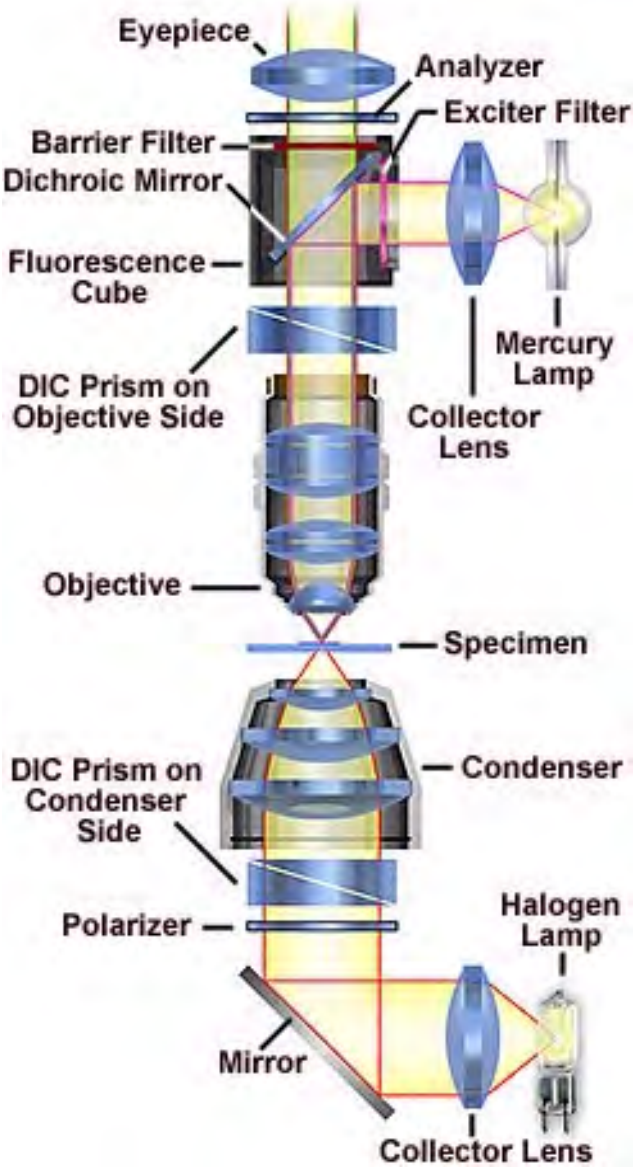

FIGURE E.2: DIC/Fluorescence combination microscope configuration

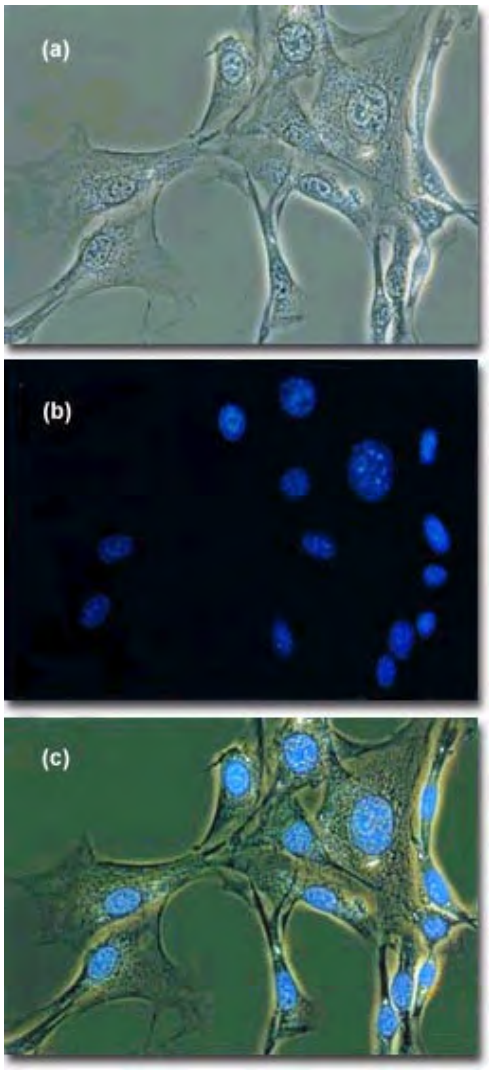

FIGURE E.3: Fluorescence with phase contrast

through the barrier filter and into the eyepieces and/or phototube. This configuration can be used to image specimens using the techniques (fluorescence and differential interference contrast) individually or in combination.

E.2 Fluorescence with Phase Contrast

The idea is to locate a specific area of interest in a specimen using the non-destructive contrast enhancing technique then, without relocating the specimen, switch the microscope to fluorescence mode. The results of a typical experiment of this type are illustrated in Figure **??**. Figure **??**(a) illustrates 3T3 fibroblasts in monolayer tissue culture imaged using phase contrast optics. The cell line was established from a National Institutes of Health line of Swiss mouse embryo cells, which are highly contact inhibited and useful for studies involving sarcoma virus formation and leukemia virus propagation. The photomicrograph in Figure **??**(b) shows the same viewfield, but this time imaged using fluorescence illu-

mination (a mercury vapor lamp and an Olympus WU filter cube) with cells stained by the fluorochrome 4',6–diamidino–2–phenylindole (DAPI), a nucleic acid specific dye with an emission maximum at 461 nanometers, which is used to selectively stain nuclei and chromatin. Figure **??**(c) illustrates the two techniques used in combination to produce a beautiful photomicrograph of fluorescent-stained 3T3 cellular nuclei superimposed on a phase contrast image of the fibroblast cell membranes and internal organelles. This image was recorded with a specialized fluorite objective designed with phase rings to permit simultaneous observation of both fluorescence and phase contrast with the same objective.

The microscope configuration typically utilized to simultaneously image specimens using both phase contrast and fluorescence illumination is illustrated in Figure **??**. Phase contrast is conducted using transmitted light provided by a tungsten-halogen lamp positioned in a lamphouse attached to the microscope base. Light passing through the field diaphragm is reflected by a mirror into the substage condenser and through a phase annulus of the proper dimensions.

Light diffracted by the specimen is first passed through a phase plate positioned in the objective rear focal plane before interfering at the intermediate image plane with light passing through the specimen undiffracted. Simultaneously, ultraviolet light emitted by a mercury burner is passed through an exciter filter, then reflected by a dichroic mirror onto the specimen from above. Secondary fluorescence emitted by the chromophore attached to the stained specimen is captured by the objective and passed through the barrier filter and into the eyepieces and/or phototube. This configuration can be used to image specimens using the techniques (fluorescence and phase contrast) individually or in combination.

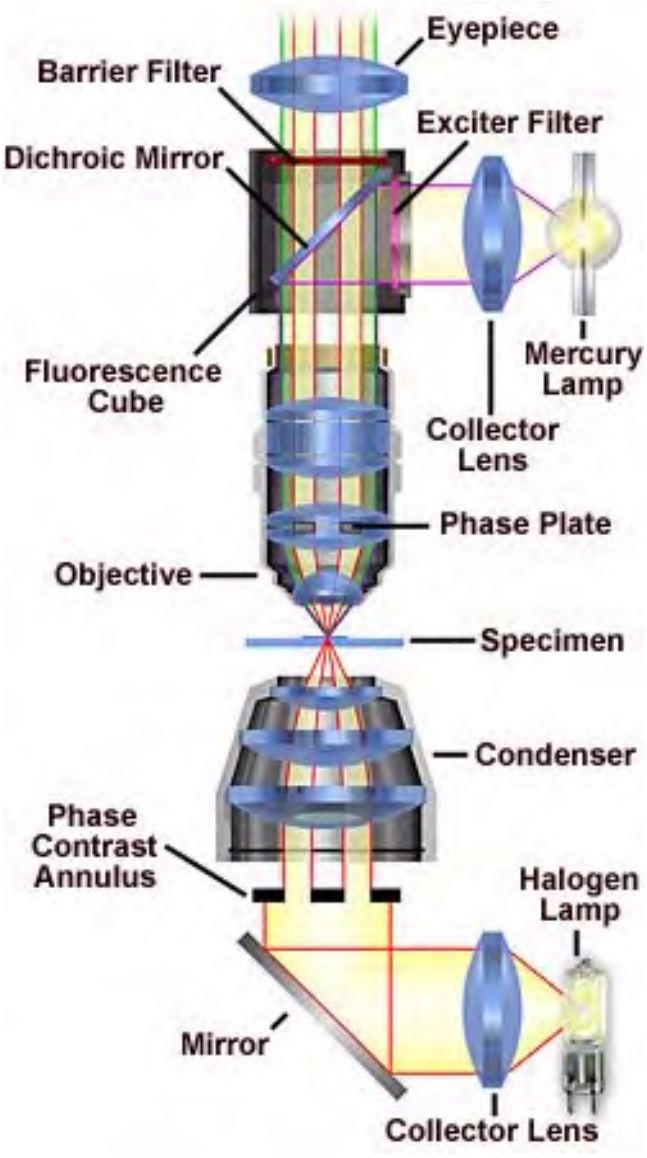

FIGURE E.4: Phase contrast/Fluorescence combination microscope configuration